Theses and Dissertations

12-1-2016

Part 1: Design, Synthesis, and Evaluation of Novel Gram-positive Antibiotics Part 2: Synthesis of Dihydrobenzofurans Via a New Transition Metal Catalyzed Reaction Part 3: Design, Synthesis, and Evaluation of Bz/gabaa A6 Positive Allosteric Modulators

Christopher Michael Witzigmann
University of Wisconsin-Milwaukee

Follow this and additional works at: https://dc.uwm.edu/etd

Part of the Organic Chemistry Commons

Recommended Citation

Witzigmann, Christopher Michael, "Part 1: Design, Synthesis, and Evaluation of Novel Gram-positive Antibiotics Part 2: Synthesis of Dihydrobenzofurans Via a New Transition Metal Catalyzed Reaction Part 3: Design, Synthesis, and Evaluation of Bz/gabaa A6 Positive Allosteric Modulators" (2016). *Theses and Dissertations*. 1429.
https://dc.uwm.edu/etd/1429

PART 1: DESIGN, SYNTHESIS, AND EVALUATION OF NOVEL

GRAM-POSITIVE ANTIBIOTICS

PART 2: SYNTHESIS OF DIHYDROBENZOFURANS VIA A NEW

TRANSITION METAL CATALYZED REACTION

PART 3: DESIGN, SYNTHESIS, AND EVALUATION OF BZ/GABA$_A$ α6

POSITIVE ALLOSTERIC MODULATORS

by

Christopher Michael Witzigmann

A Dissertation Submitted in

Partial Fulfillment of the

Requirements for the Degree of

Doctor of Philosophy

in Chemistry

at

The University of Wisconsin-Milwaukee

December 2016

ABSTRACT

PART 1: DESIGN, SYNTHESIS, AND EVALUATION OF NOVEL
GRAM-POSITIVE ANTIBIOTICS
PART 2: SYNTHESIS OF DIHYDROBENZOFURANS VIA A NEW TRANSITION METAL
CATALYZED REACTION
PART 3: DESIGN, SYNTHESIS, AND EVALUATION OF BZ/GABA$_A$ α6 POSITIVE
ALLOSTERIC MODULATORS

by

Christopher Michael Witzigmann

The University of Wisconsin-Milwaukee, 2016
Under the Supervision of Distinguished Professor James M. Cook

Part 1. Lead compound **SK-03-92** represents a new scaffold for antibiotic drug

discovery. Development of a new process for the synthesis of analogs has led to the

development of a number of new ligands with even more potent activity against gram-positive

bacteria, including drug-resistant strains of *S. aureus*. Compounds **36** and **38** represent some of

the most potent analogs developed thus far, and preliminary results indicate that they are also not

cytotoxic. Research into a Heck-mediated transition metal catalyzed pathway towards electron-

rich stilbenoid analogs has greatly expanded the scope of future SAR studies. This development

has led to 14 new analogs with minimum inhibitory concentrations (MICs) in pharmaceutically

acceptable ranges and it is presumed that further SAR expansion will lead to even more potent

compounds. Mechanism of action studies have shown that these compounds prove difficult to

induce mutations in bacteria that lead to drug-resistance. This has made determination of the

mechanism/mode of action difficult, and to date it is still not known, but is promising in that a

lack of developed resistance may show that these compounds act on pathways that are novel and

unlikely to form resistance. An enzyme catalyzed pathway involving tyrosinase is postulated as

a plausible mechanism for these stilbenoid compounds. This process would involve the

formation of quinones, which might be toxic to the bacteria, causing the observed bactericidal nature of these potent analogs. Further, this may explain some of the observed activity for a number of analogs synthesized in this study. The need for new antibiotics is clear, and these novel compounds represent a new scaffold for antibiotic drug discovery.

Part 2. Dihydrobenzofurans are an important class of compounds, a number of which are natural products and/or biologically active. A new transition metal catalyzed pathway was developed to synthesize novel dihydrobenzofurans. This new process was modified from the Heck reaction developed in Part 1. Initially, the dihydrobenzofurans synthesized by the Heck mediated process were in very low yields. Optimization of the conditions for this reaction were successful in improving the conversion to nearly quantitative levels. A preliminary examination of the scope of the reactions indicated that a number of electron-rich aryl bromides were well tolerated and high yields for nearly all attempted aryl bromides were reported. The scope of vinyl arenes includes both aryl and heteroaryl vinylic compounds, many of which were conveniently synthesized from inexpensive starting materials. This reaction sequence is similar to work reported by Larock, however differs in a number of significant ways.

Part 3. The α_6 subunits of $GABA_A$ receptors exhibit a quite restricted regional distribution in the brain. They are predominantly expressed in the granule cells of the cerebellum, and in the cochlea nuclei. Our recent study revealed that the α_6 $GABA_A$R in the cerebellum plays an important role in controlling the sensorimotor gating function, a deficit of this function is manifested in several neuropsychiatric disorders, such as schizophrenia, tic disorders, attention deficit hyperactivity disorder, obsessive compulsive disorder. We have designed a series of pyrazoloquinolinone ligands that are functionally selective for $\alpha_6\beta_{2,3}\gamma_2$ $GABA_A$ receptors and are positive allosteric modulators at this subtype. Preliminary data show

analogs such as **Compound 6** and **Compound 11** are effective in an animal model with sensorimotor gating deficit, reflecting the impairment of prepulse inhibition of the acoustic startle response (PPI) induced by methamphetamine.

Recently, the α_6 GABA$_A$R was shown to be expressed in both neurons and satellite glia of the trigeminal ganglia. The α_6 subunit positive neuronal cell bodies in the trigeminal ganglia project axons to the temporomandibular joint and likely to the trigeminal nucleus caudalis and upper cervical region (Vc–C$_1$), and might modulate orofacial pain and inflammatory temporomandibular joint nociception and might modulate orofacial pain and inflammatory temporomandibular joint nociception. Rats with 30% knock down of the α_6 subunit of GABAA receptors in trigeminal ganglia were hypersensitive to TMJ inflammation, measured by a prolong meal time. The prevalence of TMJ disorders in the United States is estimated at 4.6% and these disorders are the leading cause of chronic orofacial pain.

Importantly, trigeminal ganglia also send projections to the trigeminal nucleus caudalis (TNC) and upper cervical region (Vc–C$_1$), the trigeminal cervical complex. Activation of the TNC plays an important role in the neuropathogenesis of migraine. In an animal model of migraine, we have found a selective α_6-GABAA receptor PAM, **Compound 6**, effectively decreased the number of activated neurons in the TNC induced by intracisteral (*i.c.*) injection of capsaicin. This suggests the potential of selective α_6-GABA$_A$ receptor PAMs for the treatment of migraine.

To my family

and

For my late grandfather

Jack "Grandpa" Witzigmann

TABLE OF CONTENTS

LIST OF FIGURES

LIST OF TABLES

LIST OF SCHEMES

Part 1

DESIGN, SYNTHESIS, AND EVALUATION OF NOVEL

GRAM-POSITIVE ANTIBIOTICS

CHAPTER ONE

INTRODUCTION TO ANTIBIOTICS

I. HISTORY OF ANTIBIOTICS.

Throughout history infectious diseases have been among the most common ailments for man.[1] Historical epidemics such as the Bubonic plague, leprosy, and tuberculosis killed hundreds of millions of people and were all caused by various bacterial strains.[2-4] In the US, many of these diseases are viewed as historical, yet they still persist and are major diseases in many third-world countries to this day.[5-7] This persistence is generally due to poor living conditions, lack of access to clean water, and lack of access to antibiotics.[8]

Past countries have dealt with these epidemics through a variety of means. Usually the most successful methods were improved living conditions and access to fresh water. Quarantines were also routinely used to separate healthy individuals from the sick.[9] These methods, however, did little to help those already suffering from the disease. In fact, it wasn't until the early 20th century that the first antibiotics were discovered, the most successful of these early antibiotics was Prontosil (Scheme 1-1).[10] Prior to this discovery, vaccines were the most successful method of avoiding epidemics, however a crude understanding of pathogenicity and why vaccinations were successful led to both poor results and, similarly to recent perspectives on vaccinations, an "anti-vax" sentiment among many populations.[11] Vaccines were also not applicable to people who had already contracted a specific disease and survival rates for some of these diseases were very low. Because vaccinations were often not universal and because it was not possible to vaccinate for many infectious diseases, the discovery of antibiotics was perhaps one of the most important discoveries of the 20th century.[12]

Scheme 1-1: Prontosil and its activation to sulfanilamide.
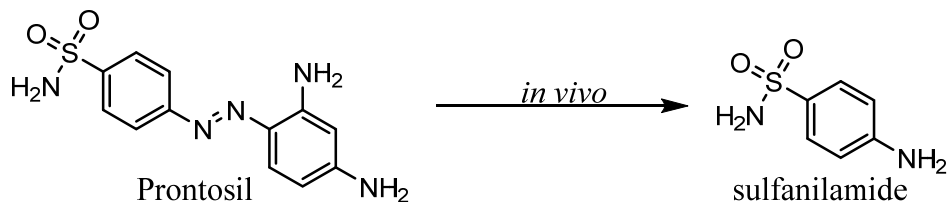
Prior to the discovery of Prontosil, Paul Erhlich, an early pioneer in bacterial staining and chemotherapeutic agents, discovered that methylene blue could be used to treat patients with malaria.[13] Methylene blue is described as the first fully synthetic drug, and it found use as an antimalarial drug due to its ability to stain the pathogenic protozoans responsible for malaria.[14] Erhlich's hypothesis was that the ability of the drug to stain the pathogens blue may lead to therapeutic potential. Indeed, when tested on two patients their fevers subsided and the parasites disappeared from their bloodstream. Methylene blue was used for many years as an antimalarial drug until the more successful chloroquine was discovered.[15]

Based on this early work by Erhlich, Gerhard Domagk continued research on dyes as possible antibiotic agents. In the early 1930's, Domagk discovered that Prontosil rubrum, named due to its deep red color, was efficacious in treating mice infected with streptococci.[16] Interestingly, the compound had no activity when used *in vitro*. Indeed, it was later found that Prontosil was an early example of a pro-drug, a compound that breaks down to the active component *in vivo*. In this case, Prontosil breaks down to sulfanilamide, a compound found to have potent antibacterial activity (Scheme 1-1).[17] Although this led to a rather short pharmaceutical duration of Prontosil, because sulfanilamide was similarly efficacious *in vivo*, this ushered in a new era of antibiotic research in the field of sulfa drugs.

Unfortunately, this new paradigm shift in medicine came with an unfortunate side-effect, **bacterial resistance**. Sulfanilamide resistance was reported as early as the late 1930's, just a few years after the discovery of Prontosil's antibacterial activity.[18] This has led to a back-and-forth struggle to design new antibiotics that can treat the growing number of resistant strains.

II.   CURRENT ANTIBIOTICS.

Since the early pioneering days of antibiotic research, many new antibiotics have been discovered. Advances in the fields of microbiology have allowed researchers to not only discover new antibiotics, but also to assess the mechanisms by which these new antibiotics target bacteria, they're mode/mechanism of action (MOA).[19-20]

Although certainly not an exhaustive list, eight different current antibiotics will be illustrated here. These include Gentamicin, Ampicillin, Oxacillin, Ciprofloxacin, Vancomycin, Erythromycin, Tetracycline, and Rifampin. These eight drugs are all used in later chapters as controls for compounds synthesized in this work.

1.   Gentamicin.

Figure 1-1: Structure of Gentamicin.
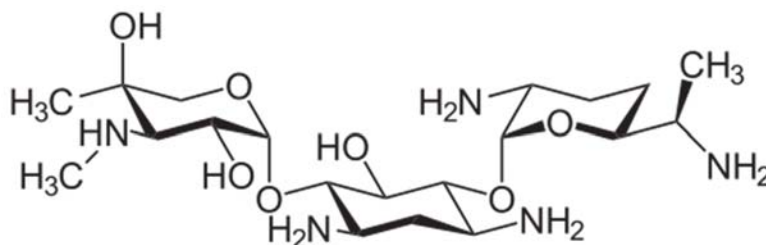
Gentamicin was discovered in 1963 as a fermentation product of the gram-positive bacteria *Micromonospora purpurea*.[21] Due to poor oral bioavailability, it is generally used either

as a topical agent or intravenously.[22-23] Gentamicin is a type of aminoglycoside which works by stopping bacterial protein synthesis, this typically kills the bacterium and is known as a bactericidal antibiotic.[24] It is also listed by the World Health Organization (WHO) as an essential medicine, one of the most important medications needed in a basic health system.

Gentamicin is generally used for gram-negative infections, especially blood-related infections.[25] Although certain gram-positive strains are susceptible to Gentamicin, most are not, so in general it is not used to treat gram-positive infections. Unfortunately, Gentamicin has several severe side-effects including nephrotoxicity (kidney damage) and ototoxicity (cochlea toxicity) which limit its use as a treatment.[22, 26] Recently due to the emergence of resistance in many gram-negative strains, Gentamicin has found renewed use since it is still effective against a number of these resistant strains.[27] This lack of resistance is directly tied to its infrequent use in the past rather than an inability for Gentamicin to confer resistance, as resistant strains are now becoming more prevalent due to this resurgence.[28]

2. Ampicillin.

Figure 1-2: Structure of Ampicillin.
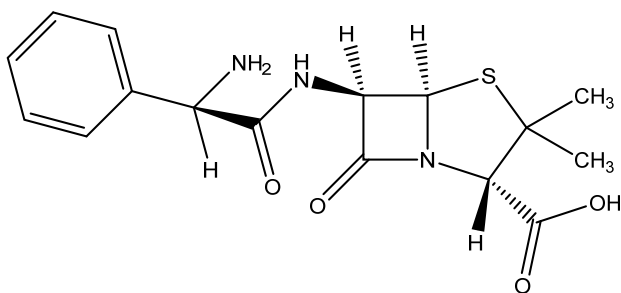
Ampicillin is a drug related to penicillin and is in the ß-lactam family of antibiotics.[29] These antibiotics inhibit transpeptidase, a protein necessary for cell wall synthesis.[30] This often

leads to cell lysis and death of the cell, so ß-lactam antibiotics are bactericidal.[30-31] Ampicillin was the first 'broad-spectrum' penicillin with activity against both gram-positive and gram-negative bacteria. It differs from penicillin G only with the inclusion of an amino group, which helps Ampicillin penetrate gram-negative bacterial cell walls.[32] It is also on the WHO's list of essential medicines for basic health systems.

Like other penicillins, Ampicillin is not effective against methicillin-resistant *S. aureus* (MRSA). The effectiveness of penicillin analogs relies on their ability to both reach penicillin-binding proteins (PBPs) and bind to the PBPs. Some bacteria are able to produce enzymes that cleave the ß-lactam rings, known as ß-lactamase or penicillinase.[33] Cleavage of the ß-lactam rings leaves the resulting compound ineffective. Another method bacteria have employed to gain resistance to ß-lactams is altering the PBPs. This is most notable in MRSA strains in which the PBP is altered to such a degree that the ß-lactam ring is no longer able to bind and the antibiotics are thus ineffective.[33-34]

In the case of ß-lactamases, it has been shown that ß-lactamase inhibitors such as clavulanic acid can increase the potency of penicillin's when co-administered.[35] However, treatment in this fashion can potentially lead to bacterial strains that possess higher levels of ß-lactamase expression which can make future treatments with ß-lactams even less effective.[36] Still, treatments with ampicillin or the closely related amoxicillin are among the most prescribed treatments for bacterial infections.[37]

3.   Oxacillin.

Similarly to Ampicillin, Oxacillin is also a ß-lactam antibiotic. They differ greatly in that Oxacillin is resistant to penicillinase[38], however, this has led to extensive use against penicillin-

resistant *S. aureus*. Unfortunately, this led to the previously mentioned resistant strains in which the PBPs active sites are altered in such a way that these ß-lactams can no longer bind, leaving drugs like Oxacillin and the related Methicillin ineffective for MRSA strains.[39]

Figure 1-3: Structure of Oxacillin.
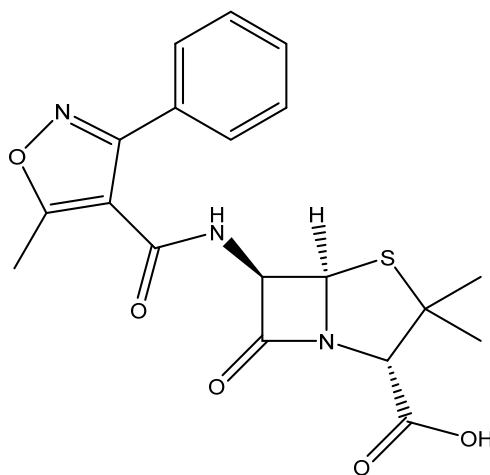
Despite these issues, Oxacillin remains a popular choice for treating bacterial infections that are penicillin resistant.[40] It is increasingly important, however, that these drugs are not over prescribed and that patients adhere to the treatment protocols to slow the emergence of new strains of MRSA.[41]

4.   Ciprofloxacin.

Ciprofloxacin, commonly known as simply Cipro, is a relatively modern antibiotic released in 1987. It is also on the list of WHO's essential medications for a basic health system. It is used for both gram-positive and gram-negative infections and works by inhibiting DNA gyrase and topoisomerase IV.[42] This prevents bacterial DNA from separating and thus inhibits cell division. Cipro has been shown to be bactericidal when used in higher concentrations, however at its MIC it is bacteriostatic.[43] It is thought this bactericidal nature is due to the release

of DNA gyrase complexes leading to chromosomal DNA fragmentation, while at lower concentrations the inhibitory effects just stop cell division.[44]

Figure 1-4: Structure of Ciprofloxacin.
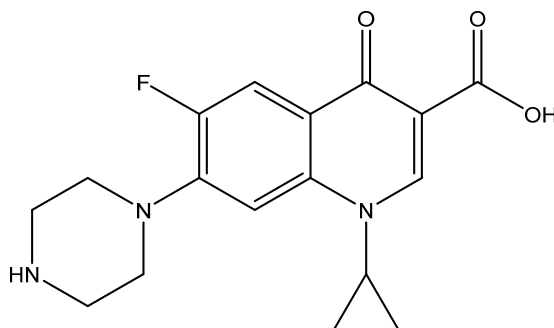
Cipro is a second generation fluoroquinolone and is derived from the original antibiotic quinolones discovered in the early 1960's. In general, these fluoroquinolones are known to quickly develop resistance, sometimes even within one course of treatment.[45] This problem was compounded with prescriptions for conditions not approved by the FDA and overuse in veterinary medicine.[46-47] Some bacteria developed efflux pumps that decrease intracellular quinolone concentration and some others developed mutations to DNA gyrase and topoisomerase IV that decreased binding affinity for quinolones.[45]

One literature source published in the late 1980's reports that clinical oral dosage of Cipro to 37 MRSA patients resulted in Cipro-resistant mutants which developed in 6 out of the 37 cases. While the article claims 91% of patients were clinically cured or their conditions improved, this rate of resistance was alarming.[48]

5.   Vancomycin.

Figure 1-5: Structure of Vancomycin.
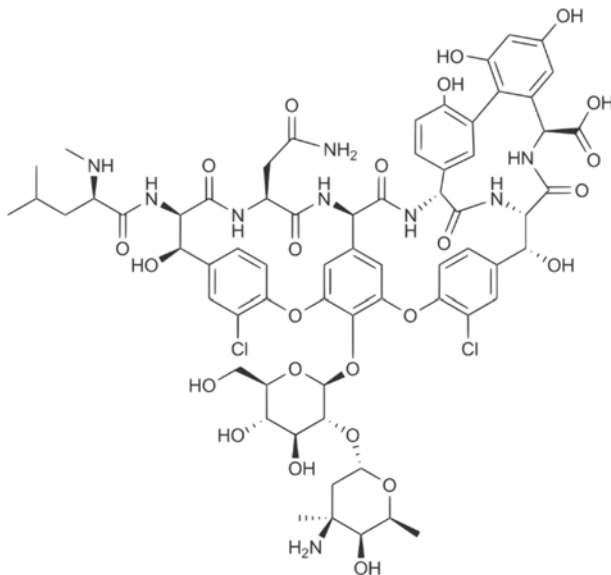
Vancomycin is a gram-positive antibiotic biosynthesized by the bacteria *Amycolatopsis orientalis*. It was first isolated in 1953 from a soil sample collected from the jungles of Borneo.[49] The mode of action is the inhibition of proper cell-wall synthesis leading to death of the cell. Due to the difference in cell wall configurations, Vancomycin is ineffective in treating bacterial infections from gram-negative bacteria.

Originally Vancomycin was developed as a solution to the penicillin-resistant *S. aureus* infections mentioned earlier, however as Methicillin and Oxacillin were developed and were both more efficacious and easier to dose, Vancomycin fell behind as a drug of last-resort. This was due in part to its low oral bioavailability, which necessitated IV administration.[50] Recently, however, Methicillin and Oxacillin resistant *S. aureus* (MRSA) have necessitated Vancomycin as a first-line treatment for a number of these infections.[51] While IV injections are necessary for

most infections, it can be orally administered for bowel or stomach infections since it has rather poor oral absorption.[52] It is now also on the WHO's list of essential medications.

Vancomycin resistance, however, is becoming more prevalent, especially in hospital settings.[51, 53] If these infections are not identified as Vancomycin resistant early enough, patients are at extreme risk. As these strains of Vancomycin-intermediate and Vancomycin-resistant *S. aureus* (VISA and VRSA respectively) become more prevalent, a new antibiotic will necessarily become the new first-line treatment for bacterial infections, with resistance likely to follow.

6.　　Erythromycin.

Figure 1-6: Structure of Erythromycin.
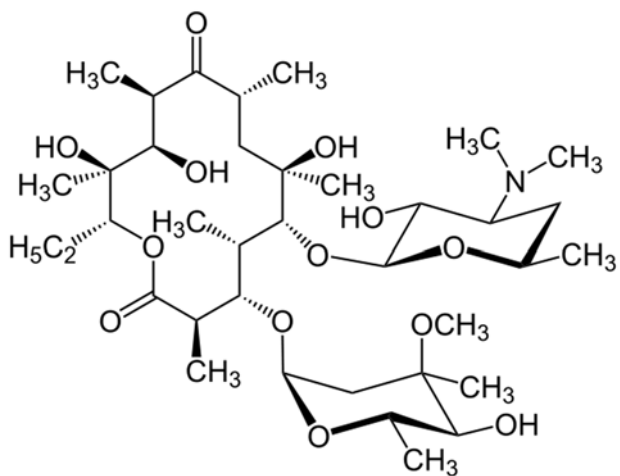
Erythromycin is yet another antibiotic that was originally separated from a natural source, in this case the bacteria *Saccharopolyspora erythraea*.[54] It is also another antibiotic listed by the WHO as an essential medication for a basic health system. It was first isolated in 1952 and was found to be active against gram-positive bacterial strains. Erythromycin is in the antibiotic class of macrolides, compounds that inhibit protein synthesis by binding to the 50S subunit of

bacterial ribosomes, humans do not have 50S ribosomal units so these compounds act selectively on the bacteria.[55]

Resistance to macrolides and Erythromycin is seen in many bacteria with mutations in the 50S subunit which inhibits binding. MRSA strains, for example, are notoriously resistant to Erythromycin and other macrolides.[56-58] Growing resistance in other species is also an alarming concern.

7. Tetracycline.

Figure 1-7: Structure of Tetracycline.
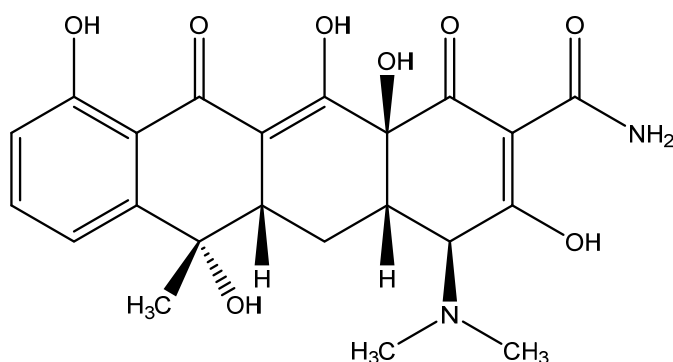
Tetracycline was also originally isolated from bacteria, in this case strains of Streptomyces produced the compound.[59] It was first isolated in 1945 and was surprisingly already prescribed as a drug as early as 1948.[60] It is yet another antibiotic listed by the WHO as an essential medicine.

Tetracycline acts by inhibiting protein synthesis by blocking the attachment of charged aminoacyl-tRNA to the A site on the ribosome.[61] Tetracycline binds to the 30S ribosomal subunit of microbial ribosomes and also binds to the 40S subunit of mammalian ribosomes. However, while bacteria actively pump Tetracycline into the cytoplasm, mammalian cells do not.

The relatively small off-site effects in humans by Tetracycline can be explained by this 40S binding.[62] The inhibition of protein synthesis is reversible and thus bacteriostatic.[59]

Bacteria actively form resistance to Tetracycline by either encoding efflux pumps that actively pump Tetracycline from the cytoplasm, or by ribosomal protection proteins that dislodge Tetracycline from the ribosome.[59, 63] Tetracyclines are sometimes prescribed for MRSA related infections, however identification of the strain and its susceptibility to Tetracycline are important factors considered before treatment.[64-66]

8.   Rifampin.

Figure 1-8: Structure of Rifampin.
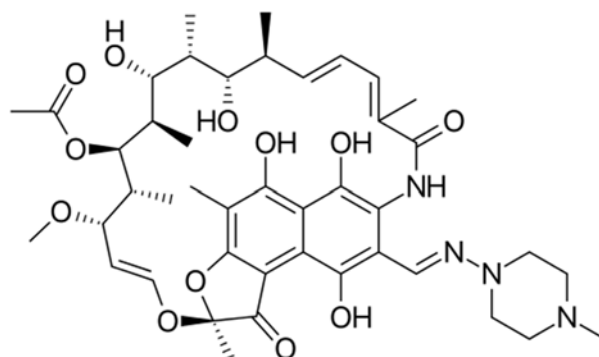
As has been the case for most antibiotics discussed above, Rifampin was also first isolated from another species of bacteria, in this case *Amycolatopsis rifamycinica*. It was first discovered in 1957 and first sold as a medication in 1971.[67] Along with most of the aforementioned antibiotics, it is also on the WHO list of essential medications, particularly for Tuberculosis (TB).[68]

Rifampin inhibits RNA polymerase halting bacterial RNA synthesis. It is extremely potent in wild-type strains of *M. Tuberculosis* and many strains of MRSA; however, resistance is

easily conferred.[69] Bacteria confer resistance through altered residues in the Rifampin binding

site on RNA polymerase.[69-71] Rifampin resistant TB is one of the most dangerous microbes in

developing countries, with TB infecting nearly 10 million people in 2014 alone. It is estimated

that ~20% of all cases involve strains resistant to at least one medication.[72-74] This often leads to

a 'cocktail' drug composed of, in many cases, three separate drugs (isoniazid, pyrazinamide, and

rifampin).[75]

Due to side-effects and the conference of resistance, Rifampin is generally not used to

treat MRSA infections, but when it is used, it is generally used in combination therapy to reduce

the likelihood of forming resistance.[76]

III.   THE NEED FOR NEW ANTIBIOTICS.

The eight aforementioned pharmaceutical drugs represent some of the most widely

prescribed medications for bacterial infections. It should be clear, however, that resistant strains

to every single one of these antibiotics has been observed. The early penicillins were the first to

lose effectiveness, followed closely by the penicillinase resistant methicillin/oxacillin drugs. The

explosion of new antibiotics in the mid-20th century slowed the spread of resistance, or at least

widened its scope, leaving a plethora of treatment options even for the deadliest infections. That

said, however, identification of strains is difficult and generally results in the use of the best

current first-line therapy to eradicate an infection and give the best chances of survival to the

patient. Indeed, choosing the wrong therapy is deadly in many cases, especially in MRSA

related infections.[77]

This problem is exacerbated since the first-line treatments slowly lose effectiveness and a

new first-line therapy is needed. Currently, Vancomycin is considered the first-line treatment for

many identified MRSA infections[78], as MRSA becomes more prevalent, the use of Vancomycin will also become more prevalent. In the past decade we have seen a surprising explosion of Vancomycin resistant related microbes, specifically VISA and VRSA.[79]

Currently, it is estimated that close to 19,000 patients die annually from MRSA related infections in the United States alone.[80-83] When VRSA becomes just as prevalent as MRSA is today, those numbers could sky-rocket. This alone is an important reason for the development of new antibiotics, but there is also a plethora of other related infections both from gram-negative bacteria and mycobacterium that also require new medications and new treatments.[84-87]

Unfortunately, bacterial infections are less enticing for pharmaceutical companies as treatment lengths are generally weeks as opposed to chronic diseases in which treatments could last years. The costs necessary to take a drug from the bench to a prescription are prohibitive with such short treatment cycles. Moreover, as current antibiotics are still effective to varying degrees, competition in the market lowers the potential profits from a new drug.[88]

With this combination of factors involved, it is not surprising that the number of new antibiotics approved by the Food and Drug Administration (FDA) has steadily declined since the 1980's. It is also important to note that new antibiotics are generally from an already known class of antibiotics, of which resistance patterns are already known. Recently the resurgence of antimicrobial research has led to the discovery of the first new class of antibiotics in 30 years, Teixobactin. Human trials of this new drug may not be started until 2017, however, and although resistant strains have not been isolated *in vitro*, experts claim that it is still possible that resistant strains will develop in clinical settings.[89]

IV. CONCLUSION.

The history of antibiotics spans just over one century. In the course of that century many new drugs have been discovered that have become essential medications in treating often deadly infections. More recently, however, the spread of resistance has led to the need for the discovery of new antibiotics. Although the economic benefits of antimicrobial research limit the overall throughput, it is exciting to see that the first new class of antibiotics in 30 years was recently discovered with Teixobactin. It is hoped that this ushers in a new wave of antimicrobial research that can potentially lead to discovery of many new novel classes of antimicrobials that are active against resistant strains. Moreover, compounds that do not confer resistance could usher in a new era of microbial treatment that no longer relies on the susceptibility patterns of different strains.

Described in this thesis is a new class of antibiotics, stilbenoids, which have been found to possess potent activity against gram-positive bacteria. These compounds were originally derived from a natural product, but synthetically modified to increase potency. While these stilbenoids exhibited potent activity against wild-type strains, it was also discovered that these compounds possess potent activity against all resistant strains tested. Additionally, mutants from a sub-lethal dosage of these agents were not observed over many trials, prompting the hypothesis that these compounds might not confer resistance. Many of these small molecules were also tested both *in vitro* and *in vivo* for cytotoxicity and were generally found to be well tolerated and safe. The mode of action for these new stilbenoid derivatives is still elusive, due in part to their lack of conference of resistance. The compounds described within this thesis may one day be useful tools or medications for gram-positive bacterial infections.

CHAPTER TWO

SYNTHESIS, SCALE-UP, AND BIOLOGICAL EVALUATION OF

SK-03-92 AND A SMALL SERIES OF DIRECT ANALOGS BASED ON AN

INTERESTING STILBENOID NATURAL PRODUCT SCAFFOLD

I.   INTRODUCTION AND BACKGROUND.

1.   Natural product identification and evaluation.

Due to the emergence of resistant pathogens, discovery of new and novel antibiotics is of utmost priority. Natural products represent one of the greatest sources for novel compounds with biological activity. These natural products can be modified and enhanced via synthetic techniques to potential drug candidates. Our interdisciplinary research team has been engaged in screening extracts of medicinal plants and fungi in search of new molecules with interesting biological profiles. This research led to the identification of (E)-3-hydroxy-5-methoxystilbene (Figure 2-1, **1**) in the leaves of a shrub native to the great lakes region. This shrub, *Comptonia Peregrina*, also known as "sweet fern", has been used in traditional herbalism to treat a number of medical issues. It is used as a tea to treat nausea or a poultice for skin conditions, which may be directly related to the antimicrobial components of the plant.

Figure 2-1: Natural product from 'sweet fern'.
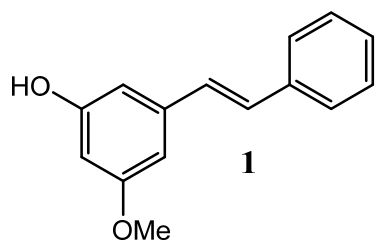
Chemical Formula: $C_{15}H_{14}O_2$
Molecular Weight: 226.28
c Log P: 3.71
tPSA: 29.46

Further pharmacological testing of the essential oils of sweet fern indicated that the oil was cytotoxic to mammalian cells.[90] This cytotoxicity, however, was likely due to other major components of the oil, for example methyl p-coumarate (Figure 2-2). The Michael-acceptor nature of this molecule is likely the cause of this cytotoxicity, and it is important to note that the compound of interest, **1**, does not have any Michael-acceptor moieties. In other work we have shown that related compounds with a Michael-acceptor moiety are both very active antimicrobials while also cytotoxic to mammalian cell lines.[91]

Figure 2-2: Methyl p-coumarate as a Michael-acceptor.
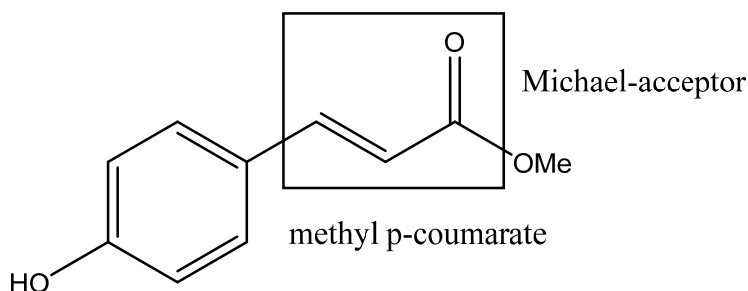
Interestingly compound **1** was also identified in a number of other plant species including *Didymochlaena* truncatula[92] and *Alpinia katsumadai*[93], however as far as one can determine the antimicrobial activity was only investigated by the LaCrosse/UWM research team. Other stilbenes have been investigated as antimicrobial agents and have been shown to exhibit activity against both gram-positive bacteria and certain fungal strains, however these stilbenes are multimeric derivatives of a basic stilbene structure. An example of such a compound is "heyneanol A", reported to have both cytotoxic character with potential use for cancer therapy as well as antimicrobial activity specific for gram-positive bacteria. These multimeric compounds may work by a similar mechanistic pathway to the natural product **1**; however, it should be noted that mechanism of action studies for both the compounds presented in this work, along with

other similarly structured compounds, such as heyneanol A, have not been unequivocally

elucidated as of yet.

Figure 2-3: Structure of heyneanol A.
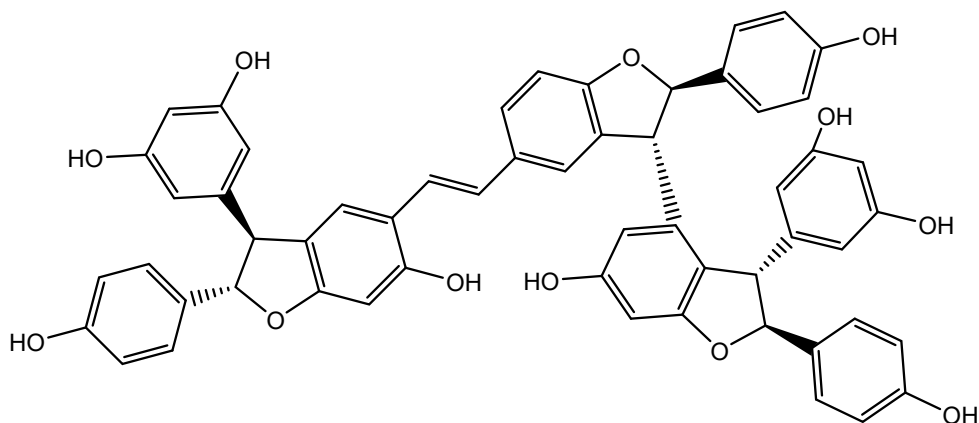
2. Initial SAR study.

Although analysis of crude extracts and extremely small heavily purified samples of a

product from natural sources may yield interesting biological data, it is imperative that these

molecules be prepared synthetically to confirm both the biological activity and also permit the

synthesis of novel analogs that may improve upon the biological activity of the parent natural

compound.

A broad SAR study was imagined that included synthesis of not only the parent

stilbenoid scaffold, but also the synthesis of analogous vinyl ethers, vinyl thioethers, and

enamines (Figure 2-4).[94]

Figure 2-4: Initial SAR targets.
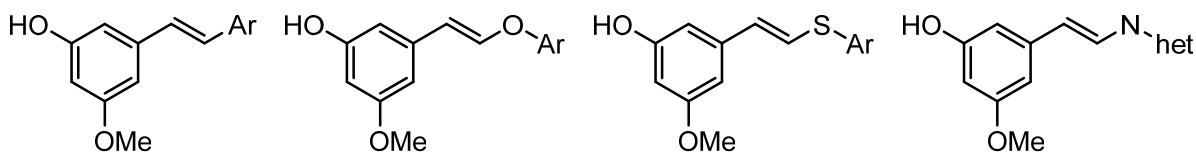
Compounds synthesized in these series were routinely assayed for Minimum Inhibitory Concentrations (MICs) against eleven standard test strains of bacteria including two gram-positive species (*S. aureus* and *E. faecalis*), two gram-negative species (*P. aeruginosa* and *E. coli*), and seven mycobacterium strains (*M. intracellulare*, *M. chelonae*, *M. fortuitum*, *M. kansasii*, *M. avium*, and *M. smegmatis*). In addition, some compounds were also tested against *B. cereus*, a safer surrogate of the deadly and high priority *B. anthracis* which has potential use as a biological weapon. *M. smegmatis* is a safer surrogate of the high risk pathogen *M. tuberculosis*, which presents a major health epidemic in third world countries.

The original synthesis of the natural product **1** and other related stilbenoid compounds was accomplished by utilizing a transition metal catalyzed Negishi cross-coupling reaction. Negishi coupling forms a C-C bond between organic halides (or triflates) and organozinc compounds with a relatively wide scope, thus it was envisioned that a wide variety of compounds could be synthesized via this method. Detailed in Scheme 2-1 is the route towards both the natural product and a number of new analogs.

Scheme 2-1: Synthesis of stilbenoids, including the natural product 1.
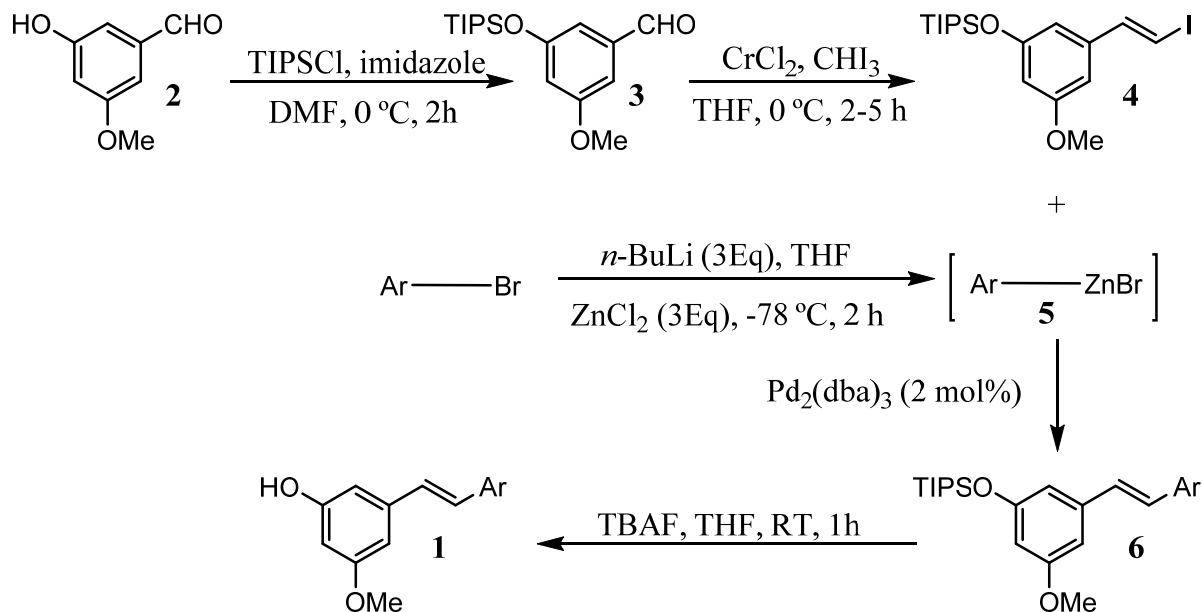
Although this method was successful in the synthesis of the natural product and a number

of related analogs, several issues with the reaction were reported. First, the starting aldehyde **2**

was both expensive and it was found that protection of the phenol to the TIPS derivative **3** was

necessary for the conversion to the vinyl iodide **4**. Additionally, the vinyl iodide **4** was unstable

at room temperature and purification required column chromatography, thus large scale reactions

were difficult and sometimes resulted in little or no yield of the product. Storage of the vinyl

iodide at -40 ºC kept it relatively stable, however, enough impurities were present after several

days/weeks that re-purification was necessary to achieve high yields in the palladium catalyzed

cross-coupling reaction.

Synthesis of the organozinc complex **5** from aryl bromides generally proceeded with no

issue and the vast number of commercially available aryl bromides provided ample substitution

patterns in this aryl unit. Finally, deprotection of the TIPS group with TBAF in THF generally

worked very well and in some cases could be done in a one-pot fashion prior to purification of the protected compound **6**.

In a similar fashion vinyl ethers, vinyl thioethers, and enamines were also synthesized from the vinyl iodide **4** using a copper catalyzed process described below (Scheme 2-2, Scheme 2-3, and Scheme 2-4).

Scheme 2-2: Synthesis of vinyl ethers.

Ar—OH

1. 5 mol% CuI, 5 mol% L
   2 eq Cs_2CO_3, DMF
   40 °C, 1-2 h
2. TBAF, one-pot, 1 h
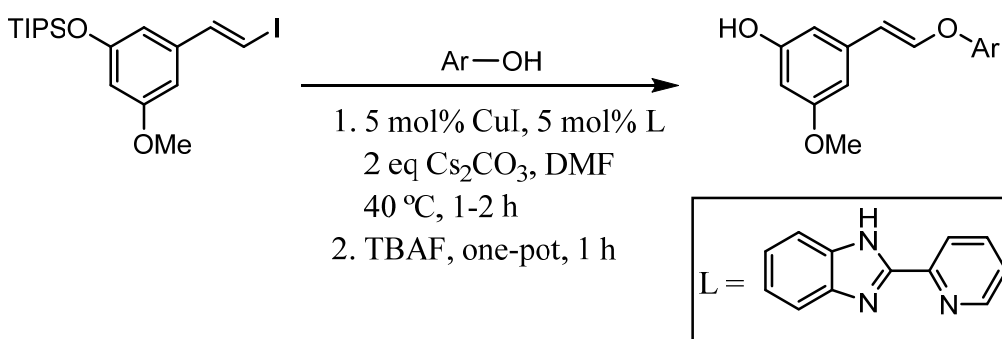
Scheme 2-3: Synthesis of vinyl thioethers.

Ar—SH

1. 10 mol% CuI, 20 mol% L
   1.5 eq K_2PO_4, DMF
   40 °C, 1-2 h
2. TBAF, one-pot, 1 h
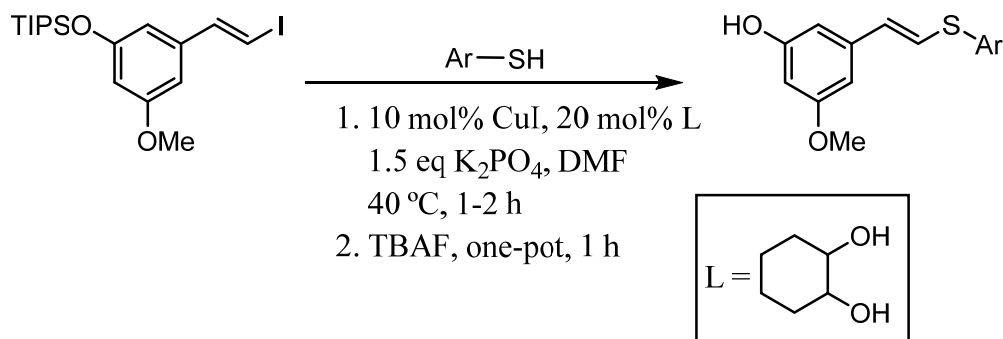
Scheme 2-4: Synthesis of enamines.
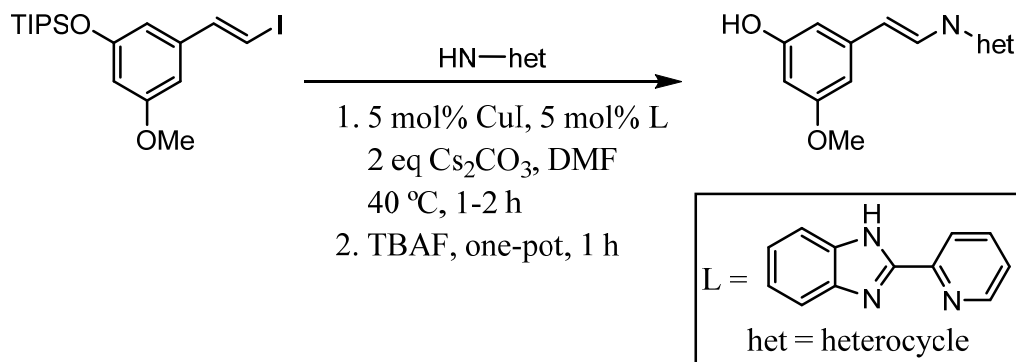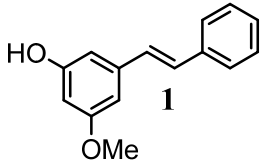
3.   Results and Discussion.

With a viable synthetic procedure in place for the synthesis of natural product **1**, enough compound was prepared to assay against of number of bacterial strains. Additional strains of bacteria were also used in the assay of the natural product as it was of highest priority. The results indicated that indeed the stilbenoid has antimicrobial properties and its activity should be explored more thoroughly (Table 2-1).

Interestingly the natural compound **1** was found to have activity against both gram-positive bacteria and mycobacterium, but no activity against gram-negative bacteria. This interesting result led to the idea that perhaps the mechanism of action was related to the cell wall, since the biggest difference between both gram-positive and mycobacterium to gram-negative bacteria is indeed the construction of the cell wall. Some of the most interesting results from this initial assay were the activity against strains that are resistant to some commercial antibiotics. These include the results from *E. faecium* VRE 1 and VRE 14 (vancomycin resistant enterococci) and *S. aureus* MRSA MC-1 and MC-4 (methicillin resistant). This was a surprising result as both methicillin and vancomycin's mode of action is directly tied to the bacterial cell

wall, suggesting that if this natural product is also acting on the cell wall, it may be acting on a

novel mechanism of action.

Table 2-1: Antimicrobial assays for natural product 1.
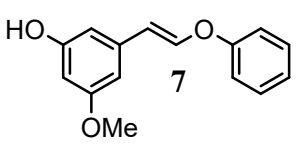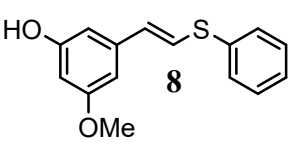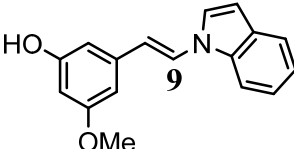
Species	Gram	MIC (µg/mL)
Bacillus anthracis	+	8
Bacillus megaterium	+	64
Bacillus cereus	+	16
Bacillus subtilis	+	16
Corynebacterium pseudodipthericum	+	16
Corynebacterium diphtheriae Tox-	+	32
Corynebacterium xerosis	+	16
Enterococcus faecium VRE 1	+	16
Enterococcus faecium VRE 14	+	16
Enterococcus faecalis ATCC 29212	+	16
Staphylococcus aureus ATCC 29213	+	32
Staphylococcus aureus ATCC 25923	+	32
Staphylococcus aureus MRSA MC-1	+	32
Staphylococcus aureus MRSA MC-4	+	32
Streptococcus mitis	+	64
Streptococcus aagalactiae	+	32
Streptococcus pyogenes	+	16
Streptococcus pneumoniae ATCC 49619	+	8
Listeria monocytogenes	+	32
Mycobacterium bovis BCG	N/A	26
Escherichia coli	–	>128
Pseudomonas aeruginosa	–	>128

+: gram-positive, -: gram-negative, N/A: mycobacterium are neither + or -

Vinyl ethers, vinyl thioethers, and enamines also showed promise when assayed against

the primary targets (Table 2-2). Other compounds synthesized within these series had equal to or

weaker activity then the compounds shown below. Because of this, more focus was put into the

synthesis of the stilbenoid compounds closely related to the natural product **1**.

Table 2-2: Antimicrobial assays for vinyl ether, vinyl thioether, and enamine analogs.[a]
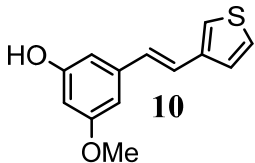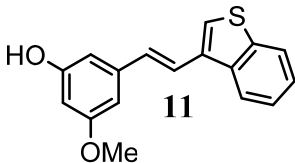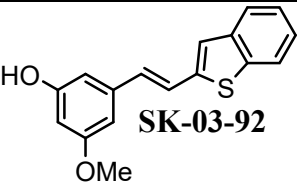
Bacterial Strain	7	8	9
S. aureus	64	16	32
E. faecalis	64	16	32
P. aeruginosa	>128	>128	>128
E. coli	>128	>128	>128
M. intracellulare	128	64	64
M. chelonae	>128	128	64
M. fortuitum	128	128	128
M. kansasii	>128	64	64
M. avium	128	128	64
M. smegmatis	128	128	32
M. marinum	>128	64	64

[a]Values in μg/mL

Synthesis of a number of stilbenoid analogs, moreover, led to a far more interesting

analog in **SK-03-92** (Table 2-3). Many other compounds in this series, however, were more

similar in activity to the natural product **1**, not potent enough for use as an antimicrobial drug candidate.

Table 2-3: Activity of some novel stilbenoid compounds, including SK-03-92.[a]

Bacterial Strain	10	11	SK-03-92
S. aureus	16	16	**2**
E. faecalis	32	16	**2**
P. aeruginosa	>128	>128	>128
E. coli	>128	>128	>128
M. intracellulare	64	64	32
M. chelonae	128	64	32
M. fortuitum	128	64	16
M. kansasii	128	64	32
M. avium	128	64	32
M. smegmatis	64	64	32
M. marinum	128	64	16

[a]Values in µg/mL

With activities below the range of 10 µg/mL, **SK-03-92** exhibited activity that was similar to some mainstream antibiotics and thus served as an excellent lead compound for further SAR studies.

II.   CHEMISTRY AND RESULTS.

1.   Scale up of SK-03-92.

Based on the initial SAR study, SK-03-92 (Table 2-3) was deemed the most promising lead compound and therefore future study required a synthesis suitable for scale-up to gram quantities. The original palladium-mediated Negishi cross-coupling reaction required not only the use of expensive transition metals, but also the use of unstable intermediates which were difficult to prepare in large quantities (Scheme 2-1). It was found that a Wittig-type approach could be used to successfully scale up SK-03-92 to gram quantities through a less expensive yet more laborious seven-step process beginning with 3,5-dihydroxybenzoic acid (Scheme 2-5).

Scheme 2-5: Scale-up of the synthesis of SK-03-92.
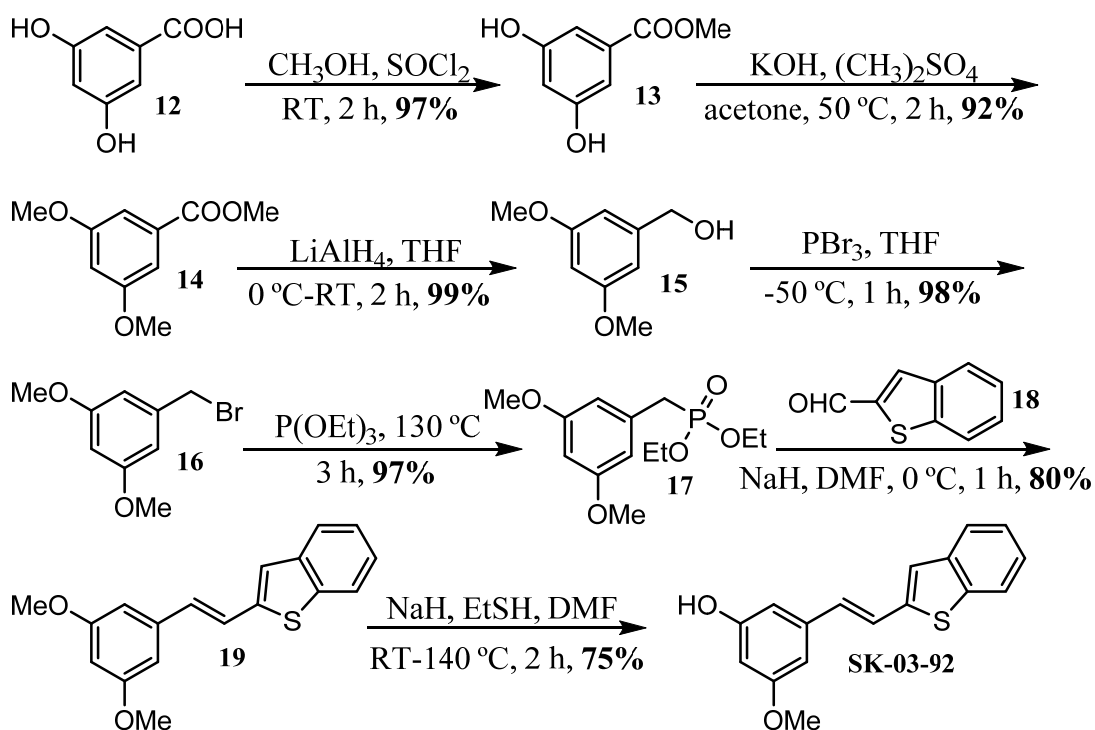
The 3,5-dihydroxybenzoic acid (**12**) was converted into the methyl ester (**13**) and subsequently protected as the dimethoxy derivative (**14**). It is worth noting that the conversion from **12** to **14** could be accomplished in one step utilizing the same conditions as **13** to **14**; however, this leads to a slightly lower overall yield. The hydride reduction of **14** with lithium aluminum hydride provided the alcohol (**15**) which was subsequently treated with phosphorous tribromide to provide the alkyl bromide (**16**). The synthesis of the diethylphosphonate (**17**) was accomplished by heating bromide **16** in neat triethylphosphite at 130 °C. The diethylphosphonate (**17**) and benzo[b]thiophene-2-carbaldehyde (**18**), in the presence of sodium hydride, gave the corresponding stilbene (**19**) in good overall yields. Mono-demethylation was accomplished by treating **19** with sodium ethanethiolate at 140 °C to furnish the final stilbene, **SK-03-92**, in an approximate overall yield of 50%. It should also be noted that the benzyl bromo derivative (**16**) was not stable and decomposed readily on the benchtop, thus storage as the alcohol (**15**) or conversion immediately to the more stable diethylphosphonate (**17**) was preferred.

One significant hurdle to scale-up via this method, however, was the price of thioaldehyde **18**. The conversion of the much less expensive thionapthene **20** to **18** was accomplished by lithiation of the 2-position with n-butyl lithium and subsequent treatment with dimethylformamide to provide the aldehyde **18** in excellent yield (Scheme 2-6).

Scheme 2-6: Scale-up of the synthesis of aldehyde 18.
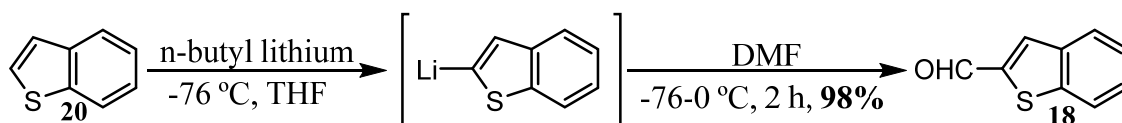
Although this route was longer than the prior Negishi cross-coupling procedure, it was successfully used to synthesize over 50 grams of **SK-03-92** in a more economical and less cumbersome manner. Purification was only necessary after synthesis of **19** (crystallized from toluene) and although chromatography was usually necessary for small scale purification of **SK-03-92**, on large scale it can be adequately purified by crystallization from isopropanol with excellent recovery. This was a major improvement in the route.

2.   Synthesis of analogs starting from SK-03-92.

The initial SAR study employing the previously discussed Negishi cross-coupling procedure focused exclusively on substitution (ring C) using a variety of aryl bromides (Figure 2-5, green portion), which left the 'left-hand-side' (Figure 2-5, red portion) substitution pattern and bridged alkene (Figure 2-5, blue portion) moieties intact. After screening a number of different aldehydes the benzo[b]thiophene moiety was found to be the most active, and thus the goal of this research was to synthetically modify both the 'left-hand-side' and the bridge in an attempt to gain more insight into the SAR of these novel stilbenoid compounds and perhaps get a clinical candidate to treat MRSA infections.

Figure 2-5: Functionality evaluation of SK-03-92.

Chemical Formula: $C_{17}H_{14}O_2S$
Molecular Weight: 282.36
c Log P: 4.74
tPSA: 29.46
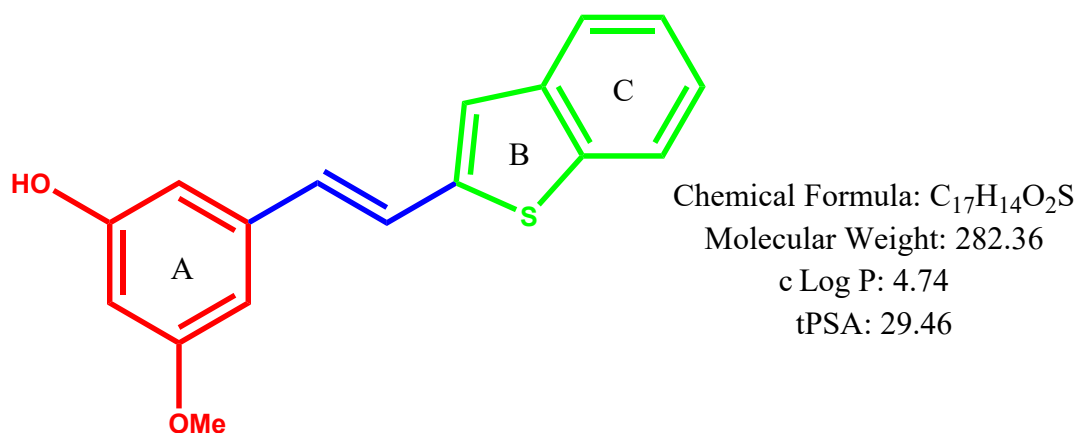
Since adequate amounts of SK-03-92 were available, direct modification of SK-03-92 was explored. The most convenient method of directly modifying the 'bridge' of SK-03-92 was to hydrogenate it via Pd/C to the saturated analog **21** (Scheme 2-7).

Scheme 2-7: Hydrogenation of SK-03-92.
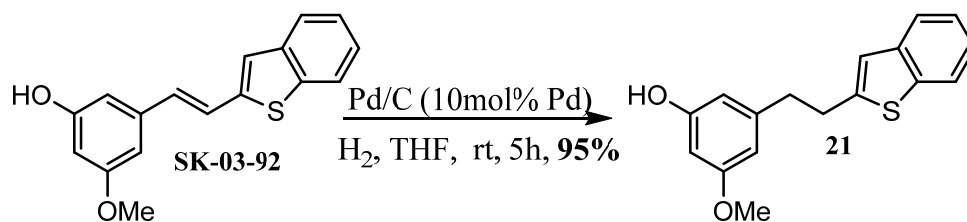
Based on the biological evaluation of this new analog, to be discussed in the upcoming section, additional modifications to the bridge were not attempted.

SK-03-92 has relatively few sites for direction manipulation, however, the phenolic group at the 3-position gave access to a few new analogs. Since the advent of transition metal chemistry a number of reactions have been developed that replace aryl halides or triflates with other desirable functionalities.[95-99] Through the initial SAR it was shown that the dimethoxy analog **19** (Scheme 2-5) was inactive and based on this it was assumed that the phenolic functionality was essential for activity. However, for the same reason mono-demethylation was successful, namely the symmetrical nature of **19**, this would also allow substitution at the phenolic site and subsequent demethylation of the methoxy group at position 5 to give structural analogs of SK-03-92 (Figure 2-6).

Figure 2-6: Phenolic substitution followed by demethylation.
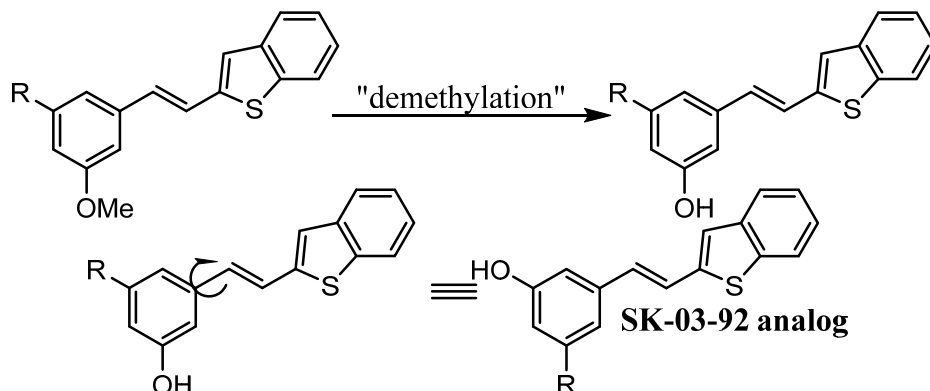
From this study, synthesis of the triflate analog of SK-03-92 was followed by substitution using transition metal catalysis. This was followed further by demethylation of the methoxy group at position 5 giving rise to other interesting analogs. Synthesis of the triflate analog of SK-03-92 from triflic anhydride proceeded smoothly in 98% yield (Scheme 2-8) and was found to be adequately stable when stored in a freezer.

Scheme 2-8: Synthesis of the triflate analog of SK-03-92.
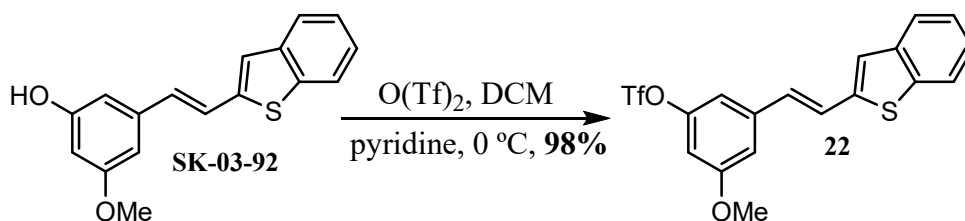
With the triflate **22** in hand, the study focused on replacement with a functional group similar in size and electronic character to the methoxy group at position 5 of **SK-03-92**. The first interesting analog planned was conversion of the triflate group to a thiol (Scheme 2-9). A number of methods existed for this transformation[100-103], however, this work focused on a method employing triisopropyl silane thiol and palladium tetrakis. Two analogs were envisioned

from this route; first the thiol depicted in Scheme 2-9, and next the thiomethoxy **25** depicted in

Scheme 2-11.

Scheme 2-9: Triflate to thiol synthesis.
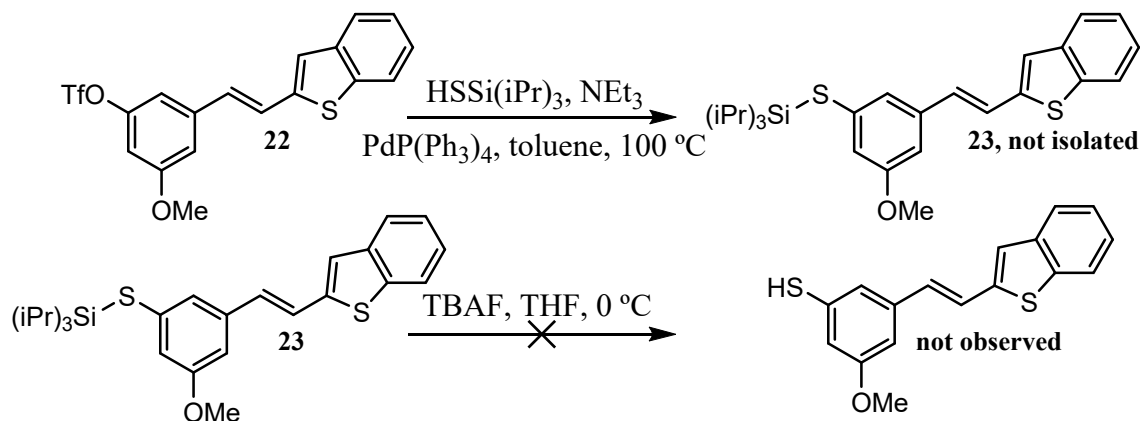
Unfortunately, although the transition metal catalyzed reaction worked flawlessly, the

simple removal of the silyl group proved troublesome. In fact, the thiol analog was never

observed even in crude samples tested by NMR. On addition of TBAF, it was noted that starting

material abruptly disappears with formation of baseline material. This material was tested by

NMR, but revealed little information on the structure of the crude material. Though synthesis of

the thiol was halted, it was found that adding 2 equivalents of iodomethane to the TBAF

conditions resulted in the thiomethyl compound **24** (Scheme 2-10). Further demethylation of **24**

led to the SK-03-92 thiomethyl analog **25** (Scheme 2-11).

Scheme 2-10: Synthesis of thiomethyl analog of 19.
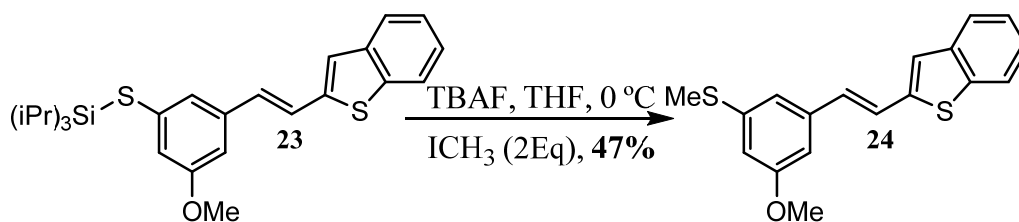
Scheme 2-11: Synthesis of the thiomethyl analog of SK-03-92.
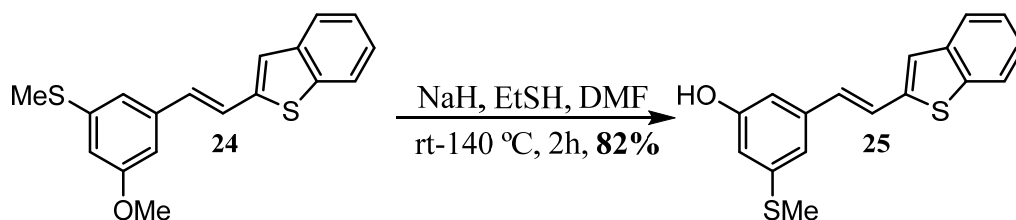
Unfortunately, the methylation reaction took place in low yield leading to an overall poor yield of the interesting SK-03-92 analog **25**. The final reaction to compound **25** took advantage of the electronic character of the thiomethyl group which was not as readily demethylated as methoxy groups, an interesting reaction considering that the thiol itself was not stable enough to isolate.

The next analog of interest was substitution of the triflate group with a nitrile group. A nitrile group is of similar size to a methoxyl group, however, they have very different electronic characteristics, so this substitution could give some insight into the SAR related to ring A of SK-03-92. A number of methods are available for such a substitution[104-106], however, in this case we started with the well-known Rosenmund-von Braun reaction (Scheme 2-12).[107] It was found that under the harsh conditions, conversion to the nitrile via this process was not possible. It is also possible that triflates are not suitable for this reaction since little literature support was found for the substitution besides those of aryl halides.

Scheme 2-12: Rosenmund-von Braun reaction.
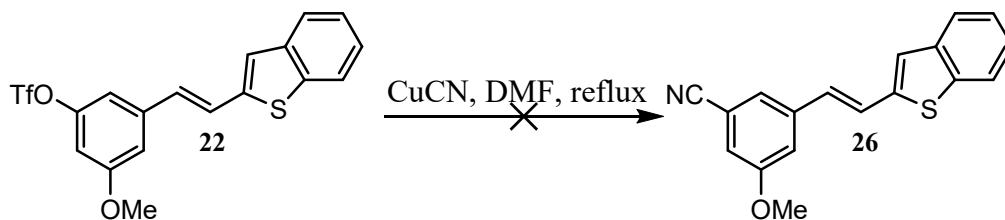
Fortunately, there are many alternatives to such reactions and it was found that in a similar manner to the thiol synthesis, palladium tetrakis was found to convert the triflate into the corresponding nitrile in the presence of copper iodide and sodium cyanide (Scheme 2-13).

Scheme 2-13: Transition metal catalyzed nitrile synthesis.
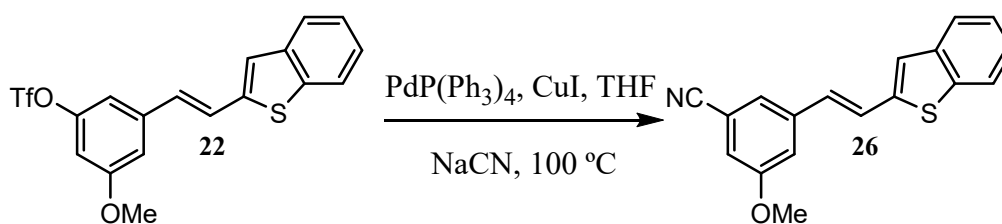
Unfortunately, low yields (35%) and difficulties in the synthesis of the phenol from the nitrile analog **26** made synthesis of the nitrile analog of SK-03-92 difficult and it was not pursued further (Scheme 2-14).

Scheme 2-14: Demethylation of the nitrile analog.
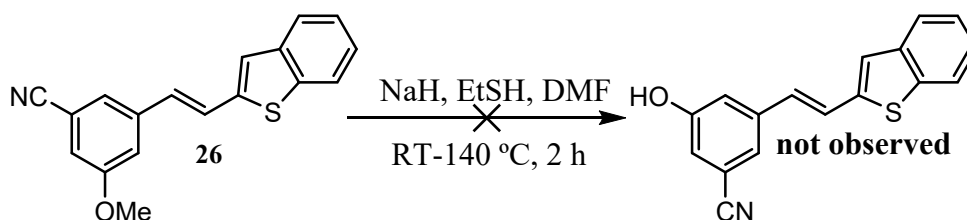
It should be noted that it is presumed that the above reaction does work, however only a small amount of **26** was synthesized and it may have decomposed under the harsh conditions of demethylation Scheme 2-14. At this time, however, it was determined that a new synthetic pathway was necessary for synthesis of analogs similar to SK-03-92. Although the triflate pathway was successful for a small number of compounds, the necessity to demethylate many of the possible analogs proved troublesome on such a small scale.

One further analog was also synthesized from the diethylphosphonate (**17**) originally discussed in Scheme 2-5. Thiophene-2-carbaldehyde (**27**) and diethylphosphonate were reacted in a similar manner to Scheme 2-5 (step 6) to give the dimethoxy analog **28**. Demethylation via sodium ethane thiol gave the desired thiophene analog **29** (Scheme 2-15). Thiophene is a known bioisostere of a benzene ring[108-110] and given the activity of SK-03-92 with a thionapthene ring, this compound is an isostere of the original natural product **1** and its activity was important to compare to **1**.

Scheme 2-15: Synthesis of the thiophene derivative of natural product 1.
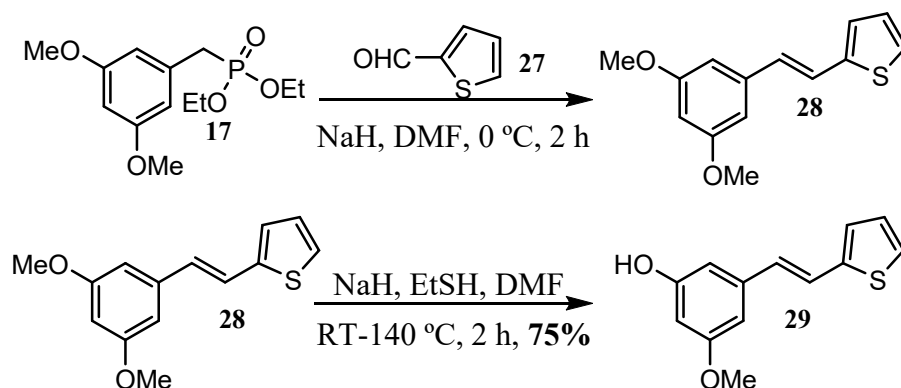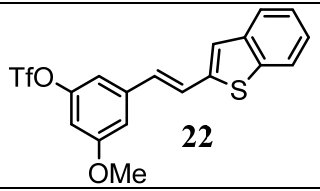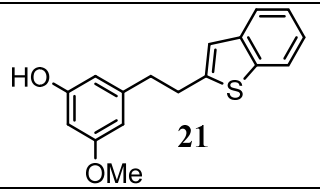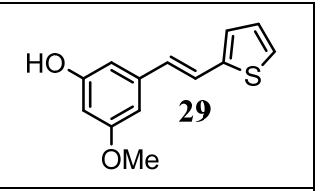
3. MIC results and discussion.

Minimum inhibitory concentrations (MICs) of new analogs were carried out according to standard protocols.[111] As previously discussed, the strains tested were two gram-positive strains, two gram-negative strains, and a series of seven different mycobacterium strains. Although MIC data for the mycobacterium strains was not within a drug-suitable range for any compounds discussed analysis of the data, in some cases, reveal interesting SAR information. For example, in some cases stilbenes exhibited activity against both gram-positive and mycobacterium strains,

yet in other cases some only exhibited activity against gram-positive strains. This may relate to the difference in the cell walls between gram-positive bacteria and mycobacterium.

Table 2-4: MIC results for compounds 22, 21, and 29.[a]

Bacterial Strain	22	21	29
S. aureus	>128	8	32
E. faecalis	>128	16	64
P. aeruginosa	>128	>128	>128
E. coli	>128	>128	>128
M. intracellulare	>128	128	64
M. chelonae	>128	>128	128
M. fortuitum	>128	128	>128
M. kansasii	>128	>128	64
M. avium	>128	128	128
M. smegmatis	>128	128	128
M. marinum	>128	>128	64

[a]Values in µg/mL

Not surprisingly, triflate **22** was found to be inactive (Table 2-4). As discussed the previous SAR indicated that a phenolic group was necessary, since dimethoxy analogs, prior to demethylation, were found to be inactive in all cases tested. Importantly, however, examination

of the MIC of the triflate analog indicated this lack of activity extended to groups other than methoxy.

The saturated analog **21** was found to retain activity (Table 2-4), although it was ~4-fold less active then the parent lead compound SK-03-92. From this it was concluded that the olefinic bridge was important, but not absolutely necessary for activity, which may prove useful for future SAR endeavors. However, rigid stilbenes with an olefinic bridge have exhibited more potent activity and thus should be investigated first. It is hypothesized that the rigidity of the unsaturated bridge may help these stilbenoid compounds penetrate the cell walls of the gram-positive bacteria more readily. Only a subtle loss of activity when the bridge was saturated supports this hypothesis. This may be of importance for later SAR advances as saturation of the bridge can reduce the likelihood of side-effects similar to that of other stilbenoid pharmaceuticals such as stilbestrol.[112]
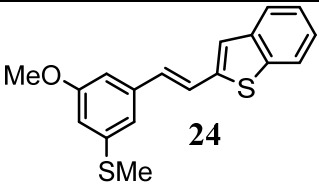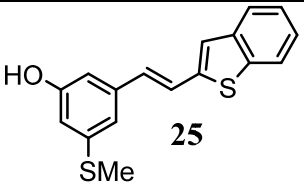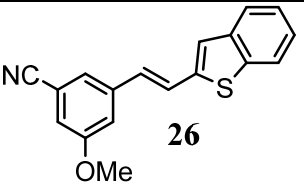
Since thiophene is a bioisostere of benzene, it was felt the thiophene analog **29** should have similar activity to the natural product **1** and that was the case (Table 2-4). Interestingly in the previous SAR it was found that substitution of a naphthene group instead the thianaphthene in SK-03-92 resulted in an 8-fold decrease in activity even though they are related bioisosteres. This led one to believe that it was perhaps the change in geometric orientation from naphthene to thianaphthene that led to the poorer MIC results (Figure 2-7). Interestingly, ring B 5-membered thiophene rings form a conserved symmetry with respect to the alkene bridge when compared to their 6-membered ring counterparts.

Figure 2-7: Orientation of ring C in stilbenoid compounds.
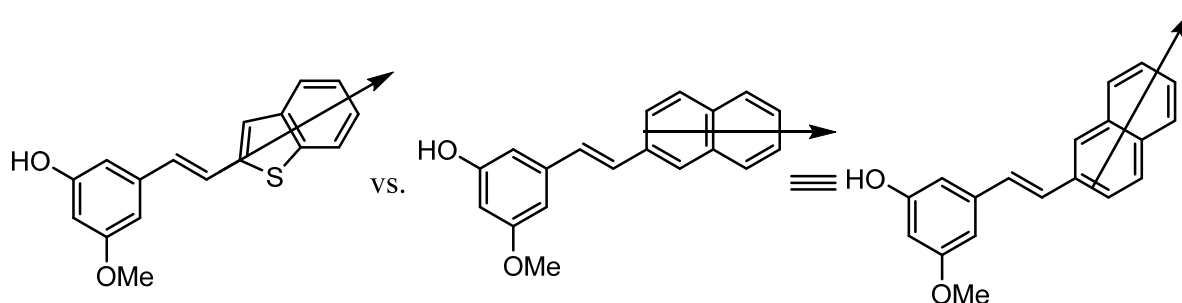
Table 2-5: MIC results for compounds 24, 25, and 26.[a]

Bacterial Strain	24	25	26
S. aureus	>128	**2**	>128
E. faecalis	>128	**8**	>128
P. aeruginosa	>128	>128	>128
E. coli	>128	>128	>128
M. intracellulare	>128	128	>128
M. chelonae	>128	64	>128
M. fortuitum	>128	64	>128
M. kansasii	>128	64	>128
M. avium	>128	64	>128
M. smegmatis	>128	64	>128
M. marinum	>128	64	>128

[a]Values in μg/mL

As previously discussed the SAR predicted that lack of a phenolic group would result in a lack of activity and ligand **24** with a thiomethyl group, devoid of a phenolic group, lacked activity (Table 2-5). Similar results were seen with triflate **22**; which indicated that the phenolic nature in ring A is necessary for the antimicrobial activity as observed in compounds such as SK-03-92.

Thiomethyl analog **25** retained activity and was as active as the parent SK-03-92 within experimental error (Table 2-5). Analysis of this result indicated that although the phenol was a necessary component for consistently potent compounds, there was room for synthetic manipulation of the methoxy group of SK-03-92 to retain or enhance potency in ring A of the stilbenoids.

Finally, the nitrile analog **26** lacked activity since it too lacked the necessary phenolic group. Synthesis of the more interesting phenolic analog of **26** failed via the current methods and was followed up in future studies to be discussed in Chapter 3.

4.   Biological and Pharmacokinetic data on SK-03-92.

Note: These data were gathered and compiled by Dr. Bill Schwan, UW-LaCrosse.

The gram quantities of SK-03-92 permitted a more robust experimental design that included more in depth *in vitro* assays as well as *in vivo* assays in mice/rats.

The preliminary efficacy testing was performed using SK-03-92 in a murine thigh abscess model.[113] Briefly, murine thigh abscesses were established with a 1 x 10^6 CFU of *S. aureus* MW2, a CA-MRSA strain. Three cohorts were established: a phosphate buffered saline control (containing DMSO), a single-dose group of 3.2 µg SK-03-92 per gram mouse, and a single-dose group of 160 µg SK-03-92 per gram mouse. On the day after the bacteria were

injected into the mice (CA-MRSA), the mice were injected with either drug or control. Two days after the drug dose (three days after injection of the bacteria), murine thighs were collected, homogenized, and plated onto brain heart infusion agar. Colony counts were taken for the homogenized thighs of the mice. Examination of the results indicated that the median CFU/thigh was one log unit lower in the low-dose (3.2 µg per g) test group, and two log units lower in the high-dose (160 µg per g) test group, as compared with the control group (Figure 2-8). It was also important to note that no adverse effects were noted in any of the mice tested with SK-03-92.

Figure 2-8: *In vivo* testing of SK-03-92 in a murine thigh abscess model.
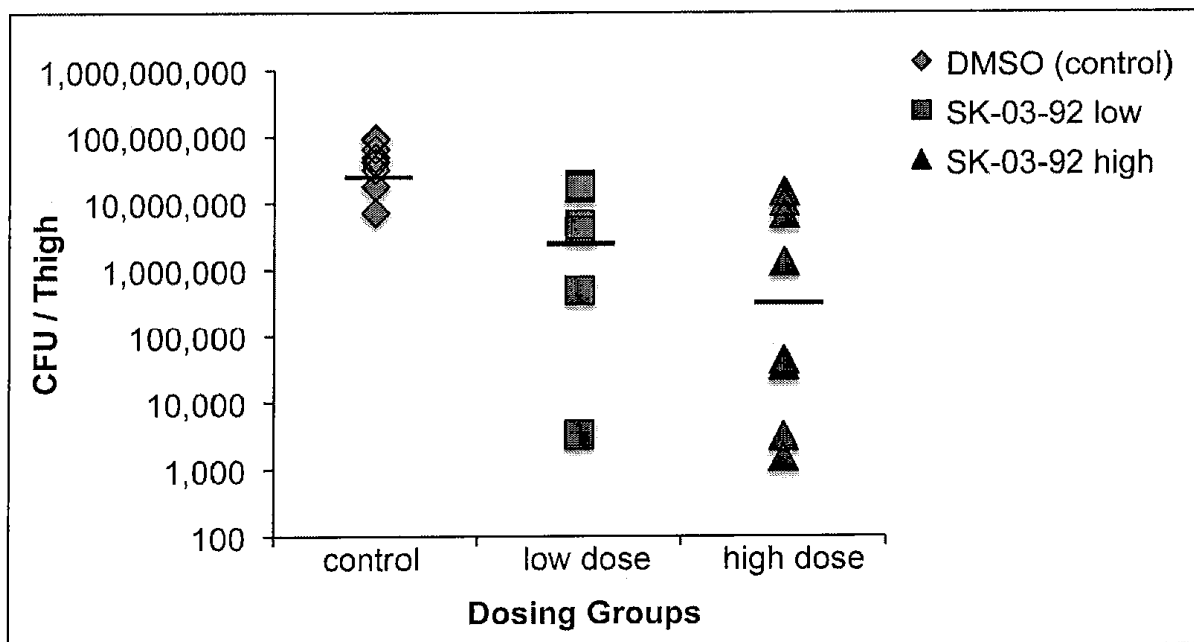
These results were encouraging, however they also indicated that a more in-depth pharmacokinetic profile of SK-03-92 was necessary.

4.1: Determining the solubility of SK-03-92 in other solutions

Because SK-03-92 had low solubility in an aqueous solution, and solubilizing the drug in DMSO would be inappropriate for oral or intravenous (IV) administration to humans, alternative vehicles were examined. The solubility of SK-03-92 was determined using high performance liquid chromatography (HPLC). The solubility of SK-03-92 in PBS was <0.0001 mg/mL, but the solubility in other suitable vehicles ranged from 4.6 mg/mL for 20% Solutol HS 15/80% PBS to 9.2 mg/mL for PEG 400. The Solutol HS 15/PBS solution was chosen for further development of a dosing solution due to the potential for use in both IV and oral administration.

4.2: Safety/cytotoxicity testing of SK-03-92

To determine the approximate safety of SK-03-92 against tissue culture cells, an MTT [3-(4,5-dimethylthiazol-2-yl)-2,5-diphenyltetrazolium bromide] assay was performed. The IC_{50} of SK-03-92 was shown to be 125 μg/mL for all four tissue culture cell lines (J774A.1, U937, 292, and T24), generating a promising relatively high therapeutic index (IC_{50}/MIC) of 62.5 for 90% of the *S. aureus* strains.

To determine if SK-03-92 was safe for use *in vivo*, an escalating dosing scheme in mice (5, 50, 300, and 2000 mg/kg) was employed. None of the mice that received a single dose of the highest drug concentration (2000 mg/kg) IP displayed any adverse effects over a two-week time frame (e.g., altered gait, ungroomed, significant weight loss), demonstrating that SK-03-92 was non-toxic at this highest dose. After initial dosing at 2000 mg/kg, a repeat dose of 2000 mg/kg was administered a week later, and again, no overt toxicity was observed for the animals. High doses of the related compounds, pterostilbene and resveratrol, have been shown to be non-toxic in mice[114], rats[115], and humans[116].

4.3: Single dose PK analysis of SK-03-92

A single dose of SK-03-92 was given to mice to assess single dose PK parameters. The observed area under the plasma concentration-time curve (AUCINF_obs), maximum plasma concentration (C_{max}), time to achieve C_{max} (T_{max}), oral clearance of drug observed (Cl_F_obs), volume of distribution of drug observed (Vz_F_obs), and half-life were calculated. Intraperitoneally administered SK-03-92 had a half-life of 22.46 min, a T_{max} of 30 min, a C_{max} of 1.64 µg/mL, a Cl_F_obs of 1.46 mL/min/g, a Vz_F_obs of 47.71 mL/g, and a AUCINF_obs of 70.15 min·mg/mL (Table 2-6). The T_{max} of 30 min when given ip and 22 min when dosed orally demonstrated rapid absorption of SK-03-92 in line with the rapid absorption of other stilbenoid drugs.[117] The maximal plasma concentration (C_{max}) was somewhat low for orally administered SK-03-92 (370 ng/mL), but was still detectable and was approximately 25% of the C_{max} observed with ip-administered drug (1.64 µg/mL). The C_{max} and $AUC_{0\text{-inf}}$ values for SK-03-92 fall between the values reported for resveratrol and pterostilbene[118]. After achieving the C_{max}, the SK-03-92 plasma concentrations dropped to negligible levels 75 min after oral gavage, which was in line with the PK results that have been observed using other stilbenoid drugs.[117-118] The relatively short half-life of SK-03-92 (22 min for ip administered, 30 min for orally administered) suggested that administration more than once a day would be needed to treat a *S. aureus* infection. The concentration of SK-03-92 reached a high of 1.641 µg/mL after 30 min and dropped to 0.149 µg/mL within 90 min of ip injection. All of the mice looked healthy, and no overt toxicity (e.g., excessive weight loss, ungroomed, altered gait) was observed, mimicking the mouse safety study above.

Table 2-6. Summary of pharmacokinetic (PK) parameters by route and schedule.

Route	Half-Life (min)	T_{max} [c] (min)	C_{max} [c] (µg/mL)	Cl_F_obs [c] (mL/min/g)	Vz_F_obs [c] (mL/g)	AUCINF_obs [c] (min*µg/mL)
ip [a]	22.46 ± 17.81	30.00 ± 0.00	1.64 ± 0.59	1.46 ± 0.26	47.71 ± 33.25	70.15 ± 12.76
oral [b]	30.40 ± 17.81	21.43 ± 11.80	0.37 ± 0.35	21.00 ± 6.71	810.67 ± 173.87	5.14 ± 1.87

a Mean ± standard deviation from three mice tested; b Mean ± standard deviation from three mice tested; c Tmax (time to achieve Cmax), Cmax (maximum plasma concentration), Cl_F-obs (oral clearance of drug observed), Vz_F-obs (volume of distribution of drug observed), and AUCINF_obs (area under the plasma concentration-time curve observed).

4.4: Relative bioavailability of SK-03-92

To determine the relative bioavailability of the SK-03-92 lead compound, 100 µg/g of Solutol HS 15/PBS formulated SK-03-92 was administered orally to the mice. After 15 min, 0.740 µg/g was detected in the mouse plasma, and by 30 min that level had dropped to 0.126 µg/g. All of the mice looked healthy, and no signs of toxicity were observed. The relative bioavailability (AUC_{oral}/AUC_{IP}) was approximately 8%, which indicated that oral delivery of the drug would not provide therapeutic concentrations for treating *S. aureus* infections. Other studies that have examined stilbenoid compounds have also observed low to very low bioavailability for those agents.[117-119]

4.5: Multi-dose effects and protein analyses of SK-03-92

Examination of the single dose PK analysis indicated that the SK-03-92 lead compound was safe, but the plasma concentration was somewhat low. Multi-dose experiments were performed to assess adverse effects associated with chronic dosing as well as pharmacokinetics. Given that adverse effects do not correlate linearly with plasma concentrations, animals could experience adverse effects when plasma concentrations were undetectable with repeated dosing. Pharmacokinetic evaluations were performed to determine if changes in pharmacokinetic profiles with chronic dosing (e.g., reduced clearance) were associated with adverse effects.

To determine how multiple doses of SK-03-92 affected the health of the mice, as well as the PK parameters, an extended five-day PK study was undertaken. Plasma concentrations ranged from a high of 0.086 µg/mL after 15 min to a low of 0.027 µg/mL after 75 min. In the PK study which extended to two-weeks following oral administration, the plasma SK-03-92 concentrations ranged from 0.144 µg/mL after 15 min to 0.01 µg/mL after 75 min. On average, the treated mice lost about 1.5% of their weight after two-days, but after one week, the weight of treated mice increased on average by 5.16% on day 9 and went up further to 9.75% by day 12. Two doses of SK-03-92 given four hours apart for three days achieved a maximum SK-03-92 plasma concentration of only 2.12 µg/mL.

4.6: Protein binding by SK-03-92

The degree of protein binding by SK-03-92 in plasma was also determined. It was found that 84.4% of the SK-03-92 drug bound to plasma proteins. Consequently, most of the SK-03-92 lead compound bound to plasma proteins, which could affect its bioavailability.

This was the first study to examine the PK properties of a new lead compound labeled SK-03-92. Other studies have examined the PK properties of stilbenoid-based compounds, but none of these other studies have done PK analysis with the expressed goal of using a drug with a stilbene scaffold to treat bacterial infections. The absence of overt symptoms in mice following dosing with SK-03-92 suggests that SK-03-92 may have a very good safety margin. High concentrations of SK-03-92 given daily to mice did not appear to have gross adverse effects on the mice, which is in line with animal studies done using resveratrol and pterostilbene.[117] Both the SK-03-92 ip and oral administration pharmacokinetic profiles were low; likewise, low plasma concentrations of resveratrol (<1 µg/mL) and pterostilbene (<8 µg/mL) have been observed in animals. The maximum SK-03-92 plasma concentration in the mice was only 2.12 µg/mL. Several properties

of SK-03-92 probably contribute to its low plasma/tissue concentrations in mice. Aqueous solubility appeared to be one of the barriers. Stilbene compounds are hydrophobic and generally insoluble in aqueous solutions. The use of a Solutol HS 15/PBS solution improved the solubility of SK-03-92, but the solubility was still less than 10%. Another property tied to the low plasma/tissue availability of SK-03-92 was its high level of plasma protein binding (84.4%). Our previous *in vitro* study demonstrated a much higher MIC against *Streptococcus pneumoniae*, and this was probably due to SK-03-92 binding to the proteins found in the fetal calf serum added to the wells of the microtiter plate. A myriad of proteins present in the bloodstream and tissues would reduce the effective concentration of SK-03-92. Lastly, SK-03-92 exhibited a relatively short half-life in the mice, breaking down into metabolic byproducts within 15 min after ip or oral delivery. Resveratrol and pterostilbene also have short half-lives in animal plasma (15–60 min and 120 min, respectively) with substantial accumulation of metabolic byproducts.

New drugs with novel mechanisms of action are needed to keep abreast of antibiotic resistance in *S. aureus*, one of the ESKAPE pathogens. The safety profile of SK-03-92 is highly encouraging. Although the oral bioavailability of SK-03-92 may hinder use as an oral stand-alone treatment for *S. aureus* infections, the opportunity to employ it against drug resistant strains of MRSA topically or embedded in a patch still exists. We are also analyzing microarrays and performing additional assays to elucidate the mechanism(s) of action of SK-03-92. Furthermore, we are currently assessing whether SK-03-92 has a synergistic effect when co-administered with clinically useful antimicrobials such as oxacillin, clindamycin, and vancomycin. If the half-life and bioavailability problems can be solved, an analog of SK-03-92 may have a future in treating *S. aureus* skin and soft tissue infections.

III.   CONCLUSION.

In summary, a method for the scale-up of SK-03-92, a new lead compound for antimicrobial research, was completed in an overall yield of 50% from a total of seven synthetic steps. This permitted gram scale synthesis of SK-03-92 which led to a compendium of information on the biological and pharmacokinetic properties of SK-03-92.

Although initial results with SK-03-92 *in vivo* seemed promising, pharmacokinetic issues involving its absorption as well as it is half-life indicate that as a pharmaceutical candidate it is not ideal. However, it provides the impetus and direction for future synthetic endeavors discussed in future Chapters of this work.

Since the mechanism of action of SK-03-92 and related analogs is still unknown, it is not possible to design related drugs for a specific target, but rather continue with SAR studies to attempt to find the optimal substitution patterns for activity. Once a catalog of active compounds is constructed, more in depth PK analysis may lead to a novel candidate for an antimicrobial pharmaceutical drug.

Synthesis of some new analogs was successful using transition metal catalyzed substitution of a triflate group with other small nucleophiles, however the route took place in low yield and required a difficult demethylation step after the penultimate palladium catalyzed reaction. This was not ideal and was not seen as a long-term solution to advance the SAR of this interesting class of compounds. Because of this, a new one-step route was investigated.

IV.   EXPERIMENTAL.

1.   *In vitro* and *in vivo* assays. *(Completed by Dr. Bill Schwan, UW-LaCrosse)*

1.1: MIC assays.

In vitro minimum inhibitory concentration (MIC) determinations were performed according to the Clinical and Laboratory Standards Institute (CLSI) guidelines,[115] for most of the bacteria that were screened. Tetracycline, ciprofloxacin, and erythromycin controls were included as control antibiotics for the gram-positive bacteria MICs and correlated with established MIC values. All anti-mycobacterium activity evaluations (except for the anti-*Mycobacterium tuberculosis* assays) were performed using MIC assays in Middlebrook 7H9 broth with 10% oleic acid albumin dextrose complex (OADC) as previously described.[120] Rifampin was used as the positive control for the mycobacterial MICs. All MIC numbers are a compilation of the geometric means from three separate runs. For the broad characterization against *S. aureus*, strains that have been typed by a variety of means were used.[116]

1.2: Mice.

The Institutional Animal Care and Use Committees at the University of Wisconsin-La Crosse and the University of Wisconsin-Madison approved the study design and the animal handling protocols of this pharmacokinetic study. The protocol number for UW-Madison was M1732 with a start date of 23 April 2009, whereas the UW-La Crosse protocol was 3–8 with a start date of 26 March 2008. Either female BALB/c (NCI) or Swiss Webster (Harlan) mice 5–9 weeks old were used in this study.

1.3: Cytotoxicity assays.

Initial *in vitro* safety testing of SK-03-92 was performed with an MTT [3-(4,5-dimethylthiazol-2-yl)-2,5-diphenyltetrazolium bromide] assay (9, American Type Culture Collection) for several tissue culture cell lines (murine monocytic J774A.1, human monocytic U937, human kidney epithelial 293, and human bladder epithelial T24) using mitomycin C

(Sigma, St. Louis, MO, USA) and DMSO alone as positive and negative controls, respectively. Assays were done a total of three times per tissue culture cell line.

1.4: Initial Safety Testing in Mice.

Three female 5–9 week old Swiss Webster mice (Harlan) per drug concentration were injected intraperitoneally (ip) with increasing concentrations of SK-03-92: 5, 50, 300, and 2000 mg/kg according to OECD.[115] The lowest concentration of drug was used first. Overt toxicity (e.g., altered gait, ungroomed, significant weight loss) was monitored. If two of three mice showed no overt toxicity, then the next dose of drug was given.

1.5: HPLC sssay development.

An HPLC method was developed on a Halo C18 4.6 × 1.0 mm, 2.7 μm column (MAC-MOD Analytical Inc., Chadds Ford, PA, USA) for the detection and quantitation of SK-03-92. The method was developed using the information obtained from a scouting gradient of 5%–100% acetonitrile over 35 min. A UV spectrum of SK-03-92 was obtained from the scouting gradient and the observed maximum for SK-03-92 was 335 nm, with a local maximum of 224 nm also observed. The 335 nm maximum wavelength was used for the quantitation of SK-03-92, and the 224 nm local maximum wavelength was used to monitor for possible formation of degradation products not visible at the 335 nm wavelength. Flow rate was 0.750 mL/min and injection volume was 10 μL. The mobile phase was 62% acetonitrile (Fisher, Hanover Park, IL, USA):38% water (Milli-Q UV plus) and the isocratic program was 62% acetonitrile:38% water for 20 min. Acquisition time was 10 min and room temperature retention time was 5.4 min. Standards of SK-03-92 were prepared in acetonitrile at concentrations of 0.05–0.005 mg/mL.

1.6: Single Dose PK Assay.

An initial single dose PK experiment was performed using 100 μg/g of formulated SK-03-92 administered ip to twenty-one female, 5–6 week old BALB/c mice (7 per cohort for 3 cohorts, NCI) under parameters established previously. Three animals were used as a control group and received blank vehicle, whereas three mice per time point received 100 μg/g SK-03-92 ip and were sacrificed with blood collected at the 15, 30, 45, 60, 75, and 90 min time points by warming the tails of the mice in warm water, lancing the lateral saphenous tail vein, and collecting the blood (up to 150 μL) into microvette tubes (Sarstedt) containing EDTA or terminal bleed into vacucontainers containing EDTA as an anti-coagulant. Plasma was separated from packed blood cells by centrifugation ($600 \times g$) and stored at -70 °C until needed for HPLC analysis. Samples were analyzed with a Shimadzu Prominence HPLC system (Kyoto, Japan) with a Halo C18 column (MAC-MOD Analytical Inc., Chadds Ford, PA, USA). A mobile phase of 62% acetonitrile/38% water, isocratic program of 62% acetonitrile for 20 min, and flow rate of 0.75 mL/min with an injection volume of 10 μL and a retention time of 5.4 min were used. The standard curve for SK-03-92 was linear from 0.0098 to 2.5 μg/mL in plasma. Each chromatogram was collected and integrated to estimate the peak area of analyte by EZ Chrom® software (version.1.0, Agilent Technologies Inc., Santa Clara, CA, USA). The ratio of peak area of SK-03-92 was calculated to estimate the drug concentration(s) using a pre-built calibration curve. Major pharmacokinetic parameters were calculated using the noncompartmental analysis module of WinNonlin® (version 5.1, Pharsight Corp., Princeton, NJ, USA) under sparsely sampling mode.

1.7: Bioavailability assay.

A relative bioavailability study was performed using 100 μg/g of formulated SK-03-92 administered orally to six female 5–6 week old BALB/c mice (NCI) with three animals as the

control group receiving blank vehicle by the oral route. Three mice per time point had blood collected at 15 and 30 min after administration.

1.8: Multi-dose analysis.

First, a five-day PK study with SK-03-92 orally administered to female 5-6 week old BALB/c mice was conducted. Three mice received 300 μL of blank vehicle by oral administration. Doses of 100 μg/g SK-03-92 were given orally each day in the vehicle. Blood was collected from three mice at time points 15, 30, 45, 60, 75, and 90 min after administration. Body weight was monitored every day before SK-03-92 administration. Plasma was prepared and stored at −70 °C until analyzed by HPLC. In an extension of this PK study to two-weeks following oral administration of SK-03-92, six mice were dosed in the test (SK-03-92) arm and six vehicle control mice in the other arm. Lastly, a multi-dosing PK analysis was done using two 51-μg/g doses of SK-03-92 per day (given four hours apart) over the course of three days in five mice.

1.9 Protein binding assay.

Plasma collected from EDTA treated blood from six SK-03-92 dosed mice was added to methyl *tert*-butyl ether (MTBE) to precipitate the proteins. The precipitated proteins were separated from the remainder of the plasma by centrifugation (14,000× *g* for 20 min) through a Microcon 10K filter (Millipore) and dried under a stream of nitrogen gas. The dried product was suspended in 62% acetonitrile/38% ddH$_2$O and the AUC was quantified and correlated with the initial concentration of SK-03-92 present in the plasma by HPLC.

2.   Characterization data.

Both 1H and 13C NMR spectra were recorded on a Bruker DPX-300 or DRX-500 instrument where noted. HRMS scans were recorded with a Shimadzu LCMS-IT-TOF or similar

instruments run at the Shimadzu Analytical Chemistry Center of Southeastern Wisconsin. *In silico* cLogP values and topological polar surface area values (tPSA) were calculated with ChemBioDraw Ultra v. 14.

(E)-3-(2-(Benzo[b]thiophen-2-yl)vinyl)-5-methoxyphenol (SK-03-92, Table 2-3, entry 3)
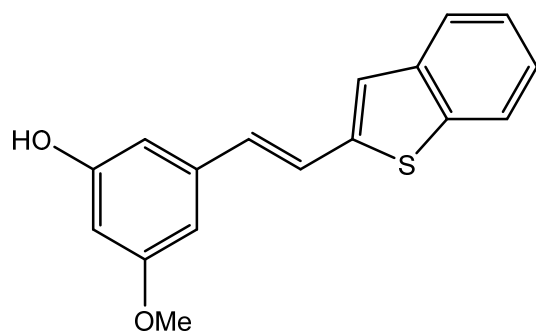
Chemical Formula: $C_{17}H_{14}O_2S$
Molecular Weight: 282.36
c Log P: 4.74
tPSA: 29.46

The NaH (60% dispersed in mineral oil, 3.6 g, 0.09 mol) was added to anhydrous DMF (100 mL) at 0° C. The CH_3CH_2SH (12.2 mL, 13.22 g, 0.12 mol) was then added dropwise and stirred at 0° C for 30 min. The temperature of the reaction mixture was allowed to rise to rt and the mixture stirred for 1 h. The temperature of the reaction mixture was raised to 140° C and (E)-2-(3,5-dimethoxystyryl)benzo[b]thiophene (8.90 g, 0.03 mol) in dry DMF (30 mL) was added dropwise to the reaction mixture. This mixture was held at 140° C and monitored by TLC (30% EtOAc in hexanes). When the starting material was no longer present by TLC (~1 hr), the reaction mixture was cooled to rt and quenched by addition of aq 0.5N HCl (500 mL). The mixture was extracted with EtOAc (3 x 200 mL). The combined organic layers were washed sequentially with aq 0.5N HCl (3x60 mL) and brine (3 x 60 mL). The organic layer was dried over Na_2SO_4 and the solvent was removed *in vacuo*. The crude solid was purified by flash column chromatography (FCC) (20% EtOAc in hexanes) to afford the pure SK-03-92 in 92% yield as a pale yellow solid (7.79g): ^{1}H NMR (300 MHz, CD$_3$COCD$_3$) δ 8.43 (s, 1H), 7.89 – 7.77 (m, 2H), 7.52 – 7.34 (m, 4H), 6.97 (d, J = 15.9 Hz, 1H), 6.72 (m, 2H), 6.40 (t, J = 2.2 Hz, 1H),

3.81 (s, 3H); ^{13}C NMR (75 MHz, CD$_3$COCD$_3$) δ 161.3, 158.7, 142.7, 140.3, 138.6, 130.8, 124.8, 124.5, 123.6, 123.4, 122.4, 122.0, 106.2, 103.4, 101.5, 54.6; HRMS (ESI) (M + H), Calcd. for C$_{17}$H$_{15}$O$_2$S 283.0793; Found 283.0797.

(E)-3-(2-(Benzo[b]thiophen-2-yl)vinyl)-5-methoxyphenyl trifluoromethanesulfonate (22, Table 2-4, entry 1)
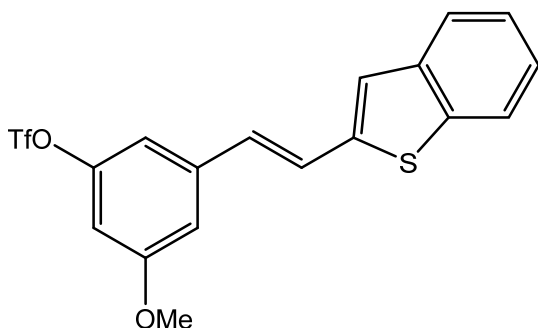
Chemical Formula: C$_{18}$H$_{13}$F$_3$O$_4$S$_2$
Molecular Weight: 414.41
c Log P: 6.21
tPSA: 52.6

The (E)-3-(2-(benzo[b]thiophen-2-yl)vinyl)-5-methoxyphenol (1.00g, 3.54mmol, 1eq) was dissolved in 50mL DCM (freshly distilled) and the pyridine (310mg, 3.90mmol, 1.1eq) was added in one portion. The solution was cooled to 0 ºC and trifluoromethanesulfonic anhydride (1.1g, 3.90mmol, 1.1eq) was added dropwise at 0 ºC. The starting material was consumed after 10 min on analysis by TLC (20% EtOAc in hexanes) and the reaction was quenched with aq 0.5N HCl (50mL). DCM (40mL) was added and the organic layer extracted. The organic layer was washed with brine (50mL) and dried over Na$_2$SO$_4$. The solvent was removed *in vacuo* leaving a crude yellow solid. The solid was purified by flash column chromatography on silica gel (10% EtOAc in hexanes) to provide the pure **22** in 98% yield as a white solid (1.44g): ^{1}H NMR (300 MHz, CDCl$_3$) δ 7.80 (dd, *J* = 8.8, 4.8 Hz, 1H), 7.75 (dd, *J* = 6.1, 3.0 Hz, 1H), 7.41 – 7.30 (m, 4H), 7.28 (s, 1H), 7.04 (s, 2H), 6.92 (d, *J* = 16.0 Hz, 1H), 6.74 (t, *J* = 2.1 Hz, 1H), 3.89 (s, 3H), 1.57 (s, 1H); ^{13}C NMR (75 MHz, CDCl$_3$) δ 160.97, 150.51, 141.74, 140.00, 139.80,

139.16, 128.56, 125.24, 124.89, 124.72, 124.68, 123.73, 122.30, 112.00, 111.19, 106.59, 55.82; HRMS (ESI) (M + H), Calcd. for $C_{18}H_{14}F_3O_4S_2$ 415.0286; Found 415.0291.

3-(2-(Benzo[b]thiophen-2-yl)ethyl)-5-methoxyphenol (21, Table 2-4, entry 2)
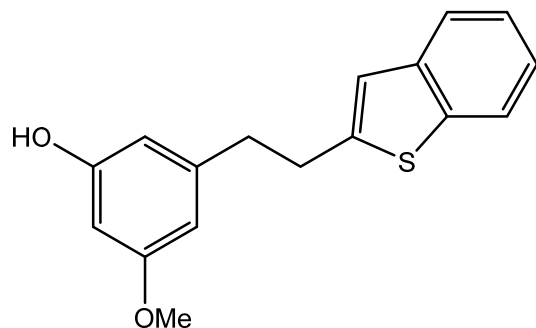
Chemical Formula: $C_{17}H_{16}O_2S$
Molecular Weight: 284.37
c Log P: 4.93
tPSA: 29.46

The (E)-3-(2-(benzo[b]thiophen-2-yl)vinyl)-5-methoxyphenol (100mg, 0.354mmol, 1eq) and 10% Pd/C (38mg, 10mol% Pd) were mixed in a sealed tube under argon. THF (4mL) was added in one portion and the sealed tube was evacuated under vacuum and backfilled with argon three consecutive times. The sealed tube was evacuated under vacuum and a balloon filled with hydrogen was attached. The starting material was consumed after 2h (TLC, silica gel) and the solution was filtered through a plug of celite. The solvent was removed in vacuo to leave a crude yellow solid. The solid was purified by flash column chromatography on silica gel (10% EtOAc in hexanes) to provide the pure **21** in 95% yield as a white solid (96 mg): ^{1}H NMR (300 MHz, CDCl$_3$) δ 7.79 (d, J = 7.6 Hz, 1H), 7.68 (d, J = 7.3 Hz, 1H), 7.42 – 7.19 (m, 2H), 7.02 (s, 1H), 6.41 (s, 1H), 6.30 (dd, J = 5.9, 3.7 Hz, 2H), 4.83 (s, 1H), 3.77 (s, 3H), 3.33 – 3.11 (m, 2H), 3.11 – 2.83 (m, 2H); ^{13}C NMR (75 MHz, CDCl$_3$) δ 160.95, 156.59, 145.28, 143.63, 140.08, 139.31, 124.12, 123.55, 122.82, 122.15, 120.93, 107.92, 106.84, 99.32, 55.29, 37.37, 32.32; HRMS (ESI) (M + H), Calcd. for $C_{17}H_{17}O_2S$ 285.0949; Found 285.0947.

(E)-3-Methoxy-5-(2-(thiophen-2-yl)vinyl)phenol (29, Table 2-4, entry 3)
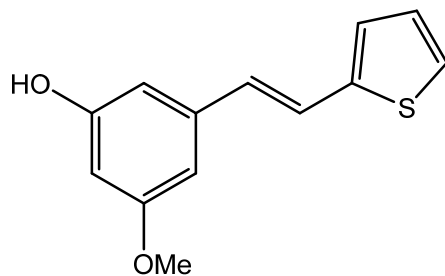
Chemical Formula: $C_{13}H_{12}O_2S$
Molecular Weight: 232.30
c Log P: 3.69
tPSA: 29.46

The NaH (60% dispersed in mineral oil, 360 mg, 0.009 mol) was added to anhydrous DMF (10 mL) at 0° C. The CH_3CH_2SH (1.22 mL, 1.32 g, 0.012 mol) was then added dropwise and stirred at 0° C for 30 min. The temperature of the reaction mixture was allowed to rise to rt and the mixture stirred for 1 h. The temperature of the reaction mixture was raised to 140° C and (E)-2-(3,5-dimethoxystyryl)thiophene (739 mg, 0.003 mol) in dry DMF (3 mL) was added dropwise to the reaction mixture. This mixture was held at 140° C and monitored by TLC (30% EtOAc in hexanes, silica gel). When starting material was no longer present by TLC (~2 h) the reaction mixture was cooled to rt and quenched by addition of aq 0.5N HCl (50 mL). The mixture was extracted with EtOAc (3 x 20 mL). The combined organic layers were washed sequentially with aq 0.5N HCl (3x15 mL) and brine (3 x 15 mL). The organic layer was dried (Na_2SO_4) and the solvent was removed *in vacuo*. The crude solid was purified by FCC (20% EtOAc in hexanes) to afford the pure **29** in 62% yield as an off-white solid (432 mg): ^{1}H NMR (300 MHz, CDCl₃) δ 7.23 – 7.17 (m, 2H), 7.09 – 7.08 (m, 1H), 7.04 – 7.00 (m, 1H), 6.84 (d, *J* = 16.2 Hz, 1H), 6.63 (s, 1H), 6.57 (s, 1H), 6.36 (t, *J* = 2.1 Hz, 1H), 5.04 (s, 1H), 3.83 (s, 3H); ^{13}C NMR (75 MHz, CDCl₃) δ 161.0, 156.7, 142.4, 139.3, 127.8, 127.5, 126.3, 124.5, 122.4, 105.7, 104.7, 101.0, 55.3; HRMS (ESI) (M + H), Calcd. for C₁₃H₁₃O₂S 233.0636; Found 233.0639.

(E)-2-(3-Methoxy-5-(methylthio)styryl)benzo[b]thiophene (24, Table 2-5, entry 1)
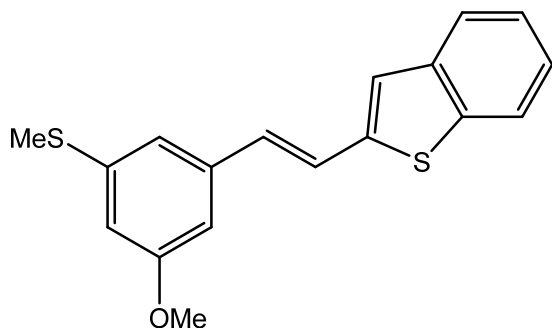
Chemical Formula: $C_{18}H_{16}OS_2$
Molecular Weight: 312.45
c Log P: 5.57
tPSA: 9.23

The (E)-3-(2-(benzo[b]thiophen-2-yl)vinyl)-5-methoxyphenyl trifluoromethanesulfonate (250mg, 0.603mmol, 1eq) and tetrakis(triphenylphosphine)palladium(0) (35mg, 5mol%) were mixed in a sealed tube under argon. Then degassed toluene (3mL), triisopropylsilanethiol (138mg, 0.724mmol, 1.2eq), and triethylamine (80mg, 0.784mmol, 1.3eq) were added and the sealed tube was heated to 100 ºC. After 2h the starting material was consumed (by TLC) and the sealed tube was cooled to rt. The solution was filtered through a plug of celite and the celite washed with EtOAc (10mL x 3). The organic layer was washed with water (10mL) and brine (10mL), then dried over Na_2SO_4, and the solvent removed *in vacuo*. The crude solid was dissolved in THF and iodomethane (171mg, 1.20mmol, 2eq) was added in one portion. Tetrabutyl-ammonium fluoride trihydrate (381mg, 1.20mmol, 2eq) was added slowly in 3 portions. Analysis by TLC (20% EtOAc in hexanes, silica gel) confirms the reaction was complete 0.5h after the addition. The reaction was quenched with water (10mL) and extracted with EtOAc (10mL x 2). The organic layer was washed with brine (10mL) and dried over Na_2SO_4. The solvent was removed *in vacuo* leaving an orange solid. The solid was purified by flash column chromatography on silica gel (10% EtOAc in hexanes) to provide the pure **24** in 47% yield as a yellow solid (89 mg): ^{1}H NMR (300 MHz, CDCl3) δ 7.85 – 7.76 (m, 1H), 7.76 – 7.69 (m, 1H), 7.42 – 7.24 (m, 4H), 7.00 (d, *J* = 10.2 Hz, 1H), 6.94 (d, *J* = 16.0 Hz, 1H), 6.84 (s,

1H), 6.80 – 6.70 (m, 1H), 3.87 (s, 3H), 2.55 (s, 3H); ^{13}C NMR (75 MHz, CDCl$_3$) δ 160.18,

142.58, 140.32, 140.15, 138.98, 138.36, 130.25, 124.88, 124.55, 123.69, 123.50, 123.18, 122.25,

117.29, 111.87, 108.61, 55.39, 15.77; HRMS (ESI) (M + H), Calcd. for C$_{18}$H$_{17}$OS$_2$ 313.0721;

Found 313.0718.

(E)-3-(2-(Benzo[b]thiophen-2-yl)vinyl)-5-(methylthio)phenol (25, Table 2-5, entry 2)
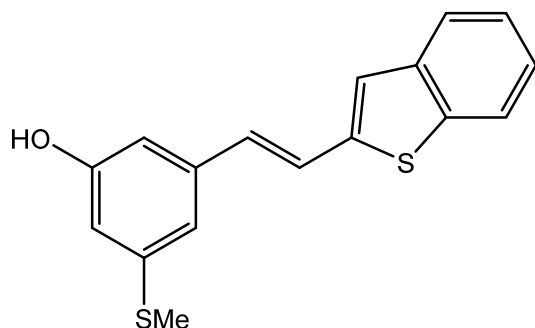
Chemical Formula: C$_{17}$H$_{14}$OS$_2$
Molecular Weight: 298.42
cLog P: 5.31
tPSA: 20.23

The NaH (60% dispersed in mineral oil, 40mg, 1.00 mmol, 8eq) was added to anhydrous DMF

(2 mL) at 0° C. Then CH$_3$CH$_2$SH (0.1 mL 1.39 mmol, 11eq) was added dropwise and stirred at

0° C for 30 min. The temperature of the reaction mixture was allowed to rise to rt and the

mixture stirred for 1 h. The temperature of the reaction mixture was raised to 140° C and (E)-2-

(3-methoxy-5-(methylthio)styryl)benzo[b]thiophene (38.7 mg, 0.124 mmol, 1eq) in dry DMF

(0.5 mL) was added dropwise to the reaction mixture. This mixture was held at 140° C and

monitored by TLC (30% EtOAc in hexanes). When the starting material was no longer present

by TLC (~1 hr) the reaction mixture was cooled to 0 ºC and quenched by addition of aq 0.5N

HCl (10 mL). The mixture was extracted with EtOAc (3 x 10 mL). The combined organic layers

were washed sequentially with aq 0.5N HCl (2 x 10 mL) and brine (2 x 10 mL). The organic

layer was dried over Na$_2$SO$_4$ and the solvent was removed *in vacuo*. The crude solid was purified

by FCC (20% EtOAc in hexanes) to afford the pure product in 82% yield as a pale yellow solid

(30 mg): ^{1}H NMR (300 MHz, CDCl$_3$) δ 7.78 (dd, *J* = 7.9, 4.8 Hz, 1H), 7.75 – 7.66 (m, 1H), 7.40

– 7.29 (m, 2H), 7.29 – 7.23 (m, 2H), 6.96 (s, 1H), 6.89 (d, J = 16.0 Hz, 1H), 6.76 (s, 1H), 6.68 (t, J = 1.8 Hz, 1H), 2.52 (s, 3H); ^{13}C NMR (75 MHz, CDCl$_3$) δ 160.52, 142.48, 140.46, 140.10, 138.76, 138.32, 130.22, 124.87, 124.45, 123.70, 123.40, 123.15, 122.20, 117.19, 111.67, 108.71, 15.57; HRMS (ESI) (M + H), Calcd. for C$_{17}$H$_{15}$OS$_2$ 299.0564; Found 299.0568.

(E)-3-(2-(Benzo[b]thiophen-2-yl)vinyl)-5-methoxybenzonitrile (26, Table 2-5, entry 3)
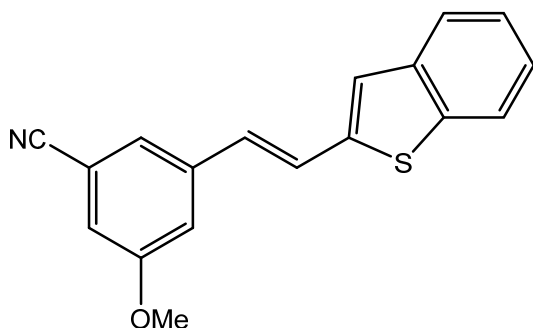
Chemical Formula: C$_{18}$H$_{13}$NOS
Molecular Weight: 291.37
cLog P: 5.17
tPSA: 33.02

The (E)-3-(2-(benzo[b]thiophen-2-yl)vinyl)-5-methoxyphenyl trifluoromethanesulfonate (250mg, 0.603mmol, 1eq), tetrakis(triphenylphosphine)palladium(0) (35mg, 5mol%), sodium cyanide (59.10mg, 1.21mmol, 2eq), and copper iodide (11.5mg, 10mol%) were mixed in a sealed tube under argon. Then degassed toluene (3mL) was added and the sealed tube was heated to 100 ºC. After 2hr the starting material was consumed (by TLC) and the sealed tube was cooled to rt. The solution was filtered through a plug of celite and the celite washed with EtOAc (10mL x 3). The organic layer was washed with water (10mL) and brine (10mL), dried over Na$_2$SO$_4$, and the solvent removed *in vacuo* to furnish a red solid. The solid was purified by flash column chromatography on silica gel (20% EtOAc in hexanes) to provide the pure **26** in 35% yield as a yellow solid (61.5 mg): ^{1}H NMR (300 MHz, CDCl$_3$) δ 7.80 (dd, J = 8.6, 5.0 Hz, 1H), 7.77 – 7.70 (m, 1H), 7.46 – 7.29 (m, 5H), 7.22 (s, 1H), 7.05 (s, 1H), 6.89 (d, J = 16.0 Hz, 1H), 3.89 (s, 3H); ^{13}C NMR (75 MHz, CDCl$_3$) δ 160.03, 141.69, 139.97, 139.36, 139.16, 128.11, 125.30, 124.98,

124.81, 124.72, 123.76, 122.52, 122.31, 118.60, 116.83, 115.88, 113.65, 55.68; HRMS (ESI) (M

+ H), Calcd. for $C_{18}H_{14}NOS$ 292.0796; Found 292.0792.

CHAPTER THREE

DEVELOPMENT OF A NEW TRANSITITION METAL CATALYZED

REACTION FOR THE SYNTHESIS OF NOVEL ANALOGS OF SK-03-92:

EXPLORATION OF THE HECK REACTION

I.   INTRODUCTION AND BACKGROUND.

1.   Negishi and Wittig couplings.

As described in the previous Chapter, the two methods that were previously employed to

synthesize novel stilbenoid analogs had numerous shortcomings from a synthetic perspective

(Scheme 3-1).

Scheme 3-1: Negishi cross-coupling and Wittig-Horner type coupling procedures.
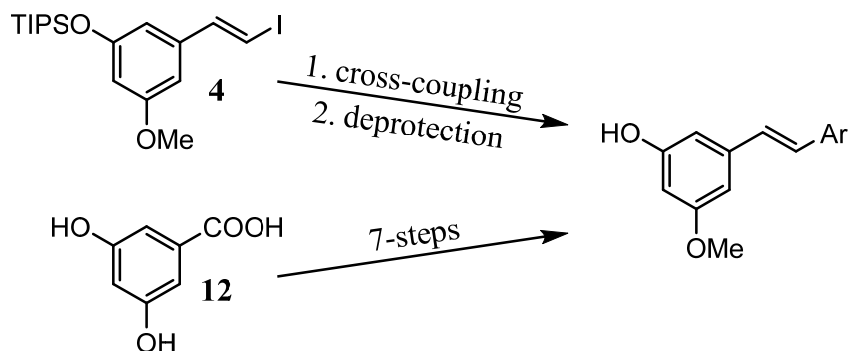
The Negishi cross-coupling procedure required synthesis of the unstable vinyl iodide **4**

and while it was useful for synthesis of analogs in which ring A (see Figure 2-4) was static, it

was not very useful for a more comprehensive analysis of the SAR. It also required deprotection

of a silyl group, which while not very difficult nor low-yielding, still added another step to the

process. The Wittig-Horner type coupling was devised for scale-up purposes of SK-03-92 and

similarly to the Negishi type coupling it was very useful when ring A was held static. However, it also required a deprotection step; in this case a mono-demethylation which was rather low-yielding and troublesome when working on small scales. A reaction with a more comprehensive scope for the synthesis of similar stilbenoid analogs was necessary.

2.   Retrosynthetic analysis.

As described earlier, it is helpful to identify and separate the three distinct structural moieties observed in these analogs: the phenolic substituted ring A, the alkene "bridge", and the non-polar aromatic region of, in general, rings B and C (see Figure 2-4). Due to the reactivity of phenols, prior synthetic procedures focused on protection, which of course resulted in the need for deprotection, generally as a final step, to obtain the desired analog. The removal of this deprotection step was a priority, directing research toward reactions that were tolerable to phenolic substituents.

Because prior results indicated that benzo[b]thiophene was the most advantageous non-polar aryl group which represented rings B and C in active analogs, it was determined that a method that focuses on this moiety, while still with the capacity to change to different structural analogs, was preferred.

The SAR also indicated that the alkene 'bridge', while not necessary for activity, seemed to show improved potency for at least 1 analog. Taken together, these stipulations resulted in the analysis illustrated in Scheme 3-2.

Scheme 3-2: Retrosynthetic analysis.
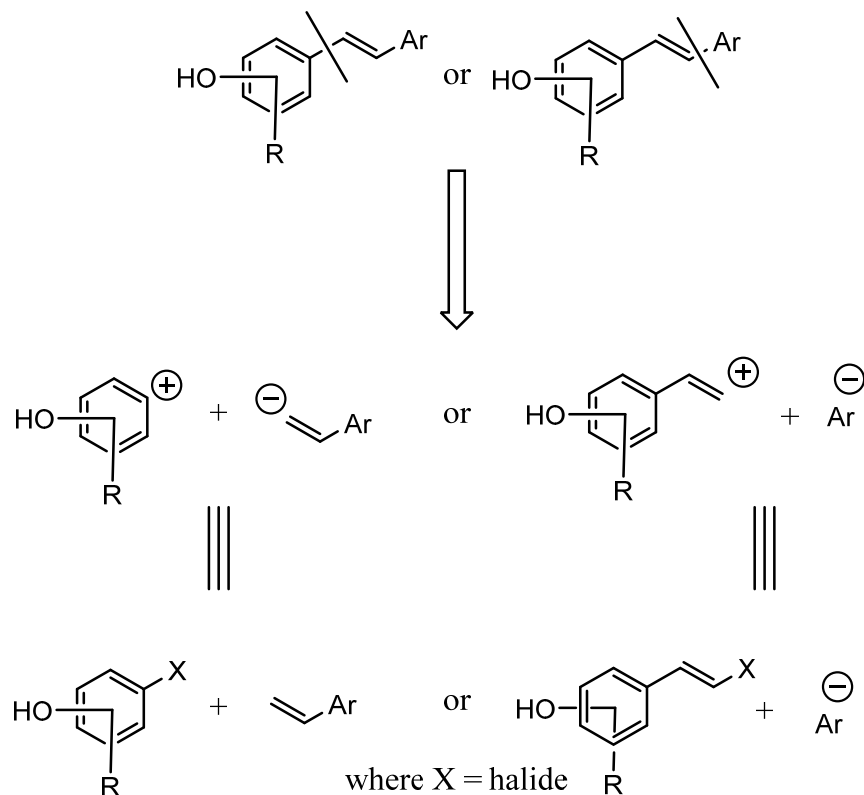
The second option in the Figure above very much resembles the prior Negishi cross-coupling reaction. The first option, however, is more interesting for a number of reasons. Firstly, aryl halides are generally commercially available and inexpensive. Secondly, if a desired bromo/iodo phenol is not available, phenols can be readily brominated with commercially available and inexpensive reagents such as Br_2 or NBS. In addition, keeping the aryl side-chain static as a benzo[b]thiophene moiety was the initial goal for the new SAR and synthesis of the vinyl analog was trivial.

Both options, however, strongly imply a transition metal catalyzed reaction. One of the most well-known transition metal reactions is the Heck-Mizoroki reaction, a reaction between an aryl halide (usually electron-poor) and an unsaturated (usually activated) styrene.[121] In this case,

however, electron-rich phenolic bromides and unactivated styrenes are not ideal candidates for such a reaction[121-122], however it was still pursued due to the scope and ease of synthesis of the starting materials.

3.   Heck-Mizoroki reaction.

3.1: Background.

In the early 1970's both Heck and Mizoroki published a nearly identical synthesis of stilbene (Scheme 3-3).[123-124] This synthesis employed iodobenzene, styrene, base, and a palladium (II) catalyst. This work was an extension of prior work done by both Fujiwara[125-126] and Heck.[127]

Scheme 3-3: Original synthesis by Mizoroki (1971) and Heck (1972).
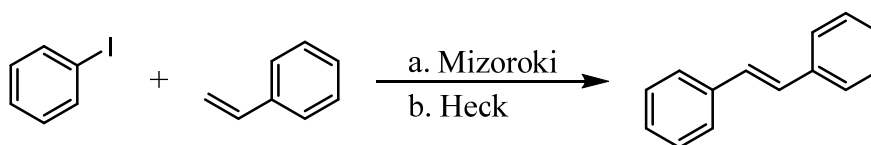
a. 1971, PdCl$_2$ (0.1 eq), KOAc, CH$_3$OH, 120 ℃, **95%**
b. 1972, Pd(OAc)$_2$ (0.1 eq), n-Bu$_3$N, neat, 100 ℃, **75%**

Heck greatly expanded the scope and utility of this reaction over the course of the next few years and made many key discoveries including the use of phosphine ligands to enhance reaction conditions.[128] As one of the first palladium mediated coupling procedures, the Heck reaction prompted the way to other widely known transition metal catalyzed reactions such as the Suzuki reaction, Sonogashira coupling, and Negishi coupling reactions.[129-131]

3.2: Catalytic cycle.

The catalytic cycle of the Heck reaction (Figure 3-1) generally starts with a palladium (II) species which is subsequently reduced to palladium (0) via a phosphine ligand and through a number of transformations, all discussed below, ends with a regeneration of the palladium (0) species which gives rise to the catalytic nature of the process.

Figure 3-1: General catalytic cycle of the Heck reaction.
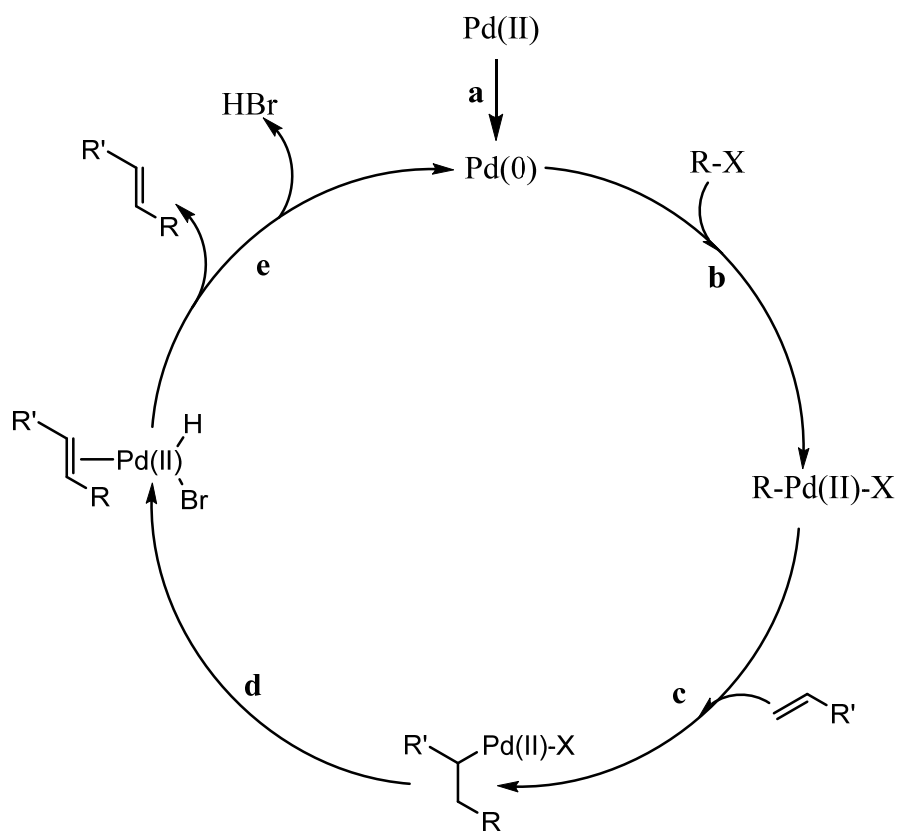
As discussed earlier a palladium (II) catalyst, if employed, is reduced to palladium (0), prior to entering the catalytic cycle (Figure 3-1).[132] While palladium (II) catalysts are routinely used based on the relative stability of palladium (II) and the ability to store for long periods of time on the benchtop, palladium (0) catalysts are also available and can be used directly without the need for pre-catalyst activation.[133-135] Many of these catalysts, including palladium tetrakis,

are not air or temperature stable, however a growing number of air and/or temperature stable palladium (0) catalysts have been discovered.[134, 136-137]

The next step, **b** (Figure 3-1), is the oxidative addition of a halide or triflate substituted aryl group (Scheme 3-4). This reaction occurs in a concerted manner (**b₁**) and though the cis and trans isomers are in equilibrium (**b₂**), it has been found that only the cis continues through the catalytic cycle.[138-140]

Scheme 3-4: Concerted mechanism of oxidative addition (Figure 3-1 "b").
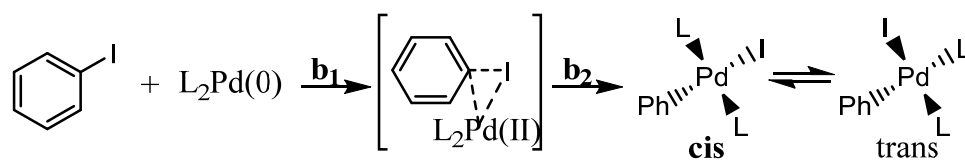
Detailed in process **c** (Figure 3-1) is the migratory insertion of an alkene into the palladium species (Scheme 3-5). Data suggests that this step also relies on a concerted mechanism (**c₁**), although other mechanisms may be possible depending on the catalyst/ligand/reactants involved.[141-142] The regioselectivity of the migratory insertion step is generally determined by steric considerations, however when electron-rich alkenes are employed in some cases electronic character can play a role.[134, 143] Regioselectivity in the original Heck/Mizoroki reaction relied exclusively on sterics due to the electron-poor nature of the alkene (styrene).

Scheme 3-5: Migratory insertion of an alkene to palladium (Figure 3-1 "c").
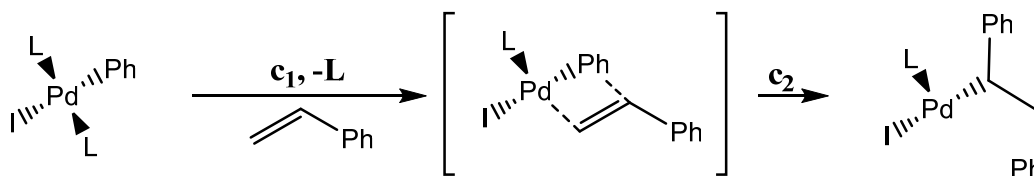
The double bond is re-introduced by ß-hydride elimination, step **d** (Scheme 3-6). Steric effects generally lead to only the E isomer; however, in some cases the Z isomer can be more prevalent.[134, 144] Base plays an essential role in reductively eliminating the remaining palladium hydride species back to palladium (0), stopping re-insertion of the alkene and allowing the catalytic cycle to continue, step **e** (Scheme 3-7).

Scheme 3-6: ß-hydride elimination (Figure 3-1 "d").
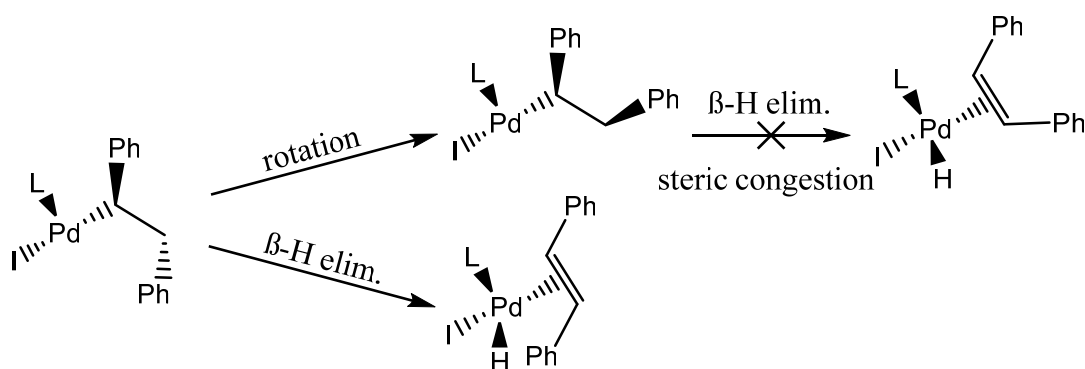
Scheme 3-7: Base promoted dehydropalladation and reductive elimination (Figure 3-1 "e").
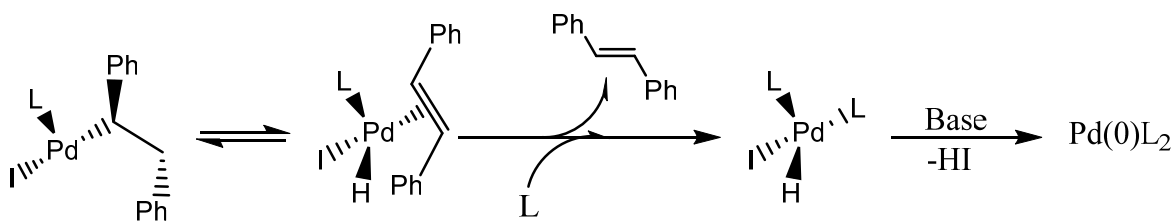
As with almost all transition metal chemistry, the above schemes are a general case and many factors may influence these micro-reactions to varying degrees. Many theories exist on the exact mechanism of oxidative addition and reductive elimination; presented here are the most well-regarded theories for a general palladium-phosphine directed reaction.[134, 138, 143]

3.3: Scope.

The scope of the Heck reaction is wide and varied. Bimolecular reactions to intramolecular reactions have been thoroughly explored over the last few decades. It was generally thought that aryl (pseudo)halides were necessary; however, recent findings suggest that even alkyl halides can undergo Heck reactions.[145-147] With some 3rd generation phosphine catalysts it is even possible to use aryl chlorides with varying degrees of success.[148-150] The most general considerations for a Heck reaction seem to be an organo-halide and an olefin, from there careful selection of both catalyst and ligand, along with reaction conditions, can potentially lead to the desired product.

II.   CHEMISTRY AND RESULTS.

1.   Heck reaction trials.

From examination of the original retrosynthetic analysis, it was determined that a Heck reaction may be useful in the synthesis of analogs of SK-03-92. The original synthesis envisioned the use of 3-bromo substituted phenols to give analogs with the same substitution pattern as SK-03-92, however, 4-bromo substituted phenols were both easier to synthesize and were generally more commercially available. For these reasons we started the original trials using 1-(5-bromo-2-hydroxyphenyl)ethan-1-one (**30**, Scheme 3-8) which had been previously purchased for another project.

Scheme 3-8: Proposed Heck reaction.
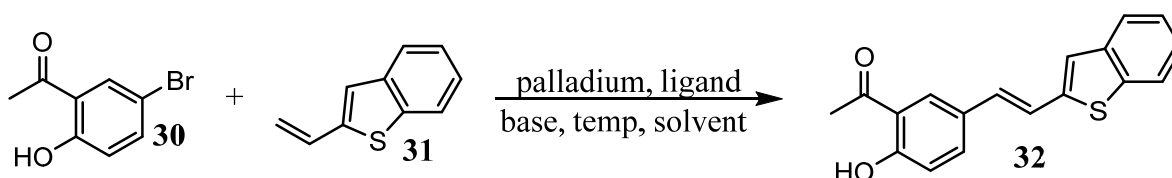
This reaction also hinged on the synthesis of the olefin **31**. This was conveniently accomplished starting from the aldehyde **18** (Scheme 3-9), previously synthesized and used for the scale-up of SK-03-92. The synthesis of olefin **31** proceeded with little difficulty from a Wittig reaction employing methyltriphenylphosphonium bromide and sodium methoxide.

Scheme 3-9: Synthesis of olefin 31.
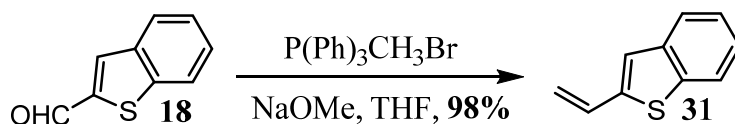
Unlike the vinyl iodides previously used, the olefin **31** was sufficiently stable at room temperature to permit a much easier purification procedure. The styrene analog was a white crystalline solid, however, it was found that storage on the benchtop over the course of several days led to decomposition to a yellow viscous oil that was assumed to be polymerization of the olefin. Storage at 0 °C kept olefin **31** analytically pure for over 6 months, thus addition of a polymerization inhibitor was unnecessary.

With both reactants in hand the conditions for the initial palladium mediated reaction were considered. In general Heck reactions prefer electron-poor (unactivated) aryl bromides and electron-rich (activated) olefins.[134, 151] In our case, however, the substituted 4-bromo phenols were electron-rich and the 2-vinylbenzo[b]thiophene **31** was electron-poor. Because of this it was assumed that heating would be necessary, so many solvents were initially tried at or above their boiling points in sealed vessels.

Although base plays many roles in the Heck reaction, the most crucial role is removing the acidic proton produced (in this case HBr) to permit the catalytic cycle to continue. Sodium

acetate has found use in a number of Heck reactions and as a weaker base was unlikely to cause problems with either the aryl bromide or olefin.

For palladium (II) species it was important to reduce the palladium to palladium (0) with phosphine ligands to initiate the catalytic process. There is an extensive library of phosphine ligands available and many are suited for specific reactions.[152] In this trial only two simple phosphine ligands were explored, triphenylphosphine and tri(o-tolyl)phosphine. The two ligands are by far the most widely used ligands in palladium catalyzed coupling reactions. Palladium (0) catalysts could be used with no additional ligand as they are already in the correct oxidation state.

Solvents were chosen mainly with regard to their ability to dissolve the starting materials as, in general, homogenous reactions are more likely to succeed. With these factors in mind, a number of reaction trials were completed (Table 3-1).

Table 3-1: Heck reaction trials.
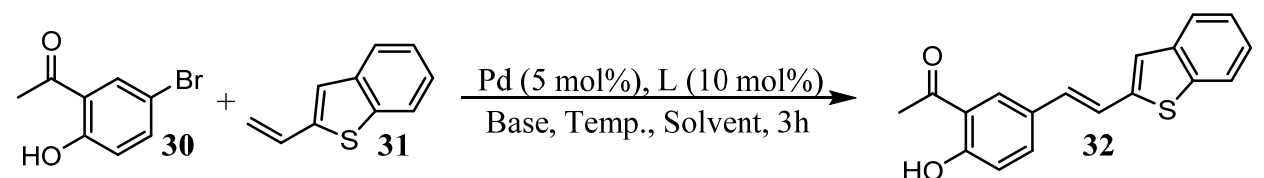
Trial	Palladium	Ligand	Base	Solvent[a]	Temp. (°C)	Conversion (%)[b]
1	Pd(OAc)$_2$	P(Ph)$_3$	NaOAc	THF	70	0
2	""	P(o-tol)$_3$	NaOAc	THF	70	0
3	""	P(Ph)$_3$	NaOAc	ACN	95	0
4	""	P(o-tol)$_3$	NaOAc	ACN	95	0
5	""	P(Ph)$_3$	NaOAc	DMA	150	0[d]
6	""	P(o-tol)$_3$	NaOAc	DMA	150	0[d]
7	PdCl$_2$	P(Ph)$_3$	NaOAc	THF	70	0
8	""	P(o-tol)$_3$	NaOAc	THF	70	0
9	""	P(Ph)$_3$	NaOAc	ACN	95	0
10	""	P(o-tol)$_3$	NaOAc	ACN	95	0
11	""	P(Ph)$_3$	NaOAc	DMA	150	0[d]
12	""	P(o-tol)$_3$	NaOAc	DMA	150	3
13	PdP(Ph$_3$)$_4$	---	NaOAc	DMA	100	5
14	""	---	NaOAc	DMA	150	0[d]
15	H.Pallad[c]	---	NaOAc	DMA	150	5
16	""	---	NaOAc	DMA/5% H$_2$O	150	95
17	""	---	NaOAc	DMA/5% H$_2$O	100	24
18	""	---	NaOH (aq.)	DMA/5% H$_2$O	150	93
19	""	---	Cs$_2$CO$_3$	DMA/5% H$_2$O	150	96
20	""	---	NaOAc	DMA/10% H$_2$O	150	96

[a] freshly distilled and degassed via freeze-thaw, [b] determined by HPLC, [c] Herrmann's palladacycle, [d] large amounts of palladium black – likely decomposition.

Analysis of the data in Table 3-1 indicated that under most conditions no conversion to

the stilbene analog was noted, however when a small amount of water was added to

dimethylacetamide as the solvent, there was nearly full conversion. The idea to add water to the

conditions was conceived from trials 12, 13, and 15 where a small but noted conversion took

place. Of all the solvents tested, dimethylacetamide was the most hygroscopic, therefore, it was thought that perhaps in the cases in which some conversion was noted, water may have somehow entered the reaction. The role of water in the reaction is not fully understood, and indeed, reports in the literature only posits that water may increase the rate of palladium catalyzed reactions in some cases,[153-155] although the reasons behind this are somewhat elusive. In general, it is thought that water can stabilize intermediates and thus accelerate the reaction,[156] although few reactions were found where water was necessary for any conversion. In the case of this reaction, 5-10% water was found to give almost full conversion. It is unclear how much water is necessary for conversion and there was no attempt to quantify this amount.

Herrmann's palladacycle (Figure 3-2) is a cyclopalladated complex discovered by Herrmann in 1997.[157] Since this catalyst exists as palladium (II) at room temperature, this catalyst exhibits far greater air and temperature stability compared to other common palladium catalysts such as palladium tetrakis which readily decomposes at room temperature. Herrmann's palladacycle has a unique property in that at elevated temperatures, approximately 80 ºC, the catalyst reduces to a form of palladium (0) suitable for Heck reactions without any additional ligand. Because of these properties, it was an interesting catalyst choice for the trial reaction. Indeed, when palladium acetate with ligands or palladium tetrakis was heated over 100 ºC, necessary for conversion, large quantities of palladium black resulted, which indicated decomposition of the catalyst. When Herrmann's palladacycle was used, however, the reaction mixture only changed color after prolonged heating at 150 ºC, and in some cases never became the dark black color which indicated catalyst decomposition.

Figure 3-2: Herrmann's palladacycle.
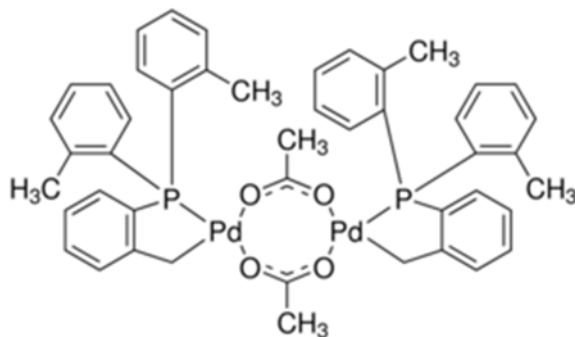
While the role of base is critical in Heck reactions, little difference was seen in switching from the relatively weak base, sodium acetate, to the relatively strong base, sodium hydroxide. It should be noted, however, that aryl bromides are not always stable in strongly basic solutions, and in these cases heating was found to cause premature decomposition of some aryl bromides which led to lower yields. In the trial case, however, the bromide was rather stable and conversion was not greatly affected. Because high conversion was seen with sodium acetate and in general the stability of aryl bromides was not investigated prior to submitting them to the reaction conditions, sodium acetate seemed to be the best choice as the base. The nitrogen-based bases are also often used in Heck reactions and many other palladium catalyzed reactions that require base, however, at the high temperature conditions necessary for conversion, nitrogen based bases were deemed too volatile and not worth investigating due to the already high conversion rate observed with sodium acetate.

It should also be noted that Herrmann's palladacycle employs P(o-tolyl)3 ligands, the same ligands employed in trials 2,4,6,8,10, and 12. In fact, Herrmann's palladacycle was conveniently synthesized in the lab by treating palladium acetate with tri(o-tolyl)phosphine under gentle heating (Scheme 3-10) on a 5 gram scale. The difference in the trials, however, was

that the phosphine ligand was added in excess which drives the conversion to Pd(P(o-tolyl)$_3$)$_4$, similar in structure to palladium tetrakis, which is also thermally unstable and readily decomposes to palladium black when subjected to high temperatures. Because of the convenient synthesis of the palladacycle and its relative stability, the attempt to use palladium acetate along with just one molar equivalent of the phosphine ligand (synthesizing the palladacycle *in situ*) was not attempted. It was assumed that such a reaction would result in similar conversion if the other conditions for trial 20 were followed.

Scheme 3-10: Synthesis of Herrmann's palladacycle.

$$\text{Pd(OAc)}_2 \text{ (1 eq)} + \text{P(o-tolyl)}_3 \text{ (1 eq)} \xrightarrow[\text{0.5-1 h}]{\text{toluene, 50 °C}} \text{Herrmann's palladacycle}$$
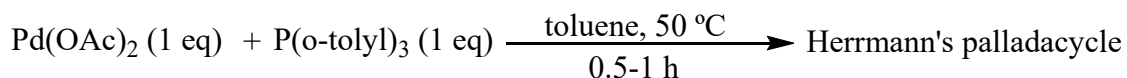
Optimization of the palladium catalyzed reaction was successful and was next attempted with a variety of other aryl bromides.

2.   New thianaphthene analogs and their SAR.

As discussed earlier, substituted 4-bromophenols are less expensive, easier to synthesize, and generally more commercially available when compared to other aryl substitution patterns; thus the initial focus of this SAR was this substitution pattern (Table 3-2). Heck reactions are extremely versatile and it should be noted that this method, now optimized for substituted phenols, should work with any substitution patterns given they are stable to the reaction conditions. In the first series of reactions, most of them employed substituted 4-bromophenols as starting materials, however, some other substitution patterns were also employed. In a later section other substitution patterns will be discussed in more detail and are of critical importance to provide potent antibacterial stilbenes.

Table 3-2: First series of analogs synthesized.

R$_2$, R$_5$, Br, R$_1$, R$_4$, R$_3$ + vinyl benzothiophene **31** → (Herrmann's palladacycle (2.5 mol%), NaOAc, 150 °C, DMA (10% H$_2$O), 3h) → product

Compound	R$_1$	R$_2$	R$_X$	Yield (%)[a]
32	OH	CHO	---	91
33	OH	F	---	91
34	OH	H	---	90
35	-OCH$_2$O-		---	95
36	OH	OMe	---	93
37	OMe	OH	---	89
38	OH	Cl	---	92
39	Cl	OH	---	90
40	OH	CN	---	91
41	OH	NO2	---	80
42	OH	Cl	R$_4$ = Cl	93
43	OH	OMe	R$_3$ = OMe	75
44	OH	OCF$_3$	---	85
45	OH	OEt	---	90
46	OH	OiPr	---	90
47	OH	COOH	---	93
48	OMe	COOH	---	91
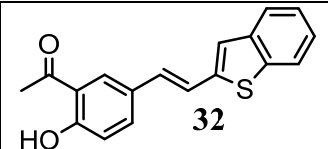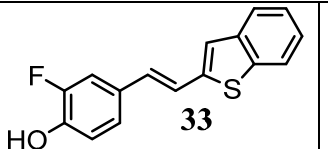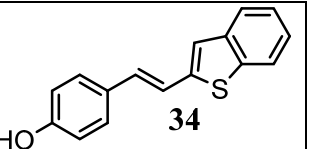
[a] Yield of isolated and purified product.

Four different compounds were prepared without a phenol in the R$_1$ position; **35**, **37**, **39**, and **48**. Additionally, compounds **42** and **43** are tri-substituted analogs, which illustrates some of the versatility of the Heck reaction. Similarly to SK-03-92, these compounds could be further purified after column chromatography by crystallization from isopropanol, however, this was only done if a larger scale synthesis was employed. Indeed, when **36** and **38** were scaled up to a 1-gram scale using identical reaction conditions to their small-scale preparation, similarly excellent yields were observed. Thus the Heck catalyzed reaction was not only an efficient

process for constructing a library of stilbenoid analogs, but also for scale-up for pharmacological studies when necessary.

From this first series of analogs several important antibacterials were identified with activity against gram-positive bacteria, some of which were more active then lead compound SK-03-92. Summarized in the following tables are the structures and MIC values for novel antimicrobials synthesized utilizing Heck coupling detailed in Table 3-2.
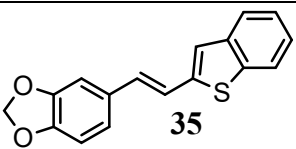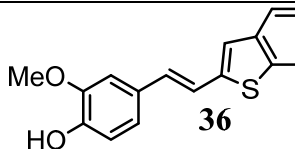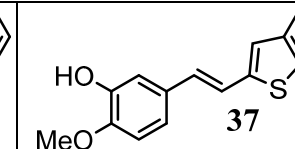
Table 3-3: MICs for compounds 32, 33, and 34[a].

Bacterial Strain	32	33	34
S. aureus	>128	>128	32
E. faecalis	>128	>128	32
P. aeruginosa	>128	>128	>128
E. coli	>128	>128	>128
M. intracellulare	>128	>128	>128
M. chelonae	>128	>128	>128
M. fortuitum	>128	>128	128
M. kansasii	>128	>128	>128
M. avium	>128	>128	>128
M. smegmatis	>128	>128	128
M. marinum	>128	>128	>128

[a]Values in µg/mL

Unfortunately, the trial ketone **32** previously discussed was not active against any bacterial strains. The fluorine analog **33** was also inactive and the simple phenol **34** demonstrated only meager activity on the gram-positive strains. Initial setbacks such as this were expected, however, and the SAR continued with another group of compounds (Table 3-4).

Table 3-4: MICs for compounds 35, 36, and 37[a].

Bacterial Strain	35	36	37
S. aureus	>128	1	>128
E. faecalis	>128	1	128
P. aeruginosa	>128	>128	>128
E. coli	>128	>128	>128
M. intracellulare	>128	16	>128
M. chelonae	>128	16	>128
M. fortuitum	>128	8	>128
M. kansasii	>128	32	>128
M. avium	>128	16	>128
M. smegmatis	>128	8	>128
M. marinum	>128	8	>128

[a]Values in μg/mL
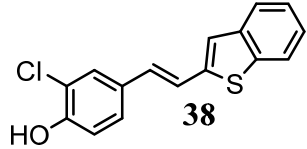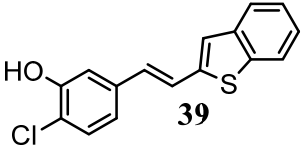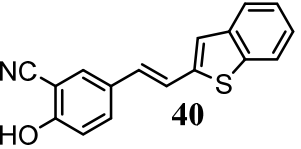
Similarly to the prior SAR, lack of a phenol in the case of the 1,3-dioxole ligand **35** resulted in no activity. In general, a few compounds which lack phenolic groups were

synthesized and screened to both validate the SAR, as well as test the theory that a phenol was necessary for potency. Analog **36** is indeed very similar to SK-03-92, however, it differed in the position of the phenol. However, the phenol in this position increased the activity about 2-4 fold against gram-positive and mycobacterium species. Perhaps more interesting, however, was the lack of activity of **37**, which was very similar in structure to both SK-03-92 and **36**. This small change seemed to indicate that the target can accept the phenol changing position, but not the methoxy group. This may indicate that the active site for these ligands has a larger space to accommodate hydrogen bond donors, but has a conserved space for functional groups ortho to the phenol.

The next set of analogs (Table 3-5) was prepared to determine the effects of changes in the position of substituents as well. The chloro analog **38** represents one of the most active compounds developed, to date. The chlorine group differs from methoxy group at the same position in a number of notable fashions. First, chlorine is an electron withdrawing group by induction while the methoxy group is an electron donating group by resonance. Secondly, chlorine is at best a weak hydrogen bond acceptor while the methoxy group is a very strong hydrogen bond acceptor. Thus, electronic character and H-bond acceptor character do not seem to influence the activity in a meaningful way. Another difference between the chloro and methoxy groups is size, with chloro being smaller; this may explain the similar activity between these two compounds. Ligand **39**, with a similar switching of positions of chloro and hydroxy groups seen earlier, also exhibited a much weaker MIC value. The basis for this selective activity is still undetermined, but it seems that it points to interactions between the small molecule and a specific target in the bacteria. This is interesting as earlier findings suggested

75

that these compounds may act on more than one target, however, extreme activity loss from a
simple substitution points to a specific target or selective metabolic step instead.

Table 3-5: MICs for compounds 38, 39, and 40[a].

Bacterial Strain	38	39	40
S. aureus	0.5	64	32
E. faecalis	0.5	64	32
P. aeruginosa	>128	>128	>128
E. coli	>128	>128	>128
M. intracellulare	>128	>128	>128
M. chelonae	>128	>128	>128
M. fortuitum	>128	>128	>128
M. kansasii	>128	>128	>128
M. avium	>128	>128	>128
M. smegmatis	>128	>128	>128
M. marinum	>128	>128	>128

[a]Values in µg/mL
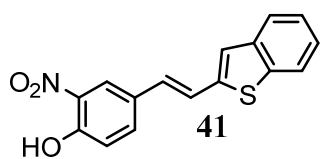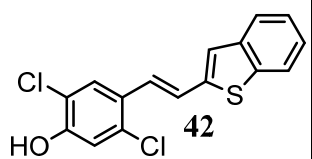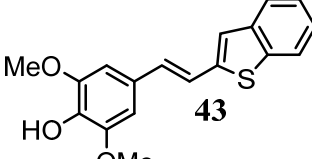
In regard to active chloro **38**, it is also of interest that the chloro substitution greatly
diminished activity against the mycobacterium species as compared to the similar methoxy
analog **36**. This was interesting considering that activity against gram-positive bacteria from the
prior SAR almost always was followed by a linear-type activity against mycobacterium species.

Given the similar nature of gram-positive bacteria and mycobacterium, this activity was not surprising. Given that no compounds from the prior SAR were active against gram-negative bacteria, it was hypothesized that the mode of action was somehow related to the cell walls of both the gram-positive bacteria and mycobacteria. Thus the lack of activity of **38** to mycobacterium could give some insight into the cellular target, whether it is a single target or multiple targets.

Finally, synthesis of the cyano compound **40** was similar to the nitrile analog **26**, however, in this case the phenol was easy to prepare in one step. While it showed some activity, it was not active enough to warrant synthesis of the nitrile at other positions at this time.

Table 3-6: MICs for compounds 41, 42, and 43[a].

Bacterial Strain	**41**	**42**	**43**
S. aureus	128	32	32
E. faecalis	128	8	32
P. aeruginosa	>128	>128	>128
E. coli	>128	>128	>128
M. intracellulare	>128	>128	>128
M. chelonae	>128	>128	>128
M. fortuitum	>128	>128	>128
M. kansasii	>128	>128	>128
M. avium	>128	>128	>128
M. smegmatis	>128	>128	>128
M. marinum	>128	>128	>128
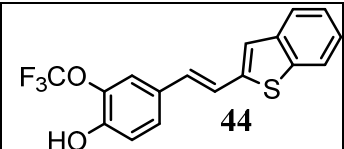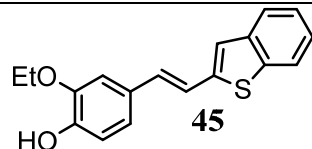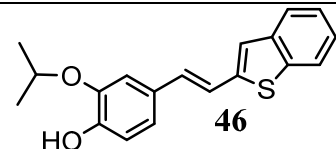
[a]Values in µg/mL

Outlined in Table 3-6 are the details of the SAR of three more analogs of interest. The nitro analog **41** was synthesized to test whether or not a strong electron withdrawing group in the R_2 position increased activity similar to the chloro group. It was found, however, that the nitro analog **41** was not very active at all with MIC's of 128 µg/mL against the gram-positive strains. Both **42** and **43** probe the idea of tri-substituted analogs. Both, however, exhibited weaker activity then their disubstituted parent compounds. In future SAR studies it may be beneficial to

try a range of tri-substituted analogs to improve solubility, metabolism, and other pharmaceutical parameters, however, this remains to be seen.

The next set of compounds were prepared to attempt to demonstrate that size was directly related to activity (Table 3-7).

Table 3-7: MICs for compounds 44, 45, and 46[a].

Bacterial Strain	F$_3$CO... 44	EtO... 45	...O... 46
S. aureus	>128	8	>128
E. faecalis	>128	8	>128
P. aeruginosa	>128	>128	>128
E. coli	>128	>128	>128
M. intracellulare	>128	32	16
M. chelonae	>128	32	16
M. fortuitum	>128	32	16
M. kansasii	>128	32	8
M. avium	>128	32	16
M. smegmatis	>128	16	32
M. marinum	8	16	4

[a]Values in μg/mL

The trifluoromethoxy analog **44** was inactive in all assays except that of *M. marinum*, however, this could be a case of experimental error or a bad strain. It was interesting that the

trifluoromethoxy analog was far less active even though fluoride is generally a good bioisostere for hydrogen, however, CF_3 is more similar in size to isopropyl and thus sterics may play a large role in the potency of this analog. The electronic character of trifluoromethoxy also differs from that of a methoxy group, which may also explain the loss of activity.
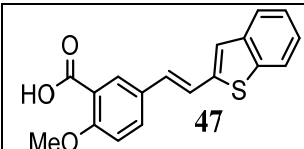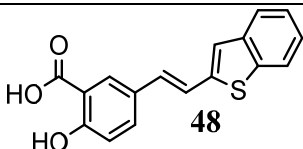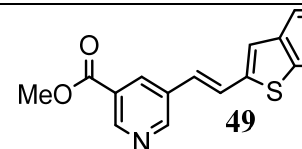
The ethoxy analog **45** retained some activity, however was less active then both the methoxy and chloro analogs. Ethoxy, similar to methoxy, also retained activity in the mycobacterium assays, however.

Finally, the isopropoxy analog **46** was seemingly the most interesting of the set even given it had no activity on the gram-positive strains tested. Ligand **46** was found to retain mycobacterium activity even though it exhibited no gram-positive activity. Since the chloro derivative was very active against gram-positive bacteria, but had no activity against mycobacterium, the isopropoxy was inversely active against mycobacterium but not gram-positive bacteria. This seems to suggest that the mode of action for gram-positive bacteria is independent of the mycobacterium species.

This suggests, as suggested from earlier work, that some of these compounds act on multiple targets. The targets in gram-positive and mycobacterium strains, however, could be very similar as indeed they share an evolutionary past. Uncovering these targets, however, remains a struggle and will be detailed in future sections.

The final table from this first series of compounds (Table 3-8) includes two carboxylic acid derivatives **47** and **48**. The third compound included, **49**, is from the next series of compounds discussed in Table 3-9.

Table 3-8: MICs for compounds 47, 48, and 49[a].

Bacterial Strain	47	48	49
S. aureus	>128	8	>128
E. faecalis	>128	8	>128
P. aeruginosa	>128	>128	>128
E. coli	>128	>128	>128
M. intracellulare	>128	>128	>128
M. chelonae	>128	>128	>128
M. fortuitum	>128	>128	>128
M. kansasii	>128	>128	>128
M. avium	>128	>128	>128
M. smegmatis	>128	>128	>128
M. marinum	>128	>128	>128
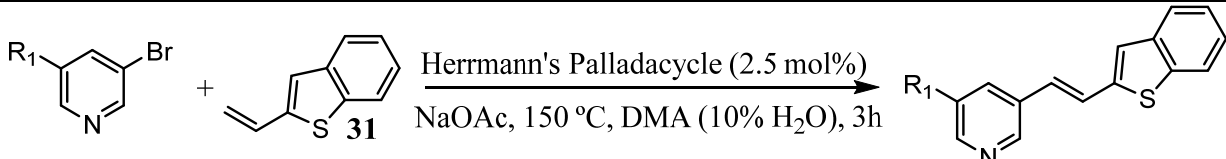
[a]Values in µg/mL

Similar to prior results, the non-phenolic analog **47** was not active. The para-phenolic acid **48**, however, was active against gram-positive bacteria, while similarly to the chloro derivative lacked activity on the mycobacterium strains. Similarly to chloro, the carboxylic acid is electron withdrawing, which may play a role in this activity profile.

The pyridine derivative **49**, though inactive, led to the next series of compounds, the pyridines. Pyridine analogs were synthesized in the hope of discovering a more water soluble

active analog that would be more useful for future *in vivo* work. The optimized Heck reaction

was found to work with good to excellent yields of these pyridine derivatives. Only four

pyridine analogs were prepared for this study, but these pyridine analogs may prove useful for

future SAR studies, especially if more *in vivo* work is planned because of increased water

solubility which should enhance bioavailability.

Table 3-9: Pyridine series of analogs synthesized.
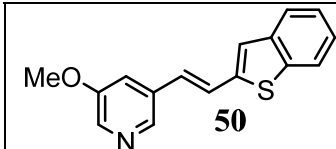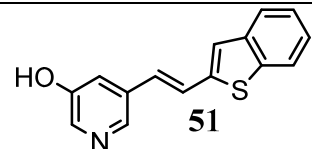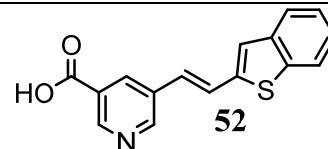
Compound	R$_1$	Yield (%)
49	COOMe	82
50	OMe	90
51	OH	90
52	COOH	87

Although only four analogs were prepared, based on the yields it seems likely that a great

deal of other N-containing analogs are possible. It was found that phenolic analog **51** was rather

unstable and over the course of several days on the benchtop it was no longer analytically pure,

therefore it is best stored in the freezer. In general, the work-up procedure for the stilbenoid

derivatives involved washing with dilute acid; in the case of pyridines this would obviously be

problematic. However, washing with just water only led to a negligible loss of yield. Analysis

of the data in Table 3-8 illustrated pyridine **49** had no activity in any strains tested. Indeed it was

assumed that perhaps only the phenol derivative **51** would show activity based on the past SAR.

It was surprising to find that **51** also lacked activity, but the carboxylic acid derivative **52** was

still active in both gram-positive and mycobacterium strains (Table 3-10). In the case of the

meta-phenol **51**, it is conceivable that the unstable nature of this analog causes it to degrade prior

to exerting any antibacterial properties.

Table 3-10: MICs for compounds 50, 51, and 52ª.

Bacterial Strain	MeO...**50**	HO...**51**	HO...**52**
S. aureus	>128	128	8
E. faecalis	>128	128	8
P. aeruginosa	>128	>128	>128
E. coli	>128	>128	>128
M. intracellulare	>128	>128	32
M. chelonae	>128	>128	32
M. fortuitum	>128	>128	64
M. kansasii	>128	>128	32
M. avium	>128	>128	64
M. smegmatis	>128	>128	64
M. marinum	>128	>128	32

ªValues in µg/mL

The meta-carboxy pyridine analog **52** was the first case of a non-phenolic derivative to

show activity. Two possibilities exist for this activity. First, perhaps the acidic -OH in the

carboxylate is a good replacement for the acidic phenolic -OH. Second, it is possible this

compound acts as a zwitterion and the NH+ mimics the phenol (Figure 3-3). This zwitterionic

form may more closely mimic the structure of SK-03-92. In any case, an active pyridine analog is promising for future SAR studies and if an ~8-fold more active pyridine analog is discovered, and it has suitable PK properties, it may be a viable lead compound for preclinical studies.

Figure 3-3: Zwitterionic form of 52.
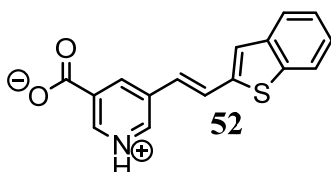
3. New styrenes and substitution patterns.

Although this optimized Heck reaction was an excellent method to synthesize stilbenes from a wide selection of aryl bromides, after a number of active analogs were discovered it was prudent to again modify the 'right-hand-side' to see if potency could be further enhanced. As previously described (Scheme 3-9) synthesis of styrenes was quick and in high yields from aldehydes. Some styrenes of interest were even commercially available, for example 4-vinyl-1,1'-biphenyl (**58**). Thus a number of new styrenes were synthesized to be used in the Heck reaction to provide a growing variety of stilbenoid compounds in rational drug design.

The first new styrene derivative investigated was the indole (Scheme 3-11). Indoles are widely known for exhibiting excellent PK properties and are privileged substructures of a number of pharmaceutical drugs.[158-161] Because of the previously discussed poor ADME properties of SK-03-92, analogs that can perhaps improve these properties were pursued.

Scheme 3-11: Synthesis of 2-vinylindole.
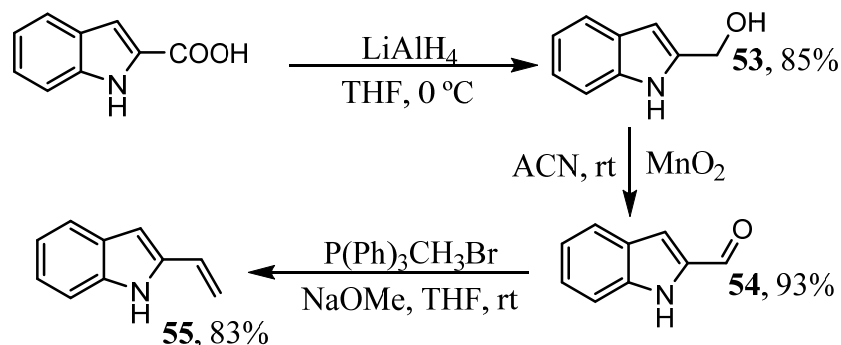
Since the 1H-indole-2-carboxylic acid starting material was inexpensive, the first two steps, first to the alcohol **53** and then to the aldehyde **54** were scaled up to gram-scale from the start. Similarly to the thianaphthene analog **31**, 2-vinylindole **55** was synthesized in high yield. One striking difference between **31** and **53**, however, was their acid stability. The indole **53** readily decomposed and gave a deep purple color when treated with even minimal amounts of acid. This is commonly observed with benzylic alcohol analogs of indoles at position 2 via loss of water.

The N-methyl derivative of aldehyde **54** was also synthesized, which gave the N-methyl indole derivative **57** (Scheme 3-12). This was done to probe the substitution of the NH indole position for future possible analogs.

Scheme 3-12: Synthesis of 1-methyl-2-vinyl-1H-indole 57.
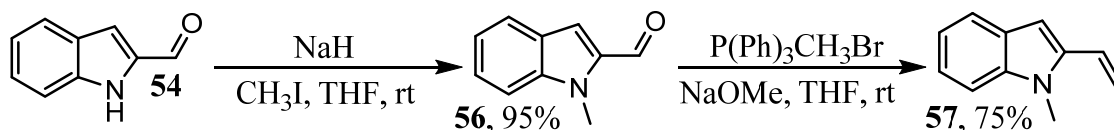
Another styrene of interest was the 2-vinylbenzofuran (**60**), since it is very similar to the lead styrene 2-vinylbenzo[b]thiophene **31 31**. Synthesis of this analog followed similarly to the

route for the thianaphthene derivative in that the aldehyde (**59**) was preferably synthesized since it was expensive to purchase commercially (Scheme 3-13).

Scheme 3-13: Synthesis of 2-vinylbenzofuran 60.
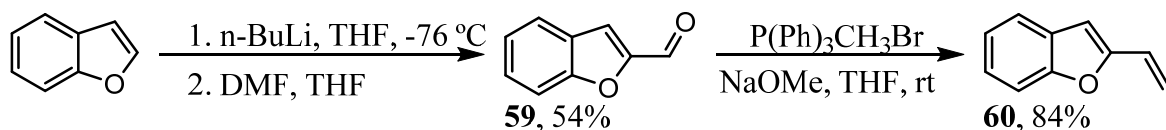
Substitution of new groups on the original thianaphthene analog **31** itself was also explored. The most easily substituted position seemed to be the 5-position and substitution with both fluoro and chloro groups were explored. Unfortunately, substituted thianaphthenes are expensive and it was necessary to synthesize them from substituted thiols (Scheme 3-14). These reactions were found to be messy and low-yielding, however, the substituted thiols were inexpensive enough to scale the reactions up to get enough material to continue on to the desired final substituted styrenes.

Scheme 3-14: Synthesis of substituted thianaphthenes.
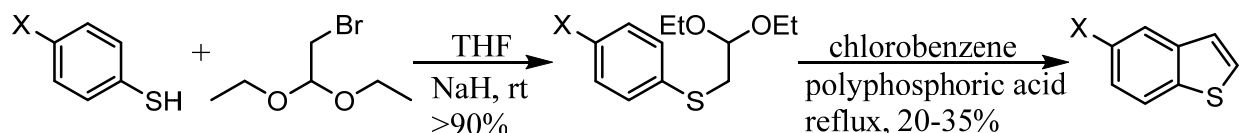
where X = Cl, F

Once the substituted thianaphthenes were synthesized, synthesis of the 2-vinyl analogs followed the same route to the lead vinyl analog **31** (Scheme 3-15). Similarly to **31**, high yields of the substituted 2-vinylthianaphthenes **61** and **62** were obtained and the material was similar in terms of stability and appearance. Future SAR studies may also focus on substitution in both this 5-position and other positions based on availability of substituted thiols. It should be noted that

3-substituted thiols will likely generate two different isomers when cyclized that may prove very difficult to separate, thus focus initially on 4-substituted thiols (this work) or 2-substituted thiols would be preferred.

Scheme 3-15: Synthesis of substituted styrenes.

1. n-BuLi, THF, -76 °C
2. DMF, THF

X = Cl, 88%
X = F, 85%

P(Ph)₃CH₃Br
NaOMe, THF, rt

X = Cl, **61**, 96%
X = F, **62**, 95%
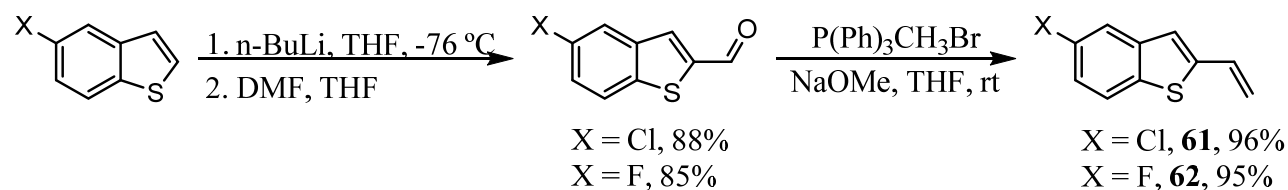
Summarized in Figure 3-4 are the styrenes that are now available for synthesis of stilbenes via the optimized Heck reaction.

Figure 3-4: Styrenes synthesized and/or commercially available.
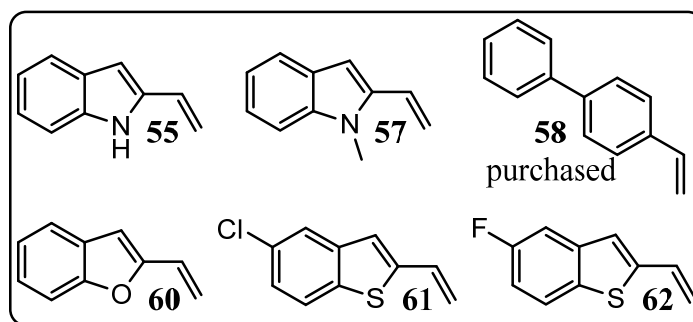
Synthesis using a new substitution pattern was also investigated in this second series of compounds. Using the convenient hydroxy/methoxy substitution pattern found to lead to active compounds, depicted in Figure 3-5 below are all of the possible substitution patterns that can be explored using the Heck reaction.

Figure 3-5: Substitution patterns.
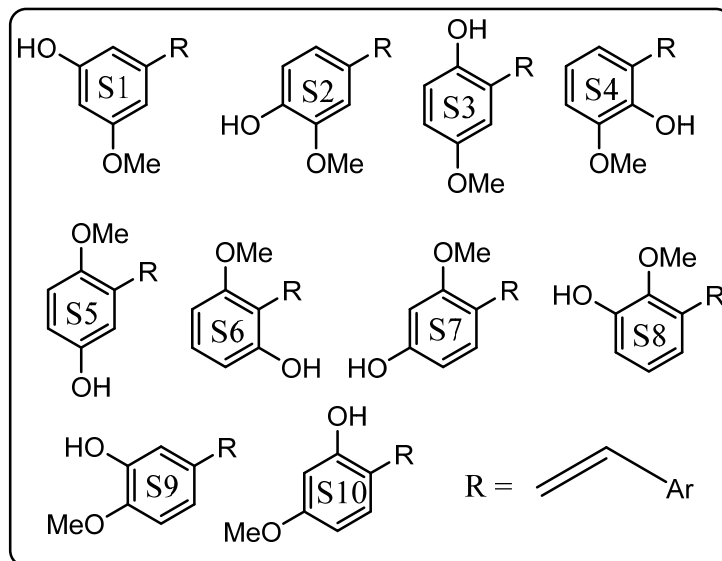
Previously it was shown that the methoxy group was preferably meta to the "R" group (S1-S4), therefore, these were the preferred substitution patterns to try first. Pattern S1 was the substitution pattern employed in the synthesis of SK-03-92 while S2 was the substitution pattern employed for the optimized Heck reaction described in this chapter. Pattern S3 was a novel substitution pattern and given the ortho/para directing nature of the phenol, synthesis of the substituted aryl bromide was routine (Scheme 3-16). Synthesis of S4 was completed on a small-scale for another project, however, as of yet it has not been applied to this project. Pattern S9 has also been partially explored with two compounds lacking activity, while S5-8 and S10 might be considered for future SAR studies.

Scheme 3-16: Synthesis of 2-bromo-4-methoxyphenol.
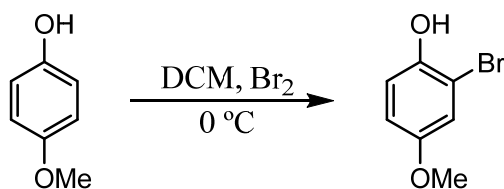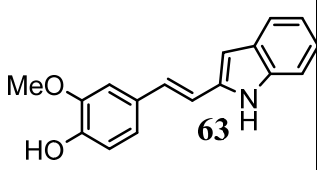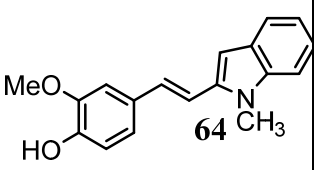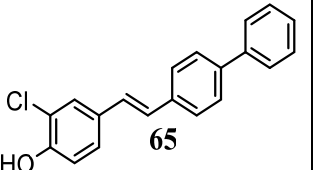
With these new starting materials in hand, the synthesis of another series of analogs was accomplished. Summarized in Table 3-11 is the synthesis of these new analogs.

Table 3-11: Second series of analogs synthesized.

Compound	R_1	R_2	R_X	Styrene	Yield (%)
63	OH	OMe	---	**55**	83
64	OH	OMe	---	**57**	89
65	OH	Cl	---	**58**	84
66	H	OMe	R_4 = OH	**31**	86
67	H	OMe	R_4 = OH	**55**	81
68	H	OMe	R_4 = OH	**60**	86
69	OH	OMe	---	**61**	87
70	OH	Cl	---	**61**	87
71	OH	Cl	---	**62**	92
72	OH	OMe	---	**62**	88
73	NH2	OMe	R_4 = Cl	**31**	75
74	H	OMe	R_3 = OH	**62**	92

The indole analogs **63** and **67** were both not acid sensitive, unlike their parent styrene **55**. The N-methyl analog **57** was also not acid sensitive. This is of importance because acid stability *in vivo* is an important quality for a drug-candidate. Compounds that readily decompose when subjected to changes in pH are likely to quickly decompose *in vivo* (stomach, 2; gut, 9-10) and likely not reach their target in time to elicit an effect. The relative instability of the styrene indole, in this case, is likely simply related to the relative reactivity of the olefin, which is quenched on annulation with the aryl bromides. Polymerization reactions with styrenes, likely the major mode of decomposition, is well known.[162-164]

Table 3-12: MICs for compounds 63, 64, and 65[a].

Bacterial Strain	63	64	65
S. aureus	4	32	>128
E. faecalis	4	32	>128
P. aeruginosa	>128	>128	>128
E. coli	>128	>128	>128
M. intracellulare	32	32	>128
M. chelonae	32	32	>128
M. fortuitum	32	32	>128
M. kansasii	32	32	>128
M. avium	16	32	>128
M. smegmatis	16	32	>128
M. marinum	32	32	>128

[a]Values in µg/mL

The major focus from this series of compounds were phenolic derivatives with either methoxy or chloro substituents, since in the first series these were found to be the most potent. Yields were generally high for all the analogs prepared, again showing the utility of the optimized Heck reaction in the synthesis of a wide variety of analogs with Herrmann's catalyst.

A number of new analogs were discovered that exhibited activity against gram-positive bacteria from this second series. Based on these findings it is clear that the SAR is honing in on
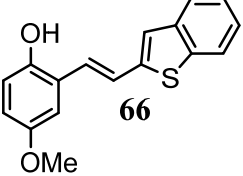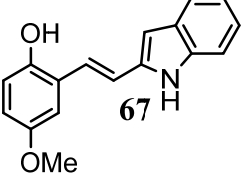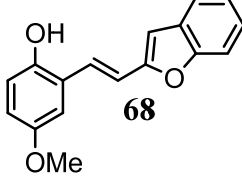
the, as of yet, unknown targets and future SAR studies should be successful in discovering even more active analogs.

Described in Table 3-12, the indole derivative **63** had similar activity to the two lead compounds **36** and **38**. Although the activity of **63** is somewhere between 4-8-fold lower then lead compounds **36** and **38**, it is well within the margins for an antibiotic drug candidate. The indole moiety may also prove to have better ADME properties and thus have better *in vivo* performance compared to other analogs. The N-methyl analog **64** was much less active, and thus it seems the N-methyl styrene is not a good choice for future SAR studies. The commercially available styrene **58** was used to synthesize compound **65**, which was found to have no activity for any tested strains, thus this styrene is also a poor choice for future SAR studies.

It is also worth noting that like the other hydroxy/methoxy derivatives, both **63** and **64** retained mycobacterium activity. Interestingly, the mycobacterium activity of **64** was found to be the same as its activity against gram-positive bacteria (32 µg/mL) and very similar to the activity of **63** on these same mycobacterium species. This again may indicate that a similar yet distinct mode of action is involved between the two different subspecies of bacteria.

Detailed in Table 3-13 are both a new substitution pattern as well as use of different styrenes in an attempt to gain more insight into the SAR. Across the board these three analogs (**66**, **67**, and **68**) seem to display similar activities with the different styrenes employed. In a previous SAR, a derivative with the benzofuran substitution pattern was found to be inactive. Regardless, benzofurans should also be explored in any future SAR based on these data.

Table 3-13: MICs for compounds 66, 67, and 68[a].
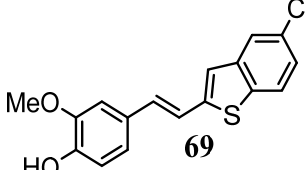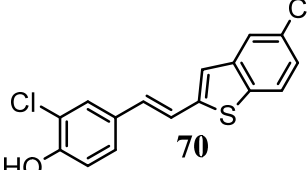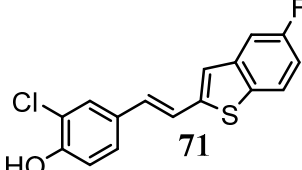
Bacterial Strain	66	67	68
S. aureus	4	4	4
E. faecalis	4	8	4
P. aeruginosa	>128	>128	>128
E. coli	>128	>128	>128
M. intracellulare	32	64	32
M. chelonae	64	32	64
M. fortuitum	32	64	32
M. kansasii	64	32	32
M. avium	64	64	64
M. smegmatis	32	64	32
M. marinum	32	64	32

[a]Values in μg/mL

The new substitution pattern, phenol ortho to the bridge, was also found to retain activity. Although the activity was slightly lower, again it is within the range of other pharmaceutical antibiotics. Although not quantified, the solubility of this new substitution pattern in water and aqueous acidic soliutions seemed to be higher than that of past compounds, perhaps due to the influence of the phenol which is in close proximity to the hydrophobic side chain.

Table 3-14: MICs for compounds 69, 70, and 71[a].
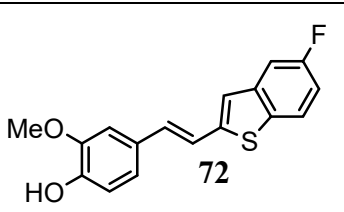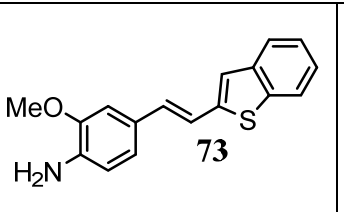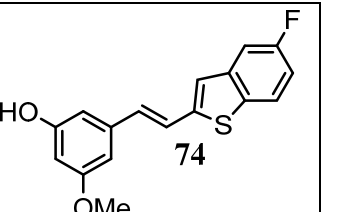
Bacterial Strain	69 (Cl / MeO / HO)	70 (Cl / Cl / HO)	71 (F / Cl / HO)
S. aureus	128	32	4
E. faecalis	128	4	2
P. aeruginosa	>128	>128	>128
E. coli	>128	>128	>128
M. intracellulare	>128	>128	>128
M. chelonae	>128	>128	>128
M. fortuitum	>128	>128	>128
M. kansasii	>128	>128	>128
M. avium	>128	>128	>128
M. smegmatis	>128	>128	>128
M. marinum	>128	>128	>128

[a]Values in µg/mL

Detailed in Table 3-14 are some of the substituted thianaphthene analogs synthesized. Interestingly the ring D chloro substituted **69** lost all activity when compared to the related active analog **36**. This may indicate that the molecular volume must not be increased too drastically. Indeed **70** and **71** show similar trends. The ring D chloro analog **70** was less active then the ring D fluoro analog **71**, and both are less active then the related parent analog **38**. It was also

interesting to note that similar to what has been observed in the SAR, the ring A chloro analogs **70** and **71** again lack mycobacterium activity but still show gram-positive activity.

Table 3-15: MICs for compounds 72, 73, and 74[a].

Bacterial Strain	72	73	74
S. aureus	8	>128	0.5
E. faecalis	32	>128	0.5
P. aeruginosa	>128	>128	>128
E. coli	>128	>128	>128
M. intracellulare	>128	>128	64
M. chelonae	>128	>128	64
M. fortuitum	>128	>128	32
M. kansasii	>128	>128	64
M. avium	>128	>128	64
M. smegmatis	>128	>128	32
M. marinum	>128	>128	64

[a]Values in µg/mL

Detailed in Table 3-15 are the values for the final set of compounds from this second series. The ring D fluoro analog **72** again seems to indicate that molecular volume is important because it is more active than then ring D chloro analog **69**, yet less active then the related

compound **36**. A more detailed analysis of molecular volume will be discussed in an upcoming chapter. The analog **73** attempted to replace the phenolic function with a more soluble amine, which lost all activity as the SAR would predict. Gratifyingly, ring D fluoro analog **74** showed increased activity when compared to its parent compound SK-03-92 and similar activity to the important lead compounds **36** and **38**.

III. CONCLUSION.

In summary, a new transition metal catalyzed Heck reaction was optimized for the synthesis of novel stilbenoid analogs. This method was found to be extremely versatile in the one-step synthesis of a number of structurally similar, yet distinct analogs. Moreover, the starting materials necessary for the reaction were either commercially available or easily synthesized in the lab with common starting materials.

This reaction was found to work best with 'Herrmann's palladacycle', a cyclic palladium dimer that, at room temperature, exists as the relatively stable and air tolerable palladium (II) species. At elevated temperatures, generally over 80 ºC, studies indicated that the palladacycle was altered and reduced to the active palladium (0) catalyst, which was found to be stable enough for use at 150 ºC, a temperature at which other Pd catalysts readily decomposed.

A break-through in this reaction was the addition of water which permitted nearly full conversion of the starting materials with Herrmann's catalyst at 150 ºC. Without the addition of water conversions were generally less than 10%, with many reactions resulting in zero conversion.

Using this reaction, a number of new antibiotic analogs were prepared that had potent activity less than 10 µg/mL against gram-positive bacterial strains, a general target for new drug

95

candidates. These include analogs **36**, **38**, **45**, **48**, **52**, **63**, **66**, **67**, **68**, **71**, and **74**. Many of these new lead compounds were assayed against drug-resistant strains of gram-positive bacteria, the results of which will be discussed in a later section.

A significant number of new analogs can be prepared via the method outlined in this chapter and the general idea behind this SAR was both to advance our current understanding of the SAR as well as provide potential new directions for future SAR work, with the final aim of a clinical candidate with activity against MDR MRSA, VISA, VRSA, etc.

IV.   EXPERIMENTAL

1.   *In vitro* MIC assays.

In vitro minimum inhibitory concentration (MIC) determinations were performed according to the Clinical and Laboratory Standards Institute (CLSI) guidelines,[115] for most of the bacteria that were screened. Tetracycline, ciprofloxacin, and erythromycin controls were included as control antibiotics for the gram-positive bacteria MICs and correlated with established MIC values. All anti-Mycobacterium activity evaluations were performed using MIC assays in Middlebrook 7H9 broth with 10% oleic acid albumin dextrose complex (OADC) as previously described[114]. Rifampin was used as the positive control for the mycobacterial MICs. All MIC numbers are a compilation of the geometric means from three separate runs. For the broad characterization against *S. aureus*, strains that have been typed by a variety of means were used[116].

2.   General procedure for the optimized Heck reaction.

As previously noted Herrmann's palladacycle is both air and temperature stable and thus it was not necessary to weigh it under an inert atmosphere. All solid materials were charged to a

10 mL sealable reaction vessel under argon with a magnetic stir-bar. The vessel was purged by vacuum three times, backfilling with argon after each evacuation.

In a separate flask dimethylacetamide mixed with 10% water was frozen under argon via dry ice/acetone. Once frozen, the flask was evacuated with high vacuum and slowly warmed to rt. Vigorous evolution of bubbles confirmed removal of gases from the solvent. This was repeated three times or until minimal evolution of bubbles was observed. The solvent was kept under argon and was found suitable for use over many weeks as long as it was kept under an inert gas.

The solvent (3mL) was added to the reaction vessel under argon and the flask was immediately heated to 150 ºC in an oil bath. In many cases the color of the reaction mixture slowly darkened over a period of 3h, at which time it was generally a dark black color. After 3h the reaction vessel was cooled to rt, diluted with EtOAc (10mL), filtered through a plug of celite, washed with dilute acid (or water where acidic solutions were problematic), dried (Na2SO4), and solvent was removed to a crude residue. In general compounds were purified by FCC as described, but if necessary they could be further purified by crystallization from isopropanol.

3.   Characterization data.

Both 1H and 13C NMR spectra were recorded on a Bruker DPX-300 or DRX-500 instrument where noted. HRMS scans were recorded with a Shimadzu LCMS-IT-TOF or similar instruments run at the Shimadzu Analytical Chemistry Center of Southeastern Wisconsin. *In silico* cLogP values and topological polar surface area values (tPSA) were calculated with ChemBioDraw Ultra v. 14.

(E)-1-(5-(2-(Benzo[b]thiophen-2-yl)vinyl)-2-hydroxyphenyl)ethan-1-one (32, Table 3-3, entry 1)
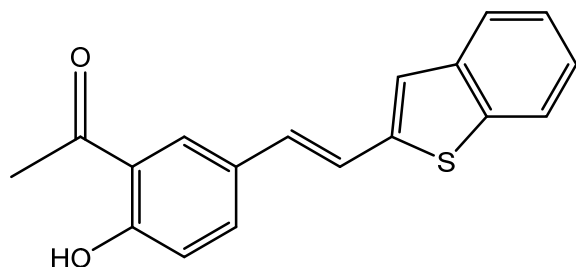
Chemical Formula: $C_{18}H_{14}O_2S$
Molecular Weight: 294.37
c Log P: 4.18
tPSA: 37.3

The general procedure was followed (3 h). The 1-(5-bromo-2-hydroxyphenyl)ethan-1-one **30** (134.2 mg, 0.624 mmol, 1 eq), 2-vinylbenzo[b]thiophene **31** (100 mg, 0.624 mmol, 1 eq), sodium acetate (102.4 mg, 1.248 mmol, 2 eq), and Herrmann's palladacycle (14.6 mg, 0.016 mmol, 0.025 eq) were charged to a vial containing oxygen free solvent (10% water in dimethylacetamide, 3 mL) under an argon atmosphere. The vial was sealed with a septum and the mixture was heated to 150 ºC for 3h, cooled to rt, and EtOAc (10mL) was added in one portion. The suspension was filtered through a plug of celite and the filtrate was washed successively with 0.5 N aq HCl (2 x 10 mL) and brine (2 x 10 mL). The organic layer was dried (Na_2SO_4) and solvent was removed *in vacuo* to provide a crude red solid. The solid was purified by flash column chromatography on silica gel (30% EtOAc in hexanes) to provide the pure ketone **32** in 91% yield as an off-white solid (167 mg): ^{1}H NMR (300 MHz, CDCl3) δ 12.36 (s, 1H), 7.81 (d, *J* = 1.7 Hz, 1H), 7.79 (d, *J* = 2.6 Hz, 1H), 7.72 (dd, *J* = 6.0, 2.8 Hz, 2H), 7.39 – 7.30 (m, 2H), 7.29 – 7.25 (m, 2H), 7.03 (d, *J* = 8.7 Hz, 1H), 6.96 (d, *J* = 16.0 Hz, 1H), 2.72 (s, 3H); ^{13}C NMR (75 MHz, CDCl3) δ 146.75, 145.98, 143.22, 140.33, 138.71, 130.90, 129.29, 124.54, 124.48, 123.25, 122.49, 122.19, 120.62, 120.21, 114.69, 108.39, 55.95; HRMS (ESI) (M - H), Calcd. for $C_{18}H_{13}O_2S$ 293.0636; Found 293.0625.

(E)-4-(2-(Benzo[b]thiophen-2-yl)vinyl)-2-fluorophenol (33, Table 3-3, entry 2)
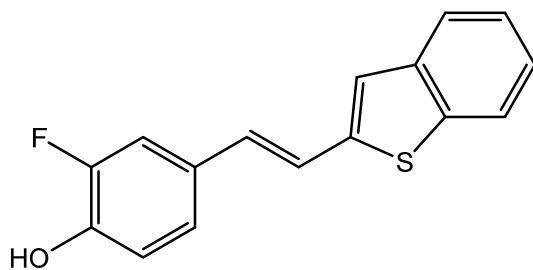
Chemical Formula: $C_{16}H_{11}FOS$
Molecular Weight: 270.32
c Log P: 5.03
tPSA: 20.23

The general procedure was followed (3 h). The 4-bromo-2-fluorophenol (119.2 mg, 0.624 mmol, 1 eq), 2-vinylbenzo[b]thiophene **31** (100 mg, 0.624 mmol, 1 eq), sodium acetate (102.4 mg, 1.248 mmol, 2 eq), and Herrmann's palladacycle (14.6 mg, 0.016 mmol, 0.025 eq) were charged to a vial containing oxygen free solvent (10% water in dimethylacetamide, 3 mL) under an argon atmosphere. The vial was sealed with a septum and the mixture was heated to 150 °C for 3h, cooled to rt, and EtOAc (10mL) was added in one portion. The suspension was filtered through a plug of celite and the filtrate was washed successively with 0.5 N aq HCl (2 x 10 mL) and brine (2 x 10 mL). The organic layer was dried (Na_2SO_4) and solvent was removed *in vacuo* to provide a yellow solid. The solid was purified by flash column chromatography on silica gel (20% EtOAc in hexanes) to provide the pure fluoro analog **33** in 91% yield as a white solid (153 mg): ^{1}H NMR (500 MHz, DMSO) δ 10.14 (s, 1H), 7.96 – 7.85 (m, 1H), 7.84 – 7.74 (m, 1H), 7.51 (dd, J = 12.7, 1.9 Hz, 1H), 7.45 (d, J = 16.5 Hz, 1H), 7.42 (s, 1H), 7.34 (pd, J = 7.1, 1.4 Hz, 2H), 7.27 (dd, J = 8.3, 1.7 Hz, 1H), 6.98 (d, J = 8.8 Hz, 1H), 6.93 (d, J = 16.5 Hz, 1H); ^{13}C NMR (126 MHz, DMSO) δ 151.70 (d, J = 240.8 Hz), 145.60 (d, J = 12.5 Hz), 143.17 (s), 140.48 (s), 138.45 (s), 130.09 (s), 128.81 (d, J = 6.4 Hz), 125.26 (s), 125.18 (s), 124.15 (s), 123.92 (s), 123.52 (s), 122.81 (s), 121.24 (s), 118.33 (s), 114.31 (d, J = 18.6 Hz); HRMS (ESI) (M + H), Calcd. for $C_{16}H_{12}FOS$ 271.0593; Found 271.0599.

(E)-4-(2-(Benzo[b]thiophen-2-yl)vinyl)phenol (34, Table 3-3, entry 3)
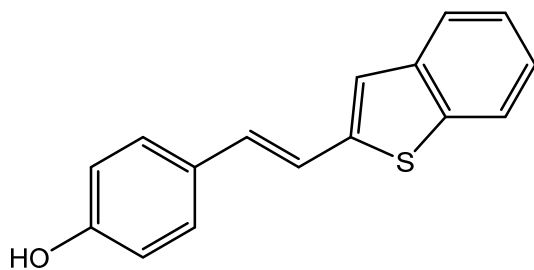
Chemical Formula: $C_{16}H_{12}OS$
Molecular Weight: 252.33
c Log P: 4.87
tPSA: 20.23

The general procedure was followed (3 h). The 4-bromophenol (108 mg, 0.624 mmol, 1 eq), 2-vinylbenzo[b]thiophene **31** (100 mg, 0.624 mmol, 1 eq), sodium acetate (102.4 mg, 1.248 mmol, 2 eq), and Herrmann's palladacycle (14.6 mg, 0.016 mmol, 0.025 eq) were charged to a vial containing oxygen free solvent (10% water in dimethylacetamide, 3 mL) under an argon atmosphere. The vial was sealed with a septum and the mixture was heated to 150 ºC for 3h, cooled to rt, and EtOAc (10mL) was added in one portion. The suspension was filtered through a plug of celite and the filtrate was washed successively with 0.5 N aq HCl (2 x 10 mL) and brine (2 x 10 mL). The organic layer was dried (Na_2SO_4) and solvent was removed *in vacuo* to provide an off-white solid. The solid was purified by flash column chromatography on silica gel (20% EtOAc in hexanes) to provide the pure p-phenol **34** in 90% yield as a white solid (142 mg): ^{1}H NMR (300 MHz, DMSO-d6) δ 9.70 (s, 1H), 7.94 – 7.84 (m, 1H), 7.76 (dd, *J* = 6.4, 2.3 Hz, 1H), 7.47 (d, *J* = 8.5 Hz, 2H), 7.42 – 7.27 (m, 4H), 6.93 (d, *J* = 16.1 Hz, 1H), 6.79 (d, *J* = 8.5 Hz, 2H); ^{13}C NMR (75 MHz, DMSO-d6) δ 158.26, 143.58, 140.55, 138.27, 131.19, 128.65, 127.74, 125.12, 125.06, 123.75, 122.88, 122.75, 119.63, 116.13; HRMS (ESI) (M + H), Calcd. for $C_{16}H_{13}OS$ 253.0687; Found 253.0681.

(E)-5-(2-(Benzo[b]thiophen-2-yl)vinyl)benzo[d][1,3]dioxole (35, Table 3-4, entry 1)

Chemical Formula: $C_{17}H_{12}O_2S$
Molecular Weight: 280.34
c Log P: 5.04
tPSA: 18.46

The general procedure was followed (3 h). The 5-bromobenzo[d][1,3]dioxole (125.5 mg, 0.624 mmol, 1 eq), 2-vinylbenzo[b]thiophene **31** (100 mg, 0.624 mmol, 1 eq), sodium acetate (102.4 mg, 1.248 mmol, 2 eq), and Herrmann's palladacycle (14.6 mg, 0.016 mmol, 0.025 eq) were charged to a vial containing oxygen free solvent (10% water in dimethylacetamide, 3 mL) under an argon atmosphere. The vial was sealed with a septum and the mixture was heated to 150 ºC for 3h, cooled to rt, and EtOAc (10mL) was added in one portion. The suspension was filtered through a plug of celite and the filtrate was washed successively with 0.5 N aq HCl (2 x 10 mL) and brine (2 x 10 mL). The organic layer was dried (Na_2SO_4) and solvent was removed *in vacuo* to provide a yellow solid. The solid was purified by flash column chromatography on silica gel (10% EtOAc in hexanes) to provide the pure dioxole **35** in 95% yield as a white solid (166 mg): ^{1}H NMR (300 MHz, DMSO-d6) δ 7.96 – 7.86 (m, 1H), 7.79 (dd, J = 6.0, 2.8 Hz, 1H), 7.47 (d, J = 16.1 Hz, 1H), 7.42 (s, 1H), 7.39 – 7.28 (m, 3H), 7.09 (d, J = 8.1 Hz, 1H), 6.97 (d, J = 10.1 Hz, 1H), 6.93 (d, J = 1.5 Hz, 1H), 6.06 (s, 2H); ^{13}C NMR (75 MHz, DMSO-d6) δ 148.41, 147.86, 143.19, 140.46, 138.43, 131.23, 130.83, 125.25, 125.17, 123.90, 123.52, 122.79, 122.57, 121.19, 108.94, 105.93, 101.68; HRMS (ESI) (M - H), Calcd. for $C_{17}H_{13}O_2S$ 281.0636; Found 282.0638.

(E)-4-(2-(Benzo[b]thiophen-2-yl)vinyl)-2-methoxyphenol (36, Table 3-4, entry 2)

Chemical Formula: $C_{17}H_{14}O_2S$
Molecular Weight: 282.36
c Log P: 4.74
tPSA: 29.46

The general procedure was followed (3 h). The 4-bromo-2-methoxyphenol (126.7 mg, 0.624 mmol, 1 eq), 2-vinylbenzo[b]thiophene **31** (100 mg, 0.624 mmol, 1 eq), sodium acetate (102.4 mg, 1.248 mmol, 2 eq), and Herrmann's palladacycle (14.6 mg, 0.016 mmol, 0.025 eq) were charged to a vial containing oxygen free solvent (10% water in dimethylacetamide, 3 mL) under an argon atmosphere. The vial was sealed with a septum and the mixture was heated to 150 ºC for 3h, cooled to rt, and EtOAc (10mL) was added in one portion. The suspension was filtered through a plug of celite and the filtrate was washed successively with 0.5 N aq HCl (2 x 10 mL) and brine (2 x 10 mL). The organic layer was dried (Na_2SO_4) and solvent was removed *in vacuo* to provide a yellow solid. The solid was purified by flash column chromatography on silica gel (20% EtOAc in hexanes) to provide the pure methoxy phenol **36** in 93% yield as a white solid (164 mg): ^{1}H NMR (300 MHz, CDCl3) δ 7.83 – 7.77 (m, 1H), 7.75 – 7.66 (m, 1H), 7.40 – 7.29 (m, 2H), 7.23 (s, 1H), 7.20 (d, *J* = 16.2 Hz, 1H), 7.06 (d, *J* = 10.2 Hz, 2H), 6.95 (dd, *J* = 12.0, 3.9 Hz, 2H), 5.70 (s, 1H), 3.98 (s, 3H); ^{13}C NMR (75 MHz, CDCl3) δ 146.75, 145.98, 143.22, 140.33, 138.71, 130.90, 129.29, 124.54, 124.48, 123.25, 122.49, 122.19, 120.62, 120.21, 114.69, 108.39, 55.95; HRMS (ESI) (M - H), Calcd. for $C_{17}H_{13}O_2S$ 281.0636; Found 281.0629.

(E)-5-(2-(Benzo[b]thiophen-2-yl)vinyl)-2-methoxyphenol (37, Table 3-4, entry 3)

Chemical Formula: $C_{17}H_{14}O_2S$
Molecular Weight: 282.36
c Log P: 4.74
tPSA: 29.46

The general procedure was followed (3 h). The 5-bromo-2-methoxyphenol (126.7 mg, 0.624 mmol, 1 eq), 2-vinylbenzo[b]thiophene **31** (100 mg, 0.624 mmol, 1 eq), sodium acetate (102.4 mg, 1.248 mmol, 2 eq), and Herrmann's palladacycle (14.6 mg, 0.016 mmol, 0.025 eq) were charged to a vial containing oxygen free solvent (10% water in dimethylacetamide, 3 mL) under an argon atmosphere. The vial was sealed with a septum and the mixture was heated to 150 ºC for 3h, cooled to rt, and EtOAc (10mL) was added in one portion. The suspension was filtered through a plug of celite and the filtrate was washed successively with 0.5 N aq HCl (2 x 10 mL) and brine (2 x 10 mL). The organic layer was dried (Na_2SO_4) and solvent was removed *in vacuo* to provide a yellow solid. The solid was purified by flash column chromatography on silica gel (20% EtOAc in hexanes) to provide the pure methoxy phenol **37** in 89% yield as a white solid (157 mg): ^{1}H NMR (300 MHz, DMSO-d6) δ 9.11 (s, 1H), 7.89 (d, J = 7.0 Hz, 1H), 7.76 (d, J = 8.1 Hz, 1H), 7.42 (s, 1H), 7.38 – 7.25 (m, 3H), 7.07 (s, 1H), 7.02 (d, J = 8.4 Hz, 1H), 6.93 (d, J = 9.4 Hz, 1H), 6.88 (d, J = 16.2 Hz, 1H), 3.80 (s, 3H); ^{13}C NMR (75 MHz, DMSO-d6) δ 148.65, 147.11, 143.35, 140.50, 138.36, 131.12, 129.69, 125.16, 123.81, 123.29, 122.76, 120.48, 119.39, 113.39, 112.60, 56.08; HRMS (ESI) (M + H), Calcd. for $C_{17}H_{15}O_2S$ 283.0793; Found 283.0787

(E)-4-(2-(Benzo[b]thiophen-2-yl)vinyl)-2-chlorophenol (38, Table 3-5, entry 1)

Chemical Formula: $C_{16}H_{11}ClOS$
Molecular Weight: 286.77
c Log P: 5.43
tPSA: 20.23

The general procedure was followed (3 h). The 4-bromo-2-chlorophenol (129.5 mg, 0.624 mmol, 1 eq), 2-vinylbenzo[b]thiophene **31** (100 mg, 0.624 mmol, 1 eq), sodium acetate (102.4 mg, 1.248 mmol, 2 eq), and Herrmann's palladacycle (14.6 mg, 0.016 mmol, 0.025 eq) were charged to a vial containing oxygen free solvent (10% water in dimethylacetamide, 3 mL) under an argon atmosphere. The vial was sealed with a septum and the mixture was heated to 150 ºC for 3h, cooled to rt, and EtOAc (10mL) was added in one portion. The suspension was filtered through a plug of celite and the filtrate was washed successively with 0.5 N aq HCl (2 x 10 mL) and brine (2 x 10 mL). The organic layer was dried (Na_2SO_4) and solvent was removed *in vacuo* to provide a yellow solid. The solid was purified by flash column chromatography on silica gel (20% EtOAc in hexanes) to provide the pure chloro phenol **38** in 92% yield as a grey solid (164 mg): ^{1}H NMR (300 MHz, DMSO-d6) δ 10.44 (s, 1H), 7.90 (d, J = 6.8 Hz, 1H), 7.85 – 7.73 (m, 1H), 7.68 (s, 1H), 7.46 (d, J = 16.3 Hz, 1H), 7.43 (m, 2H), 7.40 – 7.27 (m, 2H), 6.98 (d, J = 8.4 Hz, 1H), 6.92 (d, J = 16.1 Hz, 1H); ^{13}C NMR (75 MHz, DMSO-d6) δ 153.57, 143.17, 140.45, 138.45, 129.70, 129.25, 128.42, 127.11, 125.25, 125.16, 123.91, 123.55, 122.80, 121.23, 120.69, 117.29; HRMS (ESI) (M + H), Calcd. for $C_{16}H_{12}ClOS$ 287.0297; Found 287.0298.

(E)-5-(2-(Benzo[b]thiophen-2-yl)vinyl)-2-chlorophenol (39, Table 3-5, entry 2)
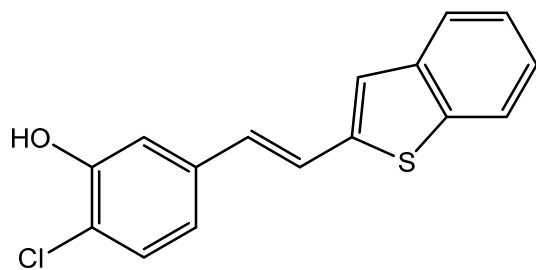
Chemical Formula: $C_{16}H_{11}ClOS$
Molecular Weight: 286.77
c Log P: 5.43
tPSA: 20.23

The general procedure was followed (3 h). The 5-bromo-2-chlorophenol (129.5 mg, 0.624 mmol, 1 eq), 2-vinylbenzo[b]thiophene **31** (100 mg, 0.624 mmol, 1 eq), sodium acetate (102.4 mg, 1.248 mmol, 2 eq), and Herrmann's palladacycle (14.6 mg, 0.016 mmol, 0.025 eq) were charged to a vial containing oxygen free solvent (10% water in dimethylacetamide, 3 mL) under an argon atmosphere. The vial was sealed with a septum and the mixture was heated to 150 ºC for 3h, cooled to rt, and EtOAc (10mL) was added in one portion. The suspension was filtered through a plug of celite and the filtrate was washed successively with 0.5 N aq HCl (2 x 10 mL) and brine (2 x 10 mL). The organic layer was dried (Na_2SO_4) and solvent was removed *in vacuo* to provide a yellow solid. The solid was purified by flash column chromatography on silica gel (20% EtOAc in hexanes) to provide the pure chloro phenol **39** in 90% yield as a yellow solid (161 mg): ^1H NMR (300 MHz, DMSO-d6) δ 10.28 (s, 1H), 7.98 – 7.85 (m, 1H), 7.85 – 7.74 (m, 1H), 7.52 (s, 1H), 7.49 (d, J = 16.4 Hz, 1H), 7.42 – 7.29 (m, 3H), 7.20 – 7.07 (m, 2H), 6.94 (d, J = 16.1 Hz, 1H); ^{13}C NMR (75 MHz, DMSO-d6) δ 153.65, 142.62, 140.34, 138.70, 136.77, 130.57, 129.99, 125.53, 125.24, 124.63, 124.11, 123.38, 122.87, 119.97, 118.93, 114.89; HRMS (ESI) (M + H), Calcd. for $C_{16}H_{12}ClOS$ 287.0297; Found 287.0291.

(E)-5-(2-(Benzo[b]thiophen-2-yl)vinyl)-2-hydroxybenzonitrile (40, Table 3-5, entry 3)
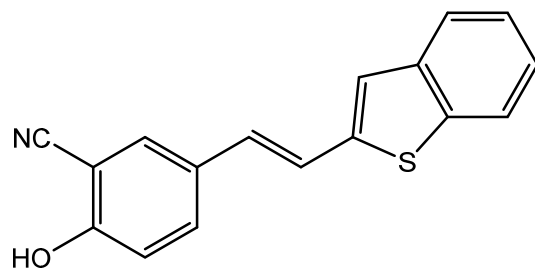
Chemical Formula: $C_{17}H_{11}NOS$
Molecular Weight: 277.34
c Log P: 4.9
tPSA: 44.02

The general procedure was followed (3 h). The 5-bromo-2-hydroxybenzonitrile (123.6 mg, 0.624 mmol, 1 eq), 2-vinylbenzo[b]thiophene **31** (100 mg, 0.624 mmol, 1 eq), sodium acetate (102.4 mg, 1.248 mmol, 2 eq), and Herrmann's palladacycle (14.6 mg, 0.016 mmol, 0.025 eq) were charged to a vial containing oxygen free solvent (10% water in dimethylacetamide, 3 mL) under an argon atmosphere. The vial was sealed with a septum and the mixture was heated to 150 ºC for 3h, cooled to rt, and EtOAc (10mL) was added in one portion. The suspension was filtered through a plug of celite and the filtrate was washed successively with 0.5 N aq HCl (2 x 10 mL) and brine (2 x 10 mL). The organic layer was dried (Na_2SO_4) and solvent was removed *in vacuo* to provide a yellow solid. The solid was purified by flash column chromatography on silica gel (20% EtOAc in hexanes) to provide the pure nitrile **40** in 91% yield as a white solid (157 mg): ^{1}H NMR (300 MHz, DMSO-d6) δ 11.33 (s, 1H), 7.96 – 7.88 (m, 2H), 7.85 – 7.74 (m, 2H), 7.52 (d, *J* = 16.1 Hz, 1H), 7.43 (s, 1H), 7.40 – 7.28 (m, 2H), 7.04 (d, *J* = 8.7 Hz, 1H), 6.95 (d, *J* = 16.1 Hz, 1H); ^{13}C NMR (75 MHz, DMSO-d6) δ 160.36, 142.91, 140.39, 138.52, 133.21, 131.87, 128.96, 128.70, 125.38, 125.20, 124.01, 123.94, 122.84, 122.05, 117.23, 117.07, 99.82; HRMS (ESI) (M + H), Calcd. for $C_{17}H_{12}NOS$ 278.0640; Found 278.0642.

(E)-4-(2-(Benzo[b]thiophen-2-yl)vinyl)-2-nitrophenol (41, Table 3-6, entry 1)
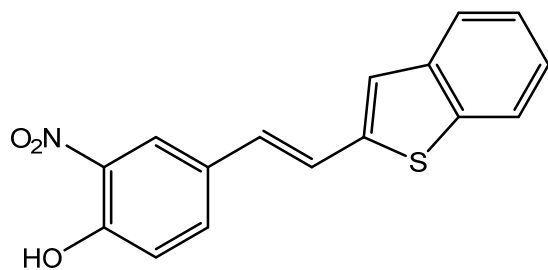
Chemical Formula: $C_{16}H_{11}NO_3S$
Molecular Weight: 297.33
tPSA: 72.04

The general procedure was followed (3 h). The 4-bromo-2-nitrophenol (136.1 mg, 0.624 mmol, 1 eq), 2-vinylbenzo[b]thiophene **31** (100 mg, 0.624 mmol, 1 eq), sodium acetate (102.4 mg, 1.248 mmol, 2 eq), and Herrmann's palladacycle (14.6 mg, 0.016 mmol, 0.025 eq) were charged to a vial containing oxygen free solvent (10% water in dimethylacetamide, 3 mL) under an argon atmosphere. The vial was sealed with a septum and the mixture was heated to 150 °C for 3h, cooled to rt, and EtOAc (10mL) was added in one portion. The suspension was filtered through a plug of celite and the filtrate was washed successively with water (2 x 10 mL) and brine (2 x 10 mL). The organic layer was dried (Na_2SO_4) and solvent was removed *in vacuo* to provide a yellow solid. The solid was purified by flash column chromatography on silica gel (50% EtOAc in hexanes) to provide the pure nitrophenol **41** in 80% yield as a brown solid (148 mg): ^{1}H NMR (300 MHz, DMSO-d6) δ 8.15 (d, *J* = 1.5 Hz, 1H), 7.96 – 7.89 (m, 1H), 7.86 (dd, *J* = 8.8, 1.7 Hz, 1H), 7.83 – 7.75 (m, 1H), 7.57 (d, *J* = 16.1 Hz, 1H), 7.47 (s, 1H), 7.41 – 7.30 (m, 2H), 7.15 (d, *J* = 8.7 Hz, 1H), 7.03 (d, *J* = 16.1 Hz, 1H). [phenol 1H not observed]; ^{13}C NMR (75 MHz, DMSO-d6) δ 152.24 (phenolic), 142.79, 140.37, 138.62, 137.63, 133.16, 128.74, 128.43, 125.44, 125.21, 124.21, 124.06, 123.61, 122.86, 122.69, 119.99; HRMS (ESI) (M + H), Calcd. for $C_{16}H_{12}NO_3S$ 298.0538; Found 298.0535.

(E)-4-(2-(Benzo[b]thiophen-2-yl)vinyl)-2,5-dichlorophenol (42, Table 3-6, entry 2)
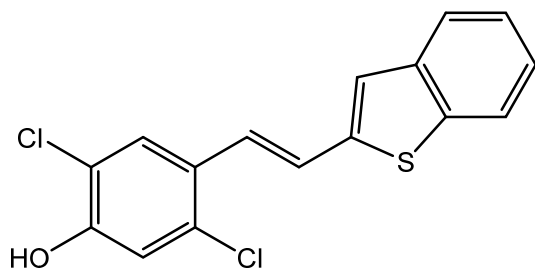
Chemical Formula: $C_{16}H_{10}Cl_2OS$
Molecular Weight: 321.22
c Log P: 5.99
tPSA: 20.23

The general procedure was followed (3 h). The 4-bromo-2,5-dichlorophenol (151 mg, 0.624 mmol, 1 eq), 2-vinylbenzo[b]thiophene **31** (100 mg, 0.624 mmol, 1 eq), sodium acetate (102.4 mg, 1.248 mmol, 2 eq), and Herrmann's palladacycle (14.6 mg, 0.016 mmol, 0.025 eq) were charged to a vial containing oxygen free solvent (10% water in dimethylacetamide, 3 mL) under an argon atmosphere. The vial was sealed with a septum and the mixture was heated to 150 °C for 3h, cooled to rt, and EtOAc (10mL) was added in one portion. The suspension was filtered through a plug of celite and the filtrate was washed successively with 0.5 N aq HCl (2 x 10 mL) and brine (2 x 10 mL). The organic layer was dried (Na_2SO_4) and solvent was removed *in vacuo* to provide a yellow/grey solid. The solid was purified by flash column chromatography on silica gel (20% EtOAc in hexanes) to provide the pure dichlorophenol **42** in 93% yield as a grey solid (186 mg): ^{1}H NMR (300 MHz, DMSO-d6) δ 10.99 (s, 1H), 7.97 (s, 1H), 7.94 – 7.89 (m, 1H), 7.85 – 7.79 (m, 1H), 7.63 (d, *J* = 16.0 Hz, 1H), 7.49 (s, 1H), 7.36 (p, *J* = 5.5 Hz, 2H), 7.09 (d, *J* = 16.3 Hz, 1H), 7.06 (s, 1H); ^{13}C NMR (75 MHz, DMSO-d6) δ 154.12, 142.65, 140.36, 138.55, 131.36, 127.84, 126.20, 125.63, 125.29, 124.76, 124.47, 124.23, 124.20, 122.89, 120.48, 117.32; HRMS (ESI) (M + H), Calcd. for $C_{16}H_{11}Cl_2OS$ 320.9908; Found 320.9912.

(E)-4-(2-(Benzo[b]thiophen-2-yl)vinyl)-2,6-dimethoxyphenol (43, Table 3-6, entry 3)
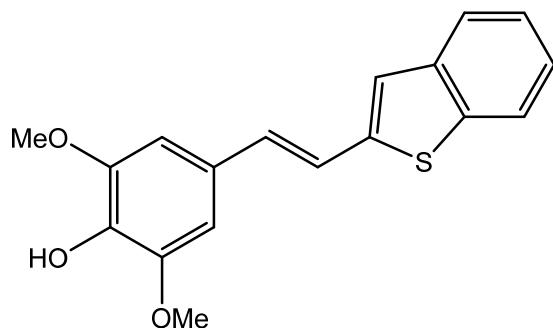
Chemical Formula: $C_{18}H_{16}O_3S$
Molecular Weight: 312.38
c Log P: 4.62
tPSA: 38.69

The general procedure was followed (3 h). The 4-bromo-2,6-dimethoxyphenol (145.4 mg, 0.624 mmol, 1 eq), 2-vinylbenzo[b]thiophene **31** (100 mg, 0.624 mmol, 1 eq), sodium acetate (102.4 mg, 1.248 mmol, 2 eq), and Herrmann's palladacycle (14.6 mg, 0.016 mmol, 0.025 eq) were charged to a vial containing oxygen free solvent (10% water in dimethylacetamide, 3 mL) under an argon atmosphere. The vial was sealed with a septum and the mixture was heated to 150 ºC for 3h, cooled to rt, and EtOAc (10mL) was added in one portion. The suspension was filtered through a plug of celite and the filtrate was washed successively with 0.5 N aq HCl (2 x 10 mL) and brine (2 x 10 mL). The organic layer was dried (Na2SO4) and solvent was removed *in vacuo* to provide a brown solid. The solid was purified by flash column chromatography on silica gel (20% EtOAc in hexanes) to provide the pure dimethoxyphenol **43** in 75% yield as a yellow solid (146 mg): ^{1}H NMR (500 MHz, DMSO) δ 8.66 (s, 1H), 7.93 – 7.89 (m, 1H), 7.79 (dd, *J* = 7.1, 1.5 Hz, 1H), 7.48 (d, *J* = 15.7 Hz, 1H), 7.41 (s, 1H), 7.39 – 7.29 (m, 2H), 6.96 (s, 2H), 6.95 (d, *J* = 16.0 Hz, 1H), 3.84 (s, 6H); ^{13}C NMR (126 MHz, DMSO) δ 148.62 (2C), 143.59, 140.59, 138.33, 136.73, 131.84, 127.19, 125.15, 125.12, 123.82, 122.93, 122.79, 120.28, 104.93 (2C), 56.51 (2C); HRMS (ESI) (M + H), Calcd. for C18H17O3S 313.0898; Found 313.0892.

(E)-4-(2-(Benzo[b]thiophen-2-yl)vinyl)-2-(trifluoromethoxy)phenol (44, Table 3-7, entry 1)

Chemical Formula: $C_{17}H_{11}F_3O_2S$
Molecular Weight: 336.33
c Log P: 6.4
tPSA: 29.46
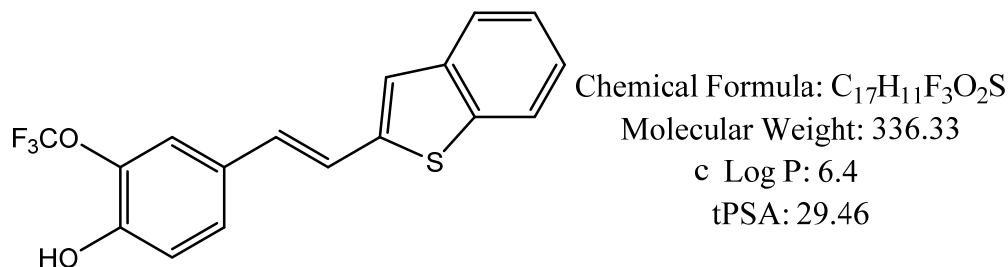
The general procedure was followed (3 h). The 4-bromo-2-(trifluoromethoxy)phenol (160.4 mg, 0.624 mmol, 1 eq), 2-vinylbenzo[b]thiophene **31** (100 mg, 0.624 mmol, 1 eq), sodium acetate (102.4 mg, 1.248 mmol, 2 eq), and Herrmann's palladacycle (14.6 mg, 0.016 mmol, 0.025 eq) were charged to a vial containing oxygen free solvent (10% water in dimethylacetamide, 3 mL) under an argon atmosphere. The vial was sealed with a septum and the mixture was heated to 150 ºC for 3h, cooled to rt, and EtOAc (10mL) was added in one portion. The suspension was filtered through a plug of celite and the filtrate was washed successively with 0.5 N aq HCl (2 x 10 mL) and brine (2 x 10 mL). The organic layer was dried (Na_2SO_4) and solvent was removed *in vacuo* to provide a brown solid. The solid was purified by flash column chromatography on silica gel (20% EtOAc in hexanes) to provide the pure trifluoromethoxy **44** in 85% yield as a white solid (178 mg): ^{1}H NMR (300 MHz, DMSO-d6) δ 10.45 (s, 1H), 7.91 (dd, *J* = 6.0, 2.9 Hz, 1H), 7.82 – 7.75 (m, 1H), 7.59 (s, 1H), 7.52-7.48 (m, 1H), 7.51-7.45 (d, *J* = 16.1 Hz, 1H), 7.44 (s, 1H), 7.39 – 7.29 (m, 2H), 7.03 (d, *J* = 8.5 Hz, 1H), 6.97 (d, *J* = 16.1 Hz, 1H); ^{13}C NMR (75 MHz, DMSO-d6) δ 150.35, 143.07, 140.43, 138.49, 136.77, 129.66, 128.74, 127.34, 125.29, 125.17, 123.94, 123.70, 122.81, 122.57, 121.77, 121.53, 118.33; HRMS (ESI) (M + H), Calcd. for $C_{17}H_{12}F_3O_2S$ 337.0510; Found 337.0513.

(E)-4-(2-(Benzo[b]thiophen-2-yl)vinyl)-2-ethoxyphenol (45, Table 3-7, entry 2)
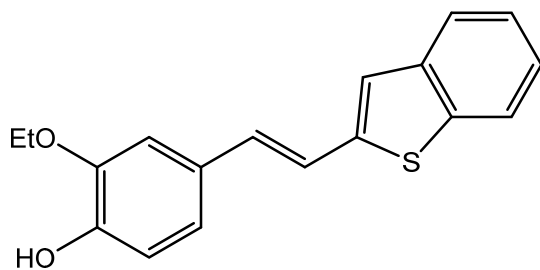
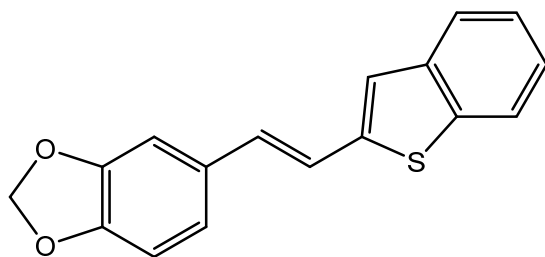Chemical Formula: $C_{18}H_{16}O_2S$
Molecular Weight: 296.38
c Log P: 5.08
tPSA: 29.46

The general procedure was followed (3 h). The 4-bromo-2-ethoxyphenol (135.5 mg, 0.624 mmol, 1 eq), 2-vinylbenzo[b]thiophene **31** (100 mg, 0.624 mmol, 1 eq), sodium acetate (102.4 mg, 1.248 mmol, 2 eq), and Herrmann's palladacycle (14.6 mg, 0.016 mmol, 0.025 eq) were charged to a vial containing oxygen free solvent (10% water in dimethylacetamide, 3 mL) under an argon atmosphere. The vial was sealed with a septum and the mixture was heated to 150 ºC for 3h, cooled to rt, and EtOAc (10mL) was added in one portion. The suspension was filtered through a plug of celite and the filtrate was washed successively with 0.5 N aq HCl (2 x 10 mL) and brine (2 x 10 mL). The organic layer was dried (Na_2SO_4) and solvent was removed *in vacuo* to provide a red solid. The solid was purified by flash column chromatography on silica gel (20% EtOAc in hexanes) to provide the pure ethoxyphenol **45** in 90% yield as a yellow solid (166 mg): ^{1}H NMR (300 MHz, DMSO-d6) δ 9.20 (s, 1H), 7.88 (d, J = 7.1 Hz, 1H), 7.76 (d, J = 7.6 Hz, 1H), 7.46 – 7.27 (m, 4H), 7.24 (s, 1H), 7.03 (d, J = 8.1 Hz, 1H), 6.92 (d, J = 16.1 Hz, 1H), 6.81 (d, J = 8.1 Hz, 1H), 4.10 (q, J = 6.9 Hz, 2H), 1.37 (t, J = 7.0 Hz, 3H); ^{13}C NMR (75 MHz, DMSO-d6) δ 147.96, 147.50, 143.64, 140.58, 138.30, 131.54, 128.28, 125.11, 125.04, 123.75, 122.81, 122.75, 120.97, 119.85, 116.17, 111.85, 64.35, 15.25; HRMS (ESI) (M + H), Calcd. for $C_{18}H_{17}O_2S$ 297.0949; Found 297.0957.

(E)-4-(2-(Benzo[b]thiophen-2-yl)vinyl)-2-isopropoxyphenol (46, Table 3-7, entry 3)
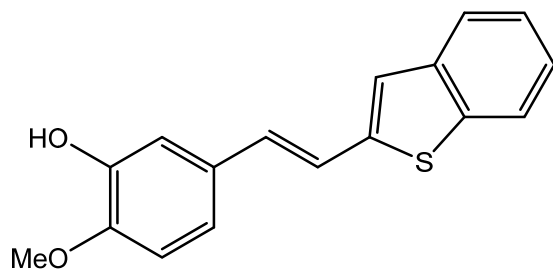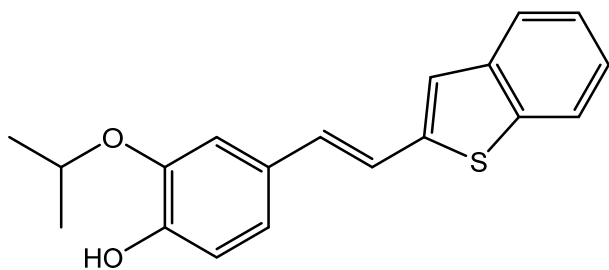

Chemical Formula: $C_{19}H_{18}O_2S$
Molecular Weight: 310.41
c Log P: 5.4
tPSA: 29.46

The general procedure was followed (3 h). The 4-bromo-2-isopropoxyphenol (144.2 mg, 0.624 mmol, 1 eq), 2-vinylbenzo[b]thiophene **31** (100 mg, 0.624 mmol, 1 eq), sodium acetate (102.4 mg, 1.248 mmol, 2 eq), and Herrmann's palladacycle (14.6 mg, 0.016 mmol, 0.025 eq) were charged to a vial containing oxygen free solvent (10% water in dimethylacetamide, 3 mL) under an argon atmosphere. The vial was sealed with a septum and the mixture was heated to 150 ºC for 3h, cooled to rt, and EtOAc (10mL) was added in one portion. The suspension was filtered through a plug of celite and the filtrate was washed successively with 0.5 N aq HCl (2 x 10 mL) and brine (2 x 10 mL). The organic layer was dried (Na_2SO_4) and solvent was removed *in vacuo* to provide a yellow oil. The oil was purified by flash column chromatography on silica gel (20% EtOAc in hexanes) to provide the pure isopropoxyphenol **46** in 90% yield as a yellow-white solid (174 mg): ^{1}H NMR (500 MHz, DMSO) δ 9.12 (s, 1H), 7.89 (d, *J* = 7.6 Hz, 1H), 7.77 (d, *J* = 7.5 Hz, 1H), 7.40 (d, *J* = 15.9 Hz, 1H), 7.39 (s, 1H), 7.37 – 7.29 (m, 2H), 7.26 (s, 1H), 7.06 (d, *J* = 8.2 Hz, 1H), 6.93 (d, *J* = 16.1 Hz, 1H), 6.82 (d, *J* = 8.2 Hz, 1H), 4.65 (dt, *J* = 12.1, 6.0 Hz, 1H), 1.30 (d, *J* = 6.0 Hz, 6H); ^{13}C NMR (126 MHz, DMSO) δ 149.07, 146.10, 143.66, 140.59, 138.31, 131.49, 128.31, 125.13, 125.07, 123.77, 122.86, 122.77, 121.26, 119.89, 116.53, 114.81, 71.15, 22.44; HRMS (ESI) (M + H), Calcd. for $C_{19}H_{19}O_2S$ 311.1106; Found 311.1110.

(E)-5-(2-(Benzo[b]thiophen-2-yl)vinyl)-2-hydroxybenzoic acid (47, Table 3-8, entry 1)
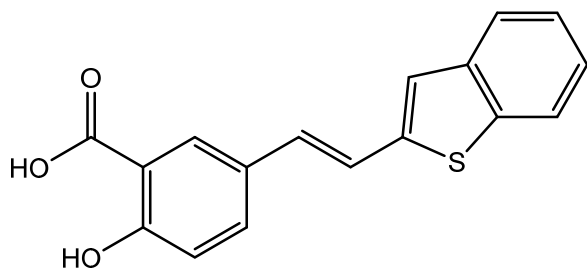
Chemical Formula: $C_{17}H_{12}O_3S$
Molecular Weight: 296.34
c Log P: 4.43
tPSA: 57.53

The general procedure was followed (3 h). The 5-bromo-2-hydroxybenzoic acid (135.4 mg, 0.624 mmol, 1 eq), 2-vinylbenzo[b]thiophene **31** (100 mg, 0.624 mmol, 1 eq), sodium acetate (102.4 mg, 1.248 mmol, 2 eq), and Herrmann's palladacycle (14.6 mg, 0.016 mmol, 0.025 eq) were charged to a vial containing oxygen free solvent (10% water in dimethylacetamide, 3 mL) under an argon atmosphere. The vial was sealed with a septum and the mixture was heated to 150 ºC for 3h, cooled to rt, and EtOAc (10mL) was added in one portion. The suspension was filtered through a plug of celite and the filtrate was washed successively with 0.5 N aq HCl (2 x 10 mL) and brine (2 x 10 mL). The organic layer was dried (Na_2SO_4) and solvent was removed *in vacuo* to provide a orange solid. The solid was purified by flash column chromatography on silica gel (50% EtOAc in hexanes) to provide the pure acid phenol **47** in 93% yield as an off-white solid (172 mg): ^{1}H NMR (300 MHz, DMSO-d6) δ 8.01 (d, $J = 1.4$ Hz, 1H), 7.89 (d, $J = 6.8$ Hz, 1H), 7.83 – 7.64 (m, 2H), 7.43 (d, $J = 16.1$ Hz, 1H), 7.42 (s, 1H), 7.37 – 7.25 (m, 2H), 6.99 (d, $J = 16.2$ Hz, 1H), 6.90 (d, $J = 8.6$ Hz, 1H). [acidic and phenolic protons not observed]; ^{13}C NMR (75 MHz, CDCl3) δ 172.13, 162.47, 143.40, 140.51, 138.42, 132.67, 130.54, 129.17, 127.02, 125.13, 125.12, 123.81, 123.30, 122.77, 120.45, 117.84, 116.20; HRMS (ESI) (M + H), Calcd. for $C_{17}H_{13}O_3S$ 297.0585; Found 297.0589.

(E)-5-(2-(benzo[b]thiophen-2-yl)vinyl)-2-methoxybenzoic acid (48, Table 3-8, entry 2)
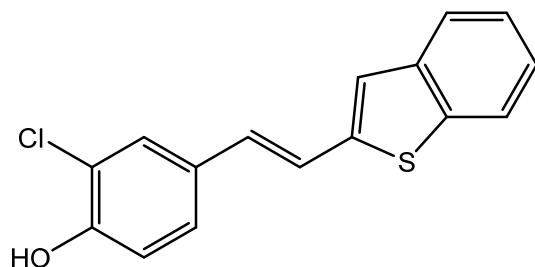

Chemical Formula: $C_{18}H_{14}O_3S$
Molecular Weight: 310.37
c Log P: 4.69
tPSA: 46.53

The general procedure was followed (3 h). The 5-bromo-2-methoxybenzoic acid (144.2 mg, 0.624 mmol, 1 eq), 2-vinylbenzo[b]thiophene **31** (100 mg, 0.624 mmol, 1 eq), sodium acetate (102.4 mg, 1.248 mmol, 2 eq), and Herrmann's palladacycle (14.6 mg, 0.016 mmol, 0.025 eq) were charged to a vial containing oxygen free solvent (10% water in dimethylacetamide, 3 mL) under an argon atmosphere. The vial was sealed with a septum and the mixture was heated to 150 °C for 3h, cooled to rt, and EtOAc (10mL) was added in one portion. The suspension was filtered through a plug of celite and the filtrate was washed successively with 0.5 N aq HCl (2 x 10 mL) and brine (2 x 10 mL). The organic layer was dried (Na_2SO_4) and solvent was removed *in vacuo* to provide a yellow solid. The solid was purified by flash column chromatography on silica gel (20% EtOAc in hexanes) to provide the pure acid methoxy **48** in 91% yield as an off-white solid (176 mg): ^{1}H NMR (300 MHz, DMSO-d6) δ 12.77 (s, 1H), 7.91 (d, J = 1.9 Hz, 2H), 7.78 (d, J = 6.9 Hz, 2H), 7.52 (d, J = 16.1 Hz, 1H), 7.45 (s, 1H), 7.34 (p, J = 7.3 Hz, 2H), 7.15 (d, J = 8.8 Hz, 1H), 7.02 (d, J = 16.1 Hz, 1H), 3.85 (s, 3H); ^{13}C NMR (75 MHz, DMSO-d6) δ 167.67, 158.27, 143.14, 140.44, 138.53, 131.50, 129.75, 129.13, 128.89, 125.29, 125.16, 123.94, 123.81, 122.82, 122.31, 121.69, 113.29, 56.38; HRMS (ESI) (M + H), Calcd. for $C_{18}H_{15}O_3S$ 311.0742; Found 311.0743.

Methyl (E)-5-(2-(benzo[b]thiophen-2-yl)vinyl)nicotinate (49, Table 3-8, entry 3)

Chemical Formula: $C_{17}H_{13}NO_2S$
Molecular Weight: 295.36
c Log P: 3.74
tPSA: 38.66

The general procedure was followed (3 h). The methyl 5-bromonicotinate (134.8 mg, 0.624 mmol, 1 eq), 2-vinylbenzo[b]thiophene **31** (100 mg, 0.624 mmol, 1 eq), sodium acetate (102.4 mg, 1.248 mmol, 2 eq), and Herrmann's palladacycle (14.6 mg, 0.016 mmol, 0.025 eq) were charged to a vial containing oxygen free solvent (10% water in dimethylacetamide, 3 mL) under an argon atmosphere. The vial was sealed with a septum and the mixture was heated to 150 ºC for 3h, cooled to rt, and EtOAc (10mL) was added in one portion. The suspension was filtered through a plug of celite and the filtrate was washed successively with water (2 x 10 mL) and brine (2 x 10 mL). The organic layer was dried (Na_2SO_4) and solvent was removed *in vacuo* to provide a brown/red solid. The solid was purified by flash column chromatography on silica gel (49% EtOAc and 1% TEA in hexanes) to provide the pure pyridine methylester **49** in 82% yield as a brown solid (151 mg): ^{1}H NMR (300 MHz, CDCl$_3$) δ 9.11 (s, 1H), 8.89 (s, 1H), 8.48 (t, $J = 1.9$ Hz, 1H), 7.81 (dd, $J = 8.1, 5.1$ Hz, 1H), 7.76 (dt, $J = 5.5, 3.2$ Hz, 1H), 7.51 (d, $J = 16.1$ Hz, 1H), 7.43 – 7.32 (m, 3H), 7.28 (s, 1H), 7.00 (d, $J = 16.1$ Hz, 1H), 4.02 (s, 3H); ^{13}C NMR (75 MHz, DMSO-d6) δ 166.96, 152.21, 149.49, 142.36, 140.60, 139.12, 133.87, 132.73, 127.40, 126.25, 125.98, 125.84, 125.53, 125.36, 124.49, 123.06, 52.82; HRMS (ESI) (M + H), Calcd. for $C_{17}H_{14}NO_2S$ 296.0745; Found 296.0739.

(E)-3-(2-(Benzo[b]thiophen-2-yl)vinyl)-5-methoxypyridine (50, Table 3-9, entry 1)
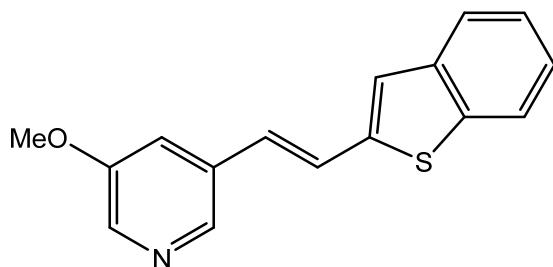
Chemical Formula: $C_{16}H_{13}NOS$
Molecular Weight: 267.35
c Log P: 3.8
tPSA: 21.59

The general procedure was followed (3 h). The 3-bromo-5-methoxypyridine (117.5 mg, 0.624 mmol, 1 eq), 2-vinylbenzo[b]thiophene **31** (100 mg, 0.624 mmol, 1 eq), sodium acetate (102.4 mg, 1.248 mmol, 2 eq), and Herrmann's palladacycle (14.6 mg, 0.016 mmol, 0.025 eq) were charged to a vial containing oxygen free solvent (10% water in dimethylacetamide, 3 mL) under an argon atmosphere. The vial was sealed with a septum and the mixture was heated to 150 ºC for 3h, cooled to rt, and EtOAc (10mL) was added in one portion. The suspension was filtered through a plug of celite and the filtrate was washed successively with water (2 x 10 mL) and brine (2 x 10 mL). The organic layer was dried (Na_2SO_4) and solvent was removed *in vacuo* to provide a yellow solid. The solid was purified by flash column chromatography on silica gel (19% EtOAc and 1% TEA in hexanes) to provide the pure methoxy pyridine **50** in 90% yield as a red/brown solid (150 mg): ^1H NMR (300 MHz, DMSO-d6) δ 8.41 (s, 1H), 8.21 (d, J = 2.6 Hz, 1H), 7.99 – 7.91 (m, 1H), 7.88 – 7.83 (m, 1H), 7.80 (d, J = 16.0 Hz, 1H), 7.70 (s, 1H), 7.57 – 7.49 (m, 1H), 7.41 – 7.32 (m, 2H), 7.06 (d, J = 16.2 Hz, 1H), 3.89 (s, 3H); ^{13}C NMR (75 MHz, CDCl₃) δ 154.29, 142.54, 140.27, 139.96, 138.79, 138.11, 133.23, 127.48, 125.65, 125.27, 124.95, 124.70, 124.23, 122.91, 118.80; HRMS (ESI) (M + H), Calcd. for $C_{16}H_{14}NOS$ 268.0796; Found 268.0789.

(E)-5-(2-(Benzo[b]thiophen-2-yl)vinyl)pyridin-3-ol (51, Table 3-9, entry 2)

Chemical Formula: $C_{15}H_{11}NOS$
Molecular Weight: 253.32
c Log P: 3.53
tPSA: 32.59

The general procedure was followed (3 h). The 5-bromopyridin-3-ol (108.6 mg, 0.624 mmol, 1 eq), 2-vinylbenzo[b]thiophene **31** (100 mg, 0.624 mmol, 1 eq), sodium acetate (102.4 mg, 1.248 mmol, 2 eq), and Herrmann's palladacycle (14.6 mg, 0.016 mmol, 0.025 eq) were charged to a vial containing oxygen free solvent (10% water in dimethylacetamide, 3 mL) under an argon atmosphere. The vial was sealed with a septum and the mixture was heated to 150 ºC for 3h, cooled to rt, and EtOAc (10mL) was added in one portion. The suspension was filtered through a plug of celite and the filtrate was washed successively with water (2 x 10 mL) and brine (2 x 10 mL). The organic layer was dried (Na_2SO_4) and solvent was removed *in vacuo* to provide a yellow solid. The solid was purified by flash column chromatography on silica gel (29% EtOAc and 1% TEA in hexanes) to provide the pure pyridine phenol **51** in 90% yield as a brown solid (142 mg): ^{1}H NMR (300 MHz, DMSO-d6) δ 10.09 (s, 1H), 8.29 (s, 1H), 8.07 (s, 1H), 7.98 – 7.90 (m, 1H), 7.85 – 7.78 (m, 1H), 7.65 (d, *J* = 16.2 Hz, 1H), 7.53 (s, 1H), 7.38 (dd, *J* = 11.7, 7.6 Hz, 3H), 7.00 (d, *J* = 16.2 Hz, 1H); ^{13}C NMR (75 MHz, CDCl₃) δ 154.29, 142.54, 140.27, 139.96, 138.79, 138.11, 133.23, 127.48, 125.65, 125.27, 124.95, 124.70, 124.23, 122.91, 118.80; HRMS (ESI) (M + H), Calcd. for $C_{15}H_{12}NOS$ 254.0640; Found 254.0645.

(E)-5-(2-(Benzo[b]thiophen-2-yl)vinyl)nicotinic acid (52, Table 3-9, entry 3)

Chemical Formula: $C_{16}H_{11}NO_2S$
Molecular Weight: 281.33
c Log P: 3.48
tPSA: 49.66
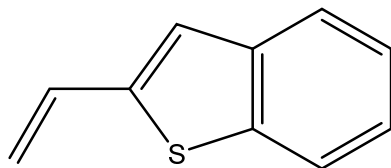
The general procedure was followed (3 h). The 5-bromonicotinic acid (126.1 mg, 0.624 mmol, 1 eq), 2-vinylbenzo[b]thiophene **31** (100 mg, 0.624 mmol, 1 eq), sodium acetate (102.4 mg, 1.248 mmol, 2 eq), and Herrmann's palladacycle (14.6 mg, 0.016 mmol, 0.025 eq) were charged to a vial containing oxygen free solvent (10% water in dimethylacetamide, 3 mL) under an argon atmosphere. The vial was sealed with a septum and the mixture was heated to 150 ºC for 3h, cooled to rt, and EtOAc (10mL) was added in one portion. The suspension was filtered through a plug of celite and the filtrate was washed successively with water (2 x 10 mL) and brine (2 x 10 mL). The organic layer was dried (Na_2SO_4) and solvent was removed *in vacuo* to provide a brown/red solid. The solid was purified by flash column chromatography on silica gel (49% EtOAc and 1% TEA in hexanes) to provide the pure pyridine acid **52** in 87% yield as a light brown solid (153 mg): ^{1}H NMR (300 MHz, $CDCl_3$) δ 13.59 (s, broad, 1H), 9.04 (s, 1H), 8.96 (s, 1H), 8.54 (s, 1H), 8.00 – 7.94 (m, 1H), 7.90 (d, *J* = 16.3 Hz, 1H), 7.87 – 7.82 (m, 1H), 7.58 (s, 1H), 7.38 (dd, *J* = 5.9, 3.2 Hz, 2H), 7.16 (d, *J* = 16.3 Hz, 1H); ^{13}C NMR (75 MHz, DMSO-d6) δ 166.66, 152.15, 149.52, 142.33, 140.20, 138.98, 133.96, 132.75, 127.29, 126.22, 126.18, 125.82, 125.62, 125.30, 124.39, 122.96; HRMS (ESI) (M + H), Calcd. for $C_{16}H_{12}NO_2S$ 282.0589; Found 282.0582.

2-vinylbenzo[b]thiophene 31 (31, Scheme 3-9)

Chemical Formula: C$_{10}$H$_8$S
Molecular Weight: 160.23

The The sodium methoxide (406.6 mg, 7.53 mmol, 1.1eq), methyltriphenylphosphonium bromide (2.69 g, 7.53 mmol, 1.1eq), and THF (25mL) were stirred under argon at rt for 0.5h. The benzo[b]thiophene-2-carbaldehyde (1.11 g, 6.84 mmol, 1eq) was dissolved in THF (5mL) and added dropwise to the solution. After 3h examination by TLC (10% EtOAc in hexanes) indicated no starting aldehyde remained and the reaction was quenched with 0.5N aq HCl (10mL). The organic layer was extracted and the aq layer was subsequently extracted with EtOAc (15mL x 2). The organic layer was washed with brine (10mL x 2), dried (Na$_2$SO$_4$), and the solvent removed *in vacuo* to yield an off-white solid. The solid was purified by flash column chromatography on silica gel (hexanes) to provide the pure thiostyrene **31** in 98% yield as a white solid (1076 mg): ^{1}H NMR (500 MHz, CDCl$_3$) δ 7.87 – 7.79 (m, 1H), 7.79 – 7.72 (m, 1H), 7.43 – 7.32 (m, 2H), 7.22 (s, 1H), 6.98 (dd, *J* = 17.3, 10.8 Hz, 1H), 5.74 (d, *J* = 17.3 Hz, 1H), 5.37 (d, *J* = 10.8 Hz, 1H); ^{13}C NMR (126 MHz, CDCl$_3$) δ 143.16, 140.08, 138.93, 130.66, 124.85, 124.48, 123.63, 123.14, 122.34, 116.00; HRMS (ESI) (M + H), Calcd. for C$_{10}$H$_9$S 161.0425; Found 161.0431.

2-Vinyl-1H-indole (55, Figure 3-4)
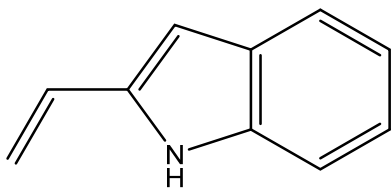
Chemical Formula: C$_{10}$H$_9$N
Molecular Weight: 143.19

The The sodium methoxide (406.6 mg, 7.53 mmol, 1.1eq), methyltriphenylphosphonium bromide (2.69 g, 7.53 mmol, 1.1eq), and THF (25mL) were stirred under argon at rt for 0.5h. The 1H-indole-2-carbaldehyde (993 mg, 6.84 mmol, 1eq) was dissolved in THF (5mL) and added dropwise to the solution. After 3h analysis by TLC (10% EtOAc in hexanes) indicated no starting aldehyde remained and the reaction mixture was quenched with water (10mL). The organic layer was extracted and the aq layer was subsequently extracted with EtOAc (15mL x 2). The organic layer was washed with brine (10mL x 2), dried (Na$_2$SO$_4$), and the solvent removed *in vacuo* to yield a yellow solid. The solid was purified by flash column chromatography on silica gel (hexanes, 1% TEA) to provide the pure indole styrene **55** in 92% yield as a yellow solid (901 mg): ^{1}H NMR (500 MHz, CDCl$_3$) δ 8.08 (s, 1H), 7.75 (d, J = 7.8 Hz, 1H), 7.44 – 7.31 (m, 2H), 7.31 – 7.23 (m, 1H), 6.82 (dd, J = 17.8, 11.2 Hz, 1H), 6.66 (s, 1H), 5.60 (d, J = 17.8 Hz, 1H), 5.38 (d, J = 11.2 Hz, 1H); ^{13}C NMR (126 MHz, CDCl$_3$) δ 136.74, 136.48, 128.88, 127.66, 122.96, 120.96, 120.28, 112.44, 110.99, 103.20; HRMS (ESI) (M + H), Calcd. for C$_{10}$H$_{10}$N 144.0813; Found 144.0845.

1-Methyl-2-vinyl-1H-indole (57, Figure 3-4)
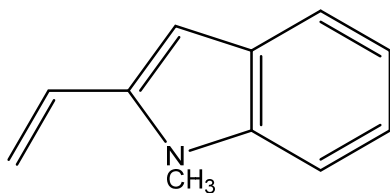
Chemical Formula: C$_{11}$H$_{11}$N
Molecular Weight: 157.22

The sodium methoxide (406.6 mg, 7.53 mmol, 1.1eq), methyltriphenylphosphonium bromide (2.69 g, 7.53 mmol, 1.1eq), and THF (25mL) were stirred under argon at rt for 0.5h. The 1-methyl-2-vinyl-1H-indole (1.07 g, 6.84 mmol, 1eq) was dissolved in THF (5mL) and added dropwise to the solution. After 3h examination by TLC (10% EtOAc in hexanes) indicated no

starting aldehyde remained and the reaction was quenched with 0.5N aq HCl (10mL). The

organic layer was extracted and the aq layer was subsequently extracted with EtOAc (15mL x 2).

The organic layer was washed with brine (10mL x 2), dried (Na_2SO_4), and the solvent removed

in vacuo to yield an off-white solid. The solid was purified by flash column chromatography on

silica gel (hexanes) to provide the pure methylindole styrene **57** in 98% yield as a white solid

(1076 mg): ^{1}H NMR (500 MHz, Acetone) δ 7.56 (d, $J = 7.8$ Hz, 1H), 7.36 (d, $J = 8.2$ Hz, 1H),

7.23 – 7.13 (m, 1H), 7.06 (t, $J = 7.4$ Hz, 1H), 6.92 (dd, $J = 17.4, 11.3$ Hz, 1H), 6.73 (s, 1H), 5.87

(dd, $J = 17.4, 1.3$ Hz, 1H), 5.36 (dd, $J = 11.3, 1.2$ Hz, 1H), 3.75 (s, 3H); ^{13}C NMR (126 MHz,

Acetone) δ 138.39, 138.06, 127.91, 126.20, 121.55, 120.24, 119.57, 115.47, 109.42, 98.63,

29.15; HRMS (ESI) (M + H), Calcd. for $C_{11}H_{12}N$ 158.0970; Found 158.0975.

2-Vinylbenzofuran (60, Figure 3-4)

Chemical Formula: $C_{10}H_8O$
Molecular Weight: 144.17

The sodium methoxide (406.6 mg, 7.53 mmol, 1.1eq), methyltriphenylphosphonium bromide

(2.69 g, 7.53 mmol, 1.1eq), and THF (25mL) were stirred under argon at rt for 0.5h. The

benzofuran-2-carbaldehyde (1.00 g, 6.84 mmol, 1eq) was dissolved in THF (5mL) and added

dropwise to the solution. After 3h examination by TLC (10% EtOAc in hexanes) indicated no

starting aldehyde remained and the reaction was quenched with 0.5N aq HCl (10mL). The

organic layer was extracted and the aq layer was subsequently extracted with EtOAc (15mL x 2).

The organic layer was washed with brine (10mL x 2), dried (Na_2SO_4), and the solvent removed

in vacuo to yield a yellow oil. The oil was purified by flash column chromatography on silica

gel (hexanes) to provide the pure benzofuran styrene **60** in 85% yield as a clear oil that slowly

solidifies in a freezer (838 mg): ^{1}H NMR (300 MHz, CDCl$_3$) δ 7.56 (d, J = 7.6 Hz, 1H), 7.49 (d, J = 8.1 Hz, 1H), 7.27 (m, 2H), 6.75 – 6.62 (dd, J = 17.4 Hz, J = 11.4 Hz, 1H), 6.63 (s, 1H), 6.00 (d, J = 17.4 Hz, 1H), 5.42 (d, J = 11.2 Hz, 1H); ^{13}C NMR (75 MHz, CDCl$_3$) δ 154.86, 154.78, 128.83, 125.30, 124.64, 122.79, 120.98, 115.71, 111.02, 104.74; HRMS (ESI) (M + H), Calcd. for C$_{10}$H$_9$O 145.0653; Found 145.0652.

5-Chloro-2-vinylbenzo[b]thiophene 31 (61, Figure 3-4)
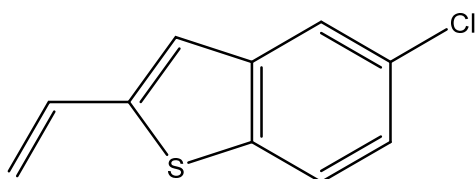
Chemical Formula: C$_{10}$H$_7$ClS
Molecular Weight: 194.68

The sodium methoxide (406.6 mg, 7.53 mmol, 1.1eq), methyltriphenylphosphonium bromide (2.69 g, 7.53 mmol, 1.1eq), and THF (25mL) were stirred under argon at rt for 0.5h. The 5-chlorobenzo[b]thiophene-2-carbaldehyde (1.35 g, 6.84 mmol, 1eq) was dissolved in THF (5mL) and added dropwise to the solution. After 3h examination by TLC (10% EtOAc in hexanes) indicated no starting aldehyde remained and the reaction was quenched with 0.5N aq HCl (10mL). The organic layer was extracted and the aq layer was subsequently extracted with EtOAc (15mL x 2). The organic layer was washed with brine (10mL x 2), dried (Na$_2$SO$_4$), and the solvent removed *in vacuo* to yield an off-white solid. The solid was purified by flash column chromatography on silica gel (hexanes) to provide the pure chloro thiostyrene **61** in 96% yield as a white solid (1278 mg): ^{1}H NMR (300 MHz, CDCl$_3$) δ 7.67 (dd, J = 5.1, 3.3 Hz, 2H), 7.29 (dt, J = 4.8, 3.9 Hz, 1H), 7.08 (s, 1H), 6.91 (dd, J = 17.3, 10.8 Hz, 1H), 5.72 (d, J = 17.3 Hz, 1H), 5.37 (d, J = 10.8 Hz, 1H); ^{13}C NMR (75 MHz, CDCl$_3$) δ 145.06, 141.16, 136.96, 130.64, 130.29, 125.13, 123.22, 123.03, 122.15, 116.78; HRMS (ESI) (M + H), Calcd. for C$_{10}$H$_8$ClS 195.0035; Found 195.0032.

5-Fluoro-2-vinylbenzo[b]thiophene 31 (62, Figure 3-4)
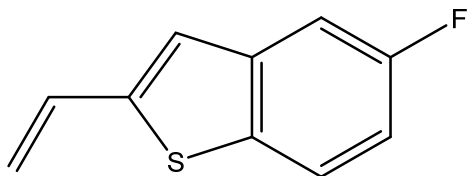
Chemical Formula: C$_{10}$H$_7$FS
Molecular Weight: 178.22

The sodium methoxide (406.6 mg, 7.53 mmol, 1.1eq), methyltriphenylphosphonium bromide (2.69 g, 7.53 mmol, 1.1eq), and THF (25mL) were stirred under argon at rt for 0.5h. The 5-fluorobenzo[b]thiophene-2-carbaldehyde (1.23 g, 6.84 mmol, 1eq) was dissolved in THF (5mL) and added dropwise to the solution. After 3h examination by TLC (10% EtOAc in hexanes) indicated no starting aldehyde remained and the reaction was quenched with 0.5N aq HCl (10mL). The organic layer was extracted and the aq layer was subsequently extracted with EtOAc (15mL x 2). The organic layer was washed with brine (10mL x 2), dried (Na$_2$SO$_4$), and the solvent removed *in vacuo* to yield an off-white solid. The solid was purified by flash column chromatography on silica gel (hexanes) to provide the pure fluoro thiostyrene **62** in 95% yield as a white solid (1159 mg): ^{1}H NMR (300 MHz, CDCl$_3$) δ 7.69 (dd, J = 8.8, 4.8 Hz, 1H), 7.38 (dd, J = 9.4, 2.4 Hz, 1H), 7.12 (s, 1H), 7.08 (dd, J = 8.8, 2.5 Hz, 1H), 6.92 (dd, J = 17.3, 10.8 Hz, 1H), 5.72 (d, J = 17.3 Hz, 1H), 5.37 (d, J = 10.8 Hz, 1H); ^{13}C NMR (75 MHz, CDCl$_3$) δ 160.94 (d, J = 241.4 Hz), 145.56 (s), 141.02 (d, J = 9.5 Hz), 134.22 (d, J = 1.5 Hz), 130.40 (s), 123.32 (d, J = 9.3 Hz), 122.60 (d, J = 4.3 Hz), 116.60 (s), 113.44 (d, J = 25.2 Hz), 109.02 (d, J = 23.0 Hz); HRMS (ESI) (M + H), Calcd. for C$_{10}$H$_8$FS 179.0331; Found 179.0334.

(E)-4-(2-(1H-Indol-2-yl)vinyl)-2-methoxyphenol (63, Table 3-11, entry 1)
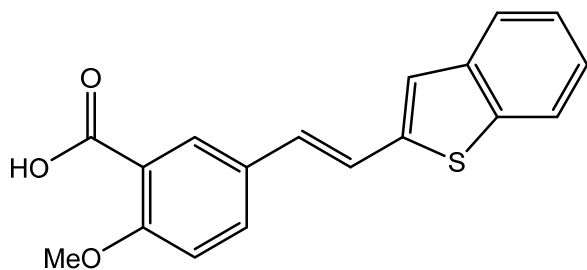

Chemical Formula: $C_{17}H_{15}NO_2$
Molecular Weight: 265.31
c Log P: 3.31
tPSA: 41.49

The general procedure was followed (3 h). The 4-bromo-2-methoxyphenol (126.7 mg, 0.624 mmol, 1 eq), 2-vinyl-1H-indole (89.4 mg, 0.624 mmol, 1 eq), sodium acetate (102.4 mg, 1.248 mmol, 2 eq), and Herrmann's palladacycle (14.6 mg, 0.016 mmol, 0.025 eq) were charged to a vial containing oxygen free solvent (10% water in dimethylacetamide, 3 mL) under an argon atmosphere. The vial was sealed with a septum and the mixture was heated to 150 ºC for 3h, cooled to rt, and EtOAc (10mL) was added in one portion. The suspension was filtered through a plug of celite and the filtrate was washed successively with water (2 x 10 mL) and brine (2 x 10 mL). The organic layer was dried (Na_2SO_4) and solvent was removed *in vacuo* to provide a yellow solid. The solid was purified by flash column chromatography on silica gel (19% EtOAc and 1% TEA in hexanes) to provide the pure indole stilbene **63** in 83% yield as a brown solid (137 mg): ^{1}H NMR (300 MHz, DMSO-d6) δ 11.27 (s, 1H), 9.18 (s, 1H), 7.47 (d, J = 7.7 Hz, 1H), 7.32 (d, J = 8.0 Hz, 1H), 7.16 (d, J = 1.4 Hz, 1H), 7.12 – 7.01 (m, 3H), 7.01 – 6.88 (m, 2H), 6.79 (d, J = 8.1 Hz, 1H), 6.49 (s, 1H), 3.85 (s, 3H); ^{13}C NMR (75 MHz, DMSO-d6) δ 148.43, 147.15, 137.79, 137.58, 129.01, 128.99, 128.17, 122.05, 120.57, 120.20, 119.55, 117.05, 116.12, 111.21, 109.60, 102.20, 56.05; HRMS (ESI) (M + H), Calcd. for $C_{17}H_{16}NO_2$ 266.1181; Found 266.1183.

(E)-2-Methoxy-4-(2-(1-methyl-1H-indol-2-yl)vinyl)phenol (64, Table 3-11, entry 2)
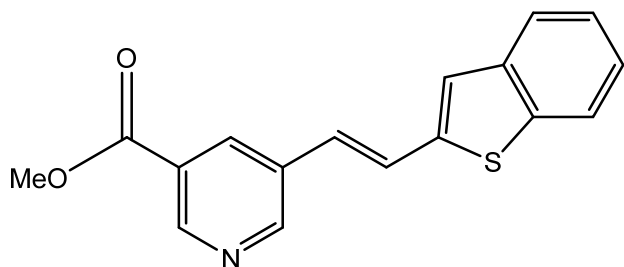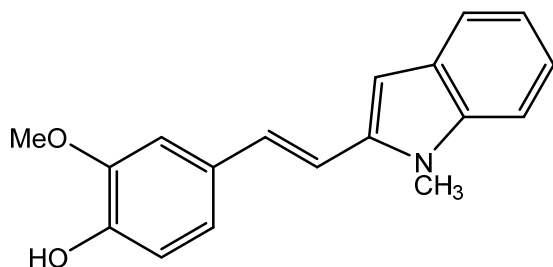

Chemical Formula: $C_{18}H_{17}NO_2$
Molecular Weight: 279.34
c Log P: 3.54
tPSA: 32.7

The general procedure was followed (3 h). The 4-bromo-2-methoxyphenol (126.7 mg, 0.624 mmol, 1 eq), 1-methyl-2-vinyl-1H-indole (98 mg, 0.624 mmol, 1 eq), sodium acetate (102.4 mg, 1.248 mmol, 2 eq), and Herrmann's palladacycle (14.6 mg, 0.016 mmol, 0.025 eq) were charged to a vial containing oxygen free solvent (10% water in dimethylacetamide, 3 mL) under an argon atmosphere. The vial was sealed with a septum and the mixture was heated to 150 ºC for 3h, cooled to rt, and EtOAc (10mL) was added in one portion. The suspension was filtered through a plug of celite and the filtrate was washed successively with water (2 x 10 mL) and brine (2 x 10 mL). The organic layer was dried (Na_2SO_4) and solvent was removed *in vacuo* to provide a brown solid. The solid was purified by flash column chromatography on silica gel (19% EtOAc and 1% TEA in hexanes) to provide the pure methylindole stilbene **64** in 89% yield as a brown solid (155 mg): ^1H NMR (300 MHz, DMSO-d6) δ 9.21 (s, 1H), 7.49 (d, *J* = 7.7 Hz, 1H), 7.42 (d, *J* = 8.2 Hz, 1H), 7.29 (d, *J* = 1.5 Hz, 1H), 7.27 – 6.94 (m, 5H), 6.84 – 6.73 (m, 2H), 3.86 (s, 3H), 3.84 (s, 3H); ^{13}C NMR (75 MHz, DMSO-d6) δ 148.33, 147.36, 139.42, 138.09, 131.45, 129.11, 128.10, 121.38, 120.91, 120.07, 119.92, 116.02, 114.64, 110.50, 110.02, 97.71, 56.20, 30.16; HRMS (ESI) (M + H), Calcd. for $C_{18}H_{18}NO_2$ 280.1338; Found 280.1345.

(E)-4-(2-([1,1'-Biphenyl]-4-yl)vinyl)-2-chlorophenol (65, Table 3-11, entry 3)
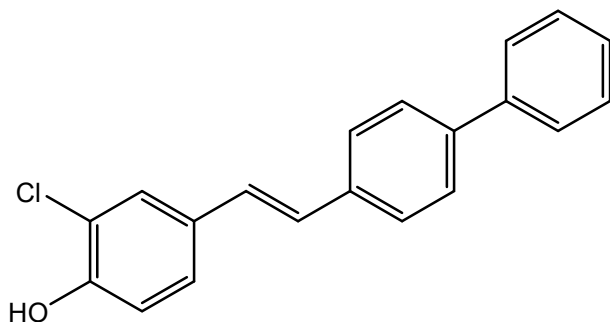
Chemical Formula: $C_{20}H_{15}ClO$
Molecular Weight: 306.79
c Log P: 6.07
tPSA: 20.23

The general procedure was followed (3 h). The 4-bromo-2-chlorophenol (129.5 mg, 0.624 mmol, 1 eq), 4-vinyl-1,1'-biphenyl (112.5 mg, 0.624 mmol, 1 eq), sodium acetate (102.4 mg, 1.248 mmol, 2 eq), and Herrmann's palladacycle (14.6 mg, 0.016 mmol, 0.025 eq) were charged to a vial containing oxygen free solvent (10% water in dimethylacetamide, 3 mL) under an argon atmosphere. The vial was sealed with a septum and the mixture was heated to 150 ºC for 3h, cooled to rt, and EtOAc (10mL) was added in one portion. The suspension was filtered through a plug of celite and the filtrate was washed successively with 0.5 N aq HCl (2 x 10 mL) and brine (2 x 10 mL). The organic layer was dried (Na_2SO_4) and solvent was removed *in vacuo* to provide a yellow oil. The oil was purified by flash column chromatography on silica gel (20% EtOAc in hexanes) to provide the pure biphenyl stilbene **65** in 84% yield as a white solid (164 mg): ^{1}H NMR (300 MHz, DMSO-d6) δ 10.35 (s, 1H), 7.75 – 7.61 (m, 7H), 7.54 – 7.31 (m, 4H), 7.27 – 7.10 (m, 2H), 6.98 (d, *J* = 8.4 Hz, 1H); ^{13}C NMR (75 MHz, DMSO-d6) δ 153.19, 140.13, 139.31, 136.91, 130.09, 129.41, 128.21, 127.88, 127.71, 127.33, 127.27, 126.88, 126.63, 120.59, 117.29; HRMS (ESI) (M + H), Calcd. for $C_{20}H_{16}ClO$ 307.0890; Found 307.0885.

(E)-2-(2-(Benzo[b]thiophen-2-yl)vinyl)-4-methoxyphenol (66, Table 3-12, entry 1)

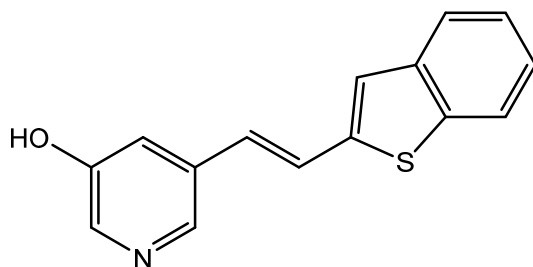Chemical Formula: $C_{17}H_{14}O_2S$
Molecular Weight: 282.36
c Log P: 4.74
tPSA: 29.46

The general procedure was followed (3 h). The 2-bromo-4-methoxyphenol (126.7 mg, 0.624

mmol, 1 eq), 2-vinylbenzo[b]thiophene **31** (100 mg, 0.624 mmol, 1 eq), sodium acetate (102.4

mg, 1.248 mmol, 2 eq), and Herrmann's palladacycle (14.6 mg, 0.016 mmol, 0.025 eq) were

charged to a vial containing oxygen free solvent (10% water in dimethylacetamide, 3 mL) under

an argon atmosphere. The vial was sealed with a septum and the mixture was heated to 150 ºC

for 3h, cooled to rt, and EtOAc (10mL) was added in one portion. The suspension was filtered

through a plug of celite and the filtrate was washed successively with 0.5 N aq HCl (2 x 10 mL)

and brine (2 x 10 mL). The organic layer was dried (Na$_2$SO$_4$) and solvent was removed *in vacuo*

to provide a yellow solid. The solid was purified by flash column chromatography on silica gel

(20% EtOAc in hexanes) to provide the pure o-hydroxy stilbene **66** in 86% yield as a bright

yellow-green solid (151 mg): ^{1}H NMR (300 MHz, DMSO-d6) δ 9.48 (s, 1H), 7.90 (d, J = 8.3 Hz,

1H), 7.84 – 7.73 (m, 1H), 7.59 (d, J = 16.2 Hz, 1H), 7.44 (s, 1H), 7.34 (p, J = 7.5 Hz, 2H), 7.21

(d, J = 16.1 Hz, 1H), 7.17 (s, 1H), 6.82 (d, J = 8.8 Hz, 1H), 6.75 (dd, J = 8.8, 2.7 Hz, 1H), 3.74

(s, 3H); ^{13}C NMR (75 MHz, DMSO-d6) δ 152.86, 149.69, 143.83, 140.53, 138.40, 126.27,

125.26, 125.16, 123.94, 123.70, 123.59, 122.81, 122.43, 117.19, 116.11, 110.99, 55.92; HRMS

(ESI) (M + H), Calcd. for C$_{17}$H$_{15}$O$_2$S 283.0793; Found 283.0790.

(E)-2-(2-(1H-Indol-2-yl)vinyl)-4-methoxyphenol (67, Table 3-12, entry 2)
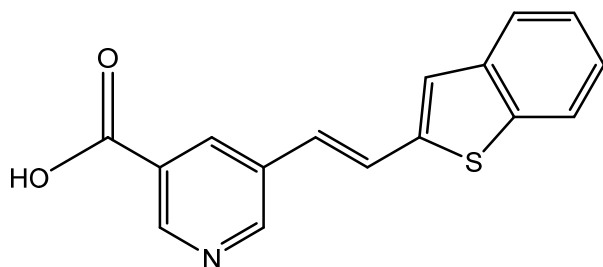
Chemical Formula: $C_{17}H_{15}NO_2$
Molecular Weight: 265.31
c Log P: 3.31
tPSA: 41.49

The general procedure was followed (3 h). The 2-bromo-4-methoxyphenol (126.7 mg, 0.624 mmol, 1 eq), 2-vinyl-1H-indole (89.4 mg, 0.624 mmol, 1 eq), sodium acetate (102.4 mg, 1.248 mmol, 2 eq), and Herrmann's palladacycle (14.6 mg, 0.016 mmol, 0.025 eq) were charged to a vial containing oxygen free solvent (10% water in dimethylacetamide, 3 mL) under an argon atmosphere. The vial was sealed with a septum and the mixture was heated to 150 ºC for 3h, cooled to rt, and EtOAc (10mL) was added in one portion. The suspension was filtered through a plug of celite and the filtrate was washed successively with water (2 x 10 mL) and brine (2 x 10 mL). The organic layer was dried (Na_2SO_4) and solvent was removed *in vacuo* to provide a yellow solid. The solid was purified by flash column chromatography on silica gel (19% EtOAc and 1% TEA in hexanes) to provide the pure indole stilbene **67** in 81% yield as a bright green solid (134 mg): ^{1}H NMR (300 MHz, DMSO-d6) δ 11.39 (s, 1H), 9.38 (s, 1H), 7.48 (d, *J* = 7.7 Hz, 1H), 7.39 (d, *J* = 16.7 Hz, 1H), 7.33 (d, *J* = 8.1 Hz, 1H), 7.23 (d, *J* = 16.7 Hz, 1H), 7.16 – 7.02 (m, 1H), 6.96 (t, *J* = 7.3 Hz, 1H), 6.81 (d, *J* = 8.8 Hz, 1H), 6.71 (dd, *J* = 8.7, 2.7 Hz, 1H), 6.52 (s, 1H), 3.74 (s, 3H); ^{13}C NMR (75 MHz, DMSO-d6) δ 152.86, 149.45, 137.91, 137.79, 128.91, 124.68, 123.08, 122.18, 120.30, 119.61, 119.56, 117.01, 115.13, 111.37, 110.70, 102.84, 55.86; HRMS (ESI) (M + H), Calcd. for $C_{17}H_{16}NO_2$ 266.1181; Found 266.1178.

(E)-2-(2-(Benzofuran-2-yl)vinyl)-4-methoxyphenol (68, Table 3-12, entry 3)
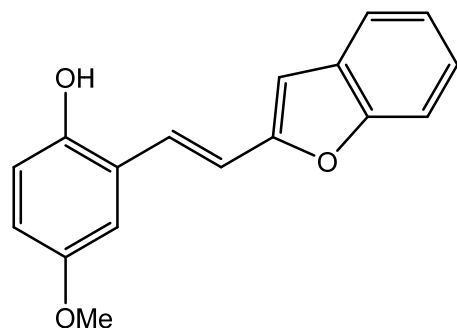
Chemical Formula: $C_{17}H_{14}O_3$
Molecular Weight: 266.30
c Log P: 3.38
tPSA: 38.69

The general procedure was followed (3 h). The 2-bromo-4-methoxyphenol (126.7 mg, 0.624 mmol, 1 eq), 2-vinylbenzofuran (90 mg, 0.624 mmol, 1 eq), sodium acetate (102.4 mg, 1.248 mmol, 2 eq), and Herrmann's palladacycle (14.6 mg, 0.016 mmol, 0.025 eq) were charged to a vial containing oxygen free solvent (10% water in dimethylacetamide, 3 mL) under an argon atmosphere. The vial was sealed with a septum and the mixture was heated to 150 ºC for 3h, cooled to rt, and EtOAc (10mL) was added in one portion. The suspension was filtered through a plug of celite and the filtrate was washed successively with 0.5 N aq HCl (2 x 10 mL) and brine (2 x 10 mL). The organic layer was dried (Na_2SO_4) and solvent was removed *in vacuo* to provide a yellow solid. The solid was purified by flash column chromatography on silica gel (20% EtOAc in hexanes) to provide the pure benzofuran stilbene **68** in 86% yield as a bright yellow solid (143 mg): ^{1}H NMR (500 MHz, DMSO) δ 9.53 (s, 1H), 7.61 (d, *J* = 7.4 Hz, 1H), 7.59 (d, *J* = 8.0 Hz, 1H), 7.51 (d, *J* = 16.4 Hz, 1H), 7.32 (d, *J* = 16.4 Hz, 1H), 7.33 – 7.29 (m, 1H), 7.26 – 7.21 (m, 1H), 7.18 (d, *J* = 3.0 Hz, 1H), 6.92 (s, 1H), 6.83 (d, *J* = 8.8 Hz, 1H), 6.76 (dd, *J* = 8.8, 3.0 Hz, 1H), 3.75 (s, 3H); ^{13}C NMR (126 MHz, DMSO) δ 155.89, 154.66, 152.85, 150.01, 129.38, 125.75, 125.10, 123.60, 123.54, 121.41, 117.24, 116.52, 116.37, 111.24, 111.06, 105.41, 55.91; HRMS (ESI) (M + H), Calcd. for $C_{17}H_{15}O_3$ 267.1021; Found 267.1026.

(E)-4-(2-(5-Chlorobenzo[b]thiophen-2-yl)vinyl)-2-methoxyphenol (69, Table 3-13, entry 1)

Chemical Formula: $C_{17}H_{13}ClO_2S$
Molecular Weight: 316.80
c Log P: 5.3
tPSA: 29.46
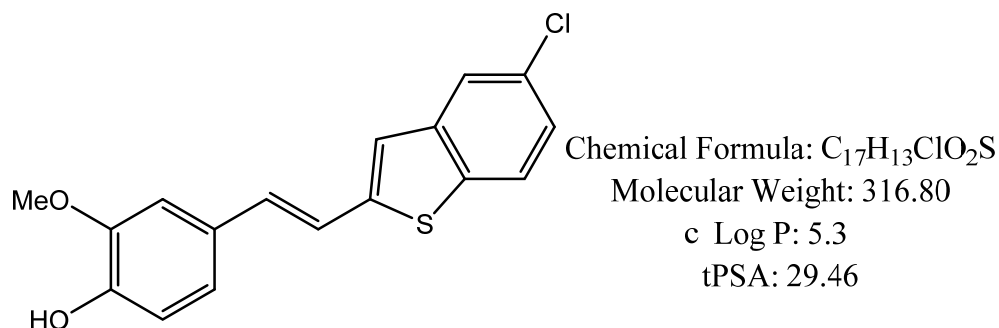
The general procedure was followed (3 h). The 4-bromo-2-methoxyphenol (127 mg, 0.624 mmol, 1 eq), 5-chloro-2-vinylbenzo[b]thiophene **31** (121.5 mg, 0.624 mmol, 1 eq), sodium acetate (102.4 mg, 1.248 mmol, 2 eq), and Herrmann's palladacycle (14.6 mg, 0.016 mmol, 0.025 eq) were charged to a vial containing oxygen free solvent (10% water in dimethylacetamide, 3 mL) under an argon atmosphere. The vial was sealed with a septum and the mixture was heated to 150 ºC for 3h, cooled to rt, and EtOAc (10mL) was added in one portion. The suspension was filtered through a plug of celite and the filtrate was washed successively with 0.5 N aq HCl (2 x 10 mL) and brine (2 x 10 mL). The organic layer was dried (Na_2SO_4) and solvent was removed *in vacuo* to provide a yellow solid. The solid was purified by flash column chromatography on silica gel (20% EtOAc in hexanes) to provide the pure 5-chlorothiophenyl analog **69** in 87% yield as a yellow solid (174 mg): ^{1}H NMR (300 MHz, DMSO-d6) δ 9.31 (s, 1H), 7.92 (d, *J* = 8.5 Hz, 1H), 7.86 (d, *J* = 1.4 Hz, 1H), 7.42 (d, *J* = 16.1 Hz, 1H), 7.37 (s, 1H), 7.33 (dd, *J* = 8.6, 1.7 Hz, 1H), 7.27 (s, 1H), 7.05 (d, *J* = 8.1 Hz, 1H), 6.97 (d, *J* = 16.1 Hz, 1H), 6.79 (d, *J* = 8.1 Hz, 1H), 3.85 (s, 3H); ^{13}C NMR (75 MHz, DMSO-d6) δ 148.37, 147.89, 145.93, 141.99, 136.78, 132.40, 130.13, 128.10, 124.87, 124.37, 123.00, 121.94, 121.22, 119.52, 116.08, 110.61, 56.12; HRMS (ESI) (M + H), Calcd. for $C_{17}H_{14}ClO_2S$ 317.0403; Found 317.0404.

(E)-2-Chloro-4-(2-(5-chlorobenzo[b]thiophen-2-yl)vinyl)phenol (70, Table 3-13, entry 2)

Chemical Formula: $C_{16}H_{10}Cl_2OS$
Molecular Weight: 321.22
c Log P: 5.99
tPSA: 20.23

The general procedure was followed (3 h). The 4-bromo-2-chlorophenol (129.5 mg, 0.624 mmol, 1 eq), 5-chloro-2-vinylbenzo[b]thiophene **31** (121.5 mg, 0.624 mmol, 1 eq), sodium acetate (102.4 mg, 1.248 mmol, 2 eq), and Herrmann's palladacycle (14.6 mg, 0.016 mmol, 0.025 eq) were charged to a vial containing oxygen free solvent (10% water in dimethylacetamide, 3 mL) under an argon atmosphere. The vial was sealed with a septum and the mixture was heated to 150 ºC for 3h, cooled to rt, and EtOAc (10mL) was added in one portion. The suspension was filtered through a plug of celite and the filtrate was washed successively with 0.5 N aq HCl (2 x 10 mL) and brine (2 x 10 mL). The organic layer was dried (Na_2SO_4) and solvent was removed *in vacuo* to provide a yellow solid. The solid was purified by flash column chromatography on silica gel (20% EtOAc in hexanes) to provide the pure 5-chlorothiophenyl analog **70** in 87% yield as an off-white solid (174 mg): ^{1}H NMR (300 MHz, DMSO-d6) δ 10.47 (s, 1H), 7.93 (d, J = 8.6 Hz, 1H), 7.87 (d, J = 1.9 Hz, 1H), 7.69 (d, J = 1.8 Hz, 1H), 7.54 – 7.28 (m, 4H), 6.98 (d, J = 8.4 Hz, 1H), 6.96 (d, J = 16.1 Hz, 1H); ^{13}C NMR (75 MHz, DMSO-d6) δ 153.77, 145.47, 141.86, 136.94, 130.59, 130.16, 129.05, 128.59, 127.27, 125.07, 124.42, 123.14, 122.66, 120.85, 120.72, 117.29; HRMS (ESI) (M + H), Calcd. for $C_{16}H_{11}Cl_2OS$ 320.9908; Found 320.9914.

(E)-2-Chloro-4-(2-(5-fluorobenzo[b]thiophen-2-yl)vinyl)phenol (71, Table 3-13, entry 3)

Chemical Formula: $C_{16}H_{10}ClFOS$
Molecular Weight: 304.76
c Log P: 5.59
tPSA: 20.23

The general procedure was followed (3 h). The 4-bromo-2-chlorophenol (129.5 mg, 0.624 mmol, 1 eq), 5-fluoro-2-vinylbenzo[b]thiophene **31** (111 mg, 0.624 mmol, 1 eq), sodium acetate (102.4 mg, 1.248 mmol, 2 eq), and Herrmann's palladacycle (14.6 mg, 0.016 mmol, 0.025 eq) were charged to a vial containing oxygen free solvent (10% water in dimethylacetamide, 3 mL) under an argon atmosphere. The vial was sealed with a septum and the mixture was heated to 150 ºC for 3h, cooled to rt, and EtOAc (10mL) was added in one portion. The suspension was filtered through a plug of celite and the filtrate was washed successively with 0.5 N aq HCl (2 x 10 mL) and brine (2 x 10 mL). The organic layer was dried (Na_2SO_4) and solvent was removed *in vacuo* to provide a yellow solid. The solid was purified by flash column chromatography on silica gel (20% EtOAc in hexanes) to provide the pure 5-fluorothiophenyl analog **71** in 92% yield as an off-white solid (175 mg): ^{1}H NMR (500 MHz, DMSO) δ 10.48 (s, 1H), 7.94 (dd, J = 8.8, 5.0 Hz, 1H), 7.70 (d, J = 2.0 Hz, 1H), 7.62 (dd, J = 9.8, 2.5 Hz, 1H), 7.47 (d, J = 15.9 Hz, 1H), 7.45 (dd, J = 8.3, 2.2 Hz, 1H), 7.40 (s, 1H), 7.20 (td, J = 9.0, 2.6 Hz, 1H), 6.99 (d, J = 8.4 Hz, 1H), 6.96 (d, J = 16.1 Hz, 1H); ^{13}C NMR (126 MHz, DMSO) δ 160.87 (d, J = 239.2 Hz), 153.75 (s), 145.89 (s), 141.64 (d, J = 9.9 Hz), 134.15 (s), 130.38 (s), 129.11 (s), 128.57 (s), 127.28 (s), 124.41 (d, J = 9.5 Hz), 123.15 (d, J = 4.2 Hz), 121.02 (s), 120.73 (s), 117.30 (s),

113.54 (d, J = 24.8 Hz), 109.32 (d, J = 23.0 Hz); HRMS (ESI) (M + H), Calcd. for $C_{16}H_{11}ClFOS$ 305.0203; Found 305.0210.

(E)-4-(2-(5-Fluorobenzo[b]thiophen-2-yl)vinyl)-2-methoxyphenol (72, Table 3-14, entry 1)

Chemical Formula: $C_{17}H_{13}FO_2S$
Molecular Weight: 300.35
c Log P: 4.9
tPSA: 29.46

The general procedure was followed (3 h). The 4-bromo-2-methoxyphenol (126.7 mg, 0.624 mmol, 1 eq), 5-fluoro-2-vinylbenzo[b]thiophene **31** (111 mg, 0.624 mmol, 1 eq), sodium acetate (102.4 mg, 1.248 mmol, 2 eq), and Herrmann's palladacycle (14.6 mg, 0.016 mmol, 0.025 eq) were charged to a vial containing oxygen free solvent (10% water in dimethylacetamide, 3 mL) under an argon atmosphere. The vial was sealed with a septum and the mixture was heated to 150 ºC for 3h, cooled to rt, and EtOAc (10mL) was added in one portion. The suspension was filtered through a plug of celite and the filtrate was washed successively with 0.5 N aq HCl (2 x 10 mL) and brine (2 x 10 mL). The organic layer was dried (Na_2SO_4) and solvent was removed *in vacuo* to provide a yellow solid. The solid was purified by flash column chromatography on silica gel (20% EtOAc in hexanes) to provide the pure 5-fluorothiophenyl analog **72** in 88% yield as a yellow solid (165 mg): ^{1}H NMR (300 MHz, DMSO-d6) δ 9.31 (s, 1H), 7.92 (dd, J = 8.7, 5.0 Hz, 1H), 7.60 (dd, J = 9.9, 2.1 Hz, 1H), 7.42 (d, J = 16.1 Hz, 1H), 7.37 (s, 1H), 7.26 (s, 1H), 7.18 (td, J = 9.1, 2.3 Hz, 1H), 7.05 (d, J = 8.2 Hz, 1H), 6.96 (d, J = 16.1 Hz, 1H), 6.79 (d, J = 8.1 Hz, 1H), 3.85 (s, 3H); ^{13}C NMR (75 MHz, DMSO-d6) δ 160.86 (d, J = 239.0 Hz), 148.36 (s), 147.84 (s), 146.33 (s), 141.75 (d, J = 9.8 Hz), 133.97 (s), 132.18 (s), 128.13 (s), 124.33 (d, J

= 9.4 Hz), 122.40 (d, J = 4.3 Hz), 121.17 (s), 119.65 (s), 116.07 (s), 113.29 (d, J = 25.1 Hz), 110.60 (s), 109.16 (d, J = 23.2 Hz), 56.11 (s); HRMS (ESI) (M + H), Calcd. for $C_{17}H_{14}FO_2S$ 301.0699; Found 301.0692.

(E)-4-(2-(Benzo[b]thiophen-2-yl)vinyl)-2-methoxyaniline (73, Table 3-14, entry 2)
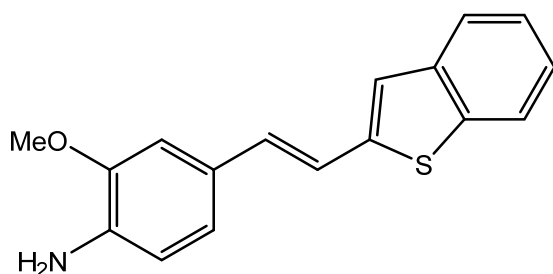
Chemical Formula: $C_{17}H_{15}NOS$
Molecular Weight: 281.37
c Log P: 4.33
tPSA: 35.25

The general procedure was followed (3 h). The 4-bromo-2-methoxyaniline (126.1 mg, 0.624 mmol, 1 eq), 2-vinylbenzo[b]thiophene **31** (100 mg, 0.624 mmol, 1 eq), sodium acetate (102.4 mg, 1.248 mmol, 2 eq), and Herrmann's palladacycle (14.6 mg, 0.016 mmol, 0.025 eq) were charged to a vial containing oxygen free solvent (10% water in dimethylacetamide, 3 mL) under an argon atmosphere. The vial was sealed with a septum and the mixture was heated to 150 ºC for 3h, cooled to rt, and EtOAc (10mL) was added in one portion. The suspension was filtered through a plug of celite and the filtrate was washed successively with water (2 x 10 mL) and brine (2 x 10 mL). The organic layer was dried (Na2SO4) and solvent was removed *in vacuo* to provide a yellow solid. The solid was purified by flash column chromatography on silica gel (20% EtOAc in hexanes) to provide the pure amine **73** in 75% yield as a brown solid (131 mg): ^{1}H NMR (300 MHz, DMSO-d6) δ 7.87 (d, J = 7.2 Hz, 1H), 7.79 – 7.69 (m, 1H), 7.40 – 7.24 (m, 4H), 7.12 (s, 1H), 6.96 (d, J = 8.1 Hz, 1H), 6.88 (d, J = 16.1 Hz, 1H), 6.62 (d, J = 8.0 Hz, 1H), 5.09 (s, 2H), 3.84 (s, 3H); ^{13}C NMR (75 MHz, DMSO-d6) δ 146.80, 144.13, 140.72, 139.15,

138.07, 132.32, 125.07, 124.91, 124.78, 123.53, 122.68, 121.85, 121.59, 117.66, 113.74, 108.72, 55.81; HRMS (ESI) (M + H), Calcd. for $C_{17}H_{16}NOS$ 282.0953; Found 282.0956.

(E)-3-(2-(5-Fluorobenzo[b]thiophen-2-yl)vinyl)-5-methoxyphenol (74, Table 3-14, entry 3)


Chemical Formula: $C_{17}H_{13}FO_2S$
Molecular Weight: 300.35
cLog P: 4.9
tPSA: 29.46

The general procedure was followed (3 h). The 3-bromo-5-methoxyphenol (126.7 mg, 0.624 mmol, 1 eq), 5-fluoro-2-vinylbenzo[b]thiophene **31** (111 mg, 0.624 mmol, 1 eq), sodium acetate (102.4 mg, 1.248 mmol, 2 eq), and Herrmann's palladacycle (14.6 mg, 0.016 mmol, 0.025 eq) were charged to a vial containing oxygen free solvent (10% water in dimethylacetamide, 3 mL) under an argon atmosphere. The vial was sealed with a septum and the mixture was heated to 150 ºC for 3 h, cooled to rt, and EtOAc (10mL) was added in one portion. The suspension was filtered through a plug of celite and the filtrate was washed successively with 0.5 N aq HCl (2 x 10 mL) and brine (2 x 10 mL). The organic layer was dried (Na_2SO_4) and solvent was removed *in vacuo* to provide a yellow solid. The solid was purified by flash column chromatography on silica gel (20% EtOAc in hexanes) to provide the pure 5-fluorothiophenyl analog **74** in 92% yield as an off-white solid (172 mg): ^1H NMR (300 MHz, DMSO-d6) δ 9.54 (s, 1H), 7.97 – 7.93 (m, 1H), 7.65 – 7.61 (m, 1H), 7.54 – 7.43 (m, 2H), 7.25 – 7.19 (m, 1H), 6.93 (d, J = 15.9 Hz, 1H), 6.70 (s, 1H), 6.62 (s, 1H), 6.31 (s, 1H), 3.75 (s, 3H); ^{13}C NMR (75 MHz, DMSO-d6) δ 160.86 (d, J = 237.75 Hz), 161.15 (s), 159.14 (s), 145.55 (s), 141.54 (d, J = 9.75 Hz), 138.42 (s),

134.31 (s), 131.87 (s), 124.46 (d, J = 9.75 Hz), 123.87 (d, J = 3.75 Hz), 122.78 (s), 113.74 (d, J =

24.75 Hz), 109.42 (d, J = 22.5 Hz), 106.94 (s), 103.63 (s), 102.18 (s), 55.53 (s); HRMS (ESI) (M

+ H), Calcd. for $C_{17}H_{14}FO_2S$ 301.0699; Found 301.0703.

CHAPTER FOUR

ALDOL CONDENSATION PRODUCTS AND THEIR ANTIMICROBIAL PROPERTIES: STRUCTURALLY SIMILAR TO BOTH STILBENOID AND ACRYLATE ACTIVE COMPOUNDS

I. INTRODUCTION AND BACKGROUND.
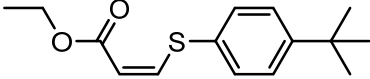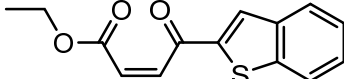
The aldol condensation is a carbon-carbon bond forming reaction in which an enol or enolate anion reacts with a carbonyl compound, followed by dehydration to give a conjugated enone (Scheme 4-1).[165] This reaction was discovered in the late 19th century and is still one of the most important C-C bond forming reactions in organic chemistry.[165-166] It is particularly useful for large-scale preparation of materials due to the inexpensive reagents involved.

Scheme 4-1: Aldol condensation mechanisms.
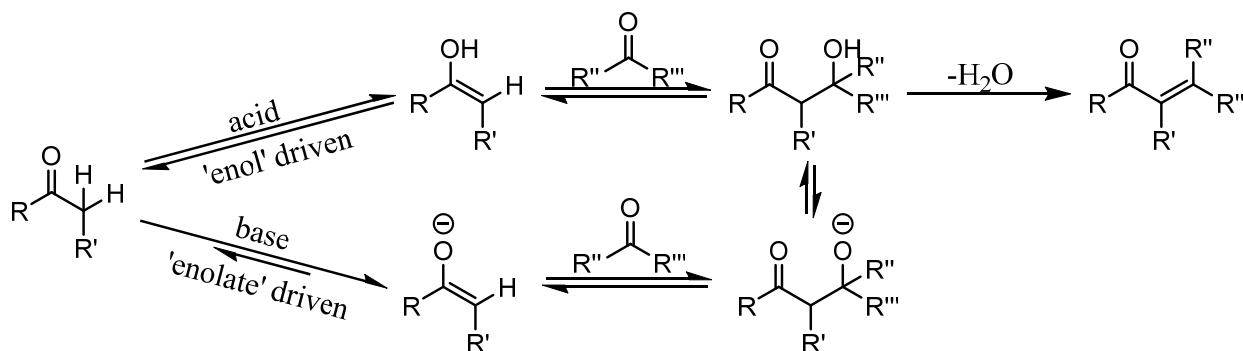
Earlier in the SAR of stilbenoid compounds it was discovered that another class of compounds, acrylates, also showed activity against mycobacteria with lead compound **SK-04-57ac**.[120] These acrylates were further investigated through a second SAR and compounds with potent activity against gram-positive bacteria and mycobacteria were discovered, the most active being **TI-01-37ac** (Table 4-1).[91]

Table 4-1: Acrylate activity[a].

Bacterial Strain	SK-04-57ac	TI-01-37ac
S. aureus	>512	1
E. faecalis	>512	2
P. aeruginosa	>128	64
E. coli	>512	16
M. intracellulare	N.T.	4
M. chelonae	N.T.	8
M. fortuitum	N.T.	16
M. kansasii	N.T.	8
M. avium	N.T.	16
M. smegmatis	16	4
M. marinum	N.T.	4

[a]Values in µg/mL, N.T. = not tested

Interestingly **TI-01-37ac** was the first compound synthesized that had broad activity against gram-positive, gram-negative, and mycobacterium species. This activity, however, was later linked to the cytotoxic nature of these compounds, which was likely due to the Michael-acceptor nature of the α,ß-unsaturated carbonyl system.[167-170] In fact, when the carbon double-bond was saturated, the compound which resulted had no activity for all strains tested – unlike saturation of the stilbene double-bond which, while it decreased potency, were still active (see

Chapter 2). Analysis of further NMR studies confirmed that various anilines formed Michael adducts with these acrylate compounds in an irreversible manner.

Regardless, modification of the stilbenoid core structure to include this α,ß-unsaturated function was still explored to see if further modification of the bridge portion was advantageous, accompanied by less cytotoxicity.

II.   CHEMISTRY AND RESULTS.

As discussed in the Introduction, the aldol condensation can lead to α,ß-unsaturated compounds with a wide variety of substituents. In this case, the focus was on modification of the current lead compounds by changing the 'bridge' portion to include this α,ß-unsaturated function (Figure 4-1).

Figure 4-1: Target compounds.
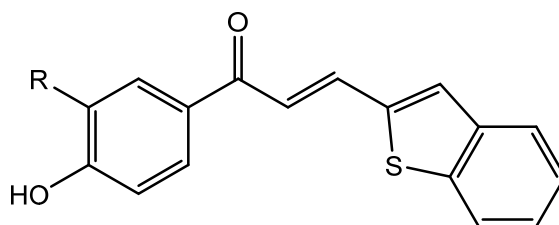
Synthesis of such compounds would require an aldehyde and a methyl ketone, and since benzo[b]thiophene-2-carbaldehyde (**18**) was already synthesized and the phenolic methyl ketones were commercially available and relatively inexpensive, a series of three new analogs were prepared (Table 4-2).

Synthesis of these analogs was found to proceed smoothly and purification by crystallization from ethanol resulted in isolation of analytically pure material with no need of flash column chromatography. These enone compounds, however, were found to be less soluble

then the already rather insoluble stilbenoid compounds in suitable *in vitro*/*in vivo* solvent preparations.
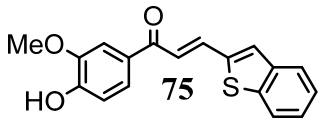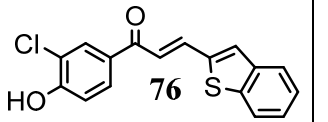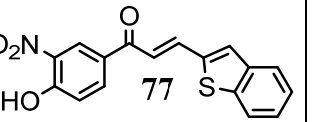
Table 4-2: Synthesis of enone analogs.

Compound	R	Yield (%)
75	OMe	89
76	Cl	93
77	NO$_2$	81

Examination of the data in Table 4-3 details the activity of these enone analogs against the standard bacterial strains tested. The methoxy analog **75** retained similar activity to its related stilbenoid analog **36** while the chloro analog **76** does not retain activity compared to the potent stilbenoid analog **38**. This variability might be explained by the poor solubility of these compounds, however, since considerable effort is required to keep them in solution. The nitro analog **77**, for example, readily precipitates out of a DMSO/water solution even at very low concentrations which certainly could hinder MIC screens. However, it is important to note that both the methoxy analog **75** and the nitro analog **77** were potent antimicrobials against *S. aureus*.

Table 4-3: Enone analog activities.[a]

Bacterial Strain	MeO... HO... **75** S	Cl... HO... **76** S	O₂N... HO... **77** S
S. aureus	0.5	128	2
E. faecalis	1	64	128
P. aeruginosa	>128	>128	>128
E. coli	>128	>128	>128
M. intracellulare	16	32	64
M. chelonae	32	32	64
M. fortuitum	16	64	128
M. kansasii	8	128	>128
M. avium	16	64	128
M. smegmatis	32	>128	128
M. marinum	4	16	64

[a]Values in µg/mL

Synthesis of more analogs in this series was halted due to a number of reasons. First and foremost, availability of substituted methyl ketones, although generally inexpensive, was low. Secondly, the low solubility exhibited by these compounds was not promising, since they seemed even less soluble then the related stilbenoid derivatives. Finally, cytotoxicity concerns from both studies on **75** (to be discussed in the next chapter) and previous studies on **SK-04-57ac** and **TI-01-37ac** were considered a hurdle based on the Michael acceptor pharmacophore in these analogs.

III. CONCLUSION.

In conclusion, a synthesis of enone compounds structurally similar to the lead stilbenoid compounds was accomplished using an aldol condensation reaction. Three different analogs were synthesized, one of which had similar activity to the best current lead compounds. This analog, **75**, was structurally related to an earlier lead compound **36**. Given this potent activity, **75** was also considered a lead compound in this work, however it may not be as desirable as the related stilbene analogs due to cytotoxicity and solubility issues.

These issues, however, could be addressed in future SAR work by removing the α,ß-unsaturated nature of this compound via various methods to determine whether or not activity can be retained, especially if this substitution leads to better water solubility.

As also noted, selection of methyl ketones was rather low, however they could also be conveniently synthesized via a Fries rearrangement reaction or other similar reactions. Attempts to synthesize the enone analogs of the stilbenoids with different substitution patterns (**66**, **67**, and **68** for example) may also prove useful in future work.

IV. EXPERIMENTAL.

1. *In vitro* MIC assays. (completed by Dr. Bill Schwan)

In vitro minimum inhibitory concentration (MIC) determinations were performed according to the Clinical and Laboratory Standards Institute (CLSI) guidelines,[115] for most of the bacteria that were screened. Tetracycline, ciprofloxacin, and erythromycin were included as control antibiotics for the gram-positive bacterial MIC values and correlated with established MIC values. All anti-Mycobacterium activity evaluations were performed using MIC assays in

Middlebrook 7H9 broth with 10% oleic acid albumin dextrose complex (OADC) as previously described.[114] Rifampin was used as the positive control for the mycobacterial MIC values. All MIC numbers are a compilation of the geometric means from three separate runs. For the broad characterization against *S. aureus*, strains that have been typed by a variety of means were used by Schwan et al[116].

2. Characterization data.

Both 1H and 13C NMR's were recorded on a Bruker DPX-300 or DRX-500 instrument where noted. HRMS scans were recorded on a Shimadzu LCMS-IT-TOF or similar instruments run at the Shimadzu Analytical Chemistry Center of Southeastern Wisconsin. *In silico* cLogP values and topological polar surface area values (tPSA) were calculated with ChemBioDraw Ultra v. 14.

(E)-3-(Benzo[b]thiophen-2-yl)-1-(4-hydroxy-3-methoxyphenyl)prop-2-en-1-one (75, Table 4-3, entry 1)
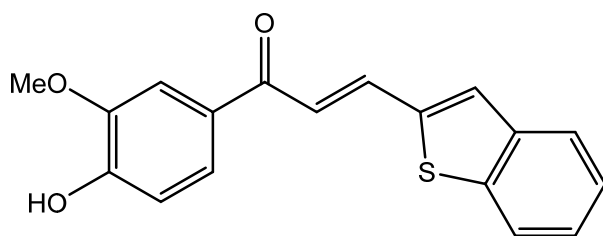
Chemical Formula: $C_{18}H_{14}O_3S$
Molecular Weight: 310.37
c Log P: 4.1
tPSA: 46.53

The 1-(4-hydroxy-3-methoxyphenyl)ethan-1-one (500mg, 3 mmol, 1eq) and benzo[b]thiophene-2-carbaldehyde (500mg, 3.08 mmol, 1.02eq) were dissolved in acetone (20mL) at rt. Potassium hydroxide (338mg, 6 mmol, 2eq, crushed) was added in one portion and the slurry heated to reflux. The reaction was followed by TLC (50% EtOAc in hexanes, silica gel) and was complete after 3 h. The mixture was cooled with an ice bath and quenched with excess aq 0.5N HCl (50mL). The solution which resulted was extracted with EtOAc (50mL x 2), washed with brine

(50mL x 2), and the organic layer was dried (Na$_2$SO$_4$). The solvent was removed *in vacuo* which resulted in in a yellow solid (921mg, 99% yield). The solid was further purified by crystallization from hot EtOH to give yellow microcrystals of the enone **75** (834mg, 90.5% recovery, 89% overall yield):^{1}H NMR (300 MHz, DMSO-d6) δ 10.14 (s, 1H), 7.98 (d, *J* = 15.1 Hz, 1H), 8.04 – 7.92 (m, 2H), 7.92 – 7.84 (m, 1H), 7.74 (dd, *J* = 8.3, 1.8 Hz, 1H), 7.60 (d, *J* = 1.7 Hz, 1H), 7.60 (d, *J* = 15.3 Hz, 1H), 7.49 – 7.37 (m, 2H), 6.95 (d, *J* = 8.3 Hz, 1H), 3.88 (s, 3H); ^{13}C NMR (75 MHz, DMSO-d6) δ 186.84, 152.62, 148.35, 140.52, 140.11, 139.95, 136.35, 130.33, 129.62, 126.89, 125.54, 125.03, 124.20, 123.52, 123.16, 115.55, 111.97, 56.13; HRMS (ESI) (M + H), Calcd. for C$_{18}$H$_{15}$O$_3$S 311.0742; Found 311.0749.

(E)-3-(Benzo[b]thiophen-2-yl)-1-(3-chloro-4-hydroxyphenyl)prop-2-en-1-one (76, Table 4-3, entry 2)
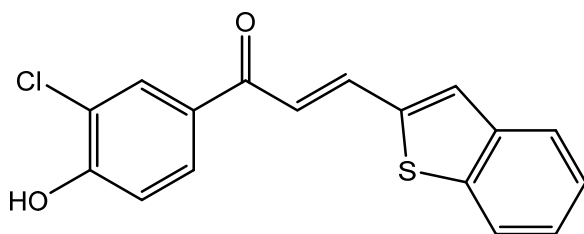
Chemical Formula: C$_{17}$H$_{11}$ClO$_2$S
Molecular Weight: 314.78
cLog P: 4.79
tPSA: 37.3

The 1-(3-chloro-4-hydroxyphenyl)ethan-1-one (512mg, 3 mmol, 1eq) and benzo[b]thiophene-2-carbaldehyde (500mg, 3.08 mmol, 1.02eq) were dissolved in acetone (20mL) at rt. Potassium hydroxide (338mg, 6 mmol, 2eq, crushed) was added in one portion and the slurry heated to reflux. The reaction was followed by TLC (50% EtOAc in hexanes, silica gel) and was complete after 3 h. The mixture was cooled with an ice bath and quenched with excess aq 0.5N HCl (50mL). The solution which resulted was extracted with EtOAc (50mL x 2), washed with brine (50mL x 2), and the organic layer was dried (Na$_2$SO$_4$). The solvent was removed *in vacuo* which resulted in a yellow solid (932mg, 98.6% yield). The solid was further purified by crystallization

from hot EtOH to give yellow microcrystals of enone **76** (878mg, 94% recovery, 93% overall

yield): ^{1}H NMR (300 MHz, DMSO-d6) δ 11.32 (s, 1H), 8.16 (d, J = 2.0 Hz, 1H), 8.06 – 7.95 (m,

3H), 8.00 (d, J = 14.6 Hz, 1H), 7.95 – 7.85 (m, 1H), 7.61 (d, J = 15.3 Hz, 1H), 7.51 – 7.37 (m,

2H), 7.12 (d, J = 8.5 Hz, 1H); ^{13}C NMR (75 MHz, DMSO-d6) δ 186.22, 158.46, 140.38, 140.31,

139.90, 137.07, 131.19, 130.67, 130.03, 129.89, 126.99, 125.57, 125.11, 123.20, 123.16, 120.87,

116.97; HRMS (ESI) (M + H), Calcd. for $C_{17}H_{12}ClO_2S$ 315.0247; Found 315.0243.

(E)-3-(Benzo[b]thiophen-2-yl)-1-(4-hydroxy-3-nitrophenyl)prop-2-en-1-one (77, Table 4-3,

entry 3)
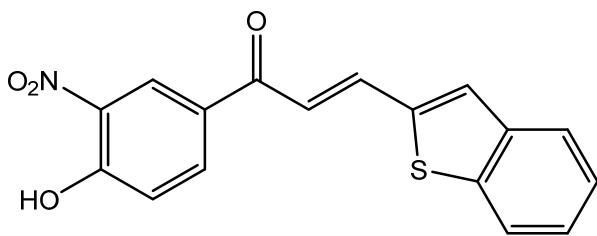
Chemical Formula: $C_{17}H_{11}NO_4S$
Molecular Weight: 325.34
tPSA: 89.11

The 1-(4-hydroxy-3-nitrophenyl)ethan-1-one (543.5mg, 3 mmol, 1eq) and benzo[b]thiophene-2-

carbaldehyde (500mg, 3.08 mmol, 1.02eq) were dissolved in acetone (20mL) at rt. Potassium

hydroxide (338mg, 6 mmol, 2eq, crushed) was added in one portion and the slurry heated to

reflux. The reaction was followed by TLC (50% EtOAc in hexanes, silica gel) and was complete

after 3 h. The mixture was cooled with an ice bath and quenched with excess aq 0.5N HCl

(50mL). The solution which resulted was extracted with EtOAc (50mL x 2), washed with brine

(50mL x 2), and the organic layer was dried (Na2SO4). The solvent was removed *in vacuo* which

resulted in a yellow solid (898mg, 92% yield). The solid was further purified by trituration in

hot EtOH to give a yellow powder of enone **77** (795mg, 88.5% recovery, 81% overall yield): [1]H

NMR (300 MHz, DMSO-d6) δ 12.04 (s, 1H), 8.62 (d, J = 2.0 Hz, 1H), 8.27 (dd, J = 8.8, 2.1 Hz,

1H), 8.03 (d, J = 15.3 Hz, 1H), 7.98 (d, J = 10.2 Hz, 2H), 7.92 – 7.85 (m, 1H), 7.60 (d, J = 15.2

Hz, 1H), 7.50 – 7.36 (m, 2H), 7.26 (d, J = 8.8 Hz, 1H); ^{13}C NMR (75 MHz, DMSO-d6) δ

185.98, 156.13, 140.40, 140.22, 139.84, 137.75 (2C), 135.05, 131.09, 128.84, 127.08, 126.66,

125.56, 125.16, 123.18, 122.69, 119.63; HRMS (ESI) (M + H), Calcd. for $C_{17}H_{12}NO_4S$

326.0487; Found 326.0483.

CHAPTER FIVE

ACTIVITY OF THE MOST ACTIVE COMPOUNDS AGAINST RESISTANT

STRAINS, PRELIMINARY CYTOXICITY DATA, PRELIMINARY *IN VIVO*

DATA, MECHANISM OF ACTION STUDIES, AND PRELIMINARY

PHARMACOPHORE MODELING

I.   INTRODUCTION.

As previously discussed, twelve new compounds with activity averaging below 10

µg/mL for gram-positive strains were identified in this SAR study. These compounds, pictured

below (Figure 5-1), represent potential targets for further pharmaceutical development.

Figure 5-1: Most active compounds from this SAR.
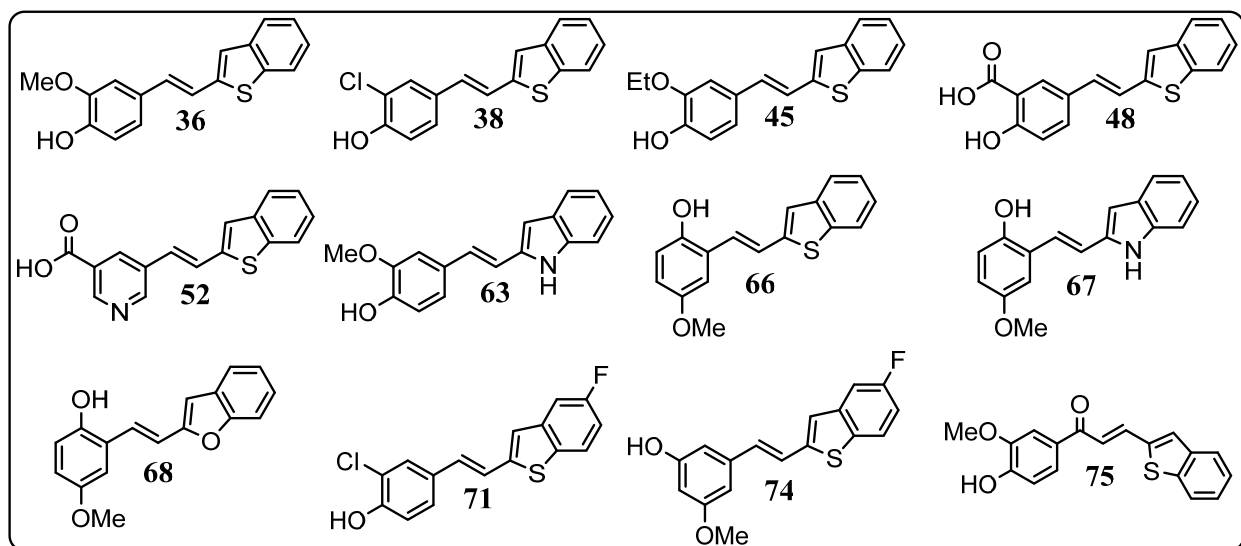
The two gram-positive strains tested, however, were not antibiotic resistant strains and

are very susceptible to current antibiotics on the market. This necessitates screening these

compounds against tested against drug-resistant strains to confirm they have potential use as a new and novel therapy for bacterial infections which may not develop resistance.

A combination of eight antibiotic resistant strains were used by Schwan et al. in a follow-up assay to test many of the most active compounds from this series. These include three strains of multi-drug resistant *S. aureus* (MDR-MRSA), rifampin resistant *S. aureus* (RifR-MRSA), vancomycin intermediate resistant *S. aureus* (VISA-MRSA), community-acquired methicillin resistant *S. aureus* (MW2-MRSA), and two strains of vancomycin resistant enterococci (VRE). These strains represent some of the most highly virulent and deadly gram-positive bacterial strains and many are contracted and isolated directly from hospitalized patients.

Controls in the form of commercial pharmaceutical antibiotics were also tested in these same assays. These eight doctor-prescribed antibiotics are Gentamicin, Ampicillin, Oxacillin, Ciprofloxacin, Vancomycin, Erythromycin, Tetracycline, and Rifampin. These drugs were earlier described in Chapter 1 and represent some of the most prescribed drugs that are currently on the market.

It was previously determined (Chapter 2) that SK-03-92, a parent compound to the analogs described in this work, was not cytotoxic both *in vitro* and *in vivo*, even up to doses as high as 2000 mg/kg. While these results only indicate that SK-03-92 is not cytotoxic, it also implies that analogs of SK-03-92 should not be cytotoxic as well, especially if no known cytotoxic moieties are introduced into the core structure. Preliminary cytotoxicity studies were still initiated with five of the most active analogs along with vancomycin as a control. These analogs were tested in a CellTiter-Glo toxicity assay to determine cell viability after incubation with the compounds of interest.

Preliminary *in vivo* work has also been done on both compounds **36** and **38**. This work involved a lung infection model with mice dosed either intranasal (IN) or intraperitoneal (IP). The results from this preliminary work are somewhat promising, but it is clear much work has yet to be done in this area to confirm it with a reasonable n value.

Mechanism/mode of action studies were also initiated on both compounds **36** and **38**. In general, the most convenient method of determining the mode of action is by first isolating strains that acquire resistance via repeated sub-MIC dosing. Genomic information on these resistant strains can then be used to determine the mode of action and perhaps even the mechanism of action.

Finally, a preliminary pharmacophore model was constructed from compounds synthesized in this work. Pharmacophore models can be extremely helpful in the design of new compounds and in the elucidation of a binding site, if one exists.

II. RESULTS AND DISCUSSION.

1. *In vitro* data on resistant strains.

As mentioned five compounds were selected for preliminary cytotoxicity studies. These five compounds were some of the mostactive compounds found via this new SAR and include compounds **36**, **38**, **45**, **48**, and **75** (Table 5-1). Of these compounds **36**, **38**, and **75** are by far the most active with MIC values around 1 μg/mL, rivaling that of Vancomycin and other commercial antibiotics. Excitingly, all compounds tested were equipotent against the drug-resistant strains, with no significant variability. **In fact, for the particularly dangerous Vancomycin resistant enterococci (VRE) strains, the analogs prepared via this SAR were more active then every commercial antibiotic tested aside from Rifampin.** As discussed

earlier, Rifampin develops resistance very quickly and thus is used only in the most dire situations, generally co-administered with another antibiotic.

The variability of commercialized antibiotics seen in Table 5-1 is also alarming and speaks to the delicate nature of antibiotic use in infections. These strains are prevalent in hospital settings and it is unnerving to know that a particularly resistant strain could be the cause of an infection. It is not possible by visible inspection to discern whether or not a particular infection is caused by drug-resistant bacteria or susceptible non-drug resistant strains. The choice of the wrong treatment can both increase the likelihood of spreading the infection to other patients, as well as conferring additional resistance to the bacteria in question. Doctors must choose the best course of treatment and wait for biological testing of the bacterial strain in question to determine whether it is drug-resistant or not; this is valuable time and, unfortunately, the cause for the alarming number of deaths from MRSA infections.[171-173]

Table 5-1: MICs and Cell Viability of some of the most active compounds developed in this work.

Compound	Minimum Inhibitory Concentration (Values in µg/mL)								Cell Viability (Values in µM)
	MC7827 MDR MRSA	MC7769 RifR MRSA	MC7606 MDR MRSA	MC7846 VISA MRSA	MC7583 MDR MRSA	MW2 MRSA	VRE 1	VRE 14	IC50 HEK293-T
36	**1**	**1**	**1**	**1**	**0.5**	**0.5**	**1**	**1**	**>150**
38	**0.5**	**0.5**	**0.5**	**1**	**0.5**	**0.5**	**0.5**	**0.5**	**>150**
75	**1**	**1**	**1**	**1**	**0.5**	**0.5**	**1**	**1**	**48.18**
45	8	8	16	8	8	8	16	32	>150
47	8	8	8	8	4	8	4	4	>150
Gentamicin	8	32	16	32	ND	ND	128	128	ND
Ampicillin	32	>128	>128	8	ND	ND	128	128	ND
Oxacillin	4	4	4	4	ND	ND	128	128	ND
Ciprofloxacin	>128	>128	32	128	ND	ND	8	64	ND
Vancomycin	1	1	1	4	ND	ND	32	128	>150
Erythromycin	>128	>128	128	>128	ND	ND	>128	128	ND
Tetracycline	32	0.5	64	0.25	ND	ND	4	64	ND
Rifampin	0.015	>128	0.003	0.006	ND	ND	0.25	0.006	ND
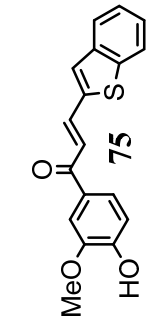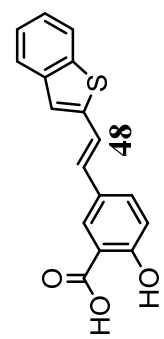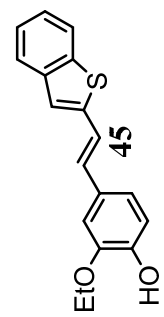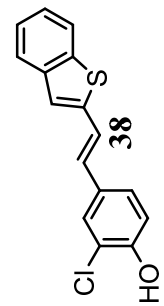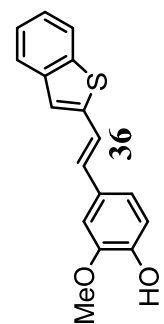
Examination of the data in Table 5-1 clearly indicated that of the five compounds tested, all were very potent against the dangerous drug-resistant strains of gram-positive bacteria. Particularly interesting is the potent activity against VRE strains of which only rifampin was found to be more active than four of the five selected analogs. In fact, the MIC of chloro stilbene analog **38** was almost universally under 1 μg/mL, better then all controls except for rifampin. **However, in the rifampin resistant strain, MC7769 RifR MRSA, compound 38 was 256-fold more active than rifampin!**

The methoxy enone analog **75** was also very active against all strains tested, similarly to compound **38**, however **75** was also slightly cytotoxic. This was almost certainly due to the Michael-acceptor nature of this compound, similar to the acrylate compounds discussed earlier. It should be noted, however, that 1 μg/mL for **75** is a MIC value of approximately 3 μM, therefore the antimicrobial activity was still 16-fold greater than the IC_{50} of the cytotoxicity. This indicated that while cytotoxicity might be a problem *in vivo*, the activity of the compound is likely due, in major part, to the antibiotic properties rather than the cytotoxic properties. Alternative analogs such as **36** and **38** are both very potent and also show no inherent cytotoxicity, so they remain as promising treatment options which require further testing.

An additional thirteen analogs were also tested against these resistant strains (Table 5-2). A number of these analogs were earlier found to be active against the non-resistant strains, but some were also tested as negative controls, for example phenol analog **34** and chloro analog **39**. These compounds have not yet been tested for cytotoxicity, but again it is important to note that prior data heavily implies that these compounds, none of which are Michael-acceptors, should be safe and non-cytotoxic.

Of these analogs, many were found to exhibit average MIC values of less than 10 µg/mL against these resistant strains. This is potent enough to explore further. The ring D chloro analogs **69** and **70** interestingly exhibited very potent activity against MC7606 MDR MRSA, however, were clearly less active against the other strains. This strange behavior has not yet been explained, however difficulty solubilizing these compounds was noted and perhaps the lack of activity is due more to solubility issues, further testing of these compounds is on-going in bacterial assays that do not rely upon aqueous dissolution of an analog prior to treatment. The ring D fluoro analog **74** was the most active compound to date, with some MIC value in the 0.25 µg/mL range.

Table 5-2: MIC values of some other active (and inactive) compounds from this work.

Compound	Minimum Inhibitory Concentrations (values in μg/mL)							
	MC7827 MDR MRSA	MC7769 RifR MRSA	MC7606 MDR MRSA	MC7846 VISA MRSA	MC7583 MDR MRSA	MW2 MRSA	VRE 1	VRE 14
34	>128	>128	64	>128	128	>128	>128	>128
39	>128	>128	>128	>128	>128	>128	>128	>128
42	16	2	16	32	16	32	1	16
63	8	2	1	2	16	1	4	4
64	16	4	2	4	16	4	32	32
66	4	1	2	2	8	4	4	4
67	8	4	2	4	8	4	8	8
68	8	2	4	4	16	4	4	4
69	>128	>128	1	>128	16	8	>128	128
70	128	32	0.25	64	64	>128	4	4
71	8	4	0.5	8	4	4	4	2
72	16	8	1	8	4	4	32	64
74	0.25	0.5	0.25	0.5	0.5	0.5	1	1

34 39 42 63 64 66, X = S 67, X = O 68, X = NH 69 70 71 72 74
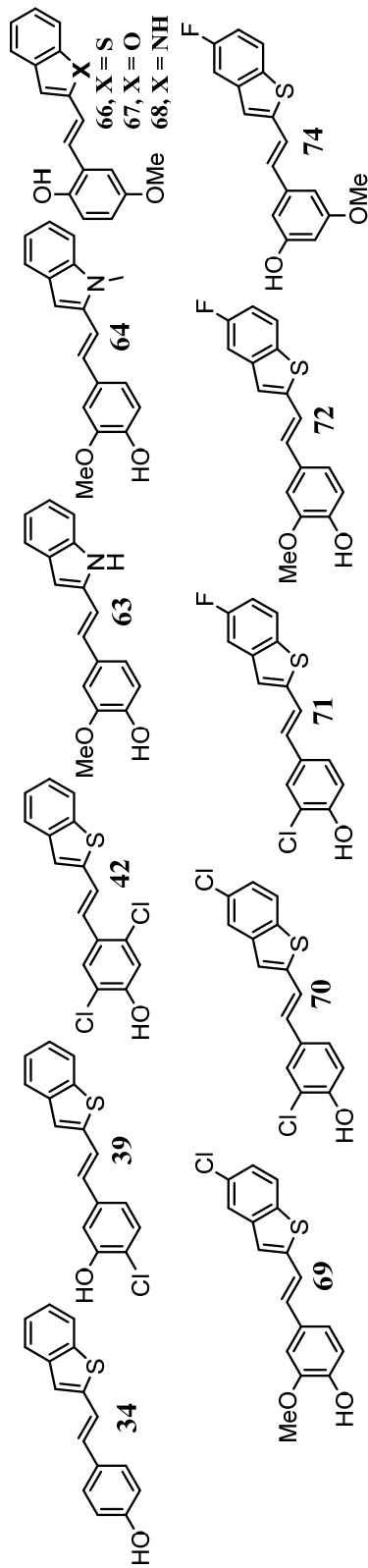
## 2.	Preliminary *in vivo* data on 36 and 38.

While this *in vitro* data is promising, *in vivo* data is also necessary since potential drugs must be efficacious in mammalian systems. Preliminary *in vivo* studies were completed on two of the most active compounds that were developed early in this SAR, **36** and **38**.

These compounds were tested in a *S. aureus* lung infection model at a dosage of 10 mg/kg intranasally. The results from this preliminary *in vivo* exposure indicate that a number of problems still exist with these compounds *in vivo* in regard to vehicle choice, similarly to SK-03-92, however they seemed to be at least partially efficacious (Table 5-3).

Table 5-3: Preliminary *in vivo* data from a lung infection model.

Trial	Mouse 1	Mouse 2	Mouse 3	Mouse 4
Vehicle	0	0	0	---
Vehicle + MRSA	D	D	D	4
36 + MRSA	D	3-4	4	D
38 + MRSA	D	D	4	D

D = dead; 0=healthy; 1=less active; 2=hunched, less active;
3=ruffled, hunched, inactive; 4- ruffled, hunched, inactive, gaunt

A major problem in this experiment was dissolving the compound prior to treatment, as mentioned. According to the team administering the compound, in this particular experiment compound **36** seemed more soluble in the vehicle whereas **38** was not fully dissolved. For intranasal exposure undissolved solids entering the lungs can cause lung trauma which can actually increase the spread of infection and indeed **38** was found to not be particularly efficacious in this experiment. The compound **36**, which was seemingly more well-dissolved, appeared to have a small effect on the outcome of the mice. Two mice survived as opposed to just one and one of the mice had a better clinical score then what was seen in the MRSA control.

Based on these findings, another preliminary *in vivo* experiment was planned using these two compounds.

A second *in vivo* experiment followed in a similar fashion to the first, however in this case compounds were also administered intraperitoneal (IP) as well as intranasal (IN) (Figure 5-2). Similarly to the first trial, our collaborators had issues fully dissolving the compounds, in this case the 'more soluble' solution obtained was that of compound **38**.

Figure 5-2: *In vivo* lung infection model data.

Intranasal route
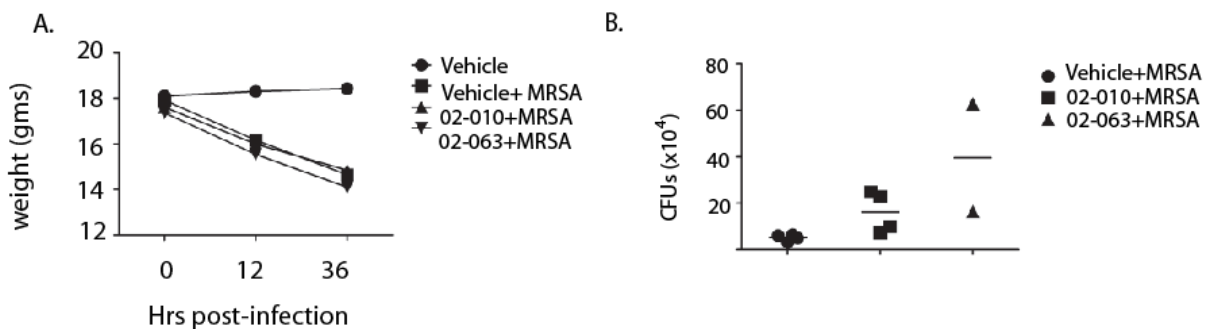
Intraperitoneal Route
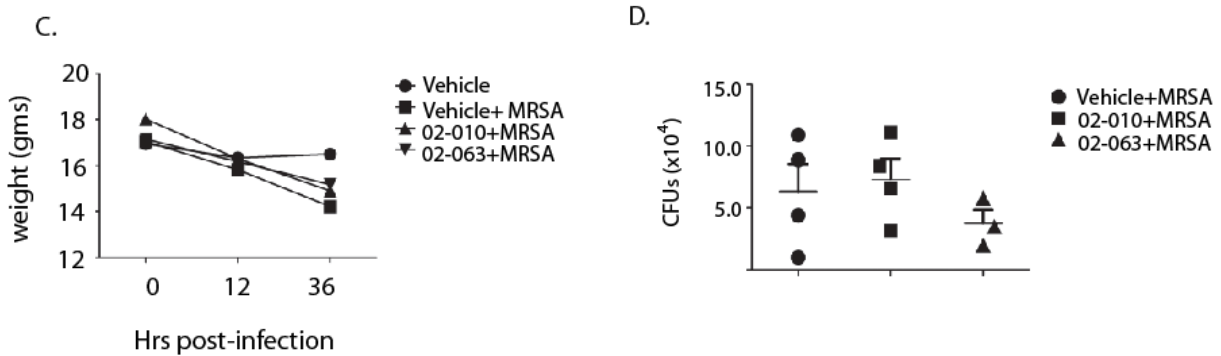
02-010 = **36**; 02-063 = **38**

Our collaborators again noted that the poor results of IN exposure were likely due to solids left undissolved in the administered vehicle. In this case, however, a modest decrease in CFUs was noted when the 'better dissolved' **38** was administered IP. Although these results are far from ideal, they at least show that these compounds have some efficacy *in vivo* and if explored with a better vehicle or if more active compounds with a better pharmacokinetic profile are discovered these could potentially lead to a drug that is efficacious in these *in vivo* lung infection models.

3.   Mechanism of action studies.

One of the original goals of this work was to not only develop more potent analogs, but also study the mode and/or mechanism of action (MoA) of these compounds. Mode of action refers to the cellular site of action, such as cell walls or protein synthesis. Mechanism of action refers to the actual cellular target, such as a specific protein target. As an example, penicillin's mode of action is inhibition of bacterial cell wall synthesis, while it is mechanism of action is inhibition of penicillin-binding proteins (PBPs). This distinction is often not clarified in sources and the acronym MoA is used interchangeably to discuss the cellular response to these compounds. It should be noted that resistance to a mode of action for a specific compound is never observed, but rather resistance to its mechanism of action. Consequently, there is an important distinction between the two in terms of actual cellular response. In the case of this work, no distinction is necessary since data on both mode and mechanism of action have proven difficult to obtain for the reasons described below.

MoA studies are often carried out dosing a bacterial colony several times with the compound of interest in a concentration slightly lower than its MIC value. In theory, the bacteria

that survive these repeated exposures may have some desirable trait that permits them to be resistant or at least partially resistant to the compounds employed. The repeated exposure helps ensure that these resistant groups are allowed to reproduce and repopulate faster than the drug susceptible groups.[174-176] Once a resistant colony is grown, genomic testing can reveal definitive differences between them and the wild-type susceptible strains, these differences can help identify the mode of action and perhaps even the mechanism of action.[177]

Although this general method is useful for determining MoA, it has one critical problem – if resistance can be easily conferred *in vitro*, it will inevitably be conferred in nature. This indeed has been a major problem for antibiotics, as previously noted, the number of resistant strains is growing at an incredible rate.

In the case of these novel stilbenoid compounds, however, many repeated *in vitro* experiments have been attempted over the course of several years and resistant strains have not been produced. **This may indicate that these compounds act on a number of different pathways and that when one builds resistance, the others are still susceptible to the compounds. It may also indicate that the target itself cannot, or at least does not easily, confer resistance.**

While this is exciting in terms of actual pharmaceutical use, it has made determining the mechanism of action much more difficult and in fact not possible, to date. As of yet, no MoA has been determined for these compounds, however as mentioned earlier based on the lack of activity against gram-negative bacteria they may prove to act on a target associated with cell walls. One important result from this work, however, was the determination that both methoxy analog **36** and chloro analog **38** were both bactericidal on all tested strains of *S. aureus*.

Bactericidal non-cytotoxic agents are far more advantageous since they have the ability to clear the infection rather than simply slowing it down in contrast to bacteriostatic agents.

A survey of recent literature[178] suggests that "macromolecular synthesis assay" studies can be used to help deduce plausible modes of action. Administration of an increasing *in vitro* dose of a compound and measuring the bacterial production of key cellular products such as DNA, RNA, protein, cell wall and lipid synthesis can be used along with a known control antibiotic that acts on those pathways to help determine if the compound acts on any of those specific sites. Methods such as these can potentially help lead to the discovery of the MoA for this new and novel library of compounds. These studies rely on radioactive biomarkers, such as tritiated thymidine, to determine bacterial uptake after treatment.

One potential target for these novel compounds, however, are tyrosinases. Tyrosinases are enzymes that catalyze the formation of quinones, leading to a downstream process that ends with the synthesis of melanin. Stilbenes and other similar structures are known tyrosinase inhibitors[179]. In mammals, tyrosinases are known to be restrictive and selective to only L-form tyrosines, however is other life forms, bacteria for example, they are much less restrictive[180]. This mechanism can explain the similar activity seen with analogs **36** and **SK-03-92** (see Scheme 5-1).

Scheme 5-1: Potential reaction of tyrosinase with 36 and SK-03-92.
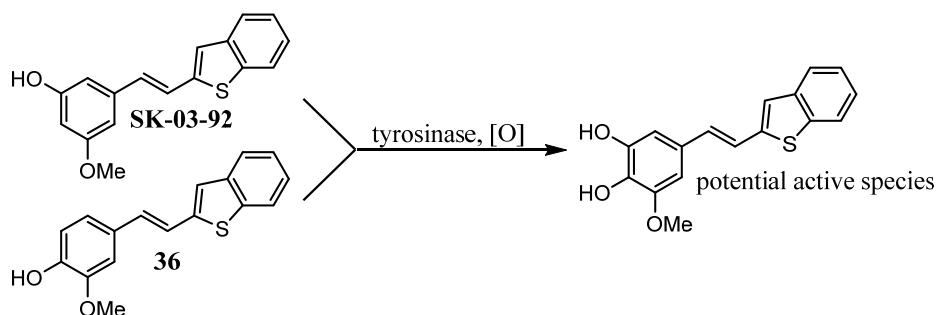
4.   Preliminary pharmacophore model and size/volume discussion.

It was previously noted that an increase/decrease in activity was seen when certain characteristics such as substitution pattern or size of the molecule was altered in a number of ways. A pharmacophore model can take these activities and correlate them with the structure of the compound to help elucidate clear structural similarities between active compounds and inactive compounds. This model can also estimate positions of key molecular sites, assuming these compounds act on a specific target, which can permite a more directed SAR study. All of the compounds from this work along with a number of compounds from the previous SAR were used to create a preliminary pharmacophore model (Figure 5-3).

Figure 5-3: Pharmacophore model of all compounds described in this work.
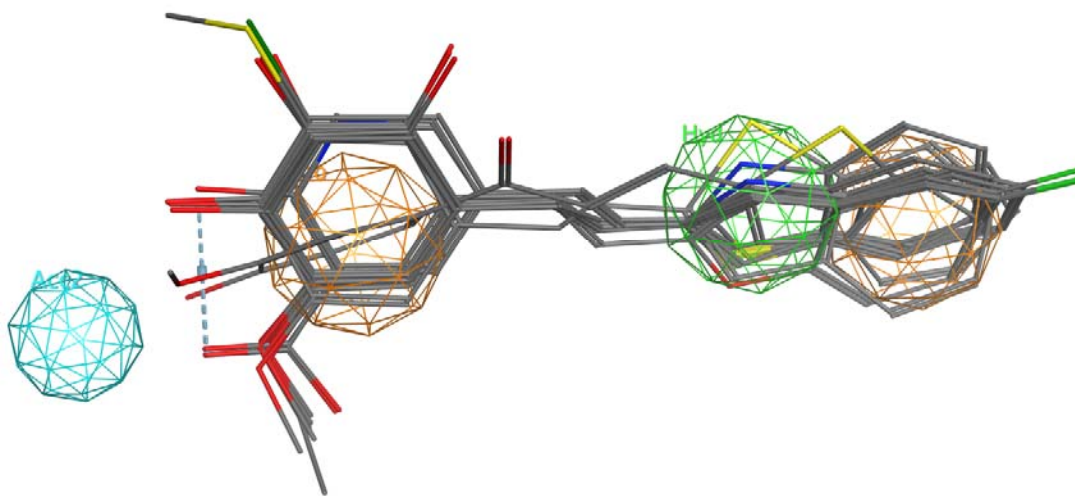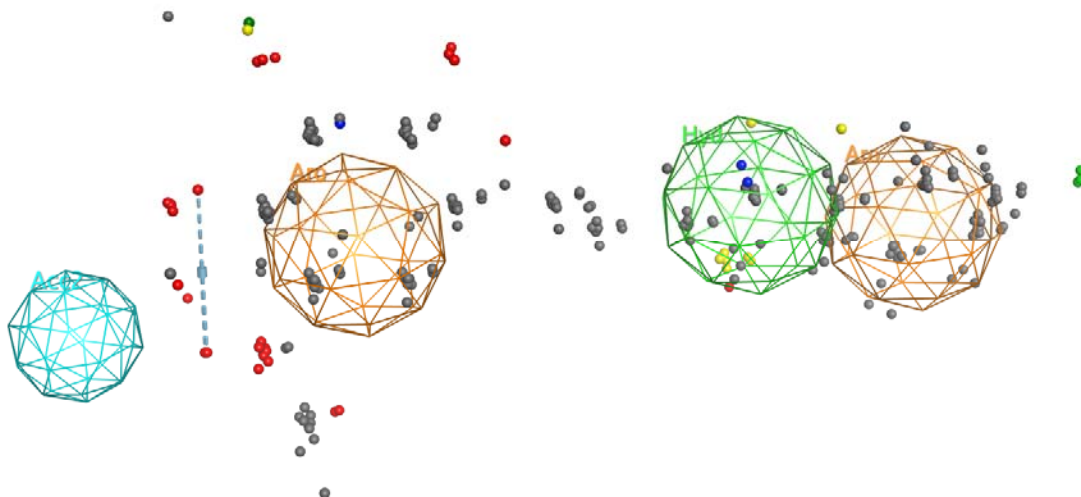
This model is based on a selection of 52 different ligands, many from this work, including active and inactive ligands. The software used to construct this pharmacophore (MOE) applies a binary selection process; consequently, for this study any compounds with activity under 10 µg/mL were considered active while any compounds with activity over 10 µg/mL were considered inactive. The consideration of all compounds with an MIC equal to or less than 32 µg/mL as active has resulted in much lower accuracy scores. Although the sample size is low and it is still unclear whether or not these compounds act via a specific site, the pharmacophore analysis still appears rather accurate. "Acc2" (teal) refers to an acceptor site, which satisfies the phenolic H-bond donor seen in most active compounds. "Hyd" (green) refers to a hydrophobic area while "Aro" (orange) refers to aromatic regions. Because the "bridge" portion and ring B/C portion were for the most part kept static, it is not clear that these regions are necessarily hydrophobic or aromatic regions in terms of the target.

What is most interesting with the model is the orientation of ring A in comparison to ring B/C. Analysis of the model indicated that these areas are preferably at a slight angle to each other rather than planar. Earlier in Figure 2-6 the idea that orientation of rings B/C was briefly discussed. It should be noted if a naphthene group were slightly rotated, as in the pharmacophore model above, the fit would not be as strong as the 5-membered ring heterocycles. This may explain the lower activity seen in the case of naphthene and other related 6-member rings. This model is at best a coarse simplification of a potential binding site, assuming again that it is only one specific site. However, if in the future a mode of action is determined, pharmacophore analysis may be useful in determining the exact mechanism of action. Additionally, this model can potentially help with future SAR studies.

Earlier the activities of **36**, **44**, **45**, and **46** were compared based on the size of alkoxy substituents; this is easier to view with 3D energy minimized conformers as shown in Figure 5-4. The orientation of these ligands was calculated in a similar manner to the pharmacophore model discussed above.

Figure 5-4: Alkoxy size and activity comparison.
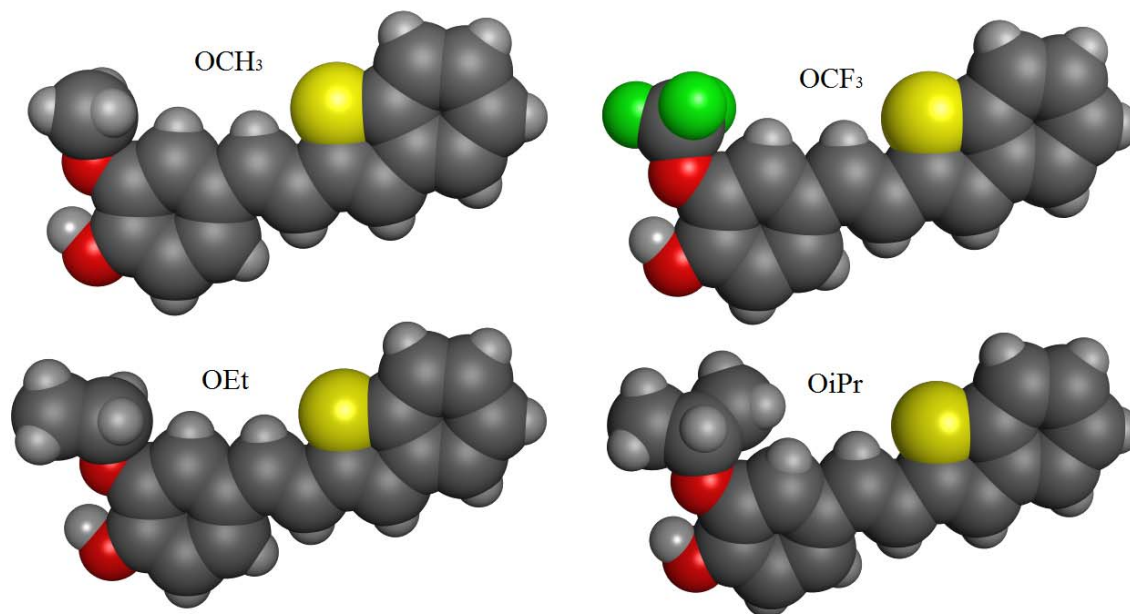
At the top-left is compound **36**, one of the most active compounds discovered with an MIC of 1 µg/mL. At the top-right is compound **44**, the CF$_3$ analog of **36** that was found to be completely inactive. The CF$_3$ group is of similar size to isopropyl, with some studies placing it in between the size of ethyl and isopropyl groups.[181] This is in agreement with the lack of activity observed for this compound. The bottom-right is the ethoxy analog **45**, which still retains potent activity of 8 µg/mL. From the 3D structure one can see that the ethyl group is off-set from ring A, however it is somewhat in-line with ring B/C, giving an overall smaller molecular volume then the isopropoxy **46** (bottom-left). Based on this analysis, it seems that one of the methyl groups in the isopropyl analog **46** may push out into an undesirable space that greatly affects the activity, whereas the methyl group in the ethoxy analog **45** does not to such an extent.

It was also postulated earlier that the activity of the enone compounds was also based on size or volume. Analysis of the energy minimization and alignment of these molecules indicated that they are all relatively similar, thus the stark difference in activity (Table 4-3) is likely due to electronic character or perhaps even solubility issues (Figure 5-5). Indeed, it was observed that these compounds were very insoluble, and incomplete solvation prior to plating could lead to a discrepancy in the results.

Figure 5-5: Overlay of enone compounds 75, 76, and 77.
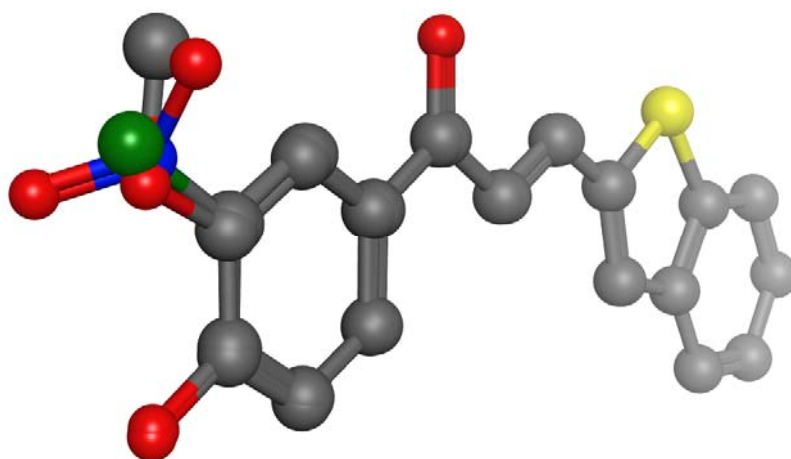
The red with grey represents the OCH$_3$ group from compound **75**, green represents the chloro group from compound **76**, and blue with red represents the NO$_2$ group from compound **77**. Although the NO$_2$ is slightly larger and out-of-plane, it was still found to retain activity against *S. aureus* whereas the smaller chloro group was completely inactive. These factors may revolve around solubility issues as well, so these compounds have also been sent to a screening

system which should be able to perform the assay in 100% DMSO, limiting any issues related to solubility. These results are still pending.

5. Future SAR studies.

From the results gathered from this SAR, it is believed that further SAR development should lead to both a more diverse selection of active compounds and even more potent analogs. Preferably a new SAR should also focus on the solubility issues observed from this study. Particular focus on the indole analogs may lead to active compounds with better overall PK characteristics as well.

As discussed, this was the second SAR study executed on this antimicrobial project. In the first SAR study, just <u>four</u> compounds were discovered with MIC values below 10 µg/mL. In this work <u>fourteen</u> new analogs with average MIC values below 10 µg/mL have been developed. As the SAR develops, it is clear a higher percentage of active compounds can be discovered, hopefully with a better solubility profile.

Considerable effort was taken in this SAR to make broad new changes to discover the scope of activity. It was found that two different new substitution patterns from this work resulted in very active antimicrobials, while the original substitution patterns also retains activity. These patterns, shown below (Figure 5-6), should be priorities for future SAR work.

Figure 5-6: Ring A lead fragments.
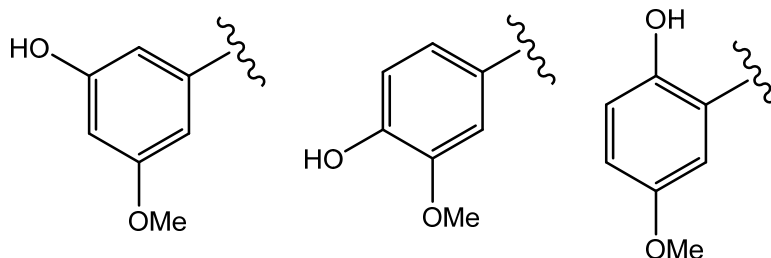
Additionally, new ring B/C ligands were also tested with positive results. Benzofuran substituted and indole substituted ligands both proved to provide active analogs, substituted thianaphthenes also gave potent compounds. Substitution of the thianapthene at other positions is of importance and awaits further study. Some of these ring B/C lead fragments are shown in Figure 5-7.

Figure 5-7: Ring B/C lead fragments.

R = F, Cl, OMe, etc...
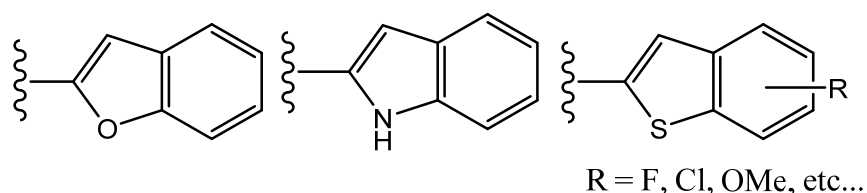
Based on this alone, many new compounds can be synthesized. The focus on more soluble pyridine analogs may also be approached. Since analog **52** already exhibited some activity, substitution on the various ring B/C fragments may prove valuable in the ring A pyridine series (Figure 5-8).

Figure 5-8: Pyridine suggestions.

R = F, Cl, OMe, etc...
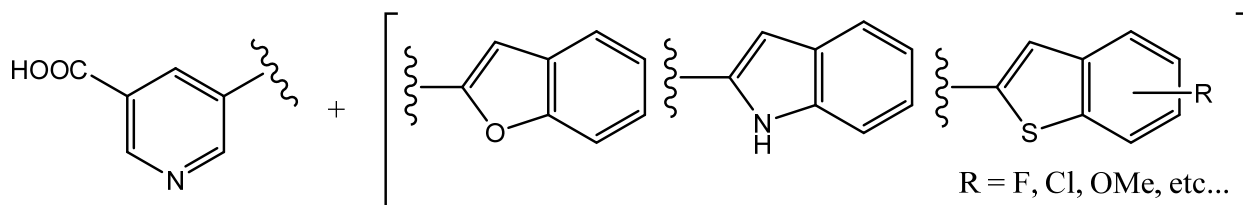
It was also earlier determined that SK-03-92 had poor metabolic stability and was rapidly metabolized in rodents. A more thorough analysis of metabolic products through *in vitro* metabolism studies may shed light on the positions which are most readily metabolized. Techniques can be used to substitute these positions (F, for example) in the hope that a more

metabolically stable analog still retains potent activity. These compounds may be more advantageous in *in vivo* applications.

III.   CONCLUSION.

In conclusion, stilbenes with potent activity against wild-type gram-positive bacteria were assayed against a number of resistant strains of gram-positive bacteria and were found to be very potently active against all drug-resistant strains tested. Analysis of these results suggest that these compounds may be a new class of antibiotics and perhaps even work by a novel mechanism of action. Controls in the form of commercial antibiotics were also tested against the same strains and the compounds synthesized in this work show a clear significance when compared to each control.

Some preliminary *in vivo* testing of two of the most active compounds discovered in this work was also initiated. The results from this preliminary work were mixed. The compounds did seem to show efficacy in infection models, but solubility issues were a problem and currently it is unknown whether the new compounds also have other poor PK properties similar to the first lead compound SK-03-92. The results do indicate that further testing with different analogs may prove beneficial, especially analogs with improved solubility. The metabolism of these compounds should also be investigated to determine if other simple substitutions can both inhibit metabolism while also retaining activity.

Pharmacophore analysis of the ligands discovered in this work was also explored. The model itself seems accurate with respect to our SAR approach and can potentially help lead a new SAR in developing more potent analogs. Additionally, 3D energy-minimized models can

clearly identify activity relationships between different analogs. These issues must be constantly weighed when deciding on which new analogs to synthesize.

Finally, this SAR has opened up a new pathway for further SAR development. Suggestions on which compounds may prove to be potently active and/or more soluble were discussed. A focus on the three main substitution patterns seems most prudent, along with the active pyridine ring A substitution pattern. The coupling of these factors with a diverse set of ring B/C ligands should both enrich the SAR and give rise to a number of new active compounds with better clinical qualities.

REFERENCES

1. Brachman, P. S., Infectious diseases--past, present, and future. *Int J Epidemiol* **2003,** *32* (5), 684-6.

2. Durrant, R. E., The bubonic plague. *Sci Am* **1988,** *259* (1), 8.

3. Cunha, C.; Pedrosa, V. L.; Dias, L. C.; Braga, A.; Chrusciak-Talhari, A.; Santos, M.; Penna, G. O.; Talhari, S.; Talhari, C., A historical overview of leprosy epidemiology and control activities in Amazonas, Brazil. *Rev Soc Bras Med Trop* **2015,** *48 Suppl 1*, 55-62.

4. Daniel, T. M., The history of tuberculosis. *Respir Med* **2006,** *100* (11), 1862-70.

5. Riedel, S., Plague: from natural disease to bioterrorism. *Proc (Bayl Univ Med Cent)* **2005,** *18* (2), 116-24.

6. Legendre, D. P.; Muzny, C. A.; Swiatlo, E., Hansen's disease (Leprosy): current and future pharmacotherapy and treatment of disease-related immunologic reactions. *Pharmacotherapy* **2012,** *32* (1), 27-37.

7. Hamzaoui, A.; Yaalaoui, S.; Tritar Cherif, F.; Slim Saidi, L.; Berraies, A., Childhood tuberculosis: a concern of the modern world. *Eur Respir Rev* **2014,** *23* (133), 278-91.

8. Utzinger, J.; Keiser, J., Urbanization and tropical health--then and now. *Ann Trop Med Parasitol* **2006,** *100* (5-6), 517-33.

9. Tognotti, E., Lessons from the history of quarantine, from plague to influenza A. *Emerg Infect Dis* **2013,** *19* (2), 254-9.

10. Aminov, R. I., A brief history of the antibiotic era: lessons learned and challenges for the future. *Front Microbiol* **2010,** *1*, 134.

11.   Dube, E.; Vivion, M.; MacDonald, N. E., Vaccine hesitancy, vaccine refusal and the anti-vaccine movement: influence, impact and implications. *Expert Rev Vaccines* **2015,** *14* (1), 99-117.

12.   Davies, J.; Davies, D., Origins and evolution of antibiotic resistance. *Microbiol Mol Biol Rev* **2010,** *74* (3), 417-33.

13.   Atamna, H.; Krugliak, M.; Shalmiev, G.; Deharo, E.; Pescarmona, G.; Ginsburg, H., Mode of antimalarial effect of methylene blue and some of its analogues on Plasmodium falciparum in culture and their inhibition of P. vinckei petteri and P. yoelii nigeriensis in vivo. *Biochem Pharmacol* **1996,** *51* (5), 693-700.

14.   Wright, P. M.; Seiple, I. B.; Myers, A. G., The evolving role of chemical synthesis in antibacterial drug discovery. *Angew Chem Int Ed Engl* **2014,** *53* (34), 8840-69.

15.   Krafts, K.; Hempelmann, E.; Skorska-Stania, A., From methylene blue to chloroquine: a brief review of the development of an antimalarial therapy. *Parasitol Res* **2012,** *111* (1), 1-6.

16.   Bentley, R., Different roads to discovery; Prontosil (hence sulfa drugs) and penicillin (hence beta-lactams). *J Ind Microbiol Biotechnol* **2009,** *36* (6), 775-86.

17.   Finkelstein, R.; Birkeland, J. M., The Mode of Action of Sulfanilamide and Prontosil. *Science* **1938,** *87* (2263), 441-2.

18.   Skold, O., Sulfonamide resistance: mechanisms and trends. *Drug Resist Updat* **2000,** *3* (3), 155-160.

19.   O'Grady, F. W., Mode of action of antibacterial agents. *Proc R Soc Med* **1971,** *64* (5), 529-33.

20.   Moellering, R. C., Jr., Mechanism of action of antimicrobial agents. *Clin Obstet Gynecol* **1979,** *22* (2), 277-83.

21.   Weinstein, M. J.; Luedemann, G. M.; Oden, E. M.; Wagman, G. H.; Rosselet, J. P.; Marquez, J. A.; Coniglio, C. T.; Charney, W.; Herzog, H. L.; Black, J., Gentamicin, a New Antibiotic Complex from Micromonospora. *J Med Chem* **1963,** *6*, 463-4.

22.   Bath, A. P.; Walsh, R. M.; Bance, M. L.; Rutka, J. A., Ototoxicity of topical gentamicin preparations. *Laryngoscope* **1999,** *109* (7 Pt 1), 1088-93.

23.   Choi, J. S.; Kim, C. K.; Lee, B. J., Administration-time differences in the pharmacokinetics of gentamicin intravenously delivered to human beings. *Chronobiol Int* **1999,** *16* (6), 821-9.

24.   Kotra, L. P.; Haddad, J.; Mobashery, S., Aminoglycosides: perspectives on mechanisms of action and resistance and strategies to counter resistance. *Antimicrob Agents Chemother* **2000,** *44* (12), 3249-56.

25.   Darmstadt, G. L.; Miller-Bell, M.; Batra, M.; Law, P.; Law, K., Extended-interval dosing of gentamicin for treatment of neonatal sepsis in developed and developing countries. *J Health Popul Nutr* **2008,** *26* (2), 163-82.

26.   Mingeot-Leclercq, M. P.; Tulkens, P. M., Aminoglycosides: nephrotoxicity. *Antimicrob Agents Chemother* **1999,** *43* (5), 1003-12.

27.   Xie, J.; Talaska, A. E.; Schacht, J., New developments in aminoglycoside therapy and ototoxicity. *Hear Res* **2011,** *281* (1-2), 28-37.

28.   Johnson, A. P.; Burns, L.; Woodford, N.; Threlfall, E. J.; Naidoo, J.; Cooke, E. M.; George, R. C., Gentamicin resistance in clinical isolates of Escherichia coli encoded by genes of veterinary origin. *J Med Microbiol* **1994,** *40* (3), 221-6.

29. Acred, P.; Brown, D. M.; Turner, D. H.; Wilson, M. J., Pharmacology and chemotherapy of ampicillin--a new broad-spectrum penicillin. *Br J Pharmacol Chemother* **1962,** *18*, 356-69.

30. Wilkins, J.; Fareau, G. E.; Patzakis, M. J., The mechanisms of action for beta-lactam antibiotics and inhibitors of bacterial protein synthesis. *Clin Orthop Relat Res* **1984,** (190), 23-30.

31. Westh, H.; Frimodt-Moller, N.; Gutschik, E., Bactericidal effect of penicillin, ampicillin, and amoxicillin alone and in combination with tobramycin against Enterococcus faecalis as determined by kill-kinetic studies. *Infection* **1991,** *19* (3), 170-3.

32. Kennedy, W. P.; Wallace, A. T.; Murdoch, J. M., Ampicillin in Treatment of Certain Gram-Negative Bacterial Infections. *Br Med J* **1963,** *2* (5363), 962-5.

33. Sabath, L. D., Mechanisms of resistance to beta-lactam antibiotics in strains of Staphylococcus aureus. *Ann Intern Med* **1982,** *97* (3), 339-44.

34. Hartman, B.; Tomasz, A., Altered penicillin-binding proteins in methicillin-resistant strains of Staphylococcus aureus. *Antimicrob Agents Chemother* **1981,** *19* (5), 726-35.

35. Heerema, M. S.; Musher, D. M.; Williams, T. W., Jr., Clavulanic acid and penicillin treatment of Staphylococcus aureus renal infection in mice. *Antimicrob Agents Chemother* **1979,** *16* (6), 798-800.

36. Schweizer, H. P., Mechanisms of antibiotic resistance in Burkholderia pseudomallei: implications for treatment of melioidosis. *Future Microbiol* **2012,** *7* (12), 1389-99.

37. Mikic, S. S.; Sabo, A.; Jakovljevic, V.; Fabri, M.; Stefan, Z.; Vukadinovic, I.; Dulejic, V., [Use of aminopenicillins in hospitals and outpatient facilities]. *Med Pregl* **2001,** *54* (11-12), 547-51.

38. Auhagen, E.; Gloxuber, C.; Hecht, G.; Knott, T.; Otten, H.; Rauenbusch, E.; Schmid, J.; Scholtan, W.; Walter, A. M., [Oxacillin-Stapenor, a penicillinase-resistant oral penicillin]. *Arzneimittelforschung* **1962,** *12*, 781-91.

39. Stapleton, P. D.; Taylor, P. W., Methicillin resistance in Staphylococcus aureus: mechanisms and modulation. *Sci Prog* **2002,** *85* (Pt 1), 57-72.

40. Rayner, C.; Munckhof, W. J., Antibiotics currently used in the treatment of infections caused by Staphylococcus aureus. *Intern Med J* **2005,** *35 Suppl 2*, S3-16.

41. Mollema, F. P.; Richardus, J. H.; Behrendt, M.; Vaessen, N.; Lodder, W.; Hendriks, W.; Verbrugh, H. A.; Vos, M. C., Transmission of methicillin-resistant Staphylococcus aureus to household contacts. *J Clin Microbiol* **2010,** *48* (1), 202-7.

42. LeBel, M., Ciprofloxacin: chemistry, mechanism of action, resistance, antimicrobial spectrum, pharmacokinetics, clinical trials, and adverse reactions. *Pharmacotherapy* **1988,** *8* (1), 3-33.

43. Heifets, L. B.; Lindholm-Levy, P. J., Bacteriostatic and bactericidal activity of ciprofloxacin and ofloxacin against Mycobacterium tuberculosis and Mycobacterium avium complex. *Tubercle* **1987,** *68* (4), 267-76.

44. Silva, F.; Lourenco, O.; Queiroz, J. A.; Domingues, F. C., Bacteriostatic versus bactericidal activity of ciprofloxacin in Escherichia coli assessed by flow cytometry using a novel far-red dye. *J Antibiot (Tokyo)* **2011,** *64* (4), 321-5.

45. Hooper, D. C., Mechanisms of fluoroquinolone resistance. *Drug Resist Updat* **1999,** *2* (1), 38-55.

46. Llor, C.; Bjerrum, L., Antimicrobial resistance: risk associated with antibiotic overuse and initiatives to reduce the problem. *Ther Adv Drug Saf* **2014,** *5* (6), 229-41.

47.   Sumano, L. H.; Gomez, R. B.; Gracia, M. I.; Ruiz-Ramirez, L., The use of ciprofloxacin in veterinary proprietary products of enrofloxacin. *Vet Hum Toxicol* **1994,** *36* (5), 476-7.

48.   Piercy, E. A.; Barbaro, D.; Luby, J. P.; Mackowiak, P. A., Ciprofloxacin for methicillin-resistant Staphylococcus aureus infections. *Antimicrob Agents Chemother* **1989,** *33* (1), 128-30.

49.   Griffith, R. S., Introduction to vancomycin. *Rev Infect Dis* **1981,** *3 suppl*, S200-4.

50.   Estes, K. S.; Derendorf, H., Comparison of the pharmacokinetic properties of vancomycin, linezolid, tigecyclin, and daptomycin. *Eur J Med Res* **2010,** *15* (12), 533-43.

51.   van Hal, S. J.; Fowler, V. G., Jr., Is it time to replace vancomycin in the treatment of methicillin-resistant Staphylococcus aureus infections? *Clin Infect Dis* **2013,** *56* (12), 1779-88.

52.   Rao, S.; Kupfer, Y.; Pagala, M.; Chapnick, E.; Tessler, S., Systemic absorption of oral vancomycin in patients with Clostridium difficile infection. *Scand J Infect Dis* **2011,** *43* (5), 386-8.

53.   Uttley, A. H.; George, R. C.; Naidoo, J.; Woodford, N.; Johnson, A. P.; Collins, C. H.; Morrison, D.; Gilfillan, A. J.; Fitch, L. E.; Heptonstall, J., High-level vancomycin-resistant enterococci causing hospital infections. *Epidemiol Infect* **1989,** *103* (1), 173-81.

54.   Preston, D. A., Microbiological aspects of erythromycin. *Pediatr Infect Dis* **1986,** *5* (1), 120-3.

55.   Tenson, T.; Lovmar, M.; Ehrenberg, M., The mechanism of action of macrolides, lincosamides and streptogramin B reveals the nascent peptide exit path in the ribosome. *J Mol Biol* **2003,** *330* (5), 1005-14.

56.   Desjardins, M.; Delgaty, K. L.; Ramotar, K.; Seetaram, C.; Toye, B., Prevalence and mechanisms of erythromycin resistance in group A and group B Streptococcus: implications for reporting susceptibility results. *J Clin Microbiol* **2004,** *42* (12), 5620-3.

57.   Misko, M. L.; Terracina, J. R.; Diven, D. G., The frequency of erythromycin-resistant Staphylococcus aureus in impetiginized dermatoses. *Pediatr Dermatol* **1995,** *12* (1), 12-5.

58.   Lowy, F. D., Antimicrobial resistance: the example of Staphylococcus aureus. *J Clin Invest* **2003,** *111* (9), 1265-73.

59.   Chopra, I.; Roberts, M., Tetracycline antibiotics: mode of action, applications, molecular biology, and epidemiology of bacterial resistance. *Microbiol Mol Biol Rev* **2001,** *65* (2), 232-60 ; second page, table of contents.

60.   Nelson, M. L.; Levy, S. B., The history of the tetracyclines. *Ann N Y Acad Sci* **2011,** *1241*, 17-32.

61.   Siegel, D., Tetracyclines: new look at old antibiotic. I. Clinical pharmacology, mechanism of action, and untoward effects. *N Y State J Med* **1978,** *78* (6), 950-6.

62.   Budkevich, T. V.; El'skaya, A. V.; Nierhaus, K. H., Features of 80S mammalian ribosome and its subunits. *Nucleic Acids Res* **2008,** *36* (14), 4736-44.

63.   Li, W.; Atkinson, G. C.; Thakor, N. S.; Allas, U.; Lu, C. C.; Chan, K. Y.; Tenson, T.; Schulten, K.; Wilson, K. S.; Hauryliuk, V.; Frank, J., Mechanism of tetracycline resistance by ribosomal protection protein Tet(O). *Nat Commun* **2013,** *4*, 1477.

64.   Bhambri, S.; Kim, G., Use of Oral Doxycycline for Community-acquired Methicillin-resistant Staphylococcus aureus (CA-MRSA) Infections. *J Clin Aesthet Dermatol* **2009,** *2* (4), 45-50.

65. Ruhe, J. J.; Menon, A., Tetracyclines as an oral treatment option for patients with community onset skin and soft tissue infections caused by methicillin-resistant Staphylococcus aureus. *Antimicrob Agents Chemother* **2007,** *51* (9), 3298-303.

66. Ruhe, J. J.; Monson, T.; Bradsher, R. W.; Menon, A., Use of long-acting tetracyclines for methicillin-resistant Staphylococcus aureus infections: case series and review of the literature. *Clin Infect Dis* **2005,** *40* (10), 1429-34.

67. Sensi, P., History of the development of rifampin. *Rev Infect Dis* **1983,** *5 Suppl 3*, S402-6.

68. Schonell, M.; Dorken, E.; Grzybowski, S., Rifampin. *Can Med Assoc J* **1972,** *106* (7), 783-6.

69. Wehrli, W., Rifampin: mechanisms of action and resistance. *Rev Infect Dis* **1983,** *5 Suppl 3*, S407-11.

70. Campbell, E. A.; Korzheva, N.; Mustaev, A.; Murakami, K.; Nair, S.; Goldfarb, A.; Darst, S. A., Structural mechanism for rifampicin inhibition of bacterial rna polymerase. *Cell* **2001,** *104* (6), 901-12.

71. White, R. J.; Lancini, G. C.; Silvestri, L. G., Mechanism of action of rifampin on Mycobacterium smegmatis. *J Bacteriol* **1971,** *108* (2), 737-41.

72. Kurbatova, E. V.; Cavanaugh, J. S.; Shah, N. S.; Wright, A.; Kim, H.; Metchock, B.; Van Deun, A.; Barrera, L.; Boulahbal, F.; Richter, E.; Martin-Casabona, N.; Arias, F.; Zemanova, I.; Drobniewski, F.; Santos Silva, A.; Coulter, C.; Lumb, R.; Cegielski, J. P., Rifampicin-resistant Mycobacterium tuberculosis: susceptibility to isoniazid and other anti-tuberculosis drugs. *Int J Tuberc Lung Dis* **2012,** *16* (3), 355-7.

73.   Mukinda, F. K.; Theron, D.; van der Spuy, G. D.; Jacobson, K. R.; Roscher, M.; Streicher, E. M.; Musekiwa, A.; Coetzee, G. J.; Victor, T. C.; Marais, B. J.; Nachega, J. B.; Warren, R. M.; Schaaf, H. S., Rise in rifampicin-monoresistant tuberculosis in Western Cape, South Africa. *Int J Tuberc Lung Dis* **2012,** *16* (2), 196-202.

74.   Ridzon, R.; Whitney, C. G.; McKenna, M. T.; Taylor, J. P.; Ashkar, S. H.; Nitta, A. T.; Harvey, S. M.; Valway, S.; Woodley, C.; Cooksey, R.; Onorato, I. M., Risk factors for rifampin mono-resistant tuberculosis. *Am J Respir Crit Care Med* **1998,** *157* (6 Pt 1), 1881-4.

75.   Pinto, L.; Menzies, D., Treatment of drug-resistant tuberculosis. *Infect Drug Resist* **2011,** *4*, 129-35.

76.   Forrest, G. N.; Tamura, K., Rifampin combination therapy for nonmycobacterial infections. *Clin Microbiol Rev* **2010,** *23* (1), 14-34.

77.   Tarai, B.; Das, P.; Kumar, D., Recurrent Challenges for Clinicians: Emergence of Methicillin-Resistant Staphylococcus aureus, Vancomycin Resistance, and Current Treatment Options. *J Lab Physicians* **2013,** *5* (2), 71-8.

78.   Tverdek, F. P.; Crank, C. W.; Segreti, J., Antibiotic therapy of methicillin-resistant Staphylococcus aureus in critical care. *Crit Care Clin* **2008,** *24* (2), 249-60, vii-viii.

79.   Conly, J. M.; Johnston, B. L., VISA, hetero-VISA and VRSA: the end of the vancomycin era? *Can J Infect Dis* **2002,** *13* (5), 282-4.

80.   Klein, E.; Smith, D. L.; Laxminarayan, R., Hospitalizations and deaths caused by methicillin-resistant Staphylococcus aureus, United States, 1999-2005. *Emerg Infect Dis* **2007,** *13* (12), 1840-6.

81.   Nair, R.; Ammann, E.; Rysavy, M.; Schweizer, M. L., Mortality among patients with methicillin-resistant Staphylococcus aureus USA300 versus non-USA300 invasive infections: a meta-analysis. *Infect Control Hosp Epidemiol* **2014,** *35* (1), 31-41.

82.   Quezada Joaquin, N. M.; Diekema, D. J.; Perencevich, E. N.; Bailey, G.; Winokur, P. L.; Schweizer, M. L., Long-term risk for readmission, methicillin-resistant Staphylococcus aureus (MRSA) infection, and death among MRSA-colonized veterans. *Antimicrob Agents Chemother* **2013,** *57* (3), 1169-72.

83.   Song, X.; Cogen, J.; Singh, N., Incidence of methicillin-resistant Staphylococcus aureus infection in a children's hospital in the Washington metropolitan area of the United States, 2003 - 2010. *Emerg Microbes Infect* **2013,** *2* (10), e69.

84.   Gillespie, S. H., Evolution of drug resistance in Mycobacterium tuberculosis: clinical and molecular perspective. *Antimicrob Agents Chemother* **2002,** *46* (2), 267-74.

85.   Musser, J. M., Antimicrobial agent resistance in mycobacteria: molecular genetic insights. *Clin Microbiol Rev* **1995,** *8* (4), 496-514.

86.   Slama, T. G., Gram-negative antibiotic resistance: there is a price to pay. *Crit Care* **2008,** *12 Suppl 4*, S4.

87.   Vasoo, S.; Barreto, J. N.; Tosh, P. K., Emerging issues in gram-negative bacterial resistance: an update for the practicing clinician. *Mayo Clin Proc* **2015,** *90* (3), 395-403.

88.   Outterson, K.; Powers, J. H.; Daniel, G. W.; McClellan, M. B., Repairing the broken market for antibiotic innovation. *Health Aff (Millwood)* **2015,** *34* (2), 277-85.

89.   Ling, L. L.; Schneider, T.; Peoples, A. J.; Spoering, A. L.; Engels, I.; Conlon, B. P.; Mueller, A.; Schaberle, T. F.; Hughes, D. E.; Epstein, S.; Jones, M.; Lazarides, L.; Steadman, V. A.; Cohen, D. R.; Felix, C. R.; Fetterman, K. A.; Millett, W. P.; Nitti, A.

G.; Zullo, A. M.; Chen, C.; Lewis, K., A new antibiotic kills pathogens without detectable resistance. *Nature* **2015,** *517* (7535), 455-9.

90.   Sylvestre, M.; Pichette, A.; Lavoie, S.; Longtin, A.; Legault, J., Composition and cytotoxic activity of the leaf essential oil of Comptonia peregrina (L.) Coulter. *Phytother Res* **2007,** *21* (6), 536-40.

91.   Tiruveedhula, V. V.; Witzigmann, C. M.; Verma, R.; Kabir, M. S.; Rott, M.; Schwan, W. R.; Medina-Bielski, S.; Lane, M.; Close, W.; Polanowski, R. L.; Sherman, D.; Monte, A.; Deschamps, J. R.; Cook, J. M., Design and synthesis of novel antimicrobials with activity against Gram-positive bacteria and mycobacterial species, including M. tuberculosis. *Bioorg Med Chem* **2013,** *21* (24), 7830-40.

92.   Cao, S.; Radwan, M. M.; Norris, A.; Miller, J. S.; Ratovoson, F.; Mamisoa, A.; Andriantsiferana, R.; Rasamison, V. E.; Rakotonandrasana, S.; Kingston, D. G., Cytotoxic and other compounds from Didymochlaena truncatula from the Madagascar rain forest. *J Nat Prod* **2006,** *69* (2), 284-6.

93.   Ngo, K.-S.; Brown, G. D., Stilbenes, monoterpenes, diarylheptanoids, labdanes and chalcones from Alpinia katsumadai. *Phytochemistry* **1998,** *47* (6), 1117-1123.

94.   Kabir, M. S.; Monte, A.; Cook, J. M., An efficient palladium-catalyzed Negishi cross-coupling reaction with arylvinyl iodides: facile regioselective synthesis of E-stilbenes and their analogues. *Tetrahedron Letters* **2007,** *48* (41), 7269-7273.

95.   Chinchilla, R.; Najera, C., The Sonogashira reaction: a booming methodology in synthetic organic chemistry. *Chem Rev* **2007,** *107* (3), 874-922.

96.   Gogsig, T. M.; Kleimark, J.; Lill, S. O.; Korsager, S.; Lindhardt, A. T.; Norrby, P. O.; Skrydstrup, T., Mild and efficient nickel-catalyzed Heck reactions with electron-rich olefins. *J Am Chem Soc* **2012,** *134* (1), 443-52.

97.   Han, C.; Buchwald, S. L., Negishi coupling of secondary alkylzinc halides with aryl bromides and chlorides. *J Am Chem Soc* **2009,** *131* (22), 7532-3.

98.   Roy, A. H.; Hartwig, J. F., Oxidative addition of aryl tosylates to palladium(0) and coupling of unactivated aryl tosylates at room temperature. *J Am Chem Soc* **2003,** *125* (29), 8704-5.

99.   Wolfe, J. P.; Buchwald, S. L., Scope and limitations of the Pd/BINAP-catalyzed amination of aryl bromides. *J Org Chem* **2000,** *65* (4), 1144-57.

100.   Fernández-Rodríguez, M. A.; Shen, Q.; Hartwig, J. F., A General and Long-Lived Catalyst for the Palladium-Catalyzed Coupling of Aryl Halides with Thiols. *Journal of the American Chemical Society* **2006,** *128* (7), 2180-2181.

101.   Itoh, T.; Mase, T., A General Palladium-Catalyzed Coupling of Aryl Bromides/Triflates and Thiols. *Organic Letters* **2004,** *6* (24), 4587-4590.

102.   McWilliams, J. C.; Fleitz, F. J.; Zheng, N.; Armstrong, J. D., Preparation of n-Butyl 4-Chlorophenyl Sulfide. In *Organic Syntheses*, John Wiley & Sons, Inc.: 2003.

103.   Mispelaere-Canivet, C.; Spindler, J.-F.; Perrio, S.; Beslin, P., Pd2(dba)3/Xantphos-catalyzed cross-coupling of thiols and aryl bromides/triflates. *Tetrahedron* **2005,** *61* (22), 5253-5259.

104.   Shim, Y. J.; Lee, H. J.; Park, S., Water-soluble complexes MX2L2 (M = Pd, Pt; L = PPh2(C6H4-p-SO3K)): Synthesis, stereoisomerism, and catalytic activities for

aromatic cyanation in n-heptane/water biphasic solution. *Journal of Organometallic Chemistry* **2012,** *696* (26), 4173-4178.

105.   Ushkov, A. V.; Grushin, V. V., Rational Catalysis Design on the Basis of Mechanistic Understanding: Highly Efficient Pd-Catalyzed Cyanation of Aryl Bromides with NaCN in Recyclable Solvents. *Journal of the American Chemical Society* **2011,** *133* (28), 10999-11005.

106.   Yang, C.-T.; Han, J.; Liu, J.; Gu, M.; Li, Y.; Wen, J.; Yu, H.-Z.; Hu, S.; Wang, X., "One-pot" synthesis of amidoxime via Pd-catalyzed cyanation and amidoximation. *Organic & Biomolecular Chemistry* **2015,** *13* (9), 2541-2545.

107.   Rosenmund, K. W.; Struck, E., Das am Ringkohlenstoff gebundene Halogen und sein Ersatz durch andere Substituenten. I. Mitteilung: Ersatz des Halogens durch die Carboxylgruppe. *Berichte der deutschen chemischen Gesellschaft (A and B Series)* **1919,** *52* (8), 1749-1756.

108.   Barillari, C.; Brown, N., Classical Bioisosteres. In *Bioisosteres in Medicinal Chemistry*, Wiley-VCH Verlag GmbH & Co. KGaA: 2012; pp 15-29.

109.   Brown, N., Bioisosterism in Medicinal Chemistry. In *Bioisosteres in Medicinal Chemistry*, Wiley-VCH Verlag GmbH & Co. KGaA: 2012; pp 1-14.

110.   Kilbourn, M. R., Thiophenes as phenyl bio-isosteres: application in radiopharmaceutical design--I. Dopamine uptake antagonists. *Int J Rad Appl Instrum B* **1989,** *16* (7), 681-6.

111.   Jenkins, S. G.; Schuetz, A. N., Current concepts in laboratory testing to guide antimicrobial therapy. *Mayo Clin Proc* **2012,** *87* (3), 290-308.

112.   Wingard, D. L.; Turiel, J., Long-term effects of exposure to diethylstilbestrol. *West J Med* **1988,** *149* (5), 551-4.

113.   Craig, W. A.; Redington, J.; Ebert, S. C., Pharmacodynamics of amikacin in vitro and in mouse thigh and lung infections. *J Antimicrob Chemother* **1991,** *27 Suppl C*, 29-40.

114.   Shahjahan Kabir, M.; Engelbrecht, K.; Polanowski, R.; Krueger, S. M.; Ignasiak, R.; Rott, M.; Schwan, W. R.; Stemper, M. E.; Reed, K. D.; Sherman, D.; Cook, J. M.; Monte, A., New classes of Gram-positive selective antibacterials: inhibitors of MRSA and surrogates of the causative agents of anthrax and tuberculosis. *Bioorg Med Chem Lett* **2008,** *18* (21), 5745-9.

115.   Clinical and Laboratory Standards Institute. Performance standards for antimicrobial susceptibility testing, 16th informational supplement. NCCLS document M100-S16. Wayne: National Committee for Clinical Laboratory Standards; 2006.

116.   Shukla, S. K.; Karow, M. E.; Brady, J. M.; Stemper, M. E.; Kislow, J.; Moore, N.; Wroblewski, K.; Chyou, P. H.; Warshauer, D. M.; Reed, K. D.; Lynfield, R.; Schwan, W. R., Virulence genes and genotypic associations in nasal carriage, community-associated methicillin-susceptible and methicillin-resistant USA400 Staphylococcus aureus isolates. *J Clin Microbiol* **2010,** *48* (10), 3582-92.

117.   Roupe, K. A.; Yanez, J. A.; Teng, X. W.; Davies, N. M., Pharmacokinetics of selected stilbenes: rhapontigenin, piceatannol and pinosylvin in rats. *J Pharm Pharmacol* **2006,** *58* (11), 1443-50.

118.   Frombaum, M.; Le Clanche, S.; Bonnefont-Rousselot, D.; Borderie, D., Antioxidant effects of resveratrol and other stilbene derivatives on oxidative stress and *NO bioavailability: Potential benefits to cardiovascular diseases. *Biochimie* **2012,** *94* (2), 269-76.

119. Wenzel, E.; Somoza, V., Metabolism and bioavailability of trans-resveratrol. *Mol Nutr Food Res* **2005,** *49* (5), 472-81.

120. Kabir, M. S.; Namjoshi, O. A.; Verma, R.; Polanowski, R.; Krueger, S. M.; Sherman, D.; Rott, M. A.; Schwan, W. R.; Monte, A.; Cook, J. M., A new class of potential anti-tuberculosis agents: Synthesis and preliminary evaluation of novel acrylic acid ethyl ester derivatives. *Bioorg Med Chem* **2010,** *18* (12), 4178-86.

121. de Meijere, A.; Meyer, F. E., Fine Feathers Make Fine Birds: The Heck Reaction in Modern Garb. *Angewandte Chemie International Edition in English* **1995,** *33* (23-24), 2379-2411.

122. Beletskaya, I. P.; Cheprakov, A. V., The heck reaction as a sharpening stone of palladium catalysis. *Chem Rev* **2000,** *100* (8), 3009-66.

123. Heck, R. F.; Nolley, J. P., Palladium-catalyzed vinylic hydrogen substitution reactions with aryl, benzyl, and styryl halides. *The Journal of Organic Chemistry* **1972,** *37* (14), 2320-2322.

124. Mizoroki, T.; Mori, K.; Ozaki, A., Arylation of Olefin with Aryl Iodide Catalyzed by Palladium. *Bulletin of the Chemical Society of Japan* **1971,** *44* (2), 581-581.

125. Fujiwara, Y.; Noritani, I.; Danno, S.; Asano, R.; Teranishi, S., Aromatic substitution of olefins. VI. Arylation of olefins with palladium(II) acetate. *Journal of the American Chemical Society* **1969,** *91* (25), 7166-7169.

126. Moritanl, I.; Fujiwara, Y., Aromatic substitution of styrene-palladium chloride complex. *Tetrahedron Letters* **1967,** *8* (12), 1119-1122.

127. Heck, R. F., Mechanism of arylation and carbomethoxylation of olefins with organopalladium compounds. *Journal of the American Chemical Society* **1969,** *91* (24), 6707-6714.

128. Dieck, H. A.; Heck, R. F., Organophosphinepalladium complexes as catalysts for vinylic hydrogen substitution reactions. *Journal of the American Chemical Society* **1974,** *96* (4), 1133-1136.

129. Miyaura, N.; Yamada, K.; Suzuki, A., A new stereospecific cross-coupling by the palladium-catalyzed reaction of 1-alkenylboranes with 1-alkenyl or 1-alkynyl halides. *Tetrahedron Letters* **1979,** *20* (36), 3437-3440.

130. Sonogashira, K.; Tohda, Y.; Hagihara, N., A convenient synthesis of acetylenes: catalytic substitutions of acetylenic hydrogen with bromoalkenes, iodoarenes and bromopyridines. *Tetrahedron Letters* **1975,** *16* (50), 4467-4470.

131. Baba, S.; Negishi, E., A novel stereospecific alkenyl-alkenyl cross-coupling by a palladium- or nickel-catalyzed reaction of alkenylalanes with alkenyl halides. *Journal of the American Chemical Society* **1976,** *98* (21), 6729-6731.

132. Crabtree, R. H., Carbonyls, Phosphine Complexes, and Ligand Substitution Reactions. In *The Organometallic Chemistry of the Transition Metals*, John Wiley & Sons, Inc.: 2005; pp 87-124.

133. Coulson, D. R.; Satek, L. C.; Grim, S. O., Tetrakis(triphenylphosphine)palladium(0). In *Inorganic Syntheses*, John Wiley & Sons, Inc.: 2007; pp 121-124.

134. Negishi, E.-i.; Meijere, A. d., Handbook of organopalladium chemistry for organic synthesis. **2002**.

135. Pierpont, C. G.; Mazza, M. C., Crystal and molecular structure of tris(dibenzylideneacetone)dipalladium(0). *Inorganic Chemistry* **1974,** *13* (8), 1891-1895.

136. Jakab, A.; Dalicsek, Z.; Holczbauer, T.; Hamza, A.; Pápai, I.; Finta, Z.; Timári, G.; Soós, T., Superstable Palladium(0) Complex as an Air- and Thermostable Catalyst for Suzuki Coupling Reactions. *European Journal of Organic Chemistry* **2015,** *2015* (1), 60-66.

137. Li, G. Y., Highly Active, Air-Stable Palladium Catalysts for the C−C and C−S Bond-Forming Reactions of Vinyl and Aryl Chlorides: Use of Commercially Available [(t-Bu)2P(OH)]2PdCl2, [(t-Bu)2P(OH)PdCl2]2, and [[(t-Bu)2PO···H···OP(t-Bu)2]PdCl]2 as Catalysts. *The Journal of Organic Chemistry* **2002,** *67* (11), 3643-3650.

138. Crabtree, R. H., Oxidative Addition and Reductive Elimination. In *The Organometallic Chemistry of the Transition Metals*, John Wiley & Sons, Inc.: 2005; pp 159-182.

139. Halpern, J., Oxidative-addition reactions of transition metal complexes. *Accounts of Chemical Research* **1970,** *3* (11), 386-392.

140. Amatore, C.; Pfluger, F., Mechanism of oxidative addition of palladium(0) with aromatic iodides in toluene, monitored at ultramicroelectrodes. *Organometallics* **1990,** *9* (8), 2276-2282.

141. Abelman, M. M.; Oh, T.; Overman, L. E., Intramolecular alkene arylations for rapid assembly of polycyclic systems containing quaternary centers. A new synthesis of spirooxindoles and other fused and bridged ring systems. *The Journal of Organic Chemistry* **1987,** *52* (18), 4130-4133.

142. Crabtree, R. H., Insertion and Elimination. In *The Organometallic Chemistry of the Transition Metals*, John Wiley & Sons, Inc.: 2005; pp 183-206.

143.   Hanley, P. S.; Hartwig, J. F., Intermolecular migratory insertion of unactivated olefins into palladium-nitrogen bonds. Steric and electronic effects on the rate of migratory insertion. *J Am Chem Soc* **2011,** *133* (39), 15661-73.

144.   Werner, H., Principles and Applications of Organotransition Metal Chemistry. Von J. P. Collman, L. G. Hegedus, J. R. Norton und R. G. Finke. Oxford University Press, Oxford 1987. XII, 989 S., geb. £ 40.00. – ISBN 0-935702-51-2. *Angewandte Chemie* **1988,** *100* (8), 1145-1146.

145.   Bloome, K. S.; McMahen, R. L.; Alexanian, E. J., Palladium-Catalyzed Heck-Type Reactions of Alkyl Iodides. *Journal of the American Chemical Society* **2011,** *133* (50), 20146-20148.

146.   Firmansjah, L.; Fu, G. C., Intramolecular Heck Reactions of Unactivated Alkyl Halides. *Journal of the American Chemical Society* **2007,** *129* (37), 11340-11341.

147.   Zou, Y.; Zhou, J., Palladium-catalyzed intermolecular Heck reaction of alkyl halides. *Chemical Communications* **2014,** *50* (28), 3725-3728.

148.   Lee, D.-H.; Taher, A.; Hossain, S.; Jin, M.-J., An Efficient and General Method for the Heck and Buchwald–Hartwig Coupling Reactions of Aryl Chlorides. *Organic Letters* **2011,** *13* (20), 5540-5543.

149.   Littke, A. F.; Fu, G. C., A Versatile Catalyst for Heck Reactions of Aryl Chlorides and Aryl Bromides under Mild Conditions. *Journal of the American Chemical Society* **2001,** *123* (29), 6989-7000.

150.   Xu, H.-J.; Zhao, Y.-Q.; Zhou, X.-F., Palladium-Catalyzed Heck Reaction of Aryl Chlorides under Mild Conditions Promoted by Organic Ionic Bases. *The Journal of Organic Chemistry* **2011,** *76* (19), 8036-8041.

151. Shaikh, T. M.; Hong, F. E., Palladium(II)-catalyzed Heck reaction of aryl halides and arylboronic acids with olefins under mild conditions. *Beilstein J Org Chem* **2013,** *9*, 1578-88.

152. Allen, D. W., Chapter 1 Phosphines and related P-C-bonded compounds. In *Organophosphorus Chemistry: Volume 43*, The Royal Society of Chemistry: 2014; Vol. 43, pp 1-51.

153. Bykov, V. V.; Bumagin, N. A., Effect of water on the palladium-catalyzed reaction of styrene with iodobenzene. *Russian Chemical Bulletin* **1997,** *46* (7), 1346-1349.

154. Kamal, A.; Srinivasulu, V.; Seshadri, B. N.; Markandeya, N.; Alarifi, A.; Shankaraiah, N., Water mediated Heck and Ullmann couplings by supported palladium nanoparticles: importance of surface polarity of the carbon spheres. *Green Chemistry* **2012,** *14* (9), 2513-2522.

155. Yoon, B.; Yen, C. H.; Mekki, S.; Wherland, S.; Wai, C. M., Effect of Water on the Heck Reactions Catalyzed by Recyclable Palladium Chloride in Ionic Liquids Coupled with Supercritical CO2 Extraction. *Industrial & Engineering Chemistry Research* **2006,** *45* (12), 4433-4435.

156. Hagiwara, H.; Sugawara, Y.; Hoshi, T.; Suzuki, T., Sustainable Mizoroki-Heck reaction in water: remarkably high activity of Pd(OAc)2 immobilized on reversed phase silica gel with the aid of an ionic liquid. *Chemical Communications* **2005,** (23), 2942-2944.

157. Herrmann, W. A.; Brossmer, C.; Reisinger, C.-P.; Riermeier, T. H.; Öfele, K.; Beller, M., Palladacycles: Efficient New Catalysts for the Heck Vinylation of Aryl Halides. *Chemistry – A European Journal* **1997,** *3* (8), 1357-1364.

158.   Banister, S. D.; Moir, M.; Stuart, J.; Kevin, R. C.; Wood, K. E.; Longworth, M.; Wilkinson, S. M.; Beinat, C.; Buchanan, A. S.; Glass, M.; Connor, M.; McGregor, I. S.; Kassiou, M., Pharmacology of Indole and Indazole Synthetic Cannabinoid Designer Drugs AB-FUBINACA, ADB-FUBINACA, AB-PINACA, ADB-PINACA, 5F-AB-PINACA, 5F-ADB-PINACA, ADBICA, and 5F-ADBICA. *ACS Chemical Neuroscience* **2015,** *6* (9), 1546-1559.

159.   Chen, K. X.; Vibulbhan, B.; Yang, W.; Sannigrahi, M.; Velazquez, F.; Chan, T. Y.; Venkatraman, S.; Anilkumar, G. N.; Zeng, Q.; Bennet, F.; Jiang, Y.; Lesburg, C. A.; Duca, J.; Pinto, P.; Gavalas, S.; Huang, Y.; Wu, W.; Selyutin, O.; Agrawal, S.; Feld, B.; Huang, H. C.; Li, C.; Cheng, K. C.; Shih, N. Y.; Kozlowski, J. A.; Rosenblum, S. B.; Njoroge, F. G., Structure-activity relationship (SAR) development and discovery of potent indole-based inhibitors of the hepatitis C virus (HCV) NS5B polymerase. *J Med Chem* **2012,** *55* (2), 754-65.

160.   de Sa Alves, F. R.; Barreiro, E. J.; Fraga, C. A., From nature to drug discovery: the indole scaffold as a 'privileged structure'. *Mini Rev Med Chem* **2009,** *9* (7), 782-93.

161.   Zhang, M. Z.; Chen, Q.; Yang, G. F., A review on recent developments of indole-containing antiviral agents. *Eur J Med Chem* **2015,** *89*, 421-41.

162.   Cohen, S. G., The Effects of Temperature on the Polymerization of Styrene. *Journal of the American Chemical Society* **1945,** *67* (1), 17-20.

163.   Goldfinger, G.; Skeist, I.; Mark, H., On the Mechanism of Inhibition of Styrene Polymerization. *The Journal of Physical Chemistry* **1943,** *47* (8), 578-587.

164. Khuong, K. S.; Jones, W. H.; Pryor, W. A.; Houk, K. N., The Mechanism of the Self-Initiated Thermal Polymerization of Styrene. Theoretical Solution of a Classic Problem. *Journal of the American Chemical Society* **2005,** *127* (4), 1265-1277.

165. Claisen, L.; Claparède, A., Condensationen von Ketonen mit Aldehyden. *Berichte der deutschen chemischen Gesellschaft* **1881,** *14* (2), 2460-2468.

166. Nielsen, A. T.; Houlihan, W. J., The Aldol Condensation. In *Organic Reactions*, John Wiley & Sons, Inc.: 2004.

167. Doan Thi Mai, H.; Gaslonde, T.; Michel, S.; Koch, M.; Tillequin, F.; Bailly, C.; David-Cordonnier, M. H.; Pfeiffer, B.; Leonce, S.; Pierre, A., Design, synthesis, and cytotoxic activity of Michael acceptors and enol esters in the benzo[b]acronycine series. *Chem Pharm Bull (Tokyo)* **2005,** *53* (8), 919-22.

168. Heller, L.; Schwarz, S.; Perl, V.; Kowitsch, A.; Siewert, B.; Csuk, R., Incorporation of a Michael acceptor enhances the antitumor activity of triterpenoic acids. *Eur J Med Chem* **2015,** *101*, 391-9.

169. Mulliner, D.; Wondrousch, D.; Schuurmann, G., Predicting Michael-acceptor reactivity and toxicity through quantum chemical transition-state calculations. *Org Biomol Chem* **2011,** *9* (24), 8400-12.

170. Wondrousch, D.; Böhme, A.; Thaens, D.; Ost, N.; Schüürmann, G., Local Electrophilicity Predicts the Toxicity-Relevant Reactivity of Michael Acceptors. *The Journal of Physical Chemistry Letters* **2010,** *1* (10), 1605-1610.

171. Hanberger, H.; Walther, S.; Leone, M.; Barie, P. S.; Rello, J.; Lipman, J.; Marshall, J. C.; Anzueto, A.; Sakr, Y.; Pickkers, P.; Felleiter, P.; Engoren, M.; Vincent, J. L.; Investigators, E. I. G. o., Increased mortality associated with methicillin-resistant

Staphylococcus aureus (MRSA) infection in the intensive care unit: results from the EPIC II study. *Int J Antimicrob Agents* **2011,** *38* (4), 331-5.

172.   Pastagia, M.; Kleinman, L. C.; Lacerda de la Cruz, E. G.; Jenkins, S. G., Predicting risk for death from MRSA bacteremia. *Emerg Infect Dis* **2012,** *18* (7), 1072-80.

173.   Vendrell, E.; Capdevila, J. A.; Barrufet, P.; Force, L.; Sauca, G.; Martinez, E.; Palomera, E.; Serra-Prat, M.; Cornudella, J.; Llopis, A.; Robledo, M. A.; Vazquez, C., Mortality among methicillin-resistant Staphylococcus aureus carriers in long-term care facilities. *Rev Esp Quimioter* **2015,** *28* (2), 92-7.

174.   Andersson, D. I.; Hughes, D., Microbiological effects of sublethal levels of antibiotics. *Nat Rev Micro* **2014,** *12* (7), 465-478.

175.   Gullberg, E.; Cao, S.; Berg, O. G.; Ilbäck, C.; Sandegren, L.; Hughes, D.; Andersson, D. I., Selection of Resistant Bacteria at Very Low Antibiotic Concentrations. *PLoS Pathog* **2011,** *7* (7), e1002158.

176.   Nonejuie, P.; Burkart, M.; Pogliano, K.; Pogliano, J., Bacterial cytological profiling rapidly identifies the cellular pathways targeted by antibacterial molecules. *Proceedings of the National Academy of Sciences of the United States of America* **2013,** *110* (40), 16169-16174.

177.   Nijman, S. M. B., Functional genomics to uncover drug mechanism of action. *Nat Chem Biol* **2015,** *11* (12), 942-948.

178.   Thangamani, S.; Mohammad, H.; Abushahba, M. F. N.; Sobreira, T. J. P.; Hedrick, V. E.; Paul, L. N.; Seleem, M. N., Antibacterial activity and mechanism of action of auranofin against multi-drug resistant bacterial pathogens. *Scientific Reports* **2016,** *6*, 22571.

179.   Chang, T. S., An updated review of tyrosinase inhibitors. *Int J Mol Sci* **2009,** *10* (6), 2440-75.

180.   Hearing, V. J., Jr.; Ekel, T. M.; Montague, P. M.; Nicholson, J. M., Mammalin tyrosinase. Stoichiometry and measurement of reaction products. *Biochim Biophys Acta* **1980,** *611* (2), 251-68.

181.   Jagodzinska, M.; Huguenot, F.; Candiani, G.; Zanda, M., Assessing the Bioisosterism of the Trifluoromethyl Group with a Protease Probe. *ChemMedChem* **2009,** *4* (1), 49-51.

Part 2

SYNTHESIS OF DIHYDROBENZOFURANS VIA A NEW

TRANSITION METAL CATALYZED REACTION

CHAPTER SIX

INTRODUCTION TO DIHYDROBENZOFURANS

I.   INTRODUCTION.

Dihydrobenzofurans are ubiquitous in nature and represent a vast array of natural products, many that are also bioactive[1]. The dihydrobenzofuran skeleton is comprised of a benzene ring fused to a 5-member oxygen heterocycle (Figure 6-1). In 2009 alone more than 500 dihydrobenzofuran-containing natural products were reported according to a reaxys search.[2] Dihydrobenzofuran containing natural products have been reported to exhibit activity against a number of diseases including, but not limited to, cancer[3], tuberculosis[4], malaria[5], and cataracts.[6] The compounds that act on direct targets such as HIF-1[7], α-glucosidase[8], aldose reductase[7], 5-LOX[9], COX-2[9], NF-κß[10], and the muscarinic M3 receptor[11] are also known. Some other dihydrobenzofuran natural products have shown antioxidant behavior and cytoprotective properties.[12] A number of others exert insecticidal activity.[13] A selection of some dihydrobenzofuran natural products can be found in Figure 6-2.

Many synthetic dihydrobenzofurans have been found to possess biological activity, some of which are currently used as pharmaceutical drugs. A selection of some synthetic dihydrobenzofuran compounds are depicted below in Figure 6-3. This diverse biological activity and ubiquity in nature make dihydrobenzofurans an interesting structural target for future synthetic work.

Figure 6-1: Structure of Dihydrobenzofuran.
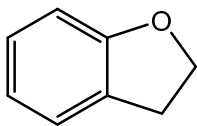
Due to the diversity of dihydrobenzofuran natural products and a growing library of bioactive synthetic dihydrobenzofurans, they represent an interesting avenue for studies of new synthetic methods. Reviewed in this chapter is a summary of some of the current methods to synthesize the dihydrobenzofuran skeleton, whereas the next chapter will detail a new and interesting one-step route to novel dihydrobenzofurans.

Figure 6-2: Some dihydrobenzofuran natural products.

cedralin A

benfur

liliflol A

fomannoxin

natural product from *Senecio vulgaris*

natural product from *Microglossa pyrifolia*
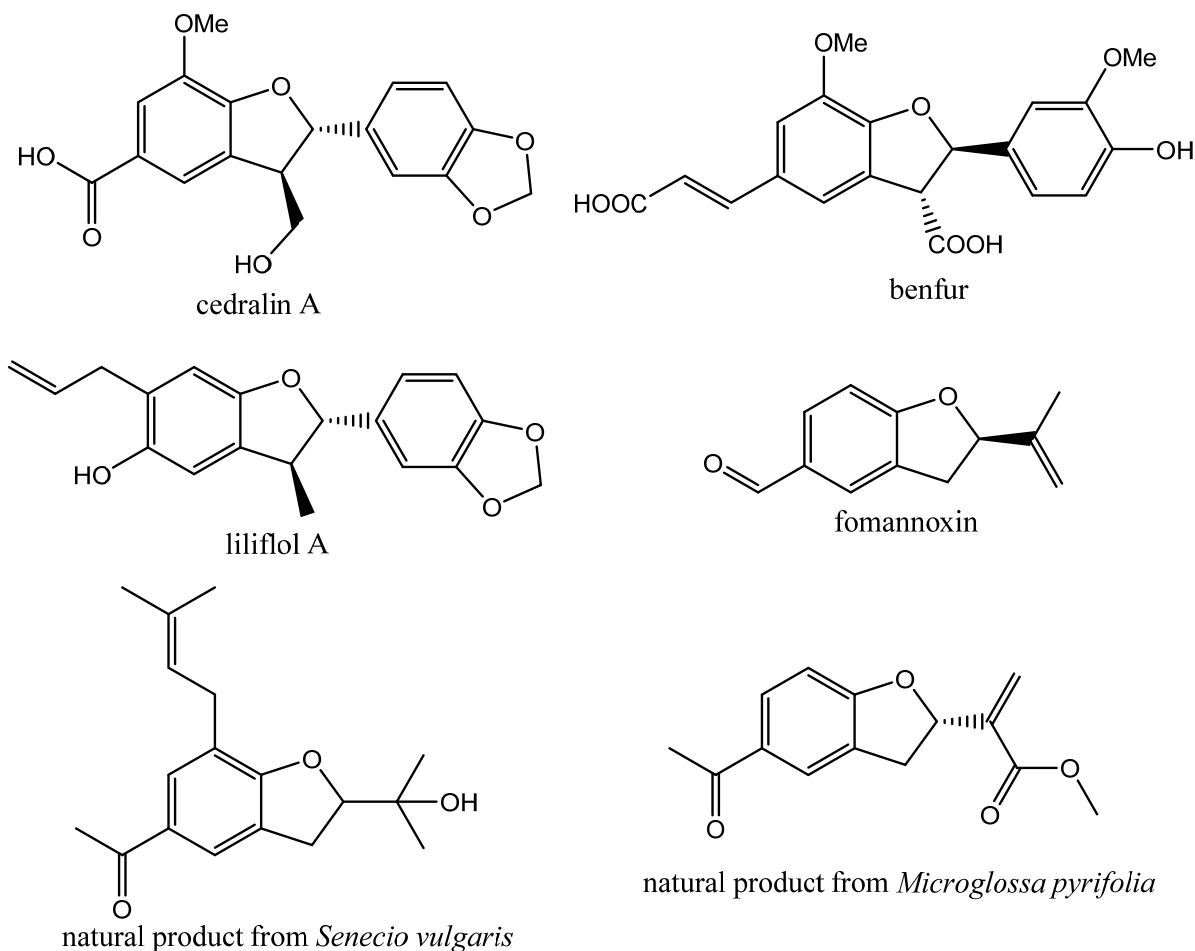
Many of the natural products shown in Figure 2 possess bioactivity. Cedralin A is active against two cancer cell lines (HL-60 and K562) and was isolated from *Cedrela sinensis*, a broadleaf tree native to China and Korea.[14] The leaves, fruit, and roots of this tree have been used in oriental medicine since ancient times for a number of diseases.[15] Benfur is a known antimitotic agent active against a number of cancer cell lines and was isolated from a species of shrub (*Dracaena*).[16] The resin from these shrubs was used in traditional medicine as an anticancer agent[17], of which benfur was found to be the active component. It is particularly interesting since it induces cell death in malignant T-cells, but does not harm primary T-cells. Liliflol A was isolated from *Magnolia liliiflora*, a flowering tree native to China.[18-19] It was found to inhibit both COX-2 and 5-LOX, targets for non-steroidal anti-inflammatory drugs (NSAIDs) and potential treatments for asthma, respectively.[9] Fomannoxin was isolated from *Heterobasidion occidentale*, a pathogenic fungus.[20] It is a potent phytotoxin that aids in the root rotting process associated with *H. occidentale* infection in trees.[21] The last two dihydrobenzofuran natural products are isolates from *Senecio vulgaris* and *Microglossa pyrifolia* respectively, extracts of which both show bioactivity.[22-23] These two recently isolated dihydrobenzofurans have not been tested for bioactivity as of yet.

The biodiversity of dihydrobenzofurans also led to the synthesis of a diverse selection of synthetic derivatives in which some are used as pharmaceutical drugs.

Figure 6-3: Some synthetic dihydrobenzofurans.

5-APDB

Efaroxan

Prucalopride

Anti-cancer compound
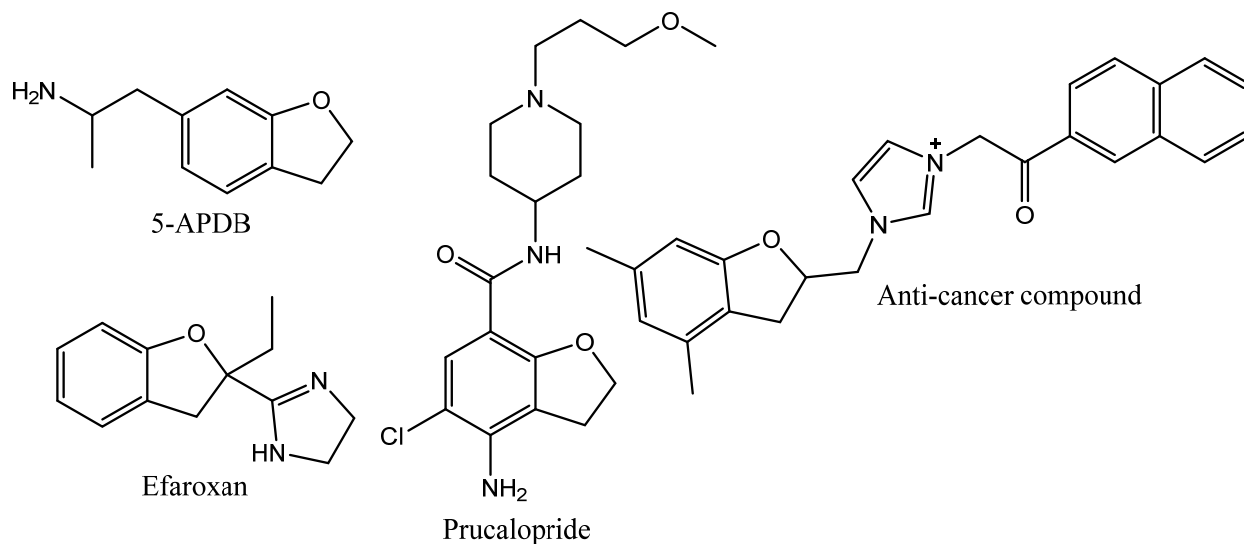
The 5-APDB is a known psychoactive compound similar to MDMA (colloquially known as ecstasy).[24-26] *In vitro* studies show 5-APDB is a selective serotonin releasing agent (SSRA) with an IC_{50} value of 130 nM.[25] Although there are reports of recreational use, anecdotal reports describe the effects of 5-APDB as much milder then related amphetamines and 5-APDB may represent an interesting scaffold for future drug development. Efaroxan is an α2-adrenergic receptor antagonist and imidazoline receptor antagonist that was initially thought to be useful in the treatment of progressive supranuclear palsy.[27] Later double-blind human trials showed no significant cognitive enhancement in patients given the drug.[28] It is still routinely used, however, as an α2-blocker for *in vitro*/*in vivo* studies.[29] Prucalopride is a first-in-class 5-HT4 receptor agonist used in patients with chronic constipation.[30] It is currently approved for use in Europe, Canada, and Israel under the brand name Resolor.[31] Other 5-HT4 receptor agonists have experienced issues with selectivity at therapeutic dosages, many of which act on 5-HT1B/D or the hERG channel and have associated cardiovascular side-effects.[32] Prucalopride is effectively selective for only 5-HT4 with >150-fold lower affinity for other receptors. The final compound

196

listed as 'anti-cancer' has been found to be cytotoxic to a number of cancer cell lines. *In vitro* studies have shown that this cytotoxic activity is even greater than the anti-cancer drug cisplatin, routinely used for a number of chemotherapies.[33]

These are just a small selection of bioactive synthetic dihydrobenzofurans from the literature. It should also be noted that natural and synthetic opiates, such as morphine, also contain the dihydrobenzofuran skeleton (Figure 6-4). These represent some of the most prescribed drugs on the market.[34] While synthetic opiates are generally synthesized from a natural opiate such as morphine or codeine, in which the dihydrobenzofuran skeleton has already been formed through biological processes, the total synthesis of natural opiates often revolves around formation of the benzofuran ring and will be discussed in this chapter as well.[35]

Figure 6-4: Structure of Morphine.

Morphine
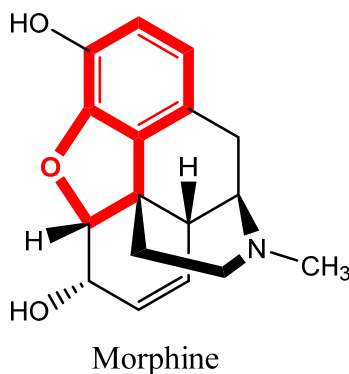
II.   SYNTHESIS OF DIHYDROBENZOFURANS.

Chemists have developed an array of methods for accessing the dihydrobenzofuran skeleton. Many of which, however, require starting materials that are not commercially available and must be synthesized through multi-step procedures. This review of the literature will focus

on some of the main pathways to construct the dihydrobenzofuran skeleton, although the list is not exhaustive by any means.

1. Synthesis by Dehydration.

If a route begins with a molecule which contains both a phenol and an alcohol functionality in the designated positions (**1**), intramolecular dehydration can yield dihydrobenzofurans (Scheme 6-1). The use of a Mitsunobu type dehydration to perform this transformation was first reported by Aristoff in 1984.[36] The near complete inversion of configuration together with high yields are major advantages of the Mitsunobu reaction.[37] In the case shown below, p-toluenesulfonic acid (p-TsOH) catalyzed the reaction giving an inseperable 68/32 mixture of diastereomeric cis and trans dihydrobenzofurans **2** and **3** respectively, whereas the Mitsunobu protocol involving triphenylphosphine (PPh3) and diethyl azodicarboxylate (DEAD) resulted in both a high yield (80%) and high diastereomeric control of **2** (95:5).[38]

Scheme 6-1: Mistunobu type dehydration/cyclization.

i. PPh$_3$, DEAD, THF, rt   dr > 95 : 5
ii. p-TsOH, toluene, reflux   dr = 68 : 32
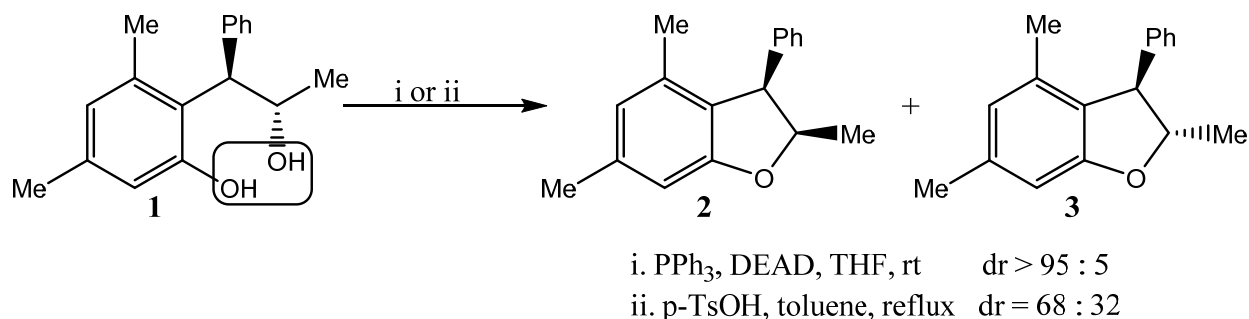
Disadvantages of the above reaction were the limited scope with substituted phenols and the necessity to synthesize many of these phenols prior to the cyclization. DEAD is also unstable and potentially explosive and the amount of by-products produced by this reaction,

triphenylphosphine oxide and diethyl hydrazinedicarboxylate are of considerable mass and render the reaction not suitable for scale-up because of waste disposal.

One solution to these issues was resolved with the use of a Vilsmeier reagent and this was followed by trimethylamine (TEA) for the cyclization of hydroxyphenols to afford dihydrobenzofurans via formation of an imidate ester, followed by displacement with phenoxide.[39] This method was particularly useful for scale-up, and has been used for the scale-up of the synthesis of 4-vinyl-2,3-dihydrobenzofuran by Bristol-Myers Squibb.[40] Outlined in Scheme 6-2 below is depicted an example of this reaction process.

Scheme 6-2: Vilsmeier cyclization method.
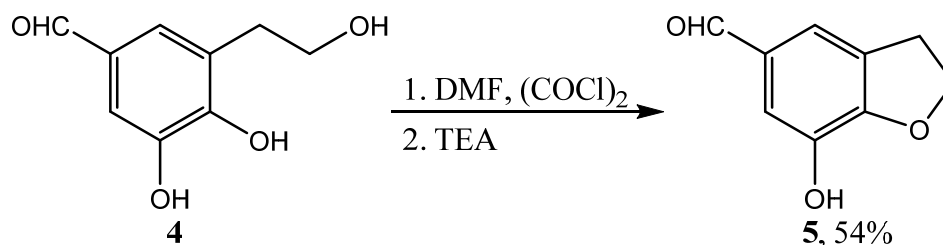
When the Mitsunobu cyclodehydration conditions were used with aldehyde **4** there was no conversion to the desired dihyrobenzofuran **5**. By contrast, the Vilsmeier method was successful in the synthesis of the dihydrobenzofuran analog in 54% yield.[41] Similarly to the Mitsunobu method, the Vilsmeier method also requires highly specific starting materials that in general are not commercially available, although it does offer an expanded scope in comparison.

2.   Synthesis by radical cyclizations.

An interesting radical reaction which involved substituted 2-bromophenols as starting materials, which are also used in the new work to be discussed in the next chapter, is

accomplished by first synthesis of **8**, which was subsequently cyclized via a radical mechanism to the dihydrobenzofuran **9** (Scheme 6-3).[42]

Scheme 6-3: Radical cyclization to dihydrobenzofurans.

i. K$_2$CO$_3$ (aq), reflux, 48h
ii. Bu$_3$SnH, AIBN (cat), benzene, reflux
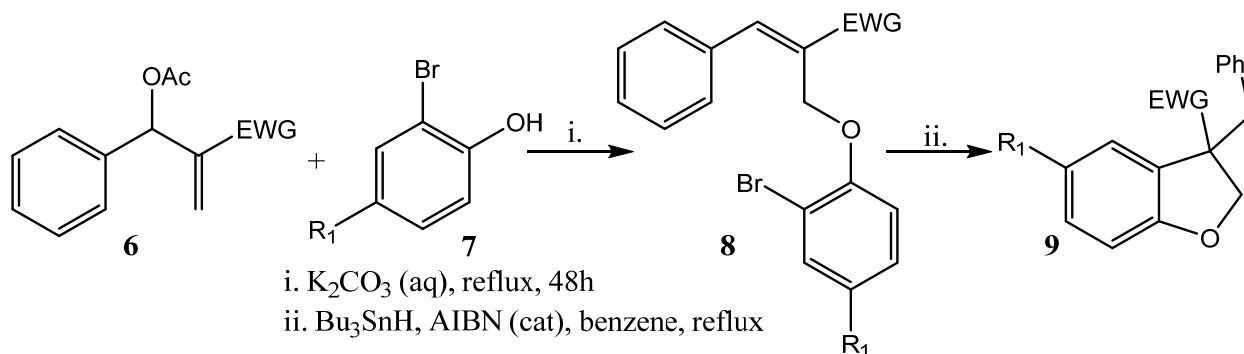
The disadvantage to reactions of this nature are of course the toxicity of tin reagents and the necessity to both synthesize bromide **8** prior to cyclization, as well as the necessity to prepare **6**. Moreover, radical reactions are known to readily dimerize on some occasions. The 2-bromophenols are advantageously commercially available, however, and used in the next chapter to synthesize related dibydrobenzofurans using a very different transition metal catalyzed prodedure.

It is important to note that the synthesis of bromide **8** required an electron-withdrawing-group (EWG), typical of most Bayliss-Hillman reactions.[43] This further limited the scope of these reactions. In addition, it was noted by the authors that use of tributyltinhydride leads to tin by-products that are sometimes difficult to separate from the reaction products; this is a common problem when employing tributyltinhydride.[44]

Other radical type reactions involving similar pathways are also available in the literature.[45-48] Many of these reactions are low-yielding and/or have a restricted scope, similar to the reaction detailed above.

3.   Biomimetic synthesis.

Biomimetic synthesis aims to use the very same biosynthetic pathways that are used in biological systems to synthesize compounds. Use of biomimetic synthesis has grown over the years and is used extensively for the synthesis of many natural products.[49-51] It is also a common approach to form the distinct dihydrobenzofuran skeleton in a number of biologically active compounds.[52]

Biological systems make extensive use of the ability of phenols and related analogs to form reactive quinones *in situ*. This process can be extended to benchtop chemistry using oxidants. Synthesis of benzofuran neo-lignans could be obtained in good yields and high stereoselectivities by oxidation of para-methoxy substituted phenols with iodobenze bis-trifluoroacetate in the presence of electron-rich styrene derivatives (Scheme 6-4).[53] This approach, which couples a quinone and a styryl moiety has been extensively adopted and has been used in the preparation of a number of dihydrobenzofurans.[54-57]

Scheme 6-4: Quinone mediated synthesis.
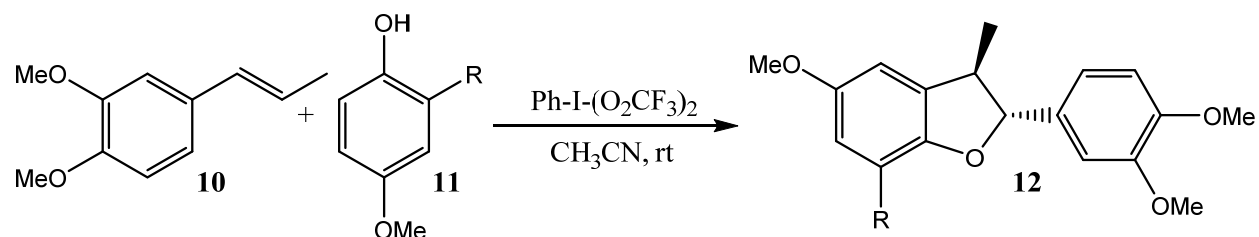
As described earlier, a number of similar methods to synthesize dihydrobenzofurans via a similar oxidative method exists. These methods, however, rely on formation of quinones and in general low yields are observed when the substitution pattern of the phenol is altered in such a way that formation of the quinone is supressed.

4.   Synthesis by epoxide ring opening.

Asymmetric synthesis of epoxides is a well-known and versatile method of synthesizing

novel compounds pioneered by Sharpless and Jacobsen among others.[58] In the case of

dihydrobenzofurans, it was found that ring opening in the presence of an intramolecular phenol

gave excellent yields and excellent ee of the corresponding dihydrobenzofurans. Detailed in

Scheme 6-5 is a reaction scheme in which Shi epoxidation led to the enantioenriched silane **14**

which was subsequently deprotected with tetrabutylammonium fluoride (TBAF). The ring

opening was quickly followed by cyclization to the dihydrobenzofuran **15**.[59] This approach was

used in the total synthesis of the dihydrobenzofuran containing natural product (+)-marmesin

(Figure 6-5) found to be a novel inhibitor of angiogenesis.[60]

Scheme 6-5: Enantioselective synthesis using Shi epoxidation.
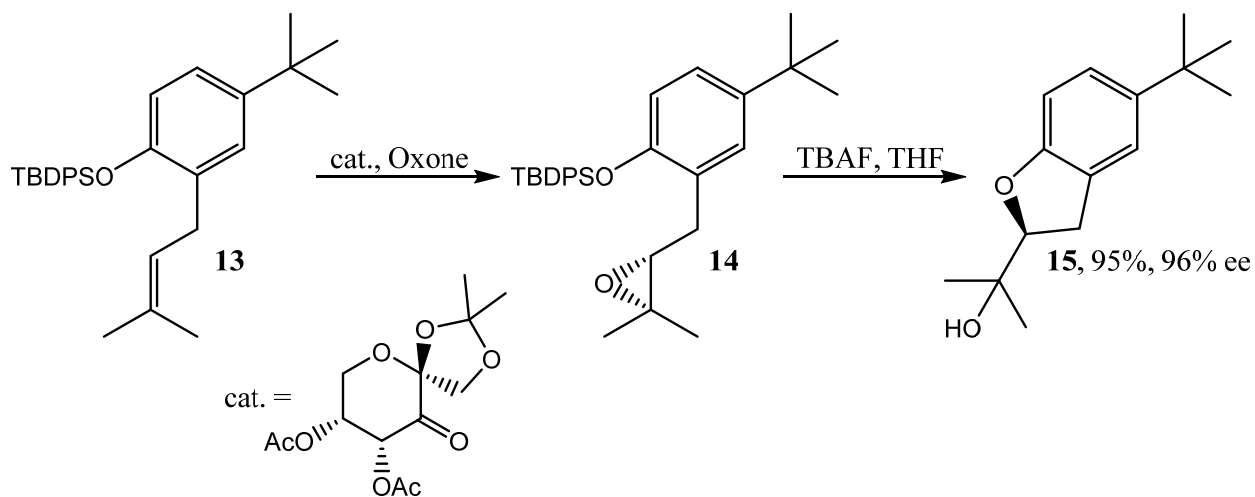
Figure 6-5: Structure of (+)-marmesin.

(+)-marmesin
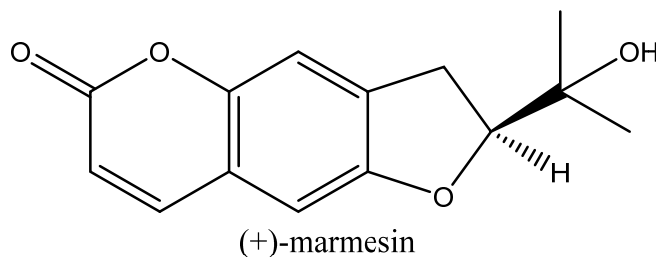
In a similar manner, Sharpless asymmetric epoxidation (SAE) has also been used to

construct the dihydrobenzofuran skeleton by a ring opening cyclization method (Scheme 6-6).[61]

This method was successfully used in the total synthesis of the dihydrobenzofuran natural

product heliannuol G (Figure 6-6).[62] These methods are advantageous for total synthesis,

however, as with other methods discussed thus far, they require very specialized starting

materials to form the 5-membered furan ring.

Scheme 6-6: Sharpless asymmetric epoxidation method.
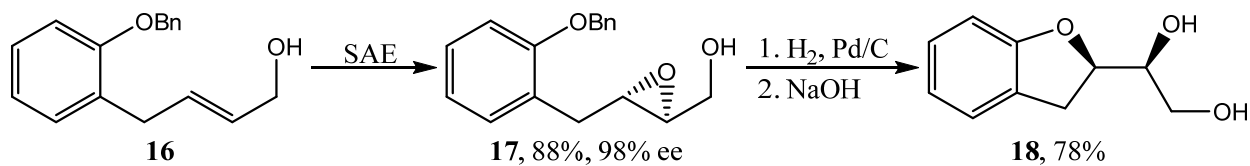
After asymmetric induction, deprotection of the phenol followed by ring opening/closure

catalyzed by base gave the dihydrobenzofuran diol **18** in good yield with inversion of symmetry.

The natural product heliannuol G was originally identified in sunflower (*Helianthus annuus*)

seed extracts of which were found to be bioactive, however there is no evidence in the literature

that the dihydrobenzofuran is the bioactive component of the extract.[63]

Figure 6-6: Structure of heliannuol G.

heliannuol G
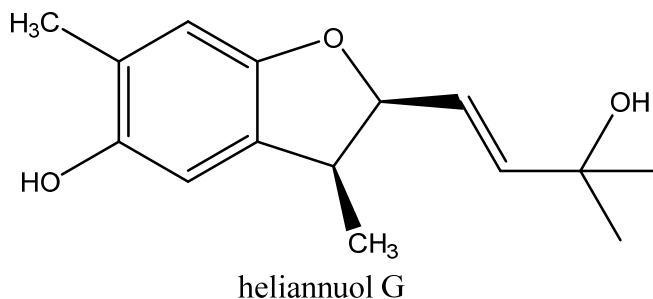
A final similar approach to the cyclization via the epoxidation ring opening is a method which involved Sharpless asymmetric dihydroxylation (Scheme 6-7).[64]

Scheme 6-7: Synthesis of 23 via the Sharpless asymmetric dihydroxylation.
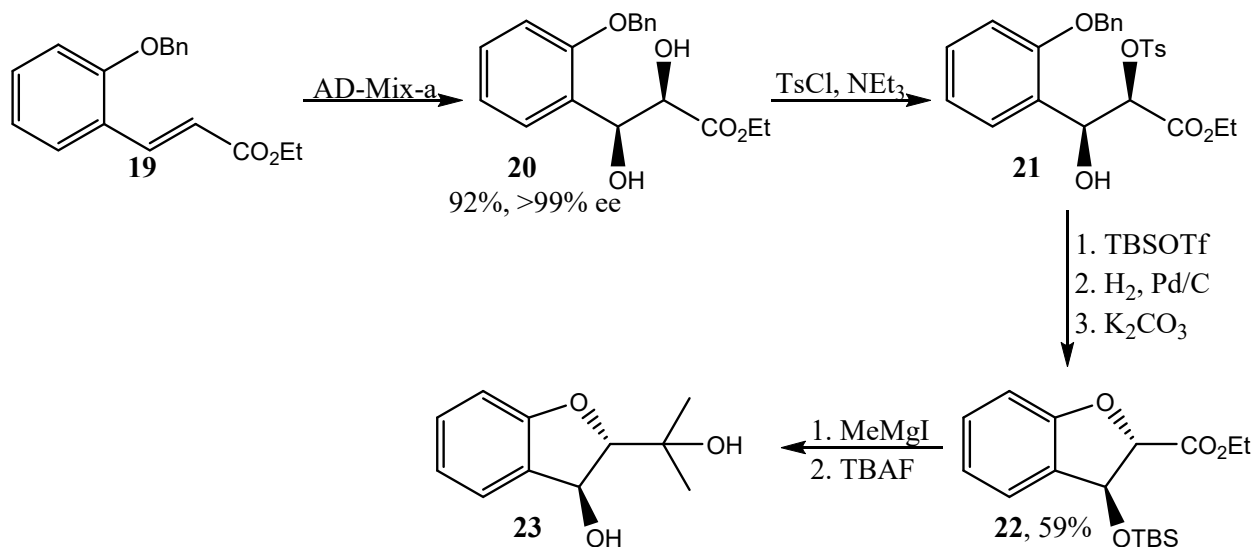
This method was successful in the synthesis of **23**, a core structure of a variety of natural products including avicenol A[65] and brosimacutin G.[66]

5.   Total synthesis of Morphine.

Morphine is an opioid alkaloid that acts directly on the central nervous system (CNS) to reduce pain.[67] In 2013 an estimated 523,000 kilograms of morphine were produced from natural

sources, many of which were used to synthesize related analogs such as codeine and oxycodone. These are pain medications routinely prescribed.[68] Morphine, as earlier described, also contains the dihydrobenzofuran skeleton and many total synthetic routes have been developed to construct this functionality.

The first total synthesis of morphine was reported by Gates in 1952, with an overall yield of 0.06% over 31 steps. The dihydrobenzofuran skeleton was introduced after the so-called "Gates intermediate" was constructed; this is illustrated in Scheme 6-8.[69] Bromination of the "Gates Intermediate" followed by conversion to the hydrazino intermediate **24** was followed by acid catalyzed conversion to the cyclized ether **25** in a yield of 8% over the three steps.

Scheme 6-8: Gates total synthesis of morphine, C-O bond forming step.
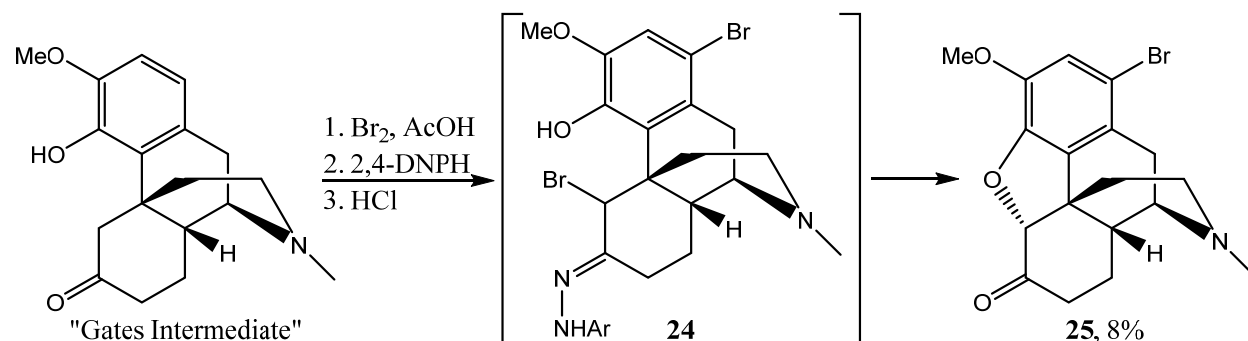
The "Gates Intermediate" was subsequently used in a number of total syntheses of morphine.[70] As shown, construction of the dihydrobenzofuran ring system occurred in very low yield and this was subsequently improved by Rice from a similar starting position. The Rice synthesis of the dihydrobenzofuran skeleton is illustrated in Scheme 6-9.[71]

Scheme 6-9: Rice total synthesis of morphine, C-O bond forming step.

1. Br$_2$, AcOH
2. NaOH, CHCl$_3$
3. H$_2$, Pd/C, CH$_2$O, NaOAc

26

27, 79%
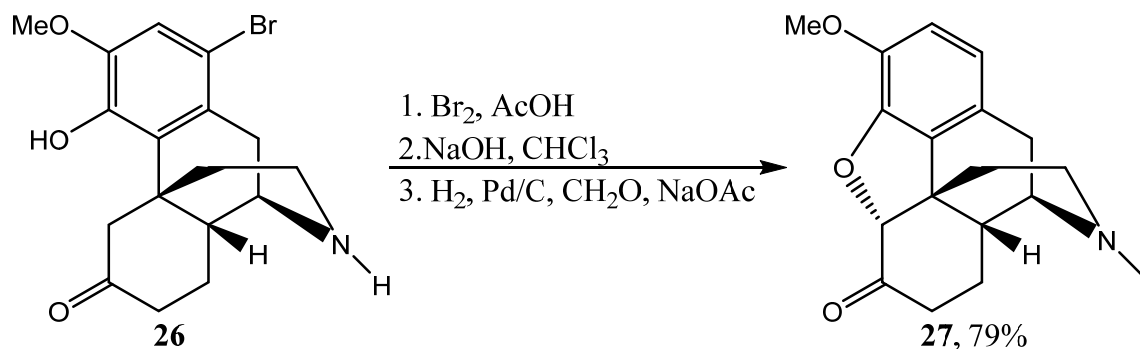
In this case, Rice formed the C-O ring of the ether by first brominating in the same position as shown in hydrazone **24** followed by base catalyzed cyclization. This was followed by debromination and N-methylation which resulted in an overall yield of **27** in 79% yield over the three steps, a clear advantage compared to the prior synthesis by Gates.

This much higher yield of the dihydrobenzofuran system was an important factor in the Rice synthesis which was known as the most efficient synthetic route to morphine.[72] The Rice synthesis was also a more efficient route with only 18 linear steps. Later, Rice developed the famous NIH synthesis of morphine which was later licensed by Mallinkroft to prepare morphine or codeine on kilogram scales, if necessary.

More recent examples of the total synthesis of morphine have focused attention on transition metal catalyzed reactions.[73] Trost reported an interesting route which involved an intramolecular Heck coupling as a key step in formation of the dihydrobenzofuran skeleton (Scheme 6-10).[74] Trost's synthesis included four transition metal catalyzed steps in a 13-step linear synthesis, which illustrated the utility of transition metal catalyzed reactions as useful tools for shortening synthetic routes. The Trost synthesis is one of the shortest total synthetic routes to morphine, but employs toxic metals that may limit its use in pharmaceutical grade preparation.

Scheme 6-10: Trost total synthesis of morphine, C-O bond forming step.
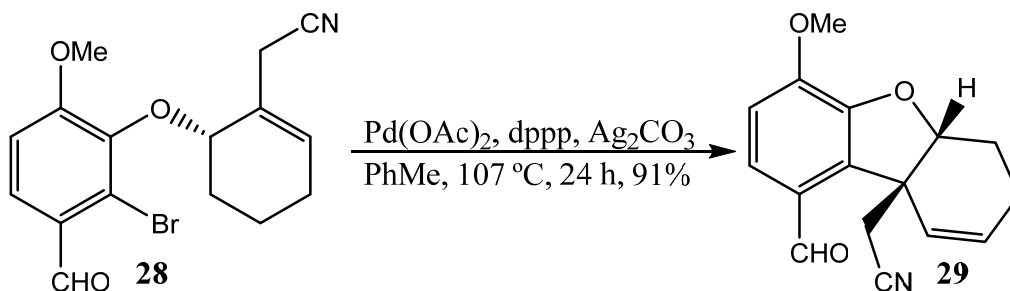
This traditional Heck-mediated intramolecular reaction from bromide **28** employed the phosphine ligand 1,3-bis(diphenylphosphino)propane (dppp) to form the active palladium zero catalyst; dihydrofuran **29** was formed in excellent yield of (91%). This led to the shortest nonbiomimetic total synthesis of (-)-galanthamine to date.

6.   Synthesis via transition metal catalysis.

Since the reactions described in the next chapter are transition metal catalyzed, a more thorough description of transition metal catalyzed reactions from the literature which led to dihydrobenzofurans will be presented. This is also by no means an exhaustive list of transition metal catalyzed reactions leading to dihydrobenzofurans, but is a description of some major pathways.

The first reaction discussed will be the Ullman reaction, generally used to couple aryl halides at high temperatures.[75] It also represents a well-known and widely used method for the synthesis of aryl ethers, although the intramolecular version of these reactions are less widely used. In general, these reactions have a relatively small scope, however they do represent possible strategies for the synthesis of dihydrobenzofurans. Described in Scheme 6-11 are an

Ullman type reaction which employed catalytic copper chloride to provide an excellent yield of dihydrobenzofuran **23**.[76]

Scheme 6-11: Intramolecular Ullman cyclization.
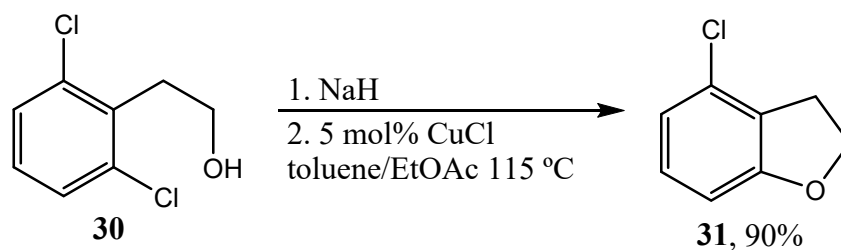
Advances in this type of intramolecular conversion were reported more recently which involved reactions between an aldehyde and a silane to furnish a silyl ether which could be converted into the corresponding alkoxide (Scheme 6-12).[77] This approach avoided the formation of hydrated products, and greatly increased the overall yield of dihydrobenzofurans compared to the earlier route (Scheme 6-11). This method also permitted construction of more substituted dihydrobenzofurans as a variety of aldehydes could be employed. It should be noted, however, that the overall scope of these reactions were still relatively small as the Ullman type coupling conditions were rather harsh.

Scheme 6-12: Advances in the Ullman reaction.
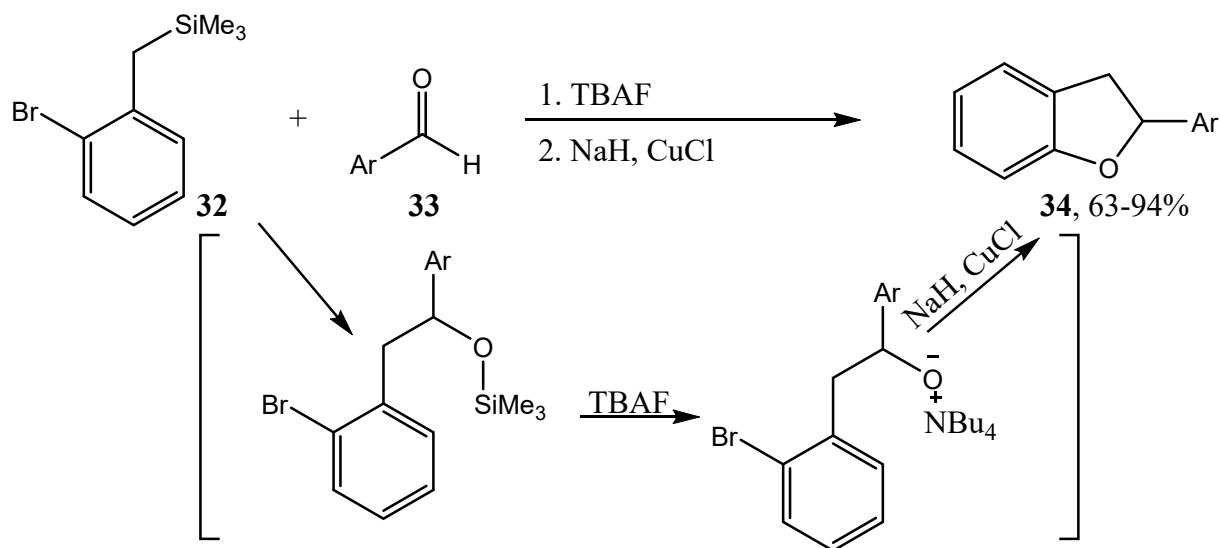
While copper catalyzed reactions were ideal from a cost perspective, other transition

metals such as palladium gave access to a wider scope of transition metal catalyzed processes.[78]

Decades of research into palladium mediated reactions has led to an ever evolving number of

new reactions to synthesize interesting chemical entities.[79] Two decades ago Buchwald

developed an intramolecular C-O bond formation process with an aryl bromide and an alcohol.

This reaction was carried out using catalytic amounts of palladium acetate along with a bidentate

phosphorous based ligand (generally Tol-BINAP or DPPF) and a base (generally K_2CO_3 or

tBuONa) in toluene between 80-100 ºC to give the corresponding heterocycles, including

dihydrobenzofurans (n = 1) in fair to very good yields (Scheme 6-13).[80]

This approach, however, was only efficient when tertiary alcohol substrates were used,

wherein R_1 and R_2 were both not hydrogen.

Scheme 6-13: Buchwald C-O coupling.
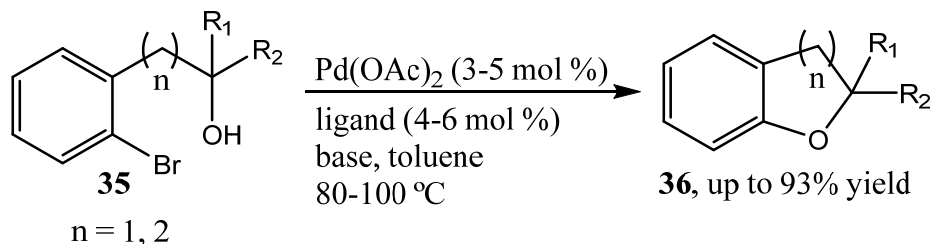
When primary or secondary alcohols were used significant amounts of the corresponding

debrominated aldehydes ($R_1 = R_2 = H$) and ketones ($R_1 = H$), respectively, were formed in place

of the cyclization. This occurred after coordination of palladium to the alcohol and ß-hydride

elimination took place, effectively stopping the reductive elimination to the desired cyclized

dihydobenzofuran **36**. This process is illustrated in Scheme 6-14.

Scheme 6-14: ß-Hydride elimination in primary/secondary alcohols.
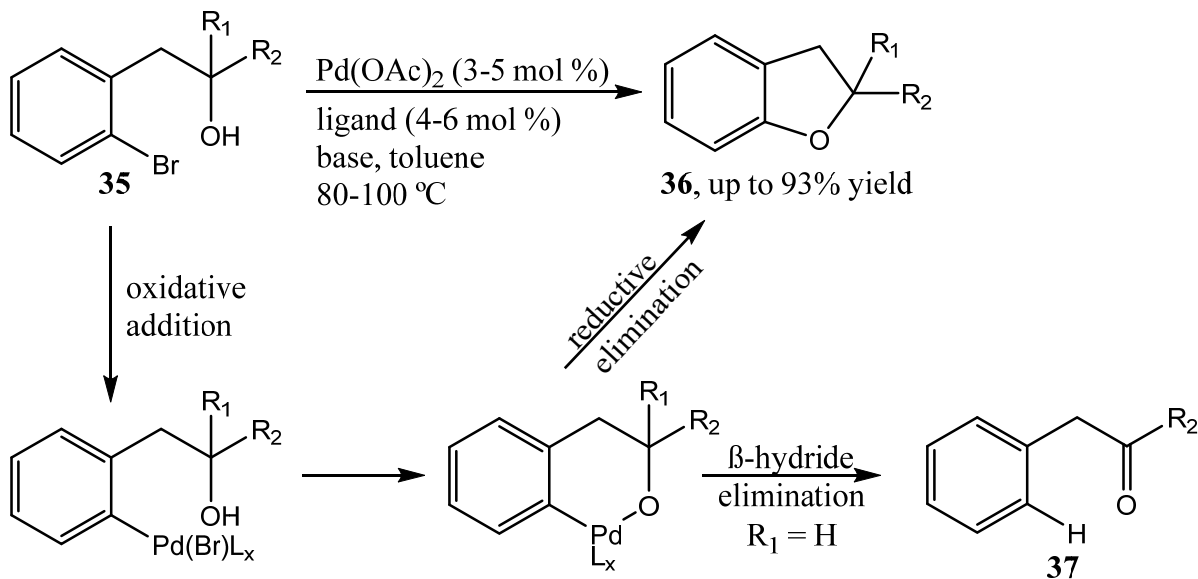
This problem was overcome by the investigation of several different phosphorous based

ligands, of which it was found that bulky, electron-rich ligands could be successfully employed

even with primary or secondary alcohols.[81] The ligand of choice for this conversion was the tert-

butyl binaphthyl ligand **38** depicted in Figure 6-7.

Figure 6-7: Buchwald ligand for use with primary/secondary alcohols.
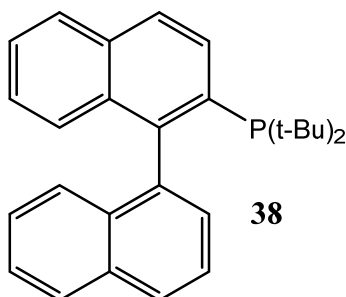
Yields from 71-85% were reported using this ligand in similar reactions to those outlined

in Scheme 6-13 involving both primary and secondary alcohols, although it was noted that yields

with secondary alcohols were generally lower and required higher temperatures. Electron-rich

and bulky ligands are excellent choices for restricting ß-hydride elimination since reductive

elimination favors electron-rich ligands and bulky ligands can help prevent ß-hydride elimination

by shielding a coordination site from hydrogen.[82]

More recently, similar reactions which involved palladium-mediated C-H activation have

been reported. Similar to the original Buchwald method, these reactions work best with tertiary

alcohols and lower yields were observed for secondary alcohols.[83] The report did not mention

the use of primary alcohols. Regardless, this is a novel method for the synthesis of

dihydrobenzofurans. This reaction process is illustrated in Scheme 6-15. Interestingly, this

method permits the use of aryl bromides, for example **39**, which after C-H activation/cyclization

can permit further substitution on the aromatic ring via use of the bromide.[84]

Scheme 6-15: C-H activation of homo-benzylic alcohols.
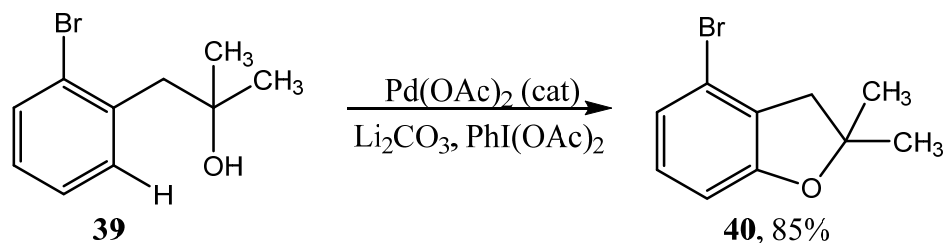
Heck-type chemistry was explored in part 1 of this work, however, it is also applicable in the synthesis of dihydrobenzofurans. One interesting example is the reductive Heck cyclization reaction, which permits stereoselective preparation of the framework for the natural product furaquinocin A (Scheme 6-16).[85]

Scheme 6-16: Reductive Heck cyclization pathway to furaquinocin A.

furaquinocin A
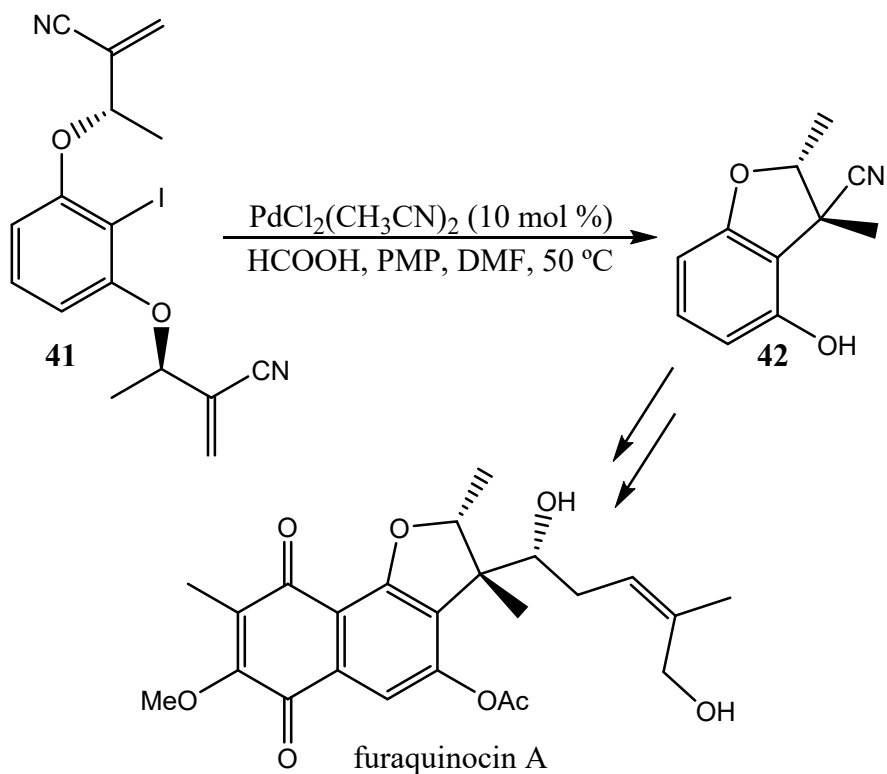
Oxidative Heck coupling generally involves the reaction of an unfunctionalized arene

directly with an olefin, which differs from the traditional Heck reaction in that a halogen is not

necessary.[86] This is attractive for highly substituted arenes where halogenation may not proceed

smoothly. Recent work has expanded the scope of these reaction to include dihydrobenzofurans

and benzofurans from electron-rich arenes (Scheme 6-17).[87]

Scheme 6-17: Oxidative Heck reactions.
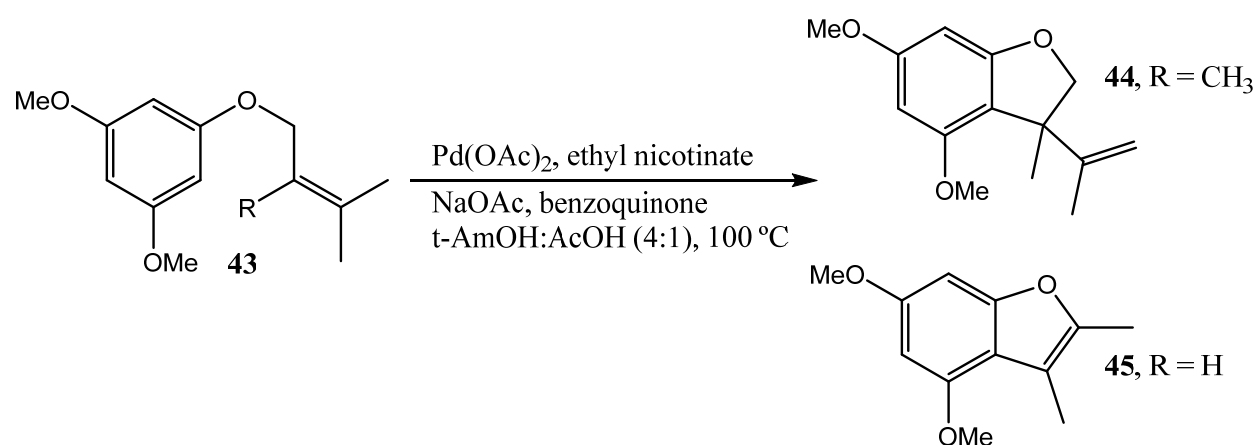
When tetrasubstituted olefins are employed (R ≠ H), synthesis of the dihydrobenzofuran

was favored, whereas when R = H, formation of the benzofuran was favored. Unfortunately,

because electrophilic Pd(II) is involved in the reaction mechanism, this method is limited to the

use of very electron-rich aromatic systems and low to 0% yields were reported with electron

deficient systems.

Detailed in Scheme 6-18 are four other Heck-type reactions that lead to

dihydrobenzofurans. The first reaction details the intramolecular coupling of an allylic ether of

o-halophenols, which advantageously leaves an unsaturated side chain that can be further

substituted if desired.[88] The next reaction involves the intramolecular carbonylative Heck

cyclization of aryldiazonium salts leaving a carboxylic acid side chain that can be modified by

various means.[89] Aryl bromides, for example **42**, were investigated in a number of

cyclization/coupling reactions. Heck cyclization followed by Stille coupling in the presence of

1,3-dimethyl-1,2-imidazolidinone (DMI) yielded the 3,3 disubstituted dihydrobenzofuran **43** in

good yield.[90] Finally, a reaction involving Heck cyclization and concomitant cyanation with

$K_4Fe(CN)_6$ as a cyanide source was reported.[91] In general, these reactions are important due to

the ability to further functionalize the products after formation of the dihydrobenzofuran

skeleton.

Scheme 6-18: Various Heck catalyzed dihydrobenzofuran reactions.
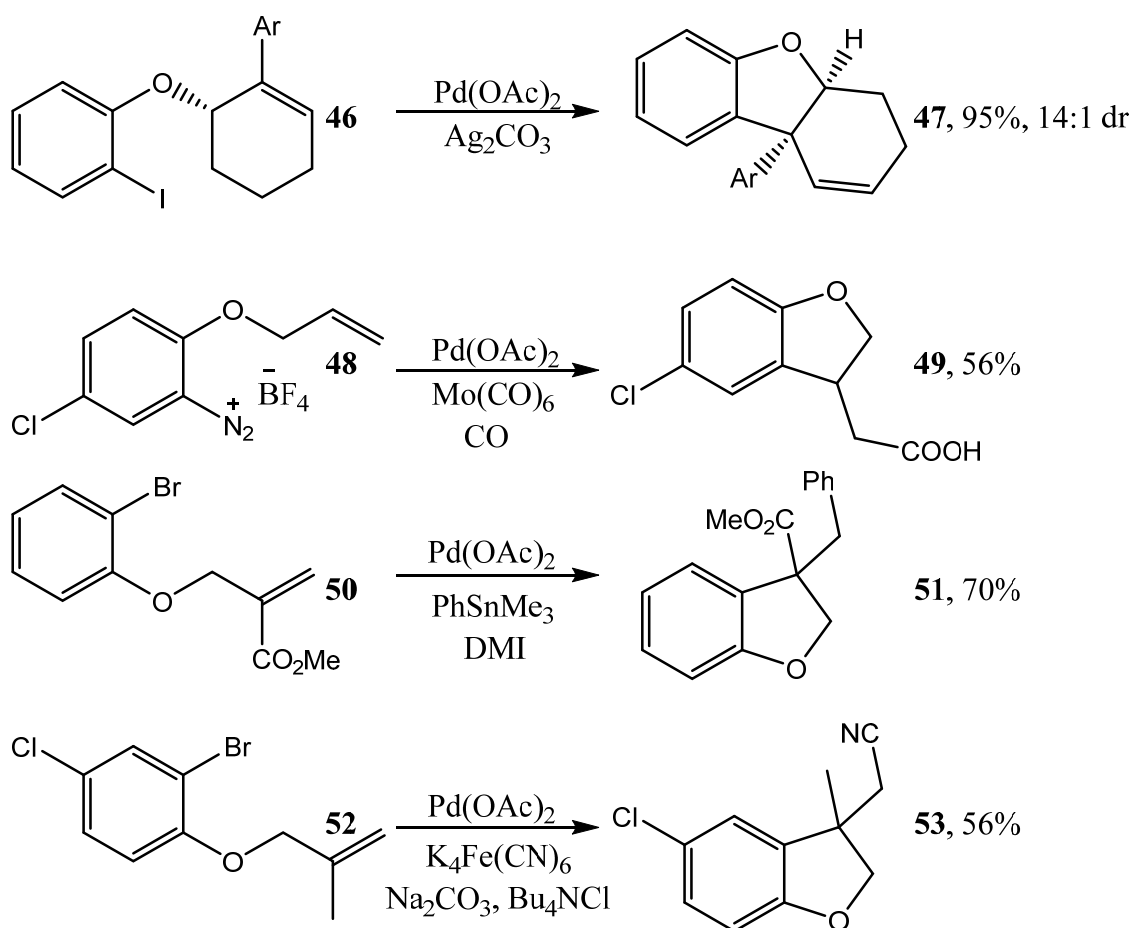
6.   The Larock dihydrobenzofuran method.

In the early 1980's Dieck reported that 1,3-dienes coordinated with palladium zero complexes which permitted nucleophilic substitution to take place (Scheme 6-19).[92] Larock capitalized on this work and reported the heteroannulation of 1,3-dienes with substituted iodophenols in the presence of catalytic amount of palladium acetate to give dihydrobenzofurans in good yields in 1990.[93] This reaction is perhaps the most similar to the work to be presented in the next chapter, thus a more critical analysis of its mechanism and scope will be presented.

Scheme 6-19: Dieck's 1,3-diene reaction.
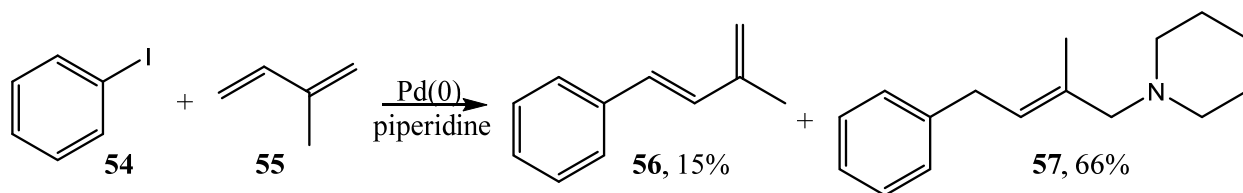
Dieck also reported that reactions with an o-iodoaniline, in place of the iodobenzene and an amine, gave the corresponding dihydroindoles (Scheme 6-20). This was the work that led directly to the future work which resulted in the Larock indole synthesis.

Scheme 6-20: Dieck's dihydroindole reaction.
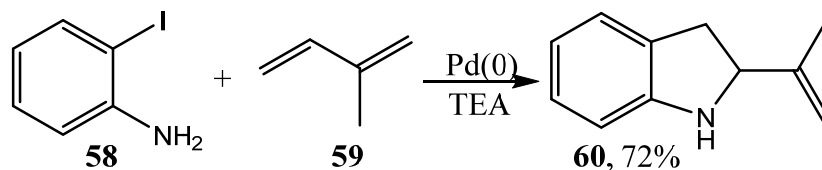
An in-depth analysis of this reaction mechanism was not reported by Dieck, rather they simply postulated that the close proximity of the amino group to the π-allylic moiety in the intermediate complex was necessary for intramolecular cyclization since experiments with

iodobenzene **46**, isoprene **47**, and aniline resulted in only the butadiene **48** with no amine

formation. As previously noted, Larock expanded on this cyclization involving 1,3-dienes and

synthesized a number of dihydrobenzofurans along with a few nitrogen-containing heterocycles.

Detailed in Scheme 6-21 is this reaction process and includes, as reported, a likely mechanism

for this transformation.

Scheme 6-21: Larock 1,3-diene cyclization.
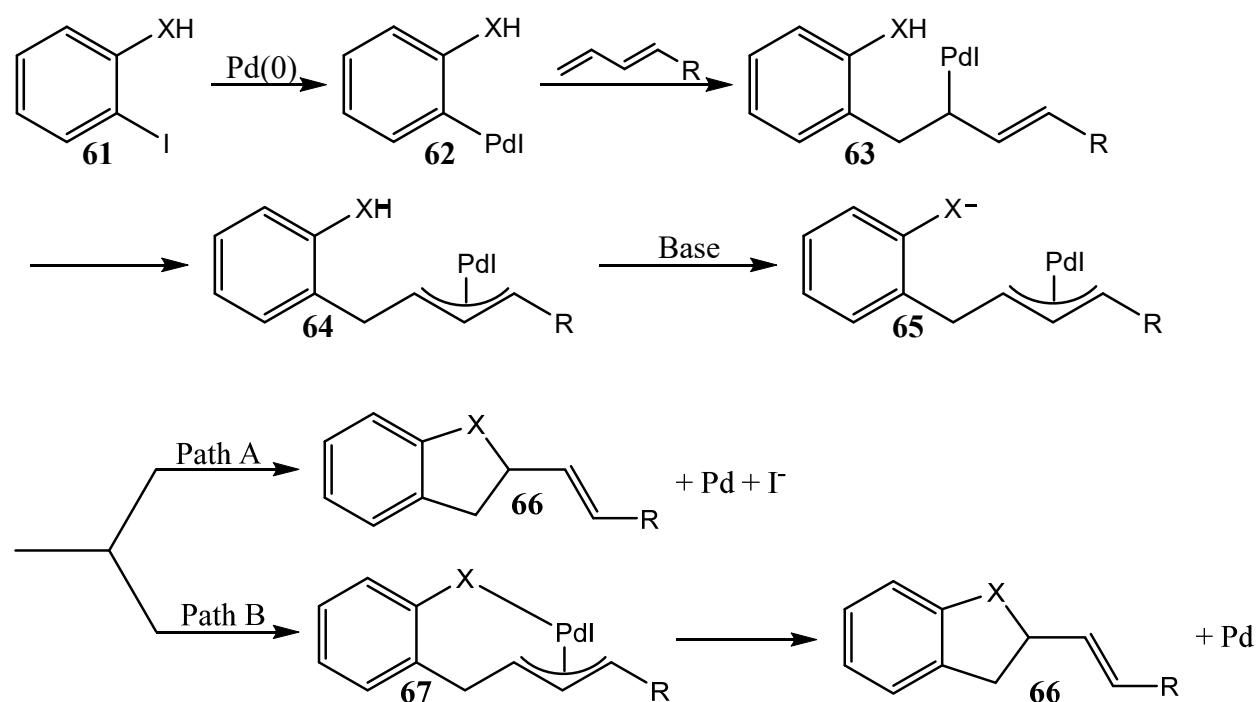
Based on this work there was little doubt that the heteroannulation proceeded via the

intermediate aryl- and π-allylpalladium intermediates depicted in Scheme 6-21 (ligands on

palladium omitted for clarity). However, it was impossible to tell whether or not the

intramolecular palladium displacement was proceeding through a direct back-side displacement

(path A) or via front-side halide displacement and subsequent reductive elimination (path B).

From studies involving 1,3-cyclohexadienes it was determined, at least in the case of 1,3-

cyclohexadiene, when 5-membered rings were formed, path B was the major pathway which involved reductive elimination.

This study was revisited by Larock in 2010[94], at which point certain advancements were made which permitted higher yields and an expanded scope. A more thorough mechanistic study was also employed and a catalytic cycle was proposed for the formation of dihydrobenzofurans. Outlined in Scheme 6-22 is this advancement, which principally revolved around the use of 2-iodo acetates instead of the prior 2-iodophenols. A more advanced bidentate ligand (dppe) was also employed in this reaction.

Scheme 6-22: Advancements in the Larock 1,3-diene cyclization.
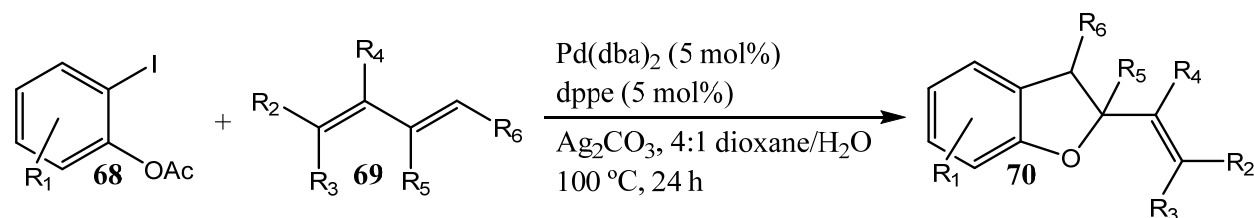
It was shown that these new conditions which involved the acetate gave consistently higher yields compared to the phenol under identical reaction conditions. The prior reaction (Scheme 6-21) also suffered from a rather poor scope in which electron-rich aryl iodides either gave low yields or did not react at all; with the acetates good yields with more electron-rich aryl iodides were observed. For example, in the prior reaction 2-iodo-4-methoxyphenol afforded mainly dehalogenated product and only negligible amounts of the desired dihydrobenzofuran **73**. However, 2-iodo-4-methoxyphenyl acetate with **72** gave a yield of 58% of the desired dihydrobenzofuran **73** when used in the updated and optimized Larock process (Scheme 6-23).

Scheme 6-23: Dihydrobenzofurans from electron-rich aryl iodides.

71 + 72 → Pd(dba)₂ (5 mol%), dppe (5 mol%), Ag₂CO₃, 4:1 dioxane/H₂O, 100 °C, 24 h → 73
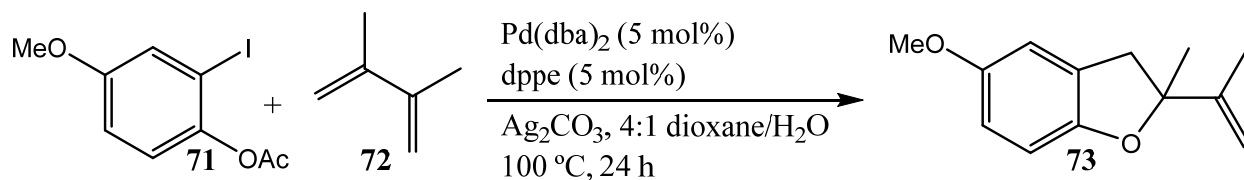
Similar results were obtained with other electron-rich aryl iodides in this report; however, in the text only 2-iodo-4-methoxyphenol was mentioned in reference to failures with electron-rich iodophenols. A proposed mechanism detailing the influence of these acetate groups was also reported (Figure 6-8). It should be noted, however, that none of the proposed aryl-palladium intermediates in this catalytic cycle have been isolated and confirmed.

Figure 6-8: Proposed catalytic cycle for the Larock's synthesis of dihydrobenzofurans.[94]

S = Solvent
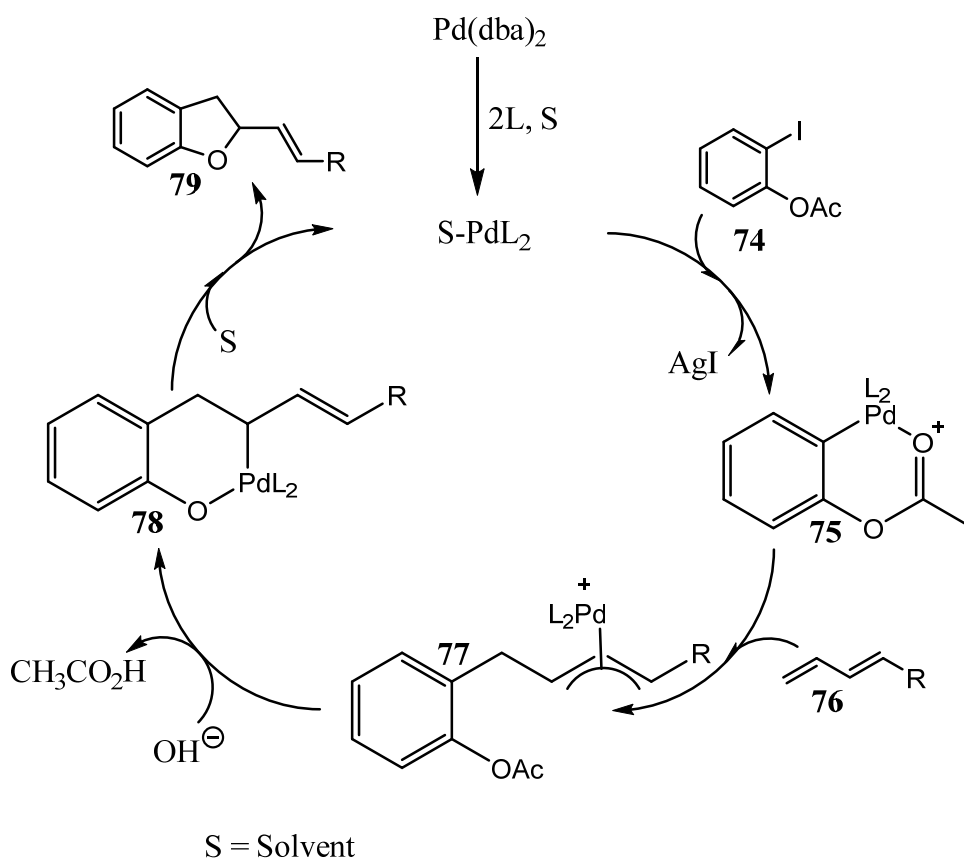
Initial oxidative addition of the iodoarene **61** to the palladium zero active catalyst provides the aryl-palladium intermediate **62** after abstraction of the iodide by Ag_2CO_3. It was postulated by Larock that this coordination led to higher reactivity towards alkene **63**, which was presumably responsible for the high yields observed in some trials. This cationic arylpalladium complex **62** next adds to the 1,3-diene **63** in a *syn*-fashion to give the π-allylpalladium complex **64** which coordinated with the acetoxy oxygen atom leading to the formation of the cyclical aryl palladium complex. This proposed coordination of the acetate was likely the mechanism that slows formation of the undesired stilbene via a normal Heck coupling mechanism. This coordination restricted rotation of the allyl C-C bonds, presumably, and was postulated to be responsible for the stereoselectivity observed when *trans-trans*-2,4-hexadiene was utilized. Deacylation of the starting iodoarene **61** was not observed under the reaction conditions, hence why it was reported that deacylation occured between **64** and **65**. A high correlation was seen between the acidity of the phenolic precursors of the iodoarenes and annulation yields, which further supported the deacylation at this step. Finally, complex **65** underwent reductive elimination to give the desired dihydrobenzofuran **66** with regeneration of the palladium zero catalyst.

It should be noted that of the 15 examples given in the report of Larock, many were under 70% yield. In general, these lower yields were associated with more electron-rich iodoarenes, similar to issues seen prior to this method which involved the use of iodophenols instead of iodoacetates. The byproducts of this reaction, similarly to the previous reaction, were the Heck-type stilbene products.

III.   CONCLUSION.

In conclusion, a number of natural and synthetic dihydrobenzofurans have proven to possess biological activity for a wide variety of disease indications; some are used as potent and selective pharmaceutical drugs. Interest in the identification of natural dihydrobenzofurans, the total synthesis of dihydrobenzofuran natural products, medicinal chemistry SAR applications involving dihydrobenzofurans, and new methods for the synthesis of dihydrobenzofurans are increasingly popular areas of study.

Detailed in this introduction are a number of both natural and synthetic dihydrobenzofurans, many of which have biological activity. A scifinder search of the dihydrobenzofuran skeleton revealed thousands of natural products with the dihydrobenzofuran functionality, many of which also possess bioactivity. These compounds are novel scaffolds for future research and methods for synthesis of these or similar analogs are of importance.

A number of methods for the synthesis of dihydrobenzofurans were also detailed. Some of these methods were described only in reference to the synthesis of some natural products, however, some were more general. Even in the general cases, many of these reactions had a rather small scope due to the complex nature of the starting material employed. In many cases, synthesis of the dihydrobenzofuran skeleton was only accomplished after a multi-step synthetic procedure. In many of these cases the placement of substituents in the starting materials, especially on the arene side chain of the dihydrobenzofuran, was either not explored or required specific moieties. For example, in many cases, some presented here, methoxy groups in the 4-position are necessary to help facilitate quinone formation. Although many natural dihydrobenzofurans also contain a methoxy group in this position, and likely follow similar

biological processes for formation of the dihydrobenzofuran core structure, this restriction can be resolved via transition metal catalyzed reactions.

Larock published a method very similar to the method to be described in this work; however, there are many core differences that will be described below. Based on our findings, it is unlikely that the mechanism involved in the work of Larock is the same as the mechanism to be described herein, however the similarity in starting materials is interesting. Dieck and Larock both reported that coordination of palladium to a phenolic system can influence the cyclization to dihydrobenzofurans and other heteroannulations. This method led to a diverse selection of dihydrobenzofurans, although issues with electron-rich arenes were noted. The work to be presented in the next chapter aims to expand the scope of transition metal catalyzed reactions in a similar manner to obtain dihydrobenzofurans, but by a 1-step mechanism which involves commercially available and easily accessible starting materials.

A NEW TRANSITION METAL CATALYZED PROCESS FOR THE

SYNTHESIS OF DIHYDROBENZOFURANS

I.   INTRODUCTION.

Detailed in Chapter 3 the Heck reaction was employed in the synthesis of a number of stilbenoid compounds with antibiotic activity. The catalytic cycle for the Heck reaction was studied in detail, but is shown again in Figure 7-1 for reference. For a more detailed explanation of the steps depicted below please see Chapter 3.

Figure 7-1: General catalytic cycle of the Heck reaction.
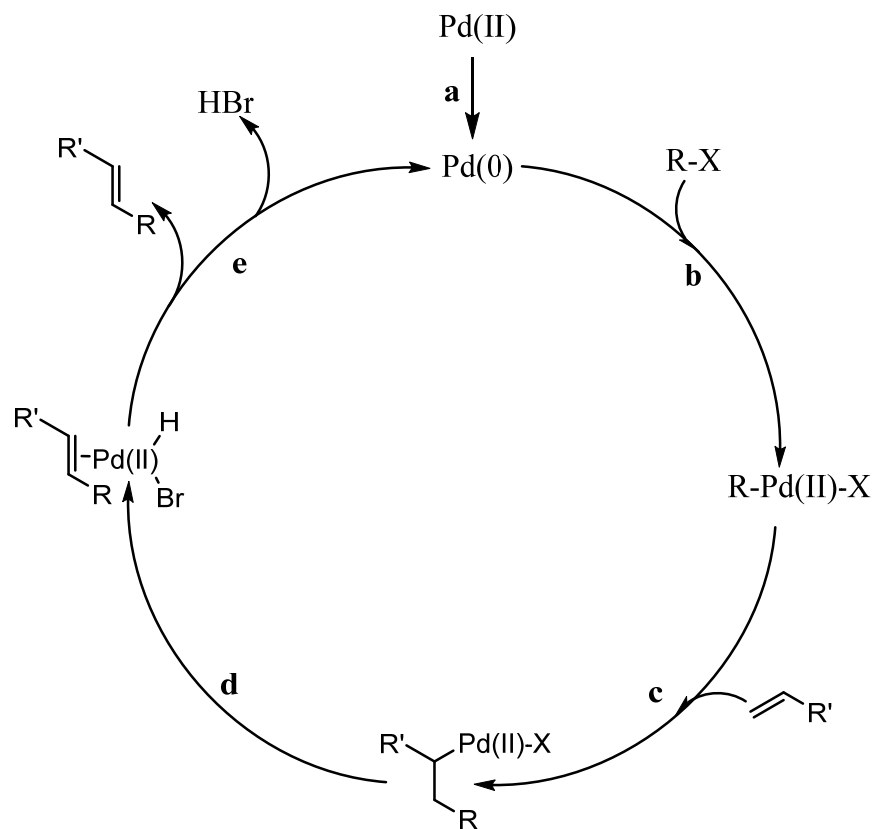
In summary, step **a** represents activation of a precatalyst to an active palladium zero catalyst, this step can be avoided if a direct palladium zero source was used. Detailed in process **b** was the oxidative addition, followed by syn-addition in step **c**. This was followed by ß-hydride elimination **d** and reductive elimination **e** to give the desired compound while reactivating the catalyst to continue in the catalytic cycle.

In general, as described in Chapter 3, both high conversion and excellent yields were observed for many of the stilbenes synthesized. In a few particular cases, however, while yields were still generally high, a prominent and easily purified dihydrobenzofuran byproduct was observed. These cases involved the reaction of 2-bromo-4-methoxyphenol **67** with styrenes under the same catalytic conditions employed for the synthesis of the stilbenes (Scheme 7-1).

Scheme 7-1: 2-bromo-4-methoxyphenol in the Heck reaction.
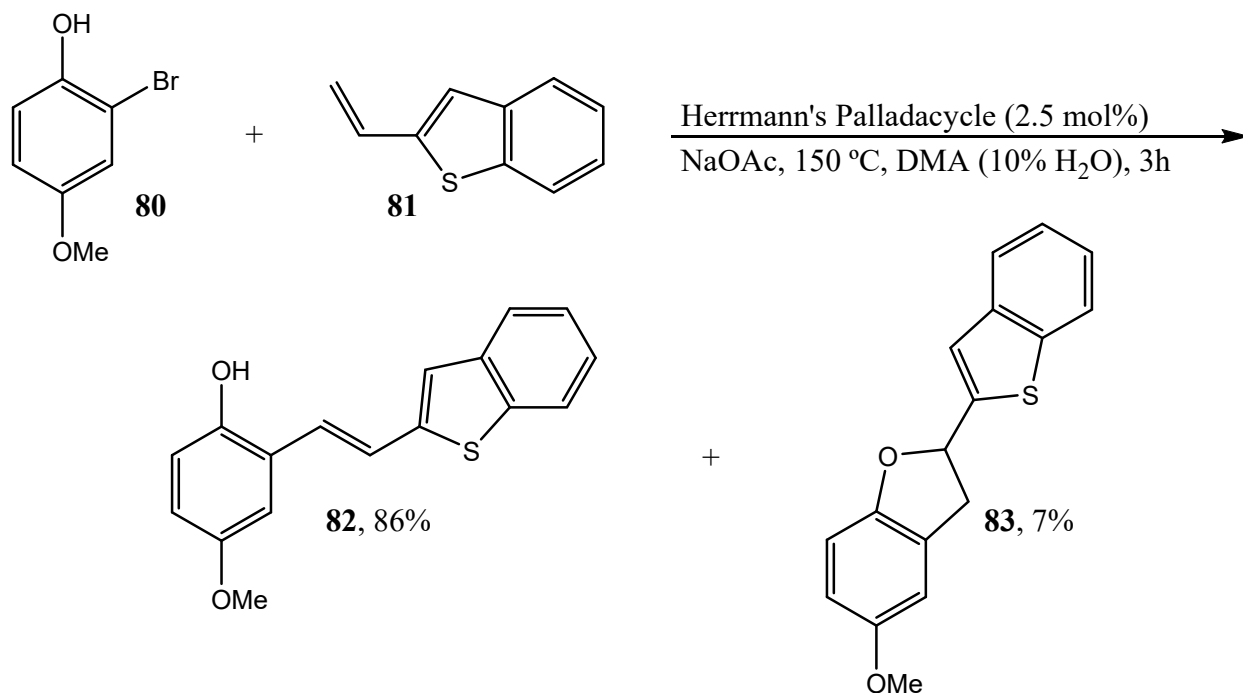
It should be noted that some of these compounds appear in part 1 of this work, however they have been re-numbered for clarity in this section.

The interesting dihydrobenzofuran **83** was purified and was the only major byproduct in this reaction. Since they were less polar than the stilbenoid derivatives, these dihydrobenzofurans were easily purified by flash column chromatography. However, with only a 7% yield this conversion was not high enough to be considered a new method for the synthesis of dihydrobenzofurans.

II.   CHEMISTRY AND RESULTS.

It was originally thought that the reaction mechanism for this process was similar to that which Larock had previously published.[94] In this case, palladium would have inserted into the heterocyclic aromatic thiophene ring system to form the aryl palladium species presented in Chapter 6. Although this did not seem very plausible, synthesis of the methyl ester acetate **85**, used in Larock's synthesis, was tested under the reaction conditions to ascertain whether or not it affected the yield of the dihydrobenzofuran (Scheme 7-2).

Scheme 7-2: Synthesis of the Larock acetate 85.
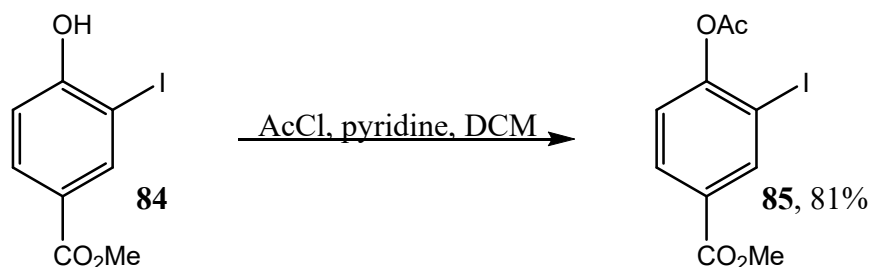
The acetate **85** was purified by crystallization from isopropanol and the ^{1}H/^{13}C NMR spectra were identical to the published reports.[94] When **85** was reacted under the same reaction

conditions of Scheme 7-1, however, this resulted in only synthesis of the stilbenoid acetate derivative **86** (Scheme 7-3) with no dihydrobenzofuran **87** observed even on examination of the crude material by NMR spectroscopy. While this does not rule out a similar mechanism to prior works reported by Larock, it certainly suggests a different mechanism may be operating in this transformation.

Scheme 7-3: Palladium catalyzed reaction with acetate 85.
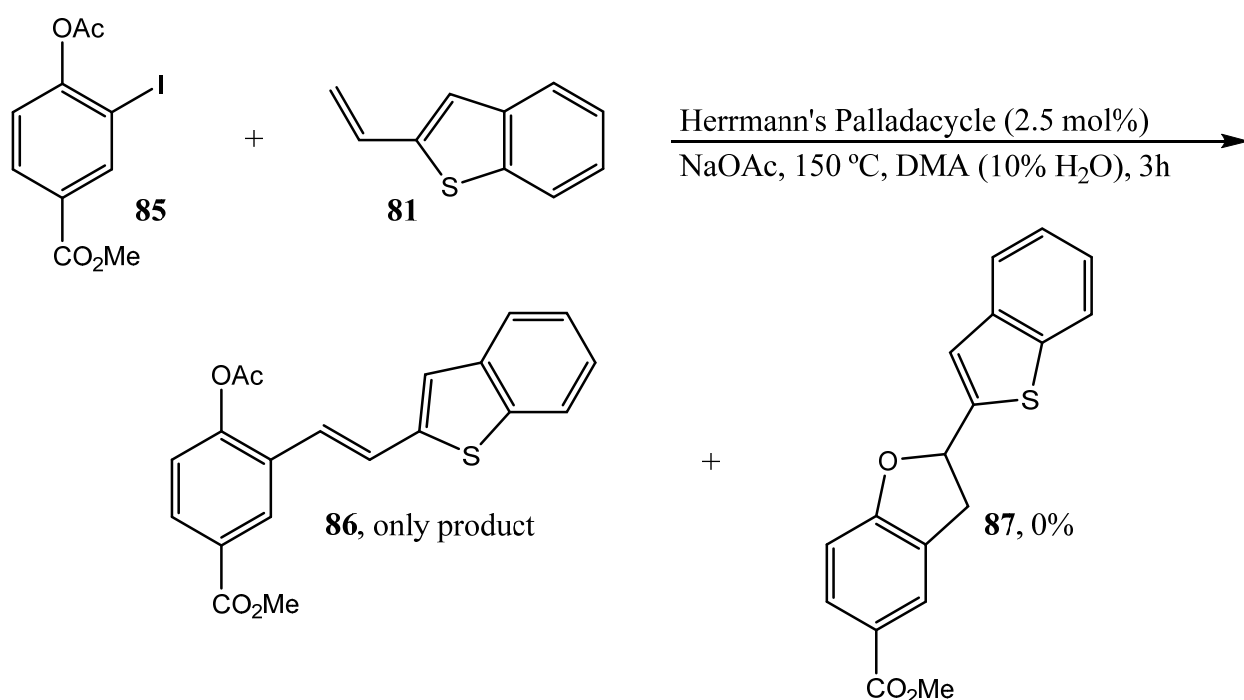
Following this work, a more thorough investigation of the reaction conditions was initiated to attempt to improve the yield of the dihydrobenzofuran product while minimizing the yield of the stilbene. The successful results from this study are detailed in Table 7-1 (see entry 13).

Table 7-1: Optimization trials.
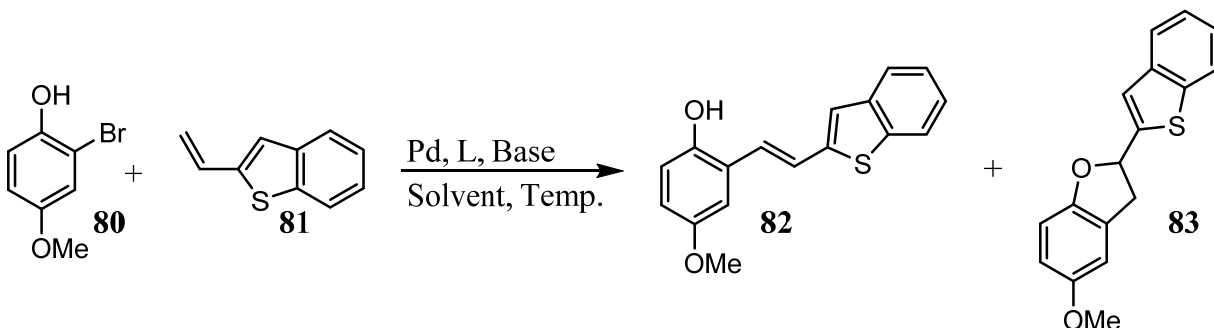
#	Pd[a]	L	Base	Solvent[b]	Temp (°C)	82 (%)[c]	83 (%)[c]
1	H.P.[d]	---	NaOAc	DMA/10% H_2O	150	86[e]	7[e]
2	""	---	NaOAc	DMA/10% H_2O	200	84	9
3	""	---	NaOAc	DMA/10% H_2O	100	0	0
4	""	---	NaOAc	DMA/10% H_2O	130	45	22
5	""	---	NaOH (aq.)	DMA/10% H_2O	130	42	15
6	""	---	NaOH (aq.)	DMA/10% H_2O	100	0	0
7	$PdCl_2$	---	NaOAc	DMA/10% H_2O	150	10	trace
8	$Pd(OAc)_2$	---	NaOAc	DMA/10% H_2O	150	11	trace
9	$PdP(Ph_3)_4$	---	NaOAc	DMA/10% H_2O	150	0	0
10	H.P.[d]	---	Cs_2CO_3	DMA/10% H_2O	150	89	10
11	""	---	Cs_2CO_3	DMA/10% H_2O	130	45	42
12	""	---	Cs_2CO_3	DMA	150	14	75
13	**""**	**---**	**Cs_2CO_3**	**DMA**	**130**	**trace**	**95**

[a] 5 mol% Pd used, [b] all solvents were degassed by freeze/thaw prior to use, [c] conversion determined by HPLC, [d] H.P. = Herrmann's palladacycle, [e] isolated yield

Gratifyingly, optimization indicated that indeed the dihydrobenzofuran **83** could be synthesized in excellent yields while minimizing the conversion of the undesired stilbene byproduct. More surprisingly, however, was that the dihydrobenzofuran was synthesized more readily at lower temperatures and without the inclusion of water, which was necessary for optimal conversion to the stilbenes in the earlier work. It was interesting to note, however, that conversion to the stilbene was noted in trial 12 even in the absence of water. It was presumed

that the change in substitution pattern from earlier Heck trials in Chapter 3 permitted this conversion to **82**, although it was still rather low.

It was also interesting to note that in trials 7 and 8, palladium (II) species still gave the desired stilbenoid product, although again in low yield. Palladium (II) species were not investigated in the absence of a ligand in the original Heck reaction trials in Chapter 3, although the low yield for these cases did not warrant further investigation. It was interesting to note, however, that palladium (II) species were able to catalytically provide the stilbenes, whereas the catalytic cycle dictates that palladium zero must be the active catalyst. This can be rationalized by the ability of palladium (II) species to undergo conversion to palladium zero just prior to formation of palladium black – which can essentially be described as clusters of ligandless palladium. Just after de-ligation of ligands, but prior to clustering, these ligandless palladium species have been previously shown to catalytically promote palladium zero reactions such as the Heck reaction.[95]

Herrmann's palladacycle (Figure 7-2) was again found to be the most suitable catalyst for this conversion. It is apparent that this palladacycle is inherently well-suited for reactions with these electron-rich aryl bromides.

Figure 7-2: Herrmann's palladacycle.
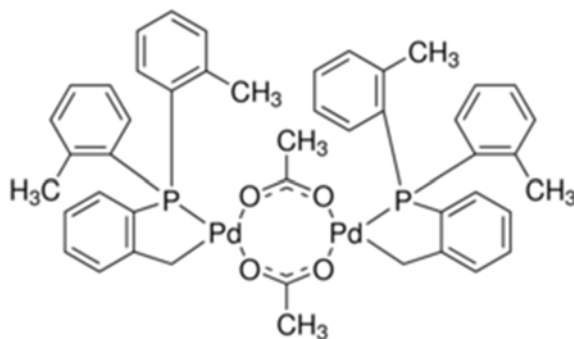
Gratifyingly, nearly complete conversion to the desired dihydrobenzofuran was observed by simply changing the base, removing water, and lowering the temperature slightly. It was presumed that this effect of temperature was related to either the reductive elimination of the stilbene or the ß-hydride elimination step, both of which would presumably lead to the stilbene product. When that critical temperature was not reached, palladium had the ability to coordinate with the phenol and conversion to the dihydrobenzofuran was accomplished. A more thorough description of a proposed mechanism will be presented later in the Chapter.

In fact, it was found the influence of temperature was incredibly important for these reactions. Four different styrenes were employed in this study (Figure 7-3) and it was found that careful control of the temperature from 100-130 °C was critical for high yields with minimization of the undesired stilbene products.

Figure 7-3: Styrenes employed in this study.
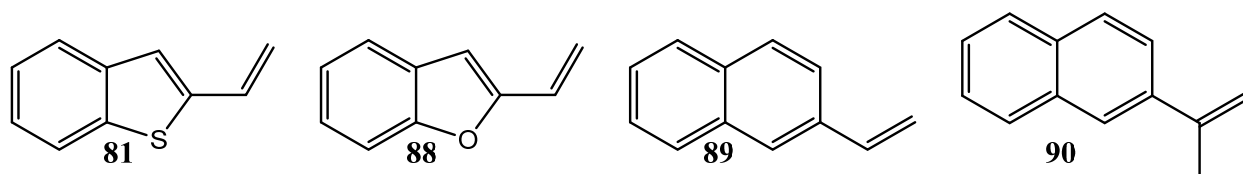
Both styrenes **81** and **88** were used in the prior SAR study described in Part 1. Styrene **89** was commercially available and styrene **90** was conveniently synthesized from ethanone **91** (Scheme 7-4).

Scheme 7-4: Synthesis of 90.
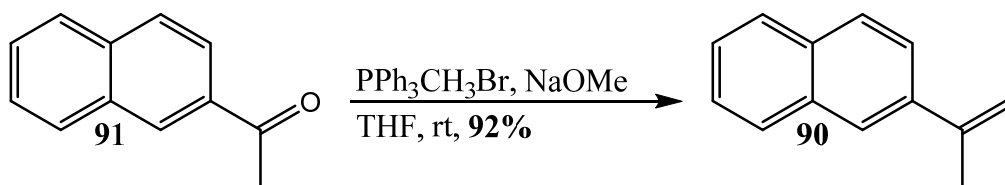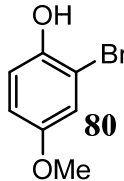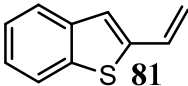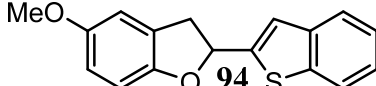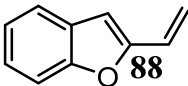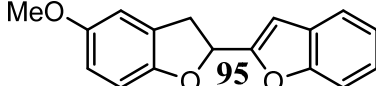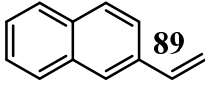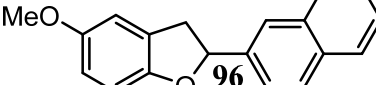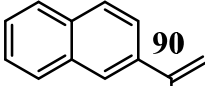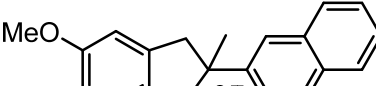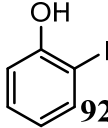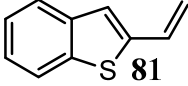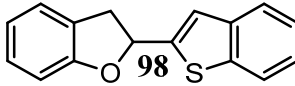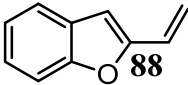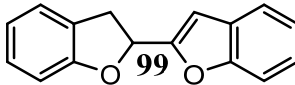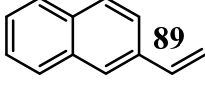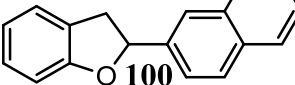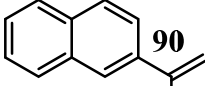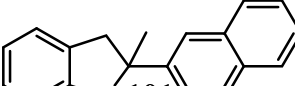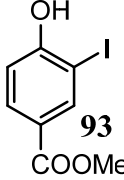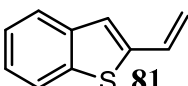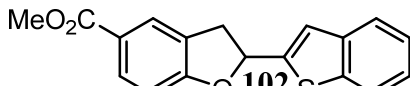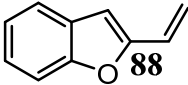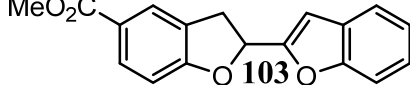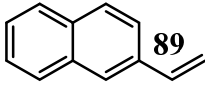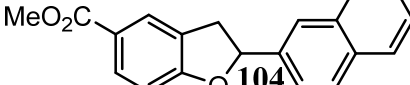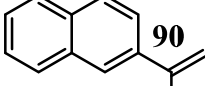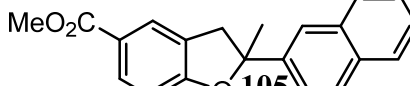
Three different aryl halides were also employed in the initial study, the previously mentioned 2-bromo-4-methoxyphenol **80** along with 2-iodophenol **92** and the iodomethyl ester **93** (Figure 7-4). Thus twelve new and novel dihydrobenzofurans were synthesized via this method. Further work and an interesting byproduct from the styrene **89** will also be described below.

Figure 7-4: Aryl halides used in this study.
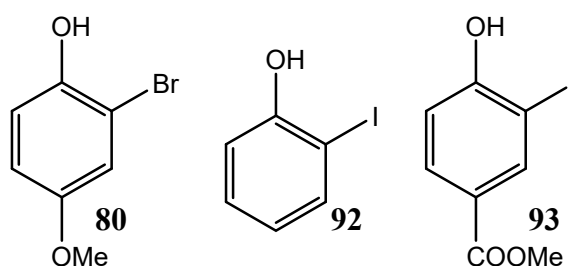
It should be noted that 2-bromophenol was also employed in the process and works as well as 2-iodophenol, however 2-bromophenol is a liquid which is more difficult to handle at room temperature then the solid 2-iodophenol. In the case of the iodomethyl ester **93**, it was available in the lab from a previous project, consequently, the bromo derivative was not employed. A subsequent study to be discussed later used three different aryl bromides similar to **80** with no issues, moreover, it seems that bromides are just as suitable as iodides for this new reaction to dihydrobenzofurans. **This is in contrast to method of Larock[94] which only employed aryl iodides, presumably out of necessity.**

Table 7-2: Scope of the reaction.[a]

Entry	Arene	Styrene	Temp. (ºC)	Product	Yield[b]
1	**80**	**81**	130	**94**	87%
2	**80**	**88**	110	**95**	75%
3	**80**	**89**	100	**96**	89%
4	**80**	**90**	130	**97**	90%
5	**92**	**81**	130	**98**	86%
6	**92**	**88**	110	**99**	73%
7	**92**	**89**	100	**100**	92%
8	**92**	**90**	130	**101**	94%
9	**93**	**81**	130	**102**	72%
10	**93**	**88**	110	**103**	77%
11	**93**	**89**	100	**104**	82%
12	**93**	**90**	130	**105**	91%

[a] Cs_2CO_3, DMA, Herrmann's palladacycle [b] isolated yield

The iodomethyl ester **93** was also an interesting substrate since it bears an electron withdrawing group, in constrast to the electron donating nature of the methoxy analog **80**. It should also be noted that under the basic reaction conditions, the methyl ester remained intact in all cases with no trace of the carboxylic acid even on examination of the crude material by NMR spectroscopy. The acetate version of **93** was the most prominent aryl iodide employed in the Larock publication (4 of 15 examples), therefore, it also served as a direct comparison to that work.

Examination of the initial study illustrated the scope of this reaction (Table 7-2). Clearly aryl bromides are applicable, as opposed to the report of Larock which seemingly required aryl iodides[94]. Furthermore, excellent yields with electron-rich arenes are easily accessible with no need to first synthesize the acetate of the phenol. Although this mechanism likely differs from that in Larock's work, these important distinctions were considered when developing the reaction to assess its novelty and importance.

It was also important to note that the original hypothesis in the study by Larock that the heterocyclic nature of the reactant was necessary for conversion with some coordination between the aromatic 1,3 diene system seemed to be less plausible here, when the reactions between the naphthyl styrenes **89** and **90** are considered. Although the thiophene and benzofuran systems are aromatic in nature, they are considerably more reactive than naphthalene, and this fact was considered early in the study here. The commercially available 2-vinylnaphthalene **89** was reacted under a number of catalytic systems to attempt to determine the best possible conditions and catalyst for the conversion. Subsequently it was determined that the original conditions (Table 7-2 and 100 ºC) with Herrmann's palladacycle gave the best yields of dihydrobenzofuran, although even in this case low conversion to the stilbene was still observed.

Detailed in Table 7-3 are some of the catalytic systems and conditions employed with 2-vinylnaphthalene **89**.

Table 7-3: Catalytic systems employed with naphthyl styrene 89.

#	Pd^a	L	Base	Additive	$89\ (\%)^b$	$106\ (\%)^b$	$96\ (\%)^b$
1	H.P.^{c}	---	Cs_2CO_3	---	1	5	86
2	Pd(OAc)$_2$	p(otolyl)$_3$	Cs_2CO_3	---	29	18	44
3	""	dppf	Cs_2CO_3	---	35	34	30
4	""	R-BINAP	Cs_2CO_3	---	45	15	25^d
5	Pd(dba)$_2$	---	Cs_2CO_3	---	75	15	10
6	PdCl$_2$	---	Cs_2CO_3	---	41	11	44
7	PdCl$_2$ (1 eq)	---	Cs_2CO_3	---	51	31	18
8	Wilk. cat.^{e}	---	Cs_2CO_3	---	91	5	4
9	Pd(PPh$_3$)$_4$	---	Cs_2CO_3	---	72	20	8
10	H.P.^{c}	---	Cs_2CO_3	LiCl	15	11	65
11	""	---	NaH	---	50	0.5	0
12	""	---	Cs_2CO_3	$K_2S_2O_8$	80	10	10
13	""	---	Cs_2CO_3	4-TBC	100	0	0

^{a} 5 mol% Pd used unless otherwise noted, ^{b} conversion determined by HPLC, ^{c} H.P. = Herrmann's palladacycle, ^{d} no asymmetric induction observed by chiral HPLC, ^{e} Wilk. cat. = Wilkinson's catalyst

Although analysis of all of the reactions in table 7-3 provide some insight into the reaction mechanism and scope, none were as useful as the original conditions in Table 7-2, which gave excellent conversion and yield of the naphthyl dihydrobenzofuran **96**. It was interesting to note that palladium zero catalysts such as Pd(dba)$_2$ and Pd(PPh$_3$)$_4$ (trials 5 and 9)

both gave low conversions to both the stilbene and the cyclized product, whereas palladium (II) catalysts (trials 2, 3, 4, 6, and 7) with or without ligands gave better overall conversions. The use of PdCl$_2$ also exhibited little difference in conversion when used stoichiometrically or catalytically, however, ratios of stilbene to dihydrobenzofuran were almost inverse to one another. There is no current explanation for this behavior. Sodium hydride as a base was found to decompose the starting styrene **89** and only trace conversion was noted. From examination of the above data the future focus should center on Pd(OAc)$_2$, PdCl$_2$, and especially Herrmann's palladacycle as catalysts of choice.

Preliminary attempts to observe asymmetric induction using R-BINAP were also unsuccessful leading to a 50:50 mixture of enantiomers (trial 4). It should be noted that in the R-BINAP case, the reaction turned black after a few minutes at 100 ºC which presumably indicated conversion to palladium black. As described earlier, palladium (II) can decompose to form active palladium zero catalysts at elevated temperature. It is possible that the palladium BINAP complex was not formed or decomposed under the reaction conditions and the conversion noted was due to the formation of these palladium black active catalysts.

In parallel with this work, a novel new compound was also observed in the synthesis of the dihydrobenzofuran **104**, and is pictured below in Table 7-4. Strangely, the benzofuran **107** was observed in higher yields with lower reaction temperatures. This was not observed in other cases and may represent an unusual characteristic of this specific reaction, however, it was still interesting to note the formations of these different products based on temperatures changes alone.

Table 7-4: Reactions with methyl ester 93 and napthene 89.

Entry	Temp. (ºC)	107 (%)[a]	104 (%)[a]	108 (%)[a]
1	70	75	25	0
2	110	15	82	0
3	140	<5	<5	86

[a] determined by HPLC

Because conversion to the benzofuran **107** at low temperatures was not expected, a crystal structure was obtained to be certain that this was the material (Figure 7-5).

Figure 7-5: Crystal structure of 107.
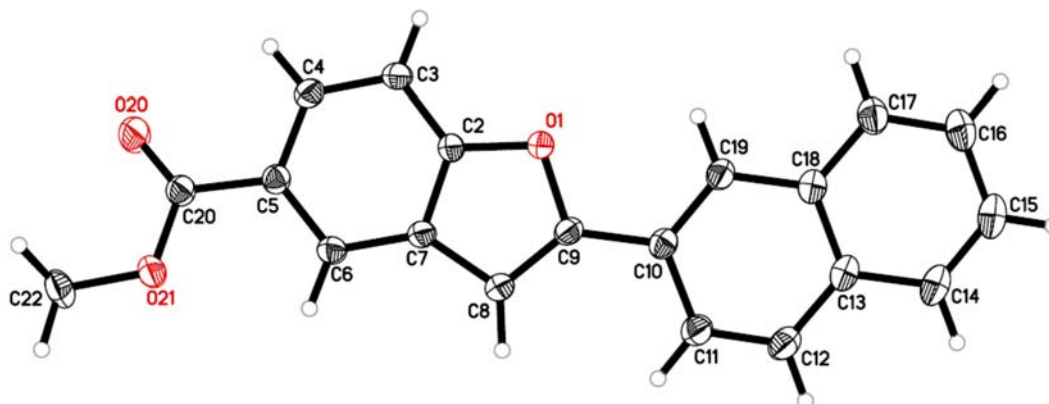
Examination of the crystal structure of benzofuran **107** indicated that the assigned structure was correct, however as noted, similar behavior with other arenes and styrenes has not yet been observed. This reaction was repeated with similar results and might represent a strange case of palladium based chemistry. A plausible mechanism for ligand **107** will be discussed in a future section.

Detailed in the introduction are a number of reactions that had restrictions on the substitution patterns of the arene ring. Many of these reactions focus on the ability to form quinones of phenols and required methoxy groups in the 4-position for good yields. It has been shown that this new reaction process works well with 4-methoxy bromophenols, however, substitution at other positions had not yet been evaluated. Based on the necessity of an ortho-halophenol, there are four different suitable positions for mono-substitution of the ring system. These are shown in Figure 7-6.

Figure 7-6: Possible substitution patterns for bromophenols.
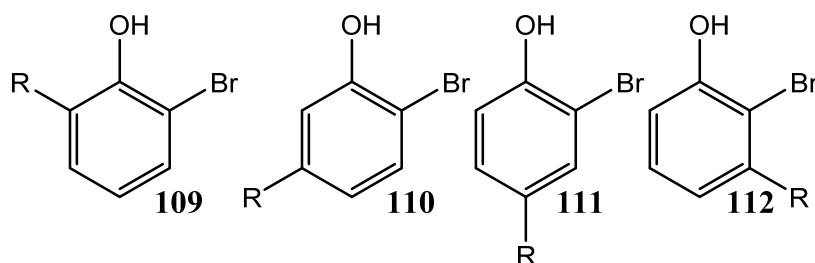
For this initial study methoxy groups were chosen as the most suitable R-group due to both the availability of the substituted phenols and its electronic characteristics. As previously discussed, transition metal chemistry in general experiences problems with the oxidative addition of electron-rich substrates, consequently the use of methoxy as a general guideline to test the scope of this reaction was deemed appropriate.

The 2-bromo-4-methoxyphenol **80** was already employed with a number of different styrenes in excellent yields (Table 7-2), therefore R = methoxy **111** was already adequately tested. This left R = methoxy **109**, **110**, and **112**. Although these aryl bromides are commercially available, the starting materials necessary for synthesis were already in hand for R = methoxy **109** and **110**, consequently while waiting to receive R = methoxy **112** the other bromides were quickly and conveniently synthesized.

In general, synthesis of aryl bromides was carried out with a brominating agent. Given the electronic character of phenols, the ortho and para positions were the most activated sites for bromination. There are many literature reports for mono-bromination of phenols and a number of pathways towards these compounds involve inexpensive reagents in high yields.[96] The synthesis of 2-bromo-6-methoxyphenol **114** was carried out with 2-methoxyphenol **113** by slowly adding it to a suspension of tert-butylamine (tBuNH$_2$) and bromine (Br$_2$) at -78 °C (Scheme 7-5). The low temperature and addition of tert-butylamine slows the reaction down considerably, halting the formation of other brominated derivatives while also promoting ortho bromination. In contrast, the same reaction at room temperature in the absence of tert-butylamine resulted in almost full conversion to the para-directed bromide 4-bromo-2-methoxy phenol, employed earlier in Part 1 for the synthesis of potent antimicrobials.

Scheme 7-5: Synthesis of ortho-substituted aryl bromide 114.
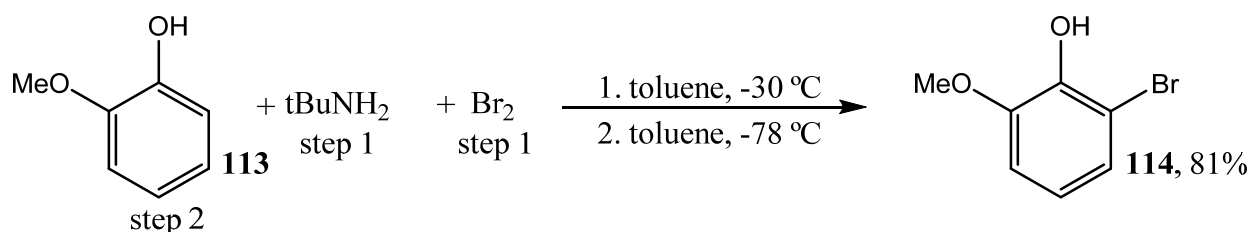
The bromide was further purified by flash column chromatography with a final yield of 81%. It should be noted that column chromatography was only used as a precaution, since after the work-up the bromide was nearly analytically pure. Palladium mediated reactions can sometimes be poisoned by extremely small quantities of (in)organic materials[97], consequently, one had to insure the starting materials were as pure as possible prior to use; this was of utmost importance for these trial reactions.
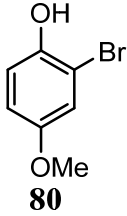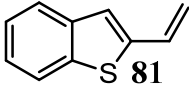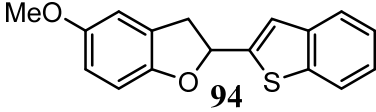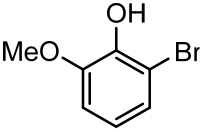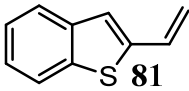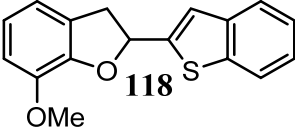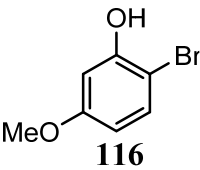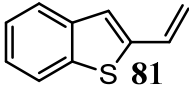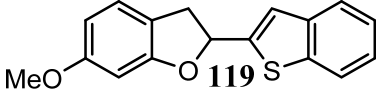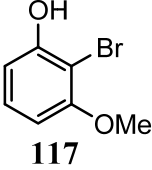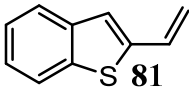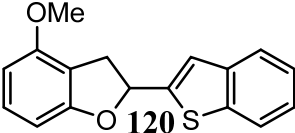
Synthesis of **116** was accomplished by starting with 3-methoxyphenol **115** and adding N-bromosuccinimide (NBS) (Scheme 7-6). To control the bromination, NBS was added in portions over a period of 4 hours. The yields were similarly high, 92% for aryl bromide **116**, even after purification by flash column chromatography.

Scheme 7-6: Synthesis of aryl bromide 116.
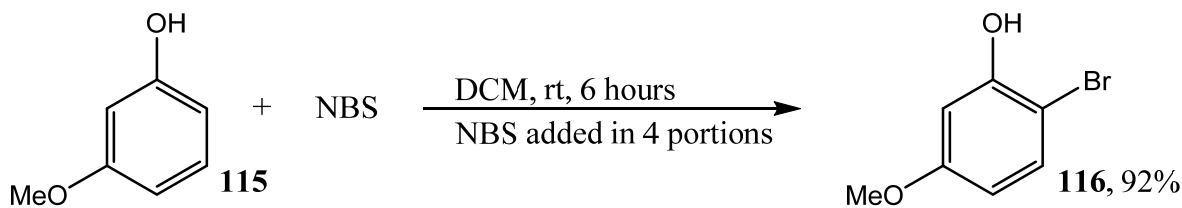
It was determined that the best styrene to use for these trial reactions was 2-vinylbenzo[b]thiophene **81**, since these reactions produced the smallest amount of stilbenoid byproduct and generally provided the best overall yields of the dihydrobenzofurans. As illustrated in Table 7-2, high yields were afforded for all styrenes tested, therefore it was deemed unnecessary to synthesize an exhaustive library using these new bromides. The details from these experiments are depicted in Table 7-5.

Table 7-5: Experiments between an ortho bromophenol and a thienyl styrene.

Entry	Arene	Styrene	Temp. (ºC)	Product	Yield[a]
1	**80**	**81**	130	**94**	87%
2	**114**	**81**	130	**118**	83%
3	**116**	**81**	130	**119**	84%
4	**117**	**81**	130	**120**	65%

[a] isolated yield

Examination of the data in this Table illustrated that substitution on the arene ring was well tolerated. The lowest yields were noted for arene **120**, which was not surprising considering the proximity of the electron-donating methoxy group to the site of coordination to palladium. In this case more careful control of the temperature may lead to higher yields, however a comprehensive optimization of this reaction was not investigated. It was clear from this process that this reaction sequence exhibited a wide scope for arenes, even electron-rich substituted aryl bromides, however, some difficulties were noted in the scope of the styrenes.

The natural product corsifuran **121** (Figure 7-7) was a prime target for a 1-step synthesis via the reaction process detailed in this work. However, under these conditions, only the

stilbenoid product was obtained. A number of different catalytic systems were attempted, but none with much success, however, future work may uncover the right conditions for this transformation.

Figure 7-7: Structure of corsifuran.

corsifuran, **121**
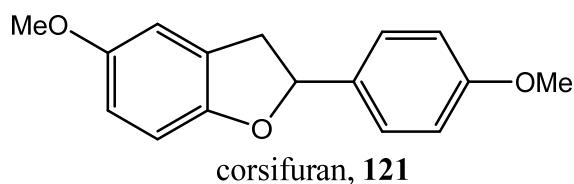
Earlier it was determined that careful reduction of the temperature could lead to enrichment of the dihydrobenzofuran over the undesired stilbenoid. This was not successful in this reaction as conversion to the stilbene was noted even at 70 °C while no conversion was observed prior to reaching this temperature. A number of different phosphine-based ligands were also investigated; however, synthesis of the natural product has not been accomplished by this method as of yet. Similar trials were also attempted with vinylbenzene with similarly negative results. Presumably the 4-methoxystyrene is a poor substrate for this reaction sequence and when employed high conversion to the stilbenoid byproduct was observed at all temperature ranges tested.

It was postulated earlier that control of the temperature led to the dihydrobenzofurans and points to an activation energy difference between the expected stilbenoid product (ß-hydride elimination followed by reductive elimination) and the cyclized product. In the case of unactivated styrenes, such as the styrenes employed in this study, presumably the activation energy for formation of the cyclized product was slightly lower than the activation energy necessary for ß-hydride elimination and thus the cyclized products are major products at lower

temperatures. In contrast, more activated styrenes such as 4-methoxystyrene and vinylbenzene may have lower activation energies for ß-hydride elimination, thus at any temperature the stilbenoid products are the major products whereas the cyclized products are not observed.

Careful selection of reagents, especially phosphine-based ligands, may be able to alter this behavior for more activated olefins. It is unclear which ligands might be most beneficial, however, bulky ligands that may help block coordination of hydrogen might be of use. Currently the exact mechanism by which this reaction occurs is not known, however future mechanistic work may provide useful strategies for use of activated olefins.

III.   PROPOSED MECHANISM.

When first discovered, these reactions were thought to be correlated to the reactions detailed earlier by Larock. Investigation into the scope of the reaction revealed this may not be the case. In the reaction process of Larock, aryl iodides were necessary and conversion of the phenol to an acetate facilitated better yields and a more extensive scope with electron-rich arenes. The reaction developed here, however, was suitable for aryl bromides and electron-rich phenols without the need to synthesize the acetates. In fact, the acetates themselves only led to conversion to the undesired stilbene, with no conversion to the dihydrobenzofuran of interest. Consideration of all these factors combined, it is believed that this reaction goes by a related, but distinct mechanism.

Synthesis of the stilbene compounds likely occurred via the normal Heck reaction mechanism discussed earlier. When the temperature was lowered, conversion to the stilbene was retarded and conversion to the desired dihydrobenzofuran was observed. From this perspective, this new mechanism certainly acts prior to the reductive elimination of the stilbene and also must

occur after migratory insertion of the styrene. Between these steps it is clear that palladium must

coordinate to the phenol to help facilitate the formation of the 5-membered heterocyclic ring.

If this coordination occurred after migratory insertion, the dihydrobenzofuran can be

obtained. The palladium complex **122** exists after migratory insertion of the alkene. In a normal

Heck reaction this would be followed by ß-hydride elimination and reductive elimination to a

stilbene product. In this case, however, coordination of the phenol to palladium (**123**) followed

by base mediated abstraction of the phenolic hydrogen atom may lead to the palladium complex

124. Subsequent reductive elimination (r.e.) would lead to the desired dihydrobenzofuran **125**.

This mechanism, however, does not account for the removal of the halide, which is generally

removed in Heck reactions by formation of H-X and neutralization with base. The Larock

mechanism presumes the removal of halide after oxidative addition of the arene (figure 6-7). If

this were the case in this reaction, it would seem a similar mechanism to that reported by Larock

would be plausible (Scheme 7-7).

Scheme 7-7: Coordination after migratory insertion.
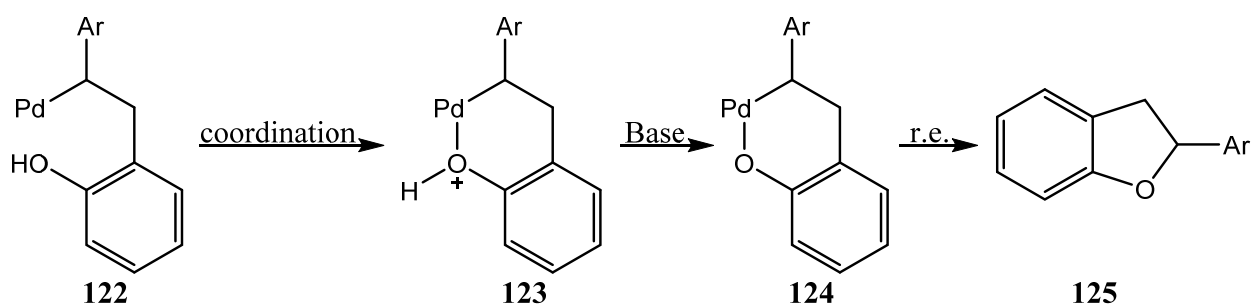
Accounting for hydrogen atoms is important for both this mechanistic process, and attempts to discuss the mechanism of the benzofuran **107**. In the dihydrobenzofuran case, the reaction process starts with 4 hydrogen atoms and ends up with 3 (Scheme 7-8).

Scheme 7-8: Hydrogen accounting, dihydrobenzofuran.
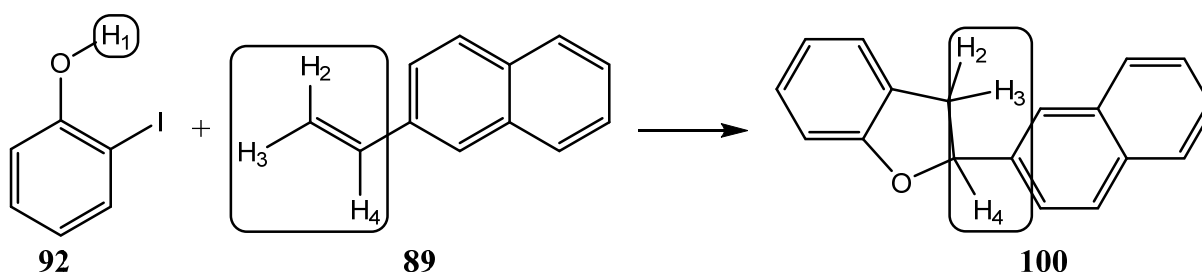
The mechanism detailed in Scheme 7-7 assumes that the phenolic H_1 is the lone hydrogen atom that does not end up in the final product **100**. This is logical since the phenolic hydrogen is the most acidic hydrogen and it also presumes that ß-hydride elimination does not occur, giving the dihydrobenzofuran. Accounting for hydrogens in the other reaction which resulted in the synthesis of the benzofuran **107** is more difficult (Scheme 7-9).

Scheme 7-9: Hydrogen accounting, benzofuran 107.
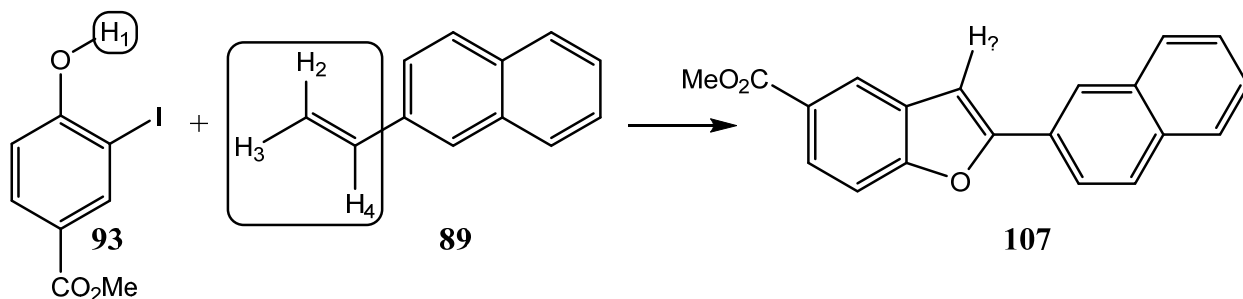
As shown, 3 hydrogen atoms are lost under the reaction conditions and only 1 remains in the final benzofuran product **107**. It can be assumed that 1 hydrogen atom is lost via ß-hydride elimination, and perhaps the phenolic hydrogen by base, however the loss of the third hydrogen

atom is troubling. Another possibility is the loss of H_2 by dehydrogenation, however subjecting the cyclized dihydrobenzofuran product **104** to the identical reaction conditions does not result in formation of the benzofuran product **107**. Perhaps before reductive elimination, H_2 is somehow removed from the organo-complex and inserted into palladium, followed by reductive elimination of the benzofuran. This would necessarily have to occur in the intermediate palladium complex **126**, since the cyclized product itself does not seem to dehydrogenate when resubmitted to the reaction conditions.

Scheme 7-10: Benzofuran proposed mechanism.
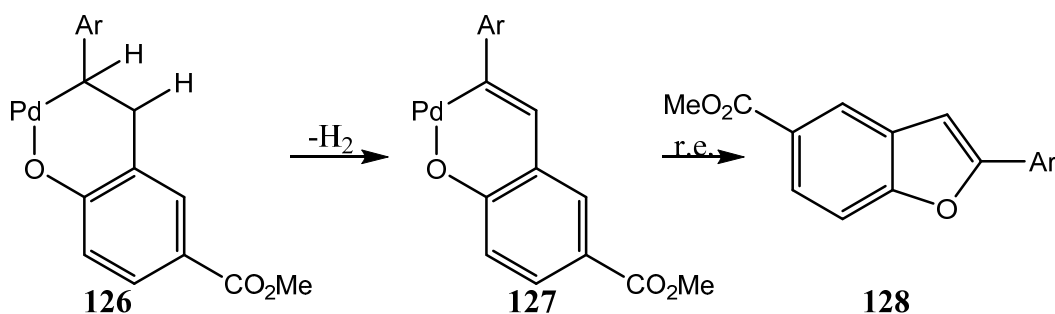
Further work in this area must be carried out to understand this. Some support in the literature for oxidation of phenols to dihydrobenzofurans and benzofurans has previously been reported[98], however, as discussed resubmission of the dihydrobenzofuran product **104** to the reaction conditions did not result in formation of any benzofuran product **107** by HPLC, therefore it would necessarily have to occur either when complexed to palladium prior to reductive elimination or perhaps through some oxidative reaction that may occur during the catalytic cycle.

IV. FUTURE WORK.

Methods that can help to prove the mechanism, both for the dihydrobenzofurans and the more difficult benzofuran **107**, might also help improve the scope of the reaction by directing optimization of reaction conditions. One potential method for experimentally determining the mechanism would be to subject deuterium labeled styrenes to the reaction conditions. This can be accomplished using relatively inexpensive starting materials such as DMF-d7 and the readily synthesized methyl-d3-triphenylphosphonium bromide. These starting materials can be used to synthesize a wide variety of deuterated styrenes that can presumably shed light on the exact reaction mechanism by monitoring the inclusion of deuterium in the final products. Some of the more easily accessible deuterated sytrenes are shown below in Figure 7-8.

Figure 7-8: Deuterated styrenes.
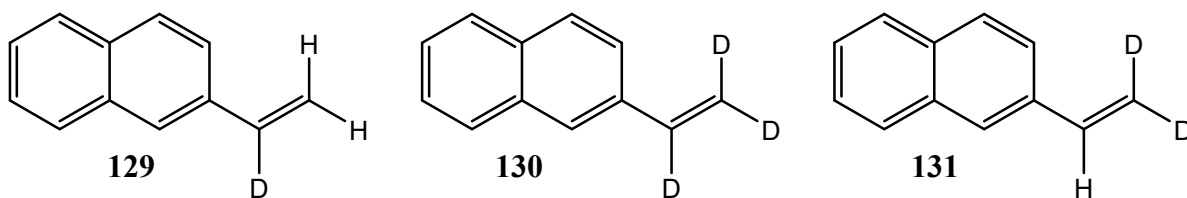
Furthermore, deuteration of the phenol, although very difficult because of exchange with water in the air, might also be possible to ascertain the fate of the phenolic hydrogen atom in this new reaction. This can perhaps be accomplished by heating the acidic phenol in deuterium oxide and removing water *in vacuo* several times under vacuum. Since the solvent and base employed are both aprotic, exchange back to hydrogen under the reaction conditions should not occur if moisture is completely eliminated.

Elucidation of an accurate mechanism can also be pursued in parallel to attempts to introduce asymmetry into the dihydrobenzofuran ring system. Palladium catalyzed reactions

generally act via mechanisms that can permit asymmetric induction by careful selection of asymmetric ligands and/or precatalysts.[99] As detailed earlier, R-BINAP as a ligand was employed without success. A large library of phosphine based asymmetric ligands exists, however, and many asymmetric precatalysts are also routinely used. Particular focus on asymmetric palladacycles like Herrmann's palladacycle that have similar palladium (II) to palladium zero chemistry presumably would be the most interesting selections.

Extending the scope of these reactions by introduction of new and interesting styrenes may also be attempted. The current scope involves rather unactivated styrenes, and trials with more activated styrenes were met with less success. Introduction of additives or different ligands could help expand the scope of the styrenes to also include activated styrenes. This aim would benefit greatly, however, from a mechanism that rests on more experimental proof.

V.   CONCLUSION.

In conclusion, a new and novel transition metal catalyzed reaction to form dihydrobenzofurans was discovered in the process of synthesizing novel small molecule antibiotics. This reaction was further successfully optimized to afford excellent yields of the novel dihydrobenzofurans while minimizing the conversion to the less interesting stilbene by-products. Synthesis of a variety of styrenes expanded the scope of the reaction process to include both heterocyclic styrenes and carbocycles; an important distinction as initially it was felt the reaction would only be applicable to heterocycles.

The proposed mechanism of this new reaction may be very similar to the mechanism postulated in the prior work of Larock, however, if so it would represent a significant expansion of the scope. The original reaction was only suitable for aryl iodides and focused solely on 1,3-

dienes, whereas the reaction detailed in this work gave excellent yields with aryl bromides and styrenes.

Another new and interesting reaction was also discovered in the case of methyl ester **93** and the napthyl styrene **89**. The benzofuran **107** was a major product under low temperature reaction conditions whereas the dihydrobenzofuran **104** was obtained at slightly higher temperatures. Furthermore, high temperature reactions favored the stilbene product **108** over both the benzofuran **107** and the dihydrobenzofuran **104**. A mechanism for this conversion was proposed, however, with a word of caution as it does not seem to match any known mechanisms of Pd chemistry, on the other hand it may be new.

Finally, substitution of the arene ring in the dihydrobenzofurans was tested by moving a methoxy group around the ring. These electron-rich arenes all gave good yields, with only the methoxy analog **117** giving a yield under 70%. This was likely due to the ortho positioning of the methoxy group which may restrict oxidative addition to the palladium species, which is seemingly unrelated to the ring forming mechanism of this reaction.

This reaction offers a new route to interesting dihydrobenzofurans and with further optimization may lead to an expanded scope that includes a more diverse selection of styrenes as well as asymmetric induction.

VI. EXPERIMENTAL.

Both ^{1}H and ^{13}C NMR spectra were recorded on a Bruker DPX-300 or DRX-500 instrument where noted. HRMS scans were recorded with a Shimadzu LCMS-IT-TOF or similar instruments.

2-Vinylbenzo[b]thiophene (81, Figure 7-3)

Chemical Formula: $C_{10}H_8S$
Molecular Weight: 160.23

The sodium methoxide (406.6 mg, 7.53 mmol, 1.1 eq), methyltriphenylphosphonium bromide (2.69 g, 7.53 mmol, 1.1 eq), and THF (25mL) were stirred under argon at rt for 0.5h. The benzo[b]thiophene-2-carbaldehyde (1.11 g, 6.84 mmol, 1 eq) was dissolved in THF (5mL) and added dropwise to the solution. After 3h, analysis by TLC (10% EtOAc in hexanes, silica gel) indicated no starting aldehyde remained and the reaction was quenched with aq 0.5N HCl (10mL). The organic layer was extracted and the aq layer was subsequently extracted with EtOAc (15mL x 2). The combined organic layers were washed with brine (10mL x 2), dried (Na2SO4), and the solvent was removed *in vacuo* to give an off-white solid. The solid was purified by flash column chromatography on silica gel (hexanes) to provide the pure 2-vinylthianaphthene **81** in 98% yield as a white solid (1076 mg): ^{1}H NMR (500 MHz, CDCl3) δ 7.87 – 7.79 (m, 1H), 7.79 – 7.72 (m, 1H), 7.43 – 7.32 (m, 2H), 7.22 (s, 1H), 6.98 (dd, J = 17.3, 10.8 Hz, 1H), 5.74 (d, J = 17.3 Hz, 1H), 5.37 (d, J = 10.8 Hz, 1H); ^{13}C NMR (126 MHz, CDCl3) δ 143.16, 140.08, 138.93, 130.66, 124.85, 124.48, 123.63, 123.14, 122.34, 116.00; HRMS (ESI) (M + H), Calcd. for $C_{10}H_9S$ 161.0425; Found 161.0431

2-Vinylbenzofuran (88, Figure 7-3)

Chemical Formula: $C_{10}H_8O$
Molecular Weight: 144.17

The sodium methoxide (406.6 mg, 7.53 mmol, 1.1 eq), methyltriphenylphosphonium bromide (2.69 g, 7.53 mmol, 1.1 eq), and THF (25mL) were stirred under argon at rt for 0.5h. The benzofuran-2-carbaldehyde (1.00 g, 6.84 mmol, 1 eq) was dissolved in THF (5mL) and added dropwise to the solution. After 3h, analysis by TLC (10% EtOAc in hexanes, silica gel) indicated no starting aldehyde remained and the reaction was quenched with aq 0.5N HCl (10mL). The organic layer was extracted and the aq layer was subsequently extracted with EtOAc (15mL x 2). The combined organic layers were washed with brine (10mL x 2), dried (Na$_2$SO$_4$), and the solvent was removed *in vacuo* to give a yellow oil. The oil was purified by flash column chromatography on silica gel (hexanes) to provide the pure 2-vinylbenzofuran **88** in 85% yield as a clear oil that slowly solidifies in a freezer to a white solid (838 mg): ^{1}H NMR (300 MHz, CDCl$_3$) δ 7.56 (d, *J* = 7.6 Hz, 1H), 7.49 (d, *J* = 8.1 Hz, 1H), 7.27 (m, 2H), 6.75 – 6.62 (dd, *J* = 17.4 Hz, *J* = 11.4 Hz, 1H), 6.63 (s, 1H), 6.00 (d, *J* = 17.4 Hz, 1H), 5.42 (d, *J* = 11.2 Hz, 1H); ^{13}C NMR (75 MHz, CDCl$_3$) δ 154.86, 154.78, 128.83, 125.30, 124.64, 122.79, 120.98, 115.71, 111.02, 104.74; HRMS (ESI) (M + H), Calcd. for C$_{10}$H$_9$O 145.0653; Found 145.0652

2-(Prop-1-en-2-yl)naphthalene (90, Figure 7-3)
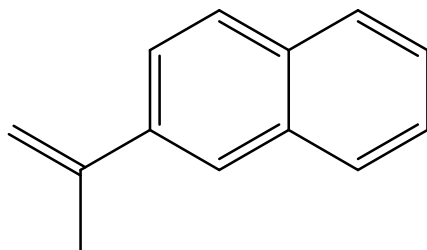
Chemical Formula: C$_{13}$H$_{12}$
Molecular Weight: 168.24

The sodium methoxide (406.6 mg, 7.53 mmol, 1.1 eq), methyltriphenylphosphonium bromide (2.69 g, 7.53 mmol, 1.1eq), and THF (25mL) were stirred under argon at rt for 0.5hr. The 1-(naphthalen-2-yl)ethan-1-one (1.16 g, 6.84 mmol, 1 eq) was dissolved in THF (5mL) and added dropwise to the solution. After 3h analysis by TLC (10% EtOAc in hexanes, silica gel) indicated

no starting aldehyde remained and the reaction was quenched with aq 0.5N HCl (10mL). The organic layer was extracted and the aq layer was subsequently extracted with EtOAc (15mL x 2). The combined organic layers were washed with brine (10mL x 2), dried (Na$_2$SO$_4$), , and the solvent was removed *in vacuo* to give an off-white solid. The solid was purified by flash column chromatography on silica gel (hexanes) to provide the pure methyl naphthyl styrene **90** in 92% yield as a white solid (1059 mg): ^{1}H NMR (500 MHz, CDCl$_3$) δ 7.97 – 7.83 (m, 4H), 7.79 – 7.73 (m, 1H), 7.57 – 7.49 (m, 2H), 5.62 (s, 1H), 5.28 (s, 1H), 2.35 (s, 3H); ^{13}C NMR (126 MHz, CDCl$_3$) δ 143.06, 138.40, 133.45, 132.87, 128.31, 127.76, 127.58, 126.18, 125.89, 124.33, 123.96, 113.09, 21.95; HRMS (ESI) (M + H), Calcd. for C$_{13}$H$_{13}$ 169.1017; Found 169.1012

Methyl 4-acetoxy-3-iodobenzoate (85, Scheme 7-2)
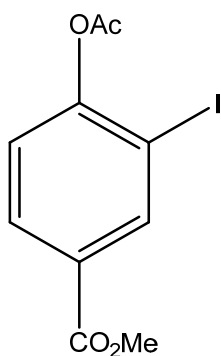
Chemical Formula: C$_{10}$H$_9$IO$_4$
Molecular Weight: 320.08

The methyl 4-hydroxy-3-iodobenzoate (**84**, 1.00g, 3.6 mmol, 1 eq) was stirred in DCM (10 mL) at rt. Then pyridine (570mg, 7.2 mmol, 2 eq) was added in one portion and the solution was stirred for 5 min. Acetyl chloride (314mg, 4 mmol, 1.1 eq) was then added dropwise by syringe over a period of 30 min. The solution was stirred for 2 h, analyzed by TLC (30% EtOAc in hexanes, silica gel) which indicated the starting material was consumed, and the mixture was quenched by addition of water (10 mL). The organic layer was extracted and the aq layer was extracted with DCM (10 mL x 2). The combined organic layers were washed with water (10

mL), brine (10 mL), dried over dried (Na$_2$SO$_4$), , and the solvent was removed *in vacuo* to give a white solid. The white solid was recrystallized from IPA to give the acetate **85** as pure white needles (935mg, 81%): mp: 153-156 ºC; ^{1}H NMR (300 MHz, CDCl3) δ 8.26 (d, J = 1.9 Hz, 1H), 7.97 (dd, J = 8.4, 2.0 Hz, 1H), 7.18 (d, J = 8.4 Hz, 1H), 3.88 (s, 3H), 2.33 (s, 3H); ^{13}C NMR (75 MHz, CDCl3) δ 167.87, 164.99, 151.86, 134.68, 129.86, 129.30, 123.74, 116.36, 52.43, 20.71. The spectral data of **85** were identical to the reported values.[94]

2-Bromo-6-methoxyphenol (114, Scheme 7-5)
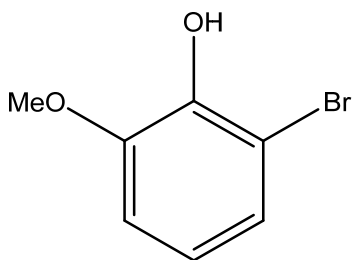
Chemical Formula: C$_7$H$_7$BrO$_2$
Molecular Weight: 203.04

The tert-butylamine (3.53g, 0.048 mol, 2 eq) was dissolved in toluene (10 mL) at -30 ºC. Bromine (3.86g, 0.024 mol, 1 eq) was slowly added to the solution at -30 ºC which resulted in a slightly turbid solution. The solution was further cooled to -78 ºC with dry ice/acetone and the 2-methoxyphenol (**113**, 3.00g, 0.24 mol, 1 eq), dissolved in toluene (5 mL), was added dropwise over 30 min. The reaction was monitored by TLC (10% EtOAc in hexanes, silica gel) and was complete after 4 h at -78 ºC. The solution was warmed to rt, quenched with a sat. aq Na$_2$S$_2$O$_4$ solution (2 mL) mixed with water (15 mL), and extracted. The aq layer was then extracted with DCM (10 mL x 2). The combined organic layers were washed with water (15 mL), brine (15 mL), and dried (Na$_2$SO$_4$). The solvent was removed *in vacuo* to provide an off-white powder. The solid was further purified by flash column chromatography (silica gel, 5% EtOAc in hexanes) to furnish aryl bromide **114** in 81% yield as a white powder (4.0g). The mp (63ºC) was in excellent agreement with the literature value.[100]

2-Bromo-5-methoxyphenol (116, Scheme 7-6)
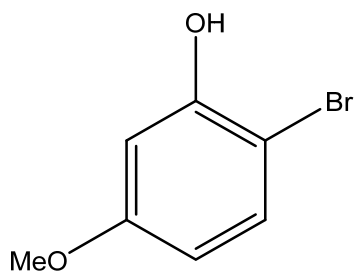
Chemical Formula: $C_7H_7BrO_2$
Molecular Weight: 203.04

The 3-methoxyphenol (**115**, 3.00g, 0.24 mol, 1 eq) was dissolved in DCM (600 mL) and N-bromosuccinimide (NBS, 4.3 g, 0.024 mol, 1 eq) was added in 4 equal portions over a period of 2 h. After the final addition of NBS, the solution was stirred for 2 additional h and monitored by TLC (20% EtOAc in hexanes). After 2 h analysis by TLC indicated the reaction was complete and the solvent was removed *in vacuo* to give an off-white powder. The crude solid was purified by flash column chromatography (silica gel, 20% EtOAc in hexanes) to furnish aryl bromide **116** in 92% yield as a white powder (4.5g): ^{1}H NMR (300 MHz, CDCl$_3$) δ 7.33 (d, J = 8.8 Hz, 1H), 6.62 (d, J = 2.9 Hz, 1H), 6.43 (dd, J = 8.8, 2.9 Hz, 1H), 5.64 (bs, 1H), 3.78 (s, 3H).

(E)-2-(2-(Benzo[b]thiophen-2-yl)vinyl)-4-methoxyphenol (82, Scheme 7-1)
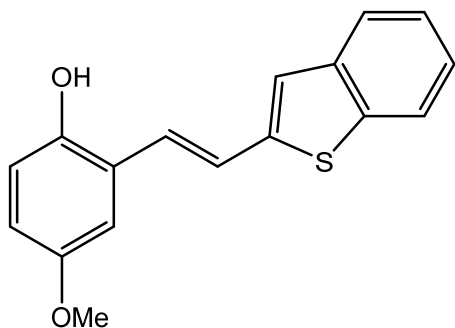
Chemical Formula: $C_{17}H_{14}O_2S$
Molecular Weight: 282.36
c Log P: 4.74
tPSA: 29.46

The 2-bromo-4-methoxyphenol (126.7 mg, 0.624 mmol, 1 eq), 2-vinylbenzo[b]thiophene (100 mg, 0.624 mmol, 1 eq), sodium acetate (102.4 mg, 1.248 mmol, 2 eq), and Herrmann's palladacycle (14.6 mg, 0.0156 mmol, 0.025 eq) were charged to a vial containing oxygen free

solvent (10% water in dimethylacetamide, 3 mL) under an argon atmosphere. The vial was

sealed with a septum and the mixture was heated to 150 ºC for 3 h, cooled to rt, and EtOAc

(10mL) was added in one portion. The suspension was filtered through a plug of celite and the

filtrate was washed successively with aq 0.5 N HCl (2 x 10 mL) and brine (2 x 10 mL). The

organic layer was dried (Na$_2$SO$_4$) and the solvent was removed *in vacuo* to provide a crude

yellow solid. The solid was purified by flash column chromatography on silica gel (20% EtOAc

in hexanes) to provide the pure hydroxyl stilbene **82** in 86% yield as a bright yellow-green solid

(151 mg): ^{1}H NMR (300 MHz, DMSO) δ 9.48 (s, 1H), 7.90 (d, *J* = 8.3 Hz, 1H), 7.84 – 7.73 (m,

1H), 7.59 (d, *J* = 16.2 Hz, 1H), 7.44 (s, 1H), 7.34 (p, *J* = 7.5 Hz, 2H), 7.21 (d, *J* = 16.1 Hz, 1H),

7.17 (s, 1H), 6.82 (d, *J* = 8.8 Hz, 1H), 6.75 (dd, *J* = 8.8, 2.7 Hz, 1H), 3.74 (s, 3H); ^{13}C NMR (75

MHz, DMSO) δ 152.86, 149.69, 143.83, 140.53, 138.40, 126.27, 125.26, 125.16, 123.94, 123.70,

123.59, 122.81, 122.43, 117.19, 116.11, 110.99, 55.92; HRMS (ESI) (M + H), Calcd. for

C$_{17}$H$_{15}$O$_2$S 283.0793; Found 283.0790

2-(Benzo[b]thiophen-2-yl)-5-methoxy-2,3-dihydrobenzofuran (94, Table 7-2, entry 1)

Chemical Formula: C$_{17}$H$_{14}$O$_2$S
Molecular Weight: 282.36

The 2-bromo-4-methoxyphenol (126.7 mg, 0.624 mmol, 1 eq), 2-vinylbenzo[b]thiophene (100

mg, 0.624 mmol, 1 eq), cesium carbonate (407 mg, 1.248 mmol, 2 eq), and Herrmann's

palladacycle (14.6 mg, 0.0156 mmol, 0.025 eq) were charged to a vial which contained dry and

oxygen free dimethylacetamide (3 mL) under an argon atmosphere. The vial was sealed with a

septum and the mixture was heated to 130 ºC for 3 h, cooled to rt, and EtOAc (10mL) was added

in one portion. The suspension was filtered through a plug of celite and the filtrate was washed

successively with aq 0.5 N HCl (2 x 10 mL) and brine (2 x 10 mL). The organic layer was dried (Na$_2$SO$_4$) and the solvent was removed *in vacuo* to provide a crude yellow solid. The solid was purified by flash column chromatography on silica gel (5% EtOAc in hexanes) to provide the pure methoxy dihydrobenzofuran **94** in 87% yield as a white solid (153 mg): mp: 100-102 ºC; ^{1}H NMR (300 MHz, CDCl$_3$) δ 7.85 – 7.78 (m, 1H), 7.78 – 7.71 (m, 1H), 7.42 – 7.29 (m, 1H), 6.81 (d, *J* = 8.6 Hz, 1H), 6.74 (dd, *J* = 8.7, 2.5 Hz, 1H), 6.09 – 5.98 (m, 1H), 3.80 (s, 1H), 3.69 (dd, *J* = 15.7, 9.2 Hz, 1H), 3.41 (dd, *J* = 15.7, 7.3 Hz, 1H); ^{13}C NMR (75 MHz, DMSO) δ 154.57, 152.84, 146.17, 139.39, 139.20, 127.67, 125.08, 125.00, 124.23, 123.06, 122.05, 113.57, 111.62, 109.68, 80.22, 56.05, 38.36; HRMS (ESI) (M + H), Calcd. for C$_{17}$H$_{15}$O$_2$S 283.0793; Found 283.0794

5-Methoxy-2,3-dihydro-2,2'-bibenzofuran (95, Table 7-2, entry 2)
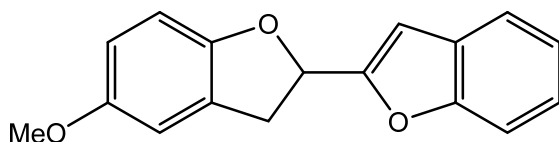
Chemical Formula: C$_{17}$H$_{14}$O$_3$
Molecular Weight: 266.30

The 2-bromo-4-methoxyphenol (126.7 mg, 0.624 mmol, 1 eq), 2-vinylbenzofuran (90 mg, 0.624 mmol, 1 eq), cesium carbonate (407 mg, 1.248 mmol, 2 eq), and Herrmann's palladacycle (14.6 mg, 0.0156 mmol, 0.025 eq) were charged to a vial which contained dry and oxygen free dimethylacetamide (3 mL) under an argon atmosphere. The vial was sealed with a septum and the mixture was heated to 130 ºC for 3 h, cooled to rt, and EtOAc (10mL) was added in one portion. The suspension was filtered through a plug of celite and the filtrate was washed successively with aq 0.5 N HCl (2 x 10 mL) and brine (2 x 10 mL). The organic layer was dried (Na$_2$SO$_4$) and the solvent was removed *in vacuo* to provide a crude yellow solid. The solid was purified by flash column chromatography on silica gel (5% EtOAc in hexanes) to provide the

pure methoxy dihydrobenzofuran **95** in 75% yield as a white solid (125 mg): mp: 84-86 °C; [1]H

NMR (500 MHz, CDCl$_3$) δ 7.57 (d, *J* = 8.0 Hz, 1H), 7.50 (d, *J* = 8.0 Hz, 1H), 7.30-7.33 (m, 1H),

7.23-7.26 (m, 1H), 6.79-6.86 (m, 3H), 6.73 (dd, *J* = 2.5, 8.5 Hz, 1H). 5.89 (t, *J* = 8.5 Hz, 1H),

3.80 (s, 3H), 3.59 (d, *J* = 9.0 Hz, 2H); ^{13}C NMR (75 MHz, CDCl$_3$) δ 155.8, 155.2, 154.5, 153.1,

127.8, 126.9, 124.6, 122.9, 121.2, 113.1, 111.4, 111.1, 109.5, 109.5, 104.4, 77.4, 56.0, 35.0;

HRMS (ESI-TOF *m/z*) for C$_{17}$H$_{14}$O$_3$ calcd 267.1010 found 267.1016 (M+H)+.

5-Methoxy-2-(naphthalen-2-yl)-2,3-dihydrobenzofuran (96, Table 7-2, entry 3)
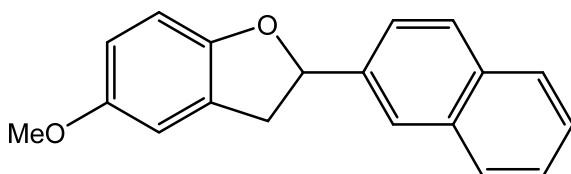
Chemical Formula: C$_{19}$H$_{16}$O$_2$
Molecular Weight: 276.34

2-bromo-4-methoxyphenol (126.7 mg, 0.624 mmol, 1 eq), 2-vinylnaphthalene (96 mg, 0.624

mmol, 1 eq), cesium carbonate (407 mg, 1.248 mmol, 2 eq), and Herrmann's palladacycle (14.6

mg, 0.0156 mmol, 0.025 eq) were charged to a vial which contained dry and oxygen free

dimethylacetamide (3 mL) under an argon atmosphere. The vial was sealed with a septum and

the mixture was heated to 130 °C for 3 h, cooled to rt, and EtOAc (10mL) was added in one

portion. The suspension was filtered through a plug of celite and the filtrate was washed

successively with aq 0.5 N HCl (2 x 10 mL) and brine (2 x 10 mL). The organic layer was dried

(Na$_2$SO$_4$) and the solvent was removed in vacuo to provide a crude yellow solid. The solid was

purified by flash column chromatography on silica gel (5% EtOAc in hexanes) to provide the

pure methoxy dihydrobenzofuran **96** in 89% yield as a white solid (153 mg): mp: 121-123 °C; [1]H

NMR (300 MHz, CDCl$_3$) δ 7.92 – 7.81 (m, 4H), 7.59 – 7.45 (m, 3H), 6.84 (dt, *J* = 6.9, 4.9 Hz,

2H), 6.77 (dd, *J* = 8.5, 2.6 Hz, 1H), 5.94 (t, *J* = 8.8 Hz, 1H), 3.81 (s, 3H), 3.70 (dd, *J* = 15.8, 9.4

Hz, 1H), 3.30 (dd, *J* = 15.7, 8.2 Hz, 1H); ^{13}C NMR (75 MHz, CDCl$_3$) δ 154.39, 153.88, 139.32,

133.23, 133.13, 128.67, 128.06, 127.73, 127.52, 126.30, 126.08, 124.68, 123.62, 113.11, 111.27, 109.29, 84.38, 56.07, 38.91; HRMS (ESI) (M + H), Calcd. for $C_{19}H_{17}O_2$ 277.1229; Found 277.1224

5-Methoxy-2-methyl-2-(naphthalen-2-yl)-2,3-dihydrobenzofuran (97, Table 7-2, entry 4)
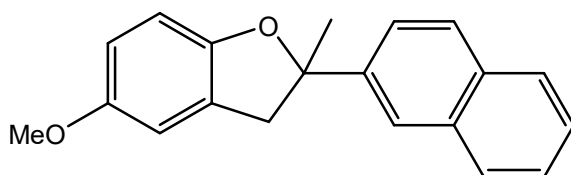
Chemical Formula: $C_{20}H_{18}O_2$
Molecular Weight: 290.36

The 2-bromo-4-methoxyphenol (126.7 mg, 0.624 mmol, 1 eq), 2-(prop-1-en-2-yl)naphthalene (105 mg, 0.624 mmol, 1 eq), cesium carbonate (407 mg, 1.248 mmol, 2 eq), and Herrmann's palladacycle (14.6 mg, 0.0156 mmol, 0.025 eq) were charged to a vial which contained dry and oxygen free dimethylacetamide (3 mL) under an argon atmosphere. The vial was sealed with a septum and the mixture was heated to 110 ºC for 3 h, cooled to rt, and EtOAc (10mL) was added in one portion. The suspension was filtered through a plug of celite and the filtrate was washed successively with aq 0.5 N HCl (2 x 10 mL) and brine (2 x 10 mL). The organic layer was dried (Na_2SO_4) and the solvent was removed in vacuo to provide a crude off-white solid. The solid was purified by flash column chromatography on silica gel (5% EtOAc in hexanes) to provide the pure methoxy dihydrobenzofuran **97** in 90% yield as a white solid (163 mg): mp: 125-127 ºC; ^{1}H NMR (300 MHz, CDCl₃) δ 8.01 – 7.80 (m, 4H), 7.62 – 7.43 (m, 3H), 6.88 (d, J = 8.3 Hz, 1H), 6.74 (d, J = 8.5 Hz, 2H), 3.77 (s, 3H), 3.53 (d, J = 15.6 Hz, 1H), 3.44 (d, J = 15.5 Hz, 1H), 1.87 (s, 3H); ^{13}C NMR (75 MHz, CDCl₃) δ 154.20, 153.08, 144.00, 133.08, 132.46, 128.27, 128.19, 127.51, 127.44, 126.17, 125.86, 123.29, 122.88, 113.09, 111.40, 109.48, 89.30, 56.03, 45.07, 29.11; HRMS (ESI) (M + H), Calcd. for $C_{20}H_{19}O_2$ 291.1385; Found 291.1382

2-(Benzo[b]thiophen-2-yl)-2,3-dihydrobenzofuran (98, Table 7-2, entry 5)
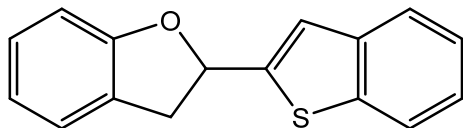
Chemical Formula: $C_{16}H_{12}OS$
Molecular Weight: 252.33

The 2-iodophenol (137.3 mg, 0.62 mmol, 1 eq), 2-vinylbenzo[b]thiophene (100 mg, 0.624 mmol, 1 eq), cesium carbonate (407 mg, 1.25 mmol, 2 eq), and Herrmann's palladacycle (14.6 mg, 0.016 mmol, 0.025 eq) were charged to a vial which contained dry and oxygen free dimethylacetamide (3 mL) under an argon atmosphere. The vial was sealed with a septum and the mixture was heated to 130 ºC for 3 h, cooled to rt, and EtOAc (10mL) was added in one portion. The suspension was filtered through a plug of celite and the filtrate was washed successively with aq 0.5 N HCl (2 x 10 mL) and brine (2 x 10 mL). The organic layer was dried (Na_2SO_4) and the solvent was removed in vacuo to provide a crude yellow solid. The solid was purified by flash column chromatography on silica gel (5% EtOAc in hexanes) to provide the pure dihydrobenofuran in 86% yield as a white solid (135.4 mg): mp: 95-96 ºC; ^{1}H NMR (500 MHz, CDCl$_3$) δ 7.82 (d, J = 8.0 Hz, 1H), 7.75 (d, J = 8.0 Hz, 1H), 7.32-7.38 (m, 3H), 7.25 (d, J = 7.0 Hz, 1H), 7.21 (t, J = 7.5 Hz, 1H), 6.91-6.96 (m, 2H), 6.07 (t, J = 8.5 Hz, 1H), 3.73 (dd, J = 9.5, 15.5 Hz, 1H), 3.47 (dd, J = 7.0, 15.5 Hz, 1H); ^{13}C NMR (75 MHz, CDCl$_3$) δ 158.9, 145.4, 139.6, 139.3, 128.4, 125.9, 124.9, 124.5, 124.4, 123.7, 122.5, 121.4, 121.0, 109.7, 80.3, 38.3; HRMS (ESI-TOF m/z) for $C_{16}H_{12}O_3S$ calcd 253.0850 found 253.0859 (M+H)+.

2,3-Dihydro-2,2'-bibenzofuran (99, Table 7-2, entry 6)
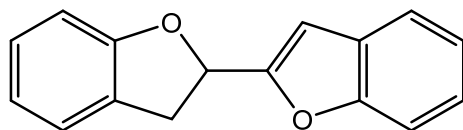
Chemical Formula: $C_{16}H_{12}O_2$
Molecular Weight: 236.27

The 2-iodophenol (137.3 mg, 0.624 mmol, 1 eq), 2-vinylbenzofuran (90 mg, 0.624 mmol, 1 eq), cesium carbonate (407 mg, 1.248 mmol, 2 eq), and Herrmann's palladacycle (14.6 mg, 0.0156 mmol, 0.025 eq) were charged to a vial which contained dry and oxygen free dimethylacetamide (3 mL) under an argon atmosphere. The vial was sealed with a septum and the mixture was heated to 130 ºC for 3 h, cooled to rt, and EtOAc (10mL) was added in one portion. The suspension was filtered through a plug of celite and the filtrate was washed successively with aq 0.5 N HCl (2 x 10 mL) and brine (2 x 10 mL). The organic layer was dried (Na_2SO_4) and the solvent was removed in vacuo to provide a crude yellow solid. The solid was purified by flash column chromatography on silica gel (5% EtOAc in hexanes) to provide the pure dihydrobenzofuran **99** in 73% yield as a white solid (107.6 mg): mp: 73-75 ºC; ^{1}H NMR (300 MHz, $CDCl_3$) δ 7.58 (d, J = 7.2 Hz, 1H), 7.49 (d, J = 8.1 Hz, 1H), 7.17-7.34 (m, 4H), 6.88-6.96 (m, 2H), 6.80 (s, 1H), 5.90 (t, J = 8.4 Hz, 1H), 3.62 (d, J = 8.7 Hz, 2H); ^{13}C NMR (75 MHz, $CDCl_3$) δ 159.0, 155.7, 155.2, 128.3, 127.8, 125.9, 124.8, 124.6, 122.9, 121.2, 120.9, 111.4, 109.7, 104.5, 77.4, 34.5; HRMS (ESI-TOF *m/z*) for $C_{16}H_{12}O_2$ calcd 237.0900 found 237.0910 (M+H)+.

2-(Naphthalen-2-yl)-2,3-dihydrobenzofuran (100, Table 7-2, entry 7)
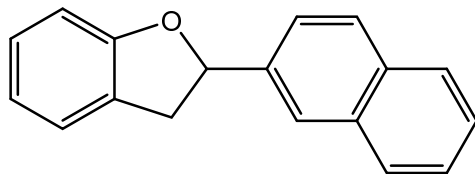
Chemical Formula: $C_{18}H_{14}O$
Molecular Weight: 246.31

The 2-iodophenol (137 mg, 0.624 mmol, 1 eq), 2-vinylnaphthalene (96 mg, 0.624 mmol, 1 eq), cesium carbonate (407 mg, 1.248 mmol, 2 eq), and Herrmann's palladacycle (14.6 mg, 0.0156 mmol, 0.025 eq) were charged to a vial which contained dry and oxygen free dimethylacetamide (3 mL) under an argon atmosphere. The vial was sealed with a septum and the mixture was

heated to 130 ºC for 3 h, cooled to rt, and EtOAc (10mL) was added in one portion. The

suspension was filtered through a plug of celite and the filtrate was washed successively with aq

0.5 N HCl (2 x 10 mL) and brine (2 x 10 mL). The organic layer was dried (Na$_2$SO$_4$) and the

solvent was removed in vacuo to provide a crude yellow solid. The solid was purified by flash

column chromatography on silica gel (5% EtOAc in hexanes) to provide the pure

dihydrobebzofuran **100** in 92% yield as a white solid (141 mg): mp: 95-97 ºC; ^{1}H NMR (500

MHz, CDCl$_3$) δ 7.94 – 7.83 (m, 4H), 7.53 (dd, J = 11.4, 6.3 Hz, 3H), 7.24 (dd, J = 12.5, 7.4 Hz,

2H), 6.95 (dd, J = 12.0, 7.7 Hz, 2H), 5.97 (t, J = 8.9 Hz, 1H), 3.74 (dd, J = 15.6, 9.6 Hz, 1H),

3.34 (dd, J = 15.6, 8.2 Hz, 1H); ^{13}C NMR (126 MHz, CDCl$_3$) δ 159.72, 139.27, 133.22, 133.15,

128.72, 128.30, 128.07, 127.75, 126.51, 126.34, 126.12, 124.95, 124.75, 123.63, 120.77, 109.48,

84.20, 38.47; HRMS (ESI) (M + H), Calcd. for C$_{18}$H$_{15}$O 247.1123; Found 247.1126

2-Methyl-2-(naphthalen-2-yl)-2,3-dihydrobenzofuran (101, Table 7-2, entry 8)
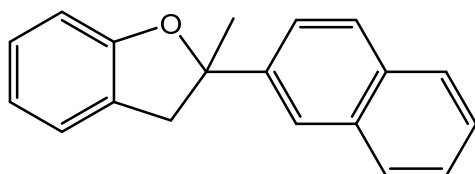
Chemical Formula: C$_{19}$H$_{16}$O
Molecular Weight: 260.34

The 2-iodophenol (137.3 mg, 0.624 mmol, 1 eq), 2-(prop-1-en-2-yl)naphthalene (105 mg, 0.624

mmol, 1 eq), cesium carbonate (407 mg, 1.248 mmol, 2 eq), and Herrmann's palladacycle (14.6

mg, 0.0156 mmol, 0.025 eq) were charged to a vial which contained dry and oxygen free

dimethylacetamide (3 mL) under an argon atmosphere. The vial was sealed with a septum and

the mixture was heated to 110 ºC for 3 h, cooled to rt, and EtOAc (10mL) was added in one

portion. The suspension was filtered through a plug of celite and the filtrate was washed

successively with aq 0.5 N HCl (2 x 10 mL) and brine (2 x 10 mL). The organic layer was dried

(Na$_2$SO$_4$) and the solvent was removed in vacuo to provide a crude off-white solid. The solid

was purified by flash column chromatography on silica gel (5% EtOAc in hexanes) to provide the pure dihydrobenzofuran **101** in 94% yield as a white solid (152 mg): mp: 103-104 °C; ^{1}H NMR (300 MHz, CDCl$_3$) δ 7.99 (s, 1H), 7.86 (m, 3H), 7.59 (dd, J = 8.6, 1.6 Hz, 1H), 7.50 (p, J = 6.5 Hz, 2H), 7.23 – 7.13 (m, 2H), 6.99 (d, J = 7.9 Hz, 1H), 6.89 (t, J = 7.4 Hz, 1H), 3.57 (d, J = 15.5 Hz, 1H), 3.47 (d, J = 15.5 Hz, 1H), 1.90 (s, 3H); ^{13}C NMR (75 MHz, CDCl$_3$) δ 158.91, 143.98, 133.12, 132.50, 128.33, 128.22, 127.55, 126.48, 126.22, 125.91, 125.11, 123.32, 122.91, 120.53, 109.68, 89.21, 44.67, 29.21; HRMS (ESI) (M + H), Calcd. for C$_{19}$H$_{17}$O 261.1279; Found 261.1281

Methyl 2-(benzo[b]thiophen-2-yl)-2,3-dihydrobenzofuran-5-carboxylate (102, Table 7-2, entry 9)
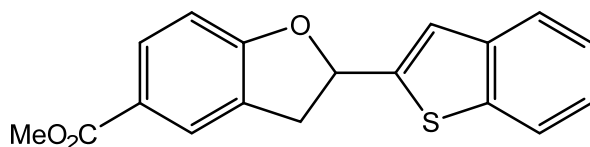
Chemical Formula: C$_{18}$H$_{14}$O$_3$S
Molecular Weight: 310.37

The methyl 4-hydroxy-3-iodobenzoate (173.53 mg, 0.624 mmol, 1 eq), 2-vinylbenzo[b]thiophene (100 mg, 0.624 mmol, 1 eq), cesium carbonate (407 mg, 1.248 mmol, 2 eq), and Herrmann's palladacycle (14.6 mg, 0.0156 mmol, 0.025 eq) were charged to a vial which contained dry and oxygen free dimethylacetamide (3 mL) under an argon atmosphere. The vial was sealed with a septum and the mixture was heated to 130 °C for 3 h, cooled to rt, and EtOAc (10mL) was added in one portion. The suspension was filtered through a plug of celite and the filtrate was washed successively with aq 0.5 N HCl (2 x 10 mL) and brine (2 x 10 mL). The organic layer was dried (Na$_2$SO$_4$) and the solvent was removed in vacuo to provide a crude yellow solid. The solid was purified by flash column chromatography on silica gel (5% EtOAc in hexanes) to provide the pure product in 72% yield as a white solid (140 mg): mp: 140-142 °C;

^{1}H NMR (300 MHz, CDCl$_3$) δ 7.95-7.97 (m, 2H), 7.52-7.83 (m, 2H), 7.32-7.40 (m, 3H), 6.91 (d,

J = 8.7 Hz, 1H), 6.16 (t, J = 7.8 Hz, 1H), 3.91 (s, 3H), 3.75 (dd, J = 9.3, 15.9 Hz, 1H), 3.47 (dd, J

= 7.2, 15.9 Hz, 1H); ^{13}C NMR (75 MHz, CDCl$_3$) δ 166.8, 162.8, 144.3, 139.6, 139.1, 131.4,

126.7, 126.4, 124.7, 124.5, 123.8, 123.3, 122.5, 121.8, 109.4, 81.4, 51.9, 37.5; HRMS (ESI-TOF

m/z) for C$_{18}$H$_{14}$O$_3$S calcd 311.0730 found 311.0736 (M+H)+.

Methyl 2,3-dihydro-[2,2'-bibenzofuran]-5-carboxylate (103, Table 7-2, entry 10)
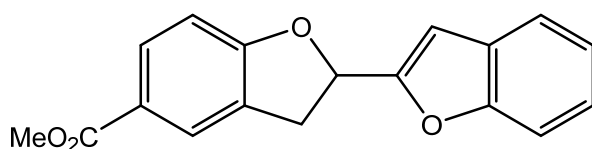
Chemical Formula: C$_{18}$H$_{14}$O$_4$
Molecular Weight: 294.31

The methyl 4-hydroxy-3-iodobenzoate (173.53 mg, 0.624 mmol, 1 eq), 2-vinylbenzofuran (90

mg, 0.624 mmol, 1 eq), cesium carbonate (407 mg, 1.248 mmol, 2 eq), and Herrmann's

palladacycle (14.6 mg, 0.0156 mmol, 0.025 eq) were charged to a vial which contained dry and

oxygen free dimethylacetamide (3 mL) under an argon atmosphere. The vial was sealed with a

septum and the mixture was heated to 130 ºC for 3 h, cooled to rt, and EtOAc (10mL) was added

in one portion. The suspension was filtered through a plug of celite and the filtrate was washed

successively with aq 0.5 N HCl (2 x 10 mL) and brine (2 x 10 mL). The organic layer was dried

(Na$_2$SO$_4$) and the solvent was removed in vacuo to provide a crude yellow solid. The solid was

purified by flash column chromatography on silica gel (5% EtOAc in hexanes) to provide the

pure methyl ester dihydrobenzofuran **103** in 77% yield as a white solid (142 mg): mp: 102-104

ºC; ^{1}H NMR (300 MHz, CDCl$_3$) δ 7.93-7.96 (m, 2H), 7.58 (d, J = 7.5 Hz, 1H), 7.48 (d, J = 7.8

Hz, 1H), 7.22-7.35 (m, 2H), 6.88 (d, J = 8.4 Hz, 1H), 6.81 (s, 1H), 5.98 (t, J = 8.7 Hz, 1H), 3.91

(s, 3H), 3.63 (d, J = 9.6 Hz, 2H); ^{13}C NMR (75 MHz, CDCl$_3$) δ 166.8, 162.9, 155.2, 154.7,

131.3, 127.7, 127.6, 126.7, 126.5, 124.3, 123.3, 123.0, 121.3, 111.5, 109.3, 105.0, 78.4, 51.9, 33.7; HRMS (ESI-TOF m/z) for $C_{18}H_{14}O_4$ calcd 295.0975 found 295.0965 (M+H)+.

Methyl 2-(naphthalen-2-yl)-2,3-dihydrobenzofuran-5-carboxylate (104, Table 7-2, entry 11)
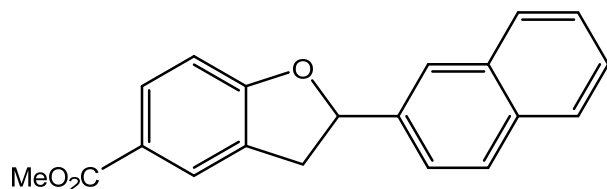
Chemical Formula: $C_{20}H_{16}O_3$
Molecular Weight: 304.35

The methyl 4-hydroxy-3-iodobenzoate (173.53 mg, 0.624 mmol, 1 eq), 2-vinylnaphthalene (96.3 mg, 0.624 mmol, 1 eq), cesium carbonate (407 mg, 1.248 mmol, 2 eq), and Herrmann's palladacycle (14.6 mg, 0.0156 mmol, 0.025 eq were charged to a vial which contained dry and oxygen free dimethylacetamide (3 mL) under an argon atmosphere. The vial was sealed with a septum and the mixture was heated to 110 ºC for 3 h, cooled to rt, and EtOAc (10mL) was added in one portion. The suspension was filtered through a plug of celite and the filtrate was washed successively with aq 0.5 N HCl (2 x 10 mL) and brine (2 x 10 mL). The organic layer was dried (Na2SO4) and the solvent was removed in vacuo to provide a crude yellow solid. The solid was purified by flash column chromatography on silica gel (5% EtOAc in hexanes) to provide the pure product in 82% yield as a white solid (155 mg): mp: 120-122 ºC; ^{1}H NMR (300 MHz, CDCl3) δ 7.84-7.96 (m, 6H), 7.44-7.48 (m, 3H), 6.92 (d, J = 8.4 Hz, 1H), 6.01 (t, J = 8.4 Hz, 1H), 3.89 (s, 3H), 3.74 (dd, J = 9.6, 15.6 Hz, 1H), 3.32 (dd, J = 7.5, 15.6 Hz, 1H); ^{13}C NMR (75 MHz, CDCl3) δ 166.9, 163.7, 138.4, 133.2, 133.1, 131.3, 128.8, 128.1, 128.0, 127.7, 126.9, 126.7, 126.4, 126.2, 124.8, 124.7, 123.3, 123.0, 109.1, 85.3, 51.8, 37.6, 29.7; HRMS (ESI-TOF m/z) for $C_{20}H_{16}O_3$ calcd 305.1160 found 305.1172 (M+H)+.

Methyl 2-methyl-2-(naphthalen-2-yl)-2,3-dihydrobenzofuran-5-carboxylate (105, Table 7-2, entry 12)
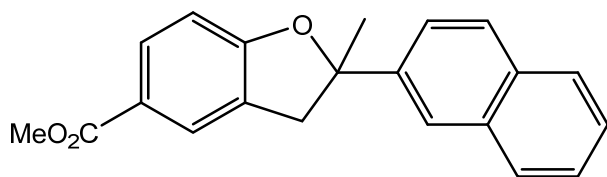
Chemical Formula: $C_{21}H_{18}O_3$
Molecular Weight: 318.37

The methyl 4-hydroxy-3-iodobenzoate (173.5 mg, 0.624 mmol, 1 eq), 2-(prop-1-en-2-yl)naphthalene (105 mg, 0.624 mmol, 1 eq), cesium carbonate (407 mg, 1.248 mmol, 2 eq), and Herrmann's palladacycle (14.6 mg, 0.0156 mmol, 0.025 eq) were charged to a vial which contained dry and oxygen free dimethylacetamide (3 mL) under an argon atmosphere. The vial was sealed with a septum and the mixture was heated to 110 ºC for 3 h, cooled to rt, and EtOAc (10mL) was added in one portion. The suspension was filtered through a plug of celite and the filtrate was washed successively with aq 0.5 N HCl (2 x 10 mL) and brine (2 x 10 mL). The organic layer was dried (Na_2SO_4) and the solvent was removed in vacuo to provide a crude off-white solid. The solid was purified by flash column chromatography on silica gel (5% EtOAc in hexanes) to provide the pure methyl ester dihydrobenzofuran **105** in 91% yield as a white solid (181 mg): mp: 125-126 ºC; ^{1}H NMR (300 MHz, CDCl$_3$) δ 8.01 – 7.91 (m, 2H), 7.91 – 7.81 (m, 4H), 7.60 – 7.46 (m, 3H), 6.98 (d, J = 8.4 Hz, 1H), 3.90 (s, 3H), 3.58 (d, J = 15.6 Hz, 1H), 3.48 (d, J = 15.6 Hz, 1H), 1.90 (s, 3H); ^{13}C NMR (75 MHz, CDCl$_3$) δ 166.98, 162.89, 143.15, 133.03, 132.55, 131.30, 128.49, 128.19, 127.55, 126.98, 126.94, 126.36, 126.09, 123.00, 122.83, 109.36, 90.95, 51.83, 43.93, 29.19; HRMS (ESI) (M + H), Calcd. for $C_{21}H_{19}O_3$ 319.1334; Found 319.1336

Methyl 2-(naphthalen-2-yl)benzofuran-5-carboxylate (107, Table 7-4, entry 1)
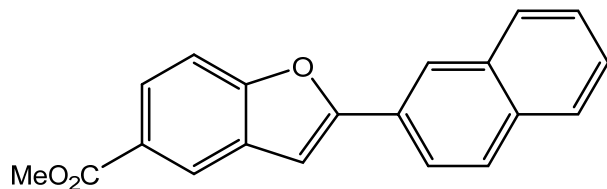
Chemical Formula: $C_{20}H_{14}O_3$
Molecular Weight: 302.33

The methyl 4-hydroxy-3-iodobenzoate (173.53 mg, 0.624 mmol, 1 eq), 2-vinylnaphthalene (96.3 mg, 0.624 mmol, 1 eq), cesium carbonate (407 mg, 1.248 mmol, 2 eq), and Herrmann's palladacycle (14.6 mg, 0.0156 mmol, 0.025 eq) were charged to a vial which contained dry and oxygen free dimethylacetamide (3 mL) under an argon atmosphere. The vial was sealed with a septum and the mixture was heated to 70 ºC for 3 h, cooled to rt, and EtOAc (10mL) was added in one portion. The suspension was filtered through a plug of celite and the filtrate was washed successively with aq 0.5 N HCl (2 x 10 mL) and brine (2 x 10 mL). The organic layer was dried (Na_2SO_4) and the solvent was removed in vacuo to provide a crude yellow solid. The solid was purified by flash column chromatography on silica gel (5% EtOAc in hexanes) to provide the pure benzofuran **107** in 75% yield as a white solid (141.5 mg): mp: 188-190 ºC; ^{1}H NMR (300 MHz, $CDCl_3$) δ 8.38 (s, 1H), 8.35 (s, 1H), 8.04 (dd, J = 1.5, 8.7 Hz, 1H), 7.84-7.95 (m, 4H), 7.49-7.60 (m, 3H), 7.18 (s, 1H), 3.96 (s, 3H); ^{13}C NMR (75 MHz, $CDCl_3$) δ 167.4, 157.6, 157.5, 133.6, 133.5, 129.4, 128.7, 128.6, 127.9, 127.2, 126.9, 126.3, 125.5, 124.3, 123.4, 122.8, 111.1, 102.2, 52.2; HRMS (ESI-TOF m/z) for $C_{20}H_{14}O_3$ calcd 303.1006 found 303.1016 (M+H)+.

Methyl (E)-4-hydroxy-3-(2-(naphthalen-2-yl)vinyl)benzoate (108, Table 7-4, entry 3)

Chemical Formula: $C_{20}H_{16}O_3$
Molecular Weight: 304.35

263

The methyl 4-hydroxy-3-iodobenzoate (173.53 mg, 0.624 mmol, 1 eq), 2-vinylnaphthalene (96.3 mg, 0.624 mmol, 1 eq), cesium carbonate (407 mg, 1.248 mmol, 2 eq), and Herrmann's palladacycle (14.6 mg, 0.0156 mmol, 0.025 eq) were charged to a vial which contained dry and oxygen free dimethylacetamide (3 mL) under an argon atmosphere. The vial was sealed with a septum and the mixture was heated to 140 ºC for 3 h, cooled to rt, and EtOAc (10mL) was added in one portion. The suspension was filtered through a plug of celite and the filtrate was washed successively with aq 0.5 N HCl (2 x 10 mL) and brine (2 x 10 mL). The organic layer was dried (Na$_2$SO$_4$) and the solvent was removed in vacuo to provide a crude yellow solid. The solid was purified by flash column chromatography on silica gel (5% EtOAc in hexanes) to provide the pure hydroxyl stilbene **108** in 86% yield as a white solid (163 mg): mp: 193-195 ºC; ^{1}H NMR (300 MHz, DMSOD$_6$) δ 10.81 (s, 1H), 8.23 (s, 1H), 8.05 (s, 1H), 7.84-7.93 (m, 4H), 7.75 (dd, *J* = 1.5, 8.4 Hz, 1H), 7.45-7.54 (m, 4H), 7.00 (d, *J* = 8.4 Hz, 1H), 3.84 (s, 3H); ^{13}C NMR (75 MHz, CDCl$_3$) δ 166.5, 159.7, 135.3, 133.7, 132.9, 130.4, 129.6, 128.7, 128.6, 128.3, 128.0, 126.8, 126.7, 126.4, 124.4, 124.0, 123.7, 121.1, 116.3, 51.9; HRMS (ESI-TOF *m/z*) for C$_{20}$H$_{16}$O$_3$ calcd 305.1180 found 305.1172 (M+H)+.

2-(Benzo[b]thiophen-2-yl)-7-methoxy-2,3-dihydrobenzofuran (118, Table 7-5, entry 2)
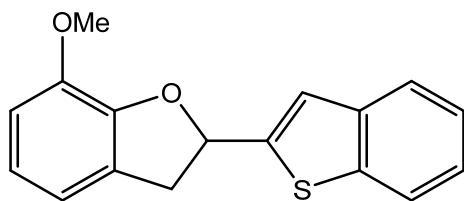
Chemical Formula: C$_{17}$H$_{14}$O$_2$S
Molecular Weight: 282.36

The 2-bromo-6-methoxyphenol (126.7 mg, 0.624 mmol, 1 eq), 2-vinylbenzo[b]thiophene (100 mg, 0.624 mmol, 1 eq), cesium carbonate (407 mg, 1.248 mmol, 2 eq), and Herrmann's palladacycle (14.6 mg, 0.0156 mmol, 0.025 eq) were charged to a vial which contained dry and

oxygen free dimethylacetamide (3 mL) under an argon atmosphere. The vial was sealed with a

septum and the mixture was heated to 130 ºC for 3 h, cooled to rt, and EtOAc (10mL) was added

in one portion. The suspension was filtered through a plug of celite and the filtrate was washed

successively with aq 0.5 N HCl (2 x 10 mL) and brine (2 x 10 mL). The organic layer was dried

(Na_2SO_4) and the solvent was removed in vacuo to provide a crude yellow solid. The solid was

purified by flash column chromatography on silica gel (5% EtOAc in hexanes) to provide the

pure methoxy dihydrobenzofuran **118** in 83% yield as a white solid (146 mg): mp: 106-107 ºC;

^{1}H NMR (300 MHz, $CDCl_3$) δ 7.87 – 7.78 (m, 1H), 7.78 – 7.72 (m, 1H), 7.43 – 7.29 (m, 3H),

6.97 – 6.79 (m, 3H), 6.18 – 6.05 (m, 1H), 3.93 (s, 3H), 3.73 (dd, J = 15.5, 9.3 Hz, 1H), 3.48 (dd,

J = 15.5, 7.6 Hz, 1H); ^{13}C NMR (75 MHz, $CDCl_3$) δ 147.32, 145.08, 144.67, 139.68, 139.26,

127.18, 124.50, 124.36, 123.68, 122.47, 121.74, 121.69, 117.07, 111.81, 80.94, 56.12, 38.75;

HRMS (ESI) (M + H), Calcd. for $C_{17}H_{15}O_2S$ 283.0793; Found 283.0789

2-(Benzo[b]thiophen-2-yl)-6-methoxy-2,3-dihydrobenzofuran (119, Table 7-5, entry 3)
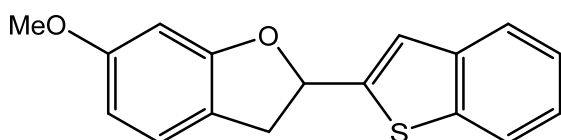
Chemical Formula: $C_{17}H_{14}O_2S$
Molecular Weight: 282.36

The 2-bromo-5-methoxyphenol (126.7 mg, 0.624 mmol, 1 eq), 2-vinylbenzo[b]thiophene (100

mg, 0.624 mmol, 1 eq), cesium carbonate (407 mg, 1.248 mmol, 2 eq), and Herrmann's

palladacycle (14.6 mg, 0.0156 mmol, 0.025 eq) were charged to a vial which contained dry and

oxygen free dimethylacetamide (3 mL) under an argon atmosphere. The vial was sealed with a

septum and the mixture was heated to 130 ºC for 3 h, cooled to rt, and EtOAc (10mL) was added

in one portion. The suspension was filtered through a plug of celite and the filtrate was washed

successively with aq 0.5 N HCl (2 x 10 mL) and brine (2 x 10 mL). The organic layer was dried

(Na$_2$SO$_4$) and the solvent was removed in vacuo to provide a crude yellow solid. The solid was purified by flash column chromatography on silica gel (5% EtOAc in hexanes) to provide the pure methoxy dihydroxybenzofuran **119** in 84% yield as a white solid (148 mg): mp: 100-101 ºC; ^{1}H NMR (300 MHz, CDCl$_3$) δ 7.87 – 7.79 (m, 1H), 7.79 – 7.68 (m, 1H), 7.41 – 7.30 (m, 3H), 7.12 (d, *J* = 7.9 Hz, 1H), 6.56 – 6.46 (m, 2H), 6.08 (dd, *J* = 9.0, 7.4 Hz, 1H), 3.81 (s, 3H), 3.65 (dd, *J* = 15.1, 9.2 Hz, 1H), 3.37 (dd, *J* = 15.1, 7.1 Hz, 1H); ^{13}C NMR (75 MHz, CDCl$_3$) δ 160.64, 160.17, 145.38, 139.61, 139.24, 124.86, 124.52, 124.40, 123.67, 122.48, 121.38, 117.76, 106.65, 96.43, 81.25, 55.53, 37.64; HRMS (ESI) (M + H), Calcd. for C$_{17}$H$_{15}$O$_2$S 283.0793; Found 283.0798

2-(Benzo[b]thiophen-2-yl)-4-methoxy-2,3-dihydrobenzofuran (120, Table 7-5, entry 4)
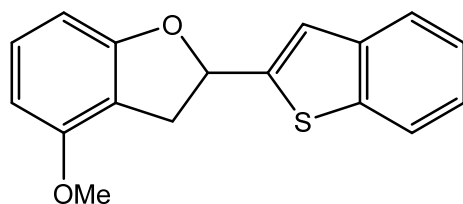
Chemical Formula: C$_{17}$H$_{14}$O$_2$S
Molecular Weight: 282.36

The 2-bromo-3-methoxyphenol (126.7 mg, 0.624 mmol, 1 eq), 2-vinylbenzo[b]thiophene (100 mg, 0.624 mmol, 1 eq), cesium carbonate (407 mg, 1.248 mmol, 2 eq), and Herrmann's palladacycle (14.6 mg, 0.0156 mmol, 0.025 eq) were charged to a vial which contained dry and oxygen free dimethylacetamide (3 mL) under an argon atmosphere. The vial was sealed with a septum and the mixture was heated to 130 ºC for 3 h, cooled to rt, and EtOAc (10mL) was added in one portion. The suspension was filtered through a plug of celite and the filtrate was washed successively with aq 0.5 N HCl (2 x 10 mL) and brine (2 x 10 mL). The organic layer was dried (Na$_2$SO$_4$) and the solvent was removed in vacuo to provide a crude yellow solid. The solid was purified by flash column chromatography on silica gel (5% EtOAc in hexanes) to provide the

pure product in 65% yield as a white solid (114 mg): mp: 110-112 ºC; ^{1}H NMR (300 MHz, CDCl$_3$) δ 7.87 – 7.79 (m, 1H), 7.79 – 7.72 (m, 1H), 7.42 – 7.29 (m, 3H), 7.17 (t, J = 8.1 Hz, 1H), 6.58 (d, J = 8.0 Hz, 1H), 6.50 (d, J = 8.3 Hz, 1H), 6.15 – 6.04 (m, 1H), 3.87 (s, 3H), 3.67 (dd, J = 15.7, 9.4 Hz, 1H), 3.39 (dd, J = 15.7, 7.2 Hz, 1H); ^{13}C NMR (75 MHz, CDCl$_3$) δ 160.20, 156.53, 145.51, 139.66, 139.28, 129.47, 124.47, 124.37, 123.67, 122.47, 121.32, 112.91, 103.49, 102.96, 80.81, 55.43, 35.71; HRMS (ESI) (M + H), Calcd. for C17H15O2S 283.0793; Found 283.0794

REFERENCES

1.   Bertolini, F.; Pineschi, M., Recent Progress in the Synthesis of 2,3-Dihydrobenzofurans. *Organic Preparations and Procedures International* **2009,** *41* (5), 385-418.

2.   Sheppard, T. D., Strategies for the synthesis of 2,3-dihydrobenzofurans. *Journal of Chemical Research* **2011,** *35* (7), 377-385.

3.   Di Micco, S.; Mazue, F.; Daquino, C.; Spatafora, C.; Delmas, D.; Latruffe, N.; Tringali, C.; Riccio, R.; Bifulco, G., Structural basis for the potential antitumour activity of DNA-interacting benzo[kl]xanthene lignans. *Organic & Biomolecular Chemistry* **2011,** *9* (3), 701-710.

4.   Huang, H.-Y.; Ishikawa, T.; Peng, C.-F.; Tsai, I.-L.; Chen, I.-S., Constituents of the Root Wood of Zanthoxylum wutaiense with Antitubercular Activity. *Journal of Natural Products* **2008,** *71* (7), 1146-1151.

5.   Zhang, H.; Qiu, S.; Tamez, P.; Tan, G. T.; Aydogmus, Z.; Hung, N. V.; Cuong, N. M.; Angerhofer, C.; Doel Soejarto, D.; Pezzuto, J. M.; Fong, H. H. S., Antimalarial Agents from Plants II. Decursivine, A New Antimalarial Indole Alkaloid from Rhaphidophora decursiva. *Pharmaceutical Biology* **2002,** *40* (3), 221-224.

6.   Saito, M.; Ueo, M.; Kametaka, S.; Saigo, O.; Uchida, S.; Hosaka, H.; Sakamoto, K.; Nakahara, T.; Mori, A.; Ishii, K., Attenuation of Cataract Progression by A-3922, a Dihydrobenzofuran Derivative, in Streptozotocin-Induced Diabetic Rats. *Biological and Pharmaceutical Bulletin* **2008,** *31* (10), 1959-1963.

7.   Ha, D. T.; Ngoc, T. M.; Lee, I.; Lee, Y. M.; Kim, J. S.; Jung, H.; Lee, S.; Na, M.; Bae, K., Inhibitors of Aldose Reductase and Formation of Advanced Glycation End-Products

in Moutan Cortex (Paeonia suffruticosa). *Journal of Natural Products* **2009,** *72* (8), 1465-1470.

8.   Kouam, S. F.; Khan, S. N.; Krohn, K.; Ngadjui, B. T.; Kapche, D. G. W. F.; Yapna, D. B.; Zareem, S.; Moustafa, A. M. Y.; Choudhary, M. I., α-Glucosidase Inhibitory Anthranols, Kenganthranols A−C, from the Stem Bark of Harungana madagascariensis. *Journal of Natural Products* **2006,** *69* (2), 229-233.

9.   Coy, E. D.; Cuca, L. E.; Sefkow, M., COX, LOX and platelet aggregation inhibitory properties of Lauraceae neolignans. *Bioorganic & Medicinal Chemistry Letters* **2009,** *19* (24), 6922-6925.

10.   Lai, P. X.; Ma, Q. L.; Row, K. H., A new acetophenone derivative and other constituents from Senecio vulgaris. *Journal of Chemical Research* **2010,** *34* (9), 514-516.

11.   Wakimoto, T.; Miyata, K.; Ohuchi, H.; Asakawa, T.; Nukaya, H.; Suwa, Y.; Kan, T., Enantioselective Total Synthesis of Aperidine. *Organic Letters* **2011,** *13* (10), 2789-2791.

12.   Chin, Y.-W.; Chai, H.-B.; Keller, W. J.; Kinghorn, A. D., Lignans and Other Constituents of the Fruits of Euterpe oleracea (Açai) with Antioxidant and Cytoprotective Activities. *Journal of Agricultural and Food Chemistry* **2008,** *56* (17), 7759-7764.

13.   Huang, Z.; Cui, Q.; Xiong, L.; Wang, Z.; Wang, K.; Zhao, Q.; Bi, F.; Wang, Q., Synthesis and Insecticidal Activities and SAR Studies of Novel Benzoheterocyclic Diacylhydrazine Derivatives. *Journal of Agricultural and Food Chemistry* **2009,** *57* (6), 2447-2456.

14.   Chang, H. C.; Hung, W. C.; Huang, M. S.; Hsu, H. K., Extract from the leaves of Toona sinensis roemor exerts potent antiproliferative effect on human lung cancer cells. *Am J Chin Med* **2002,** *30* (2-3), 307-14.

15.   Edmonds, J. M.; Staniforth, M., Plate 348. Toona sinensis. *Curtis's Botanical Magazine* **1998,** *15* (3), 186-193.

16.   Manna, S. K.; Bose, J. S.; Gangan, V.; Raviprakash, N.; Navneetha, T.; Raghavendra, P. B.; Babajan, B.; Kumar, C. S.; Jain, S. K., Novel derivative of benzofuran induces cell death mostly by G2/M cell cycle arrest through p53-dependent pathway but partially by inhibition of NF-kB. *Journal of Biological Chemistry* **2010**.

17.   Gupta, D.; Bleakley, B.; Gupta, R. K., Dragon's blood: botany, chemistry and therapeutic uses. *J Ethnopharmacol* **2008,** *115* (3), 361-80.

18.   Wang, W. S.; Lan, X. C.; Wu, H. B.; Zhong, Y. Z.; Li, J.; Liu, Y.; Shao, C. C., Lignans from the flower buds of Magnolia liliflora Desr. *Planta Med* **2012,** *78* (2), 141-7.

19.   Iida, T.; Ito, K., Four phenolic neolignans from Magnolia liliflora. *Phytochemistry* **1983,** *22* (3), 763-766.

20.   Otrosina, W. J.; Garbelotto, M., Heterobasidion occidentale sp. nov. and Heterobasidion irregulare nom. nov.: a disposition of North American Heterobasidion biological species. *Fungal Biol* **2010,** *114* (1), 16-25.

21.   Horlacher, N.; Nachtigall, J.; Schulz, D.; Sussmuth, R. D.; Hampp, R.; Fiedler, H. P.; Schrey, S. D., Biotransformation of the fungal phytotoxin fomannoxin by soil streptomycetes. *J Chem Ecol* **2013,** *39* (7), 931-41.

22.   Conforti, F.; Loizzo, M. R.; Statti, G. A.; Houghton, P. J.; Menichini, F., Biological properties of different extracts of two Senecio species. *Int J Food Sci Nutr* **2006,** *57* (1-2), 1-8.

23.   Dickson, R. A.; Houghton, P. J.; Hylands, P. J.; Gibbons, S., Antimicrobial, resistance-modifying effects, antioxidant and free radical scavenging activities of Mezoneuron

benthamianum Baill., Securinega virosa Roxb. &Wlld. and Microglossa pyrifolia Lam. *Phytother Res* **2006,** *20* (1), 41-5.

24.   Nichols, D. E.; Hoffman, A. J.; Oberlender, R. A.; Riggs, R. M., Synthesis and evaluation of 2,3-dihydrobenzofuran analogues of the hallucinogen 1-(2,5-dimethoxy-4-methylphenyl)-2-aminopropane: drug discrimination studies in rats. *J Med Chem* **1986,** *29* (2), 302-4.

25.   Monte, A. P.; Marona-Lewicka, D.; Cozzi, N. V.; Nichols, D. E., Synthesis and pharmacological examination of benzofuran, indan, and tetralin analogues of 3,4-(methylenedioxy)amphetamine. *J Med Chem* **1993,** *36* (23), 3700-6.

26.   Nichols, D. E.; Snyder, S. E.; Oberlender, R.; Johnson, M. P.; Huang, X. M., 2,3-Dihydrobenzofuran analogues of hallucinogenic phenethylamines. *J Med Chem* **1991,** *34* (1), 276-81.

27.   Chan, S. L.; Dunne, M. J.; Stillings, M. R.; Morgan, N. G., The alpha 2-adrenoceptor antagonist efaroxan modulates K+ATP channels in insulin-secreting cells. *Eur J Pharmacol* **1991,** *204* (1), 41-8.

28.   Rascol, O.; Sieradzan, K.; Peyro-Saint-Paul, H.; Thalamas, C.; Brefel-Courbon, C.; Senard, J. M.; Ladure, P.; Montastruc, J. L.; Lees, A., Efaroxan, an alpha-2 antagonist, in the treatment of progressive supranuclear palsy. *Mov Disord* **1998,** *13* (4), 673-6.

29.   Chopin, P.; Colpaert, F. C.; Marien, M., Effects of alpha-2 adrenoceptor agonists and antagonists on circling behavior in rats with unilateral 6-hydroxydopamine lesions of the nigrostriatal pathway. *J Pharmacol Exp Ther* **1999,** *288* (2), 798-804.

30.   Briejer, M. R.; Bosmans, J. P.; Van Daele, P.; Jurzak, M.; Heylen, L.; Leysen, J. E.; Prins, N. H.; Schuurkes, J. A., The in vitro pharmacological profile of prucalopride, a novel enterokinetic compound. *Eur J Pharmacol* **2001,** *423* (1), 71-83.

31.   Quigley, E. M., Prucalopride: safety, efficacy and potential applications. *Therap Adv Gastroenterol* **2012,** *5* (1), 23-30.

32.   De Maeyer, J. H.; Lefebvre, R. A.; Schuurkes, J. A., 5-HT4 receptor agonists: similar but not the same. *Neurogastroenterol Motil* **2008,** *20* (2), 99-112.

33.   Chen, W.; Yang, X.-D.; Li, Y.; Yang, L.-J.; Wang, X.-Q.; Zhang, G.-L.; Zhang, H.-B., Design, synthesis and cytotoxic activities of novel hybrid compounds between dihydrobenzofuran and imidazole. *Organic & Biomolecular Chemistry* **2011,** *9* (11), 4250-4255.

34.   Gupta, A.; Patton, C.; Diskina, D.; Cheatle, M., Retrospective review of physician opioid prescribing practices in patients with aberrant behaviors. *Pain Physician* **2011,** *14* (4), 383-9.

35.   Chida, N., Recent advances in the synthesis of morphine and related alkaloids. *Top Curr Chem* **2011,** *299*, 1-28.

36.   Aristoff, P. A.; Harrison, A. W.; Huber, A. M., Synthesis of benzopyran prostaglandins, potent stable prostacyclin analogs, via an intramolecular mitsunobu reaction. *Tetrahedron Letters* **1984,** *25* (36), 3955-3958.

37.   Mitsunobu, O.; Yamada, M., Preparation of Esters of Carboxylic and Phosphoric Acid <I>via</I> Quaternary Phosphonium Salts. *Bulletin of the Chemical Society of Japan* **1967,** *40* (10), 2380-2382.

38.	Bertolini, F.; Crotti, P.; Di Bussolo, V.; Macchia, F.; Pineschi, M., Synthesis and Cyclodehydration of Hydroxyphenols: A New Stereoselective Approach to 3-Aryl-2,3-dihydrobenzofurans. *The Journal of Organic Chemistry* **2007,** *72* (20), 7761-7764.

39.	Procopiou, P. A.; Brodie, A. C.; Deal, M. J.; Hayman, D. F., A novel cyclodehydration reaction of hydroxy-phenols using imidate esters as leaving groups. *Tetrahedron Letters* **1993,** *34* (46), 7483-7486.

40.	Rao, M.; Yang, M.; Kuehner, D.; Grosso, J.; Deshpande, R. P., A Practical Pilot-Scale Synthesis of 4-Vinyl-2,3-dihydrobenzofuran Using Imidate Ester Chemistry and Phase-Transfer Catalysis. *Organic Process Research & Development* **2003,** *7* (4), 547-550.

41.	Stafford, J. A.; Valvano, N. L., A Unified Strategy for the Synthesis of Highly Substituted Dihydrobenzofurans and Dihydrobenzopyrans. *The Journal of Organic Chemistry* **1994,** *59* (15), 4346-4349.

42.	Lee, K. Y.; Gowrisankar, S.; Lee, Y. J.; Kim, J. N., Synthesis of 2-amino-2,3-dihydrobenzofurans and fully substituted furans from modified Baylis–Hillman adducts. *Tetrahedron* **2006,** *62* (37), 8798-8804.

43.	Ciganek, E., The Catalyzed α-Hydroxyalkylation and α-Aminoalkylation of Activated Olefins (The Morita—Baylis—Hillman Reaction). In *Organic Reactions*, John Wiley & Sons, Inc.: 2004.

44.	Clive, D. L. J.; Wang, J., A Tin Hydride Designed To Facilitate Removal of Tin Species from Products of Stannane-Mediated Radical Reactions. *The Journal of Organic Chemistry* **2002,** *67* (4), 1192-1198.

45.	Beckwith, A. L. J.; Easton, C. J.; Serelis, A. K., Some guidelines for radical reactions. *Journal of the Chemical Society, Chemical Communications* **1980,** (11), 482-483.

46. Boisvert, G.; Giasson, R., Induction of radical cyclizations with the 10-methyl-9,10-dihydroacridine / NaBH4 photocatalytic system. *Tetrahedron Letters* **1992,** *33* (44), 6587-6590.

47. Kurono, N.; Honda, E.; Komatsu, F.; Orito, K.; Tokuda, M., Regioselective synthesis of substituted 1-indanols, 2,3-dihydrobenzofurans and 2,3-dihydroindoles by electrochemical radical cyclization using an arene mediator. *Tetrahedron* **2004,** *60* (8), 1791-1801.

48. Lin, H.; Schall, A.; Reiser, O., Cyclization Reactions of Vinyl Radicals via 1,6-H-Atom Transfer: Facile Access to 2,3-Disubstituted Dihydrobenzofurans. *Synlett* **2005,** *2005* (17), 2603-2606.

49. Layton, M. E.; Morales, C. A.; Shair, M. D., Biomimetic synthesis of (-)-longithorone A. *J Am Chem Soc* **2002,** *124* (5), 773-5.

50. Lecerf-Schmidt, F.; Haudecoeur, R.; Peres, B.; Ferreira Queiroz, M. M.; Marcourt, L.; Challal, S.; Ferreira Queiroz, E.; Sotoing Taiwe, G.; Lomberget, T.; Le Borgne, M.; Wolfender, J. L.; De Waard, M.; Robins, R. J.; Boumendjel, A., Biomimetic synthesis of Tramadol. *Chem Commun (Camb)* **2015,** *51* (77), 14451-3.

51. Min, L.; Zhang, Y.; Liang, X.; Huang, J.; Bao, W.; Lee, C. S., A biomimetic synthesis of (+/-)-basiliolide B. *Angew Chem Int Ed Engl* **2014,** *53* (42), 11294-7.

52. Kuethe, J. T.; Wong, A.; Journet, M.; Davies, I. W., A Rapid Synthesis of 2-Aryl-5-substituted-2,3-dihydrobenzofurans. *The Journal of Organic Chemistry* **2005,** *70* (9), 3727-3729.

53.   Wang, S.; Gates, B. D.; Swenton, J. S., A convergent route to dihydrobenzofuran neolignans via a formal 1,3-cycloaddition to oxidized phenols. *The Journal of Organic Chemistry* **1991,** *56* (6), 1979-1981.

54.   Engler, T. A.; Chai, W.; LaTessa, K. O., Lewis Acid-Controlled Regioselectivity in Reactions of Styrenyl Systems with Benzoquinone Monoimides: New Regioselective Syntheses of Substituted 2-Aryl-2,3-dihydrobenzofurans, 2-Aryl-2,3-dihydroindoles, and 2-Arylindoles. *The Journal of Organic Chemistry* **1996,** *61* (26), 9297-9308.

55.   Engler, T. A.; Combrink, K. D.; Ray, J. E., Stereoselective 3 + 2 and stereospecific 2 + 2 cycloaddition reactions of alkenes and quinones. *Journal of the American Chemical Society* **1988,** *110* (23), 7931-7933.

56.   Lomberget, T.; Baragona, F.; Fenet, B.; Barret, R., [3+2] versus [4+2] Cycloadditions of Quinone Monoimide with Azadienes: A Lewis Acid-Free Access to 5-Amino-2,3-dihydrobenzofuranes. *Organic Letters* **2006,** *8* (18), 3919-3922.

57.   Nair, V.; Rajesh, C.; Dhanya, R.; Rath, N. P., Lewis Acid Promoted Annulation of p-Quinoneimines by Allylsilanes: A Facile Entry into Benzofused Heterocycles. *Organic Letters* **2002,** *4* (6), 953-955.

58.   Porter, M. J.; Skidmore, J., Asymmetric Epoxidation of Electron-Deficient Alkenes. In *Organic Reactions*, John Wiley & Sons, Inc.: 2004.

59.   Jiang, H.; Sugiyama, T.; Hamajima, A.; Hamada, Y., Asymmetric Synthesis of 2-Substituted Dihydrobenzofurans and 3-Hydroxydihydrobenzopyrans through the Enantioselective Epoxidation of O-Silyl-Protected ortho-Allylphenols. *Advanced Synthesis & Catalysis* **2011,** *353* (1), 155-162.

60.   Kim, J. H.; Kim, J. K.; Ahn, E. K.; Ko, H. J.; Cho, Y. R.; Lee, C. H.; Kim, Y. K.; Bae, G.
        U.; Oh, J. S.; Seo, D. W., Marmesin is a novel angiogenesis inhibitor: Regulatory effect
        and molecular mechanism on endothelial cell fate and angiogenesis. *Cancer Lett* **2015,**
        369 (2), 323-30.

61.   Dinda, S. K.; Das, S. K.; Panda, G., Application of Phenolate Ion Mediated
        Intramolecular Epoxide Ring Opening in the Enantioselective Synthesis of
        Functionalized 2,3-Dihydrobenzofurans and 1-Benzopyrans. *Synthesis* **2009,** *2009* (11),
        1886-1896.

62.   Macías, F. A.; Varela, R. M.; Torres, A.; Molinillo, J. M. G., New Bioactive Plant
        Heliannuols from Cultivar Sunflower Leaves. *Journal of Natural Products* **1999,** *62* (12),
        1636-1639.

63.   Macias, F. A.; Torres, A.; Galindo, J. L.; Varela, R. M.; Alvarez, J. A.; Molinillo, J. M.,
        Bioactive terpenoids from sunflower leaves cv. Peredovick. *Phytochemistry* **2002,** *61* (6),
        687-92.

64.   Das, S. K.; Panda, G., β-Hydroxy-α-tosyloxy esters as chiral building blocks for the
        enantioselective synthesis of benzo-annulated oxa-heterocycles: scope and limitations.
        Tetrahedron **2008,** *64* (19), 4162-4173.

65.   Ito, C.; Katsuno, S.; Kondo, Y.; Tan, H. T. W.; Furukawa, H., Chemical Constituents of
        Avicennia alba. Isolation and Structural Elucidation of New Naphthoquinones and Their
        Analogues. *CHEMICAL & PHARMACEUTICAL BULLETIN* **2000,** *48* (3), 339-343.

66.   Takashima, J.; Ohsaki, A., Brosimacutins A−I, Nine New Flavonoids from Brosimum
        acutifolium. *Journal of Natural Products* **2002,** *65* (12), 1843-1847.

67.   Lipp, J., Possible mechanisms of morphine analgesia. *Clin Neuropharmacol* **1991,** *14* (2), 131-47.

68.   Walsh, S. L.; Nuzzo, P. A.; Lofwall, M. R.; Holtman, J. R., Jr., The relative abuse liability of oral oxycodone, hydrocodone and hydromorphone assessed in prescription opioid abusers. *Drug Alcohol Depend* **2008,** *98* (3), 191-202.

69.   Gates, M.; Tschudi, G., The Synthesis of Morphine. *Journal of the American Chemical Society* **1956,** *78* (7), 1380-1393.

70.   Zezula, J.; Hudlicky, T., Recent Progress in the Synthesis of Morphine Alkaloids. *Synlett* **2005,** *2005* (03), 388-405.

71.   Rice, K. C., Synthetic opium alkaloids and derivatives. A short total synthesis of (.+-.)-dihydrothebainone, (.+-.)-dihydrocodeinone, and (.+-.)-nordihydrocodeinone as an approach to a practical synthesis of morphine, codeine, and congeners. *The Journal of Organic Chemistry* **1980,** *45* (15), 3135-3137.

72.   Reed, J. W.; Hudlicky, T., The Quest for a Practical Synthesis of Morphine Alkaloids and Their Derivatives by Chemoenzymatic Methods. *Accounts of Chemical Research* **2015,** *48* (3), 674-687.

73.   Rinner, U.; Hudlicky, T., Synthesis of morphine alkaloids and derivatives. *Top Curr Chem* **2012,** *309*, 33-66.

74.   Trost, B. M.; Tang, W., Enantioselective Synthesis of (−)-Codeine and (−)-Morphine. *Journal of the American Chemical Society* **2002,** *124* (49), 14542-14543.

75.   Ullmann, F.; Bielecki, J., Ueber Synthesen in der Biphenylreihe. *Berichte der deutschen chemischen Gesellschaft* **1901,** *34* (2), 2174-2185.

76. Zhu, J.; Price, B. A.; Zhao, S. X.; Skonezny, P. M., Copper(I)-catalyzed intramolecular cyclization reaction of 2-(2′-chlorophenyl)ethanol to give 2,3-dihydrobenzofuran. *Tetrahedron Letters* **2000,** *41* (21), 4011-4014.

77. Pan, C.; Ma, Z.; Yu, J.; Zhang, Z.; Hui, A.; Wang, Z., Efficient One-Pot Synthesis of 2-Aryldihydrobenzofuran. *Synlett* **2005,** *2005* (12), 1922-1926.

78. Beletskaya, I. P.; Cheprakov, A. V., The Complementary Competitors: Palladium and Copper in C–N Cross-Coupling Reactions. *Organometallics* **2012,** *31* (22), 7753-7808.

79. Johansson Seechurn, C. C. C.; Kitching, M. O.; Colacot, T. J.; Snieckus, V., Palladium-Catalyzed Cross-Coupling: A Historical Contextual Perspective to the 2010 Nobel Prize. *Angewandte Chemie International Edition* **2012,** *51* (21), 5062-5085.

80. Palucki, M.; Wolfe, J. P.; Buchwald, S. L., Synthesis of Oxygen Heterocycles via a Palladium-Catalyzed C−O Bond-Forming Reaction. *Journal of the American Chemical Society* **1996,** *118* (42), 10333-10334.

81. Kuwabe, S.-i.; Torraca, K. E.; Buchwald, S. L., Palladium-Catalyzed Intramolecular C−O Bond Formation. *Journal of the American Chemical Society* **2001,** *123* (49), 12202-12206.

82. Aranyos, A.; Old, D. W.; Kiyomori, A.; Wolfe, J. P.; Sadighi, J. P.; Buchwald, S. L., Novel Electron-Rich Bulky Phosphine Ligands Facilitate the Palladium-Catalyzed Preparation of Diaryl Ethers. *Journal of the American Chemical Society* **1999,** *121* (18), 4369-4378.

83. Wang, X.; Lu, Y.; Dai, H.-X.; Yu, J.-Q., Pd(II)-Catalyzed Hydroxyl-Directed C−H Activation/C−O Cyclization: Expedient Construction of Dihydrobenzofurans. *Journal of the American Chemical Society* **2010,** *132* (35), 12203-12205.

84. Ioffe, D.; Kampf, A., Bromine, Organic Compounds. In *Kirk-Othmer Encyclopedia of Chemical Technology*, John Wiley & Sons, Inc.: 2000.

85. Trost, B. M.; Thiel, O. R.; Tsui, H.-C., Total Syntheses of Furaquinocin A, B, and E. *Journal of the American Chemical Society* **2003,** *125* (43), 13155-13164.

86. Li, Y.; Qi, Z.; Wang, H.; Fu, X.; Duan, C., Palladium-Catalyzed Oxidative Heck Coupling Reaction for Direct Synthesis of 4-Arylcoumarins Using Coumarins and Arylboronic Acids. *The Journal of Organic Chemistry* **2012,** *77* (4), 2053-2057.

87. Zhang, H.; Ferreira, E. M.; Stoltz, B. M., Direct Oxidative Heck Cyclizations: Intramolecular Fujiwara–Moritani Arylations for the Synthesis of Functionalized Benzofurans and Dihydrobenzofurans. *Angewandte Chemie International Edition* **2004,** *43* (45), 6144-6148.

88. Sunden, H.; Olsson, R., Asymmetric synthesis of a tricyclic benzofuran motif: a privileged core structure in biologically active molecules. *Organic & Biomolecular Chemistry* **2010,** *8* (21), 4831-4833.

89. Siqueira, F. A.; Taylor, J. G.; Correia, C. R. D., The first intramolecular Heck–Matsuda reaction and its application in the syntheses of benzofurans and indoles. *Tetrahedron Letters* **2010,** *51* (16), 2102-2105.

90. Szlosek-Pinaud, M.; Diaz, P.; Martinez, J.; Lamaty, F., Efficient synthetic approach to heterocycles possessing the 3,3-disubstituted-2,3-dihydrobenzofuran skeleton via diverse palladium-catalyzed tandem reactions. *Tetrahedron* **2007,** *63* (16), 3340-3349.

91. Lee, H.-S.; Kim, K.-H.; Lim, J.-W.; Kim, J.-N., Palladium-Catalyzed Domino Heck-Cyanation Cascade to 3-Cyanomethyl 2,3-Dihydrobenzofuran and 2,3-Dihydroindoles. *Bulletin of the Korean Chemical Society* **2011,** *32* (3), 1083-1086.

92. O'Connor, J. M.; Stallman, B. J.; Clark, W. G.; Shu, A. Y. L.; Spada, R. E.; Stevenson, T. M.; Dieck, H. A., Some aspects of palladium-catalyzed reactions of aryl and vinylic halides with conjugated dienes in the presence of mild nucleophiles. *The Journal of Organic Chemistry* **1983,** *48* (6), 807-809.

93. Larock, R. C.; Berrios-Pena, N.; Narayanan, K., Palladium-catalyzed heteroannulation of 1,3-dienes by functionally substituted aryl halides. *The Journal of Organic Chemistry* **1990,** *55* (11), 3447-3450.

94. Rozhkov, R. V.; Larock, R. C., Synthesis of Dihydrobenzofurans via Palladium-Catalyzed Annulation of 1,3-Dienes by o-Iodoaryl Acetates. *The Journal of Organic Chemistry* **2010,** *75* (12), 4131-4134.

95. de Vries, A. H. M.; Mulders, J. M. C. A.; Mommers, J. H. M.; Henderickx, H. J. W.; de Vries, J. G., Homeopathic Ligand-Free Palladium as a Catalyst in the Heck Reaction. A Comparison with a Palladacycle. *Organic Letters* **2003,** *5* (18), 3285-3288.

96. Pearson, D. E.; Wysong, R. D.; Breder, C. V., Ortho bromination of phenols. *The Journal of Organic Chemistry* **1967,** *32* (7), 2358-2360.

97. Bartholomew, C. H., Mechanisms of catalyst deactivation. *Applied Catalysis A: General* **2001,** *212* (1–2), 17-60.

98. Schofield, K.; Ward, R. S.; Choudhury, A. M., Phenol oxidation. The formation of benzofuran and 2,3-dihydrobenzofuran derivatives by oxidation of 1-(2-hydroxyphenyl)-2-(4-hydroxyphenyl)ethanes. *Journal of the Chemical Society C: Organic* **1971,** (0), 2834-2837.

99. Guiry, P. J.; Hennessy, A. J.; Cahill, J. P., The asymmetric Heck reaction: recent developments and applications of new palladium diphenylphosphinopyrrolidine complexes. *Topics in Catalysis* **1997,** *4* (3), 311-326.

100. Hsin, L.-W.; Chang, L.-T.; Chen, C.-W.; Hsu, C.-H.; Chen, H.-W., Stereoselective synthesis of morphine fragments trans- and cis-octahydro-1H-benzo[4,5]furo[3,2-e]isoquinolines. *Tetrahedron* **2005,** *61* (2), 513-520.

Part 3

DESIGN, SYNTHESIS, AND EVALUATION OF BZ/GABA$_A$

α6 POSITIVE ALLOSTERIC MODULATORS

INTRODUCTION AND BACKGROUND

I. INTRODUCTION TO GABA AND GABA RECEPTORS.

Gamma (γ)-aminobutyric acid (GABA, Figure 8-1) is the chief inhibitory neurotransmitter in the mammalian central nervous system.[1] GABA binding to specific transmembrane receptors in the plasma membrane is associated with the opening of ion channels that allow the flow of either negatively charged chloride ions into the cell or positively charged potassium ions out of the cell.[2] This negative change in transmembrane potential generally causes hyperpolarization of the neuron.[3] Three receptor classes for GABA are known, the GABA$_A$ receptor[4], in which the receptor is part of a ligand-gated ion channel complex and the GABA$_B$ receptor[5], G protein-coupled receptors that open or close ion channels via intermediary G proteins. There are also GABA$_C$ receptors that are ligand gated, but devoid of the allosteric benzodiazepine binding site of interest; GABA$_C$ receptors are also known as GABA$_A$-rho receptors and some consider them a subset of GABA$_A$[6]. Discussed in this work are ligands that selectively activate specific $\alpha_6\beta_3\gamma_2$ GABA$_A$ receptors via the allosteric benzodiazepine binding site to provide important physiological effects.

Figure 8-1: Structure of Gamma (γ)-Aminobutyric acid (GABA).
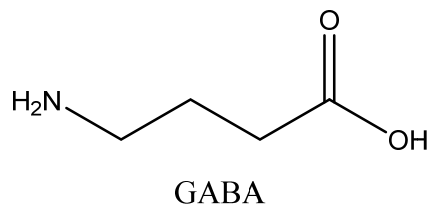
GABA

GABAergic neurons, neurons that produce GABA, exhibit chiefly inhibitory action at receptors in adult vertebrates.[7] Medium spiny neurons, depicted in Figure 8-2, are a typical example of GABAergic cells in the central nervous system (CNS).[8] GABA is synthesized in these neurons and others via enzyme catalyzed decarboxylation of glutamic acid (Scheme 8-1) and does not readily pass the blood-brain-barrier.[9]

Figure 8-2: Medium spiny cells (mouse brain).[10] (Modified from the Figure in reference 10)
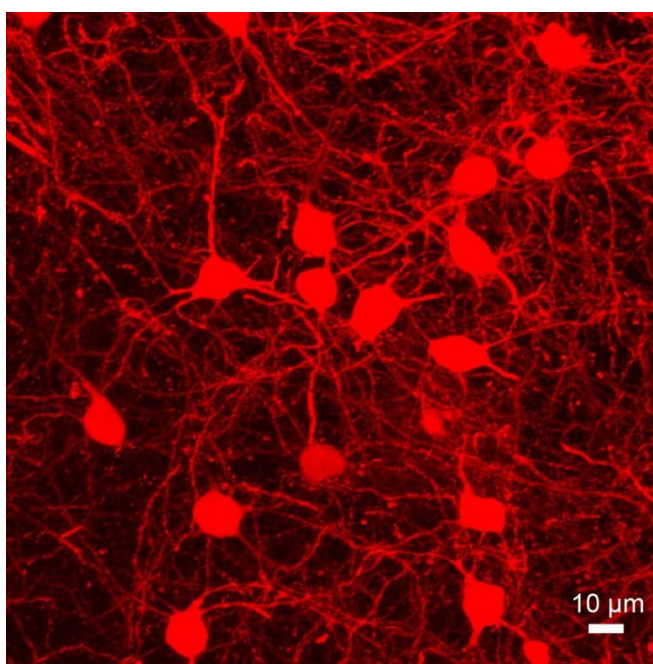
Scheme 8-1: Biosynthesis of GABA.
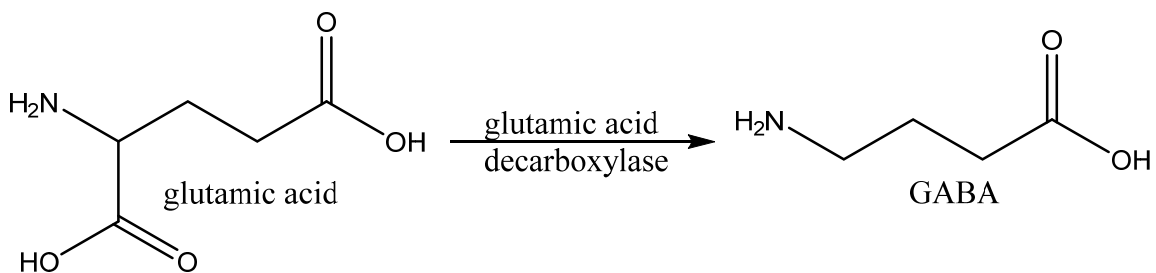
The GABA$_A$ receptor, a transmembrane heteropentameric ion channel, has been shown to affect a number of pharmacological responses when activated.[11] These include, but are not limited to, anxiety,[12] epilepsy,[13] insomnia,[14] depression,[15] bipolar disorder,[16-17] schizophrenia,[18] and Alzheimer's disease[19]. The response is dependent on the specific composition of GABA$_A$ subunits which make up the GABA$_A$ receptor.[20-21] To date, there are currently 19 individual GABA$_A$ receptor subunits which have been identified; α_{1-6}, β_{1-3}, γ_{1-3}, δ, ε, θ, π, and ρ_{1-3}[22] with additional unidentified subunits plausible. These subunits can arrange in either a hetero- or homo-pentameric ring. Currently, only a small handful of subunit formations have been positively identified to form a functional receptor, with many others highly likely or plausible.[23-24] The most common and intensively studied arrangement of the GABA$_A$ receptor consists of $\alpha_{1-6}\beta_{1-3}\gamma_2$ in a 2:2:1 stoichiometric ratio.[25]

The GABA$_A$ receptor, much like other members of the cys-loop superfamily, possesses a characteristic loop formed by 13 highly conserved amino acids between two cysteine (Cys) residues which form a disulfide bond near the N-terminal extracellular domain of the alpha subunit pictured in Figure 8-3.[12, 26] These monomeric units form the pentameric chloride ion channel also pictured in Figure 8-3.

Figure 8-3: Structure of the GABA$_A$ receptor.
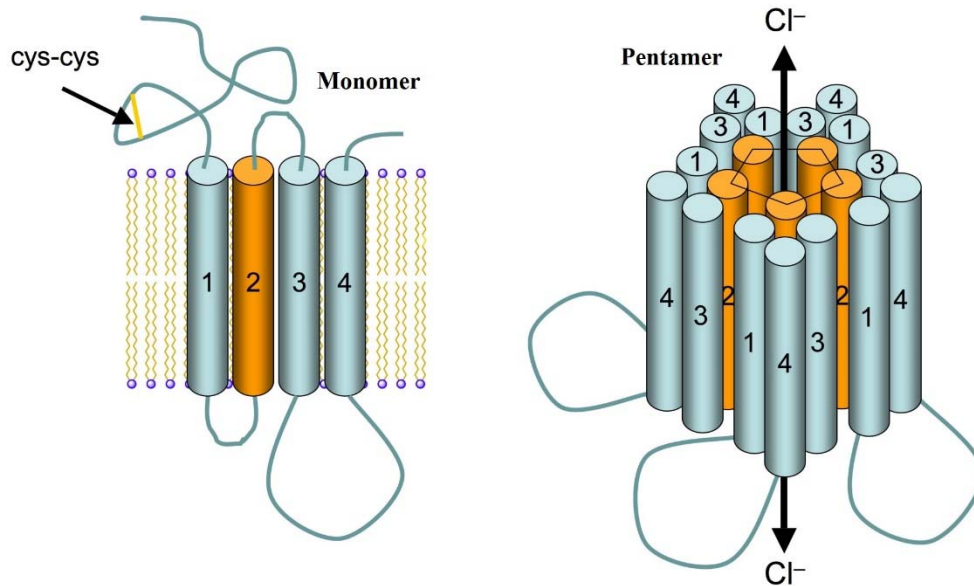
The GABA$_A$ receptor has numerous binding sites located at the synaptic cleft and also within the pore. Activation of the GABA$_A$ receptor complex can occur from the binding of a variety of compound classes at these various sites including β-carbolines[27], barbiturates[28], ethanol[29], and benzodiazepines[30], as well as pyrazoloquinolinones among others.[31-32] Located at the synaptic cleft of the abundant $\alpha_{1-6}\beta_{1-3}\gamma_2$ receptors, arranged αβαβγ clockwise when viewed from the extracellular region (Figure 8-4), are the GABA binding sites at the α-β+ interfaces; the benzodiazepine binding site (BZs) is found at the γ-α+ interface.[33-35] The more recently discovered CGS 9895 binding site is located at the β-α+ interface in which a number of pyrazoloquinolinones have been shown to bind to and activate the GABA$_A$ receptor.[36-37] In addition, neurosteroids[38], ethanol[39], and other compounds may also bind in the interior of the pore.

Figure 8-4: Binding sites on the GABA_A receptor.
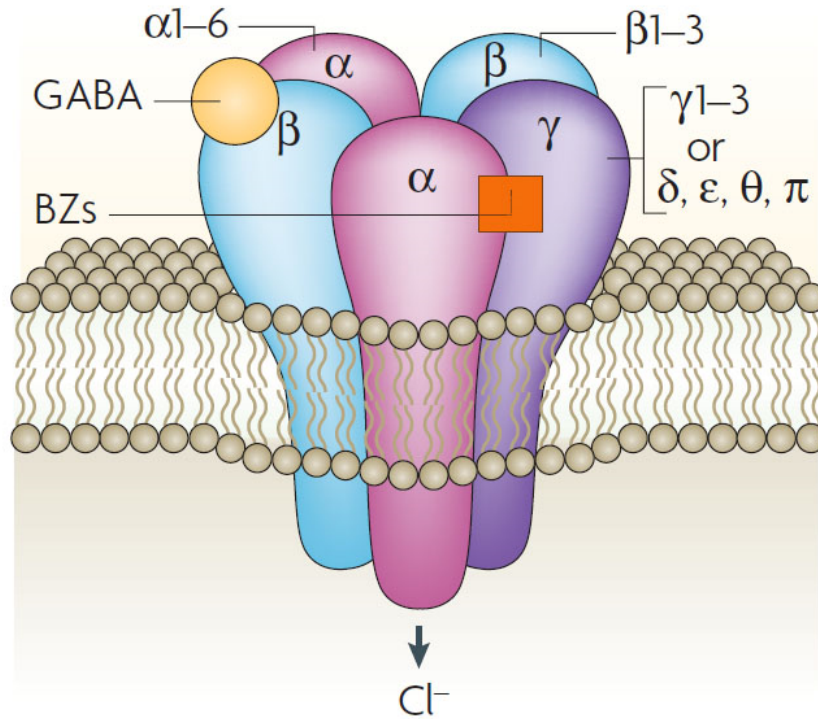
Figure 8-5: Structures of diazepam and flumazenil.

Diazepam   Flumazenil
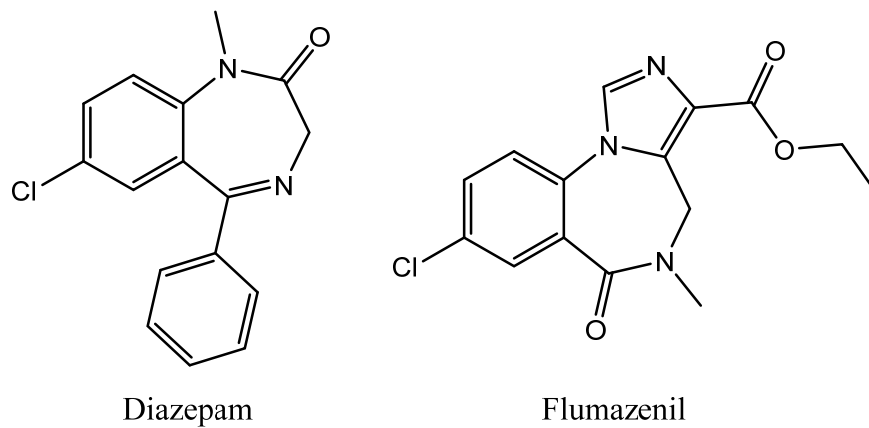
Traditional benzodiazepines such as diazepam (Figure 8-5) which contain the pendent phenyl C ring, tend to bind non-selectively to the $\alpha_{1-3,5}\beta_{1-3}\gamma_2$ GABA_A receptors at the BZ site.[34, 40]

This class of compounds has been frequently prescribed as a medication for various CNS disorders such as anxiety and convulsions for over half a century.[41-42] They offer many advantages in drug therapy since they are rapidly absorbed though the gastrointestinal tract when taken orally and generally reach maximum blood concentrations within a couple hours of ingestion.[43-44] In addition, benzodiazepines are able to readily cross the blood-brain-barrier and be distributed throughout the brain.[45] When used as an emergency anticonvulsant, certain benzodiazepines can reach levels of detection within five minutes, but tolerance to this effect develops very rapidly in humans.[46] Other advantages of benzodiazepines include minimal liver microsomal enzyme inhibition which can cause drug-drug interactions[47], and they lack serious toxicity concerns even at high concentrations[48]. Unfortunately, there are also a number of adverse effects that can be produced by benzodiazepines such as drowsiness, sedation, ataxia, muscle-relaxation, amnesia, dependence, withdrawal issues, as well as tolerance to the anticonvulsant effects limiting their use for chronic treatment of convulsions.[49-51] These adverse effects are a result of benzodiazepines which are non-selective and activate multiple GABA$_A$ receptor subtypes simultaneously.

The pharmacological response to the activation of the $\alpha_{1-6}\beta_{1-3}\gamma_2$-GABA$_A$ receptors is dependent on the composition of the subunits that form the receptor (Table 8-1), where the α subunit in regard to Bz modulation is the major determining factor.[52] Over the past decades, studies using GABA$_A$ receptor single-point knock-in mice have been able to identify the actions of the different α subunits located within the brain by rendering particular benzodiazepine receptors insensitive to modulation with benzodiazepines.[23] These studies have been done by replacing a single histidine amino acid of the α subunit with an arginine. In both α_1 and α_2

subunits, the replacement is a H101R, while the replacements are H126R for α_3 and H105R in α_5 subunits.[53]

Table 8-1: Subtype selective effects of GABA$_A$ receptors.

Subtype	Associated Effect
α_1	Sedation, anterograde amnesia, some anticonvulsant action, ataxia, tolerance, and addiction.
α_2	Anxiolytic, perhaps hypnotic (EEG), maybe some muscle relaxation at higher doses, antihyperalgesic effects.
α_3	Some anxiolytic action, anticonvulsant action at higher doses. Maybe some muscle relaxation at higher doses.
α_4	Diazepam-insensitive (DI) site.
α_5	Cognition, temporal and spatial memory (Maybe memory component of anxiety).
α_6	Diazepam-insensitive (DI) site.

GABA$_A$ receptors which contain the α_1 subunit have been shown to mediate anterograde amnesia, motor impairment, and sedative effects, as well as part of the anticonvulsant action.[21] The anxiolytic action and some anticonvulsant activity stems from the activation of the α_2 subunits[54], while contribution to the anxiolytic-like effects and possible muscle relaxation at higher receptor occupancy appear to involve agonist action at the α_3 subunit.[55] Memory and spatial learning, as well as other cognitive effects, are influenced by the α_5 subtype.[56] Antihyperalgesic effects also stem from the α_2 subunit[57]; however, the site of this action appears to occur, at least with Hz-166, from activation of the GABA$_A$ receptors that are located primarily in the spinal cord as opposed to the brain.[57] A recent triple-point knock-in mutation study was

carried out and was shown to confirm that the specific α_2 subunit was the source of the antihyperalgesic response.[58]

The abundance of specific α subtype of the $\alpha_{1-6}\beta_{2/3}\gamma_2$ GABA$_A$ receptors are not equally distributed throughout the brain. Many studies have reported using [3H]-muscimol binding studies that are followed by immunoprecipitation with specific subunit antibodies in rat brains[59], immunohistochemistry[60], or by monitoring the total decrease in GABA$_A$ receptors after knockout studies in mice[61]. The α_1 subtype is the most prevalent throughout the brain and accounts for 40-50% of the α GABA$_A$ subtypes.[62] The α_2 and α_3 subtype assemblies account for up to, but not more than, 35% and 14%, respectively and are found in the mesolimbic system.[63] Receptors containing the α_5 subtype are the least abundant of the diazepam-sensitive GABA$_A$ receptors accounting for about 5% of all α subtypes within the brain, the majority of which are located in the hippocampus.[64]

In addition to the diazepam-sensitive GABA$_A$ receptor subtypes ($\alpha_{1-3,5}\beta_{2/3}\gamma_2$), there are also two diazepam-insensitive sites in which the binding pocket cannot accommodate the pendent phenyl (C) ring of various benzodiazepines. Benzodiazepines, such as flumazenil (Figure 8-5), which lack the pendent C ring can bind to both the diazepam-sensitive and diazepam-insensitive GABA$_A$ receptor binding sites. These two DI subtypes are the α_4 and α_6 subtypes and they account for a smaller percentage of functional GABA$_A$ receptors than the diazepam-sensitive subtypes. The α_4 subtype makes up 6% of all subtypes[65] and the α_6 subtype is found primarily in the cerebellum and the olfactory bulb.[66] Although these have been studied, the pharmacological effects that are affected by benzodiazepines at these two subtypes are still relatively unknown.[67] GABA$_A$ receptors are also found in the peripheral nervous system. A major effect of GABA here involves tonic inhibition,[68] but potential uses of benzodiazepines

targeting GABA$_A$ receptors in the peripheral nervous system have been noted within the lungs, intestines, and other areas of the body.[69-70]

The diazepam-insensitive sites are of particular interest due to the lack of data on the role they play *in vivo*. The work herein targets the α6 diazepam-insensitive site and aims to determine the biological response of the first α6 selective compounds discovered, compounds originally prepared at Milwaukee as potential selective GABA$_A$ receptor agents.[71] These compounds are related to the earlier discussed pyrazoloquinoline 'CGS' compounds discovered in the 1970's and 1980's that were found to elicit similar effects to other GABA$_A$ receptor ligands. The CGS 8216 and CGS 9896 ligands (Figure 8-6) represent some of the most investigated pyrazoloquinolines of the CGS series.[72] Both were found to elicit long-lived anxiolytic effects with less sedation when compared to traditional benzodiazepines. The radioligand binding assays on CGS 8216 confirm potent binding at all receptor subtypes α$_{1-6}$ß$_3$γ$_2$, with the least potent K$_i$ found to be at the α$_6$ receptor subtype (Table 8-2). CGS 9896 was found to also bind strongly to brain membranes, with an average K$_i$ of 0.5 nM (Table 8-1).

Figure 8-6: Structures of CGS 8216 and CGS 9896.

CGS 8216   CGS 9896
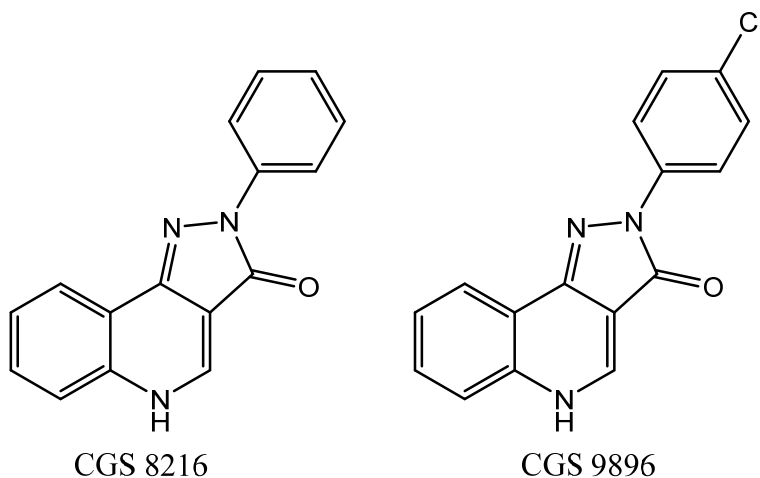
Table 8-2: Binding profiles of CGS compounds.

			Ki (nM)			
Compound	α1ß3γ2	α2ß3γ2	α3ß3γ2	α4ß3γ2	α5ß3γ2	α6ß3γ2
CGS 8216	0.05	0.08	0.12	35	0.25	17
CGS 9896			0.5 ± 0.1 (brain membranes)			

Receptor binding, however, does not necessarily cause an allosteric change in the binding site necessary for activation of the chloride ion channel. Based on *in vivo* data in mice, it was determined that CGS 8216 exhibited the properties of a weak inverse agonist while CGS 9896 exhibited properties of a mixed agonist/antagonist, very different activities for compounds that clearly bound well to most receptor subtypes. Further *in vitro* testing via frog oocytes revealed that CGS 8216 activated the ion channel weakly across the spectrum of α_{1-5}ß3γ2 subtypes while it was somewhat selective for the α_6ß3γ2 subtype (Figure 8-7). CGS 9896, on the other hand, exhibited a lack of selectivity, which presumably leads to its classification as a mixed agonist/antagonist *in vivo* (Figure 8-7). The *in vivo* properties observed for both CGS 8216 and CGS 9896 could also be mediated through other receptor subtypes that have not yet been tested.

Figure 8-7: Alpha selectivity of CGS 8216 and CGS 9896 at α_{1-6}ß3γ2 GABA$_A$ receptors.

CGS 8216   CGS 9896
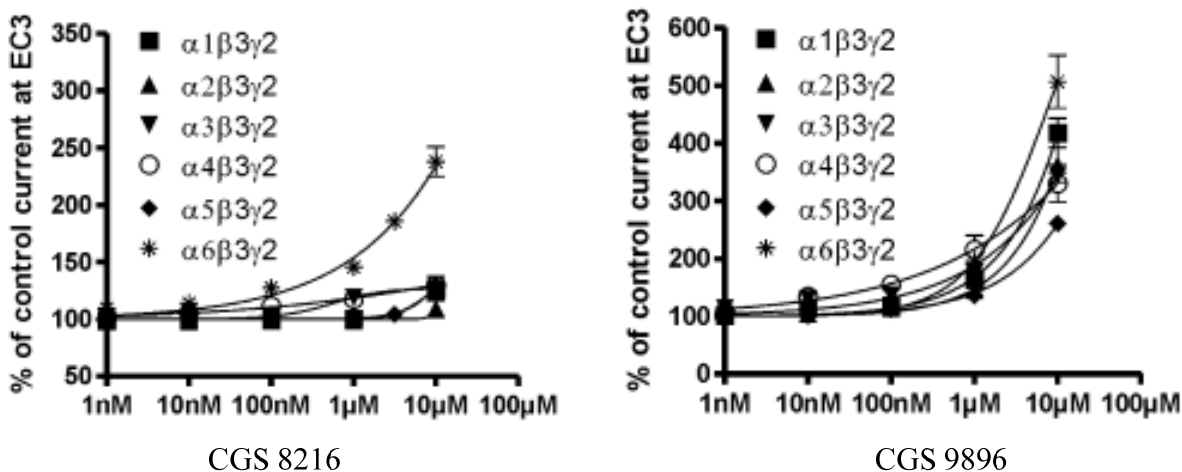
The pharmacological response due to the modulation of ligands is dependent not only on which α receptor subtype the ligand binds to, but also the effect it has on the concentration influx of chloride ions through the receptor pore.[21] Under normal physiological conditions, a neuron may become hyperpolarized leading to an action potential and a signal is fired (Figure 8-8). As GABA binds to the GABA$_A$ receptor and causes a conformational change in the receptor, chloride ions are allowed to travel through the pore. These chloride ions flow into the postsynaptic area and lower the membrane potential, which decreases the likelihood of an action potential being reached and inhibits neuronal signaling. Benzodiazepines and other allosteric ligands can influence the chloride ion flux in three separate ways; however, GABA must also be present since these ligands alone cannot induce a channel opening themselves.[73] A positive allosteric modulator (PAM) alters the conformation of the GABA$_A$ receptor which results in an increase of chloride ion flux, further inhibiting neuronal firing. PAMs are different from orthosteric agonists such as muscimol, since agonists bind to the GABA binding site while all allosteric modulators bind at a separate site.[74] Negative allosteric modulators (NAMs) are also termed "inverse agonists" because the influx of chloride ions is reduced, increasing the chance of the action potential being reached and firing.[75] The third class of ligands are null modulators, more commonly referred to as antagonists, which have no discernable effect on the influx of chloride ions. Instead, these antagonists generally have a strong binding affinity for the benzodiazepine receptor and limit the ability for other ligands to bind and influence the membrane potential.[37]

Figure 8-8: Membrane potential over time.
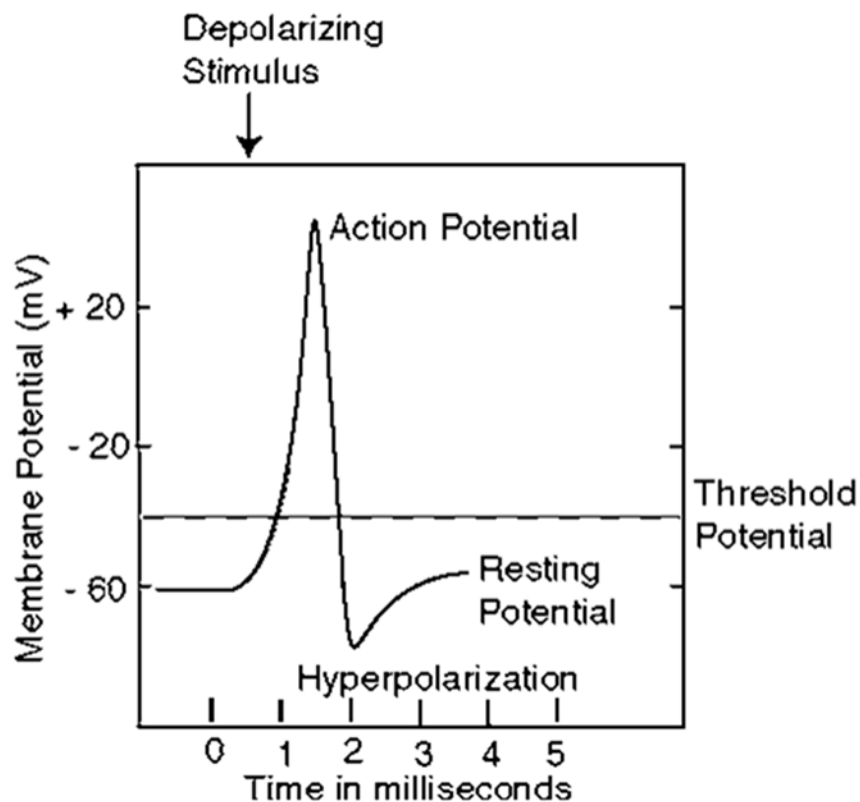
II.   ALPHA 6 Bz/GABA(A) POTENTIAL BIOLOGICAL ACTIVITY.

Prior to the synthesis and discovery of α_6 selective PAMs, which are to be discussed in the next chapter, determination of the biological response attributed to α_6 GABA$_A$ receptors was generally accomplished by gene knockout experiments in mice.[76] These gene-disruption methods leave mice with the inability to construct the α_6 polypeptide. Binding studies which involved [^{3}H]Ro15-4513 (Figure 8-9) revealed that the homozygous $\alpha6$ knockout mice still have many binding sites for benzodiazepines, however, the displacement via diazepam was markedly different in the homozygous $\alpha6$ knockout mice compared to wild-type (Figure 8-10).

Figure 8-9: Structure and binding of Ro15-4513 to BZ/GABA$_A$ receptors.

Ro15-4513

	Ki (nM)					
Compound	α1ß3γ2	α2ß3γ2	α3ß3γ2	α4ß3γ2	α5ß3γ2	α6ß3γ2
Ro15-4513	4.8±1.2	7.3±3.2	2.4±1.4	0.13±0.05	5.1±0.9	8.2±1.7

Examination of these binding data indicate that Ro15-4513 binds relatively strongly to all α$_{1-6}$ß$_3$γ$_2$ receptors, unlike diazepam which does not bind strongly to the diazepam-insensitive α$_4$ and α$_6$ sites.[77] Saturation with diazepam can therefore help distinguish the presence of diazepam-insensitive sites via displacement studies. Analysis of Figure 8-10 shows the displacement of Ro15-4513 by diazepam in both wild-type (+/+), heterozygous α6 knockout mice (+/-), and homozygous α$_6$ knockout mice. Row "a" is total binding of [3H]Ro15-4513, row "b" is displacement via diazepam, and row "c" is thionin staining.[76] Examination of the results show that in the homozygous knockout mice (-/-) Ro15-4513 was completely displaced by diazepam whereas in the wild-type (+/+) mice Ro15-4513 was displaced in most regions, but not in the cerebral granule cell layer. The cerebral granule layer is thought to contain the highest concentration of α6 receptors. It is important to note, however, that data collected from the homozygous α6 knockout mice suggested that the total number of GABA$_A$ receptors was not significantly different from wild-type, which suggested that other GABA$_A$ subunits substitute for

the missing α_6 subunits via compensatory effects. This up-regulation of other subunits could cause changes in the behavior of the mice that renders the genetic study incomplete.

Figure 8-10: [3H]Ro15-4513 binding and displacement with diazepam.
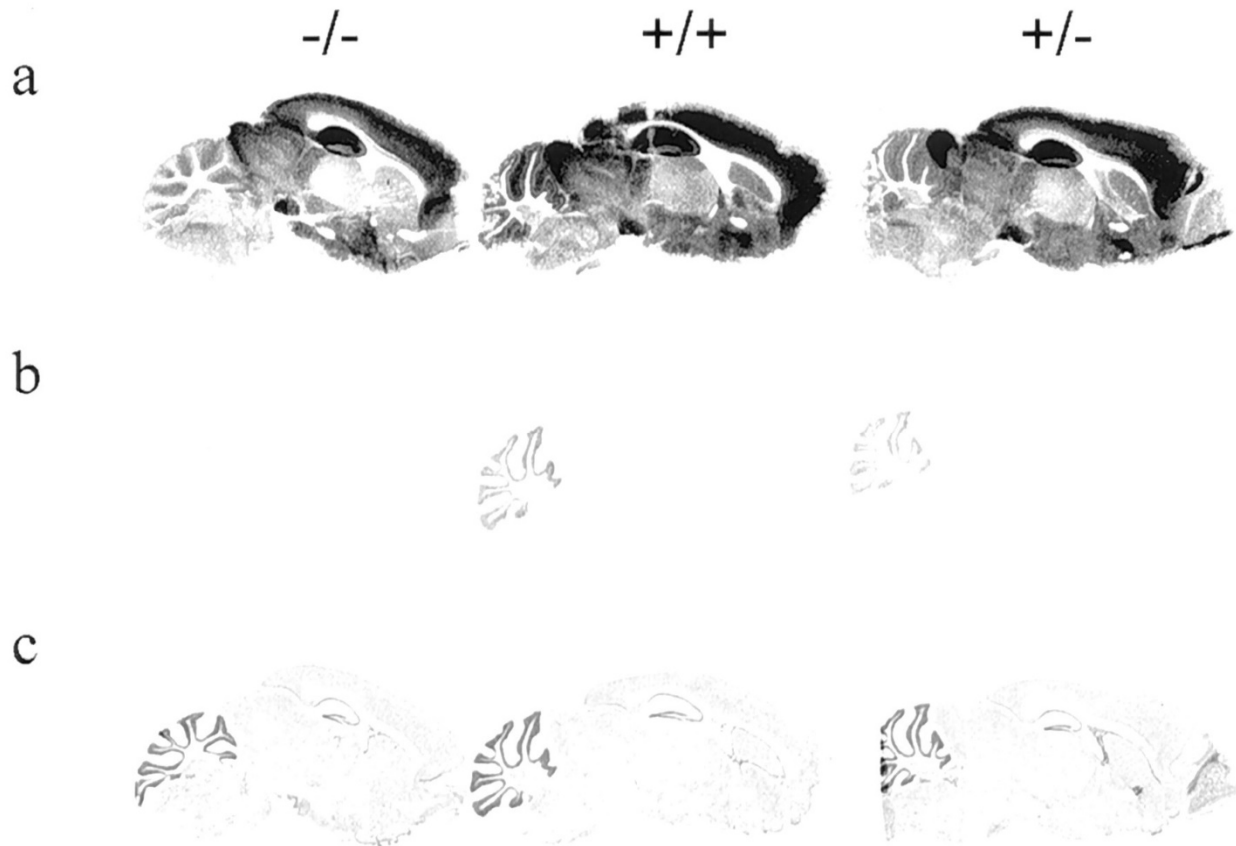
Many of these studies have focused on ethanol tolerance in mice, with mixed results.[78] Some other studies have shown an increased level of ataxia and impairment from diazepam in the α_6 knockout mice.[79]

Identification of mutations in the α_6 gene in humans has also led to possible disease treatments for childhood absence epilepsy[80], psychological stress[81], alcoholism[82], and obesity[83]. These mutations effectively cause a down-regulation in the number of α_6 receptors in the CNS,

and the wide variety of diseases associated with these mutations suggests that the α_6 site may be an important target for future drug discovery research.[84]

III.   CONCLUSION.

GABA$_A$ receptors are a diverse set of receptors located in the CNS that mediate a number of different biological processes. The pentameric transmembrane receptor consists of 5 subunits arranged around a central pore. The pore opening and closing mediates the flow of chloride anions into and out of the cells, causing an inhibitory response. The bulk of these receptors are comprised of $\alpha_{1-6}\text{ß}_3\gamma_2$ subunits, and each α unit effects distinct biological effects. This work is focused on the α_6 receptor, a so-called diazepam-insensitive receptor subclass that has only been studied by *in vivo* knockout experiments in mice or population studies that have identified mutations in the α_6 gene.

Novel pyrazoloquinolines ligands similar to the CGS series have been discovered that, unlike the prior CGS series, are subtype selective for the $\alpha_6\text{ß}_3\gamma_2$ receptor. These ligands have proven that the α_6 subtype, much like the other GABA$_A$ subtypes, has a diverse and interesting biological profile. The SAR and biological effects of these ligands will be presented in the next chapter.

CHAPTER NINE

DESIGN, SYNTHESIS, AND SCALE-UP OF NOVEL PYRAZOLOQUINOLINONES: α6 SUBTYPE SELECTIVE POSITIVE ALLOSTERIC MODULATORS

I.   INTRODUCTION TO PYRAZOLOQUINOLINONES

Drug discovery efforts into the CGS series of compounds led to a variety of pyrazoloquinilones synthesized in an attempt to discover new and interesting subtype selective ligands. Many of these compounds bound to BzR with extremely high affinity, some of which with greater affinity then diazepam such as the previously discussed CGS 9896. After this discovery, a wide range of pyrazoloquinolinones have been designed and synthesized to correlate the substitution pattern and structure with the intrinsic activity of a ligand. Thienyl-pyrazoloquinolinone (**S-135**, Figure 9-1) was reported by Takada and Shindo as a potent and orally active inverse agonist at BzR, however the related regioisomers **S1** and **S2** (Figure 9-1) demonstrated weak inverse agonist and agonist activity, respectively. The agonistic activity of **S2** (R = methyl) was also less potent then CGS 9896. A more thorough structure-activity relationship (SAR) study into introduction of alkyl substituents of increasing size onto the parent thienyl-pyrazoloquinolinone nucleus indicated that activity varied from inverse agonist, to antagonist/null modulator, to agonist depending on the size of the alkyl group.

Figure 9-1: Structure of S-135 and other related thienyl-pyrazoloquinolinones.

S-135	**S1**	**S2**
potent inverse agonist	weak inverse agonist	agonist
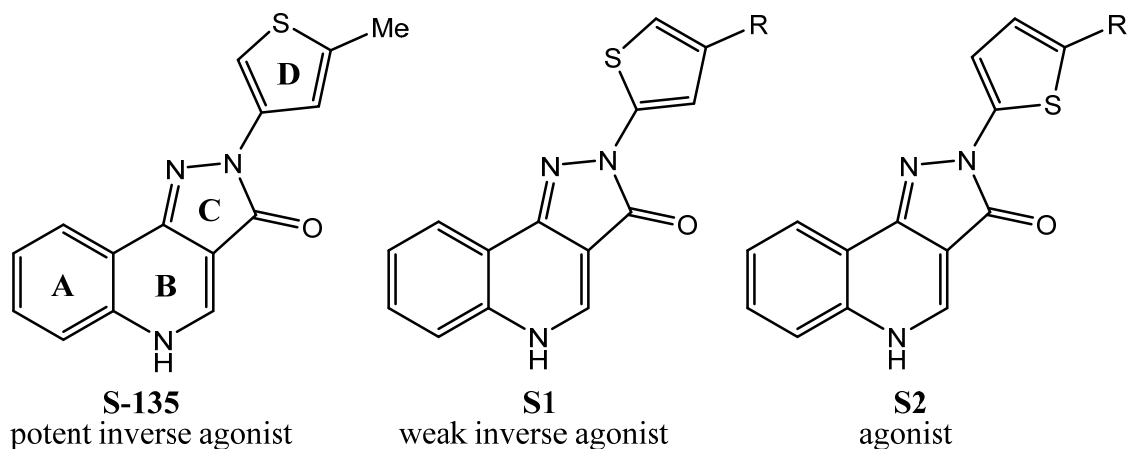
Although many of these original pyrazoloquinolinone ligands were active *in vivo* as anxiolytic/anticonvulsant agents and were well absorbed and crossed the blood-brain-barrier, the future for this series as clinical agents was limited due to very poor water solubility. However, the unique topology of the pyrazoloquinolinone core structure accompanied with potent *in vitro* affinity made them an excellent template for further refinement of pharmacophore models for the GABA$_A$ receptor. Depicted in Figure 9-2 is CGS 9896 (dotted line) and diazepam (thick line) in a unified pharmacophore model based on the binding affinity of numerous other ligands. Brackets (i.e. [A]) represent each ring system (see Figure 9-1) for clarity. Sites H1 and H2 represent hydrogen bond donor sites on the receptor protein complex while A2 represents a hydrogen bond acceptor site necessary for potent inverse activity *in vivo*. L1, L2, L3 and LDi are four lipophilic regions in the binding pharmacophore. Descriptors S1, S2, and S3 are regions of negative steric repulsion with the protein.

Figure 9-2: The Milwaukee-based unified pharmacophore model.
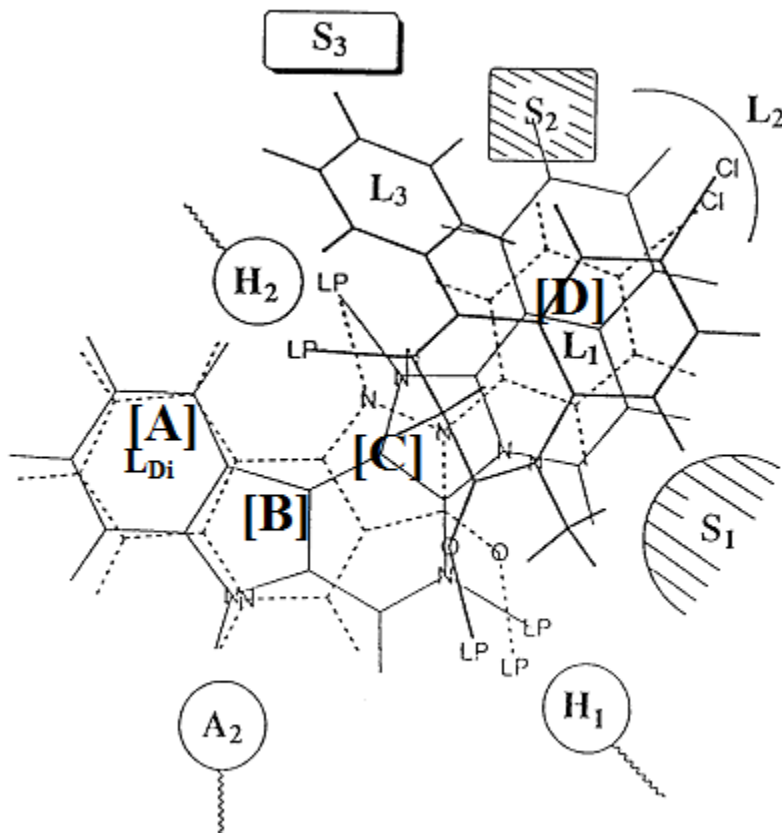
Based on this fit, the anchor points A2, H1, H2, and L1 could be employed to estimate the distance between the various receptor descriptors. The pyrazoloquinilinones fit into this model almost perfectly, compared to other ligands. Moreover, SAR studies aimed at modifying the hydrogen bond donor characteristics of the NH in ring B gave compounds with 3 orders of magnitude less binding affinity, reinforcing the idea that the A2 site is a hydrogen bond acceptor. The H1 site, thought to be hydrogen bond donor site, was also investigated by an SAR by replacing the carbonyl group in ring C with other non-hydrogen bond accepting functional groups. This also resulted in a loss of binding affinity. This strong *in silico* based evidence
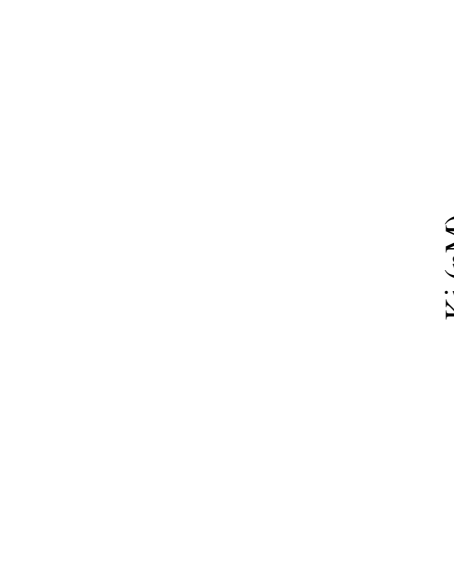
prompted further SAR studies into novel pyrazoloquinilinones via use of the unified

pharmacophore/receptor model.[68]

Figure 9-3: Schematic representation of pyrazoloquinolinones in the receptor model.

L_1 is 0.5 Å above the plane of the pyrazoloquinoline ring system.

H_2 is 0.1 Å below the plane of the pyrazoloquinoline ring system

H_1 is on the plane of the pyrazoloquinoline ring system

A_2 is on the plane of the pyrazoloquinoline ring system

a = 6.735Å; b = 9.980Å; c = 5.860Å
d = 5.734Å; e = 5.218Å; f = 7.317Å
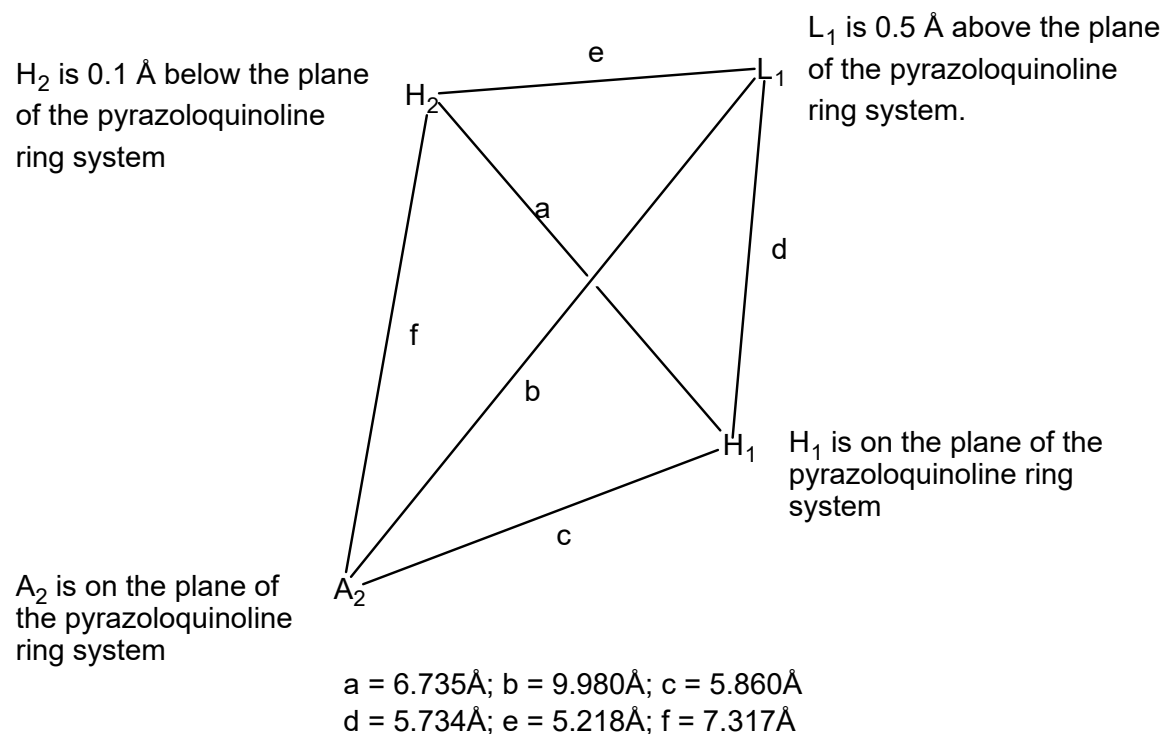
Based on the strong fit of the pyrazoloquinilinone backbone to the A2, H1, H2, and L1

receptor descriptors, synthesis of ligands that probe the LDi and L2 regions were explored. A

number of ligands were prepared with different substituents on both ring A and ring D.

Table 9-1: Binding affinity of some novel pyrazoloquinilinones.

	Compound	R8	R7	R6	R4'	Ki (nM)					
						α1β3γ2	α2β3γ2	α3β3γ2	α4β3γ2	α5β3γ2	α6β3γ2
1	CGS 8216	H	H	H	H	0.05	0.08	0.12	35	0.25	17
2	CGS 9896	H	H	H	Cl		0.5 ± 0.1 (brain membranes)				
3	PWZ-009A1	H	OMe	H	H	1.3	1.3	1.3	ND	0.8	2
4	Xhe-II-087c	H	H	tBu	Br	7000	7000	2000	ND	4000	7000
5	Xhe-III-006c	H	Br	H	Br	34	44	29	210	23	319
6	PWZ-II-029	H	OMe	H	OMe	0.3	ND	0.8	ND	0.5	10
7	Xhe-II-094	tBu	H	H	C≡CSiMe3	329	1098	1156	>1000	2462	>3000
8	PWZ-007A	OMe	H	H	H	0.1	0.1	0.1	ND	0.2	>10
9	Xhe-III-24	tBu	H	H	F	0.25	ND	8	ND	10	328
10	Xhe-II-17	tBu	H	H	C≡CH	3.3	10	7	258	17	294
11	PZ-II-028	Cl	H	H	OMe	0.2	ND	0.2	ND	0.3	1.9
12	Xhe-II-019	tBu	H	H	C≡C-C≡CtBu	273	428	762	ND	1464	>3000

Depicted in Table 9-1 are a number of ligands which bound strongly to most receptor subtypes, however selective binding was not observed. As previously discussed, binding affinity data only accesses whether or not a ligand binds to a receptor, not the effect that the ligand has on the receptor. Oocyte data, however, can distinguish between positive allosteric modulators, negative allosteric modulators (inverse agonists), and antagonists/null modulators. The oocyte graphs for CGS 8216 and CGS 9896 are found in Chapter 8, the graphs for the rest of the compounds listed in Table 9-1 can be found below in Figure 9-4.

Figure 9-4: Oocyte graphs for compounds listed in Table 9-1.
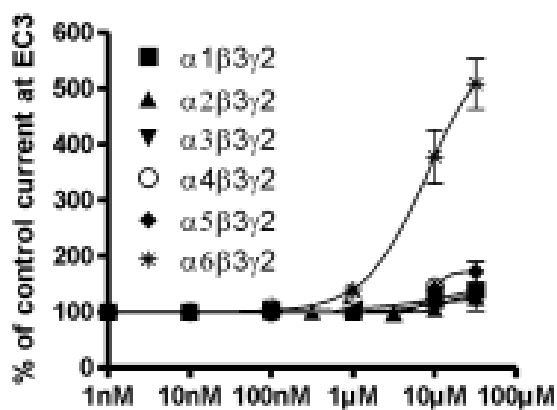
Compound 3 (PWZ-009A1)
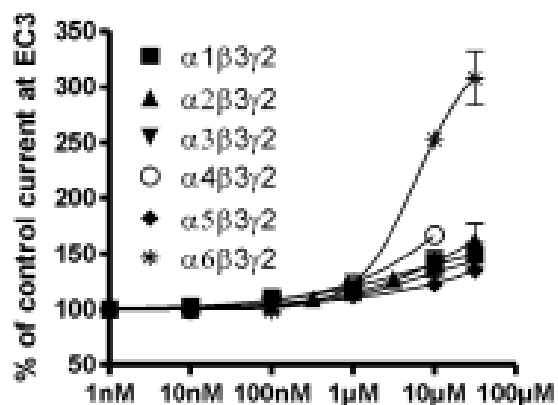
Compound 4 (Xhe-II-087c
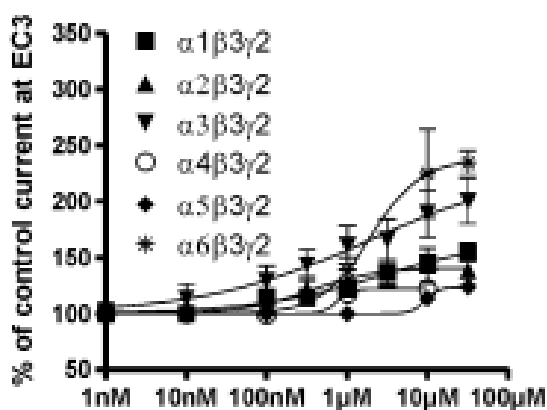
Compound 5 (Xhe-III-006c)

Compound 6 (PWZ-II-029)

Compound 7 (Xhe-II-094)

Compound 8 (PWZ-007A)

Compound 9 (Xhe-III-24)

Compound 10 (Xhe-II-17)

Compound 11 (PZ-II-028)
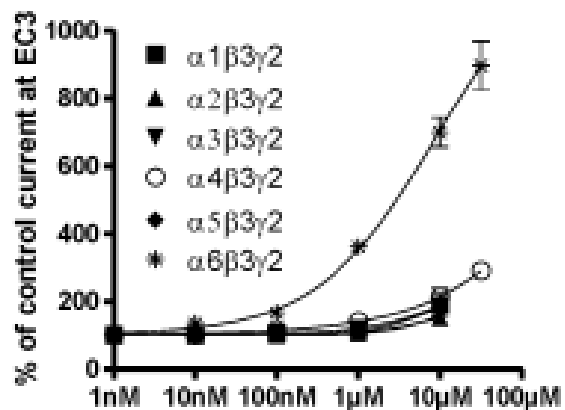
Compound 12 (Xhe-II-019)
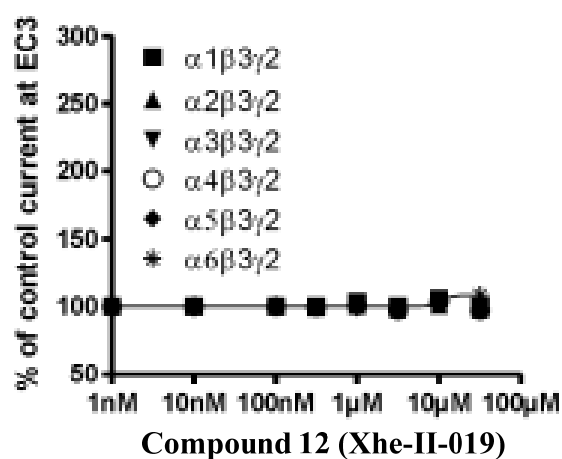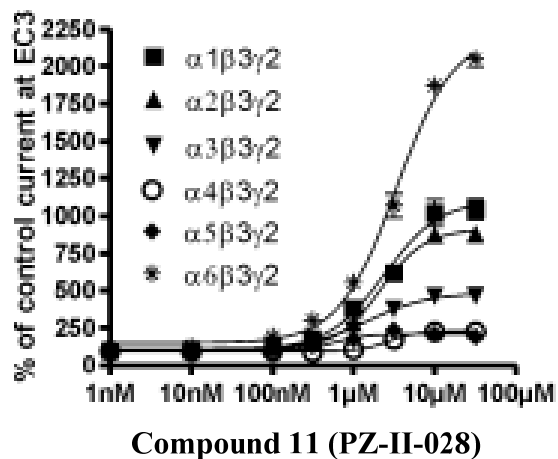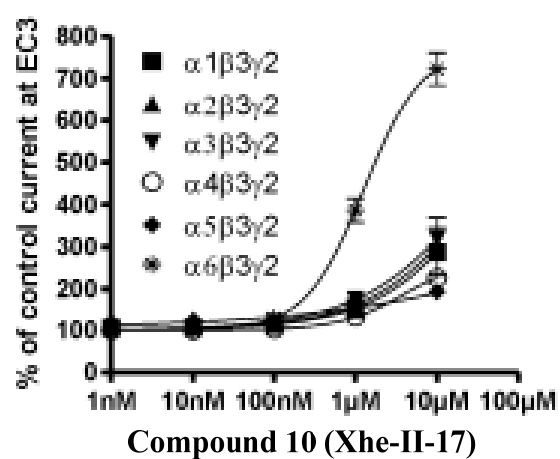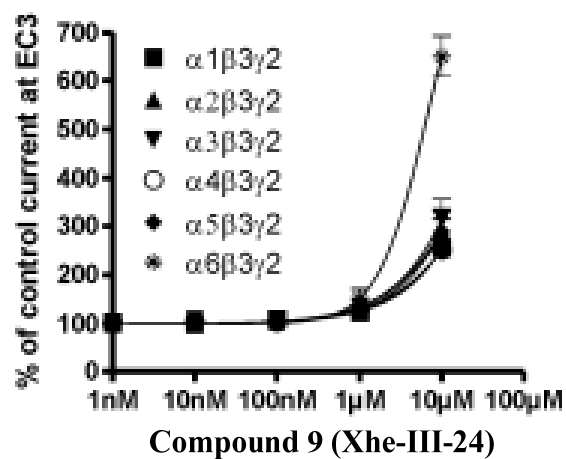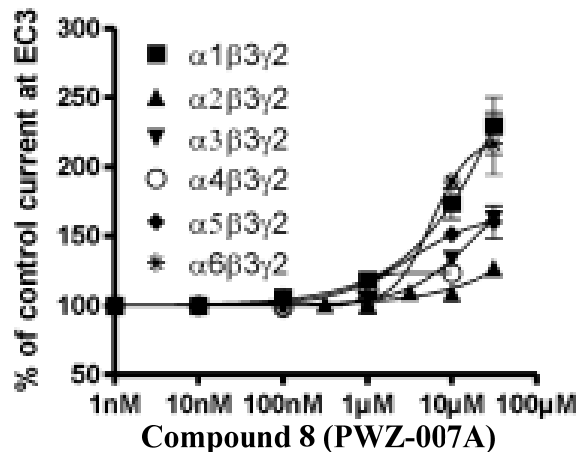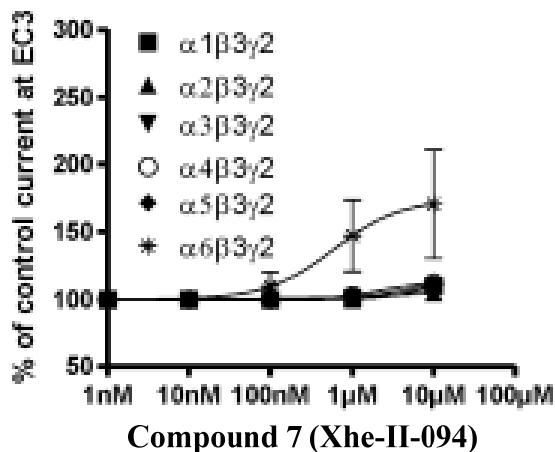
Based on examination of these oocyte graphs, a variety of compounds showed some

selectivity for α6 receptors including compounds 3, 4, 6, 7, 9, 10, and 11. However, in many

cases these activities were either weak or only applicable at high concentrations. In the case of

Compound 6, however, this α6 selectivity was potent even down to the 100nM concentration,

clearly the most selective α6 ligand discovered so far. Importantly, 100-200nM was felt to be a

pharmacologically relevant concentration. **Compound 11** was also of interest, although it was

clearly not as selective at α6 at high concentrations, the strong agonist effect on α6 receptors at or

around druggable ranges (100nM – 1 μM) also made it an interesting candidate for future work.

II.   SYNTHESIS OF PYRAZOLOQUINOLINONES

1.   Synthesis and scale-up of Compound 6 for pharmaceutical evaluation.

The pyrazoloquinilinones discussed thus far were all synthesized in the past via the same

method starting with the use of substituted amines followed later by heating with substituted aryl

hydrazines. This method is described in Scheme 9-1 below representing the synthesis of

Compound 6.

Scheme 9-1: Original synthesis of Compound 6.
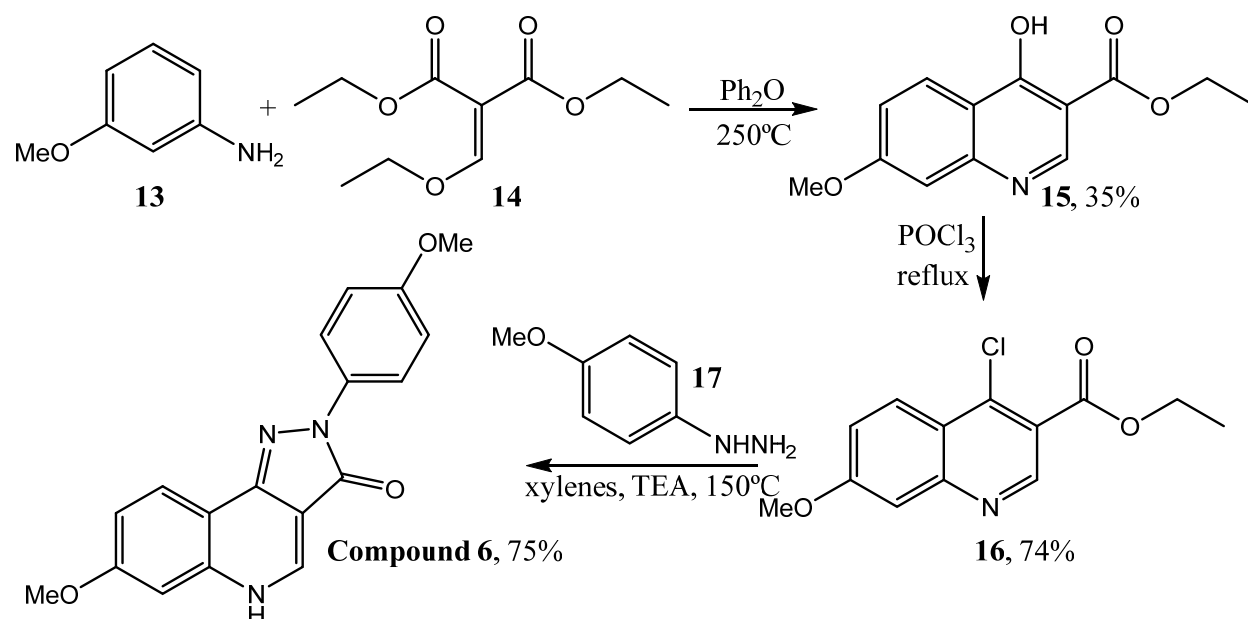
Since both **Compound 6** and **Compound 11** were of interest due to their α₆ agonist subtype selective activity, scale-up to multi-gram quantities for more extensive *in vivo* biological screening was necessary. The original synthesis, however, suffered from low yields that made scale-up difficult. Several strategies were employed to increase the yield to a degree at which it was possible to synthesize multi-gram quantities of ligands **6** and **11** in a timely fashion.

The first process improvement, depicted in Scheme 9-2, centered around simply isolating the intermediate product **18** in the first step. This was accomplished by heating amine **13** and diester **14** at 120 ºC under vacuum to afford **18** in nearly stoichiometric amounts. After the reaction was complete, the mixture was cooled, which led to the precipitation of the product. This was followed by slurrying the solids in hexanes to permit filtration of the intermediate **18**.

Scheme 9-2: Process improvement in the synthesis of Compound 6 – first step.
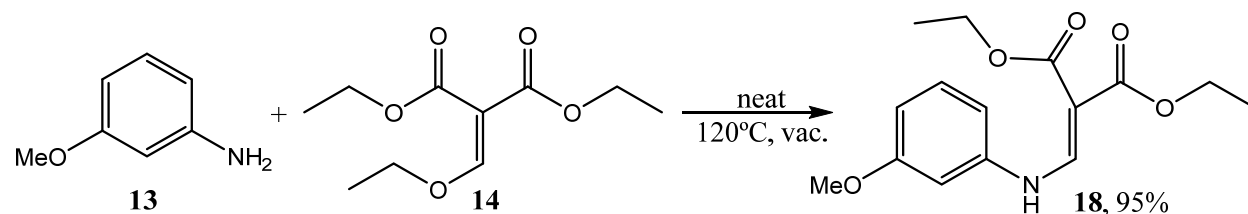
The intermediate **18** was then slurried in diphenyl ether and heated to 250 ºC with a small amount of 4-tert-butylcatechol (4TBC) added as a potential antioxidant, which seemed to increase the overall yields for this step (Scheme 9-3). The 4TBC also inhibits polymerization, which may also play a role at such high temperatures.

Scheme 9-3: Process improvements – second step.
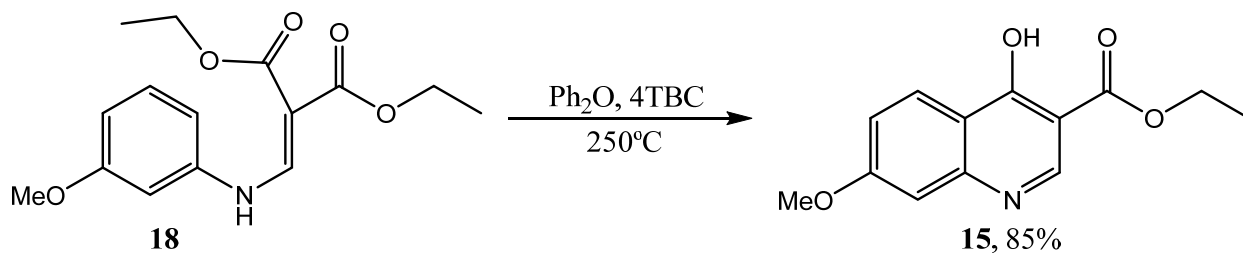
Compound **15** was found to be incredibly insoluble in most solvents and was therefore

used as is without further purification. The original procedure involved heating in neat POCl$_3$

which generally led to excellent yields, however on a larger scale the removal of POCl$_3$ was less

practical and it was found that similarly excellent yields were obtained when using 2 equivalents

of POCl$_3$ in toluene (Scheme 9-4). In this case, the chlorinated product **16**, was simply isolated

by removal of toluene after the reaction was complete. Further purification could be

accomplished by column chromatography or crystallization from EtOAc/hexanes if necessary;

however, in general the product was pure enough at this stage to continue to the next step.

Scheme 9-4: Process improvements – third step.
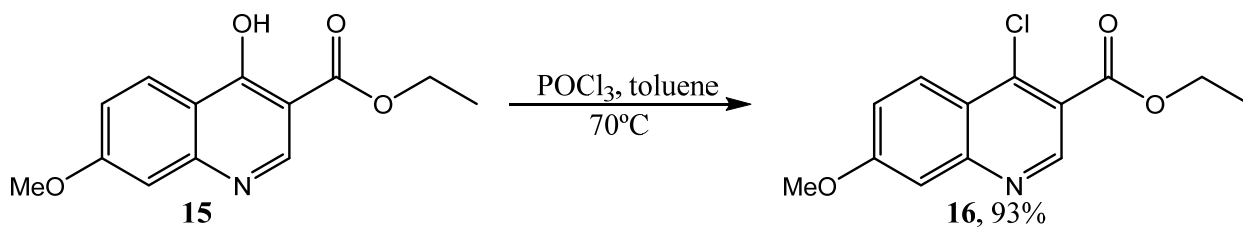
In the original synthesis free-base phenyl hydrazines were used to form the 5-member

heterocyclic ring (Scheme 9-1). While this worked well for many new analogs on small-scale,

on scale-up low yields were observed and suspected to be due to decomposition of the phenyl

hydrazine prior to conversion to the product. Many phenylhydrazines, including **17**, are more

readily purchased as the hydrochloride salts which are far more stable at room temperature. It was found that using the hydrochloride salt and generating the free-base *in situ* by the addition of excess triethylamine (TEA) gave high yields of the final target ligand **Compound 6** (Scheme 9-5). Problems associated with this step, however, included the production of 2 equivalents of triethylamine hydrochloride which could be difficult to fully remove from the final product.

Scheme 9-5: Process improvements – final step.
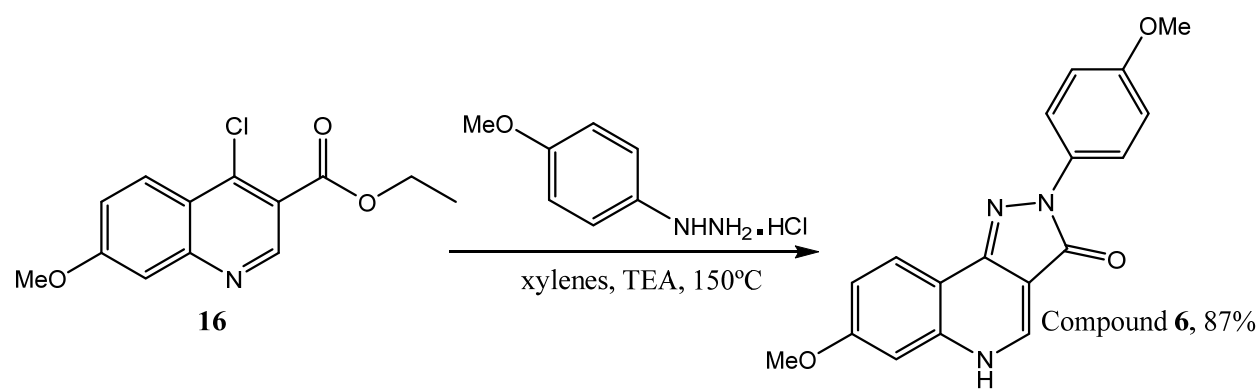
Removal of triethylamine hydrochloride was generally accomplished via an aqueous crystallization method. The **Compound 6** was slurried and heated in ethanol (1g **Compound 6** /10mL EtOH) and water was slowly titrated into the slurry at reflux until a clear solution was obtained (generally 10-15% water by volume). The solution was then cooled to room temperature and microcrystals began to form. At room temperature the volume was doubled by addition of water, the slurry cooled to 0 ºC, and filtered. In most cases this removed all traces of triethylamine hydrochloride. In the case of **Compound 11**, purification by dissolution in DMSO and precipitation with water, however, was sometimes necessary to remove trace amounts of triethylamine hydrochloride.

These improvements permitted the efficient scale-up of both **Compound 6** and **Compound 11**, necessary for synthesis of sufficient quantities for *in vivo* experiments to help

elucidate the role α_6 subtypes play in the central nervous system. In total, about 25 grams of both **Compound 6** and **Compound 11** were prepared via these methods.

2. Design and synthesis of new analogs.

This new process permitted a more efficient synthesis of a number of new ligands. These new ligands were designed to enhance potency, enhance metabolic stability, and/or increase water solubility by the addition of new functional groups to the ring A and/or ring D portions. Earlier SAR work had shown the core ring B/C functionalities were necessary for potent binding to the BZ receptor and thus were kept constant for this new SAR. As previously discussed, based on the pharmacophore receptor model it seems as though functionalities in ring A and ring D protrude into a lipophilic pocket that is, in general, more accepting of a variety of functionalities. The ligands synthesized in this work are detailed in Table 9-2.

Table 9-2: New analogs synthesized for α_6 subtype selective activity.
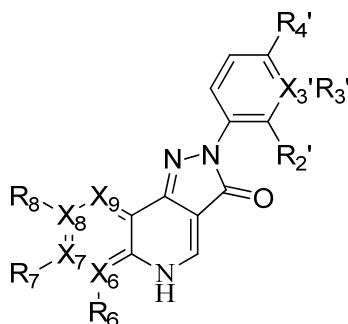
	Compound	R_8	R_7	R_6	X_9	X_8	X_7	X_6	R_4'	R_3'	R_2'	X_3'
	Compound 6	H	OCH3	H	C	C	C	C	OCH3	H	H	C
	Compound 11	Cl	H	H	C	C	C	C	OCH3	H	H	C
19	DK-I-56-1	H	OCH3	H	C	C	C	C	OCD3	H	H	C
20	RV-I-029	H	OCD3	H	C	C	C	C	OCH3	H	H	C
21	DK-I-60-3	H	OCD3	H	C	C	C	C	OCD3	H	H	C
22	DK-I-94-1	H	OCD3	H	C	C	C	C	H	OCD3	H	C
23	DK-I-88-1	H	OCH3	H	C	C	C	C	H	H	OCD3	C
24	DK-I-90-1	H	OCD3	H	C	C	C	C	H	H	OCD3	C

25	CW-03-030	H	OCH3	H	C	N	C	C	OCH3	H	H	C
26	DK-II-13-1	H	OCH3	H	C	C	C	C	OCH3	H	H	N
27	DK-I-86-1	H	OCD3	H	C	C	C	C	OCH3	H	H	N
28	DK-II-60-1	H	OCH3	H	C	C	C	C	OCD3	H	H	N
29	RV-I-37	H	OCD3	H	C	C	C	C	H	H	H	C
30	MM-I-03	Br	H	F	C	C	C	C	OCH3	H	H	C
31	DK-I-93-1	Cl	H	H	C	C	C	C	OCD3	H	H	C
32	LAU 159	Cl	H	H	C	C	C	C	H	OCH3	H	C
33	DK-I-59-1	Cl	H	H	C	C	C	C	H	OCD3	H	C
34	LAU 165	Cl	H	H	C	C	C	C	H	H	OCH3	C
35	DK-I-87-1	Cl	H	H	C	C	C	C	H	H	OCD3	C
36	DK-II-18-1	Cl	H	H	C	C	C	C	OCH3	H	H	N
37	DK-II-59-1	Cl	H	H	C	C	C	C	OCD3	H	H	N
38	LAU 463	H	Br	H	C	C	C	C	OCH3	H	H	C
39	DK-I-58-1	H	Br	H	C	C	C	C	OCD3	H	H	C
40	DK-I-92-1	H	Br	H	C	C	C	C	H	OCD3	H	C
41	DK-I-89-1	H	Br	H	C	C	C	C	H	H	OCD3	C
42	DK-II-48-1	H	Br	H	C	C	C	C	OCH3	H	H	N
43	DK-II-58-1	H	Br	H	C	C	C	C	OCD3	H	H	N
44	LAU 176	OCH3	H	H	C	C	C	C	OCH3	H	H	C
45	DK-I-95-3	OCD3	H	H	C	C	C	C	OCD3	H	H	C
46	DK-I-97-1	OCD3	H	H	C	C	C	C	H	OCD3	H	C
47	DK-98-1	OCD3	H	H	C	C	C	C	H	H	OCD3	C
48	RV-I-071	H	H	H	N	C	C	C	OCH3	H	H	H
49	MM-I-06	H	CF3	H	C	C	C	C	OCH3	H	H	C
50	MM-I-08	H	CF3	H	C	C	C	C	Cl	H	H	C
51	MM-I-09	H	CF3	H	C	C	C	C	NO2	H	H	C
52	MM-I-10	H	CF3	H	C	C	C	C	OCF3	H	H	C
53	MM-I-11	H	CF3	H	C	C	C	C	F	H	H	C
54	MM-I-12	H	CF3	H	C	C	C	C	H	OCH3	H	C
55	MM-I-13	Br	H	F	C	C	C	C	Cl	H	H	C
56	MM-I-18	Br	H	F	C	C	C	C	F	H	H	C
57	CW-02-073	H	OCH3	CH3	C	C	C	C	OCH3	H	H	C
58	CW-02-078	H	OCH3	CH3	C	C	C	C	H	H	H	C
59	CW-02-079	H	OCH3	CH3	C	C	C	C	OCF3	H	H	C
60	CW-02-082	H	OCH3	H	C	C	C	C	OCF3	H	H	C
61	CW-03-033	H	Cl	H	C	N	C	C	OCH3	H	H	C

Early efforts to enhance metabolic stability by introduction of a deuterated methoxy group were gratifyingly successful, a more in-depth analysis of this increased stability will be presented in Chapter 10. Ligands **19-24**, **27-29**, **31**, **33**, **35**, **37**, **39-41**, **43**, and **45-47** all contain a deuterated methoxy group in either ring A, ring D, or both rings. Examination of early *in vitro* experiments indicated that the deuterated methoxy analogs had the same/very similar agonistic activity as the parent methoxy analogs (OCH_3), as expected, thus many future analogs included deuterated methoxy groups to enhance metabolic stability.

Introduction of pyridine rings in either ring A or ring D was also explored in the hope of enhancing water solubility by synthesis of the hydrochloride salts, generally known to be more water soluble. The pyridine analogs were indeed much more soluble in water then the related parent ligand, however, as of this report synthesis of the hydrochloride salts has proven difficult. Early *in vitro* testing, to also be presented in Chapter 10, showed that ring A pyridines, at least in the case of compound **25**, do not retain potent α_6 activity/selectivity. Analogs substituted with ring D pyridine groups have been shown to retain activity and selectivity to α_6, which provides potentially new more soluble compounds for *in vivo* experimentation. In general, the pyridine analogs were found to ~20 times more soluble then the related analogs. This is thought to be exclusively due to the polarity of the pyridine compounds, generally with in silico clogP values much lower than their parent counterparts. For example, the clogP of **Compound 6** is 2.06 while the pyridine analog **26** has a clogP of 1.43, a significant difference on a logarithmic scale.

In general, CNS drugs tend to have high clogP values (~3). This high lipophilicity permits these drugs to more easily cross the blood-brain-barrier, thus lowering the clogP in the case of pyridine analogs may influence *in vivo* activity negatively, however the rather rigid nature of these small organic molecules may allow them to still easily cross the blood-brain-

barrier in lieu of lower lipophilicity, at which point the increased water solubility may prove useful.

A variety of other analogs were also prepared that probe different sites on ring A and ring D by substitution with typical medicinal chemistry techniques. These included altering the electronic nature of the functionalities and/or altering the size of different functionalities.

It should be noted that this study is still in its infancy and many of the compounds reported have not yet been tested yet in the *in vitro* oocyte assay to determine activity and selectivity at α_6 subtypes. All biological data compiled thus far will be presented in Chapter 10 for the compounds discussed above.

III.   CONCLUSION

In conclusion, ligands were discovered for the first time that are selectively active at α_6 subtype selective GABA(A) receptors. These receptors, up to this point, exhibited a relatively unknown function in the CNS that was only explored by experiments which involved mutations. The lead compounds, **Compound 6** and **Compound 11** were scaled up in sufficient quantities for extensive *in vivo* work and the important process improvements permitted for more efficient preparation of the lead compounds as well as new analogs.

New analogs were designed with the goal of enhancing potency, metabolic stability, and water solubility. The original CGS compounds (prepared by Ciba Geigy) discussed in Chapter 8 also had very poor water solubility, this was part of the reason they were never marketed as replacements for benzodiazepines. Work on the *in vitro* activity of many of these compounds is still on-going, however, a number of additional analogs with interesting *in vitro* properties have

been discovered since the initial discovery of **Compound 6** and **Compound 11** in Milwaukee. These new compounds will be discussed in the next chapter.

IV.   EXPERIMENTAL

Both ^{1}H and ^{13}C NMR spectra were recorded on a Bruker DPX-300 or DRX-500 instrument where noted. HRMS scans were recorded with a Shimadzu LCMS-IT-TOF mass spectrometer or similar instruments. Silica gel, unless otherwise noted, was employed for flash chromatography and TLC. Anhydrous solvents were employed unless otherwise noted.

Synthesis of Compounds by General Procedure A: A substituted aniline (1 mmol) was mixed thoroughly with DEEMM (1 mmol) and heated under argon to 120 ºC, at which point ethanol was distilled and removed from the reaction vessel. After heating the mixture for 2-3h and examination by TLC (30% EtOAc in hexanes) indicated complete consumption of the starting aniline, diphenyl ether was added and the reaction vessel was heated to 250 ºC for 2-3h. After complete cyclization to the desired quinoline the reaction vessel wass cooled to rt, hexanes were added, and the solid material which formed was filtered. No further purification was performed on this material. To the quinoline (1 mmol) was added POCl$_3$ (10 eq) and the mixture was stirred at an appropriate temperature to give the chlorinated quinoline. The chlorinated quinoline was further purified by flash column chromatography (20% EtOAc in hexanes, silica gel) generally to furnish a white/off-white solid. The chlorinated quinoline (1 mmol) was mixed with xylene, triethylamine (2.5 mmol), and an appropriate hydrazine hydrochloride salt (1.5 mmol) and heated to reflux for 3-24h. When the reaction was complete by TLC (10% MeOH in EtOAc) the mixture was cooled to 0 ºC, filtered, and the solid was washed with copious amounts of water. The solid was then washed with hexanes and allowed to dry. The solid was then recrystallized,

generally from a 5:1 mixture of EtOH:water, to furnish fluffy yellow/orange/red microcrystals of suitable purity for biological testing. Further purification can be accomplished by dissolving the solid in DMSO and slowly adding water and/or dissolving it in a basic solution (pH > 10) and slowly acidifying to pH < 6 to precipitate out the product.

Ethyl-4-hydroxy-7-methoxy (d3) quinolone-3-carboxylate. A mixture of 3-(methoxy-d3)aniline (1.26 g, 0.01 mol) and diethyl ethoxy methylenemalonate (DEMM, 4.32 g, 0.02 mol) in 50 mL of diphenyl ether were heated to 120°C for 1h. The ethanol which formed was distilled off. The solution was then heated to 245-250°C. The heating was continued for 4h. The contents were cooled to room temperature and hexane (50 mL) was added and the solids were collected by filtration. The compound was washed with ethyl acetate:hexane [(2:1), 50 mL] and dried. The yield was 2.37 g, 95%. Compound is off white and has very poor solubility. The compound was used as such for the next reaction: 1H NMR (300 MHz, DMSO) 12.123 (s, 1H), 8.489(s, 1H), 8.072-8.040(d, 1H, J= 9.6), 7.018-6.996(s, 2H), 4.239-4.170(q, 2H, J= 6.9), 1.301-1.254(t, 3H, J= 6.9), 3.876(s, 3H); 13C (75 MHz, DMSO) 165.29, 162.74, 145.27, 141.24, 127.99, 121.78, 114.63, 100.58, 59.95 and 14.80; HRMS m/z calculated for $C_{13}H_{11}D_3NO_4$ 251.1111 found 251.1110.

4-Chloro-7-methoxy (d3) quinolin-3-carboxylate. The starting Ethyl-4-hydroxy-7-methoxy (d3) quinolone-3-carboxylate (2.5 grams, 0.01 mol) was heated in neat $POCl_3$ at 80°C for 2h. The excess $POCl_3$ was distilled off under reduced pressure. The residue was dissolved in dry dichloromethane (25mL) and the solvent was distilled off under reduced pressure. The cycle was repeated 3 times to remove all the HCl and $POCl_3$. Due to unstable nature of this compound it was used without further purification (2.55 g, 95%): 1H NMR (500 MHz, $CDCl_3$) 9.19 (s, 1H), 8.32-8.30(d, 1H, J= 10.0), 7.48 (s, 1H), 7.36-7.34(t, 1H), 4.52-4.48(q, 2H, J= 10), 1.301-1.49-

1.46(t, 3H, J= 10); 13C (75 MHz, CDCl₃)164.46, 162.87, 151.28, 150.63, 143.94, 126.86, 121.73, 121.36, 120.69, 107.27, 61.95, 55.14, 14.29; HRMS m/z calculated for $C_{13}H_{10}D_3ClNO_3$ 269.0772 found 269.0770.

A general procedure for the synthesis of pyrazoloquinolinones. A mixture of 4-chloro-7-methoxy(d3)quinolin-3-carboxylate **3** (0.01 mol, 0.324g), substituted phenylhydrazine hydrochloride (0.012 mol) and TEA (0.012 m,0.12 g) in xylene (40mL) was heated to reflux for 4h. The reaction mixture was cooled to rt. The precipitated compound was collected by filtration and purified by crystallization.

Synthesis of LAU159, LAU165, and LAU463: 8-Chloro-2-(3-methoxyphenyl)-2H-pyrazolo[4,3-c]quinolin-3(5H)-one (LAU159). In a 8 mL-vial with magnetic stirrer and screw cap, ethyl 4,8-dichloroquinoline-3- carboxylate (135mg, 0.5 mmol, 1 eq), 3-(methoxy)phenyl hydrazine (83mg, 0.6 mmol, 1.2 eq) and triethylamine (61 mg, 0.6 mmol, 1.2 eq) were dissolved in dry N,Ndimethylacetamide (3 mL). The reaction mixture was heated to 140°C for 16 hours. After completion of the reaction the volatiles were removed by evaporation and the solid residue was washed with acetone and water to afford the pure product as a yellow solid (108mg, 66%): m.p.: ~ 340°C, with partial decomposition above 300°C; 1H NMR (200 MHz, DMSO-d6): 12.95 (bs, 1H), 8.72 (d, J = 5.2Hz, 1H), 8.15 (s, 1H), 7.84 - 7.70 (m, 4H), 7.33 (t, J = 8.1Hz, 1H), 6.75 (d, J = 8.1Hz, 1H), 3.80 (s, 3H); 13C NMR (50 MHz, DMSO-d6): δ= 161.5 (s), 159.5 (s), 141.9 (s), 141.0 (s), 139.5 (d), 134.2 (s), 130.6 (s), 130.2 (d), 129.5 (d), 121.6 (d), 121.1 (d), 119.9 (s), 110.9 (d), 109.5 (d), 106.3 (s), 104.4 (d), 55.1 (q); HRMS: [M+H]+ m/z (predicted) = 326.0691, m/z (measured) = 326.0688.

8-Chloro-2-(2-methoxyphenyl)-2H-pyrazolo[4,3-c]quinolin-3(5H)-one (LAU165). In an 8 mL vial with magnetic stirrer and screw cap, ethyl 4,6-dichloroquinoline- 3-carboxylate (135

mg, 0.5 mmol, 1 eq), 2-methoxyphenylhydrazine (83 mg, 0.6 mmol, 1.2 eq) and triethylamine (63 mg, 0.6 mmol, 1.2 eq) were dissolved in dry N,Ndimethylacetamide (3 mL). The reaction mixture was heated to 140 °C for 16h. After completion of the reaction the reaction mixture was evaporated to dryness. The crude product was purified by flash-column chromatography (45 g silica 60, eluent EtOAc/MeOH 5%), the co-eluting triethylamine hydrochloride was subsequently removed by washing with water. Yield: 28% (0.14 mmol, 46 mg, 28%) as a yellow solid: m.p. 310 - 313 °C with partial decomposition; 1H-NMR (200 MHz, DMSO-d6) δ = 3.73 (s, 3H), 7.03 (t, J = 7.5 Hz, 1H), 7.16 (d, J = 8.2 Hz, 1H), 7.29-7.45 (m, 2H), 7.62-7.73 (m, 2H), 8.01 (d, J = 1.6 Hz, 1H), 8.65 (s, 1H), 12.78 (s, 1H); 13C-NMR (50 MHz, DMSO-d6) δ = 55.6 (q), 105.3 (s), 112.5 (d), 120.2 (d), 120.3 (s), 120.9 (d), 121.4 (d), 127.7 (s), 129.3 (d), 129.4 (d), 129.7 (d), 130.3 (s), 134.0 (s), 139.1 (d), 141.4 (s), 155.1 (s), 161.6 (s); HRMS: [M+H] calcd 326.0691 m/z 326.0678.

7-Bromo-2-(4-methoxyphenyl)-2H-pyrazolo[4,3-c]quinolin-3(5H)-one (LAU463). The ethyl 7-bromo-4-chloroquinoline-3-carboxylate (200 mg, 0.64 mmol, 1 eq) and (4-methoxyphenyl)hydrazine (110 mg, 0.80 mmol, 1.2 eq) were dissolved in dimethylacetamide (5mL). The reaction was carefully purged with argon several times, triethylamine (1 eq) was added, and the reaction was heated to 140°C for 24 hours. The solvent was removed via Kugelrohr distillation of the crude mixture. Washing of the residue with acetone gave the product as an orange-yellow solid (121mg, 51%): m.p.: >330 °C with decomposition; 1H NMR (400 MHz, DMSO-d6) δ 12.78 (s, 1H), 8.74 (d, J = 5.8 Hz, 1H), 8.13 (d, J = 8.5 Hz, 1H), 8.06 (d, J = 8.6 Hz, 2H), 7.89 (d, J = 2.0 Hz, 1H), 7.69 (dd, J = 8.5, 2.0 Hz, 1H), 7.02 (d, J = 8.6 Hz, 2H), 3.79 (s, 3H); 13C NMR (101 MHz, DMSO) δ 161.3 (s), 156.5 (s), 142.4 (s), 140.1 (d),

136.9 (s), 133.8 (s), 129.7(d), 124.5 (d), 123.0 (s), 122.2 (d), 120.9 (d), 118.2 (s), 114.3 (d), 107.2 (s), 55.7 (q).

7-Methoxy-2-(pyrazin-2-yl)-2,5-dihydro-3H-pyrazolo[4,3-c]quinolin-3- one (DCBS126). In a 8 mL vial equipped with a magnetic stirrer and screw cap, the ethyl 4-chloro-7-methoxyquinoline-3-carboxylate (70 mg, 0.26 mmol, 1 eq) and 2-hydrazinopyrazine (32 mg, 0.29 mmol, 1.1 eq) were dispersed in 1.5 mL ethanol, triethylamine (40 μL, 0.29 mmol, 1.1 eq) was added, and the reaction mixture was heated to reflux under argon. After 20 h the reaction mixture was rinsed with water (4mL), filtered, and the precipitate was washed with EtOAc:PE (1:1, 15mL). The yellow solid was dried under reduced pressure to give the desired product giving a yellow solid (45mg, 58%): m.p.: >300 °C with decomposition; 1H NMR (400 MHz, DMSOd6) δ 3.88 (s, 3H), 7.16 – 7.23 (m, 2H), 8.13 (dd, J = 8.5, 0.8 Hz, 1H), 8.44 (d, J = 2.5 Hz, 1H), 8.56 (dd, J = 2.5, 1.5 Hz, 1H), 8.75 (s, 1H), 9.51 (d, J = 1.4 Hz, 1H), 12.74 (br s, 1H); 13C NMR (101 MHz, DMSO-d6) δ 55.6 (q), 102.1 (d), 105.0 (s), 112.2 (s), 115.5 (d), 123.9 (d), 136.6 (d), 137.3 (s), 140.0 (d), 140.1 (d), 142.8 (d), 144.9 (s), 148.0 (s), 160.8 (s), 162.4 (s); HRMS: Calc.[M+H]+ m/z 294.0992, m/z (measured) = 294.0992.

N-(4-Hydroxyphenyl)acetamide [DK-I-2-1]. To a mixture of 4-aminophenol (50.0 g, 458.2 mmol) and tetrahydrofuran (200 mL) acetic anhydride (49.1 g, 481.1 mmol) was added dropwise over 30 min while keeping the temperature below 50 ºC. The reaction mixture was then stirred for 30 min at 50 ºC and then cooled to rt. The reaction mixture was then diluted with hexanes (200 mL) to precipitate the product. After stirring for 1 h, the solid product was filtered and washed twice with hexanes (50 mL x 2). The solid was dried to afford the product as a white crystalline solid DK-I-2-1 (62.7 g, 90.0%)**:** mp 170-171 ºC; 1H NMR (300 MHz, DMSO) δ 9.64 (s, 1H), 9.13 (s, 1H), 7.34 (d, J = 8.8 Hz, 2H), 6.67 (d, J = 8.8 Hz, 2H), 1.98 (s, 3H); 13C NMR

(75 MHz, DMSO) δ 167.95, 153.57, 131.49, 121.26, 115.44, 24.19; LRMS m/z calculated for C$_8$H$_{10}$NO$_2$ (M + H)+ 152.17 found 152.15. This material was used in a later step.

N-(3-Hydroxyphenyl)acetamide [DK-I-3-1]. To a mixture of 3- aminophenol (25.0 g, 229.1 mmol) and tetrahydrofuran (100 mL) acetic anhydride (24.5 g, 240.5 mmol) was added dropwise over 30 min while keeping the temperature below 50 ºC. The reaction mixture was then stirred for 30 min at 50ºC and then cooled to rt. The reaction mixture was then diluted with hexanes (100 mL) to precipitate the product. After stirring for 1 h, the solid product was filtered and washed twice with hexanes (25 mL x 2). The solid was dried to afford the product as a white crystalline solid DK-I-3-1 (33.2 g, 96.0%)**:** mp 145-148 ºC; 1H NMR (300 MHz, DMSO) δ 9.77 (s, 1H), 9.32 (s, 1H), 7.18 (s, 1H), 7.04 (t, *J* = 8.0 Hz, 1H), 6.92 (d, *J* = 8.1 Hz, 1H), 6.42 (dd, *J* = 7.9, 2.1 Hz, 1H), 2.01 (s, 3H); 13C NMR (75 MHz, DMSO) δ 168.60, 158.01, 140.81, 129.72, 110.55, 110.18, 106.60, 24.50; LRMS m/z calculated for C$_8$H$_{10}$NO$_2$ (M + H)+ 152.17 found 152.15. This material was used in a later step.

N-(2-Hydroxyphenyl)acetamide [DK-I-30-1]. To a mixture of 2- aminophenol (25.0 g, 229.1 mmol) and tetrahydrofuran (100 mL) acetic anhydride (24.5 g, 240.5, mmol) was added dropwise over 30 min while keeping the temperature below 50 ºC. The reaction mixture was then stirred for 30 min at 50ºC and then cooled to rt. The reaction mixture was then diluted with hexanes (100 mL) to precipitate the product. After stirring for 1 h, the solid product was filtered and washed twice with hexanes (25 mL x 2). The solid was dried to afford the product as a light brown solid DK-I-30-1 (33.1 g, 95.7%)**:** mp 211-213 ºC; 1H NMR (300 MHz, DMSO) δ 9.75 (s, 1H), 9.31 (s, 1H), 7.67 (d, *J* = 7.7 Hz, 1H), 6.85 (ddd, *J* = 33.6, 14.6, 7.2 Hz, 3H), 2.10 (s, 3H); 13C NMR (75 MHz, DMSO) δ 169.44, 148.34, 126.88, 125.08, 122.80, 119.40, 116.38, 24.05;

LRMS m/z calculated for $C_8H_{10}NO_2$ (M + H)+ 152.17 found 152.15. This material was used in a later step.

N-(4-Methoxy-d3-phenyl)acetamide [DK-I-6-1]. To a mixture of N-(4-hydroxyphenyl)acetamide DK-I-2-1 (62.0 g, 410.1 mmol), potassium carbonate (113.4 g, 615.2 mmol) and acetone (230 mL) methyl iodide (D3) (100 g, 689.8 mmol) was added dropwise over 30 min. The reaction mixture was then stirred for 24 h at 20-25 ºC. The reaction mixture was then diluted with ethyl acetate (300 mL) and water (300 mL). The biphasic mixture which resulted was allowed to stand for 15 min and the layers were separated. The aq layer was extracted with ethyl acetate (200 mL) and then the combined organic layers were washed with 10% potassium carbonate solution (200 mL). The organic layer was then dried over magnesium sulfate. The solvents were then removed *in vacuo* and the product residue was slurried with hexanes (200 mL). The solid product was then filtered and washed twice with hexanes (50 mL x 2). The solid was dried to afford the product as an off-white solid DK-I-6-1 (71.7 g, 99%)**:** mp 125-126 ºC; 1H NMR (300 MHz, DMSO) δ 9.77 (s, 1H), 7.48 (d, *J* = 9.0 Hz, 2H), 6.85 (d, *J* = 9.0 Hz, 2H), 3.38 (s, 3H), 2.00 (s, 3H); 13C NMR (75 MHz, DMSO) δ 168.20, 155.48, 132.94, 121.01, 114.21, 24.23; LRMS m/z calculated for $C_9H_9D_3NO_2$ (M + H)+ 169.20 found 169.20. This material was used in a later step.

N-(3-Methoxy-d3-phenyl)acetamide [DK-I-8-1]. To a mixture of N-(3-hydroxyphenyl)acetamide DK-I-3-1 (35.0 g, 231.5 mmol), potassium carbonate (64.0 g, 463.1 mmol) and acetone (140 mL) methyl iodide (D3) (50.3 g, 347.3 mmol) was added dropwise over 30 min. The reaction mixture was then stirred for 24 h at 20-25 ºC. The reaction mixture was then diluted with ethyl acetate (150 mL) and water (150 mL). The biphasic mixture which resulted was allowed to stand for 15 min and the layers were separated. The aq layer was

extracted with ethyl acetate (100 mL) and then the combined organic layers were washed with 10% potassium carbonate solution (100 mL). The organic layer was then dried over magnesium sulfate. The solvents were then removed *in vacuo* and the product residue was slurried with hexanes (100 mL). The solid product was then filtered and washed twice with hexanes (50 mL x 2). The solid was dried to afford the product as an off-white solid DK-I-8-1 (38.9 g, 99%)**:** mp 89-91 ºC; 1H NMR (300 MHz, DMSO) δ 9.89 (s, 1H), 7.27 (s, 1H), 7.18 (t, *J* = 8.1 Hz, 1H), 7.10 (d, *J* = 8.2 Hz, 1H), 6.60 (dd, *J* = 7.8, 2.0 Hz, 1H), 2.03 (s, 3H); 13C NMR (75 MHz, DMSO) δ 168.76, 159.93, 140.96, 129.89, 111.71, 108.76, 105.30, 24.53; LRMS m/z calculated for $C_9H_9D_3NO_2$ (M + H)+ 166.20 found 166.15. This material was used in a later step.

N-(2-Methoxy-d3-phenyl)acetamide [DK-I-31-1]. To a mixture of N-(2-hydroxyphenyl)acetamide DK-I-30-1 (30.0 g, 198.5 mmol), potassium carbonate (54.9 g, 396.9 mmol) and acetone (140 mL) methyl iodide (D3) (50.3 g, 347.3 mmol) was added dropwise over 30 min. The reaction mixture was then stirred for 24 h at 20-25 ºC. The reaction mixture was then diluted with ethyl acetate (150 mL) and water (150 mL). The biphasic mixture which resulted was allowed to stand for 15 min and the layers were separated. The aq layer was extracted with ethyl acetate (100 mL) and then the combined organic layers were washed with 10% potassium carbonate solution (100 mL). The organic layer was then dried over magnesium sulfate. The solvents were then removed *in vacuo* and the product residue was slurried with hexanes (100 mL). The solid product was then filtered and washed twice with hexanes (50 mL x 2). The solid was dried to afford the product as an off-white solid DK-I-31-1 (31.9 g, 99%)**:** mp 82-83 ºC; 1H NMR (300 MHz, DMSO) δ 9.10 (s, 1H), 7.93 (d, *J* = 7.8 Hz, 1H), 7.22 – 6.97 (m, 2H), 6.97 – 6.79 (m, 1H), 2.08 (s, 3H); 13C NMR (75 MHz, DMSO) δ 168.87, 149.98, 127.87,

124.63, 122.45, 120.57, 111.50, 24.30; LRMS m/z calculated for $C_9H_9D_3NO_2$ (M + H)+ 166.20 found 169.19. This material was used in a later step.

4-Methoxy-d3-aniline [DK-I-67-1]. A mixture of N-(4-methoxy-d3- phenyl)acetamide DK-I-6-1 (20.0 g, 118.9 mmol), 12 M hydrochloric acid (20 mL, 240 mmol), and water (60 mL) was heated at 90-95 ºC for 2 h. The reaction mixture was then cooled to 20-25 ºC and the pH was adjusted to 14 with a solution of sodium hydroxide (20g, 500 mmol) and water (20 mL). The product was then extracted from the aqueous layer four times with dichloromethane (50 mL x 4). The combined organic layers were then dried over magnesium sulfate. Evaporation of the solvents on a rotovap afforded the product as a dark orange oil DK-I-67-1 (14.4 g, 96%)**:** 1H NMR (300 MHz, DMSO) δ 5.75 – 5.62 (m, 2H), 5.62 – 5.47 (m, 2H), 3.50 (s, 2H); 13C NMR (75 MHz, DMSO) δ 150.34, 141.51, 114.62, 113.89; LRMS m/z calculated for $C_7H_7D_3NO$ (M + H)+ 127.25 found 127.25. This material was used in a later step.

3-Methoxy-d3-aniline [DK-I-41-1]. A mixture of N-(3-methoxy-d3- phenyl)acetamide DK-I-8-1 (20.0 g, 118.9 mmol), 12 M hydrochloric acid (20 mL, 240 mmol), and water (60 mL) was heated at 90-95 ºC for 2 h. The reaction mixture was then cooled to 20-25 ºC and the pH was adjusted to 14 with a solution of sodium hydroxide (20g, 500 mmol) and water (20 mL). The product was then extracted from the aqueous layer four times with dichloromethane (50 mL x 4). The combined organic layers were then dried over magnesium sulfate. Evaporation of the solvents on a rotovap afforded the product as a golden yellow oil DK-I-41-1 (13.5 g, 90%)**:** 1H NMR (300 MHz, CDCl₃) δ 7.10 (t, J = 8.0 Hz, 1H), 6.35 (dddd, J = 11.9, 11.2, 3.4, 2.0 Hz, 3H), 4.00 (s, 2H); 13C NMR (75 MHz, CDCl₃) δ 160.78, 147.54, 130.16, 108.14, 104.22, 101.28; LRMS m/z calculated for $C_7H_6D_3NO$ (M + H)+ 127.25 found 127.25. This material was used in a later step.

Ethyl-6-chloro-4-hydroxyquinoline-3-carboxylate [DK-I-34-1]. A mixture of 4-chloroaniline (45.5 g, 356.7 mmol), diethyl ethoxymethylenemalonate (80.9 g, 374.1 mmol) and diphenyl ether (200 mL) was slowly heated to 230 ºC. The evolved ethanol was collected in a Dean-Stark trap. Once the ethanol formation ceased, the reaction mixture was heated for an additional 30 min at 230 ºC. The reaction mixture was then cooled to 80 ºC and diluted with ethanol (200 mL). Upon cooling to 20-25ºC the solid product was collected by filtration and washed twice with ethanol (50 mL x 2) and twice with hexanes (50 mL x 2). The solid was dried to afford the product as an off-white crystalline solid DK-I-34-1 (85.1 g, 95%)**:** 1H NMR (300 MHz, TFA) δ 11.66 (s, 1H), 9.32 (d, *J* = 4.5 Hz, 1H), 8.62 (d, *J* = 2.5 Hz, 1H), 8.12 (d, *J* = 13.0 Hz, 2H), 4.82 – 4.55 (m, 2H), 1.53 (dd, *J* = 11.8, 7.0 Hz, 3H); 13C NMR (75 MHz, TFA) δ 172.51, 167.19, 144.95, 138.35, 137.62, 137.58, 123.58, 121.35, 120.82, 105.30, 64.70, 11.96; LRMS m/z calculated for $C_{12}H_{11}ClNO_3$ (M+H)+ 252.10 found 252.10. This material was used in a later step.

Ethyl-4-hydroxy-7-methoxyquinoline-3-carboxylate [DK-I-39-1]. A mixture of 3-methoxyaniline (50.0 g, 406.0 mmol), diethyl ethoxymethylenemalonate (87.8 g, 406.0 mmol) and diphenyl ether (200 mL) was slowly heated to 230 ºC. The evolved ethanol was collected in a Dean-Stark trap. Once the ethanol formation ceased, the reaction mixture was heated for an additional 30 min at 230ºC. The reaction mixture was then cooled to 80 ºC and diluted with ethanol (200 mL). Upon cooling to 20-25 ºC the solid product was collected by filtration and washed twice with ethanol (50 mL x 2) and twice with hexanes (50 mL x 2). The solid was dried to afford the product as a light brown solid DK-I-39-1 (37.1 g, 37%)**:** 1H NMR (300 MHz, TFA) δ 11.63 (s, 1H), 9.22 (d, *J* = 6.3 Hz, 1H), 8.56 (dd, *J* = 9.1, 6.7 Hz, 1H), 7.66 – 7.54 (m, 1H), 7.47 (d, *J* = 4.2 Hz, 1H), 4.69 (dd, *J* = 13.8, 6.9 Hz, 2H), 4.13 (d, *J* = 6.4 Hz, 3H), 1.57 (q, *J* = 6.8 Hz, 3H); 13C NMR (75 MHz, TFA) δ 171.88, 167.91, 167.62, 144.49, 142.43, 126.28,

121.92, 114.05, 103.81, 99.24, 64.28, 55.45, 12.00; LRMS m/z calculated for $C_{13}H_{14}NO_4$

(M+H)+ 248.15 found 248.15. This material was used in a later step.

Ethyl-7-bromo-4-hydroxyquinoline-3-carboxylate [DK-I-49-1]. A mixture of 3-bromoaniline

(8.7 g, 58.1 mmol), diethyl ethoxymethylenemalonate (10.9 g, 58.1 mmol) and diphenyl ether

(40 mL) was slowly heated to 230 ºC. The evolved ethanol was collected in a Dean-Stark trap.

Once the ethanol formation ceased, the reaction mixture was heated for an additional 30 min at

230 ºC. The reaction mixture was then cooled to 80 ºC and diluted with ethanol (40 mL). Upon

cooling to 20-25 ºC the solid product was collected by filtration and washed twice with ethanol

(10 mL x 2) and twice with hexanes (10 mL x 2). The solid was dried to afford the product as a

light brown solid DK-I-49-1 (11.5 g, 77%)**:** 1H NMR (300 MHz, TFA) δ 11.64 (s, 1H), 9.38 (s,

1H), 8.57 (d, *J* = 8.9 Hz, 1H), 8.43 (s, 1H), 8.15 (d, *J* = 8.9 Hz, 1H), 4.75 (q, *J* = 7.1 Hz, 2H),

1.60 (t, *J* = 7.2 Hz, 3H); 13C NMR (75 MHz, TFA) δ 173.48, 167.33, 145.75, 139.71, 134.19,

134.06, 125.60, 122.70, 118.57, 105.08, 64.74, 12.01; LRMS m/z calculated for $C_{12}H_{10}BrNO_3$

(M+H)+ 296.12 found 296.05. This material was used in a later step.

Ethyl-4-hydroxy-7-methoxy-d3-quinoline-3-carboxylate [DK-I-54-1]. A mixture of 3-

methoxy-d3-aniline DK-I-41-1 (10 g, 81.2 mmol), diethyl ethoxymethylenemalonate (21.1 g,

97.4 mmol) and diphenyl ether (100 mL) was slowly heated to 230 ºC. The evolved ethanol was

collected in a Dean-Stark trap. Once the ethanol formation ceased, the reaction mixture was

heated for an additional 30 min at 230 ºC. The reaction mixture was then cooled to 80 ºC and

diluted with hexanes (100 mL). Upon cooling to 20-25 ºC the solid product was collected by

filtration and washed twice with hexanes (50 mL x 2). The solid was dried to afford the product

as a brown solid DK-I-54-1 (13.0 g, 64%)**:** 1H NMR (300 MHz, TFA) δ 11.64 (s, 1H), 9.23 (s,

1H), 8.57 (d, *J* = 9.3 Hz, 1H), 7.59 (dd, *J* = 9.4, 2.3 Hz, 1H), 7.48 (d, *J* = 2.2 Hz, 1H), 4.71 (q, *J*

= 7.2 Hz, 2H), 1.58 (t, *J* = 7.2 Hz, 3H); 13C NMR (75 MHz, TFA) δ 171.89, 167.92, 167.64, 144.50, 142.44, 126.28, 121.93, 114.05, 103.81, 99.25, 64.29, 12.01; LRMS m/z calculated for $C_{13}H_{11}D_3NO_4$ (M+H)+ 251.25 found 251.20. This material was used in a later step.

Ethyl-4-hydroxy-6-methoxy-d3-quinoline-3-carboxylate [DK-I-70-1]. A mixture of 4-methoxy-d3-aniline DK-I-67-1 (10 g, 81.2 mmol), diethyl ethoxymethylenemalonate (21.1 g, 97.4 mmol) and diphenyl ether (100 mL) was slowly heated to 230 ºC. The evolved ethanol was collected in a Dean-Stark trap. Once the ethanol formation ceased, the reaction mixture was heated for an additional 30 min at 230 ºC. The reaction mixture was then cooled to 80 ºC and diluted with hexanes (100 mL). Upon cooling to 20-25 ºC the solid product was collected by filtration and washed twice with hexanes (50 mL x 2). The solid was dried to afford the product as a light brown solid DK-I- 70-1 (9.9 g, 49%). 1H NMR (300 MHz, TFA) δ 11.66 (s, 1H), 9.15 (s, 1H), 8.05 (d, *J* = 9.2 Hz, 1H), 7.97 – 7.74 (m, 2H), 4.67 (q, *J* = 7.1 Hz, 2H), 1.67 – 1.39 (m, 3H); 13C NMR (75 MHz, TFA) δ 171.68, 167.54, 160.89, 141.86, 134.62, 129.91, 121.73, 121.28, 104.58, 102.17, 64.41, 11.97; LRMS m/z calculated for $C_{13}H_{11}D_3NO_4$ (M+H)+ 251.25 found 251.20. This material was used in a later step.

Ethyl 6-bromo-8-fluoro-4-hydroxyquinoline-3-carboxylate [MM-I-01]. 3- Bromo-5-fluoroaniline (10 g, 52.6 mmol) was heated with diethyl ethoxymethylene malonate (11.2 mL, 55.3 mmol) at 125°C. After heating for 2 h, downtherm A (50 mL) was added and the mixture was heated up to 255°C for 2 h. The reaction was cooled to rt and diluted with hexane (50 mL). The mixture was stirred for 5 min. The precipitate was filtered and washed with hexane to yield the product as a brown colored solid MM-I-01 (13.60 g, 82%)**:** mp 285 – 286 °C; 1H NMR (300 MHz, DMSO) δ 12.65 (s, 1H; H- 11), 8.40 (s, 1H; H-8), 8.04 (s, 1H; H-6), 8.00 (dd, J = 10.1, 2.0

Hz, 1H; H-2), 4.23 (q, J = 7.1 Hz, 2H; H-18), 1.28 (t, J = 7.1 Hz, 3H; H-17); HRMS m/z calculated for $C_{12}H_9NO_3FBr$ 313.9823 found 313.9833. This material was used in a later step.

Ethyl 4-hydroxy-7-(trifluoromethyl)quinoline-3-carboxylate [MM-I-04]. 3-(Trifluoromethyl)aniline (10 g, 62.1 mmol) was heated with diethyl ethoxymethylene malonate (12.6 mL, 62 mmol) at 125 °C for 1 h. Then, downtherm A (50 mL) was added and the mixture was heated up to 255 °C for 2.5 h. After heating, the reaction was cooled to rt and diluted with hexane (50 mL). The mixture was stirred for 5 min. The precipitated was filtered and washed with hexane to provide the product as a white colored solid MM-I-04 (16.51 g, 93%)**:** mp 340 – 341 °C; 1H NMR (300 MHz, DMSO) δ 12.51 (s, 1H; H-11), 8.70 (s, 1H; H-8), 8.35 (d, J = 8.3 Hz, 1H; H-6), 8.00 (s, 1H; H-3), 7.72 (d, J = 8.1 Hz, 1H; H-1), 4.24 (q, J = 14.3, 7.1 Hz, 2H; H-20), 1.29 (t, J = 7.0 Hz, 3H; H-19); HRMS m/z calculated for $C_{13}H_{10}NO_3F_3$ 286.0686 found 286.0691. This material was used in a later step.

Ethyl-4,6-dichloroquinoline-3-carboxylate [DK-I-35-1]. A mixture of ethyl-6-chloro-4-hydroxyquinoline-3-carboxylate DK-I-34-1 (85.1 g, 338.1 mmol), N,Ndimethylformamide (1.0 mL, 12.9 mmol), and dichloromethane (640 mL) was heated to 35- 40ºC. Oxalyl chloride (47.2 g, 371.9 mmol) was added dropwise to the reaction mixture over 30 min. The reaction mixture was then heated for 6 h at reflux (38-40 ºC). The resulting pale yellow solution was then cooled to 20-25 ºC. The reaction mixture was then neutralized by slowly adding a 25% solution of potassium carbonate (75 g) in water (300 mL). The layers were then separated and the aqueous layers extracted with dichloromethane (200 mL). The combined organic layers were then washed with a 25% solution of potassium carbonate (50 g) in water (200 mL). The combined organic layers were then dried over magnesium sulfate. The solvents were then removed *in vacuo* and the product residue was slurried with hexanes (200 mL). The solid product was then filtered and

washed twice with hexanes (50 mL x 2). The solid was dried to afford the product as an offwhite

solid DK-I-35-1 (81.9 g, 90%)**:** 1H NMR (300 MHz, DMSO) δ 9.13 (s, 1H), 8.30 (d, J = 2.2 Hz,

1H), 8.14 (d, J = 9.0 Hz, 1H), 7.97 (dd, J = 9.0, 2.3 Hz, 1H), 4.44 (q, J = 7.1 Hz, 2H), 1.39 (t, J =

7.1 Hz, 3H); 13C NMR (75 MHz, DMSO) δ 164.01, 150.53, 147.73, 141.04, 134.30, 133.34,

132.20, 126.53, 124.37, 124.08, 62.59; LRMS m/z calculated for $C_{12}H_9Cl_2NO_2$ (M+H)+ 270.12

found 270.10. This material was used in a later step.

Ethyl-4-chloro-7-methoxyquinoline-3-carboxylate [DK-I-40-1]. A mixture of ethyl-4-

hydroxy-7-methoxyquinoline-3-carboxylate DK-I-39-1 (37.1 g, 150.0 mmol),

N,Ndimethylformamide (0.5 mL, 6.5 mmol), and dichloromethane (150 mL) was heated to 35-

40 ºC. Oxalyl chloride (20.9 g, 165.0 mmol) was added dropwise to the reaction mixture over 30

min. The reaction mixture was then heated for 2h at reflux (38-40 ºC). The resulting brown

solution was then cooled to 20-25 ºC. The reaction mixture was diluted with dichloromethane

(150 mL) and then neutralized by slowly adding a 25% solution of potassium carbonate (75 g) in

water (300 mL). The layers were then separated and the aqueous layers extracted with

dichloromethane (100 mL). The combined organic layers were then washed with a 25% solution

of potassium carbonate (75 g) in water (300 mL). The combined organic layers were then dried

over magnesium sulfate. The solvents were then removed *in vacuo* and the product residue was

slurried with hexanes (200 mL). The solid product was then filtered and washed twice with

hexanes (50 mL x 2). The solid was dried to afford the product as an off-white solid DK-I-40-1

(36.3 g, 91%)**:** 1H NMR (300 MHz, DMSO) δ 9.08 (s, 1H), 8.25 (d, J = 9.2 Hz, 1H), 7.57 – 7.37

(m, 2H), 4.41 (q, J = 7.1 Hz, 2H), 3.98 (s, 3H), 1.38 (t, J = 7.1 Hz, 3H); 13C NMR (75 MHz,

DMSO) δ 164.32, 162.83, 151.62, 150.81, 142.02, 126.85, 122.12, 121.11, 120.56, 108.36,

62.15, 56.45, 14.49; LRMS m/z calculated for $C_{13}H_{13}ClNO_3$ (M+H)+ 266.70 found 266.15. This material was used in a later step.

Ethyl-7-bromo-4-chloroquinoline-3-carboxylate [DK-I-52-1]. A mixture of ethyl-7-bromo-4-hydroxyquinoline-3-carboxylate DK-I-49-1 (11.0 g, 37.1 mmol), N,Ndimethylformamide (0.1 mL, 1.3 mmol), and dichloromethane (50 mL) was heated to 35-40 ºC. Oxalyl chloride (5.2 g, 40.9 mmol) was added dropwise to the reaction mixture over 30 min. The reaction mixture was then heated for 1h at reflux (38-40 ºC). The resulting brown solution was then cooled to 20-25 ºC. The reaction mixture was diluted with dichloromethane (150 mL) and then neutralized by slowly adding a 25% solution of potassium carbonate (12.5 g) in water (50 mL). The layers were then separated and the aqueous layers extracted with dichloromethane (50 mL). The combined organic layers were then washed with a 25% solution of potassium carbonate (12.5 g) in water (50 mL). The combined organic layers were then dried over magnesium sulfate. The solvents were then removed *in vacuo* and the product residue was slurried with hexanes (50 mL). The solid product was then filtered and washed twice with hexanes (25 mL x 2). The solid was dried to afford the product as an off-white solid DK-I-54-1 (7.2 g, 61%)**:** 1H NMR (300 MHz, DMSO) δ 9.15 (s, 1H), 8.36 (d, *J* = 1.9 Hz, 1H), 8.28 (d, *J* = 9.0 Hz, 1H), 7.98 (dd, *J* = 9.0, 1.9 Hz, 1H), 4.44 (q, *J* = 7.1 Hz, 2H), 1.39 (t, *J* = 7.1 Hz, 3H); 13C NMR (75 MHz, DMSO) δ 164.04, 151.40, 149.74, 142.34, 132.67, 131.88, 127.50, 126.64, 124.70, 123.96, 62.55, 14.46; LRMS m/z calculated for $C_{12}H_9BrClNO_2$ (M+H)+ 314.56 found 314.05. This material was used in a later step.

Ethyl-4-chloro-7-methoxy-d3-quinoline-3-carboxylate [DK-I-57-1]. A mixture of ethyl-4-hydroxy-7-methoxy-d3-quinoline-3-carboxylate DK-I-54-1 (13.0 g, 51.9 mmol), phosphorus oxychloride (8.8 g, 57.1 mmol) and toluene (52 mL) was heated to 80-90 ºC. The reaction

mixture was then held for 1 h at 80-90 ºC). The resulting brown solution was then cooled to 20-25 ºC. The reaction mixture was then diluted with hexanes (50 mL). The solids were collected by filtration and washed twice with hexanes (50 mL each). The solids were then dissolved in dichloromethane (100 mL) and then neutralized by slowly adding a 25% solution of potassium carbonate (12.5 g) in water (50 mL). The layers were then separated and the aqueous layers extracted with dichloromethane (50 mL). The combined organic layers were then washed with a 25% solution of potassium carbonate (12.5 g) in water (50 mL). The combined organic layers were then dried over magnesium sulfate. The solvents were then removed *in vacuo* and the product residue was slurried with hexanes (50 mL). The solid product was then filtered and washed twice with hexanes (25 mL x 2). The solid was dried to afford the product as an off-white solid DK-I-57-1 (11.5 g, 82%)**:** 1H NMR (300 MHz, DMSO) δ 9.07 (s, 1H), 8.23 (d, J = 9.2 Hz, 1H), 7.54 – 7.38 (m, 2H), 4.40 (q, J = 7.1 Hz, 2H), 1.37 (t, J = 7.1 Hz, 3H); 13C NMR (75 MHz, DMSO) δ 164.29, 162.85, 151.53, 150.75, 142.41, 126.84, 122.11, 121.07, 120.56, 108.27, 62.15, 14.49; LRMS m/z calculated for $C_{13}H_{10}D_3ClNO_3$ (M+H)+ 269.70 found 269.15. This material was used in a later step.

Ethyl-4-chloro-6-methoxy-d3-quinoline-3-carboxylate [DK-I-73-2]. A mixture of ethyl-4-hydroxy-6-methoxy-d3-quinoline-3-carboxylate DK-I-70-1 (10.0 g, 40.0 mmol), phosphorus oxychloride (6.7 g, 44.0 mmol) and toluene (40 mL) was heated to 80-90 ºC. The reaction mixture was then held for 1 h at 80-90 ºC). The resulting brown solution was then cooled to 20-25 ºC. The reaction mixture was then diluted with hexanes (40 mL). The solids were collected by filtration and washed twice with hexanes (20 mL each). The solids were then dissolved in dichloromethane (100 mL) and then neutralized by slowly adding a 25% solution of potassium carbonate (10 g) in water (40 mL). The layers were then separated and the aqueous layers

extracted with dichloromethane (50 mL). The combined organic layers were then washed with a 25% solution of potassium carbonate (10 g) in water (40 mL). The combined organic layers were then dried over magnesium sulfate. The solvents were then removed *in vacuo* and the product residue was slurried with hexanes (50 mL). The solid product was then filtered and washed twice with hexanes (25 mL x 2). The solid was dried to afford the product as an off-white solid DK-I-73- 2 (8.5 g, 79%)**:** 1H NMR (300 MHz, DMSO) δ 8.95 (s, 1H), 8.03 (d, *J* = 9.1 Hz, 1H), 7.67 – 7.45 (m, 2H), 4.42 (q, *J* = 7.1 Hz, 2H), 1.38 (t, *J* = 7.1 Hz, 3H); 13C NMR (75 MHz, DMSO) δ 164.49, 159.57, 147.25, 145.36, 139.99, 131.67, 126.91, 125.20, 123.87, 102.96, 62.36, 14.47; LRMS m/z calculated for $C_{13}H_{10}D_3ClNO_3$ (M+H)+ 269.70 found 269.15. This material was used in a later step.

Ethyl 6-bromo-4-chloro-8-fluoroquinoline-3-carboxylate [MM-I-02]. The Ethyl 6-bromo-8-fluoro-4-hydroxyquinoline-3-carboxylate MM-I-01 (1 g, 3.2 mmol) was placed in a flask with $POCl_3$ (4 mL). The mixture was heated at 70°C for 3 h. The excess of $POCl_3$ was evaporated by reduced pressure and the remaining oil was quenched with saturated solution of $NaHCO_3$. Then, the aqueous solution was extracted with CH_2Cl_2 (3 x 50 mL) and the combined organic layers were dried (Na_2SO_4). The solvent was removed under reduce pressure and the residue was purified by silica gel chromatography to give the compound as a white solid MM-I-02 (0.79 g, 75%)**:** 1H NMR (300 MHz, CDCl₃) δ 9.23 (s, 1H; H-8), 8.40 (s, 1H; H-6), 7.70 (dd, J = 9.1, 1.9 Hz, 1H; H-2), 4.54 (q, J = 7.1 Hz, 2H; H- 18), 1.49 (t, J = 7.1 Hz, 3H; H-17). HRMS m/z calculated for $C_{12}H_8NO_2FClBr$ 331.9484 found 331.9487. This material was used in a later step.

Ethyl 4-chloro-7-(trifluoromethyl)quinoline-3-carboxylate [MM-I-05]. The reaction was performed following the same procedure as for MM-I-02 except the reaction was performed in bigger scale. Ethyl 4-hydroxy-7-(trifluoromethyl)quinoline-3- carboxylate MM-I-04 (5 g, 18

mmol) was heated with POCl$_3$ (10 mL) at 70°C for 3 h. MM-I- 05 was obtained as a white solid (5.1 g, 93%)**:** mp 71 – 73 °C; 1H NMR (300 MHz, CDCl$_3$) δ 9.30 (s, 1H; H-8), 8.56 (d, J = 8.9 Hz, 1H; H-6), 8.46 (s, 1H; H-3), 7.89 (dd, J = 8.9, 1.5 Hz, 1H; H-1), 4.54 (q, J = 7.1 Hz, 2H; H-20), 1.50 (t, J = 7.1 Hz, 3H; H-19); 13C NMR (75 MHz, CDCl$_3$) δ 163.96 (s), 151.35 (s), 148.54 (s), 143.47 (s), 133.53 (q), 127.84 (s), 127.60 (q), 126.92 (s), 124.69 (s), 124.01 (q), 118.86 (s), 62.45 (s), 14.21 (s); HRMS m/z calculated for C$_{13}$H$_9$NO$_2$F$_3$Cl 304.0347 found 304.0353. This material was used in a later step.

2-Methoxy-d3-5-nitropyridine [DK-II-44-1]. To a mixture of potassium tert-butoxide (13.3 g, 11.8 mmol) and methanol-d4 (50 mL) was slowly added 2-chloro-5- nitropyridine (15.0 g, 94.6 mmol). The exothermic reaction warmed to 50 ºC and then was refluxed at 65ºC for 2 h to complete the reaction. The reaction mixture was then cooled to 20-25 ºC and poured into water (750 mL). After stirring the mixture for 1 h the solid product was filtered and washed twice with water (25 mL x 2). The solid was dried to afford the product as a light yellow powder DK-II-44-1 (13.0g, 87%). 1H NMR (300 MHz, DMSO) δ 9.08 (s, 1H), 8.47 (d, *J* = 9.1 Hz, 1H), 7.03 (d, *J* = 9.1 Hz, 1H); 13C NMR (75 MHz, DMSO) δ 167.45, 145.02, 139.99, 135.01, 111.67; LRMS m/z calculated for C$_6$H$_4$D$_3$N$_2$O$_3$ (M+H)+ 158.19 found 158.20. This material was used in a later step.

5-Amino-2-methoxy-d3-pyridine [DK-II-45-1]. A mixture of 2-methoxy-d3- 5-nitropyridine DK-II-44-1 (13.0 g, 82.7 mmol), iron powder (15.9 g, 284.7 mmol), water (5 mL) and ethanol (50 mL) was heated to reflux (78 ºC). Once at reflux, concentrated hydrochloric acid (1 mL, 83.3 mmol) was added dropwise. The reaction mixture was then refluxed for 4 h to complete the reaction. Upon cooling to 20-25 ºC, the mixture was filtered to remove the iron and the solids were washed 3 times with ethanol (25 mL x 3). Sodium bicarbonate (5.0 g) was added to the

filtrate and the ethanol was removed *in vacuo*. Water (50 mL) and dichloromethane (50 mL) were added to dissolve the residue. The layers were separated and the aq layer was extracted twice with dichloromethane (50 mL x 2). The combined organic layers were dried over magnesium sulfate. The solvents were then removed *in vacuo* and the product was obtained as a clear orange-red oil DK-II-45-1 (10.0 g, 95.1%)**:** 1H NMR (300 MHz, DMSO) δ 7.57 (d, *J* = 2.7 Hz, 1H), 7.05 (dd, *J* = 8.6, 2.9 Hz, 1H), 6.56 (d, *J* = 8.7 Hz, 1H), 4.74 (s, 2H); 13C NMR (75 MHz, DMSO) δ 156.29, 139.77, 131.63, 126.85, 110.42; LRMS m/z calculated for $C_6H_6D_3N_2O$ (M+H)+ 128.15 found 128.15. This material was used in a later step.

4-Methoxy-d3-phenylhydrazine [DK-I-29-2]. A mixture of N-(4-methoxyd3-phenyl)acetamide DK-I-6-1 (30 g, 178.4 mmol), concentrated hydrochloric acid (72 mL), and water (72 mL) was heated to and held at 90 ºC for 2 h to hydrolyze the amide functionality. The reaction mixture was then cooled to 0 to 5ºC and a solution of sodium nitrite (12.9 g, 187.7 mmol) and water (25 mL) was slowly added dropwise to the reaction mixture. Upon completion of the addition, the reaction mixture was stirred for an additional 15 min at 0 to 5 ºC. The reaction mixture was then cooled to -25 to -20ºC and a solution of tin (II) chloride (74.4 g, 392.4 mmol) and concentrated hydrochloric acid (150 mL) was added dropwise to the reaction mixture over 30 min. Upon completion of the addition, the reaction mixture was stirred for an additional 4 h at -25 to -20 ºC. The reaction mixture was then diluted with diethyl ether (300 mL) and the solids were filtered and washed three times with diethyl ether (100 mL x 3). The tin adduct of the product was then dissolved in a mixture of sodium hydroxide (60 g), water (250 mL) and dichloromethane (250 mL). After stirring for 2 h at 0 to 5 ºC, the solids completely dissolved. The layers were separated and the aq layer was extracted three times with dichloromethane (100mL x 3). The combined organic layers were then dried over magnesium sulfate. The

solvents were then removed *in vacuo* and the product residue was slurried with hexanes (50 mL). The solid product was then filtered and washed twice with hexanes (50 mL x 2). The solid was dried to afford the product as a pale orange crystalline solid DK-I-29-2 (16.6 g, 66%)**:** 1H NMR (300 MHz, MeOD) δ 6.91 – 6.85 (m, 2H), 6.85 – 6.78 (m, 2H), 4.88 (s, 3H); 13C NMR (75 MHz, DMSO) δ 152.05, 147.27, 114.60, 113.38; LRMS m/z calculated for $C_7H_8D_3N_2O$ (M+H)+ 142.25 found 142.25. This material was used in a later step.

3-Methoxy-d3-phenylhydrazine [DK-I-26-3]. A mixture of N-(3-methoxyd3-phenyl)acetamide DK-I-8-1 (25 g, 148.6 mmol), concentrated hydrochloric acid (60 mL), and water (60 mL) was heated to and held at 90 ºC for 2 h to hydrolyze the amide functionality. The reaction mixture was then cooled to 0 to 5 ºC and a solution of sodium nitrite (10.8 g, 156.1 mmol) and water (21 mL) was slowly added dropwise to the reaction mixture. Upon completion of the addition, the reaction mixture was stirred for an additional 15 min at 0 to 5 ºC. The reaction mixture was then cooled to -25 to -20 ºC and a solution of tin (II) chloride (62.0 g, 327.0 mmol) and concentrated hydrochloric acid (125 mL) was added dropwise to the reaction mixture over 30 min. Upon completion of the addition, the reaction mixture was stirred for an additional 2 h at -25 to -20 ºC. The reaction mixture was then diluted with diethyl ether (250 mL) and the solids were filtered and washed three times with diethyl ether (100 mL x 3). The tin adduct of the product was then dissolved in a mixture of sodium hydroxide (20 g), water (100 mL) and dichloromethane (100 mL). After stirring for 1 h at 0 to 5 ºC, the solids completely dissolved. The layers were separated and the aq layer was extracted three times with dichloromethane (50mL x 3). The combined organic layers were then dried over magnesium sulfate. The solvents were then removed *in vacuo* to afford the product as an orange-red oil DK-I-26-3 (5.4 g, 26%)**:** 1H NMR (300 MHz, DMSO) δ 6.98 (t, *J* = 8.0 Hz, 1H), 6.65 (s, 1H), 6.51 – 6.27 (m, 2H), 6.16

(d, J = 7.9 Hz, 1H), 3.91 (s, 2H); 13C NMR (75 MHz, DMSO) δ 160.68, 154.54, 129.69, 104.96, 102.72, 97.52; LRMS m/z calculated for $C_7H_8D_3N_2O$ (M+H)+ 142.14 found 142.15. This material was used in a later step.

2-Methoxy-d3-phenylhydrazine [DK-I-43-3]. A mixture of N-(2-methoxyd3-phenyl)acetamide DK-I-31-1 (25 g, 148.6 mmol), concentrated hydrochloric acid (60 mL), and water (60 mL) was heated to and held at 90 ºC for 2 h to hydrolyze the amide functionality. The reaction mixture was then cooled to 0 to 5 ºC and a solution of sodium nitrite (10.7 g, 156.1 mmol) and water (21 mL) was slowly added dropwise to the reaction mixture. Upon completion of the addition, the reaction mixture was stirred for an additional 15 min at 0 to 5 ºC. The reaction mixture was then cooled to -25 to -20 ºC and a solution of tin (II) chloride (62.0 g, 327.0 mmol) and concentrated hydrochloric acid (125 mL) was added dropwise to the reaction mixture over 30 min. Upon completion of the addition, the reaction mixture was stirred for an additional 2 h at -25 to -20 ºC. The reaction mixture was then diluted with diethyl ether (300 mL) and the solids were filtered and washed three times with diethyl ether (100 mL x 3). The tin adduct of the product was then dissolved in a mixture of sodium hydroxide (20 g), water (100 mL) and dichloromethane (100 mL). After stirring for 1 h at 0 to 5 ºC, the solids completely dissolved. The layers were separated and the aq layer was extracted three times with dichloromethane (100mL x 3). The combined organic layers were then dried over magnesium sulfate. The solvents were then removed *in vacuo* and the product residue was slurried with hexanes (50 mL). The solid product was then filtered and washed twice with hexanes (25 mL x 2). The solid was dried to afford the product as a pale pink solid DK-I-43-3 (12.5 g, 60%)**:** 1H NMR (300 MHz, DMSO) δ 7.01 (dd, J = 7.8, 1.3 Hz, 1H), 6.92 – 6.71 (m, 2H), 6.61 (td, J = 7.7, 1.4 Hz, 1H), 5.92 (s, 1H), 3.92 (s, 2H); 13C NMR (75 MHz, DMSO) δ 146.33, 141.94, 121.26, 117.23, 111.20,

110.07; LRMS m/z calculated for $C_7H_8D_3N_2O$ (M+H)+ 142.30 found 142.30. This material was used in a later step.

5-Hydrazinyl-2-methoxypyridine [DK-I-82-3]. A mixture of 5-amino-2- methoxypyridine (10 g, 80.6 mmol), concentrated hydrochloric acid (24 mL), and water (24 mL) was cooled to 0 to 5 ºC and a solution of sodium nitrite (5.8 g, 84.6 mmol) and water (12 mL) was slowly added dropwise to the reaction mixture. Upon completion of the addition, the reaction mixture was stirred for an additional 15 min at 0 to 5 ºC. The reaction mixture was then cooled to -25 to -20 ºC and a solution of tin (II) chloride (33.6 g, 177.2 mmol) and concentrated hydrochloric acid (70 mL) was added dropwise to the reaction mixture over 30 min. Upon completion of the addition, the reaction mixture was stirred for an additional 2 h at -25 to -20 ºC. The reaction mixture was then diluted with dichloromethane (100 mL). A solution of potassium hydroxide (100 g) in water (200 mL) was added dropwise to the reaction mixture at 0 to 5 ºC over 30 min. After stirring for 1 h at 0 to 5 ºC, the solids completely dissolved. The layers were separated and the aq layer was extracted four times with dichloromethane (50mL x 4). The combined organic layers were then dried over magnesium sulfate. The solvents were then removed *in vacuo* and the product residue was slurried with hexanes (20 mL). The slurry was placed in a freezer at -20 ºC for 24 h to fully precipitate the product. The solid product was then filtered and washed twice with hexanes (10 mL x 2). The solid was dried to afford the product as a pale yellow-brown solid DK-I-82-3 (7.8 g, 70%)**:** 1H NMR (300 MHz, DMSO) δ 7.70 (s, 1H), 7.20 (d, *J* = 8.7 Hz, 1H), 6.61 (d, *J* = 8.8 Hz, 1H), 6.41 (s, 1H), 3.97 (s, 2H), 3.73 (s, 3H); 13C NMR (75 MHz, DMSO) δ 156.98, 144.09, 129.85, 125.25, 110.22, 53.19; LRMS m/z calculated for $C_6H_{10}N_3O$ (M+H)+ 140.24 found 140.25. This material was used in a later step.

5-Hydrazinyl-2-methoxy-d3-pyridine [DK-II-56-1]. A mixture of 5-amino- 2-methoxy-d3-pyridine DK-II-45-1 (10 g, 78.6 mmol), concentrated hydrochloric acid (24 mL), and water (24 mL) was cooled to 0 to 5ºC and a solution of sodium nitrite (5.7 g, 82.5 mmol) in water (12 mL) was slowly added dropwise to the reaction mixture. Upon completion of the addition, the reaction mixture was stirred for an additional 15 min at 0 to 5 ºC. The reaction mixture was then cooled to -25 to -20 ºC and a solution of tin (II) chloride (32.8 g, 173.0 mmol) and concentrated hydrochloric acid (70 mL) was added dropwise to the reaction mixture over 30 min. Upon completion of the addition, the reaction mixture was stirred for an additional 2 h at -25 to -20 ºC. The reaction mixture was then diluted with dichloromethane (100 mL). A solution of potassium hydroxide (100 g), water (200 mL) was added dropwise to the reaction mixture at 0 to 5 ºC over 30 min. After stirring for 1 h at 0 to 5 ºC, the solids completely dissolved. The layers were separated and the aq layer was extracted four times with dichloromethane (50mL x 4). The combined organic layers were then dried over magnesium sulfate. The solvents were then removed *in vacuo* and the product residue was slurried with hexanes (20 mL). The slurry was placed in a freezer at -20 ºC for 24 h to fully precipitate the product. The solid product was then filtered and washed twice with hexanes (10 mL x 2). The solid was dried to afford the product as a pale yellow-brown solid DK-II-56-1 (6.4 g, 57%)**:** 1H NMR (300 MHz, DMSO) δ 7.70 (d, *J* = 2.8 Hz, 1H), 7.31 – 7.19 (m, 1H), 6.61 (d, *J* = 8.8 Hz, 1H), 6.42 (s, 1H), 4.00 (s, 2H); 13C NMR (75 MHz, DMSO) δ 157.01, 144.07, 129.87, 125.27, 110.22; LRMS m/z calculated for $C_6H_7D_3O$ (M+H)+ 143.25 found 143.25. This material was used in a later step.

7-Methoxy-2-(4-methoxyphenyl)-2,5-dihydro-3H-pyrazolo[4,3- c]quinolin-3-one [Compound 6]. A mixture of ethyl-4-chloro-7-methoxyquinoline-3-carboxylate DK-I-40-1 (4 g, 15.1 mmol), 4-methoxyphenylhydrazine hydrochloride (3.15 g, 18.1 mmol), triethylamine

(3.66g, 36.1 mmol) and xylenes (32 mL) was heated to reflux (138 ºC) and held at reflux for 2 h. The resulting yellow-orange slurry was cooled to 100 ºC and diluted with ethanol (32 mL). The reaction mixture was then refluxed at 80ºC for 30 min and then cooled to 20-25 ºC. The solids were collected by filtration and washed twice with a 1:1 mixture of ethanol (2.5 mL x 2) and hexanes (2.5 mL x 2) and then washed twice with hexanes (5 mL x 2). The solid was dried to afford the product as a yellow powder **Compound 6** (2.0 g, 41%)**:** 1H NMR (300 MHz, DMSO) δ 12.59 (s, 1H), 8.65 (s, 1H), 8.10 (t, J = 8.7 Hz, 3H), 7.34 – 7.12 (m, 2H), 7.01 (d, J = 9.1 Hz, 2H), 3.87 (s, 3H), 3.78 (s, 3H); 13C NMR (75 MHz, DMSO) δ 161.45, 160.85, 156.22, 143.11, 139.33, 137.42, 134.10, 124.05, 120.68, 115.77, 114.25, 112.68, 106.87, 102.26, 55.98, 55.68; LRMS m/z calculated for $C_{18}H_{16}N_3O_3$ (M+H)+ 322.25 found 322.25.

7-Methoxy-d3-2-(4-methoxyphenyl)-2,5-dihydro-3H-pyrazolo[4,3- c]quinolin-3-one [RV-I-029]. A mixture of ethyl-4-chloro-7-methoxy-d3-quinoline-3- carboxylate DK-I-57-1 (2 g, 7.4 mmol), 4-methoxyphenylhydrazine hydrochloride (1.56 g, 8.9 mmol), triethylamine (1.81g, 17.6 mmol) and xylenes (16 mL) was heated to reflux (138 ºC) and held at reflux for 2 h. The resulting yellow-orange slurry was cooled to 100 ºC and diluted with ethanol (16 mL). The reaction mixture was then refluxed at 80 ºC for 30 min and then cooled to 20-25 ºC. The solids were collected by filtration and washed twice with a 1:1 mixture of ethanol (2.5 mL x 2) and hexanes (2.5 mL x 2) and then washed twice with hexanes (5 mL x 2). The solid was dried to afford the product as a yellow powder RV-I-029 (1.0 g, 41%)**:** 1H NMR (300 MHz, DMSO) δ 12.59 (s, 1H), 8.65 (s, 1H), 8.10 (t, J = 8.7 Hz, 3H), 7.17 (d, J = 2.0 Hz, 2H), 7.01 (d, J = 8.9 Hz, 2H), 3.78 (s, 3H); 13C NMR (75 MHz, DMSO) δ 161.45, 160.86, 156.22, 143.11, 139.32, 137.42, 134.11, 124.05, 120.68, 115.76, 114.25, 112.66, 106.87, 102.25, 55.68; LRMS m/z calculated for $C_{18}H_{13}D_3N_3O_3$ (M+H)+ 325.30 found 325.30.

7-Methoxy-2-(4-methoxy-d3-phenyl)-2,5-dihydro-3H-pyrazolo[4,3- c]quinolin-3-one [DK-I-56-1]. A mixture of ethyl-4-chloro-7-methoxyquinoline-3-carboxylate DK-I-40-1 (2 g, 7.4 mmol), 4-methoxy-d3-phenylhydrazine DK-I-29-2 (1.25 g, 8.9 mmol), triethylamine (0.90g, 8.9 mmol) and xylenes (16 mL) was heated to reflux (138 ºC) and held at reflux for 2 h. The resulting yellow-orange slurry was cooled to 100 ºC and diluted with ethanol (16 mL). The reaction mixture was then refluxed at 80ºC for 30 min and then cooled to 20-25 ºC. The solids were collected by filtration and washed twice with a 1:1 mixture of ethanol (2.5 mL x 2) and hexanes (2.5 mL x 2) and then washed twice with hexanes (5 mL x 2). The solid was dried to afford the product as a yellow powder DK-I-56-1 (1.5 g, 62.5%)**:** 1H NMR (300 MHz, DMSO) δ 12.60 (s, 1H), 8.66 (s, 1H), 8.10 (t, J = 9.7 Hz, 3H), 7.18 (s, 2H), 7.01 (d, J = 8.4 Hz, 2H), 3.88 (s, 3H); 13C NMR (75 MHz, DMSO) δ 160.73, 160.43, 156.39, 143.09, 139.34, 137.43, 134.08, 124.08, 120.68, 115.80, 114.24, 112.69, 106.87, 102.28, 56.00; LRMS m/z calculated for $C_{18}H_{13}D_3N_3O_3$ (M+H)+ 325.30 found 325.30.

7-Methoxy-d3-2-(4-methoxy-d3-phenyl)-2,5-dihydro-3H-pyrazolo[4,3- c]quinolin-3-one

[DK-I-60-3]. A mixture of ethyl-4-chloro-7-methoxy-d3-quinoline-3- carboxylate DK-I-57-1 (2 g, 7.4 mmol), 4-methoxy-d3-phenylhydrazine DK-I-29-2 (1.26 g, 8.9 mmol), triethylamine (0.90g, 8.9 mmol) and xylenes (16 mL) was heated to reflux (138ºC) and held at reflux for 2 h. The resulting yellow-orange slurry was cooled to 100 ºC and diluted with ethanol (16 mL). The reaction mixture was then refluxed at 80 ºC for 30 min and then cooled to 20-25 ºC. The solids were collected by filtration and washed twice with a 1:1 mixture of ethanol (2.5 mL x 2) and hexanes (2.5 mL x 2) and then washed twice with hexanes (5 mL x 2). The solid was dried to afford the product as a yellow powder DK-I-60-3 (1.2 g, 50.0%)**:** 1H NMR (300 MHz, DMSO) δ 12.57 (s, 1H), 8.65 (s, 1H), 8.10 (t, J = 9.0 Hz, 3H), 7.17 (d, J = 5.7 Hz, 2H), 7.01 (d, J = 9.0 Hz,

2H); 13C NMR (75 MHz, DMSO) δ 161.45, 160.85, 156.21, 143.12, 139.37, 137.48, 134.10, 124.05, 120.69, 115.76, 114.24, 112.68, 106.86, 102.30; LRMS m/z calculated for $C_{18}H_{10}D_6N_3O_3$ (M+H)+ 328.15 found 328.15.

7-Methoxy-d3-2-(3-methoxy-d3-phenyl)-2,5-dihydro-3H-pyrazolo[4,3- c]quinolin-3-one [DK-I-94-1]. A mixture of ethyl-4-chloro-7-methoxy-d3-quinoline-3- carboxylate DK-I-57-1 (2 g, 7.4 mmol), 3-methoxy-d3-phenylhydrazine DK-I-26-3 (1.26 g, 8.9 mmol), triethylamine (0.90g, 8.9 mmol) and xylenes (16 mL) was heated to reflux (138 ºC) and held at reflux for 2 h. The resulting yellow-orange slurry was cooled to 100 ºC and diluted with ethanol (16 mL). The reaction mixture was then refluxed at 80 ºC for 30 min and then cooled to 20-25 ºC. The solids were collected by filtration and washed twice with a 1:1 mixture of ethanol (2.5 mL x 2) and hexanes (2.5 mL x 2) and then washed twice with hexanes (5 mL x 2). The solid was dried to afford the product as a yellow powder DK-I-94-1 (1.5 g, 62.0%)**:** 1H NMR (300 MHz, DMSO) δ 12.62 (s, 1H), 8.66 (s, 1H), 8.13 (d, J = 9.4 Hz, 1H), 7.93 – 7.73 (m, 2H), 7.34 (t, J = 8.2 Hz, 1H), 7.18 (d, J = 6.7 Hz, 2H), 6.74 (d, J = 8.2 Hz, 1H); 13C NMR (75 MHz, DMSO) δ 162.13, 161.02, 159.97, 143.50, 141.73, 139.59, 137.58, 129.94, 124.18, 115.84, 112.56, 111.30, 109.60, 106.83, 104.81, 102.32; LRMS m/z calculated for $C_{18}H_{10}D_6N_3O_3$ (M+H)+ 328.25 found 328.25.

7-Methoxy-d3-2-(2-methoxy-d3-phenyl)-2,5-dihydro-3H-pyrazolo[4,3- c]quinolin-3-one [DK-I-90-1]. A mixture of ethyl-4-chloro-7-methoxy-d3-quinoline-3- carboxylate DK-I-57-1 (2 g, 7.4 mmol), 2-methoxy-d3-phenylhydrazine DK-I-43-3 (1.26 g, 8.9 mmol), triethylamine (0.90g, 8.9 mmol) and xylenes (16 mL) was heated to reflux (138 ºC) and held at reflux for 2 h. The resulting yellow-orange slurry was cooled to 100 ºC and diluted with ethanol (16 mL). The reaction mixture was then refluxed at 80ºC for 30 min and then cooled to 20-25 ºC. The solids were collected by filtration and washed twice with a 1:1 mixture of ethanol (2.5 mL x 2) and

hexanes (2.5 mL x 2) and then washed twice with hexanes (5 mL x 2). The solid was dried to afford the product as a yellow powder DK-I-90-1 (1.8 g, 75.0%): 1H NMR (300 MHz, DMSO) δ 12.47 (s, 1H), 8.57 (s, 1H), 7.99 (d, J = 8.7 Hz, 1H), 7.51 – 7.24 (m, 2H), 7.22 – 6.93 (m, 4H); 13C NMR (75 MHz, DMSO) δ 162.19, 160.63, 155.66, 142.97, 139.04, 137.26, 129.88, 129.67, 128.51, 123.87, 120.65, 115.49, 112.96, 112.91, 105.83, 102.15; LRMS m/z calculated for $C_{18}H_{10}D_6N_3O_3$ (M+H)+ 328.30 found 328.30.

7-Methoxy-2-(2-methoxy-d3-phenyl)-2,5-dihydro-3H-pyrazolo[4,3- c]quinolin-3-one [DK-I-88-1]. A mixture of ethyl-4-chloro-7-methoxy-quinoline-3- carboxylate DK-I-40-1 (2 g, 7.5 mmol), 2-methoxy-d3-phenylhydrazine DK-I-43-3 (1.28 g, 9.0 mmol), triethylamine (0.91g, 9.0 mmol) and xylenes (16 mL) was heated to reflux (138 ºC) and held at reflux for 2 h. The resulting yellow-orange slurry was cooled to 100 ºC and diluted with ethanol (16 mL). The reaction mixture was then refluxed at 80 ºC for 30 min and then cooled to 20-25 ºC. The solids were collected by filtration and washed twice with a 1:1 mixture of ethanol (2.5 mL x 2) and hexanes (2.5 mL x 2) and then washed twice with hexanes (5 mL x 2). The solid was dried to afford the product as a yellow powder DK-I-88-1 (1.6 g, 65.6%): 1H NMR (300 MHz, DMSO) δ 12.46 (d, J = 4.9 Hz, 1H), 8.57 (d, J = 5.8 Hz, 1H), 7.99 (d, J = 8.7 Hz, 1H), 7.40 (t, J = 7.8 Hz, 1H), 7.31 (d, J = 7.6 Hz, 1H), 7.15 (dd, J = 9.7, 6.0 Hz, 3H), 7.03 (t, J = 7.5 Hz, 1H), 3.87 (s, 3H); 13C NMR (75 MHz, DMSO) δ 184.22, 162.19, 160.62, 155.66, 142.95, 139.04, 137.26, 129.88, 129.66, 128.51, 123.88, 120.65, 115.49, 112.97, 112.94, 105.83, 102.15, 55.94; LRMS m/z calculated for $C_{18}H_{13}D_3N_3O_3$ (M+H)+ 325.24 found 325.25.

8-Chloro-2-(4-methoxyphenyl)-2,5-dihydro-3H-pyrazolo[4,3-c]quinolin- 3-one [Comp 11]. A mixture of ethyl-4,6-dichloro-quinoline-3-carboxylate DK-I-35-1 (2 g, 7.4 mmol), 4-methoxyphenylhydrazine hydrochloride (1.55 g, 8.9 mmol), triethylamine (1.80g, 17.8 mmol)

339

and xylenes (16 mL) was heated to reflux (138 ºC) and held at reflux for 2 h. The resulting yellow-orange slurry was cooled to 100 ºC and diluted with ethanol (16 mL). The reaction mixture was then refluxed at 80ºC for 30 min and then cooled to 20-25 ºC. The solids were collected by filtration and washed twice with a 1:1 mixture of ethanol (2.5 mL x 2) and hexanes (2.5 mL x 2) and then washed twice with hexanes (5 mL x 2). The solid was dried to afford the product as a yellow powder Comp 11 (1.7 g, 71.0%)**:** 1H NMR (300 MHz, DMSO) δ 12.95 (d, J = 5.6 Hz, 1H), 8.72 (d, J = 6.2 Hz, 1H), 8.14 (d, J = 2.1 Hz, 1H), 8.08 (d, J = 9.0 Hz, 2H), 7.70 (dt, J = 8.9, 5.5 Hz, 2H), 7.02 (d, J = 9.1 Hz, 2H), 3.79 (s, 3H); 13C NMR (75 MHz, DMSO) δ 161.37, 156.48, 141.97, 139.79, 134.59, 133.87, 131.04, 130.46, 122.08, 121.50, 120.89, 120.48, 114.29, 106.86, 55.71; LRMS m/z calculated for $C_{17}H_{13}ClN_3O_2$ (M+H)+ 326.25 found 326.25.

8-Chloro-2-(4-methoxy-d3-phenyl)-2,5-dihydro-3H-pyrazolo[4,3- c]quinolin-3-one [DK-I-93-1]. A mixture of ethyl-4,6-dichloro-quinoline-3-carboxylate DK-I- 35-1 (2 g, 7.4 mmol), 4-methoxy-d3-phenylhydrazine DK-I-29-2 (1.25 g, 8.9 mmol), triethylamine (0.90g, 8.9 mmol) and xylenes (16 mL) was heated to reflux (138 ºC) and held at reflux for 2 h. The resulting yellow-orange slurry was cooled to 100 ºC and diluted with ethanol (16 mL). The reaction mixture was then refluxed at 80 ºC for 30 min and then cooled to 20-25 ºC. The solids were collected by filtration and washed twice with a 1:1 mixture of ethanol (2.5 mL x 2) and hexanes (2.5 mL x 2) and then washed twice with hexanes (5 mL x 2). The solids was dried to afford the product as a yellow powder DK-I-93- 1 (1.3 g, 53.6%)**:** 1H NMR (300 MHz, DMSO) δ 12.89 (s, 1H), 8.74 (s, 1H), 8.24 – 7.89 (m, 3H), 7.86 – 7.56 (m, 2H), 7.02 (d, J = 8.9 Hz, 2H); 13C NMR (75 MHz, DMSO) δ 161.38, 156.49, 141.98, 139.86, 134.59, 133.84, 131.05, 130.49, 122.09, 121.52, 120.91, 120.49, 114.29, 106.88; LRMS m/z calculated for $C_{17}H_{10}D_3ClN_3O_2$ (M+H)+ 329.15 found 329.15.

8-Chloro-2-(3-methoxyphenyl)-2,5-dihydro-3H-pyrazolo[4,3-c]quinolin- 3-one [LAU 159].

A mixture of ethyl-4,6-dichloro-quinoline-3-carboxylate DK-I-35-1 (2 g, 7.4 mmol), 3-methoxyphenylhydrazine hydrochloride (1.55 g, 8.9 mmol), triethylamine (1.80g, 17.8 mmol) and xylenes (16 mL) was heated to reflux (138 ºC) and held at reflux for 2 h. The resulting yellow-orange slurry was cooled to 100 ºC and diluted with ethanol (16 mL). The reaction mixture was then refluxed at 80 ºC for 30 min and then cooled to 20-25 ºC. The solids were collected by filtration and washed twice with a 1:1 mixture of ethanol (2.5 mL x 2) and hexanes (2.5 mL x 2) and then washed twice with hexanes (5 mL x 2). The solid was dried to afford the product as a yellow powder LAU 159 (0.7 g, 30.0%)**:** 1H NMR (300 MHz, DMSO) δ 12.85 (s, 1H), 8.69 (s, 1H), 8.15 (d, J = 1.9 Hz, 1H), 7.83 (d, J = 8.7 Hz, 2H), 7.70 (dt, J = 9.0, 5.4 Hz, 2H), 7.34 (t, J = 8.1 Hz, 1H), 6.83 – 6.65 (m, 1H), 3.81 (s, 3H); 13C NMR (75 MHz, DMSO) δ 161.99, 159.98, 142.44, 141.52, 140.02, 134.81, 131.11, 130.62, 129.97, 122.17, 121.62, 120.42, 111.47, 110.04, 106.80, 104.96, 55.59; LRMS m/z calculated for $C_{17}H_{13}ClN_3O_2$ (M+H)+ 326.20 found 326.20.

8-Chloro-2-(3-methoxy-d3-phenyl)-2,5-dihydro-3H-pyrazolo[4,3- c]quinolin-3-one [DK-I-59-1]. A mixture of ethyl-4,6-dichloro-quinoline-3-carboxylate DK-I- 35-1 (2 g, 7.4 mmol), 3-methoxy-d3-phenylhydrazine hydrochloride DK-I-26-2 (1.45 g, 8.1 mmol), triethylamine (1.87g, 18.5 mmol) and xylenes (16 mL) was heated to reflux (138 ºC) and held at reflux for 2 h. The resulting yellow-orange slurry was cooled to 100 ºC and diluted with ethanol (16 mL). The reaction mixture was then refluxed at 80 ºC for 30 min and then cooled to 20-25 ºC. The solids were collected by filtration and washed twice with a 1:1 mixture of ethanol (2.5 mL x 2) and hexanes (2.5 mL x 2) and then washed twice with hexanes (5 mL x 2). The solid was dried to afford the product as a yellow powder DK-I-59-1 (2.0 g, 87.0%)**:** 1H NMR (300 MHz, DMSO) δ

12.85 (s, 1H), 8.71 (s, 1H), 8.17 (s, 1H), 8.00 – 7.49 (m, 4H), 7.35 (t, J = 7.7 Hz, 1H), 6.77 (d, J = 7.4 Hz, 1H); 13C NMR (75 MHz, DMSO) δ 162.01, 160.01, 142.48, 141.54, 140.10, 134.76, 131.15, 130.72, 130.01, 122.14, 121.68, 120.45, 111.42, 110.04, 106.87, 104.95; LRMS m/z calculated for $C_{17}H_{10}D_3ClN_3O_2$ (M+H)+ 329.10 found 329.10.

8-Chloro-2-(2-methoxy-d3-phenyl)-2,5-dihydro-3H-pyrazolo[4,3- c]quinolin-3-one [DK-I-87-1]. A mixture of ethyl-4,6-dichloro-quinoline-3-carboxylate DK-I- 35-1 (2 g, 7.4 mmol), 2-methoxy-d3-phenylhydrazine DK-I-43-3 (1.25 g, 8.9 mmol), triethylamine (0.9g, 8.9 mmol) and xylenes (16 mL) was heated to reflux (138 ºC) and held at reflux for 2 h. The resulting yellow-orange slurry was cooled to 100 ºC and diluted with ethanol (16 mL). The reaction mixture was then refluxed at 80 ºC for 30 min and then cooled to 20-25 ºC. The solids were collected by filtration and washed twice with a 1:1 mixture of ethanol (2.5 mL x 2) and hexanes (2.5 mL x 2) and then washed twice with hexanes (5 mL x 2). The solid was dried to afford the product as a yellow powder DK-I-87-1 (1.0 g, 41.0%)**:** 1H NMR (300 MHz, DMSO) δ 12.74 (s, 1H), 8.66 (s, 1H), 8.03 (s, 1H), 7.69 (p, J = 9.0 Hz, 2H), 7.42 (t, J = 7.8 Hz, 1H), 7.32 (d, J = 7.6 Hz, 1H), 7.17 (d, J = 8.3 Hz, 1H), 7.05 (t, J = 7.5 Hz, 1H); 13C NMR (75 MHz, DMSO) δ 162.15, 155.64, 141.87, 139.59, 134.48, 130.83, 130.23, 129.91, 129.85, 128.22, 121.91, 121.40, 120.76, 120.68, 113.00, 105.81; LRMS m/z calculated for $C_{17}H_{10}D_3ClN_3O_2$ (M+H)+ 329.0882 found 329.20.

7-Bromo-2-(4-methoxyphenyl)-2,5-dihydro-3H-pyrazolo[4,3-c]quinolin- 3-one [LAU 463]. A mixture of ethyl-7-bromo-4-chloro-quinoline-3-carboxylate DK-I-52-1 (2 g, 6.3 mmol), 4-methoxyphenylhydrazine hydrochloride (1.33 g, 7.6 mmol), triethylamine (1.54g, 15.3 mmol) and xylenes (16 mL) was heated to reflux (138 ºC) and held at reflux for 2 h. The resulting yellow-orange slurry was cooled to 100 ºC and diluted with ethanol (16 mL). The reaction mixture was then refluxed at 80 ºC for 30 min and then cooled to 20-25 ºC. The solids were

collected by filtration and washed twice with a 1:1 mixture of ethanol (2.5 mL x 2) and hexanes (2.5 mL x 2) and then washed twice with hexanes (5 mL x 2). The solid was dried to afford the product as a yellow powder LAU 463 (1.4 g, 60.0%): 1H NMR (300 MHz, DMSO) δ 12.75 (s, 1H), 8.74 (s, 1H), 8.09 (dd, J = 17.7, 8.8 Hz, 3H), 7.89 (d, J = 1.6 Hz, 1H), 7.68 (dd, J = 8.6, 1.6 Hz, 1H), 7.02 (d, J = 9.1 Hz, 2H), 3.79 (s, 3H); 13C NMR (75 MHz, DMSO) δ 161.37, 156.47, 142.38, 140.08, 136.98, 133.85, 129.65, 124.51, 122.95, 122.22, 120.87, 118.22, 114.31, 107.21, 55.71; LRMS m/z calculated for $C_{17}H_{13}BrN_3O_2$ (M+H)+ 370.0191 found 370.15.

7-Bromo-2-(4-methoxy-d3-phenyl)-2,5-dihydro-3H-pyrazolo[4,3- c]quinolin-3-one [DK-I-58-1]. A mixture of ethyl-7-bromo-4-chloro-quinoline-3-carboxylate DK-I-52-1 (2 g, 6.3 mmol), 4-methoxy-d3-phenylhydrazine DK-I-29-2 (1.08 g, 7.6 mmol), triethylamine (0.77g, 7.6 mmol) and xylenes (16 mL) was heated to reflux (138 ºC) and held at reflux for 2 h. The resulting yellow-orange slurry was cooled to 100 ºC and diluted with ethanol (16 mL). The reaction mixture was then refluxed at 80 ºC for 30 min and then cooled to 20-25 ºC. The solids were collected by filtration and washed twice with a 1:1 mixture of ethanol (2.5 mL x 2) and hexanes (2.5 mL x 2) and then washed twice with hexanes (5 mL x 2). The solid was dried to afford the product as a yellow powder DK-I-58-1 (1.0 g, 42.0%): 1H NMR (300 MHz, DMSO) δ 12.75 (s, 1H), 8.74 (d, J = 4.9 Hz, 1H), 8.09 (dd, J = 17.8, 8.7 Hz, 3H), 7.88 (s, 1H), 7.69 (d, J = 8.4 Hz, 1H), 7.01 (d, J = 8.8 Hz, 2H); 13C NMR (75 MHz, DMSO) δ 161.35, 156.49, 141.88, 140.06, 136.95, 133.83, 129.65, 124.51, 122.93, 122.18, 120.86, 118.22, 114.24, 107.22; LRMS m/z calculated for $C_{17}H_{10}D_3BrN_3O_2$ (M+H)+ 373.0377 found 373.05.

7-Bromo-2-(3-methoxy-d3-phenyl)-2,5-dihydro-3H-pyrazolo[4,3- c]quinolin-3-one [DK-I-92-1]. A mixture of ethyl-7-bromo-4-chloro-quinoline-3-carboxylate DK-I-52-1 (1.5 g, 4.8 mmol), 3-methoxy-d3-phenylhydrazine DK-I-26-3 (0.81 g, 5.7 mmol), triethylamine (0.58g, 5.7

mmol) and xylenes (12 mL) was heated to reflux (138 ºC) and held at reflux for 2 h. The resulting yellow-orange slurry was cooled to 100 ºC and diluted with ethanol (12 mL). The reaction mixture was then refluxed at 80 ºC for 30 min and then cooled to 20-25 ºC. The solids were collected by filtration and washed twice with a 1:1 mixture of ethanol (2.5 mL x 2) and hexanes (2.5 mL x 2) and then washed twice with hexanes (5 mL x 2). The solid was dried to afford the product as a yellow powder DK-I-92-1 (0.7 g, 40.0%)**:** 1H NMR (300 MHz, DMSO) δ 12.78 (s, 1H), 8.76 (s, 1H), 8.15 (d, J = 8.5 Hz, 1H), 7.95 – 7.76 (m, 3H), 7.71 (d, J = 8.6 Hz, 1H), 7.35 (t, J = 8.2 Hz, 1H), 6.76 (d, J = 8.3 Hz, 1H); 13C NMR (75 MHz, DMSO) δ 162.00, 160.00, 142.81, 141.51, 140.33, 137.11, 130.03, 129.75, 124.65, 123.22, 122.26, 118.16, 111.39, 109.98, 107.20, 104.92; LRMS m/z calculated for $C_{17}H_{10}D_3BrN_3O_2$ (M+H)+ 373.0377 found 373.10.

7-Bromo-2-(2-methoxy-d3-phenyl)-2,5-dihydro-3H-pyrazolo[4,3- c]quinolin-3-one [DK-I-89-1]. A mixture of ethyl-7-bromo-4-chloro-quinoline-3-carboxylate DK-I-52-1 (2 g, 6.3 mmol), 2-methoxy-d3-phenylhydrazine DK-I-43-3 (1.08 g, 7.6 mmol), triethylamine (0.77g, 7.6 mmol) and xylenes (16 mL) was heated to reflux (138 ºC) and held at reflux for 2 h. The resulting yellow-orange slurry was cooled to 100 ºC and diluted with ethanol (16 mL). The reaction mixture was then refluxed at 80 ºC for 30 min and then cooled to 20-25 ºC. The solids were collected by filtration and washed twice with a 1:1 mixture of ethanol (2.5 mL x 2) and hexanes (2.5 mL x 2) and then washed twice with hexanes (5 mL x 2). The solid was dried to afford the product as a yellow powder DK-I-89-1 (1.2 g, 50.6%)**:** 1H NMR (300 MHz, DMSO) δ 12.60 (s, 1H), 8.64 (d, J = 16.3 Hz, 1H), 8.00 (d, J = 8.5 Hz, 1H), 7.86 (s, 1H), 7.64 (d, J = 8.5 Hz, 1H), 7.41 (t, J = 7.8 Hz, 1H), 7.32 (d, J = 7.7 Hz, 1H), 7.17 (d, J = 8.3 Hz, 1H), 7.04 (t, J = 7.5 Hz, 1H); 13C NMR (75 MHz, DMSO) δ 162.14, 158.75, 155.64, 142.23, 139.79, 136.89, 129.84,

129.45, 128.23, 124.36, 122.64, 122.04, 120.69, 118.50, 112.99, 106.18; LRMS m/z calculated for $C_{17}H_{10}D_3BrN_3O_2$ (M+H)+ 373.0377 found 373.10.

8-Methoxy-d3-2-(4-methoxy-d3-phenyl)-2,5-dihydro-3H-pyrazolo[4,3- c]quinolin-3-one [DK-I-95-3]. A mixture of ethyl-4-chloro-6-methoxy-d3-quinoline-3- carboxylate DK-I-73-2 (2 g, 7.4 mmol), 4-methoxy-d3-phenylhydrazine DK-I-29-2 (1.26 g, 8.9 mmol), triethylamine (0.90g, 8.9 mmol) and xylenes (16 mL) was heated to reflux (138 ºC) and held at reflux for 2 h. The resulting yellow-orange slurry was cooled to 100 ºC and diluted with ethanol (16 mL). The reaction mixture was then refluxed at 80 ºC for 30 min and then cooled to 20-25 ºC. The solids were collected by filtration and washed twice with a 1:1 mixture of ethanol (2.5 mL x 2) and hexanes (2.5 mL x 2) and then washed twice with hexanes (5 mL x 2). The solid was dried to afford the product as a yellow powder DK-I-95-3 (0.9 g, 37.0%)**:** 1H NMR (300 MHz, DMSO) δ 12.77 (s, 1H), 8.64 (s, 1H), 8.11 (d, J = 8.8 Hz, 2H), 7.68 (d, J = 9.1 Hz, 1H), 7.57 (s, 1H), 7.28 (d, J = 9.1 Hz, 1H), 7.02 (d, J = 8.8 Hz, 2H); 13C NMR (75 MHz, DMSO) δ 161.59, 157.98, 156.34, 143.00, 138.11, 134.10, 130.13, 121.70, 120.92, 120.50, 119.95, 114.23, 105.70, 102.96; LRMS m/z calculated for $C_{18}H_{10}D_6N_3O_3$ (M+H)+ 328.1569 found 328.25.

8-Methoxy-d3-2-(3-methoxy-d3-phenyl)-2,5-dihydro-3H-pyrazolo[4,3- c]quinolin-3-one [DK-I-97-1]. A mixture of ethyl-4-chloro-6-methoxy-d3-quinoline-3- carboxylate DK-I-73-2 (2 g, 7.4 mmol), 3-methoxy-d3-phenylhydrazine DK-I-26-3 (1.26 g, 8.9 mmol), triethylamine (0.90g, 8.9 mmol) and xylenes (16 mL) was heated to reflux (138 ºC) and held at reflux for 2 h. The resulting yellow-orange slurry was cooled to 100 ºC and diluted with ethanol (16 mL). The reaction mixture was then refluxed at 80 ºC for 30 min and then cooled to 20-25 ºC. The solids were collected by filtration and washed twice with a 1:1 mixture of ethanol (2.5 mL x 2) and hexanes (2.5 mL x 2) and then washed twice with hexanes (5 mL x 2). The solid was dried to

afford the product as a yellow powder DK-I-97-1 (1.8 g, 74.0%)**:** 1H NMR (300 MHz, DMSO) δ

12.80 (s, 1H), 8.65 (s, 1H), 7.99 – 7.80 (m, 2H), 7.67 (d, J = 9.1 Hz, 1H), 7.59 (s, 1H), 7.41 –

7.21 (m, 2H), 6.76 (d, J = 8.2 Hz, 1H); 13C NMR (75 MHz, DMSO) δ 162.25, 159.98, 158.04,

143.42, 141.76, 138.36, 130.26, 129.94, 121.73, 120.45, 120.10, 111.53, 109.64, 105.70, 105.11,

103.16; LRMS m/z calculated for $C_{18}H_{10}D_6N_3O_3$ (M+H)+ 328.1569 found 328.30.

8-Methoxy-d3-2-(2-methoxy-d3-phenyl)-2,5-dihydro-3H-pyrazolo[4,3- c]quinolin-3-one

[DK-I-98-1]. A mixture of ethyl-4-chloro-6-methoxy-d3-quinoline-3- carboxylate DK-I-73-2 (2

g, 7.4 mmol), 2-methoxy-d3-phenylhydrazine DK-I-43-3 (1.26 g, 8.9 mmol), triethylamine

(0.90g, 8.9 mmol) and xylenes (16 mL) was heated to reflux (138 ºC) and held at reflux for 2 h.

The resulting yellow-orange slurry was cooled to 100 ºC and diluted with ethanol (16 mL). The

reaction mixture was then refluxed at 80 ºC for 30 min and then cooled to 20-25 ºC. The solids

were collected by filtration and washed twice with a 1:1 mixture of ethanol (2.5 mL x 2) and

hexanes (2.5 mL x 2) and then washed twice with hexanes (5 mL x 2). The solid was dried to

afford the product as a yellow powder DK-I-98-1 (0.5 g, 20.0%)**:** 1H NMR (300 MHz, DMSO)

δ 12.65 (s, 1H), 8.57 (s, 1H), 7.65 (d, J = 9.1 Hz, 1H), 7.54 – 7.28 (m, 3H), 7.28 – 7.21 (m, 1H),

7.16 (d, J = 8.3 Hz, 1H), 7.05 (t, J = 7.5 Hz, 1H); 13C NMR (75 MHz, DMSO) δ 162.38, 157.83,

155.76, 142.92, 137.98, 130.05, 129.94, 129.83, 128.54, 121.50, 120.75, 120.65, 119.64, 112.91,

104.61, 102.88; LRMS m/z calculated for $C_{18}H_{10}D_6N_3O_3$ (M+H)+ 328.1569 found 328.30.

7-Methoxy-2-(6-methoxypyridin-3-yl)-2,5-dihydro-3H-pyrazolo[4,3- c]quinolin-3-one [DK-

II-13-1]. A mixture of ethyl-4-chloro-7-methoxy-quinoline-3- carboxylate DK-I-40-1 (2 g, 7.5

mmol), 5-hydrazinyl-2-methoxypyridine DK-I-82-3 (1.26 g, 9.0 mmol), triethylamine (0.91g, 9.0

mmol) and xylenes (16 mL) was heated to reflux (138 ºC) and held at reflux for 2 h. The

resulting yellow-orange slurry was cooled to 100 ºC and diluted with ethanol (16 mL). The

reaction mixture was then refluxed at 80 ºC for 30 min and then cooled to 20-25 ºC. The solids were collected by filtration and washed twice with a 1:1 mixture of ethanol (2.5 mL x 2) and hexanes (2.5 mL x 2) and then washed twice with hexanes (5 mL x 2). The solid was dried to afford the product as a yellow powder DK-II-13-1 (1.2 g, 49.0%)**:** 1H NMR (300 MHz, DMSO) δ 12.65 (s, 1H), 8.92 (d, J = 2.4 Hz, 1H), 8.68 (s, 1H), 8.43 (dd, J = 9.0, 2.6 Hz, 1H), 8.24 – 7.91 (m, 1H), 7.29 – 7.02 (m, 2H), 6.92 (d, J = 9.0 Hz, 1H), 3.88 (s, 6H); 13C NMR (75 MHz, DMSO) δ 161.74, 160.98, 160.43, 143.86, 139.71, 137.45, 137.37, 131.88, 130.77, 124.13, 115.94, 112.59, 110.56, 106.22, 102.30, 56.00, 53.71; LRMS m/z calculated for $C_{17}H_{15}N_4O_3$ (M+H)+ 323.1144 found 323.25.

7-Methoxy-d3-2-(6-methoxypyridin-3-yl)-2,5-dihydro-3H-pyrazolo[4,3- c]quinolin-3-one [DK-I-86-1]. A mixture of ethyl-4-chloro-7-methoxy-d3-quinoline-3- carboxylate DK-I-57-1 (2 g, 7.4 mmol), 5-hydrazinyl-2-methoxypyridine DK-I-82-3 (1.24 g, 8.9 mmol), triethylamine (0.90 g, 8.9 mmol) and xylenes (16 mL) was heated to reflux (138 ºC) and held at reflux for 2 h. The resulting yellow-orange slurry was cooled to 100 ºC and diluted with ethanol (16 mL). The reaction mixture was then refluxed at 80 ºC for 30 min and then cooled to 20-25 ºC. The solids were collected by filtration and washed twice with a 1:1 mixture of ethanol (2.5 mL x 2) and hexanes (2.5 mL x 2) and then washed twice with hexanes (5 mL x 2). The solid was dried to afford the product as a yellow powder DK-I-86-1 (1.0 g, 41.0%)**:** 1H NMR (300 MHz, DMSO) δ 12.69 (s, 1H), 8.92 (s, 1H), 8.69 (s, 1H), 8.43 (d, J = 9.0 Hz, 1H), 8.12 (d, J = 9.4 Hz, 1H), 7.18 (s, 2H), 6.92 (d, J = 9.0 Hz, 1H), 3.88 (s, 3H); 13C NMR (75 MHz, DMSO) δ 161.75, 161.01, 160.44, 143.88, 139.73, 137.46, 137.39, 131.88, 130.79, 124.15, 115.96, 112.57, 110.58, 106.22, 102.31, 53.72; LRMS m/z calculated for $C_{17}H_{12}D_3N_4O_3$ (M+H)+ 326.1330 found 326.20.

7-Methoxy-2-(6-methoxy-d3-pyridin-3-yl)-2,5-dihydro-3H-pyrazolo[4,3- c]quinolin-3-one [DK-II-60-1]. A mixture of ethyl-4-chloro-7-methoxy-quinoline-3- carboxylate DK-I-40-1 (2 g, 7.5 mmol), 5-hydrazinyl-2-methoxy-d3-pyridine DK-II-56-1 (1.28 g, 9.0 mmol), triethylamine (0.91 g, 9.0 mmol) and xylenes (16 mL) was heated to reflux (138 ºC) and held at reflux for 2 h. The resulting yellow-orange slurry was cooled to 100 ºC and diluted with ethanol (16 mL). The reaction mixture was then refluxed at 80 ºC for 30 min and then cooled to 20-25 ºC. The solids were collected by filtration and washed twice with a 1:1 mixture of ethanol (2.5 mL x 2) and hexanes (2.5 mL x 2) and then washed twice with hexanes (5 mL x 2). The solid was dried to afford the product as a yellow powder DK-II-60-1 (1.2 g, 49.0%)**:** 1H NMR (300 MHz, DMSO) δ 12.68 (s, 1H), 8.91 (d, J = 2.1 Hz, 1H), 8.68 (s, 1H), 8.42 (dd, J = 9.0, 2.4 Hz, 1H), 8.16 – 8.03 (m, 1H), 7.18 (d, J = 5.9 Hz, 2H), 6.92 (d, J = 9.0 Hz, 1H), 3.87 (s, 3H); 13C NMR (75 MHz, DMSO) δ 161.74, 160.98, 160.44, 143.85, 139.69, 137.44, 137.39, 131.86, 130.77, 124.13, 115.94, 112.58, 110.54, 106.22, 102.29, 56.00; LRMS m/z calculated for $C_{17}H_{12}D_3N_4O_3$ (M+H)+ 326.1330 found 326.30.

8-Chloro-2-(6-methoxypyridin-3-yl)-2,5-dihydro-3H-pyrazolo[4,3- c]quinolin-3-one [DK-II-18-1]. A mixture of ethyl-4,6-dichloro-7-methoxy-3-carboxylate DKI- 35-1 (2 g, 7.4 mmol), 5-hydrazinyl-2-methoxypyridine DK-I-82-3 (1.24 g, 8.9 mmol), triethylamine (0.90 g, 8.9 mmol) and xylenes (16 mL) was heated to reflux (138 ºC) and held at reflux for 2 h. The resulting yellow-orange slurry was cooled to 100 ºC and diluted with ethanol (16 mL). The reaction mixture was then refluxed at 80 ºC for 30 min and then cooled to 20-25 ºC. The solids were collected by filtration and washed twice with a 1:1 mixture of ethanol (2.5 mL x 2) and hexanes (2.5 mL x 2) and then washed twice with hexanes (5 mL x 2). The solid was dried to afford the product as a yellow powder DK-II-18-1 (1.0 g, 41.0%)**:** 1H NMR (300 MHz, DMSO) δ 12.96 (s,

1H), 8.92 (d, J = 2.6 Hz, 1H), 8.77 (s, 1H), 8.42 (dd, J = 8.9, 2.6 Hz, 1H), 8.14 (s, 1H), 7.89 –

7.60 (m, 2H), 6.93 (d, J = 9.0 Hz, 1H), 3.89 (s, 3H); 13C NMR (75 MHz, DMSO) δ 161.62,

160.64, 142.70, 140.12, 137.57, 134.58, 131.66, 131.15, 130.92, 130.64, 122.11, 121.58, 120.38,

110.59, 106.25, 53.74; LRMS m/z calculated for $C_{16}H_{12}ClN_4O_2$ (M+H)+ 327.0649 found 327.25.

8-Chloro-2-(6-methoxy-d3-pyridin-3-yl)-2,5-dihydro-3H-pyrazolo[4,3- c]quinolin-3-one

[DK-II-59-1]. A mixture of ethyl-4,6-dichloro-quinoline-3-carboxylate DKI- 35-1 (2 g, 7.4

mmol), 5-hydrazinyl-2-methoxy-d3-pyridine DK-II-56-1 (1.26 g, 8.9 mmol), triethylamine (0.90

g, 8.9 mmol) and xylenes (16 mL) was heated to reflux (138 ºC) and held at reflux for 2 h. The

resulting yellow-orange slurry was cooled to 100 ºC and diluted with ethanol (16 mL). The

reaction mixture was then refluxed at 80 ºC for 30 min and then cooled to 20-25 ºC. The solids

were collected by filtration and washed twice with a 1:1 mixture of ethanol (2.5 mL x 2) and

hexanes (2.5 mL x 2) and then washed twice with hexanes (5 mL x 2). The solid was dried to

afford the product as a yellow powder DK-II-59-1 (1.4 g, 57.0%)**:** 1H NMR (300 MHz, DMSO)

δ 12.92 (s, 1H), 8.90 (d, J = 1.7 Hz, 1H), 8.74 (d, J = 9.1 Hz, 1H), 8.40 (dd, J = 8.9, 2.4 Hz, 1H),

8.09 (s, 1H), 7.78 – 7.61 (m, 2H), 6.90 (d, J = 8.9 Hz, 1H); 13C NMR (75 MHz, DMSO) δ

161.60, 160.63, 142.67, 140.06, 137.55, 134.55, 131.64, 131.13, 130.87, 130.60, 122.07, 121.56,

120.37, 110.55, 106.26; LRMS m/z calculated for $C_{16}H_9D_3ClN_4O_2$ (M+H)+ 330.25 found

330.25.

7-Bromo-2-(6-methoxypyridin-3-yl)-2,5-dihydro-3H-pyrazolo[4,3- c]quinolin-3-one [DK-II-

48-1]. A mixture of ethyl-7-bromo-4-chloroquinoline-3-carboxylate DK-I-52-1 (2 g, 6.3 mmol),

5-hydrazinyl-2-methoxypyridine DK-I-82-3 (1.06 g, 7.6 mmol), triethylamine (0.77 g, 7.6 mmol)

and xylenes (16 mL) was heated to reflux (138 ºC) and held at reflux for 2 h. The resulting

yellow-orange slurry was cooled to 100 ºC and diluted with ethanol (16 mL). The reaction

mixture was then refluxed at 80 ºC for 30 min and then cooled to 20-25 ºC. The solids were collected by filtration and washed twice with a 1:1 mixture of ethanol (2.5 mL x 2) and hexanes (2.5 mL x 2) and then washed twice with hexanes (5 mL x 2). The solid was dried to afford the product as a yellow powder DK-II-48-1 (1.6 g, 67.0%)**:** 1H NMR (300 MHz, DMSO) δ 12.81 (s, 1H), 10.29 – 10.27 (m, 1H), 8.89 (s, 1H), 8.75 (s, 1H), 8.40 (dd, J = 8.9, 2.2 Hz, 1H), 8.09 (d, J = 8.5 Hz, 1H), 7.86 (s, 1H), 7.68 (d, J = 8.1 Hz, 1H), 6.91 (d, J = 8.9 Hz, 1H), 3.88 (s, 3H); 13C NMR (75 MHz, DMSO) δ 161.63, 160.61, 143.11, 140.38, 137.53, 136.95, 131.65, 130.88, 129.74, 124.54, 123.15, 122.26, 118.12, 110.61, 106.58, 53.74; LRMS m/z calculated for $C_{16}H_{12}BrN_4O_2$ (M+H)+ 371.19 found 371.20.

7-Bromo-2-(6-methoxy-d3-pyridin-3-yl)-2,5-dihydro-3H-pyrazolo[4,3- c]quinolin-3-one [DK-II-58-1]. A mixture of ethyl-7-bromo-4-chloroquinoline-3-carboxylate DK-I-52-1 (1.20 g, 3.8 mmol), 5-hydrazinyl-2-methoxy-d3-pyridine DK-II-56-1 (0.65 g, 4.6 mmol), triethylamine (0.46 g, 4.6 mmol) and xylenes (16 mL) was heated to reflux (138 ºC) and held at reflux for 2 h. The resulting yellow-orange slurry was cooled to 100 ºC and diluted with ethanol (16 mL). The reaction mixture was then refluxed at 80 ºC for 30 min and then cooled to 20-25 ºC. The solids were collected by filtration and washed twice with a 1:1 mixture of ethanol (2.5 mL x 2) and hexanes (2.5 mL x 2) and then washed twice with hexanes (5 mL x 2). The solid was dried to afford the product as a yellow powder DK-II-58-1 (0.5 g, 35.0%)**:** 1H NMR (300 MHz, DMSO) δ 12.77 (s, 1H), 8.88 (d, J = 2.3 Hz, 1H), 8.75 (d, J = 8.4 Hz, 1H), 8.39 (dd, J = 8.9, 2.5 Hz, 1H), 8.07 (d, J = 8.5 Hz, 1H), 7.83 (s, 1H), 7.65 (d, J = 8.6 Hz, 1H), 6.90 (d, J = 8.9 Hz, 1H); 13C NMR (75 MHz, DMSO) δ 161.60, 160.60, 143.08, 140.33, 137.51, 136.93, 131.63, 130.83, 129.70, 124.50, 123.11, 122.24, 118.10, 110.56, 106.58; LRMS m/z calculated for $C_{16}H_9D_3BrN_4O_2$ (M+H)+ 374.19 found 374.20.

7-Methoxy(d3)-2-(phenyl)-2H-pyrazolo[4,3-c]quinolin-3(5H)-one [RV-I- 37]. A mixture of ethyl-4-chloro-7-methoxy-d3-quinoline-3-carboxylate DK-I-57-1 (0.01 mol, 0.324g), phenylhydrazine hydrochloride (0.012 mol, 0.172g) and TEA (0.012 mol, 0.12 g) in 40 mL xylene was refluxed for 4h, cooled to room temperature. The precipitated compound was collected by filtration. The compound was recrystallized from methanol as a yellow colored compound RV-I-37, yield 75 %, 0.22 g**:** mp > 260°C dec. 1H NMR (500 MHz, MeOD) 8.5 (s, 1H), 8.236(d, 1H, J=9.0Hz), 8.102(d, 2H, J= 9.0), 7.492-7.236(m, 5H,); 13C (125 MHz, MeOD) 161.4, 160.8, 156.2, 143.1, 139.3, 137.4, 137.1, 134.1, 124.0, 120.6, 115.8, 114.2, 112.6, 106.8, 102.2, 78.5, 55.69; HRMS m/z calculated for $C_{17}H_{11}D_3N_3O_2$ 295.1274 found 295.1272.

2-(4-Methoxyphenyl)-2H-pyrazolo[4,3-c][1,5]naphthyridin-3(5H)-one [RV-I-071]. A mixture of ethyl 4-chloro-1,5-naphthyridine-3-carboxylate (0.01 mol, 0.236 g), 4-methoxyphenylhydrazine hydrochloride (0.012 mol, 0.153g), triethylamine (0.012mol, 0.12 g) and xylenes (40 mL) was heated to reflux (138ºC) and held at reflux for 4 hours. The resulting yellow-orange slurry was cooled to room temperature and the solids were collected by filtration. The solids washed twice with 20 ml water. Drying of the solid afforded the product as a yellow powder RV-I-071 (0.268 g)**:** 1H NMR (300 MHz, DMSO) δ 12.9 (s, 1H), 8.79 (s, 1H), 8.77 (s, 1H), 8.11-8.10(d, 2H, J= 9.0), 8.08 (s, 1H), 7.70-7.68 (m, 1H), 7.05- 7.03(d, 2H, J= 9.0), 3.80 (s, 3H); 13C NMR (75 MHz, DMSO) δ 161.49, 160.85, 156.56, 148.79.11, 143.06, 139.81, 136.60, 133.97,132.95, 127.93, 125.21, 120.91, 114.33, 109.42, 55.72; HRMS m/z calculated for $C_{16}H_{12}N_4O_2$ (M+H)+ 293.1039 found 293.1037.

8-Bromo-6-fluoro-2-(4-methoxyphenyl)-2H-pyrazolo[4,3-c]quinolin- 3(5H)-one [MM-I-03]. A mixture of 0.5 g (1.5 mmol) of ethyl 6-bromo-4-chloro-8- fluoroquinoline-3-carboxylate MM-I-02, 0.31 g (1.8 mmol) of (4-methoxyphenyl)hydrazine hydrochloride and Et3N (2 mL) was

placed in a flask with xylene (8 mL) and heated for 4 h. The reaction was cooled at rt and

filtered. The solid was washed several times with hexane and water. Then, the solid was

dissolved in a base solution 3 N NaOH and stirred for 15 min. The base solution was neutralized

with 3 N HCl and filtrated. The solid was recrystallized using hot ethanol and dried in vacuo,

affording a yellow solid MM-I-03 (0.28 g, 48%): mp 333-334°C; 1H NMR (300 MHz, DMSO) δ

8.51 (s, 1H; H-6), 8.09 (s, 1H; H-8), 8.03 (d, J = 8.9 Hz, 2H; H-15 and H-19), 7.89 (d, J = 10.5

Hz, 1H; H-2), 7.01 (d, J = 9.0 Hz, 2H; H-16 and H-18), 3.78 (s, 3H; H-24); 13C NMR (75 MHz,

DMSO) δ 161.11 (s), 156.65 (s), 140.93 (s), 139.49 (s), 133.57 (s), 124.37 (s), 124.19 (s), 122.02

(s), 121.00 (s), 120.61 (s), 119.08 (q, J = 3.3, 1.9 Hz), 118.82 (s), 118.34 (s), 118.22 (s), 114.32

(s), 107.83 (s), 55.73 (s); HRMS m/z calculated for $C_{17}H_{11}N_3O_2FBr$ 388.0091 found 388.0094.

2-(4-Methoxyphenyl)-7-(trifluoromethyl)-2H-pyrazolo[4,3-c]quinolin- 3(5H)-one [MM-I-06]. Treatment of ethyl 4-chloro-7-(trifluoromethyl)quinoline-3-carboxylate MM-I-05 (0.5 g, 1.5

mmol) with (4-methoxyphenyl)hydrazine hydrochloride (0.57 g, 1.8 mmol) and TEA (2 mL) in 8

mL of xylene under reflux for 4 h afforded the corresponding product. The reaction was cooled

at rt and filtered. The solid was washed several times with hexane and water. An acid-base

crystallization was needed to remove the triethylamine salt, and it afforded yellow crystals MM-I-06 (0.51 g, 82 %): mp 315 – 316°C; 1H NMR (300 MHz, DMSO) δ 12.93 (s, 1H; H-7), 8.84

(s, 1H; H-8), 8.40 (d, J = 8.4 Hz, 1H; H-6), 8.08 (d, J = 9.1 Hz, 2H; H-15 and H-19), 8.03 (s, 1H;

H-3), 7.83 (d, J = 8.1 Hz, 1H; H-1), 7.03 (d, J = 9.1 Hz, 2H; H-16 and H-18), 3.79 (s, 3H; H-22);

13C NMR (75 MHz, DMSO) δ 161.38 (s), 156.60 (s), 141.99 (s), 140.79 (s), 135.83 (s), 133.75

(s), 130.23 (s), 129.80 (s), 125.96 (s), 124.05 (s), 122.66 (q), 122.35 (s), 122.12 (s), 121.00 (s),

117.21 (q), 114.34 (s), 107.42 (s), 55.71 (s); HRMS m/z calculated for $C_{18}H_{12}N_3O_2F_3$ 360.0954

found 360.0943.

2-(4-Chlorophenyl)-7-(trifluoromethyl)-2H-pyrazolo[4,3-c]quinolin- 3(5H)-one [MM-I-08].

The reaction of 0.5 g (1.6 mmol) of ethyl 4-chloro-7-(trifluoromethyl)quinoline-3-carboxylate MM-I-05 with (4-chlorophenyl)hydrazine hydrochloride (0.47 g, 3.2 mmol) and 2 mL of Et3N in 8 mL of xylene at reflux for overnight afforded the product. The recrystallization of solid gave yellow crystals MM-I-08 (0.44 g, 75%)**:** mp 346 – 347°C; 1H NMR (300 MHz, DMSO) δ 12.98 (s, 1H; H-7), 8.84 (s, 1H; H-8), 8.34 (d, J = 8.3 Hz, 1H; H-1), 8.21 (d, J = 8.9 Hz, 2H; H-15 and H-19), 7.98 (s, 1H; H-3), 7.80 (d, J = 8.3 Hz, 1H; H-6), 7.47 (d, J = 8.9 Hz, 2H; H-18 and H-16); 13C NMR (75 MHz, DMSO) δ 161.92 (s), 142.71 (s), 141.03 (s), 139.11 (s), 135.84 (s), 130.51 (s), 130.08 (s), 129.08 (s), 128.45 (s), 125.88 (s), 124.11 (s), 122.72 (q), 122.27 (s), 121.92 (s), 120.40 (s), 117.15 (q), 107.15 (s). HRMS m/z calculated for $C_{17}H_9N_3OF_3Cl$ 364.0459 found 364.0453.

2-(4-Nitrophenyl)-7-(trifluoromethyl)-2H-pyrazolo[4,3-c]quinolin-3(5H)- one [MM-I-09]. In a flask containing ethyl 4-chloro-7-(trifluoromethyl)quinoline-3-carboxylate MM-I-05 (0.2 g, 0.66 mmol), (4-nitrophenyl)hydrazine (0.25 g, 1.3 mmol) and xylene (8 mL), was added 2 mL of Et3N and the flask was immediately placed in oil bath previously heated at 150°C. After 4 h of heating, the solid was collected by filtration and washed with hexane and water. The same procedure of acid-base crystallization was used affording reddish solid MM-I-09 (0.035 g, 15 %)**:** mp > 350°C; 1H NMR (300 MHz, DMSO) δ 13.09 (s, 1H; H-7), 8.89 (s, 1H; H-8), 8.41 (d, J = 9.1 Hz, 2H; H-16 and H-18), 8.35 (d, J = 8.4 Hz, 1H; H-6), 8.27 (d, J = 9.1 Hz, 2H; H-15 and H-19), 7.95 (s, 1H; H-3), 7.82 (d, J = 8.2 Hz, 1H; H-1); HRMS m/z calculated for $C_{17}H_9N_4O_3F_3$ 375.0700 found 375.0695.

2-(4-(Trifluoromethoxy)phenyl)-7-(trifluoromethyl)-2H-pyrazolo[4,3- c]quinolin-3(5H)-one [MM-I-10]. A mixture of ethyl 4-chloro-7-(trifluoromethyl)quinoline-3- carboxylate MM-I-05

(0.3 g, 1 mmol) with (4-(trifluoromethoxy)phenyl)hydrazine hydrochloride (0.48 g, 2 mmol) and Et3N (2 mL) in 8 mL of xylene was heated at reflux for overnight. The solid was collected by filtration and washed with hexane and water. The solid was dissolved in 3 N NaOH solution (10 mL) and precipitated with 3 N HCl (11 mL) solution. Then, a recrystallization using 15 mL EtOH and 2 mL of water was used and afforded yellow crystals MM-I-10 (0.25 g, 60%)**:** mp 286 – 287°C; 1H NMR (300 MHz, DMSO) δ 8.86 (s, 1H; H-8), 8.36 (d, J = 8.4 Hz, 1H; H-6), 8.29 (d, J = 9.0 Hz, 2H; H-15 and H-19), 7.99 (s, 1H; H- 3), 7.81 (d, J = 8.3 Hz, 1H; H-1), 7.43 (d, J = 8.8 Hz, 2H; H-16 and H-18); 13C NMR (75 MHz, DMSO) δ 161.98 (s), 144.85 (s), 142.85 (s), 141.22 (s), 139.27 (s), 135.96 (s), 130.54 (s), 130.11 (s), 124.12 (s), 122.78 (s), 122.29 (q, J = 2.8 Hz), 121.98 (s), 120.37 (s), 117.25 (q, J = 8.4, 4.7 Hz), 107.07 (s); HRMS m/z calculated for $C_{18}H_9N_3O_2F_6$ 414.0672 found 414.0674.

2-(4-Fluorophenyl)-7-(trifluoromethyl)-2H-pyrazolo[4,3-c]quinolin- 3(5H)-one [MM-I-11].
Treatment of ethyl 4-chloro-7-(trifluoromethyl)quinoline-3-carboxylate MM-I-05 (0.2 g, 0.66 mmol) with (4-fluorophenyl)hydrazine hydrochloride (0.22 g, 1.3 mmol) and Et3N (2 mL) in 8 mL of xylene under reflux for overnight afforded the corresponding product. The yellow crystals MM-I-11 (0.15 g, 65%) were obtained by recrystallization with hot EtOH**:** mp 296 – 297 °C; 1H NMR (300 MHz, DMSO) δ 12.98 (s, 11H; H-7), 8.84 (s, 11H; H-8), 8.36 (d, J = 8.3 Hz, 1H; H-6), 8.19 (dd, J = 9.0, 5.1 Hz, 2H; H-15 and H-19), 8.00 (s, 1H; H-3), 7.81 (d, J = 8.4 Hz, 1H; H-1), 7.27 (t, J = 8.9 Hz, 2H; H-16 and H-18); 13C NMR (75 MHz, DMSO) δ 161.69 (s), 160.85 (s), 157.66 (s), 142.41 (s), 140.94 (s), 136.74 (s), 135.78 (s), 130.21 (q), 124.09 (d), 124.07 (s), 122.73 (q), 121.99 (s), 120.97 (d), 117.14 (q), 115.95 (s), 115.65 (s), 107.21 (s); HRMS m/z calculated for $C_{17}H_9N_3OF_4$ 348.0755 found 348.0766.

2-(3-Methoxyphenyl)-7-(trifluoromethyl)-2H-pyrazolo[4,3-c]quinolin- 3(5H)-one [MM-I-12]. The reaction of 0.5 g (1.6 mmol) of ethyl 4-chloro-7- (trifluoromethyl)quinoline-3-carboxylate MM-I-05 with (3-methoxyphenyl)hydrazine hydrochloride (0.575 g, 4.1 mmol) and 2 mL of Et3N in 15 mL of xylene at reflux for overnight afforded the product. Recrystallization gave yellow crystals MM-I-12 (0.762 g, 46 %)**:** mp > 350 °C; 1H NMR (500 MHz, DMSO) δ 8.85 (s, 1H, H-8), 8.43 (d, J = 8.3 Hz, 1H, H-6), 8.04 (s, 1H, H-15), 7.88 – 7.80 (m, 3H, H-1 H-3 and H-19), 7.37 (t, J = 8.2 Hz, 1H, H-18), 6.79 (dd, J = 8.2, 2.4 Hz, 1H, H-17), 3.82 (s, 3H, H-22).

8-Bromo-2-(4-chlorophenyl)-6-fluoro-2*H*-pyrazolo[4,3-*c*]quinolin-3(5*H*)- one [MM-I-13]. A mixture of ethyl 6-bromo-4-chloro-8-fluoroquinoline-3-carboxylate MM-I-02 (0.2 g, 0.64 mmol) with (4-chlorophenyl)hydrazine hydrochloride (0.18 g, 1.2 mmol) and Et3N (2 mL) in 8 mL of xylene was heated at reflux for overnight. The solid was collected by filtration and washed with hexane and water. The solid was dissolved in 10 mL of DMSO. The solution was poured in 30 mL of H2O, and filtered in order to remove the triethylamine salt. Then, a recrystallization using 15 mL EtOH and 2 mL of water was used and afforded yellow crystals MM-I-13 (0.17 g, 70%)**:** 1H NMR (300 MHz, DMSO) δ 8.54 (s, 1H, H-8), 8.22 (d, J = 8.9 Hz, 2H, H-15 and H-19), 8.11 (s, 1H, H-6), 7.92 (dd, J = 10.6, 1.8 Hz, 1H, H-2), 7.50 (d, J = 8.9 Hz, 2H, H-16 and H-18).

8-Bromo-6-fluoro-2-(4-fluorophenyl)-2*H*-pyrazolo[4,3-*c*]quinolin-3(5*H*)- one [MM-I-18]. Treatment of ethyl 6-bromo-4-chloro-8-fluoroquinoline-3-carboxylate MM-I- 02 (0.2 g, 0.64 mmol) with (4-fluorophenyl)hydrazine hydrochloride (0.22 g, 1.3 mmol) and Et3N (2 mL) in 8 mL of xylene under reflux overnight afforded the corresponding product. The yellow crystals MM-I-18 (0.120 g, 50 %) were obtained by recrystallization with hot EtOH**:** 1H NMR (300

MHz, DMSO) δ 13.02 (s, 1H, H-7), 8.55 (s, 1H, H-8), 8.25 – 8.15 (m, 2H, H-15 and H-19), 8.12 (s, 1H, H-6), 7.93 (dd, J = 10.6, 1.9 Hz, 1H, H-2), 7.29 (t, J = 8.9 Hz, 2H, H-16 and H-18).

7-Methoxy-2-(4-(trifluoromethoxy)phenyl)-2,5-dihydro-3H-pyrazolo[4,3- c]quinolin-3-one [CW-02-082]. To a clean and dry flask ethyl 4-chloro-7-methoxyquinoline- 3-carboxylate DK-I-40-1 (531 mg, 2 mmol, 1 eq), (4-(trifluoromethoxy)phenyl)hydrazine hydrochloride (686 mg, 3 mmol, 1.5 eq), xylene (10 mL), and TEA (607 mg, 6 mmol, 3 eq) were charged. The mixture was immediately transferred to pre-heated oil bath (150 ºC) and heated for 12h at which point it was cooled to 0 ºC via ice/water bath and hexanes (20 mL) were added in one portion. The yellow solid was filtered and dried (1.35g product + TEA*HCl). The mixture was purified via general purification method A and B. The solid was dried overnight under high vacuum obtaining the pure product in 75% yield (563 mg) as a yellow powder CW-02-082**:** 1H NMR (300 MHz, DMSO) δ 12.71 (s, 1H), 8.71 (s, 1H), 8.33 (s, 2H), 8.12 (s, 1H), 7.45 (s, 2H), 7.18 (s, 2H), 3.88 (s, 3H); 13C NMR (75 MHz, DMSO) δ 162.18, 161.10, 144.50, 144.48, 143.97, 139.93, 139.60, 137.61, 124.15, 121.98, 120.12, 115.95, 112.52, 106.45, 102.37, 56.00; HRMS (ESI) (M + H),Calcd. for $C_{18}H_{13}F_3N_3O_3$ 376.0909, Found 376.0914.

7-Methoxy-2-(4-methoxyphenyl)-6-methyl-2,5-dihydro-3H-pyrazolo[4,3- c]quinolin-3-one [CW-02-073]. To a clean and dry flask ethyl 4-chloro-7-methoxy-8- methylquinoline-3-carboxylate (560 mg, 2 mmol, 1 eq), (4-methoxyphenyl) hydrazine hydrochloride (524 mg, 3 mmol, 1.5 eq), xylene (10 mL), and TEA (607 mg, 6 mmol, 3 eq) were charged. The mixture was immediately transferred to pre-heated oil bath (150 ºC) and heated overnight at which point it was cooled to 0 ºC via ice/water bath and hexanes (20 mL) were added in one portion. The yellow solid was filtered and dried (1.15g product + TEA*HCl). The mixture was purified via general purification method B. The solid was dried for 12h under high vacuum obtaining the

pure product in 70% yield (470 mg) as a yellow solid: 1H NMR (300 MHz, DMSO) δ 11.80 (s, 1H), 8.37 (s, 1H), 8.08 (dd, J = 8.9, 5.1 Hz, 3H), 7.29 (d, J = 9.0 Hz, 1H), 7.01 (d, J = 9.1 Hz, 2H), 3.92 (s, 3H), 3.78 (s, 3H), 2.36 (s, 3H); 13C NMR (75 MHz, DMSO) δ 161.39, 158.24, 156.22, 143.58, 139.11, 135.37, 134.09, 121.18, 120.66, 114.33, 114.25, 112.80, 111.11, 106.53, 56.65, 55.68, 10.03; HRMS (ESI) (M + H), Calcd. for $C_{19}H_{18}N_3O_3$ 336.1348; Found 336.1240.

7-Methoxy-6-methyl-2-phenyl-2,5-dihydro-3H-pyrazolo[4,3-c]quinolin- 3-one [CW-02-078]. To a clean and dry flask ethyl 4-chloro-7-methoxy-8-methylquinoline-3- carboxylate (560 mg, 2 mmol, 1 eq), phenylhydrazine hydrochloride (434 mg, 3 mmol, 1.5 eq), xylene (10 mL), and TEA (607 mg, 6 mmol, 3 eq) were charged. The mixture was immediately transferred to pre-heated oil bath (150 ºC) and heated overnight at which point it was cooled to 0 ºC via ice/water bath and hexanes (20 mL) were added in one portion. The yellow solid was filtered and dried (1.17g product + TEA*HCl). The mixture was purified via general purification method A. The solid was dried overnight under high vacuum obtaining the pure product in 84% yield (513 mg) as yellow crystals: 1H NMR (500 MHz, DMSO) δ 11.86 (s, 1H), 8.42 (s, 1H), 8.22 (d, J = 8.2 Hz, 2H), 8.11 (d, J = 8.8 Hz, 1H), 7.45 (t, J = 7.9 Hz, 2H), 7.33 (d, J = 8.9 Hz, 1H), 7.17 (t, J = 7.3 Hz, 1H), 3.95 (s, 3H), 2.39 (s, 3H); 13C NMR (126 MHz, DMSO) δ 162.00, 158.41, 144.04, 140.60, 139.43, 135.49, 129.15, 124.29, 121.32, 118.98, 114.42, 112.77, 111.22, 106.48, 56.71, 10.08; HRMS (ESI) (M + H), Calcd. for $C_{18}H_{16}N_3O_2$ 306.1243; Found 306.1237.

7-Methoxy-6-methyl-2-(4-(trifluoromethoxy)phenyl)-2,5-dihydro-3Hpyrazolo[4,3-c]quinolin-3-one [CW-02-079]. To a clean and dry flask ethyl 4-chloro-7- methoxy-8-methylquinoline-3-carboxylate (560 mg, 2 mmol, 1 EQ), (4-(trifluoromethoxy) phenyl) hydrazine (689 mg, 3 mmol, 1.5 eq), xylene (10 mL), and TEA (607 mg, 6 mmol, 3 eq) were charged. The mixture was immediately transferred to pre-heated oil bath (150 ºC) and heated

overnight at which point it was cooled to 0 ºC via ice/water bath and hexanes (20 mL) were added in one portion. The yellow solid was filtered and dried (1.14g product + TEA*HCl). The mixture was purified via general purification method B. The solid was dried overnight under high vacuum obtaining the pure product in 68% yield (530 mg) as a yellow powder: 1H NMR (300 MHz, DMSO) δ 11.92 (d, J = 5.8 Hz, 1H), 8.44 (d, J = 6.3 Hz, 1H), 8.33 (d, J = 9.1 Hz, 2H), 8.09 (d, J = 8.9 Hz, 1H), 7.45 (d, J = 8.9 Hz, 2H), 7.32 (d, J = 9.0 Hz, 1H), 3.94 (s, 3H), 2.37 (s, 3H); 13C NMR (75 MHz, CDCl$_3$) δ 162.11, 158.52, 144.48, 144.44, 139.74, 139.57, 135.51, 122.35, 122.00, 121.34, 120.10, 114.51, 112.64, 111.31, 106.11, 56.70, 10.05; HRMS (ESI) (M + H), Calcd. for C$_{19}$H$_{15}$F$_3$N$_3$O$_3$ 390.1066; Found 390.1068.

7-Methoxy-2-(4-methoxyphenyl)-2,5-dihydro-3H-pyrazolo[4,3- c][1,6]naphthyridin-3-one [CW-03-030]. To a clean and dry flask ethyl 4-chloro-7- methoxy-1,6-naphthyridine-3-carboxylate (78 mg, 0.29 mmol, 1 eq), (4- methoxyphenyl)hydrazine hydrochloride (76 mg, 0.435 mmol, 1.5 eq), xylene (5 mL), and TEA (89 mg, 0.87 mmol, 3 eq) were charged. The mixture was immediately transferred to pre-heated oil bath (150 ºC) and heated overnight at which point it was cooled to 0 ºC via ice/water bath and hexanes (20 mL) were added in one portion. The yellow solid was filtered and dried (product + TEA*HCl). The mixture was purified via FCC (7% MeOH in DCM) and general purification method A. The solid was dried overnight under high vacuum obtaining the pure product in 47% yield (44 mg) as orange crystals: 1H NMR (300 MHz, DMSO) δ 12.60 (s, 1H), 9.06 (s, 1H), 8.67 (s, 1H), 8.02 (d, J = 9.1 Hz, 2H), 7.02 (d, J = 9.1 Hz, 2H), 6.89 (s, 1H), 3.96 (s, 3H), 3.79 (s, 3H); 13C NMR (75 MHz, DMSO) δ 164.59, 161.30, 156.46, 144.09, 143.92, 141.36, 141.25, 133.63, 120.84, 114.32, 110.13, 108.40, 96.94, 55.72, 54.49; HRMS (ESI) (M + H), Calcd. for C$_{17}$H$_{15}$N$_4$O$_3$ 323.1144; Found 323.1138.

7-Chloro-2-(4-methoxyphenyl)-2,5-dihydro-3H-pyrazolo[4,3- c][1,6]naphthyridin-3-one

[CW-03-033]. To a clean and dry flask ethyl 4,7-dichloro-1,6- naphthyridine-3-carboxylate (120 mg, 0.443 mmol, 1 eq), (4-methoxyphenyl)hydrazine hydrochloride (116 mg, 0.664 mmol, 1.5 eq), xylene (5 mL), and TEA (135 mg, 1.33 mmol, 3 eq) were charged. The mixture was immediately transferred to pre-heated oil bath (150 ºC) and heated overnight at which point it was cooled to 0 ºC via ice/water bath and hexanes (15 mL) were added in one portion. The yellow solid was filtered and dried (product + TEA*HCl). The mixture was purified via FCC (7% MeOH in DCM) and general purification method B. The solid was dried overnight under high vacuum obtaining the pure product in 61% yield (88 mg) as an orange solid: 1H NMR (300 MHz, DMSO) δ 12.87 (s, 1H), 9.21 (s, 1H), 8.81 (s, 1H), 8.03 (d, J = 9.1 Hz, 2H), 7.61 (s, 1H), 7.03 (d, J = 9.1 Hz, 2H), 3.79 (s, 3H); 13C NMR (75 MHz, CDCl$_3$) δ 161.08, 156.70, 150.07, 146.16, 143.21, 141.60, 140.52, 133.41, 121.00, 114.38, 114.10, 113.06, 109.77, 55.73; HRMS (ESI) (M + H), Calcd. for C$_{16}$H$_{12}$ClN$_4$O$_2$ 327.0649; Found 327.0654.

Purification Method A: The crude compound was heated to reflux in ethanol (10mL/g) and a solution of ethanol/water (50% H$_2$O, 50% ethanol) was slowly added until all the compound was completely dissolved at reflux. Once dissolved, water was added dropwise at reflux until the solution became slightly cloudy. The solution was cooled slowly to rt and in most cases microcrystals began to accumulate. The solution was further cooled to 0ºC via an ice-bath, filtered, and the solids were washed with cold aq solution of ethanol/water (50% H$_2$O, 50% ethanol) and dried overnight. If necessary, compounds were further dried under high vacuum.

Purification Method B: The crude compound was dissolved in a minimal amount of DMSO and water was added until the compound was completely precipitated from the DMSO solution. The product was filtered and washed with water. The amorphous powder was ground with a mortar

and pestle and dried under high vacuum for 24h or until little trace of water was present in the

HNMR spectrum.

CHAPTER TEN

IN VITRO AND IN VIVO CHARACTERISTICS OF NOVEL, SELECTIVE, AND POTENT α6 POSITIVE ALLOSTERIC MODULATORS

I.   IN VITRO EXPERIMENTS AND RESULTS.

The first step in the determination of whether or not these novel pyrazoloquinlinones have the necessary activity/selectivity at the $\alpha_6\text{ß}_3\gamma_2$ receptor is to complete oocyte assays on the $\alpha_{1-6}\text{ß}_3\gamma_2$ receptors. Unfortunately, these oocyte assays are very time consuming, thus data on the novel compounds prepared in the earlier section is still incomplete. However, data on a number of compounds has been completed and more compounds selective to α_6 receptors have been discovered.

Where oocyte data has not yet been possible or is incomplete, other *in vitro* assays are also being used to determine other pharmalogical characteristics of these novel ligands. Currently, assays to determine water solubility and metabolic rate of these novel ligands are routinely run on new analogs. In the future, a more complete pharmacokintetic (PK) analysis of ligands identified as strong leads will also be accomplished.

1.   Oocyte data.

The oocyte data for compounds **6** and **11** are presented in Figures 10-1 and 10-2, respectively, for comparison. As described in chapter 9, **Compound 6** acts almost exclusively at α6 receptors while it is nearly silent at $\alpha_{1-5}\text{ß}_3\gamma_2$. **Compound 11**, while not as selective as **Compound 6**, exhibited much more potent activity on α_6 receptor subtypes *in vitro*.

Figure 10-1: Compound 6, oocyte efficacy data.

Compound 6
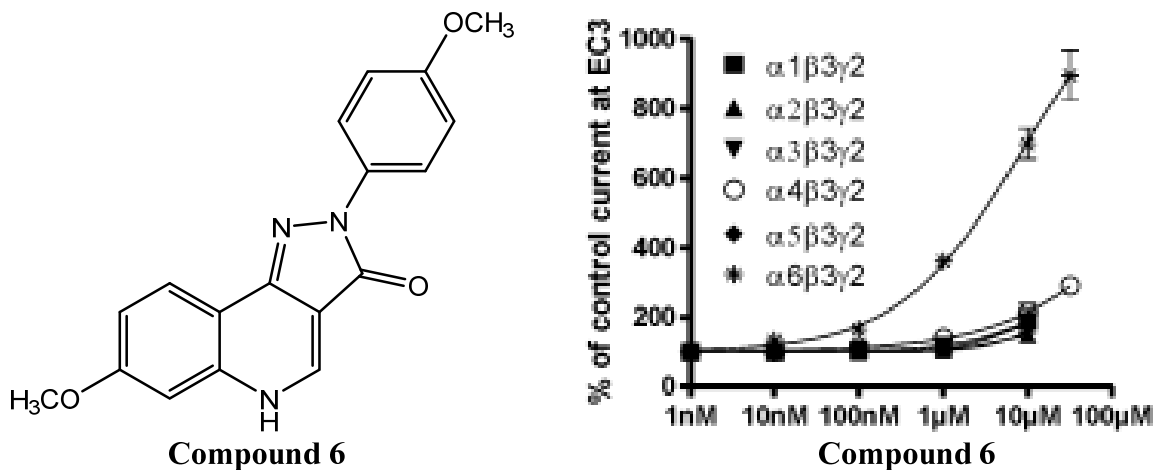
Compound 6

Figure 10-2: Compound 11, oocyte efficacy data.

Compound 11
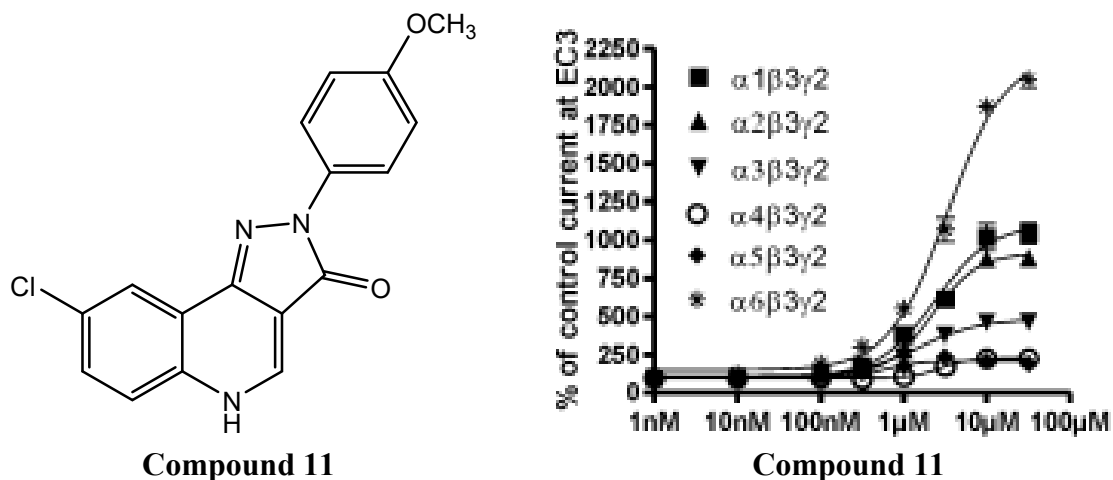
Compound 11

New compounds with complete oocyte data include LAU 159 (**32**) and LAU 463 (**38**).

These compounds along with their oocyte efficacy data are presented in Figures 10-3 and 10-4

respectively.

Figure 10-3: LAU 159, oocyte efficacy data.
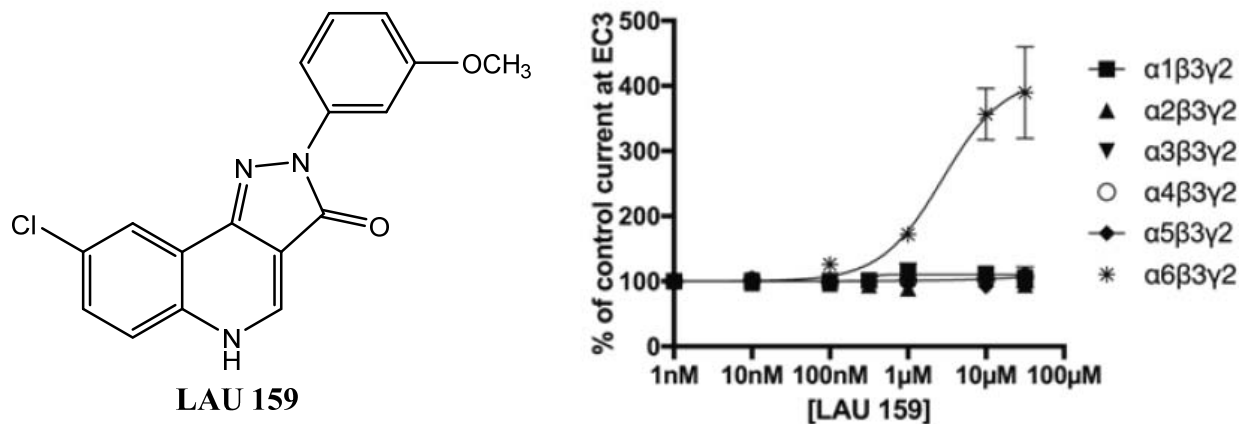
Figure 10-4: LAU 463, oocyte efficacy data.
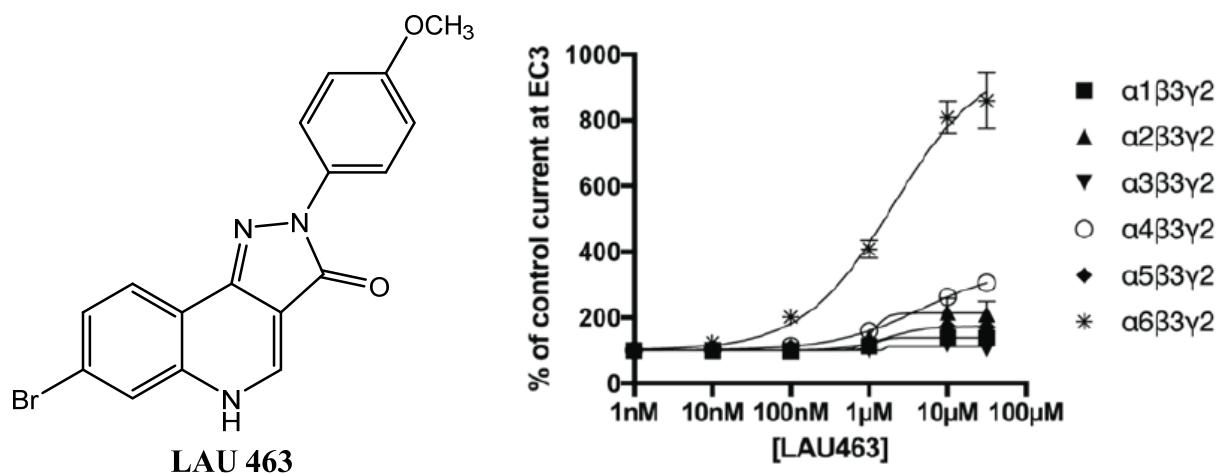
Incomplete efficacy data, that is n < 3 and/or only $\alpha_6\beta_3\gamma_2$ receptors have been determined on a variety of other novel analogs (Table 10-1). A number of these ligands act as selective α_6 agonists, including DK-I-56-1 (**19**) and RV-I-29 (**20**). Both of which are deuterated derivatives of the lead ligand **Compound 6**. The slightly lower and statistically relevant efficacy of **20** is thought to be due to a slightly impure sample. Prior to *in vivo* testing **20** was more thoroughly purified. **Compound 6** is included for reference.

Table 10-1: Oocyte efficacy data obtained; to date.

Compound at 1mM / 10 mM	$\alpha_6\beta_3\gamma_2$	$\alpha_1\beta_3\gamma_2$	$\alpha_1\beta_3$	$\alpha_5\beta_3\gamma_2$
Compound 6	**300±30** / **570±100**	NT / 140±30	NT / 180±30	NT / 220±20
DK-I-56-1 (**19**)	**270±30** / **500±80**	NT / 170±15	NT / 140±20	NT
RV-I-29 (**20**)	**190±20** / **370±40**	NT	NT	NT
DK-I-60-3 (**21**)	**280±40** / **600±100**	NT / 200±10	NT / 180±70	NT / 390±40
DK-I-94-1 (**22**)	**NT** / **~220**	NT	NT / ~200	NT
CW-03-030a (**25**)	**120±10** / **210±15**	NT / 220±20	NT	NT
DK-I-86-1 (**27**)	**160±15** / **230±30**	NT / 100±10	NT / ~110	NT / 80±10
DK-I-59-I (**33**)	**NT** / **160±30**	NT	NT / ~110	NT
DK-I-87-1 (**35**)	**~100** / **NT**	NT	~80 / NT	NT / NT
DK-I-58-1 (**39**)	**150±15** / **400±60**	NT	NT / ~140	NT / 400±25
DK-I-92-1 (**40**)	**NT** / **~220**	NT	~200	NT

NT = not tested

While it is clear that the deuterated analogs of lead ligand **Compound 6** retain α_6 activity, of the other novel ligands tested so far many are only weakly efficacious at α_6 subtypes. This adds valuable information for future SAR studies, for example comparison of **25** and **27** show a statistically relevant difference in selectivity dependent upon the position of the pyridine ring (Figure 10-5).

Figure 10-5: Pyridine ring positioning.
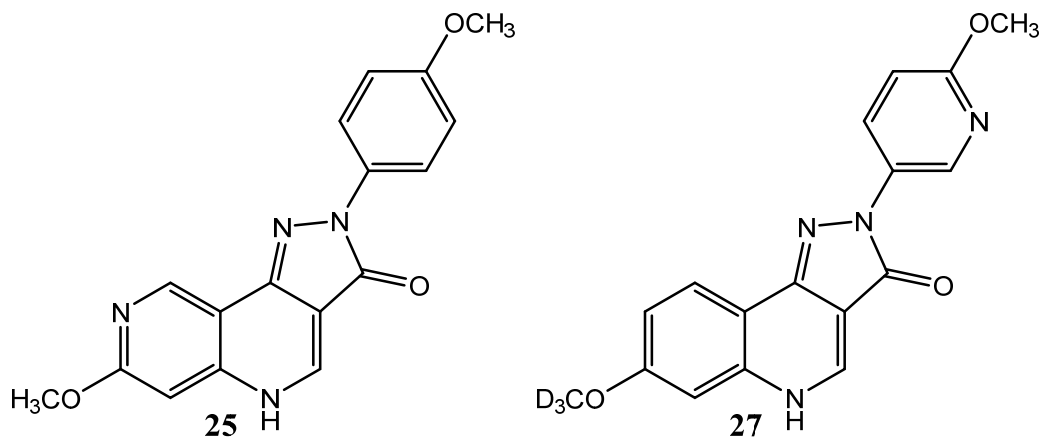
Although **27** is a deuterated analog, it has been previously shown that the deuterium atoms do not influence efficacy nor the subtype selectivity in a statistically relevant fashion. However, the position of the pyridines rings, ring A in **25** and ring D in **27**, effects a relevant change in selectivity for α_6. While both show only mild efficacy at α_6, **27** retains selectivity whereas pyridine **25** was found to also exhibit mild efficacy at the α_1 receptor subtype, which could lead to some negative side effects including sedation, ataxia, and addiction. This valuable information will aid in the future design of ring D analogs, which should lead to more soluble compounds that retain both activity and α_6 selectivity.

2.   Solubility data.

The pyridine analogs discussed above were synthesized for the sole basis to improve water solubility for future *in vivo* studies. Since the ring A pyridine **25** was found to be nonselective in preliminary *in vitro* oocyte efficacy assays, the solubility of this compound was not tested. The first four compounds examined were tested to show the enhanced solubility of pyridine analog **27**; in the future the solubility of many more analogs will be tested.

Table 10-2: Solubility data on select compounds.
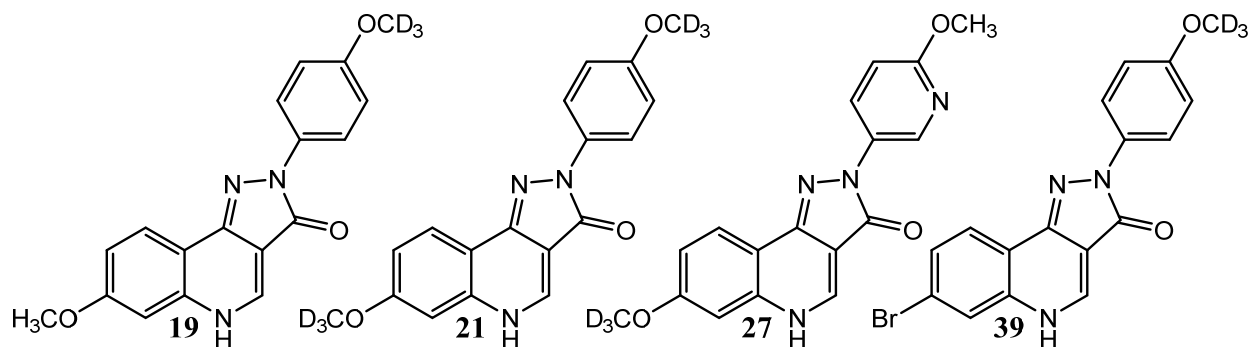
Compounds	Water solubility (ng/µL)
DK-I-56-1 (**19**)	11.40
DK-I-60-3 (**21**)	16.00
DK-I-86-1 (**27**)	211.00
DK-I-58-1 (**39**)	9.20

Determined by HPLC

From these data it can be seen that the pyridine analog **27** is nearly 20 times more water soluble then the other analogs. As described earlier, the oocyte efficacy of **27** indicated that selectivity at α6 was retained, however, it was less efficacious then the related α6 selective ligands discovered thus far. The increase in solubility, however, may be a crucial component for future *in vivo* work. Moreover, this indicated that pyridine analogs are an important target for future SAR studies since these pyridine analogs may have better oral bioavailability then other lead compounds. Unfortunately, synthesis of the hydrochloride salts of these pyridine analogs has been complicated because demethylation of the pyridine OCH$_3$ group has been observed when the compound was subjected to acidic conditions. Analogs with the pyridine nitrogen and methoxy group meta to one another are currently being prepared; synthesis of the hydrochloride salts of these analogs may be more straightforward.

3.   Metabolic data.

Deuterated methoxy groups have been shown to slow down metabolism for a number of different drug candidates. The methoxy groups present in **Compound 6** were thought to likely contribute to metabolism of these compounds. Illustrated in Table 10-3 and 10-4 are metabolic data obtained *in vitro* on both human liver microsomes and mouse liver microsomes, respectively. It was shown that deuterated analogs exhibit a significantly longer half-life then the non-deuterated analogs. The first 4 compounds in each table 10-3 and 10-4, compounds **6**, **19**, **20**, and **21** are perhaps the most indicative of this increase in metabolic stability. Illustrated in Figure 10-6 are the structures of these ligands.

Figure 10-6: Analogs with key metabolic stability.
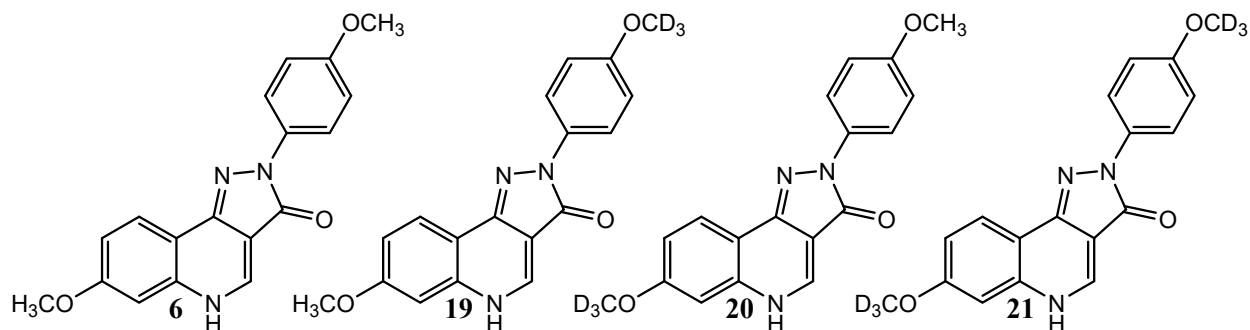
As described in Table 10-3, lead ligand **Compound 6** was shown to have a half-life of ~200 minutes, whereas the ring D mono-deuterated analog **19** was shown to have a half-life of ~500 minutes – nearly double that of the parent compound. The ring A mono-deuterated analog **20** was found to have a half-life of ~3000 minutes and the di-deuterated analog **21** was fond to have a half-life of ~700 minutes. This increase in metabolic stability is relevant and important for *in vivo* work, which should lead to a longer time of effect *in vivo* compared to **Compound 6**.

Table 10-3: *In vitro* metabolic stability on Human Liver Microsomes (HLM).

Compound	Microsome Type	Day	Half-Life (min)	STD (+/- min)	Intrinsic Clearance (mL/min/mg)	Metabolic Rate (nmol/min/mg)	% remaining at 60min	STD (+/- %)
Compound 6	HLM	1	175.00	NT	0.4	8	87.00	1.00
		2	250.00		0.277	5.6	85.20	1.00
DK-I-56-1 (**19**)	HLM	1	516.39	50.10	0.1342	2.684	91.65	0.14
		2	522.62	53.16	0.1326	2.652	91.74	0.10
RV-I-029 (**20**)	HLM	1	3387.00	693.00	0.02	0.4	95.20	1.00
		2	2558.00	792.00	0.027	0.4	95.50	1.00
DK-I-60-3 (**21**)	HLM	1	875.33	313.00	0.07917	1.5834	91.74	0.20
		2	686.13	164.00	0.101	2.02	91.28	0.17
DK-II-13-1 (**26**)	HLM	1	759.00	187.40	0.09131	1.8262	92.29	0.16
		2	828.05	177.70	0.08369	1.6738	93.41	0.13
DK-I-86-1 (**27**)	HLM	1	915.33	260.00	0.07571	1.5142	93.03	0.16
		2	589.28	261.93	0.1176	2.352	91.56	0.11
LAU 159 (**32**)	HLM	1	204.18	15.23	0.3394	6.7888	81.53	0.16
		2	209.36	15.73	0.331	6.62	81.36	0.16
DK-I-59-1 (**33**)	HLM	1	622.64	60.00	0.1113	2.226	92.85	0.07
		2	675.43	103.00	0.1026	2.052	93.13	0.11
LAU 463 (**38**)	HLM	1	96.85	2.63	0.7155	14.31	65.23	0.10
		2	110.88	5.19	0.625	12.5	68.50	0.17
DK-I-58-1 (**39**)	HLM	1	194.28	9.48	0.3567	7.134	80.55	0.11
		2	214.95	11.18	0.3224	6.448	82.35	0.11

HLM: Human Liver Microsomes, NT: not tested

Table 10-4: *In vitro* metabolic stability on Mouse Liver Microsomes (MLM).

Compound	Microsome Type	Day	Half-Life (min)	STD (+/- min)	Intrinsic Clearance (mL/min/mg)	Metabolic Rate (nmol/min/mg)	% remaining at 60min	STD (+/- %)
Compound 6	MLM	1	202.39	10.45	0.3424	6.848	81.20	0.12
		2	186.14	12.37	0.3723	7.446	79.51	0.16
DK-I-56-1 (**19**)	MLM	1	641.07	77.00	0.1081	2.161	92.66	0.10
		2	616.54	69.00	0.1124	2.248	92.94	0.09
RV-I-029 (**20**)	MLM	1	913.88	280.85	0.07583	1.5116	93.31	0.17
		2	801.80	189.52	0.08643	1.7286	93.03	0.15
DK-I-60-3 (**21**)	MLM	1	836.35	280.00	0.08286	1.6572	93.13	0.20
		2	857.35	273.00	0.0803	1.6166	93.03	0.19
DK-II-13-1 (**26**)	MLM	1	136.05	5.41	0.5095	10.19	74.14	0.12
		2	142.35	6.08	0.4868	9.736	75.40	0.13
DK-I-86-1 (**27**)	MLM	1	581.37	93.00	0.1192	2.384	91.65	0.14
		2	519.88	63.57	0.1333	2.666	91.10	0.11
LAU 159 (**32**)	MLM	1	89.72	5.12	0.7724	15.448	60.34	0.23
		2	88.42	5.32	0.7837	15.674	59.32	0.24
DK-I-59-1 (**33**)	MLM	1	154.92	7.40	0.4473	8.946	75.48	0.13
		2	176.56	7.85	0.3925	7.85	77.70	0.10
LAU 463 (**38**)	MLM	1	107.69	3.82	0.6435	12.87	67.22	0.13
		2	118.66	6.48	0.584	11.68	70.70	0.19
DK-I-58-1 (**39**)	MLM	1	138.10	8.25	0.5018	10.036	73.40	0.18
		2	140.85	6.11	0.492	9.84	74.29	0.13

MLM: Mouse Liver Microsomes

II. IN VIVO EXPERIMENTS AND RESULTS.

Novel pyrazoloquinolinones with α_6 efficacy and α_6 subtype selectivity were chosen for *in vivo* studies in a number of mouse assays to probe the neurological activity of these ligands (Figure 10-7). The first assay to be discussed is the measurement of the concentration distribution between plasma and brain of each ligand in mice. This pharmacokinetic (PK) analysis helps determine the uptake of the drug when injected intraperitoneally (i.p.), as well as the free concentration reached in the brain of the mouse. Since these ligands are presumed to only act on the central nervous system, crossing the blood-brain-barrier is necessary for a pharmacological response. The free fraction in the brain is what binds to the receptor, thus this fraction is also very important.

Since these compound bind and act via the BZ site at $\alpha_6\beta_3\gamma_2$ receptors, it was also extremely important to determine whether or not these novel selective ligands have the usual effects that are associated with benzodiazepines such as diazepam. These effects include ataxia, dependence, and sedation among others. These effects are viewed as negative side-effects for a number of indications, including those under study here. Assays that help determine whether or not benzodiazepine-like effects were seen with these novel pyrazoloquinolinone analogs were thus completed. These will also be discussed in detail in the sections to follow.

Assays that have helped elucidate the role of $\alpha6$ receptors tested for this study include pre-pulse inhibition assays, migraine assays, and IoN-CCL rat assays. These assays will be described in detail in this section. Future assays that are currently being completed or planned will also be discussed.

Figure 10-7: Ligands chosen for *in vivo* studies.

Compound 6   Compound 11   DK-I-56-1, **19**

RV-I-29, **20**   LAU 159, **32**   LAU 463, **38**
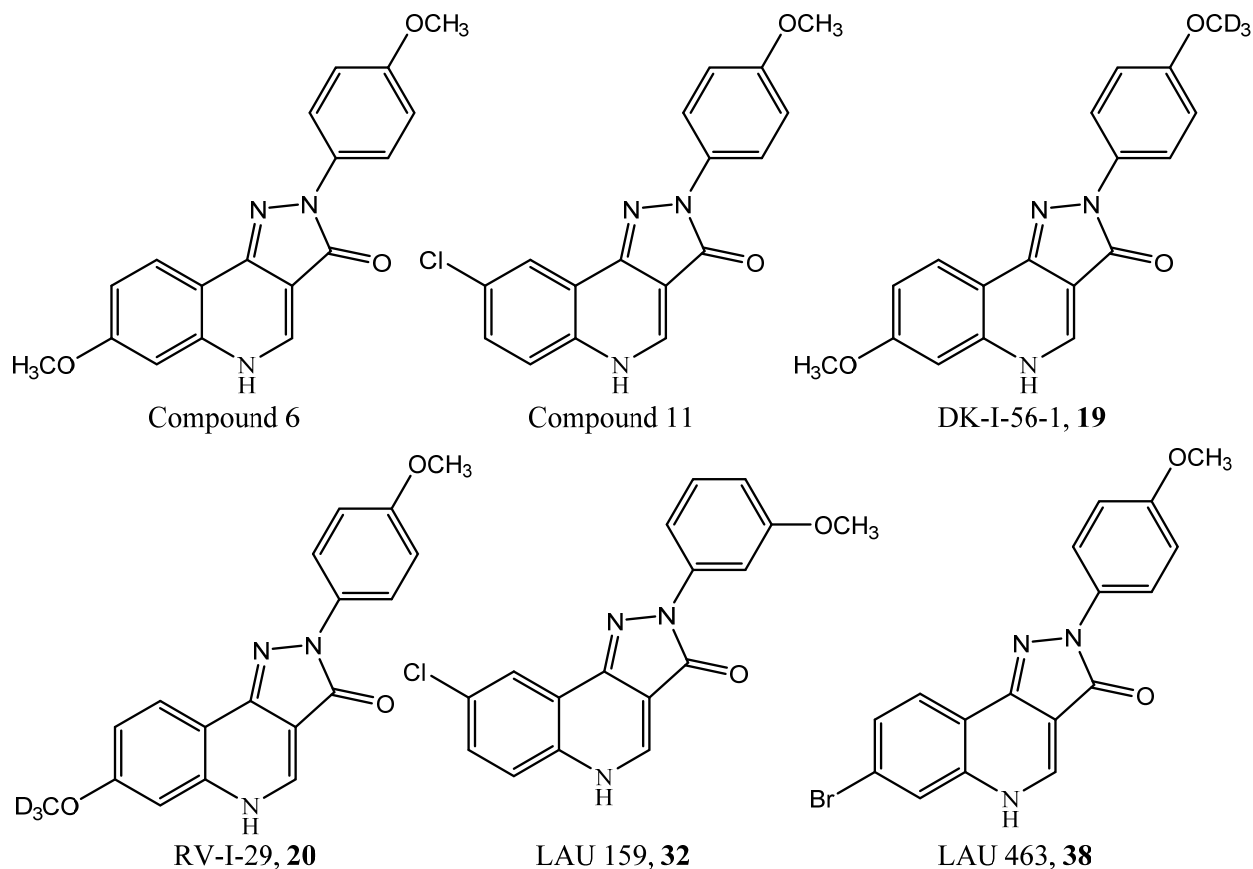
1.   Plasma/Brain distribution data.

As described earlier, blood-brain-barrier penetration is essential to potent activity for all CNS active ligands. This can be measured *in vivo* by dosing animals and at predetermined time intervals collecting blood samples from both the body and the brain. Moreover, estimates of the free brain concentration, that is the ligand not bound to proteins, can also be determined by these assays. While protein binding is a common phenomenon in CNS drugs for transport; on the other hand, when bound to protein it is unlikely that the ligand will bind to the $\alpha_6\beta_3\gamma_2$ receptor subtype in question. This binding, however, is generally reversible and often in equilibrium with

the 'free fraction' of ligand, thus moderate protein binding is often not a major concern for CNS

drugs.

Figure 10-8: Plasma/Brain distribution of Compound 6 in rats.
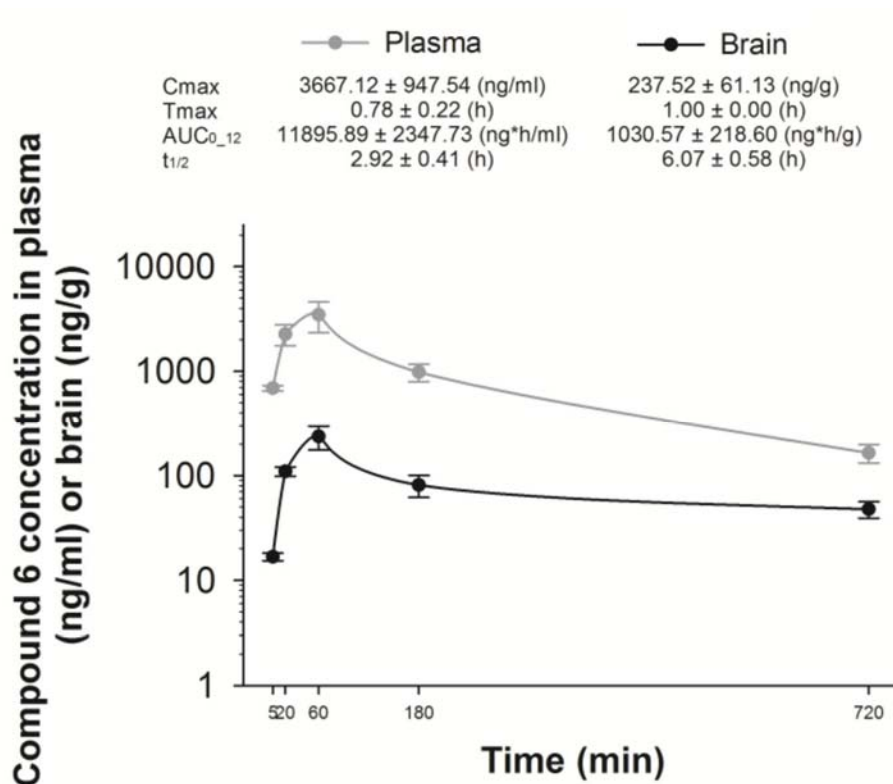
The lead compound, **Compound 6**, was found to have adequate brain concentration for a

candidate to target the CNS. Moreover, it was found that a steady concentration of ligand was

still present 12 hours post dosing. This may signify these compounds will be long-lasting *in*

vivo. Analysis of the data for the deuterated analog DK-I-56-1 indicated a similar concentration

in vivo to **Compound 6** when dosed i.p., however, with a slightly lower half-life (Figure 10-9).

Estimation of the free brain concentration indicated that a substantial amount of ligand was not

protein bound.

Figure 10-9: Plasma/Brain distribution of DK-I-56-1 in rats.
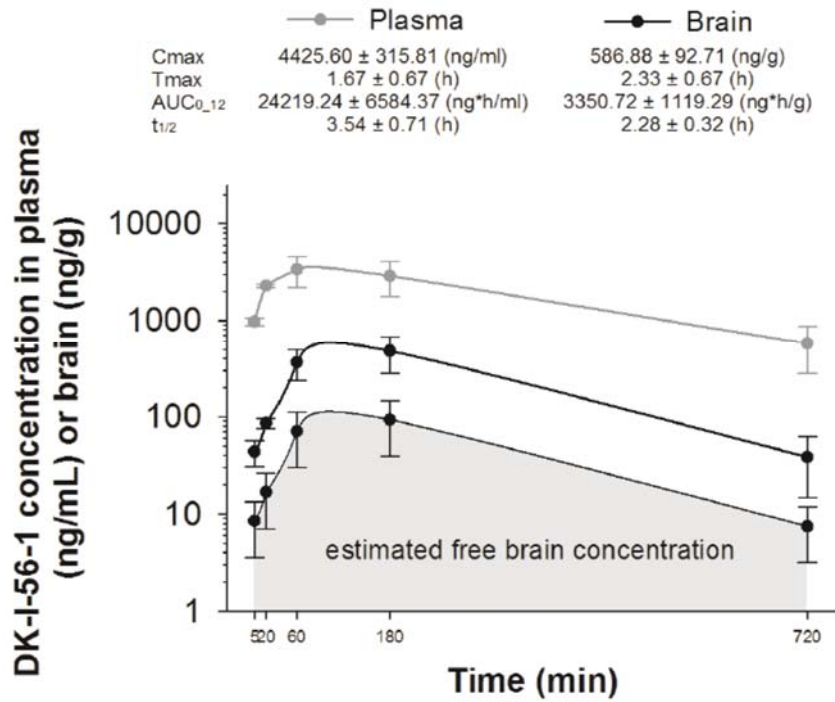
Figure 10-10: Plasma/Brain distribution of DK-I-86-1 in rats.
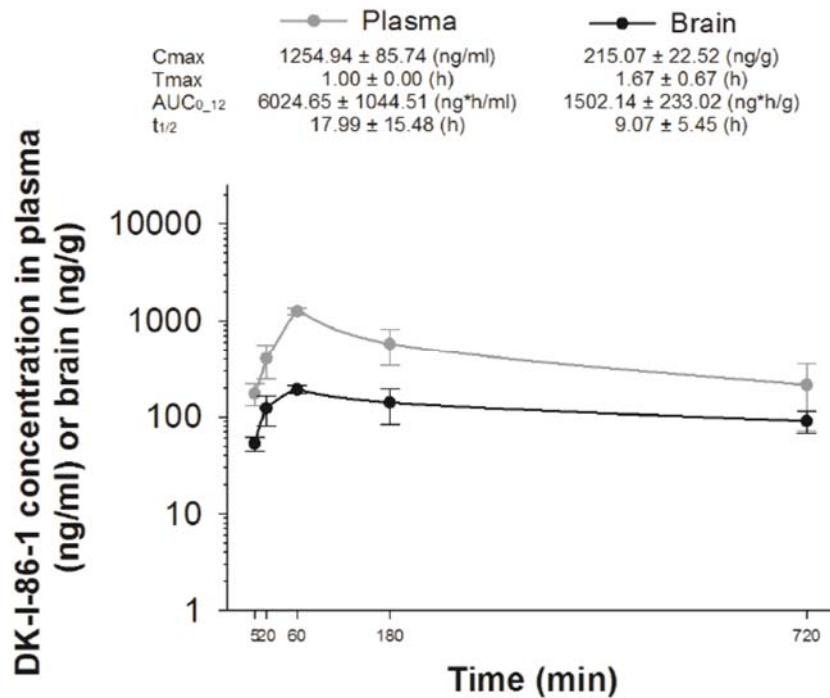
Unlike **Compound 6** and DK-I-56-1, examination of the data for the ring D pyridine analog DK-I-86-1 indicated a much lower plasma concentration with a Cmax of just 1256 ng/mL. This is compared to **Compound 6** which had a Cmax of 3667 ng/mL, nearly 3 times higher. However, analysis of the data indicated DK-I-86-1 still obtains a substantial brain concentration (Cmax = 215 ng/mL) with the longest half-life of all ligands tested (9 hours). These beneficial characteristics, along with better water solubility, make DK-I-86-1 an interesting candidate for future *in vivo* studies.

Figure 10-11: Plasma/Brain distribution of DK-I-56-1 in mice.
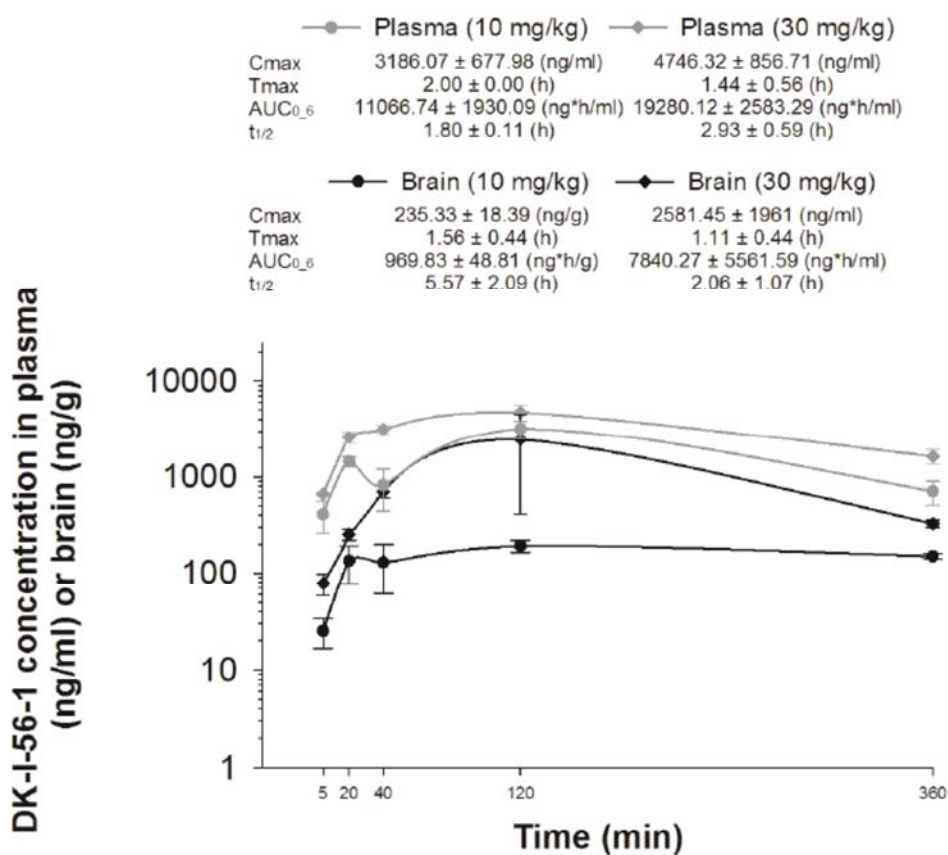
Studies of DK-I-56-1 in mice have shown a dose dependence relating to the concentration of ligand in both plasma and brain (Figure 10-11). Interesting to note is the extreme increase of brain concentration of DK-I-56-1 when a 30 mg/kg dosage was used. While these results clearly show that DK-I-56-1 is a suitable drug candidate for both rats and mice, it is clear that in mice higher doses, such as 30 mg/kg as used in this study, provided higher brain concentrations in a dose response curve manner.

2. Battery of common BZ ligand *in vivo* studies.

Since ligands that activate the BZ site have been known to elicit a number of undesirable side-effects, it was important to determine if these novel α_6 selective ligands also exhibited some of these negative side-effects especially from activation of $\alpha_1\beta_{2/3}\gamma_2$ subtypes. A number of assays have been carried out to help determine these effects and the rotorod assay is one of the most important assays to test for the α_1 receptor-mediated ataxia and sedation (Figure 10-12). While not only measuring the ability of the mouse/rat to stay on the rod, grip strength can be measured as well in regard to muscle relaxation (Figure 10-13).

Figure 10-12: Rotarod performance with Compound 6.
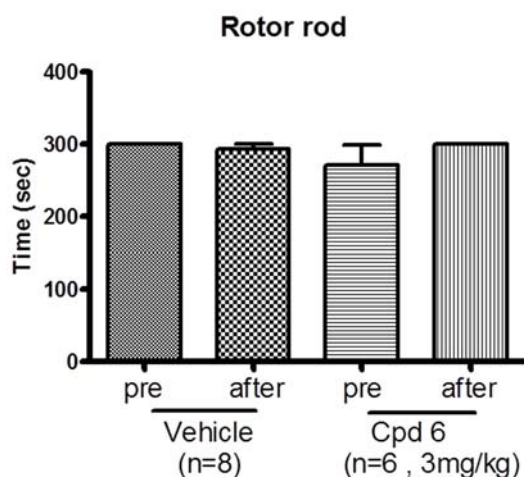
Figure 10-13: Grip strength performance with Compound 6.
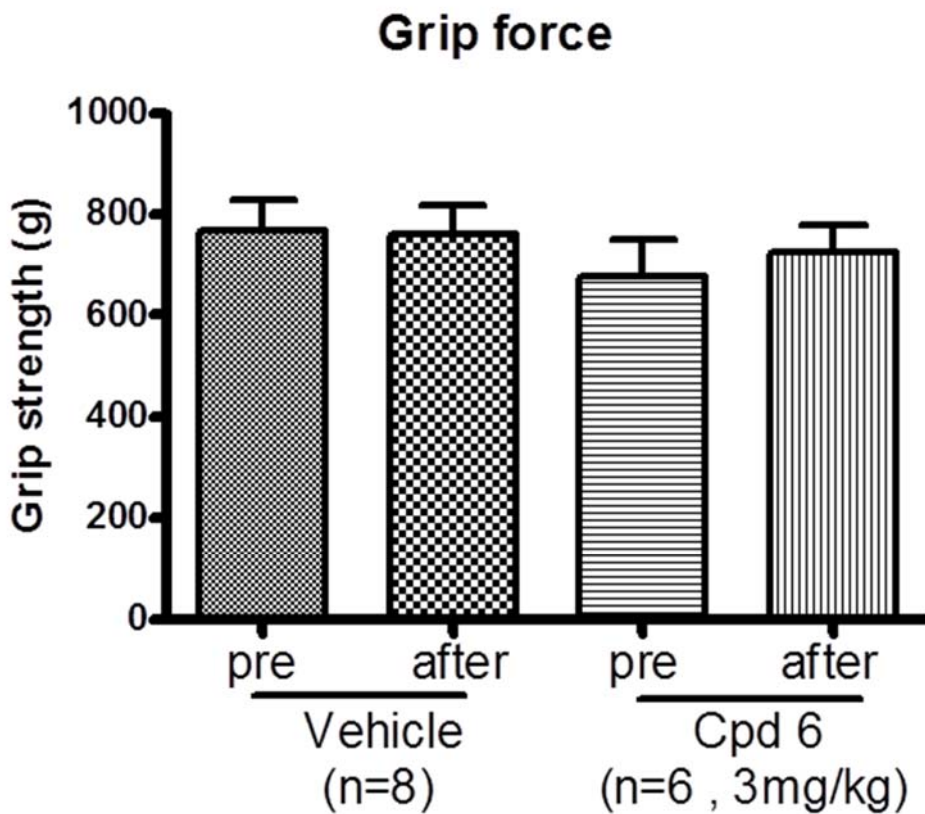
Analysis of the data from these initial tests indicated that at a dose of 3 mg/kg there was essentially no difference in rotarod timing or grip strength seen on administration of **Compound 6**. These positive results indicate that unlike a number of typical benzodiazepine drugs, **Compound 6** is unlikely to be ataxic or cause any gross motor coordination difficulties.

Figure 10-14: Test for a sedation effect of Compound 6.
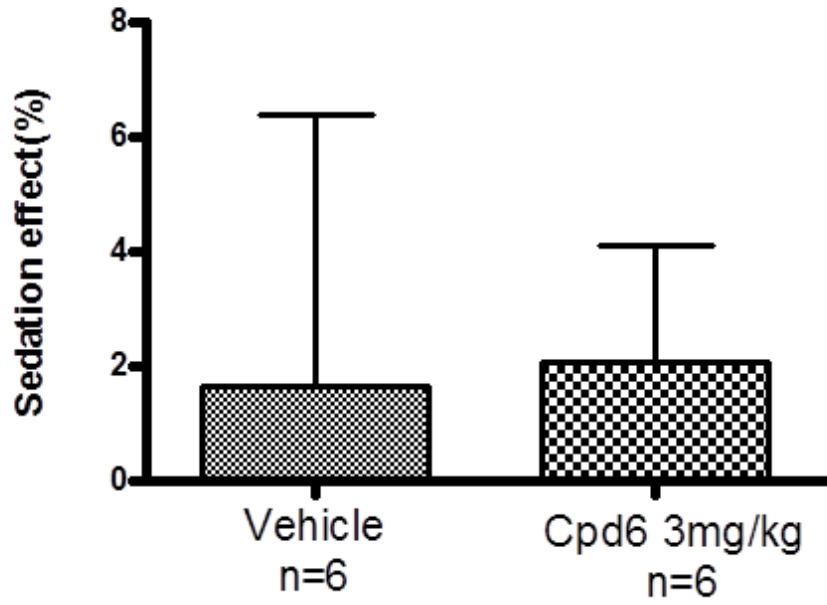
Figure 10-15: Open arms distance in elevated plus maze.
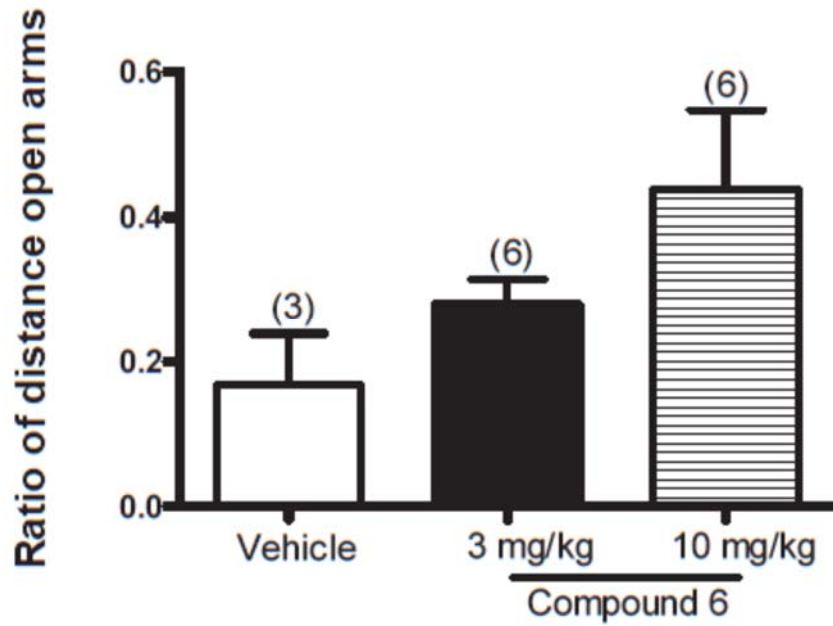
Figure 10-16: Open arms duration in elevated plus maze.
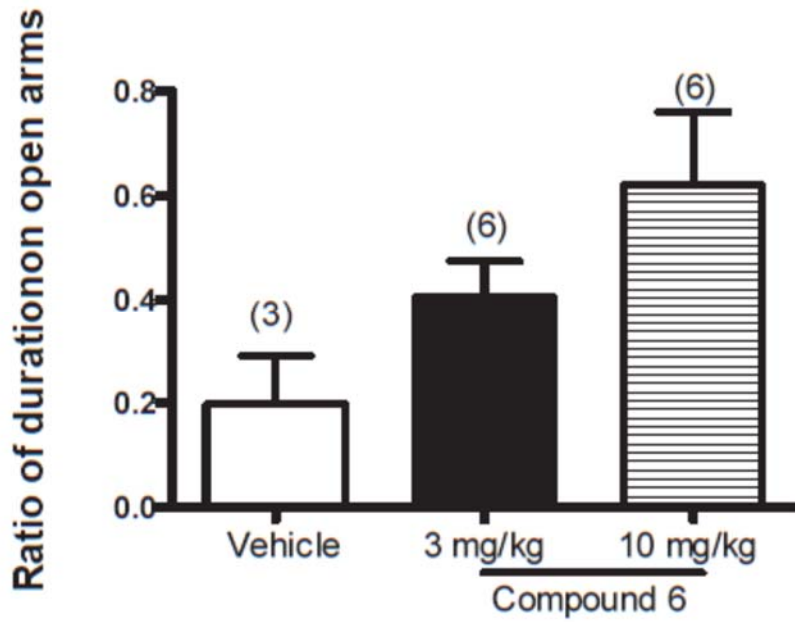
Figure 10-17: Rearing number.
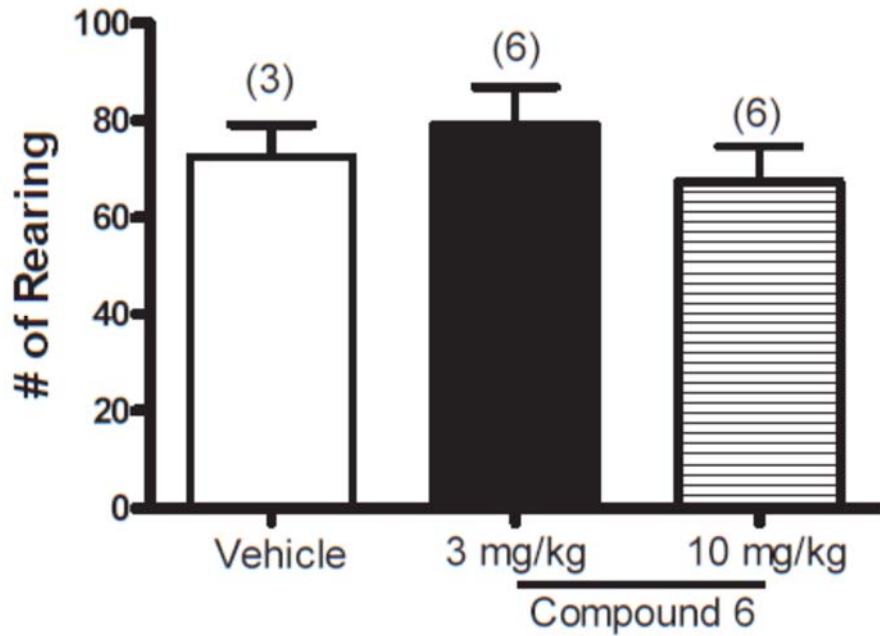
Analysis of the assays described above in Figures 10-14, 10-15, 10-16, and 10-17 detail common assays for benzodiazepine ligands. Analysis of the sedation data in Figure 10-14 confirmed that **Compound 6** has no sedative effect, in agreement with the data from the rotarod assay. The elevated plus maze assay is an attempt to assay anxiety in mice. Mice that spend more time in the "open arm" section of the elevated maze are thought to feel less anxiety then mice that stay in the "closed arm" portion. From these data, it was shown that **Compound 6** exhibited a dose-response anti-anxiety effect on mice, clearly a beneficial effect. The rearing in a closed maze pertains to the number of times a mouse goes on their rear legs to view their surroundings; analysis of the data in Figure 10-17 indicated that **Compound 6** at both 3 and 10 mg/kg exhibited little difference from vehicle.

These assays together show that **Compound 6**, and likely α_6 receptors in general, have positive biological effects while at the same time do not include the negative effects exhibited by other non-selective benzodiazepines – specifically α_1 ligands which are known to be sedative, addictive, ataxic, amnesic, and cause tolerance and addiction. The anti-anxiety effect of **Compound 6** was unexpected, since this usually emanates in mice via α_2 and α_3 receptor subtypes and will have to be verified in a Vogel conflict test of anxiolysis.

3. Studies of prepulse inhibition (PPI).

Prepulse inhibition (PPI) is a neurological phenomenon in which a weaker pulse, generally acoustic, inhibits the startle response to a subsequent stronger pulse. In this study, sensorimotor gating deficits which manifest themselves in neurological diseases such as schizophrenia, OCD, and Tourette syndrome were studied by impairing mice with methamphetamine and subsequently measuring the effect on PPI. Methamphetamine is a

recreational and addictive stimulant drug that when administered can result in a behavior similar

to symptoms of schizophrenia or other sensorimotor gating deficits. In terms of PPI, when under

the effects of methamphetamine, the 'prepulse' no longer inhibits the response to the 'pulse'

showing the mice to be experiencing more erratic behavior. Rescuing the PPI is thus defined as

reducing this erratic behavior to the point where the 'prepulse' is again able to inhibit a response

to the 'pulse' in a significant fashion. Illustrated in Figure 10-18 is an example of the

methamphetamine PPI mouse model. The designation C6 refers to **Compound 6** and C11 refers

to **Compound 11**.

Figure 10-18: PPI results with Compound 6 and Compound 11.
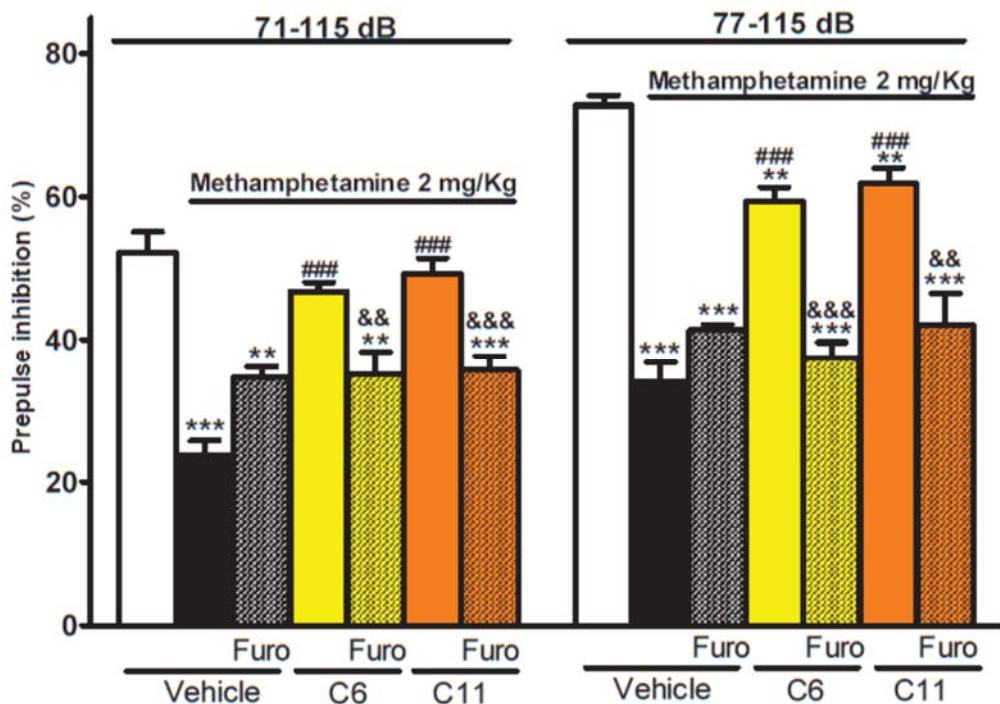
The white bars under the label "Vehicle" represent the prepulse inhibition % seen in mice

when a short prepulse (71 dB or 77 dB) was played followed by a louder pulse (115 dB). To put

the difference in noise levels in perspective 71 dB is similar to a normal conversation, 77 dB is

similar to the sound of a vacuum cleaner, and 115 dB is similar to a car horn at a short distance. From analysis of the graph it is clear that the short prepulse inhibited the response in mice to the louder pulse by about 55% for 71-115 dB and about 70% for 77-115 dB, indicating that the measured 'startle' from mice was 55-70% less intense when a prepulse was played versus when the louder 115 dB pulse was played without the prepulse.

The black bars under the label "Vehicle" represent the inhibition when mice were treated with methamphetamine. It is clear that under the effects of methamphetamine, the prepulse does not cause a significant inhibition response to the louder pulse. This more erratic behavior is what can be attributed to patients with schizophrenia, in fact studies support that almost all schizophrenic patients have a lower PPI% then non-schizophrenic control groups (eye blink test).

The grey bars labeled "Furo" represent administration of furosemide, a known $GABA_A$ antagonist/NAM that acts particularly strongly at the α_6 site. Furosemide was used as a control to assess whether or not the effects seen were the results of α_6 modulation or interactions with other sites in the brain. It was shown that furosemide given directly into the brain slightly rescued PPI% in mice under the effects of methamphetamine; however, these effects may be explained by the method in which furosemide was administered. Furosemide (pictured in Figure 10-19) does not readily cross the blood-brain-barrier because it is a very hydrophilic molecule thus necessitating direct injection into the brain. This can perhaps effect the concentration of methamphetamine in the brain which could explain the modest rescue of PPI. More importantly, however, administration of furosemide negatively affected the rescue response seen from the administration of **Compound 6** and **Compound 11**, especially in the 77-115 dB assay. This suggests that the PPI effects of **Compound 6** and **Compound 11** are mediated by α_6 subtypes.

This is an important result in terms of psychiatric diseases such as schizophrenia, OCD, and tic

diseases including Tourette syndrome among a number of other potential applications.

Figure 10-19: Structure of furosemide, an $\alpha_6\beta_3\gamma_2$ receptor antagonist.

Log P: 0.74
tPSA: 118.72

furosemide
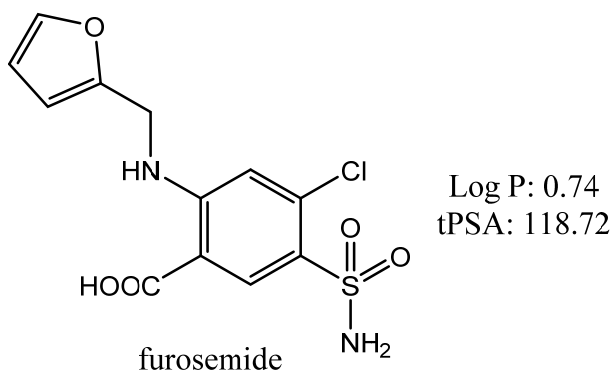
It was shown that both **Compound 6** and **Compound 11** administered i.p. at 10 mg/kg

were able to rescue PPI to a significant margin in mice under the influence of methamphetamine.

Prior data has shown that **Compound 6** was not sedative or motor impairing (Chapter 10 section

2), consequently, these results indicate that **Compound 6**, or α_6 subtypes in general, have the

ability to rescue PPI in animals with sensorimotor gating deficits. A similar assay was

subsequently completed comparing these results to some of the other new and novel α6 selective

ligands discovered thus far (Figure 10-20).

Figure 10-20: PPI rescue of other α6 PAM's.
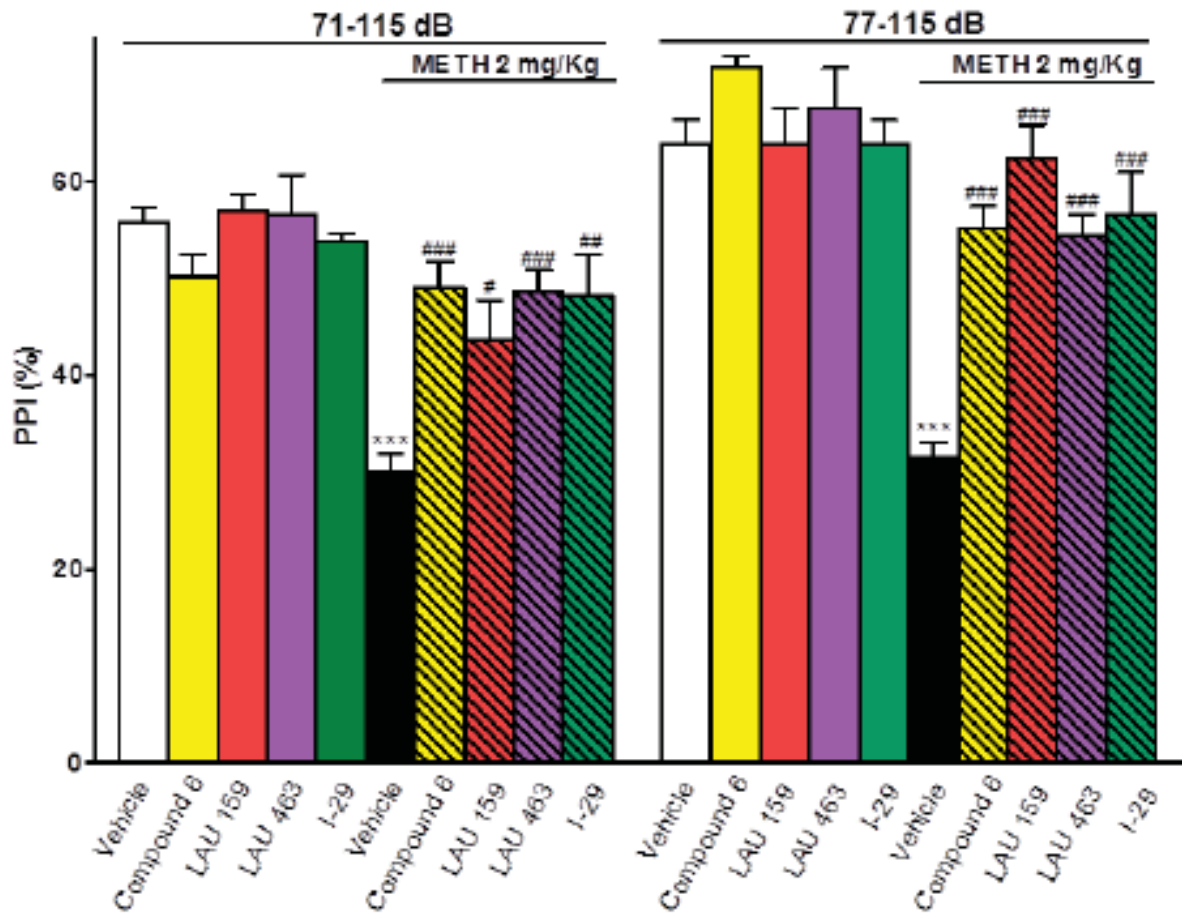
Examination of this assay indicated that the $α_6$ ligands administered i.p. at 10 mg/kg had no effect on mice that were not under the influence of methamphetamine, again showing that these selective and potent ligands have very little, if any, negative side-effects. This ability to rescue PPI while at the same time showing no negative side-effects is strong evidence that these ligands may be important pharmaceutical agents for patients with sensorimotor gating deficits.

4.   Studies on the effects of Compound 6 on migraines.

It has been demonstrated that c-Fos-ir neurons in the trigeminal nucleus caudalis (TNC) are associated with pain related to migraines. Specifically, the location of the TNC may offer an anatomical explanation to the 'back-of-the-head' pain associated with severe migraines.[85] Depicted in Figure 10-21 are data that show c-Fos positive numbers can be influenced by cranial injection of capsaicin, the chemical component of hot peppers that causes the associated burning sensation. It was found that i.p. injection of **Compound 6** at both 3 mg/kg and 10 mg/kg significantly reduced the c-Fos positive number, essentially lowering the pain sensation associated with the capsaicin vehicle. This demonstrates that these novel α6 ligands can play a potential role in negating the effects of a severe migraine.

The GABA$_A$ α$_6$ receptor has been implicated in the past as a potential inhibitor of trigeminal nociceptive pain based on gene knockout studies; these results confirm this with a true α$_6$ selective ligand with pharmaceutical potential. Examination of these results proompted further testing in an IoN-CCI model which tests for the possibility that these ligands could treat trigeminal neuralgia and trigeminal neuropathy.[86]

Figure 10-21: Reduction of c-Fos positive numbers increased by injection of capsaisin.
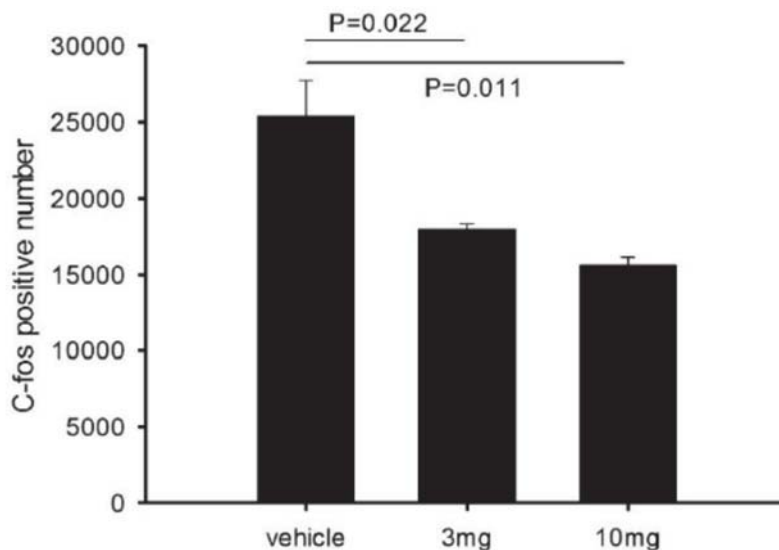
5.   IoN-CCI studies.

Infraorbital nerve chronic constriction injury (IoN-CCI) is a common neuropathic pain model. The unilateral ligature of the infraorbital nerve (IoN) in rats, as an animal model of peripheral neuropathic pain, and more specifically, trigeminal neuralgia and trigeminal neuropathy, was performed as described by Desuere and Hans.[87] The effects of subchronic treatment were tested with a nanoemulsion formulation of DK-I-56-1 (**19**) injected i.p. at 10 mg/kg. Examination of Figure 10-22 illustrates the results of this experiment.

Figure 10-22: IoN-CCI experiment results.
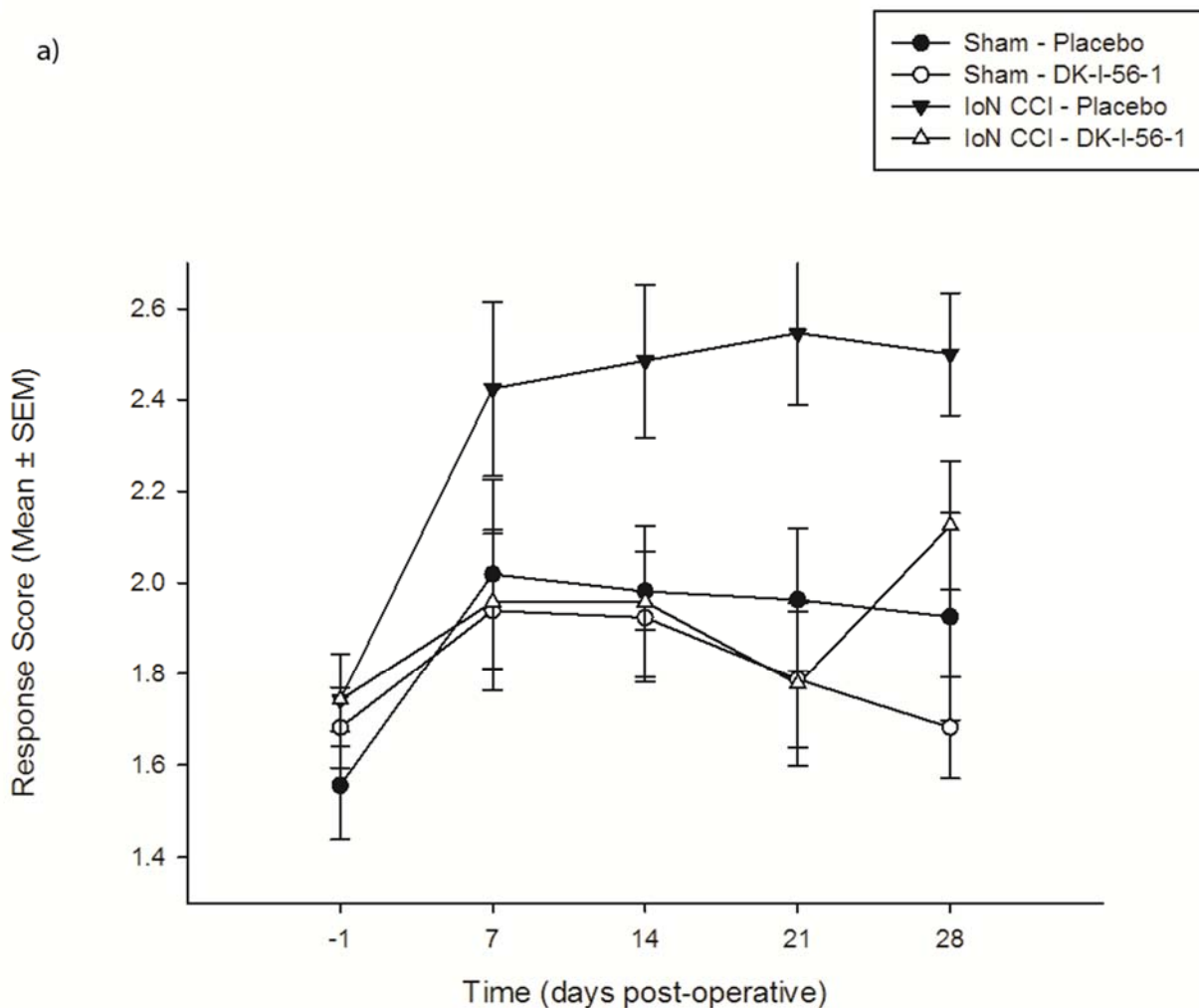
Rats were injected daily for 14 consecutive days post-surgery with DK-I-56-1 and positive effects were seen through day 21, indicating that the novel α6 selective deuterated analog of **Compound 6** (DK-I-56-1) effectively modulated pain in IoN-CCI rats. Sham surgeries (circles) represent rats that went through the entire surgical process, however, the infraorbital nerve was not ligated, thus pain associated with the surgery itself can be accounted for in the control.

Over the course of this assay face grooming in mice was also measured (Figure 10-23), another assay to assess whether or not negative side-effects of these ligands were present. It was found that the mice treated with DK-I-56-1 did not differ significantly to the other control mice. This is more confirmation that these selective ligands show no signs of the usual benzodiazepine related side-effects.

Figure 10-23: Face grooming in DK-I-56-1 treated IoN-CCI rats.
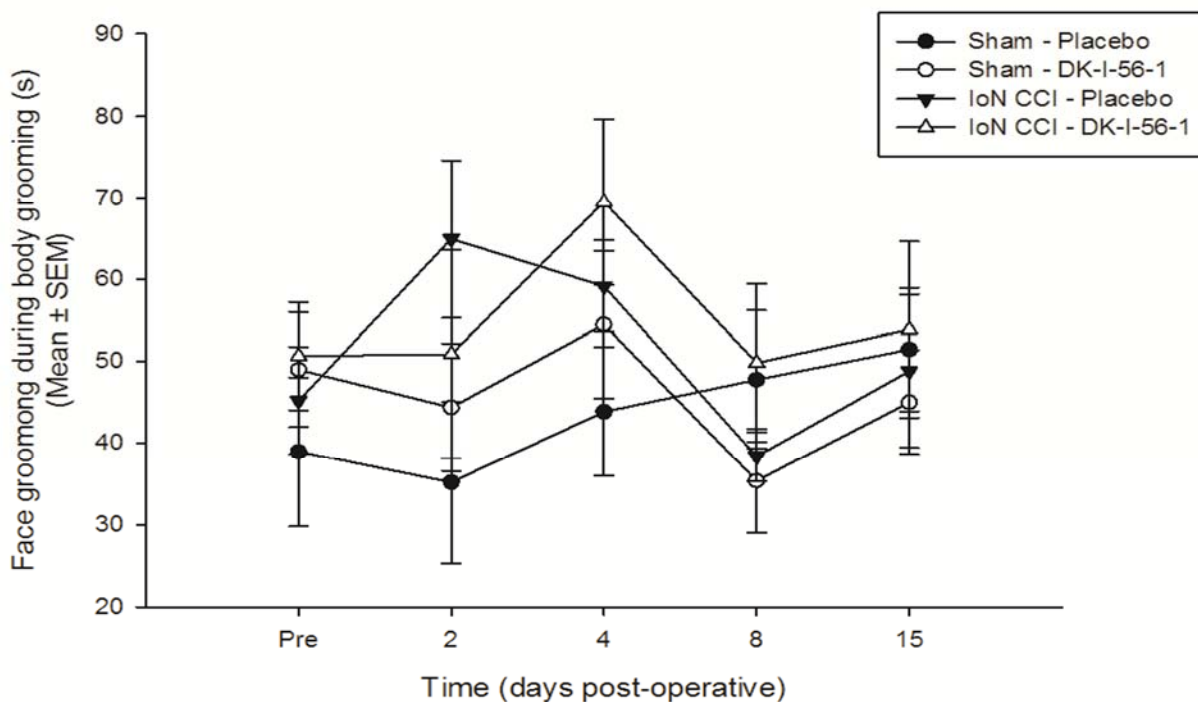
III.   CONCLUSION.

In conclusion, it has been shown that subtype selective α_6 ligands have potential as novel and selective pharmaceutical agents to treat a number of neurological disorders including nociceptive pain, OCD, Tourette syndrome, schizophrenia, and anxiety disorders among others. *In vitro* studies have shown potent efficacy at the specific $\alpha_6\beta_3\gamma_2$ subtype in oocytes, increased

solubility by addition of a pyridine ring while maintaining selectivity, and a significant increase in metabolic stability with the introduction of deuterium to ring-A or ring-D methoxy groups. These *in vitro* studies laid the ground work for *in vivo* testing in mice and rats.

The first *in vivo* studies described herein were initiated to determine some of the pharmacokinetic parameters of these compounds, principally the concentration reached in plasma and brain tissue when administered i.p. in mice. Analysis of these data indicated that these selective ligands readily passed the blood-brain-barrier and were thus good candidates for further *in vivo* work. Studies were then initiated to determine whether or not these subtype selective α_6 ligands showed any of the usual negative effects seen with benzodiazepines such as diazepam. Analysis of these studies indicated that **Compound 6**, the first reported α_6 subtype selective ligand, exhibited little or no negative side-effects when dosed i.p. in mice. In fact, a potential anti-anxiety indication was the only result that differed from vehicle (Figures 10-15 and 10-16), clearly a positive effect.

These promising results led to further *in vivo* testing in models of prepulse inhibition, migraine, and IoN-CCI assays. Analysis of all three assays showed novel potential use of these selective α_6 ligands for the treatment of different neurological diseases. Future work will include improving solubility as well as a more thorough PK study to assess drugable characteristics of these ligands. While **Compound 6** and its related deuterated analogs already show great promise in delivering a CNS drug with little to no negative side-effects, efforts to discover more soluble, selective, and potent drug candidates is still ongoing. In particular, future assays to test oral bioavailability and the design of new analogs with enhance bioavailability are particularly exciting.

REFERENCES

1. Jembrek, M. J.; Vlainic, J., GABA Receptors: Pharmacological Potential and Pitfalls. *Curr Pharm Des* **2015,** *21* (34), 4943-59.

2. Watanabe, M.; Maemura, K.; Kanbara, K.; Tamayama, T.; Hayasaki, H., GABA and GABA receptors in the central nervous system and other organs. *Int Rev Cytol* **2002,** *213*, 1-47.

3. Spitzer, N. C., How GABA generates depolarization. *J Physiol* **2010,** *588* (Pt 5), 757-8.

4. Olsen, R. W.; Tobin, A. J., Molecular biology of GABAA receptors. *FASEB J* **1990,** *4* (5), 1469-80.

5. Pinard, A.; Seddik, R.; Bettler, B., GABAB receptors: physiological functions and mechanisms of diversity. *Adv Pharmacol* **2010,** *58*, 231-55.

6. Barnard, E. A.; Skolnick, P.; Olsen, R. W.; Mohler, H.; Sieghart, W.; Biggio, G.; Braestrup, C.; Bateson, A. N.; Langer, S. Z., International Union of Pharmacology. XV. Subtypes of gamma-aminobutyric acidA receptors: classification on the basis of subunit structure and receptor function. *Pharmacol Rev* **1998,** *50* (2), 291-313.

7. McCormick, D. A., GABA as an inhibitory neurotransmitter in human cerebral cortex. *J Neurophysiol* **1989,** *62* (5), 1018-27.

8. Girault, J. A., Integrating neurotransmission in striatal medium spiny neurons. *Adv Exp Med Biol* **2012,** *970*, 407-29.

9. Thwaites, D. T.; Basterfield, L.; McCleave, P. M.; Carter, S. M.; Simmons, N. L., Gamma-Aminobutyric acid (GABA) transport across human intestinal epithelial (Caco-2) cell monolayers. *Br J Pharmacol* **2000,** *129* (3), 457-64.

10.	Reinius, B.; Blunder, M.; Brett, F. M.; Eriksson, A.; Patra, K.; Jonsson, J.; Jazin, E.; Kullander, K., Conditional targeting of medium spiny neurons in the striatal matrix. *Frontiers in Behavioral Neuroscience* **2015,** *9* (71).

11.	Johnston, G. A., GABA(A) receptor channel pharmacology. *Curr Pharm Des* **2005,** *11* (15), 1867-85.

12.	Ernst, M.; Bruckner, S.; Boresch, S.; Sieghart, W., Comparative models of GABAA receptor extracellular and transmembrane domains: important insights in pharmacology and function. *Mol Pharmacol* **2005,** *68* (5), 1291-300.

13.	Harkin, L. A.; Bowser, D. N.; Dibbens, L. M.; Singh, R.; Phillips, F.; Wallace, R. H.; Richards, M. C.; Williams, D. A.; Mulley, J. C.; Berkovic, S. F.; Scheffer, I. E.; Petrou, S., Truncation of the GABA(A)-receptor gamma2 subunit in a family with generalized epilepsy with febrile seizures plus. *Am J Hum Genet* **2002,** *70* (2), 530-6.

14.	Bateson, A. N., The benzodiazepine site of the GABAA receptor: an old target with new potential? *Sleep Med* **2004,** *5 Suppl 1*, S9-15.

15.	Mohler, H., The GABA system in anxiety and depression and its therapeutic potential. *Neuropharmacology* **2012,** *62* (1), 42-53.

16.	Petty, F., GABA and mood disorders: a brief review and hypothesis. *J Affect Disord* **1995,** *34* (4), 275-81.

17.	Ishikawa, M.; Mizukami, K.; Iwakiri, M.; Hidaka, S.; Asada, T., GABAA receptor gamma subunits in the prefrontal cortex of patients with schizophrenia and bipolar disorder. *Neuroreport* **2004,** *15* (11), 1809-12.

18.	Wassef, A.; Baker, J.; Kochan, L. D., GABA and schizophrenia: a review of basic science and clinical studies. *J Clin Psychopharmacol* **2003,** *23* (6), 601-40.

19. Solas, M.; Puerta, E.; Ramirez, M. J., Treatment Options in Alzheimer s Disease: The GABA Story. *Curr Pharm Des* **2015,** *21* (34), 4960-71.

20. Lüddens, H.; Wisden, W., Function and pharmacology of multiple GABAA receptor subunits. *Trends in Pharmacological Sciences* **1991,** *12*, 49-51.

21. Kralic, J. E.; Korpi, E. R.; O'Buckley, T. K.; Homanics, G. E.; Morrow, A. L., Molecular and pharmacological characterization of GABA(A) receptor alpha1 subunit knockout mice. *J Pharmacol Exp Ther* **2002,** *302* (3), 1037-45.

22. Simon, J.; Wakimoto, H.; Fujita, N.; Lalande, M.; Barnard, E. A., Analysis of the set of GABA(A) receptor genes in the human genome. *J Biol Chem* **2004,** *279* (40), 41422-35.

23. Sieghart, W.; Sperk, G., Subunit composition, distribution and function of GABA(A) receptor subtypes. *Curr Top Med Chem* **2002,** *2* (8), 795-816.

24. Olsen, R. W.; Sieghart, W., GABA A receptors: subtypes provide diversity of function and pharmacology. *Neuropharmacology* **2009,** *56* (1), 141-8.

25. Sieghart, W., Structure and pharmacology of gamma-aminobutyric acidA receptor subtypes. *Pharmacol Rev* **1995,** *47* (2), 181-234.

26. Vijayan, R. S.; Trivedi, N.; Roy, S. N.; Bera, I.; Manoharan, P.; Payghan, P. V.; Bhattacharyya, D.; Ghoshal, N., Modeling the closed and open state conformations of the GABA(A) ion channel--plausible structural insights for channel gating. *J Chem Inf Model* **2012,** *52* (11), 2958-69.

27. Obata, T.; Yamamura, H. I., The effect of benzodiazepines and beta-carbolines on GABA-stimulated chloride influx by membrane vesicles from the rat cerebral cortex. *Biochem Biophys Res Commun* **1986,** *141* (1), 1-6.

28. Saunders, P. A.; Ho, I. K., Barbiturates and the GABAA receptor complex. *Prog Drug Res* **1990,** *34*, 261-86.

29. Lobo, I. A.; Harris, R. A., GABA(A) receptors and alcohol. *Pharmacol Biochem Behav* **2008,** *90* (1), 90-4.

30. Di Lio, A.; Benke, D.; Besson, M.; Desmeules, J.; Daali, Y.; Wang, Z. J.; Edwankar, R.; Cook, J. M.; Zeilhofer, H. U., HZ166, a novel GABAA receptor subtype-selective benzodiazepine site ligand, is antihyperalgesic in mouse models of inflammatory and neuropathic pain. *Neuropharmacology* **2011,** *60* (4), 626-32.

31. De Deyn, P. P.; Macdonald, R. L., Effects of non-sedative anxiolytic drugs on responses to GABA and on diazepam-induced enhancement of these responses on mouse neurones in cell culture. *Br J Pharmacol* **1988,** *95* (1), 109-20.

32. Melani, F.; Cecchi, L.; Palazzino, G.; Filacchioni, G.; Martini, C.; Pennacchi, E.; Lucacchini, A., Pyrazolo[4,5-c]quinolines. 3. Synthesis, receptor binding, and 13C NMR study. *J Pharm Sci* **1986,** *75* (12), 1175-9.

33. Sigel, E.; Buhr, A., The benzodiazepine binding site of GABAA receptors. *Trends Pharmacol Sci* **1997,** *18* (11), 425-9.

34. Atack, J. R., The benzodiazepine binding site of GABA(A) receptors as a target for the development of novel anxiolytics. *Expert Opin Investig Drugs* **2005,** *14* (5), 601-18.

35. Richter, L.; de Graaf, C.; Sieghart, W.; Varagic, Z.; Morzinger, M.; de Esch, I. J.; Ecker, G. F.; Ernst, M., Diazepam-bound GABAA receptor models identify new benzodiazepine binding-site ligands. *Nat Chem Biol* **2012,** *8* (5), 455-64.

36.   Ramerstorfer, J.; Furtmuller, R.; Sarto-Jackson, I.; Varagic, Z.; Sieghart, W.; Ernst, M., The GABAA receptor alpha+beta- interface: a novel target for subtype selective drugs. *J Neurosci* **2011,** *31* (3), 870-7.

37.   Varagic, Z.; Wimmer, L.; Schnurch, M.; Mihovilovic, M. D.; Huang, S.; Rallapalli, S.; Cook, J. M.; Mirheydari, P.; Ecker, G. F.; Sieghart, W.; Ernst, M., Identification of novel positive allosteric modulators and null modulators at the GABAA receptor alpha+beta-interface. *Br J Pharmacol* **2013,** *169* (2), 371-83.

38.   Wang, M., Neurosteroids and GABA-A Receptor Function. *Front Endocrinol (Lausanne)* **2011,** *2*, 44.

39.   Aguayo, L. G.; Peoples, R. W.; Yeh, H. H.; Yevenes, G. E., GABA(A) receptors as molecular sites of ethanol action. Direct or indirect actions? *Curr Top Med Chem* **2002,** *2* (8), 869-85.

40.   Vinkers, C. H.; van Oorschot, R.; Nielsen, E. O.; Cook, J. M.; Hansen, H. H.; Groenink, L.; Olivier, B.; Mirza, N. R., GABA(A) receptor alpha subunits differentially contribute to diazepam tolerance after chronic treatment. *PLoS One* **2012,** *7* (8), e43054.

41.   Chaouloff, F.; Durand, M.; Mormede, P., Anxiety- and activity-related effects of diazepam and chlordiazepoxide in the rat light/dark and dark/light tests. *Behav Brain Res* **1997,** *85* (1), 27-35.

42.   Griffin, C. E., 3rd; Kaye, A. M.; Bueno, F. R.; Kaye, A. D., Benzodiazepine pharmacology and central nervous system-mediated effects. *Ochsner J* **2013,** *13* (2), 214-23.

43.   Mandelli, M.; Tognoni, G.; Garattini, S., Clinical pharmacokinetics of diazepam. *Clin Pharmacokinet* **1978,** *3* (1), 72-91.

44. Friedman, H.; Greenblatt, D. J.; Peters, G. R.; Metzler, C. M.; Charlton, M. D.; Harmatz, J. S.; Antal, E. J.; Sanborn, E. C.; Francom, S. F., Pharmacokinetics and pharmacodynamics of oral diazepam: effect of dose, plasma concentration, and time. *Clin Pharmacol Ther* **1992,** *52* (2), 139-50.

45. Greenblatt, D. J.; Sethy, V. H., Benzodiazepine concentrations in brain directly reflect receptor occupancy: studies of diazepam, lorazepam, and oxazepam. *Psychopharmacology (Berl)* **1990,** *102* (3), 373-8.

46. Millikan, D.; Rice, B.; Silbergleit, R., Emergency treatment of status epilepticus: current thinking. *Emerg Med Clin North Am* **2009,** *27* (1), 101-13, ix.

47. Hooper, W. D.; Watt, J. A.; McKinnon, G. E.; Reilly, P. E., Metabolism of diazepam and related benzodiazepines by human liver microsomes. *Eur J Drug Metab Pharmacokinet* **1992,** *17* (1), 51-9.

48. Buckley, N. A.; Dawson, A. H.; Whyte, I. M.; O'Connell, D. L., Relative toxicity of benzodiazepines in overdose. *BMJ* **1995,** *310* (6974), 219-21.

49. Gudex, C., Adverse effects of benzodiazepines. *Soc Sci Med* **1991,** *33* (5), 587-96.

50. Arbanas, G.; Arbanas, D.; Dujam, K., Adverse effects of benzodiazepines in psychiatric outpatients. *Psychiatr Danub* **2009,** *21* (1), 103-7.

51. Uzun, S.; Kozumplik, O.; Jakovljevic, M.; Sedic, B., Side effects of treatment with benzodiazepines. *Psychiatr Danub* **2010,** *22* (1), 90-3.

52. Uusi-Oukari, M.; Korpi, E. R., Regulation of GABA(A) receptor subunit expression by pharmacological agents. *Pharmacol Rev* **2010,** *62* (1), 97-135.

53. Rudolph, U.; Crestani, F.; Benke, D.; Brunig, I.; Benson, J. A.; Fritschy, J. M.; Martin, J. R.; Bluethmann, H.; Mohler, H., Benzodiazepine actions mediated by specific gamma-aminobutyric acid(A) receptor subtypes. *Nature* **1999,** *401* (6755), 796-800.

54. Tauber, M.; Calame-Droz, E.; Prut, L.; Rudolph, U.; Crestani, F., alpha2-gamma-Aminobutyric acid (GABA)A receptors are the molecular substrates mediating precipitation of narcosis but not of sedation by the combined use of diazepam and alcohol in vivo. *Eur J Neurosci* **2003,** *18* (9), 2599-604.

55. Atack, J. R.; Hutson, P. H.; Collinson, N.; Marshall, G.; Bentley, G.; Moyes, C.; Cook, S. M.; Collins, I.; Wafford, K.; McKernan, R. M.; Dawson, G. R., Anxiogenic properties of an inverse agonist selective for alpha3 subunit-containing GABA A receptors. *Br J Pharmacol* **2005,** *144* (3), 357-66.

56. Ling, I.; Mihalik, B.; Etherington, L. A.; Kapus, G.; Palvolgyi, A.; Gigler, G.; Kertesz, S.; Gaal, A.; Pallagi, K.; Kiricsi, P.; Szabo, E.; Szenasi, G.; Papp, L.; Harsing, L. G.; Levay, G.; Spedding, M.; Lambert, J. J.; Belelli, D.; Barkoczy, J.; Volk, B.; Simig, G.; Gacsalyi, I.; Antoni, F. A., A novel GABA(A) alpha 5 receptor inhibitor with therapeutic potential. *Eur J Pharmacol* **2015,** *764*, 497-507.

57. Paul, J.; Yevenes, G. E.; Benke, D.; Di Lio, A.; Ralvenius, W. T.; Witschi, R.; Scheurer, L.; Cook, J. M.; Rudolph, U.; Fritschy, J. M.; Zeilhofer, H. U., Antihyperalgesia by alpha2-GABAA receptors occurs via a genuine spinal action and does not involve supraspinal sites. *Neuropsychopharmacology* **2014,** *39* (2), 477-87.

58. Ralvenius, W. T.; Benke, D.; Acuna, M. A.; Rudolph, U.; Zeilhofer, H. U., Analgesia and unwanted benzodiazepine effects in point-mutated mice expressing only one benzodiazepine-sensitive GABAA receptor subtype. *Nat Commun* **2015,** *6*, 6803.

59. McKernan, R. M.; Quirk, K.; Prince, R.; Cox, P. A.; Gillard, N. P.; Ragan, C. I.; Whiting, P., GABAA receptor subtypes immunopurified from rat brain with alpha subunit-specific antibodies have unique pharmacological properties. *Neuron* **1991,** *7* (4), 667-76.

60. Fritschy, J. M.; Paysan, J.; Enna, A.; Mohler, H., Switch in the expression of rat GABAA-receptor subtypes during postnatal development: an immunohistochemical study. *J Neurosci* **1994,** *14* (9), 5302-24.

61. Suryanarayanan, A.; Liang, J.; Meyer, E. M.; Lindemeyer, A. K.; Chandra, D.; Homanics, G. E.; Sieghart, W.; Olsen, R. W.; Spigelman, I., Subunit Compensation and Plasticity of Synaptic GABA(A) Receptors Induced by Ethanol in alpha4 Subunit Knockout Mice. *Front Neurosci* **2011,** *5*, 110.

62. Mehta, A. K.; Ticku, M. K., Prevalence of the GABAA receptor assemblies containing alpha1-subunit in the rat cerebellum and cerebral cortex as determined by immunoprecipitation: lack of modulation by chronic ethanol administration. *Brain Res Mol Brain Res* **1999,** *67* (1), 194-9.

63. Fritschy, J. M.; Mohler, H., GABAA-receptor heterogeneity in the adult rat brain: differential regional and cellular distribution of seven major subunits. *J Comp Neurol* **1995,** *359* (1), 154-94.

64. Braudeau, J.; Delatour, B.; Duchon, A.; Pereira, P. L.; Dauphinot, L.; de Chaumont, F.; Olivo-Marin, J. C.; Dodd, R. H.; Herault, Y.; Potier, M. C., Specific targeting of the GABA-A receptor alpha5 subtype by a selective inverse agonist restores cognitive deficits in Down syndrome mice. *J Psychopharmacol* **2011,** *25* (8), 1030-42.

65. Benke, D.; Michel, C.; Mohler, H., GABA(A) receptors containing the alpha4-subunit: prevalence, distribution, pharmacology, and subunit architecture in situ. *J Neurochem* **1997,** *69* (2), 806-14.

66. Carlson, B. X.; Belhage, B.; Hansen, G. H.; Elster, L.; Olsen, R. W.; Schousboe, A., Expression of the GABA(A) receptor alpha6 subunit in cultured cerebellar granule cells is developmentally regulated by activation of GABA(A) receptors. *J Neurosci Res* **1997,** *50* (6), 1053-62.

67. Knoflach, F.; Benke, D.; Wang, Y.; Scheurer, L.; Luddens, H.; Hamilton, B. J.; Carter, D. B.; Mohler, H.; Benson, J. A., Pharmacological modulation of the diazepam-insensitive recombinant gamma-aminobutyric acidA receptors alpha 4 beta 2 gamma 2 and alpha 6 beta 2 gamma 2. *Mol Pharmacol* **1996,** *50* (5), 1253-61.

68. Clayton, T.; Poe, M. M.; Rallapalli, S.; Biawat, P.; Savić, M. M.; Rowlett, J. K.; Gallos, G.; Emala, C. W.; Kaczorowski, C. C.; Stafford, D. C.; Arnold, L. A.; Cook, J. M., A Review of the Updated Pharmacophore for the Alpha 5 GABA(A) Benzodiazepine Receptor Model. *International Journal of Medicinal Chemistry* **2015,** *2015*, 430248.

69. Jin, N.; Guo, Y.; Sun, P.; Bell, A.; Chintagari, N. R.; Bhaskaran, M.; Rains, K.; Baviskar, P.; Chen, Z.; Weng, T.; Liu, L., Ionotropic GABA receptor expression in the lung during development. *Gene Expr Patterns* **2008,** *8* (6), 397-403.

70. Chintagari, N. R.; Jin, N.; Gao, L.; Wang, Y.; Xi, D.; Liu, L., Role of GABA receptors in fetal lung development in rats. *PLoS One* **2010,** *5* (11), e14171.

71. Allen, M. S.; Skolnick, P.; Cook, J. M., Synthesis of novel 2-phenyl-2H-pyrazolo[4,3-c]isoquinolin-3-ols: topological comparisons with analogues of 2-phenyl-2,5-

dihydropyrazolo[4,3-c]quinolin-3(3H)-ones at benzodiazepine receptors. *J Med Chem* **1992,** *35* (2), 368-74.

72.   Boast, C. A.; Snowhill, E. W.; Simke, J. P., CGS 8216 and CGS 9896, novel pyrazoloquinoline benzodiazepine ligands with benzodiazepine agonist and antagonist properties. *Pharmacol Biochem Behav* **1985,** *23* (4), 639-44.

73.   Lummis, S. C., Locating GABA in GABA receptor binding sites. *Biochem Soc Trans* **2009,** *37* (Pt 6), 1343-6.

74.   Hansen, R. R.; Erichsen, H. K.; Brown, D. T.; Mirza, N. R.; Munro, G., Positive allosteric modulation of GABA-A receptors reduces capsaicin-induced primary and secondary hypersensitivity in rats. *Neuropharmacology* **2012,** *63* (8), 1360-7.

75.   Rigo, J. M.; Hans, G.; Nguyen, L.; Rocher, V.; Belachew, S.; Malgrange, B.; Leprince, P.; Moonen, G.; Selak, I.; Matagne, A.; Klitgaard, H., The anti-epileptic drug levetiracetam reverses the inhibition by negative allosteric modulators of neuronal GABA- and glycine-gated currents. *Br J Pharmacol* **2002,** *136* (5), 659-72.

76.   Homanics, G. E.; Ferguson, C.; Quinlan, J. J.; Daggett, J.; Snyder, K.; Lagenaur, C.; Mi, Z. P.; Wang, X. H.; Grayson, D. R.; Firestone, L. L., Gene knockout of the alpha6 subunit of the gamma-aminobutyric acid type A receptor: lack of effect on responses to ethanol, pentobarbital, and general anesthetics. *Mol Pharmacol* **1997,** *51* (4), 588-96.

77.   Turner, D. M.; Sapp, D. W.; Olsen, R. W., The benzodiazepine/alcohol antagonist Ro 15-4513: binding to a GABAA receptor subtype that is insensitive to diazepam. *J Pharmacol Exp Ther* **1991,** *257* (3), 1236-42.

78.   Sander, T.; Ball, D.; Murray, R.; Patel, J.; Samochowiec, J.; Winterer, G.; Rommelspacher, H.; Schmidt, L. G.; Loh, E. W., Association analysis of sequence

variants of GABA(A) alpha6, beta2, and gamma2 gene cluster and alcohol dependence. *Alcohol Clin Exp Res* **1999,** *23* (3), 427-31.

79.   Vekovischeva, O.; Uusi-Oukari, M.; Korpi, E. R., Tolerance to diazepam-induced motor impairment: a study with GABAA receptor alpha6 subunit knockout mice. *Neurochem Res* **2003,** *28* (5), 757-64.

80.   Hernandez, C. C.; Gurba, K. N.; Hu, N.; Macdonald, R. L., The GABRA6 mutation, R46W, associated with childhood absence epilepsy, alters 6beta22 and 6beta2 GABA(A) receptor channel gating and expression. *J Physiol* **2011,** *589* (Pt 23), 5857-78.

81.   Uhart, M.; McCaul, M. E.; Oswald, L. M.; Choi, L.; Wand, G. S., GABRA6 gene polymorphism and an attenuated stress response. *Mol Psychiatry* **2004,** *9* (11), 998-1006.

82.   Han, D. H.; Bolo, N.; Daniels, M. A.; Lyoo, I. K.; Min, K. J.; Kim, C. H.; Renshaw, P. F., Craving for alcohol and food during treatment for alcohol dependence: modulation by T allele of 1519T>C GABAAalpha6. *Alcohol Clin Exp Res* **2008,** *32* (9), 1593-9.

83.   Rosmond, R.; Bouchard, C.; Bjorntorp, P., Association between a variant at the GABA(A)alpha6 receptor subunit gene, abdominal obesity, and cortisol secretion. *Ann N Y Acad Sci* **2002,** *967*, 566-70.

84.   Thompson, C. L.; Pollard, S.; Stephenson, F. A., Developmental regulation of expression of GABAA receptor alpha 1 and alpha 6 subunits in cultured rat cerebellar granule cells. *Neuropharmacology* **1996,** *35* (9-10), 1337-46.

85.   Oshinsky, M. L.; Luo, J., Neurochemistry of trigeminal activation in an animal model of migraine. *Headache* **2006,** *46 Suppl 1*, S39-44.

86.	Kramer, P. R.; Bellinger, L. L., Reduced GABAA receptor alpha6 expression in the trigeminal ganglion enhanced myofascial nociceptive response. *Neuroscience* **2013,** *245*, 1-11.

87.	Deseure, K.; Hans, G. H., Chronic Constriction Injury of the Rat's Infraorbital Nerve (IoN-CCI) to Study Trigeminal Neuropathic Pain. *J Vis Exp* **2015,** (103).

Christopher M. Witzigmann

5456 S. Andrae Dr., New Berlin, WI 53151
chris.witzigmann@gmail.com • (414) 687-4912

EDUCATION

University of Wisconsin – Milwaukee
- PhD in Organic Chemistry   2009-2016
- Under the direction of University Distinguished Professor Dr. James M. Cook
  <u>Thesis Title</u>
  Part 1: Design, synthesis, and evaluation of novel gram-positive antibiotics
  Part 2: Synthesis of dihydrobenzofurans via a new transition metal catalyzed reaction
  Part 3: Design, synthesis, and evaluation of GABA(A) α6 positive allosteric modulators

University of Wisconsin – Milwaukee
- BS Chemistry (Course in Chemistry)   2001-2007
- Undergraduate research under Dr. Andrew Pacheco   2007
  Synthesis of organic cage ligands for heavy metals

PROFESSIONAL EXPERIENCE

Fontarome Chemical (now Apiscent Labs)
- R&D Chemist 1   2007-2008
  - Use test starting materials
  - Supervise production chemists
  - Manage GC/MS and LC/MS R&D equipment
- R&D Chemist II   2008-2009
  - Lead chemist, multiple API and F&F projects
  - Bench to production scale troubleshooting
  - Process chemistry pilot plant scale

PATENTS

1. "Stereospecific Synthesis of Acrylate Ethers and Amines for Industrial and Medicinal Applications," Kabir, M.; Cook, J.M.; Monte, A.; Rott, M.; Schwan, W.; **Witzigmann, C.**; Namjoshi, O.; Babu, V.V.N.Phani; Verma, R. Provisional filed 14 March (2012), Serial # 61/610,574.

2. "Design and Synthesis of Acrylate Esters with Activity Against Bacteria and Mycobacteria, Including M. Tuberculosis and Methicillin Resistant S. Aurerus (MRSA)., M. Kabir, J.M. Cook, A. Monte, M. Rott, W. Schwan, **C. Witzigmann**, O. Namjoshi, V.V.N. Phani Tiruveedhula, R. Verma, Provisional Patent Applied for 4/10/13. Serial # 61/810, 487.

3. "Compounds for the Treatment of Gram-positive Bacterial Infections Including Resitant Strains of Staphylococcus aureus," Cook, J.; **Witzigmann, C.**; Tiruveedhula, V.V.N.; Monte, A.; Schwan, W.; Rott, M.; Verma, R.; Verma, A. filed October 2015.

4. "Ligands selective to alpha 6 subunit-containing GABAA receptors and their methods of use," Chiou, L.; Cook, J.; Ernst, M.; Fan, P.; **Witzigmann, C.**; Knutson, D.; Meirelles, M.; Mihorilovic, M.; Varagic, Z.; Verma, R.; Savic, M. filed June, 2016.

PUBLICATIONS

1. "Design and Synthesis of Novel Antimicrobials with Activity Against Gram-Positive Bacteria and Mycro-bacterial Species, Including M. Tuberculosis", Tiruveedhula, V. V. N.; **Witzigmann, C.**; Verma, R.; Shahjahan, M.; Rott, M.; Schwan, W.; Monte, A.; Sherman, D.; Cook, J. M. Bioorg. and Med. Chem., 21, 7830-40 (2013).

2. "Pharmacokinetic/Toxicity Properties of the New Anti-Staphylococcal Lead Compound SK-03-92," Schwan, W.; Kolesar, J.; Kabir, M.S.; Elder Jr, E.; Williams, J.; Minerath, R.; Cook, J.M.; **Witzigmann, C.**; Monte, A.; Flaherty, T.; Antibiotics, 4, 617-626 (2015).

3. "Characterization of GABA(A) receptor ligands with automated patch-clamp using human neurons derived from pluripotent stem cells," Yuan, N.; Poe, M.; **Witzigmann, C.**; Cook, J. M., Stafford, D.; Arnold, L.; Journal of Pharmacological and Toxicological Methods, manuscript accepted (2016).

3 additional manuscripts in process

PROFESSIONAL MEETINGS

- ACS National Meeting; New Orleans, LA; April 7-11, 2013.
"Design and Synthesis of a New Class of Antibacterials with Activity Against Mycobacteria and Gram-Positive Bacteria", **C.M. Witzigmann**, V.V. Tiruveedhula, J.M. Cook, A. Monte, W. Schwan, (Abst. MEDI 391).

- ACS National Meeting; Dallas, TX; March 16-20, 2014.
"Design and Synthesis of Novel Small Molecule Stilbenes with Activity Against Gram-Positive Bacteria and Mycobacterium," **Witzigmann, C.**; Tiruveedhula, V.; Monte, A.; Schwan, W.; Cook, J.M., (Abst.MEDI 266).

TEACHING AND RESEARCH EXPERIENCE

- Research Assistant   2011-2016
  - Designed new and novel small molecule compounds in a comprehensive SAR approach towards potently bioactive molecules.
  - Led a cross-functional research project between three different international universities.
  - Discovered and optimized a new palladium catalyzed reaction.
- Teaching Assistant   2009-intermittent
  - Chemistry 102: General Chemistry
  - Chemistry 103: Survey of Biochemistry
  - Chemistry 344: Organic Chemistry Laboratory